

## Abstracts

# 54. Jahrestagung der Deutschen Gesellschaft für Neuroradiologie e.V. und 27. Jahrestagung der Österreichischen Gesellschaft für Neuroradiologie

9.–12. Oktober 2019  
Kap Europa, Frankfurt a. M.

**Kongresspräsidenten**  
Prof. Dr. Claus Zimmer  
(München)  
Prim. Dr. Johannes Trenkler  
(Linz)

Dieses Supplement wurde von der Deutschen Gesellschaft für Neuroradiologie finanziert.

## Inhaltsverzeichnis

<b>Abstracts</b> . . . . .	S3
1. KI – Künstliche Intelligenz . . . . .	S3
Abstracts: 73, 97, 104, 124, 163, 187, 192, 208, 230, 241, 244, 254, 262, 264, 266, 280, 286, 345, 360, 363	
2. Neuroonkologie . . . . .	S15
Abstracts: 38, 88, 98, 176, 189, 220, 245, 311	
3. Entzündliche ZNS-Erkrankungen . . . . .	S19
Abstracts: 74, 87, 101, 106, 110, 142, 166, 194, 214, 296, 303	
4. Neurodegeneration. . . . .	S27
Abstracts: 157, 171, 180, 184, 204, 211, 256, 289, 310, 358	
5. Wirbelsäule . . . . .	S34
Abstracts: 96, 111, 128, 164, 199, 205, 314	
6. Zerebrovaskuläre Erkrankungen. . . . .	S41
Abstracts: 39, 42, 53, 63, 64, 65, 68, 69, 70, 75, 79, 81, 82, 86, 89, 94, 99, 100, 103, 108, 112, 115, 117, 121, 125, 127, 129, 130, 132, 134, 135, 136, 137, 138, 139, 144, 147, 148, 158, 162, 172, 174, 181, 183, 190, 193, 195, 196, 197, 203, 218, 222, 223, 224, 225, 234, 237, 246, 249, 251, 255, 259, 260, 263, 271, 274, 276, 277, 281, 285, 287, 288, 290, 291, 292, 293, 297, 298, 300, 301, 304, 309, 313, 320, 322, 323, 324, 329, 331, 340, 341, 347, 348, 349, 355, 356, 357, 364, 365, 370	
7. Sonstiges. . . . .	S102
Abstracts: 51, 57, 62, 67, 80, 92, 105, 109, 126, 143, 145, 150, 178, 186, 188, 200, 207, 226, 229, 252, 253, 267, 268, 269, 270, 284, 294, 299, 305, 312, 321, 333, 343, 362, 367	
<b>Autorenverzeichnis</b> . . . . .	S126

## 1. KI—Künstliche Intelligenz

73

### IMPACT OF SLICE THICKNESS ON ROBUSTNESS OF ELECTRONIC ALBERTA STROKE PROGRAM EARLY COMPUTED TOMOGRAPHY SCORES (E-ASPECTS)

Ulf Neuberger<sup>\*1</sup>, Johannes Pfaff<sup>1</sup>, Simon Nagel<sup>2</sup>, Peter Arthur Ringleb<sup>2</sup>, Christian Herweh<sup>1</sup>, Martin Bendszus<sup>1</sup>, Markus Möhlenbruch<sup>1</sup>, Philipp Kickingeder<sup>1</sup>

<sup>1</sup>Universitätsklinikum Heidelberg Neurologische Klinik: Neuroradiologie, Heidelberg, Deutschland

<sup>2</sup>Universitätsklinikum Heidelberg Neurologische Klinik: Neurologie, Heidelberg, Deutschland

**Background:** The clinical utility and non-inferiority of electronically derived Alberta Stroke Program Early CT Scores (e-ASPECTS) to quantify signs of acute ischemic infarction could be demonstrated in multiple studies. Still, the impact of different slice thicknesses of CT scans on the system's robustness are not sufficiently known.

**Methods:** A consecutive series of  $n=258$  patients diagnosed between 06/2016 and 01/2019 with middle cerebral artery occlusion and availability of baseline non-contrast CT scans with 1 mm slice thickness (ST) were included. Axial multiplanar reconstructions (MPR) between 2 and 10 mm ST (increment 1 mm) and maximum-intensity-projections (MIP) of 5 and 10 mm ST were generated and used to calculate e-ASPECTS scores with Brainomix software. Parameters from all reconstructions were univariately compared against those of the 1 mm dataset (which was defined as ground truth) and correlated with baseline stroke severity (National Institutes of Health Stroke Scale, NIHSS) as well as clinical outcome (modified Rankin Scale, mRS) and hemorrhagic events using generalized logistic regressions.

**Result:** There was no significant difference of e-ASPECTS scores (median, 9; interquartile range, 8–10) derived from 1 mm ST and those from MPR with 2–6 mm or MIP with 5 or 10 mm ST. However there was a significant difference in parameters derived from MPR reconstructions with >6 mm slice thickness ( $p<0.031$ ).

There was a significant correlation of lower e-ASPECTS and increasing baseline NIHSS values for all reconstructions. In generalized logistic regressions, MIP of 10 mm yielded the overall highest effects on clinical outcome after 90 days with odds ratios and confidence intervals for moderate outcome (mRS 2–6, 0.74 [0.62–0.88]), for poor outcome (mRS 3–6, 0.69 [0.58–0.83]) and for fatal outcome (0.76 [0.64–0.90]).

**Discussion:** The implementation of electronically derived ASPECTS by fully automated software solutions has been shown to be a clinically useful tool. The purpose of this study was to test the impact of different STs of CT scans on the robustness of a widely distributed software to generate e-ASPECTS for evaluation of early ischemic changes in patients with AIS.

**Conclusion:** Brainomix software can generate robust e-ASPECTS based on axial MPR images up to 6 mm ST without additional benefit of thinner slices. Furthermore, MIP reconstructions of 10 mm ST also produced robust results and had even higher effects as predictor of the clinical outcome after 90 days.

97

### HOW TO BREAK THE BOTTLENECK OF AI-DRIVEN RADIOLOGY AND GET YOUR HANDS ON THE NEW GOLD: "RIPE" A SOLUTION FOR DATA EXTRACTION AND ANALYSIS PIPELINE

Andreas Georg Junge<sup>\*1,2,3</sup>, Chang Gyu Cho<sup>2</sup>, Johannes Böhme<sup>2</sup>, Alex Förster<sup>2</sup>, Christoph Groden<sup>2</sup>, Thomas Ganslandt<sup>3</sup>, Holger Wenz<sup>2</sup>, Máté Maros<sup>2,3</sup>

<sup>1</sup>Hochschule Mannheim—University of Applied Sciences, Technical Informatics, Mannheim, Deutschland

<sup>2</sup>Medical Faculty Mannheim, Heidelberg University, Department of Neuroradiology, Mannheim, Deutschland

<sup>3</sup>Medizinische Fakultät Mannheim der Universität Heidelberg, Abteilung für Biomedizinische Informatik am Heinrich-Lanz-Zentrum, Mannheim, Deutschland

**Hintergrund:** In the new era of AI-driven radiology, data is the new gold. Still, data extraction and generation of high-quality labeled cohorts is extremely tedious and work intensive. It takes up 90% of the total effort of most machine learning (ML) projects. Ultimately, the quality of these input data defines the usability of the final ML model.

Here, we present an open-source, customizable data extraction and pre-processing pipeline (Radiology Information and PACS Extractor; RIPE) that enables an automated bulk information retrieval tailored for consequent deployment of prognostic and predictive models using computer assisted feedback for translational research in the daily praxis.

**Methoden:** We developed a vendor-independent fully open-source solution on top of the local RIS/PACS system (Syngo, Siemens) using well-established programming environments (C++, Python), libraries and frameworks (Qt, DCMTK, and Postgres). Building upon commonly used standards enabled us to create an easily expandable framework to streamline the complete information retrieval process from data collection, filtering, preprocessing up to final model deployment.

**Ergebnisse:** We present the use case of developing a complete end-to-end pipeline based on RIPE for primary ( $n=243$ ) and metastatic ( $n=252$ ) brain tumor classification. The pipelines enabled a  $>15\times$  faster cohort ( $n=497$ ,  $t=20$  h) extraction compared to manual data ( $t=2$  months) retrieval ( $p<0.01$ ) when scanning over 7000 cases from the last 5 years. By detailed query specification, we could achieve significantly higher data purity ( $p<0.01$ ) at first retrieval, thus substantially limiting manual review and quality control efforts. Furthermore, RIPE allows for a fully automated deep learning-based segmentation, classification, and prognostic evaluation of cases.

**Diskussion:** We present a customizable open-source software solution (RIPE), that is once set up, can not only diminish the need for manual data retrieval and preprocessing but also significantly speed up the whole development and deployment process of AI algorithms.

**Fazit:** Extractor frameworks like RIPE can support radiologists to provide precision medicine and to improve patient care at the earliest stage of diagnosis.

104

### EVALUATION OF AUTOMATED MENINGIOMA SEGMENTATION USING DEEP-LEARNING ON MULTIPARAMETRIC MRI

Kai Roman Laukamp<sup>\*</sup>, Lenhard Pennig, Frank Thiele, Robert Peter Reimer, David Zopfs, Lukas Görtz, Marco Timmer, Georgy Shakirin, Michael Perkuhn, Jan Borggrefe

Uniklinik Köln, Köln, Deutschland

**Hintergrund:** In clinical management, volumetric assessment of meningiomas is valuable for surgery or radiation planning and evaluation of tumour growth, as it allows for more sensitive detection of tumour

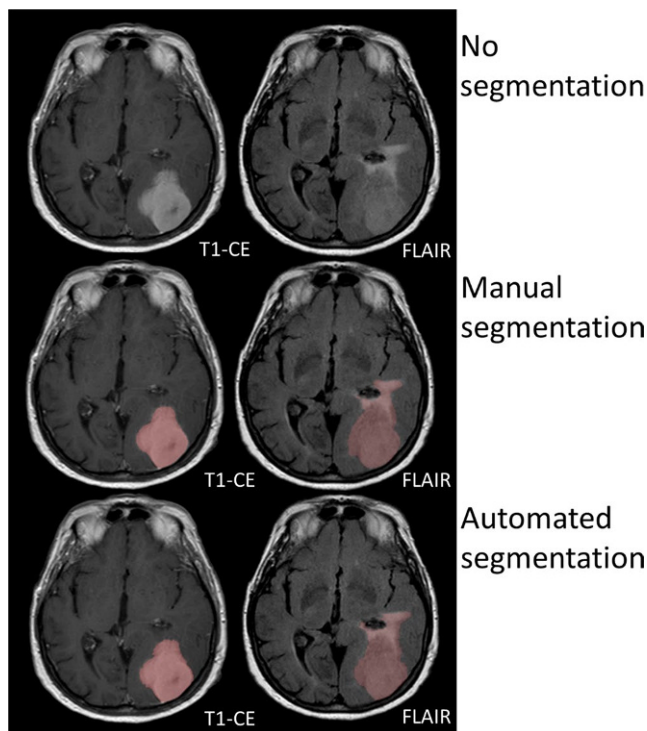


Fig. 1 | 104

growth than conventional diameter-methods. In this study, we evaluated a dedicated meningioma deep-learning-model and evaluated its performance in automated segmentation as a potential substitute for manual-segmentations.

**Methoden:** One hundred twenty-six MRI-datasets (T1-/T2-weighted, T1-weighted contrast-enhanced [T1CE], FLAIR) of patients with intracranial meningiomas (grade I: 97, grade II: 29) were included. An established deep-learning-model architecture (DeepMedic, BioMedIA) was used for automated segmentation. Two tumour components were segmented: (i) contrast-enhancing-tumour volume in T1CE and (ii) total-lesion-volume (union of lesion volume in T1CE and FLAIR [including solid tumour, necrosis and surrounding oedema]). Registration, skull-stripping, resampling, and normalization was applied for preprocessing of imaging data. Initially, the deep-learning-model was trained on manual segmentations of two independent readers from 70 patients. The trained model was then validated on 56 patients by comparison of automated to ground-truth manual segmentations, which were performed by two experienced readers in consensus.

**Ergebnisse:** Comparing automated and manual segmentations revealed average dice-coefficients of  $0.91 \pm 0.08$  for contrast-enhancing-tumour volume and  $0.82 \pm 0.12$  for total-lesion-volume depicted. In the training cohort, interreader-variabilities of manual readers were  $0.92 \pm 0.07$  for contrast-enhancing-tumour and  $0.88 \pm 0.05$  for total-lesion-volume.

**Diskussion:** Automated segmentation by deep-learning showed high segmentation accuracy, which was comparable to manual interreader-variability.

**Fazit:** In future, time-consuming manual segmentations might therefore be omitted.

#### Literatur

1. Akkus Z, Galimzianova A, Hoogi A, et al. Deep Learning for Brain MRI Segmentation: State of the Art and Future Directions. *J Digit Imaging*. 2017;:1–11.

2. Kamnitsas K, Ledig C, Newcombe VFJ, et al. Efficient Multi-Scale 3D CNN with Fully Connected CRF for Accurate Brain Lesion Segmentation. *Med Image Anal*. 2016;36:61–78.

124

#### AI IN MULTIPLE SCLEROSIS IMAGING—IMPROVING LESION DETECTION WITH SYNTHETIC DIR

Tom Finck\*<sup>1</sup>, Lioba Grundl<sup>1</sup>, Hongwei Li<sup>2</sup>, Johannes Paetzold<sup>2</sup>, Paul Eichinger<sup>1</sup>, Claus Zimmer<sup>1</sup>, Björn Menze<sup>2</sup>, Benedikt Wiestler<sup>1</sup>

<sup>1</sup>Abteilung für Diagnostische und Interventionelle Neuroradiologie, Klinikum rechts der Isar, München, Deutschland

<sup>2</sup>Department of Computer Science, Technische Universität München, München, Deutschland

**Background:** Synthetic MR imaging enables the reconstruction of various image contrasts from 1 scan and potentially allows reducing scan times and improving image quality. We have implemented a neural network which produces an artificial DIR sequence based primarily on T1, T2 and FLAIR images. Here we want to compare the artificial DIR sequence with conventional sequences in patients with multiple sclerosis (MS).

**Methods:** We have recently proposed a novel Generative Adversarial Networks (GAN) architecture, called DiamondGAN, which is capable of synthesizing images from multiple inputs, and have trained a model to create a high-contrast DIR image from T1, T2 and FLAIR input. Two-rater visual evaluation of white-matter lesion count (juxtacortical, periventricular, infratentorial and subcortical) in synthetic DIR images was performed and compared to the lesion counts on input FLAIR as well as a physically acquired DIR in 20 multiple sclerosis (MS) patients.

**Result:** Inter-rater reliability was comparable for FLAIR

**Conclusion:** A high-contrast DIR image, synthesized from standard FLAIR, T1 and T2, significantly increased lesion detection compared to input FLAIR and was comparable to a physically acquired DIR. Our method may facilitate a more widespread use of DIR sequences with only modest technical effort. Moreover, it may serve as an example of how computational methods can generate synthetic high-contrast images tailored to specific pathologies.

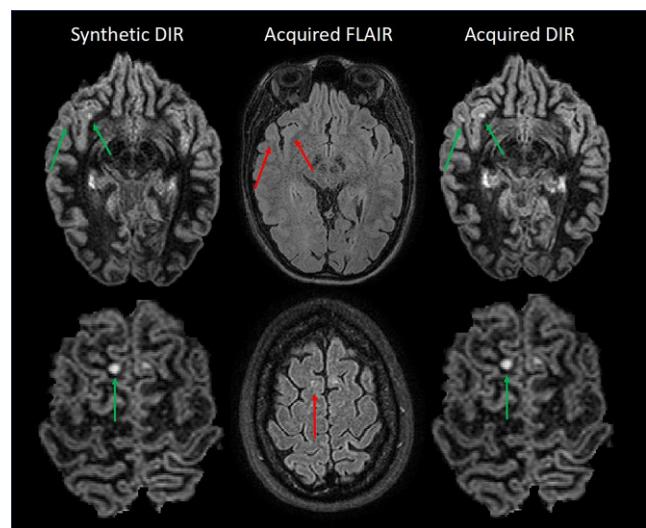


Fig. 1 | 124

163

**NEOPLASTIC AND NON-NEOPLASTIC ACUTE INTRACEREBRAL HEMORRHAGE IN CT BRAIN SCANS: MACHINE LEARNING-BASED PREDICTION OF DIGNITY USING RADIOMIC IMAGE FEATURES**

Jawed Nawabi\*<sup>1</sup>, Helge Kniep<sup>2</sup>, Reza Kabiri<sup>2</sup>, Christian Thaler<sup>2</sup>, Gabriel Broocks<sup>2</sup>, Tobias D. Faizy<sup>2</sup>, Gerhard Schoen<sup>2,3</sup>, Jens Fiehler<sup>2</sup>, Uta Hanning<sup>2</sup>

<sup>1</sup>Charité Universitätsmedizin, Radiologie, Berlin, Deutschland

<sup>2</sup>Universitätsklinikum Hamburg-Eppendorf, Diagnostische und Interventionelle Neuroradiologie, Hamburg, Deutschland

<sup>3</sup>Universitätsklinikum Hamburg-Eppendorf, Institut für Biometrie, Hamburg, Deutschland

**Background:** Early differentiation of neoplastic and non-neoplastic intracerebral hemorrhage (ICH) can be difficult in initial radiological evaluation, especially for extensive ICHs<sup>1</sup>. The aim of this study was to evaluate the potential of a machine learning based prediction of etiology for acute ICHs based on quantitative radiomic image features extracted from initial noncontrast-enhanced computed tomography (NECT) brain scans<sup>2</sup>.

**Methods:** The analysis included NECT brain scans from 77 patients with acute ICH (*n*=50 non-neoplastic, *n*=27 neoplastic). Radiomic features including shape, histogram and texture markers were extracted from non-, wavelet- and log-sigma-filtered images using regions of interest of ICH and perihematomal edema (PHE). 6090 quantitative predictors were evaluated utilizing random forest algorithms with 5-fold model-external cross-validation. Model stability was assessed through comparative analysis of 10 randomly drawn cross-validation sets. Classifier performance was compared with predictions of two radiologists employing Matthews correlation coefficient (MCC).

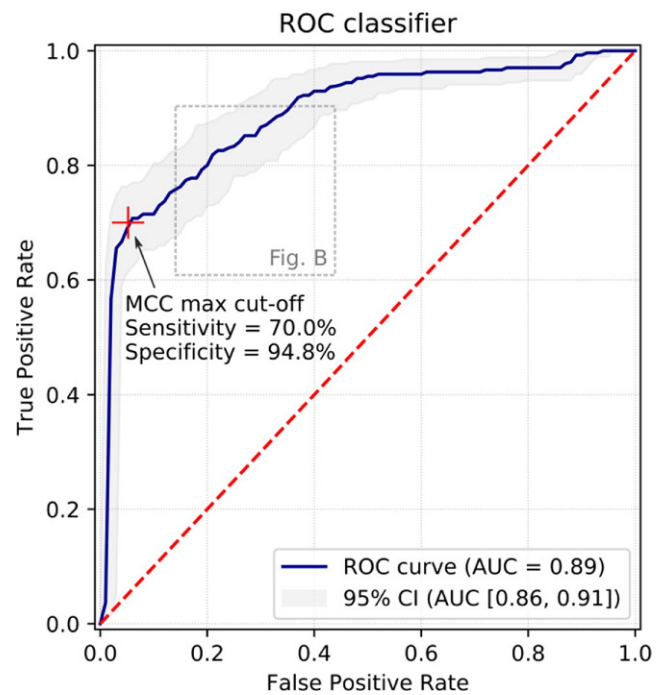
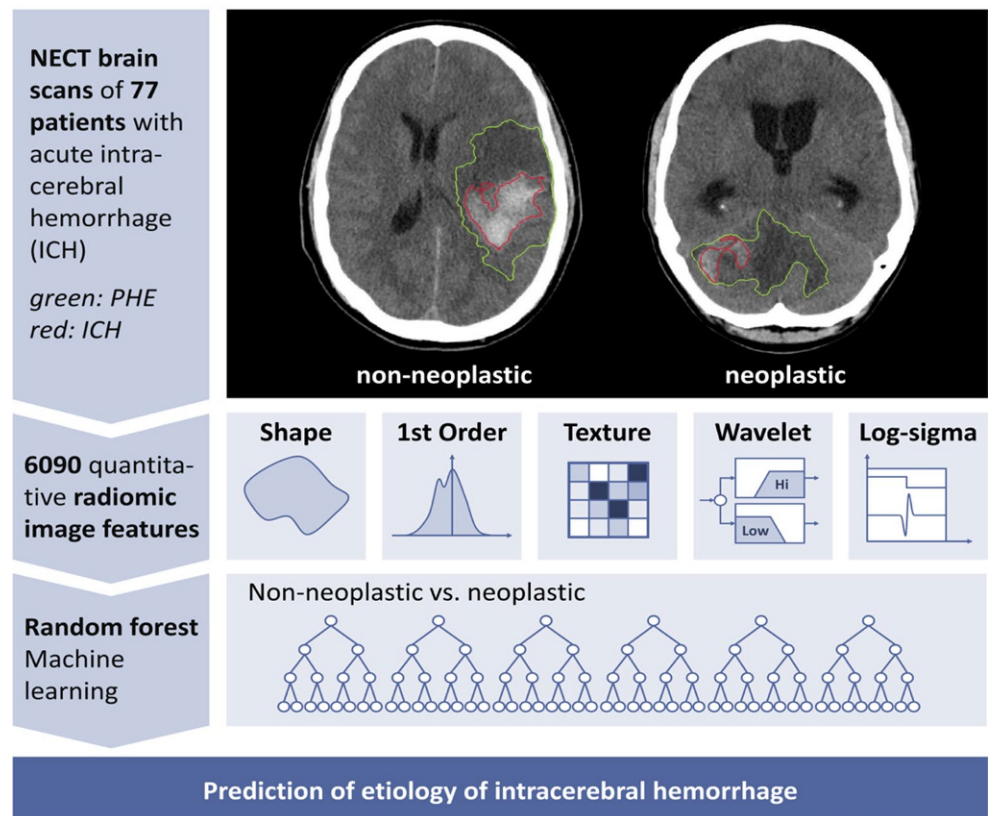


**Fig. 2 | 163** Receiver-Operating-Characteristics (ROC) curves for differentiation of neoplastic and nonneoplastic ICHs of the proposed machine learning classifier based on quantitative radiomic image features. Blue line shows ROC curve, grey area shows 95% confidence interval (CI). Red cross shows cut-off points/prediction performance.

**Fig. 1 | 163** Conceptual overview of the proposed machine learning approach showing the major processing steps: CT based image acquisition and segmentation, feature extraction (*n* = 6090), and statistical learning (random forest algorithm). NECT: Noncontrast-enhanced computed tomography; ICH: intracerebral hemorrhage; PHE: perihematomal edema.



### Feature importance contribution [%]

		Feature class		
		First order	Texture	Shape
a	Applied filter			
	Original	17.2	0.0	2.5
	Wavelet	20.5	23.0	
	Log-sigma	14.2	22.5	
b	ROI region			
	ICH + PHE	34.9	16.8	0.0
	ICH/(ICH + PHE)	0.4	12.2	1.5
	ICH/PHE	1.0	11.7	1.0
	PHE	9.8	2.6	0.0
	ICH	5.8	2.3	0.0

**Fig. 3 | 163** Feature importance contribution of 100 most important features in %. **a**) by applied filter and feature class **b**) by region and feature class. Texture feature class includes gray level size zone matrix, gray level dependence matrix, gray level run length matrix and gray level size zone. ROI: region of interest; ICH: intracerebral hemorrhage; PHE: perihematomal edema

**Results:** ROC AUC of the test sets for predicting neoplastic vs. non-neoplastic ICHs was 0.89 (95% CI [0.68; 0.99];  $P < 0.001$ ), specificities and sensitivities reached  $> 80\%$ . Compared to the radiologists' predictions, the machine learning algorithm yielded equal or superior results for all evaluated metrics. MCC of the proposed algorithm at its optimal operating point (0.69) was significantly higher than MCC of the radiologist readers (0.54);  $P = 0.01$ .

**Discussion:** Evaluating quantitative features of acute NECT images in a machine learning algorithm provided high discriminatory power in predicting non-neoplastic vs. neoplastic ICHs.

**Conclusion:** Utilized in clinical routine, the proposed approach could improve patient care at low risk and costs.

**References**

1. Nawabi, et al. Neoplastic and Non-Neoplastic Causes of Acute Intracerebral Hemorrhage on CT: The Diagnostic Value of Perihematomal Edema. Clin Neuroradiol. 2019;: Mar 21. [Epub ahead of print].
2. Kniep, et al. Radiomics of Brain MRI: Utility in Prediction of Metastatic Tumor Type. Radiology. 2019;290(2):479–87.

187

#### AUTOMATIC DETECTION OF LARGE VESSEL OCCLUSION ON CTA IN ACUTE ISCHEMIC STROKE USING AI

Fatih Seker<sup>1</sup>, Johannes Pfaff<sup>1</sup>, Christian Herweh<sup>\*1</sup>, Anne Berberich<sup>2</sup>, Yahia Mokli<sup>2</sup>, Markus Möhlenbruch<sup>1</sup>, Stephen Gerry<sup>3</sup>, Peter Arthur Ringleb<sup>2</sup>, Simon Nagel<sup>2</sup>

<sup>1</sup>Neurologische Universitätsklinik, Universität Heidelberg, Neuroradiologie, Heidelberg, Deutschland

<sup>2</sup>Neurologische Universitätsklinik, Universität Heidelberg, Neurologie, Heidelberg, Deutschland

<sup>3</sup>Centre for Statistics in Medicine, University of Oxford, Oxford, England

**Hintergrund:** Identification of large vessel occlusion (LVO) in acute ischemic stroke (AIS) is a crucial step before initiating mechanical thrombectomy (MT). This is typically done using CT angiography (CTA). However, especially in primary stroke centers this can be challenging and the decision for referring a patient might be delayed. e-CTA (Brainomix®, Oxford, UK) is an artificial intelligence-based software tool for CTA analysis and offers automatic occlusion detection.

**Methoden:** CTAs of 144 AIS patients were selected of which 74 had an LVO confirmed by angiography. Ground truth was defined by an experienced interventional neuroradiologist with unrestricted data access. LVO location was dichotomized into proximal, i.e. ICA terminus and proximal M1 segment (45 patients) and peripheral, i.e. distal M1 and proximal M2 segments (29 patients). CTAs were independently analyzed by e-CTA and four stroke physicians, 2 neuroradiologists (reader 1 & 2) and 2 neurologists (reader 3 & 4) who were blinded.

**Ergebnisse:** For proximal LVOs eCTA showed a similar performance with regard to sensitivity, specificity and accuracy as compared to the physicians who were in a close range (see table). For any LVO including 40% peripheral occlusions eCTA had a lesser sensitivity than the physicians while the specificity was comparable to the physicians and better than one of them (see table).

**Diskussion:** e-CTA shows similar performance regarding the detection of proximal LVOs as compared to stroke physicians and thereby has the potential to facilitate and accelerate decision making in AIS especially under circumstances where stroke experts may not be readily available.

		Reader 1	Reader 2	Reader 3	Reader 3	e-CTA
Prox LVO	Sensitivity	100.0%	100.0%	100.0%	100.0%	96.6% (91,9–100%)
	Specificity	100.0%	98.7% (96,1–100%)	98.6% (96–100%)	98.6% (96–100%)	97.7% (94,5–100%)
	Accuracy	100.0%	99.3%	99.3%	99.3%	97.2%
Any LVO	Sensitivity	100.0%	98.6% (95,8–100%)	100.0%	100.0%	80.0% (70,6–89,4%)
	Specificity	98.6% (96–100%)	90.5% (83,9–97,2%)	98.6% (96–100%)	98.6% (96–100%)	94.6% (89,4–99,7%)
	Accuracy	99.3%	94.4%	99.3%	99.3%	87.5%

192

#### E-ASPECTS DERIVED ACUTE ISCHEMIC VOLUMES ON NON-CONTRAST ENHANCED COMPUTED TOMOGRAPHY IMAGES

Simon Nagel<sup>\*1</sup>, Olivier Joly<sup>2</sup>, Johannes Pfaff<sup>3</sup>, Panagiotis Papanagiotou<sup>4</sup>, Klaus Fassbender<sup>5</sup>, Wolfgang Reith<sup>6</sup>, Markus Möhlenbruch<sup>3</sup>, Christian Herweh<sup>3</sup>, Iris Grundwald<sup>7</sup>

<sup>1</sup>Universitätsklinikum Heidelberg, Neurologie, Heidelberg, Deutschland

<sup>2</sup>Brainomix, Oxford, England

<sup>3</sup>Universitätsklinikum Heidelberg, Neuroradiologie, Heidelberg, Deutschland

<sup>4</sup>KLlinikum Bremen, Neuroradiologie, Bremen, Deutschland

<sup>5</sup>Universität des Saarlandes, Neurologie, Homburg, Deutschland

<sup>6</sup>Universität des Saarlandes, Neuroradiologie, Homburg, Deutschland

<sup>7</sup>Angia Ruskin University, Neuroscience, Essex, England

**Background:** e-ASPECTS is an AI supported software and here we aimed to Validate Automatically derived Acute Ischemic Volumes (AAIV) from e-ASPECTS on Non-Contrast Computed Tomography (NCCT)

**Methods:** Data from three studies were reanalyzed with e-ASPECTS Version 7. The National Institute of Health Stroke Scale (NIHSS) determined stroke severity at baseline and clinical outcome was measured with the modified Rankin Scale (mRS) between 45 to 120 days. Spearman ranked correlation coefficients (R) of AAIV and e-ASPECTS scores with NIHSS and mRS as well as Pearson correlation of AAIV with diffusion weighted imaging (DWI) and CT Perfusion (CTP) estimated infarct core volumes were calculated. Multivariate regression analysis (odds ratio, OR with 95% confidence intervals, CI) and Bland–Altman plots (BA) were performed.

**Result:** We included 388 patients. Mean AAIV was 11.6+/-18.9 ml and e-ASPECTS was 9 (8–10: median and interquartile range). AAIV, respectively e-ASPECTS correlated with NIHSS at baseline (R=0.35,  $p < 0.001$ ; R=-0.36,  $p < 0.001$ ) and follow-up mRS (R=0.29,  $p < 0.001$ ; R=-0.3,  $p < 0.001$ ). In subsets of patients AAIV within the affected hemisphere correlated strongly with DWI ( $n=37$ , R=0.68,  $p < 0.001$ ) and CTP derived infarct core ( $n=41$ , R=0.76,  $p < 0.001$ ) lesion volume and BA plots showed a bias close to zero (-2.65 ml for DWI and 0.45 ml for CTP core). Within the whole cohort the AAIV (OR 0.98 per ml, 95% CI 0.96–0.99) and e-ASPECTS scores (OR 1.3, 95%CI 1.07–1.57) were independent predictors of good outcome

**Conclusion:** AAIV on NCCT correlated moderately with clinical severity but strongly with DWI lesion and CTP infarct core volumes and predicted clinical outcome.

**208**

**ADVANCED MACHINE LEARNING IN ACTION: RADIOMIC BASED OUTCOME PREDICTION OF ACUTE INTRACRANIAL HEMORRHAGE ON COMPUTED TOMOGRAPHY**

Jawed Nawabi\*<sup>1,2</sup>, Helge Kniep<sup>2</sup>, Peter Sporns<sup>3</sup>, Sarah Elsayed<sup>2</sup>, Gabriel Brooks<sup>2</sup>, Gerhard Schoen<sup>4</sup>, Jens Fiehler<sup>2</sup>, Uta Hanning<sup>2</sup>

<sup>1</sup>Charite—Campus Mitte, Institut für Radiologie, Berlin, Deutschland

<sup>2</sup>Universitätsklinikum Hamburg-Eppendorf, Institut für Diagnostische und Interventionelle Neuroradiologie, Hamburg, Deutschland

<sup>3</sup>Universitätsklinikum Münster, Institut für Radiologie, Münster, Deutschland

<sup>4</sup>Universitätsklinikum Hamburg-Eppendorf, Institut für Biometrie, Hamburg, Deutschland

**Background:** Intracranial hemorrhage (ICH) requires prompt diagnosis to optimize patient outcomes <sup>1</sup>. We hypothesized that machine learning algorithms could automatically analyze non-contrast computed tomography (NECT) of the head and predict clinical outcome of ICH patients <sup>2</sup>.

**Methods:** 300 NECTs with acute spontaneous ICH between 2014–2019 were retrospectively included from the database at a tertiary university hospital. A binary outcome was defined as Modified Ranking Scale (mRS) 0–3 (good outcome) and mRS 4–6 (bad outcome) at discharge. Radiomic features including shape, histogram and texture markers were extracted from non-, wavelet- and log-sigma-filtered images using regions of interest of ICH. The quantitative predictors were evaluated utilizing random forest algorithms with 5-fold model-external cross-validation.

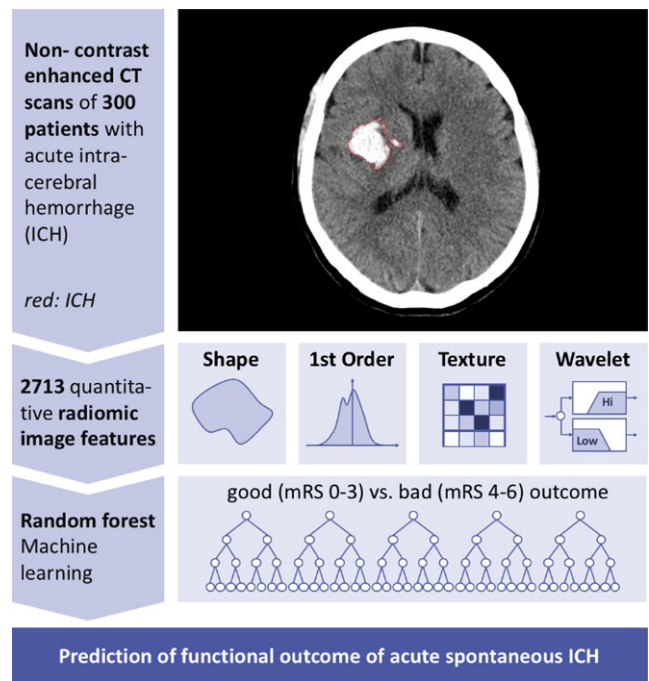


Fig. 1 | 208 Conceptual overview

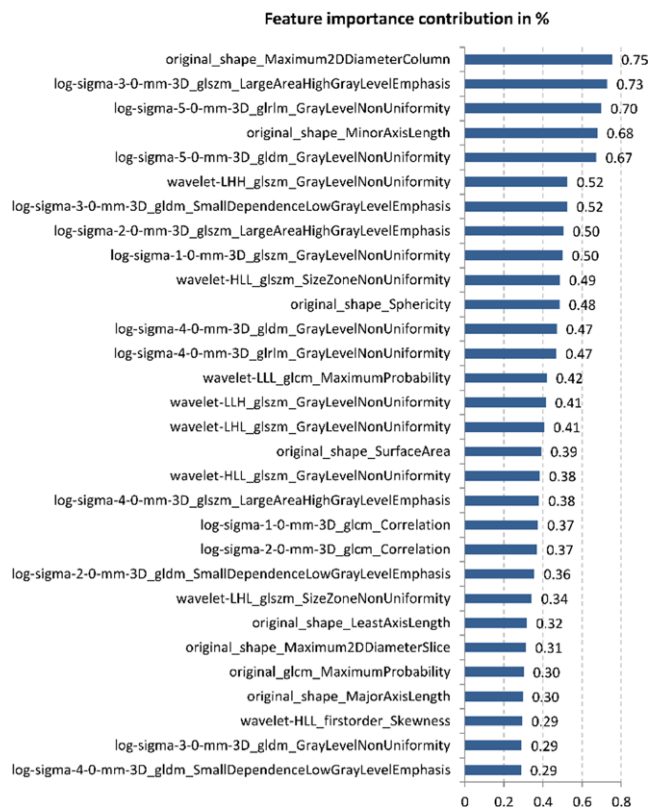


Fig. 2 | 208 Feature importance contribution

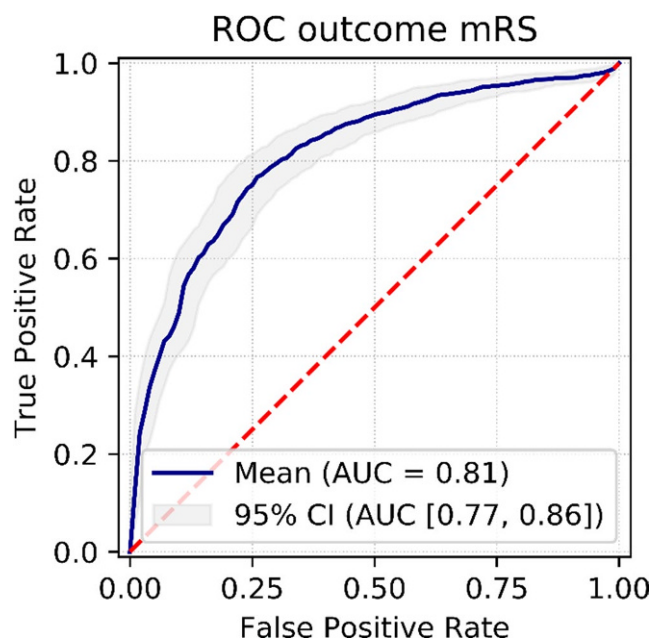


Fig. 3 | 208 ROC-Curve

**Results:** The model achieved an area under the ROC curve of 0.81 (95% CI [0.077; 0.86];  $P < 0.01$ ), specificities and sensitivities reached 78% at Youden's Index optimal cut-off point for the prediction of functional outcome at discharge (mRS).

**Discussion:** In conclusion, quantitative features of acute NECT images in a machine learning algorithm provided high discriminatory power in predicting functional outcome. In clinical routine, this proposed approach could allow early triage of high-risk patients for poor outcome.

#### References

1. Qureshi AI, et al. Intracerebral haemorrhage. *Lancet*. 2009;.
2. Arbabshirani MR, et al. Advanced machine learning in action: identification of intracranial hemorrhage on computed tomography scans of the head with clinical workflow integration. *Npj Digit Med*. 2018;.

#### 230

##### RELIABLE AUTOMATED DETECTION OF RADIOLOGIC NPH FEATURES USING MACHINE LEARNING METHODS

Suam Kim<sup>\*1</sup>, Yang S<sup>2</sup>, M Hohenhaus<sup>1</sup>, M Reiser<sup>3</sup>, E Kellner<sup>4</sup>, J Beck<sup>1</sup>, H Urbach<sup>2</sup>, K Egger<sup>2</sup>

<sup>1</sup>Klinik für Neurochirurgie, Uniklinik Freiburg, Freiburg im Breisgau, Deutschland

<sup>2</sup>Klinik für Neuroradiologie, Uniklinik Freiburg, Freiburg, Deutschland

<sup>3</sup>Medical Physics and Functional Neurosurgery, Uniklinik Freiburg, Freiburg, Deutschland

<sup>4</sup>Medical Physics, Uniklinik Freiburg, Freiburg, Deutschland

**Background:** Idiopathic Normal pressure hydrocephalus (NPH) is of special interest as a neurodegenerative condition treatable by a ventriculo-peritoneal shunt. With as of yet not comprehensively defined diagnostic criteria, the amount of patients afflicted by a possibly reversible form of dementia is unknown. In light of demographic challenges, advances in identifying the subpopulation likely to benefit from sur-

gery are required, to which radiologic features such as the DESH-sign (1) may contribute.

**Methods:** A support vector machine (SVM) was trained to detect volumetric imaging features of NPH in whole brain gray matter, white matter and CSF (Fig. 1). It was applied on MRI scans of patients with NPH ( $n=35$ ) vs a control group of patients with different neurodegenerative diseases ( $n=37$ ).

**Results:** Visual and automatic analysis showed close consistency ( $p=1.0$  on exact Fisher's test) including surgically treated patients with benefit (Fig. 2 and 3).

**Discussion:** Given the notion of imaging features preceding clinical symptoms in NPH reliable methods of routine screening for NPH-features will become a key element in a future-oriented healthcare system.

**Conclusion:** The exemplary method for automating this process enables future prospective and systematic studies of larger scale aimed at patients likely to develop NPH-symptoms at some later point in time (2) as well as benefit from therapeutic or prophylactic shunting.

#### References

1. Craven, et al. The predictive value of DESH for shunt responsiveness in idiopathic normal pressure hydrocephalus. *J Clin Neurosci*. 2016;.
2. Engel, et al. Paradigm-shift: radiological changes in the asymptomatic iNPH-patient to be: an observational study. *Fluids Barriers CNS*. 2018;.

#### 241

##### CAN WE TRUST AI? INVESTIGATING UNCERTAINTY IN UNSUPERVISED BRAIN ANOMALY DETECTION

Christoph Baur<sup>1</sup>, Shadi Albarqouni<sup>1</sup>, Claus Zimmer<sup>2</sup>, Nassir Navab<sup>1</sup>, Benedikt Wiestler<sup>\*2</sup>

<sup>1</sup>Chair for Computer Aided Medical Procedures, TUM, München, Deutschland

<sup>2</sup>Abteilung für Neuroradiologie, TUM, München, Deutschland

**Hintergrund:** Deep Learning has emerged as a powerful tool to support clinical decision-making. However, the "black box nature" of these algorithms has raised concerns about explainability and trustworthiness of AI. To better understand how neural networks learn, we investigated uncertainty in the predictions of an unsupervised neural network which was taught normal brain anatomy.

**Methoden:** Previously, we have trained a Skip-Autoencoder on normal brain MR images, thus enabling this network to learn normal brain anatomy for unsupervised anomaly delineation (UAD). To quantify uncertainty, we turned this network into a Bayesian Neural Network by placing a distribution over the network parameters  $\theta$  and calculated i) the mean ("predictive mean") and ii) the pixel-wise variance in the reconstructed images over  $n$  Monte-Carlo samples. To simulate a range of brain pathologies, we tested our network on a sample of patients with Multiple Sclerosis (MS) or Glioblastoma (GB).

**Ergebnisse:** In the averaged difference images (Fig. A4/B4), the UAD system detected both MS and GB lesions with good reliability, but also produced false-positive results, mostly located at the gyri/sulci interface. To understand how certain the network was in detecting anomalies, we further investigated the pixel-wise variance, assuming this variance to be low when the network was certain of a detection. Interestingly, this revealed that correctly detected anomalies indeed showed low variance (Fig. A5/B5), indicating high confidence of the model. In contrast, the variance was clearly higher in false-positive detections.

**Diskussion:** In a Bayesian model of our UAD system, model uncertainty was much lower for true detections than for false-positive findings. This suggests that our network indeed learns about normal brain morphology, as it is quite confident in detecting pathologies. On the

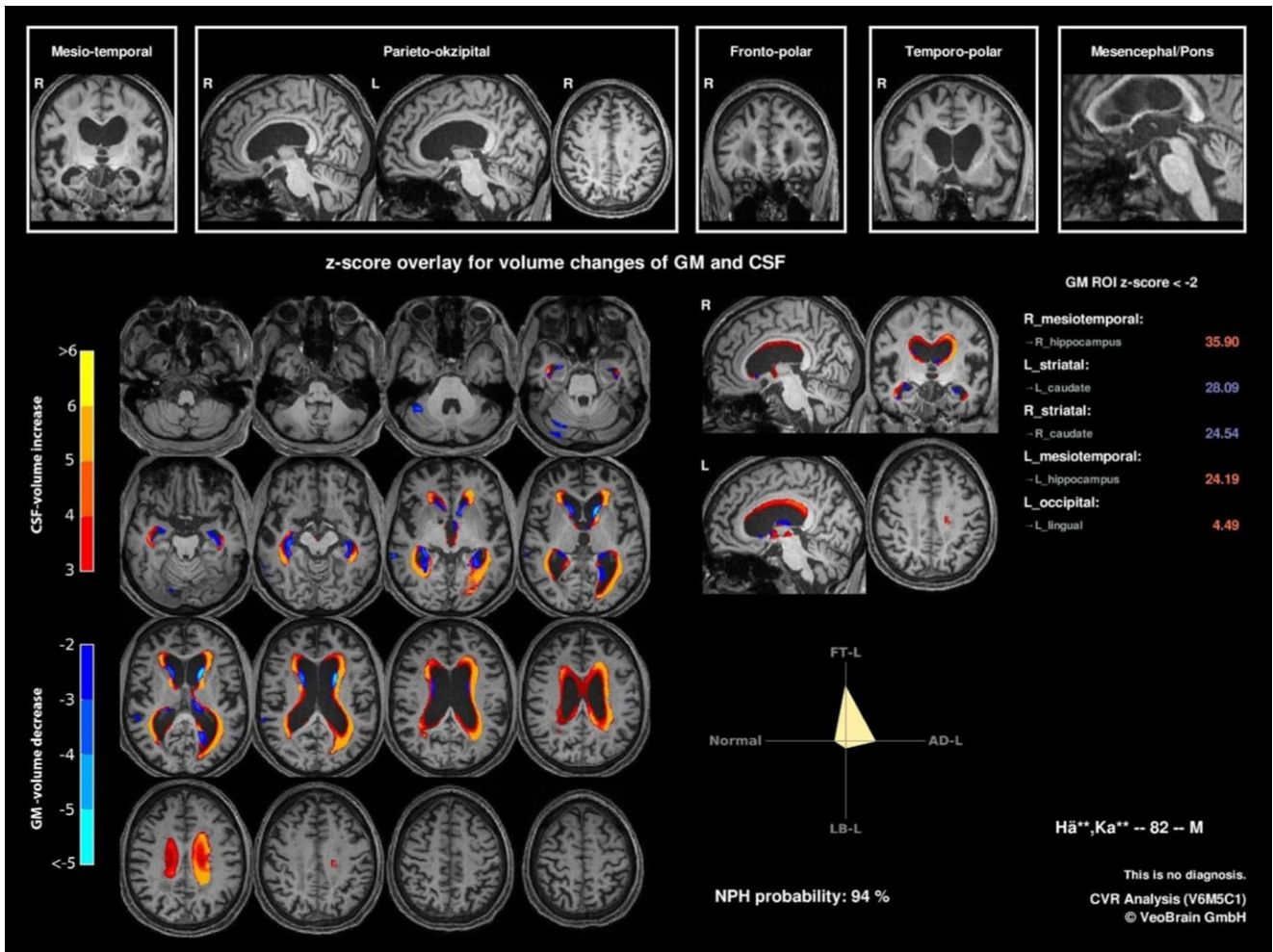


Fig. 1 | 230 VEOmorph ([www.veobrain.com](http://www.veobrain.com)) analysis results with abnormal GM and CSF voxels superimposed in color on individual 3D T1w brain MRI (increase of CSF volume in red to yellow, and decrease of GM volume in dark to light blue)

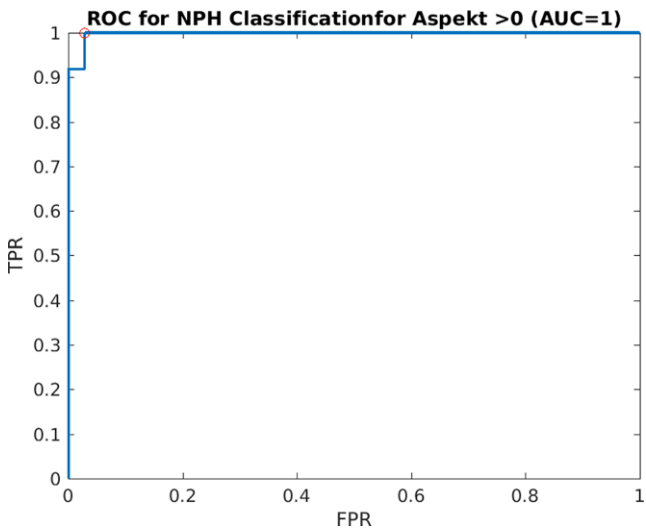


Fig. 2 | 230 ROC analysis of generated probability for NPH as shown in Fig. 1 in comparison to clinically conformed diagnosis

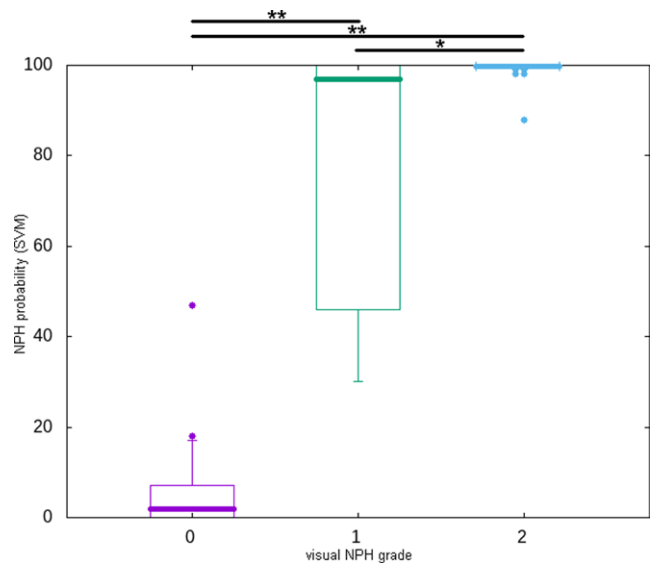
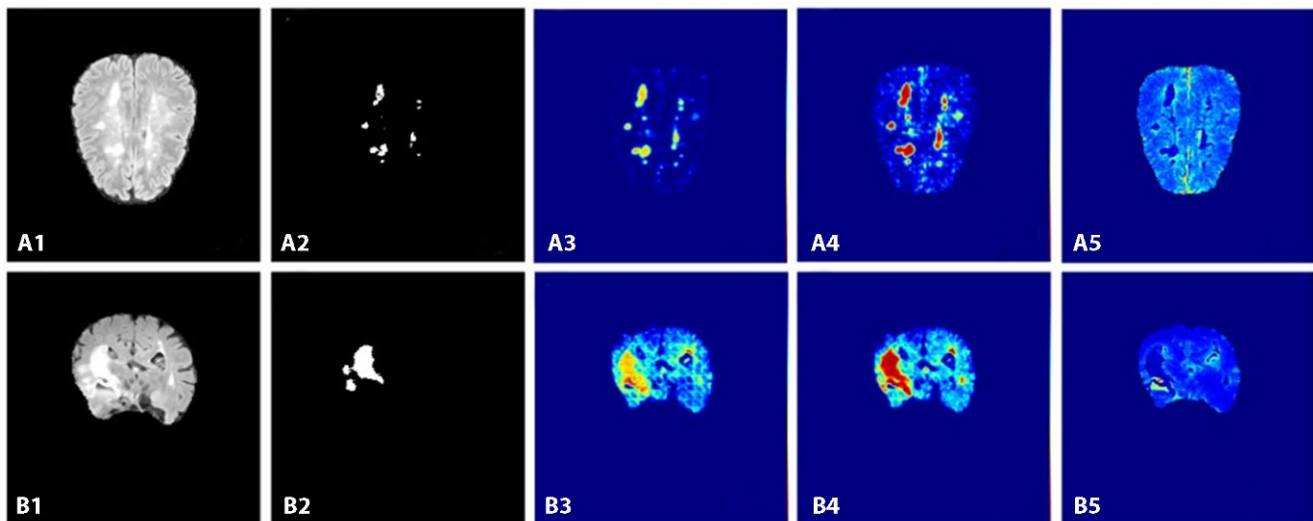


Fig. 3 | 230 NPH probability in percent against visual grade of NPH typical changes (0=no NPH typical changes, 1=probable NPH typical changes, 2=definite NPH typical changes)



**Fig. 1** | 241 Heatmap display for residuals and uncertainties. A1: input slice with MS lesions; A2: corresponding ground-truth segmentation; A3: the residual from a Skip-Autoencoder; A4: the residual computed on the predictive mean of Bayesian Autoencoder; A5: the pixel-wise uncertainty from the Bayesian Autoencoder. B1-B5: The same for a Glioblastoma sample

other hand, in areas of high anatomical variability (such as sulci), our model shows higher uncertainty.

**Fazit:** There are two important implications of our findings: i) visualizing uncertainty helps radiologists to understand the performance of AI models better and ii) explicitly incorporating uncertainty may lead to a more robust UAD system.

244

#### FULLY AUTOMATED LONGITUDINAL SEGMENTATION OF NEW OR ENLARGING MULTIPLE SCLEROSIS (MS) LESIONS USING 3D CONVOLUTION NEURAL NETWORKS

Julia Krüger<sup>\*1</sup>, Roland Opfer<sup>1</sup>, Nils Gessert<sup>2</sup>, Sven Schipling<sup>3,4</sup>, Ann-Christin Ostwaldt<sup>1</sup>, Christine Walker-Egger<sup>3,4</sup>, Praveena Manogaran<sup>3,5</sup>, Alexander Schlaefler<sup>2</sup>

<sup>1</sup>jung diagnostics GmbH, Hamburg, Deutschland

<sup>2</sup>Institute of Medical Technology, University of Technology Hamburg, Hamburg, Deutschland

<sup>3</sup>Neuroimmunology and Multiple Sclerosis Research, Department of Neurology, University Hospital Zurich and University of Zurich, Zürich, Schweiz

<sup>4</sup>Neuroscience Center Zurich, University of Zurich and Federal Institute of Technology (ETH), Zürich, Schweiz

<sup>5</sup>Department of Information Technology and Electrical Engineering (D-ITET), Swiss Federal Institute of Technology, Zürich, Schweiz

**Background:** The quantification of new and enlarging Multiple Sclerosis (MS) lesions (lesion activity) from follow-up MRI scans is an important surrogate of clinical disease activity. Manual assessment is time consuming, inter-rater variability is high, and only few fully automated methods are available so far.

**Methods:** A 3D convolution neural network (CNN) with encoder-decoder (U-Net-like) architecture was employed with four reductions of the spatial feature maps in the encoder. Input data consisted of two fluid attenuated inversion recovery (FLAIR) images (baseline (BL) and follow-up (FU)). Each image was entered into the encoder independently and the feature maps were concatenated and then fed into the decoder. The output was a 3D mask indicating new (in FU) or enlarged (compared to BL) lesions.

The encoder was pre-trained on cross-sectional MS patient data using 1,809 2D and 3D FLAIR images acquired on 156 different MRI scanners. MRI data originated from clinical routine and was sent to jung diagnostics GmbH for image analysis (Biometrica MS®). MS lesions were annotated on all images semi-automatically.

For the evaluation and the training of the decoder (with leave-9-out cross validation of 10 nets) 89 RRMS patient data acquired at University Hospital of Zurich was used. For each patient (mean age 35.6 years) a BL and FU 3D FLAIR image (3T Philips Ingenia) were used (mean follow-up 2.2 years). New or enlarging lesions were manually annotated on the FU scan of each patient by two independent raters.

**Results:** Rater 1 and 2 identified on average 1.1 new or enlarging lesions (interquartile range (IQR) [0.0,1.0]). In 55 cases no lesion activity was identified by rater 1 and in 53 cases by rater 2. Excluding these cases, mean lesion activity was 2.62 lesions per case (IQR [1.0 3.0]). For evaluation, mean and IQR of dice coefficient (DC), lesion-wise sensitivity (SEN) and false positive count (FP) were determined. We obtained the following results between raters (inter-rater) and between raters and CNN (rater-CNN):

inter-rater: DC: 0.49 [0.34 0.72] SEN: 0.60 [0 1] FP: 0.753 [0 1];

rater-CNN: DC: 0.49 [0.31 0.70] SEN: 0.58 [0.33 1] FP: 0.625 [0 1].

**Conclusions:** The low inter-rater performance signifies the complexity and uncertainty of identifying new and enlarging lesions. An automated CNN-based approach can quickly (<1 min) provide an independent and deterministic assessment of lesions from BL and FU scans to support diagnosis and potentially mitigate inter-rater variability.

254

#### SUCCESSFUL USE OF DATA ANALYSIS IN HEALTHCARE

Manuel Perfler<sup>1</sup>, Sandra Wartner<sup>1</sup>, Stephan Leitner<sup>\*1</sup>

<sup>1</sup>RISC Software GmbH, Hagenberg, Österreich

**Hintergrund:** Digitalization and automation entail extensive data acquisition in a wide variety of sectors such as industry, commerce and healthcare. As a result, large amounts of data must be stored securely and processed in a way that is beneficial to the medical expert in order to derive valuable information from them. By applying statistical methods, modern data and visual analytics methods, as well as ma-

chine learning, the existing knowledge is analyzed in context with the recorded data. Using methods from the field of artificial intelligence, knowledge is generated and recommendations for action are formulated for these experts (expert-in-the-loop).

**Methoden:** Data analyses consists of 3 steps:

Data Engineering and Modeling: Health and sensor data must be intelligently combined, filtered and linked. Checking the correctness and completeness of the data is also relevant.

Data Analytics and Artificial Intelligence: In order to gain knowledge from collected and filtered data, mathematical, statistical and artificial intelligence methods, as well as visual analytics are used.

Data Presentation: The visual processing of data and analysis results is an important tool for gaining new insights. An essential factor for the interpretation of analysis results is the strong involvement of domain experts.

In order to technically enable and guide researchers and analysts in medicine to fulfil their role in the process of data analysis, we developed an ontology-based research and analytics infrastructure. Due to its approach, the generic infrastructure can be adapted to any research domain of interest by the researchers themselves.

**Ergebnisse:** In a research cooperation we built an ontology model of stroke patients and have been gathering data for several years. We want to showcase the data analysis process and benefits of visual analytics as well as give an outlook of possible machine learning algorithms that can be performed on medical image data of stroke patients.

**Diskussion:** As a major part of our research is focused on guiding medical experts through the data analysis process, we are always looking for feedback and suggestions on the features and guidance that is required by the community.

**Fazit:** Our ontology based data analysis system combines data complexity, interface diversity and visualization with user-friendliness. Domain experts are supported by the modeling, integration, validation, processing and evaluation of their data.

262

### MORPHOMETRIE UND MACHINE LEARNING ZUR ERKENNUNG VON ALZHEIMER-DEMENZ: EIN METHODENVERGLEICH

Tobias Raffelsberger\*<sup>1</sup>, Raimund Kleiser<sup>1</sup>, Friedrich Leblhuber<sup>2</sup>, Sibylle Wimmer<sup>1</sup>, Johannes Trenkler<sup>1</sup>

<sup>1</sup>Kepler Universitätsklinikum, Neuromed Campus, Institut für Neuroradiologie, Linz, Österreich

<sup>2</sup>Kepler Universitätsklinikum, Neuromed Campus, Abteilung für Gerontologie, Linz, Österreich

**Hintergrund:** Morphometrie in Verbindung mit Support Vector Machines (SVMs) hat sich für eine automatisierte Früherkennung von Mild Cognitive Impairment (MCI) und Alzheimer-Demenz (AD) bereits als vielversprechend erwiesen [1,2]. Die vorliegende Arbeit vergleicht die diesbezügliche Performance der Morphometrie-Software CAT12 mit jenen der bereits länger etablierten Softwares FreeSurfer und SPM12.

**Methoden:** Als Trainingsgrundlage für die SVMs dienten 240 Datensätze (80 MCI, 80 AD und 80 gesunde Kontrollen (HC)) aus der ADNI-Datenbank. Für diese wurden mittels der Softwares FreeSurfer, SPM12 und CAT12 Gehirnvolumen beziehungsweise -dicke in vordefinierten Regions-of-interest (ROIs) bestimmt. Die Unterteilung in ROIs erfolgte dabei unter Verwendung von vier unterschiedlichen funktionellen Atlanten. Vektoren bestehend aus den ermittelten ROI-Daten ergänzt von Geschlecht und Alter der Versuchspersonen dienten als Trainingsdaten für binäre SVM-Klassifikatoren (HC vs. AD, HC vs. MCI und MCI vs. AD). Mittels 10-facher Kreuzvalidierung wurde die Trefferquote der Klassifikatoren ermittelt. Eine Selektion jener ROIs, die sich als am relevantesten für die Klassifikation erwiesen, erfolgte mittels Rekursiver Feature Elimination (RFE).

**Ergebnisse:** Alle untersuchten morphometrischen Methoden erzielten Trefferquoten von über 85%. Unter Verwendung der Volumenbestimmung unter CAT12 wurde mit 95.1% das Top-Resultat erzielt. Die RFE verbesserte dabei die Trefferquoten im Durchschnitt um 11.5%.

**Diskussion:** Nennenswerte Unterschiede ergeben sich einerseits zwischen den morphometrischen Methoden, andererseits zwischen den funktionellen Atlanten. CAT12 auf der einen Seite und der Atlas zur Verfügung gestellt von Neuromorphometrics Inc. auf der anderen Seite stechen positiv hervor.

**Fazit:** Erstklassige Klassifikationsergebnisse sowie eine vergleichsweise kurze Verarbeitungsdauer von zirka 45 Minuten pro Datensatz machen CAT12 zu einem weiteren vielversprechenden Kandidaten für den morphometrischen Part einer zukünftigen automatisierten Früherkennung von dementiellen Erkrankungen.

### Literatur

1. Gupta, et al. Alzheimer's Disease Diagnosis Based on Cortical and Subcortical Features. *J Healthc Eng.* 2019;2019:13.
2. Cuingnet, et al. Automatic classification of patients with Alzheimer's disease from structural MRI: A comparison of ten methods using the ADNI database. *Neuroimage.* 2011;56:766–81.

264

### ICOBRAIN'S NATURAL LANGUAGE RADIOLOGICAL REPORTING FOR MULTIPLE SCLEROSIS FOLLOW-UP

Diana Sima<sup>1</sup>, Guido Wilms<sup>1</sup>, Thijs Vande Vyvere<sup>1</sup>, Martin Seelhorst<sup>1</sup>, Wim Van Hecke<sup>1</sup>, Dirk Smeets<sup>1</sup>

<sup>1</sup>icomatrix, Leuven, Belgium

**Hintergrund:** Radiological reporting in multiple sclerosis (MS) and other neurological conditions is an important tool that facilitates the communication between radiologist and neurologist. In this work we assess the added value of automatically generated natural language radiologic reports based on the automated icobrain software for MS follow-up.

**Methoden:** Longitudinal MRI acquisitions approximately 1 year apart were collected from 25 multiple sclerosis patients. The automated software icobrain was used to compute lesion load (including new and enlarging lesions) and brain volumetry (including annualized atrophy). Natural language reports containing lesion evolution and atrophy findings were automatically generated. Each dataset was presented in random order to an experienced radiologist twice: with and without automatically generated report. Final reports were created either from scratch or by verifying and adapting the automatically generated report. The time necessary to complete each report was kept.

**Ergebnisse:** With respect to timing, the median time for conventional radiological reporting was 7min17s (interquartile range 4min40s), while the median computer-aided radiologic reporting time was 4min37s (interquartile range 3min35s), with the latter significantly faster (paired t-test and Wilcoxon signed-rank test  $p < 0.01$ ). With respect to findings, the computer-aided reports indicated 7 stable patients (normal atrophy, no lesion activity), 7 patients with slight progression (slightly abnormal atrophy rate or enlarging lesions), and 11 progressive patients (5 with new lesions, 10 with abnormal atrophy rate for their age). Conventional radiological reports indicated 19 stable patients (no lesion activity, no apparent atrophy) and 6 progressive patients (new lesion formation or lesion enlargement, also identified above as progressive).

**Diskussion:** Computer-aided radiological reports are faster than conventional reporting, with approximately 8 conventional reports per hour versus 13 computer-aided reports per hour. Stable patients identified by the computer-aided technique were also deemed stable by con-

ventional radiological reading, but the software also reported cases of subtle cerebral atrophy.

**Fazit:** Standardization of radiologic reporting and incorporation of brain atrophy are steps towards future improvements in the clinical management of MS patients.

266

### EVALUATION OF A NEW AI-BASED SINGLE-RUN 3D-ANGIOGRAPHY (3D-A) FOR VISUALIZATION OF CEREBRAL AVMS

Stefan Lang<sup>\*1</sup>, Philip Höller<sup>1</sup>, Felix Eisenhut<sup>1</sup>, Manuel Schmidt<sup>1</sup>, Christian Kaethner<sup>2</sup>, Arnd Dörfler<sup>1</sup>

<sup>1</sup>Neuroradiologie, Universitätsklinikum Erlangen, Erlangen, Deutschland

<sup>2</sup>Siemens Healthineers AG, Erlangen, Deutschland

**Background:** The AI-based 3D-A is a new postprocessing method that allows a significant reduction of the patient dose (PD) necessary for 3D-imaging of cerebral vessels. Our aim was evaluation of 3D-A for visualization of cerebral AVMs.

**Methods:** 3D-DSA datasets of cerebral AVMs have been reconstructed using conventional and prototype software (Siemens Healthineers AG, Germany). Corresponding reconstructions have been analyzed by 2 experienced neuroradiologists in consensus reading in terms of quantitative (AVM size [S] in mm) and qualitative parameters (image quality 0–4 [e.g., IQ=4 means excellent], main feeder [e.g. ACA, MCA, PCA, etc.], localization [eloquent vs. non-eloquent], venous drainage [superficial, deep, mixed]). Martin-Spetzler-Scores (MSS) were assessed in both reconstructions.

**Result:** In total 10 datasets ( $n_{\text{male}}=6; n_{\text{female}}=4; \text{age}_{\text{mean}}=54.3$  years) have been successfully reconstructed using both conventional and prototype software. In all cases corresponding reconstructions demonstrated complete congruency in terms of IQ ( $\text{IQ}_{3\text{D-DSA}/3\text{D-A}}=4$ ), localization ( $n_{\text{eloquent } 3\text{D-DSA}/3\text{D-A}}=8; n_{\text{non-eloquent } 3\text{D-DSA}/3\text{D-A}}=2$ ), main feeder ( $n_{\text{ACA } 3\text{D-DSA}/3\text{D-A}}=1; n_{\text{MCA } 3\text{D-DSA}/3\text{D-A}}=3; n_{\text{PCA } 3\text{D-DSA}/3\text{D-A}}=6$ ), venous drainage ( $n_{\text{superficial } 3\text{D-DSA}/3\text{D-A}}=4; n_{\text{deep } 3\text{D-DSA}/3\text{D-A}}=4; n_{\text{mixed } 3\text{D-DSA}/3\text{D-A}}=2$ ) and MSS ( $\text{MSS}_{1\text{D-DSA}/3\text{D-A}}=1; \text{MSS}_{2\text{D-DSA}/3\text{D-A}}=4; \text{MSS}_{3\text{D-DSA}/3\text{D-A}}=5$ ). Measurement of AVM size ( $S_{3\text{D-DSA}}=20.2 \pm 11.2$  mm;  $S_{3\text{D-A}}=19.9 \pm 10.9$  mm) correlated well ( $r=0.994; p=0.0001$ ) in both reconstructions.

**Discussion:** The AI-based 3D-A shows comparable results to 3D-DSA in terms of quantitative and qualitative parameters.

**Conclusion:** 3D-A is a promising method for visualization of AVMs and might help to reduce PD for the diagnostic work-up of AVMs.

280

### THE HIDDEN PROWESS OF NLP AND RADIOLOGICAL REPORTS: A TEXT MINING PIPELINE FOR MACHINE LEARNING-ASSISTED DIAGNOSTICS AND REPORTING

Andreas Georg Junge<sup>1,2,3</sup>, Benedikt Kämpgen<sup>4</sup>, Chang Gyu Cho<sup>2</sup>, Christoph Groden<sup>2</sup>, Thomas Ganslandt<sup>3</sup>, Holger Wenz<sup>2</sup>, Máté Maros<sup>\*2,3</sup>

<sup>1</sup>Hochschule Mannheim—University of Applied Sciences, Technical Informatics, Mannheim, Deutschland

<sup>2</sup>Heidelberg University, Medical Faculty Mannheim, Department of Neuroradiology, Mannheim, Deutschland

<sup>3</sup>Heidelberg University, Medical Faculty Mannheim, Department of Biomedical Informatics at the Heinrich Lanz Center, Mannheim, Deutschland

<sup>4</sup>Empolis, Information Management GmbH, Kaiserslautern, Deutschland

**Background:** The value of radiological reports is often neglected and advancements in natural language processing (NLP) are forced to take a backseat behind the predominance of computer vision applications of deep learning in radiology. Furthermore, the language of radiological reports is extremely heterogeneous. Efforts were put forward to unify reporting language by using structured reporting (SR). However, the adoption of SR is still incremental with controversial aspects regarding the usability of SR for data extraction. To illustrate the value of radiological texts and the prowess of NLP, we present our text mining pipeline with three use cases that include i) AI algorithm-based indexing for improved data extraction, ii) report quality assessment and iii) clinical key information content with particular focus on neurovascular emergencies.

**Methods:** We mirrored our local RIS (Syngo, Siemens) between 2014–2018 including ~48.000 CT and MRI reports, and associated billing information. All reports were RadLex® annotated using a proprietary NLP pipeline<sup>1</sup> (Empolis Information Management GmbH) that is free for research purposes. Further, we performed i) comprehensive indexing of the corpus and created language models using open-source software (Elasticsearch and PyTorch), and ii) latent space analyses to identify characteristics specific for certain clinical scenarios or styles of attending radiologists.

**Result:** We created a RadLex® annotation pipeline that can automatically provide quality score for each report based on predefined local or international guidelines<sup>2</sup>. Since its implementation the browser-embedded assistive NLP-algorithm significantly increased ( $p<0.05$ ) the occurrence of ASPECT scores in reports about vascular emergencies. Further, the pipeline can support junior readers in creating reports similar to the style of the attending radiologist by whom these are going to be signed off.

**Discussion:** Computer assisted reporting tools can speed up knowledge transfer to junior radiologists, improve their report quality and reduce the burden of signing off reports on senior radiologists.

**Conclusion:** Our use cases of NLP applied on radiological reports strongly argue for the tremendous value hidden in radiological text to streamline the reporting process and to improve its quality.

### References

- Jungmann F, et al. Radiologe. 2019.
- Maros ME, et al. In Vivo. 2018.

286

### PREVENTION OF RECURRENT STROKE: AI-BASED CLASSIFICATION OF ETIOLOGY FROM IMAGING FEATURES, HISTOPATHOLOGICAL REPORTS AND CLINICAL DATA

Helge Kniep<sup>\*1</sup>, Peter Sporns<sup>2</sup>, Moritz Wildgruber<sup>2</sup>, Astrid Jeibmann<sup>3</sup>, Jens Minnerup<sup>4</sup>, Jens Fiehler<sup>1</sup>, Uta Hanning<sup>1</sup>

<sup>1</sup>Klinik und Poliklinik für Neuroradiologische Diagnostik und Intervention, Universitätsklinikum Hamburg-Eppendorf, Hamburg, Deutschland

<sup>2</sup>Institut für Klinische Radiologie, Universitätsklinikum Münster, Münster, Deutschland

<sup>3</sup>Institut für Neuropathologie, Universitätsklinikum Münster, Münster, Deutschland

<sup>4</sup>Klinik für Neurologie mit Institut für Translationale Neurologie, Universitätsklinikum Münster, Münster, Deutschland

Stroke etiology	# patients	# males	Age mean	Age SD
Arterioembolic (TOAST 1)	34	19	69.0	12.5
Cardioembolic (TOAST 2)	75	34	73.0	11.0
Other determined course (TOAST 4)	11	9	50.1	13.8
<b>Total</b>	<b>120</b>	<b>62</b>	<b>69.7</b>	<b>13.3</b>

**Fig. 1 | 286** Demographic characteristics of study cohort; # Number of; SD standard deviation

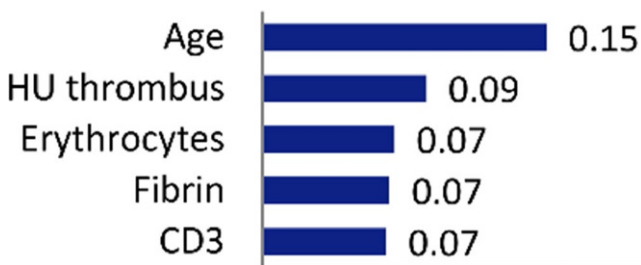


**Fig. 2 | 286** Importance of top-5 predictors (Gini impurity); HU Hounsfield units

**Background:** Second events account for 20% of all 260.000 strokes that occur annually in Germany. Targeted prevention of recurrent strokes requires a profound understanding of the underlying pathology. However, pathogenesis remains unclear in 40% of the cases (1). We hypothesized that quantitative information from images, histopathological reports and clinical data can be used for machine learning-based prediction of etiology to efficiently support differential diagnostics and prophylaxis of second ischemic strokes.

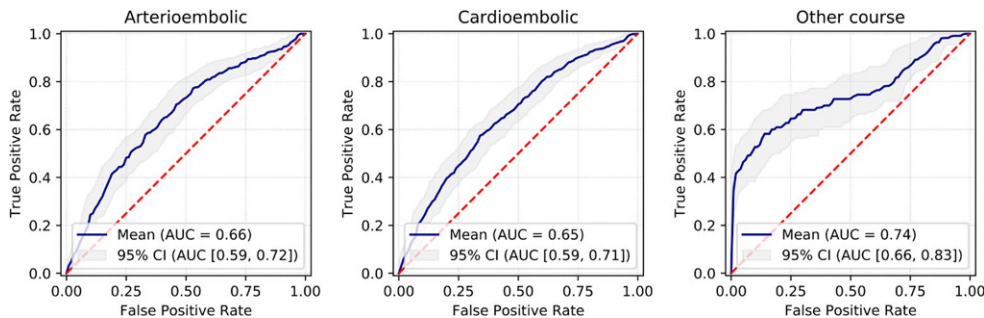
**Methods:** The analysis includes 120 patients with occlusion of the carotid-T or middle cerebral artery who underwent thrombectomy. HU densities of thrombi were evaluated in the admission non-contrast CT scans. Thrombi samples were histologically analyzed and immunohistochemistry for CD3, CD20, and CD68/KiM1P was performed. Additional clinical parameters were extracted through chart review. The final diagnosis of stroke etiology as defined by the TOAST classification was available for all included patients. A total of 20 quantitative markers including imaging features, histological information and clinical data were evaluated for their ability to predict the underlying etiology in a 3-class random forest algorithm with 5-fold cross-validation.

**Result:** 34 of the 120 included patients had arterioembolic strokes, 75 had cardioembolic strokes, and 11 had other determined strokes (Fig. 1). ROC AUCs of the validation sets were 0.66 for predicting arterioembolic etiology, 0.65 for cardioembolic etiology and 0.74 for other determined courses (Fig. 2). The most important predictors of etiology were age, thrombus density (HU) and the histological markers erythrocytes, fibrin and CD3 (Fig. 3).

**Discussion:** Our results confirm feasibility of machine learning-based etiology prediction. A significant increase in classification performance can be expected from integration of additional predictors including texture, shape and filtered imaging markers.

**Conclusion:** Quantitative markers from imaging features, histopathological analysis and clinical data employed in an artificial intelligence-based classifier may support differential diagnosis of stroke etiology. In clinical routine, such algorithm could facilitate differential diagnosis of stroke etiology and hence enable targeted prophylaxis of second events.

**Fig. 3 | 286** Receiver Operating Characteristics for validation set predictions of proposed machine learning classifier; AUC Area under the curve; CI Confidence interval



**References**

1. Grau AJ, et al. "Risk factors, outcome, and treatment in subtypes of ischemic stroke: the German stroke data bank." Stroke. 2001;32(11):2559–66.

**345**

**VOLLAUTOMATISIERTE DETEKTION UND SEGMENTIERUNG INTRAKRANIELLER METASTASEN BEI MALIGNEM MELANOM IN DER CMRT ANHAND EINES DEEP-LEARNING-MODELS**

Lenhard Pennig\*<sup>1</sup>, Simon Lennartz<sup>1</sup>, Frank Thiele<sup>2</sup>, Liliana Caldeira<sup>1</sup>, Lukas Görtz<sup>3</sup>, David Maintz<sup>1</sup>, Kai Roman Laukamp<sup>1</sup>, Jan Borggrefe<sup>1</sup>

<sup>1</sup>Uniklinik Köln, Institut für Diagnostische und Interventionelle Radiologie, Köln, Deutschland

<sup>2</sup>Philips GmbH, Aachen, Deutschland

<sup>3</sup>Uniklinik Köln, Zentrum für Neurochirurgie, Köln, Deutschland

**Hintergrund:** Das maligne Melanom stellt eine Tumorentität dar, bei der es häufig und schon im frühen Krankheitsverlauf zu einer intrakraniellen Filialisierung kommen kann<sup>1</sup>. Ziel dieser Studie ist es, intrakranielle Metastasen bei diesen Patienten in multiparametrischen MRT mittels eines Deep-Learning-Modells (DLM) vollautomatisch zu detektieren und zu segmentieren.

**Methoden:** Retrospektive monozentrische Studie, bei der von Patienten mit malignem Melanom und nachgewiesener intrakranieller Filialisierung eine durch zwei unabhängige Radiologen manuelle Segmentierung der Metastasen in multiparametrischen MRT-Bilddaten (T1 +/- KM, T2, FLAIR) zum Zeitpunkt der Erstdiagnose (05/2013–10/2018) auf der Plattform IntelliSpace Discovery (Philips Healthcare) durchgeführt wurde. Diese Ergebnisse wurden mit den vollautomatisierten Segmentierungen eines an Gliomen trainierten DLM<sup>2</sup> (DeepMedic, BioMedIA) verglichen. Folgende Ausschlusskriterien wurden angewandt: Zweite maligne Grunderkrankung, kleine Metastasen (<0,15 ml), schwere MRT-Artefakte und insuffiziente MRT-Datensätze.

**Ergebnisse/Results:** 34 Patienten (63 +/- 12 Jahre; männlich: n=20) mit 56 Metastasen konnten eingeschlossen werden. Das DLM erreichte eine Detektionsrate der Metastasen von 86%. Für die Segmentierung der Metastasen an sich betreffend konnte ein Dice-Koeffizient von 0,63 (Median), maximal 0,9, berechnet werden.

**Diskussion:** Das DLM detektierte Melanommetastasen >0,15 ml mit einer hohen Genauigkeit und segmentierte diese suffizient. Die Anwendung des DLM auf andere Tumorentitäten und auf Metastasen geringerer Größe, beispielsweise anhand weiterer Pre- und Postprocessing-Verfahren sowie Training des DLM, sollten weiter beforscht werden.

**Fazit:** Intrakranielle Filiae in der cMRT bei Patienten mit malignem Melanom lassen sich ab einer Größe von 0,15 ml mittels Deep Learning mit einer hohen Genauigkeit automatisch detektieren und suffizient segmentieren.

## Literatur

1. Zhang D, et al. Incidence and prognosis of brain metastases in cutaneous melanoma patients: a population-based study. *Melanoma Res.* 2019;29(1):77–84. Feb.
2. Perkuhn B, et al. Clinical Evaluation of a Multiparametric Deep Learning Model for Glioblastoma Segmentation Using Heterogeneous Magnetic Resonance Imaging Data From Clinical Routine. *Invest Radiol.* 2018;53(11):647–54.

## 360

### UNSUPERVISED DEEP LEARNING FOR DETECTION OF BRAIN DISEASE IN MR IMAGING

Rami Eisawy<sup>1,2</sup>, Julia Moosbauer<sup>3</sup>, Tom Finck<sup>4</sup>, Claus Zimmer<sup>4</sup>, Björn Menze<sup>1</sup>, Franz MJ Pfister<sup>\*2,3</sup>, Benedikt Wiestler<sup>4</sup>

<sup>1</sup>Department of Computer Science, Technical University of Munich, Munich, Deutschland

<sup>2</sup>Digital Helix GmbH, R&D, Munich, Deutschland

<sup>3</sup>Department of Statistics, Ludwig Maximilian University, Munich, Deutschland

<sup>4</sup>Klinikum rechts der Isar, Technical University of Munich, Munich, Deutschland

**Background:** Manual detection and interpretation of suspicious findings in radiological exams is a slow and lengthy process, requiring the highest level of attention and expertise. Introducing an automatic approach to distinguish abnormal from normal anatomy and physiology has the potential to speed up the diagnostic process and avoid errors by serving as a second read. Recently, there have been numerous attempts to solve this problem with the use of supervised machine learning. However, this poses three major limitations: Costliness of data annotation, risk of annotation errors being reproduced by the algorithm and lack of training data for rare diseases.

**Methods:** To avoid those limitations, an unsupervised, progressively growing adversarial autoencoder model is presented. The model is exclusively trained on images from a healthy cohort, thus learning the normal anatomy and signal of the brain. Subsequently, pathologies are automatically detected as deviations from this normality. We evaluate the model on datasets containing a variety of MS lesions, WMH, stroke, and GBM across the FLAIR MR sequence.

**Results:** The evaluation shows the effectiveness of the method and its ability to highlight even small abnormalities in brain MRI exams, yielding state-of-the-art results in terms of overlap error and distance-based measures (Average DSC=0.614±0.135) in diseases the network has never seen before.

**Discussion:** Qualitative results effectively show the power of the proposed autoencoder model. Reconstructed samples show high detail while simultaneously not reconstructing the pathological areas, facilitating a segmentation pipeline. Additionally, no modifications to the model are needed to allow for extensive generalisability to various applications such as detecting other white matter hyperintensities, tumors or inflammation, or even other modalities (e.g. CT) or parts of the body.

**Conclusion:** To further evaluate the model and achieved results thus far, additional experiments on a larger dataset consisting of various different pathologies are scheduled. Clinical studies proving model efficacy is subject to ongoing research and intended to substantiate the use of the model as a clinical tool.

## 363

### CAPSNETS DETECT SIGNS OF INFARCTION IN NECT STROKE PATIENTS WITH SUPER-HUMAN PERFORMANCE

Christian Riedel<sup>\*1</sup>

<sup>1</sup>Dept. of Neuroradiology, University of Göttingen, Göttingen, Deutschland

**Hintergrund/Background:** To evaluate if a hybrid approach of a convolutional neural network with a shallow capsular network can be trained to reach super-human performance in recognizing early signs of infarction and dense artery signs in NECT images of acute ischemic stroke patients.

**Methoden:** We trained a shallow capsular neural network which received inputs from 5 convolutional layers with NECT images of 150 patients with an acute stroke and 150 patients with a different pathological condition. The training used labeling for early signs of infarction derived from CTA-, CTP and subsequent NECT imaging as well as labels of hyperdense artery signs. After training, the ROC curves for correct identification of patients with acute ischemic stroke indicators were compared to those found by three expert reviewers blinded with respect to the clinical situation for a total of 80 NECT test sets.

**Ergebnisse:** The ROC curve for the correct identification of more than one early sign of infarction was found to have an area under the curve of 0.925, whereas the expert reviewers had an AUC between 0.783 and 0.854.

**Diskussion:** While classical convolutional neural networks tend to require at least several hundred training data sets for a complex task such as detection of stroke indicators from NECT images, the capsular network approach delivers high performance detection at a moderate amount of training data.

**Fazit:** Using the capsular network approach, complex spatial hierarchies in 3D medical images can be used in order to recognize early signs of infarction even with a super-human performance.

## 2. Neuroonkologie

38

### MULTIVARIATE NONINVASIVE PREDICTION OF IDH MUTATIONAL STATUS IN WHO GRADE II AND III GLIOMAS WITH ADVANCED MRI T2-MAPPING TECHNIQUES

Timo Alexander Auer\*<sup>1</sup>, Maike Kern<sup>2</sup>, Uli Fehrenbach<sup>1</sup>, Martin Misch<sup>3</sup>, Edzard Wiener<sup>4</sup>

<sup>1</sup>Klinik für Neuroradiologie, Charite—Universitätsmedizin Berlin, Klinik für Radiologie, Berlin, Deutschland

<sup>2</sup>Klinik für Neuroradiologie, Charite—Universitätsmedizin Berlin, Berlin, Deutschland

<sup>3</sup>Klinik für Neurochirurgie, Charite—Universitätsmedizin Berlin, Berlin, Deutschland

<sup>4</sup>Klinik für Neuroradiologie, Charite—Universitätsmedizin Berlin, Berlin, Deutschland

**Hintergrund:** To investigate multivariate analyses for noninvasive prediction of the IDH-mutational status in grade II and III gliomas including evaluation of T2-“Mapping”-sequences.

**Methoden:** MR examinations with pathologically proven WHO-grade II and III gliomas were retrospectively enrolled. Multivariate ROC-analyses to predict IDH mutational status were performed containing quantitative T2 mapping analyses and qualitative characteristics (sex, age, localization, heterogeneity, edema, necrosis and diameter). Relaxation times were calculated pixelwise by means of a standardized ROI-analyses. Interobserver variability also was tested.

**Ergebnisse:** Out of 32 patients (mean age: 50.7; range: 32–83) in the collective, 28% (9/32) were grade II gliomas and 72% (24/32) grade III, while 59.5% showed a positive IDH mutated-state (IDHm) and 40.5% were wildtype (IDHw). Multivariate ROC-analyses were calculated for relaxation time and range, localization and age with a cumulative **0.955 AUC** ( $p < 0.001$ ), while central T2-relaxation time had by far the highest single variable sensitivity (**AUC: 0.873; Range: 0.762; Age: 0.809; Localization: 0.713**). Age (cut off: 49 years;  $p = 0.031$ ) and localization ( $p = 0.014$ ) were the only qualitative parameters found to be significant as IDHw gliomas were older and IDHm gliomas were preferentially located fronto-temporal.

**Diskussion:** Analyses of T2-mapping relaxation times seem to be suitable for predicting the correct IDH mutational state in grade II and III glioma. To the best of our knowledge this is the first study evaluating quantitative T2-mapping sequences for prediction of the IDH mutational state in low grade gliomas. Furthermore, age and localization seem also to be reliable qualitative characteristics to correlate with the mutational state.

**Fazit:** T2-Mapping may be a promising technique for predicting the correct IDH mutational state in combination with the so far known correlating qualitative characteristics.

88

### THE CORRELATION OF (B)LOOD-(O)XYGEN-(L)EVEL-(D)EPENDENT SIGNAL AND RADIOLOGICAL DEFINED TUMOR GROWTH PATTERNS IN PATIENTS WITH GLIOBLASTOMA

Katharina Rosengarth\*<sup>1</sup>, Katharina Hense<sup>2,3</sup>, Isabel Wiesinger<sup>2</sup>, Christian Ott<sup>1</sup>, Christian Doenitz<sup>1</sup>, Alexander Brawanski<sup>1</sup>, Christina Wendl<sup>2</sup>

<sup>1</sup>Universitätsklinikum Regensburg, Institut für Neurochirurgie, Regensburg, Deutschland

<sup>2</sup>Universitätsklinikum Regensburg, Institut für Radiologie, Regensburg, Deutschland

<sup>3</sup>Universität Regensburg, Institut für Psychologie, Regensburg, Deutschland

**Hintergrund:** Functional magnetic resonance imaging (fMRI) in glioblastoma (GBM) is challenging because these tumors exhibit an impaired neurovascular coupling which decreases fMRI signal and may lead to misinterpretations of fMRI signals. In this study we wanted to investigate if a radiologically defined tumor growth pattern may influence the integrity of the fMRI signal and interact with tumor proximity in patients suffering from GBM.

**Methoden:** 62 patients with primary GBM were included. Patients were stratified in 2 groups according to their radiologically defined tumor growth pattern (R-GBM, 18 patients: rim-like tumor growth pattern; P-GBM 44 patients: palisading growth pattern). Functional imaging was performed at a 3T Siemens Scanner. During the fMRI paradigm subjects had to perform covertly a verb generation task. Data analysis was done by using SPM 12 for analysis and region of interest (ROI) definition. To assess the influence of tumor proximity and growth pattern on (language associated) fMRI-signal integrity percent signal change and finite impulse response functions in four ROIs were defined located one proximate, one peripheral and two distal (one tumor ipsilateral and one tumor contralateral) to the tumor. Results were adjusted for tumor size, necrosis size and age.

**Ergebnisse:** Qualitatively, percent signal changes showed reasonable values in all ROIs independently of their location (min=0.3% max=1.7%) but appearing lower proximal to a tumor. The peak values of the FIR-functions and % signal changes were significantly lower in ROIs close to a tumor compared to ROIs distal to a tumor independently of tumor growth pattern. The comparison of tumor proximate and tumor peripheral fMRI-signal revealed that only R-GBM patients showed significant higher peak values of the FIR-functions and % signal changes in the peripheral ROI. This was not significantly apparent in patients with P-GBMs.

**Diskussion:** Preliminary results suggest that the fMRI signal is valid in proximity of a GBM. Thereby the signal increases with growing distance to the tumor. The results also support that fMRI is among other factors strongly influenced by radiologically defined tumor growth pattern.

**Fazit:** fMRI in GBM patients should be interpreted in the context of tumor growth pattern.

98

### KORREKTUR DER WASSERKONTAMINATION IN DER DTI: VERBESSERTE VORHERSAGE DER REZIDIVLOKALISATION IN GLIOBLASTOMEN BEREITS IM PRÄOPERATIVEN MRT.

Marie-Christin Metz<sup>1</sup>, Miguel Molina-Romero<sup>2</sup>, Jana Lipkova<sup>2</sup>, Friederike Liesche<sup>3</sup>, Björn Menze<sup>2</sup>, Claus Zimmer<sup>1</sup>, Benedikt Wiestler\*<sup>1</sup>

<sup>1</sup>Abteilung für Diagnostische und Interventionelle Neuroradiologie, Technische Universität München, München, Deutschland

<sup>2</sup>Institut für Informatik, Technische Universität München, Lehrstuhl für Informatikanwendungen in der Medizin und Augmented Reality, Garching, Deutschland

<sup>3</sup>Institut für Allgemeine Pathologie und Pathologische Anatomie, Technische Universität München, Fachgebiet für Neuropathologie, München, Deutschland

**Hintergrund:** Für die Vorhersage der Lokalisation von Glioblastom-Rezidiven haben sich die Diffusions-Tensor-Bildgebung (DTI) und insbesondere die daraus ableitbare Fraktionelle Anisotropie (FA) als ein vielversprechender Ansatz herausgestellt. Ein bisher ungelöstes Problem dabei war die Wasserkontamination der DTI im Perifokalödem. Mit unserer Arbeit stellen wir einen neuen Ansatz vor, der basierend auf Deep-Learning-Methoden die Wasserkontamination korrigiert und somit eine genauere Vorhersage des Tumorrezidivs ermöglicht.

**Methoden:** Wir untersuchten die präoperativen MRT-Datensätze von 35 Glioblastompatienten unserer prospektiven Kohorte, sowie die jeweils ersten Verlaufsbilder, welche ein Tumorrezidiv zeigten. Mittels semi-automatischer Segmentierung markierten wir dabei Kontrastmit-

tel-anreichernde Tumoranteile und in der FLAIR-Sequenz hyperintense Areale. Die DTI-Datensätze wurden daraufhin vom Störfaktor des freien Wassers mittels eines neuen Modells eines neuronalen Netzwerkes befreit, welches zuvor mit synthetischen Daten trainiert worden war. Die resultierenden korrigierten FA-Werte, sowie die FA-Rohdaten unterteilten wir zum besseren Vergleich in die 10., 50. und 90. Perzentile, wobei wir Areale mit und ohne späteren Rezidivauftritts gegenüberstellten (Abb. 1).

**Ergebnisse:** Für die korrigierten FA-Werte fanden wir signifikante Unterschiede zwischen den Arealen mit und ohne späterem Tumorrezidiv in allen drei Perzentilen mit  $p_{10}=0,001111$ ,  $p_{50}=0,0031$  und  $p_{90}<0,0001$  (Wilcoxon rank-sum test; Abb. 2b). Im Gegensatz dazu zeigten sich bei den unkorrigierten FA-Daten nur in der 90. Perzentile signifikante Unterschiede, wohingegen die Werte der 10. und 50. Perzentile statistisch nicht zu unterscheiden waren ( $p_{90}=0,0003$  vs.  $p_{10}=0,07515$  und  $p_{50}=0,079$ ; Abb. 2a).

**Diskussion:** Nach der Elimination der Wasserkontamination lassen sich im Perifokalödem schon kleinste, vermutlich durch Infiltration des Tumors bedingte Veränderungen der FA-Werte feststellen. An den Stellen, an denen später ein Rezidiv auftritt, sind diese signifikant niedriger als in Arealen mit reinem Ödem. Diese Veränderungen sind in der konventionellen MRT-Bildgebung bisher nicht sichtbar und könnten deshalb wichtige Informationen für personalisierte Therapieentscheidungen liefern.

**Fazit:** Die hier vorgestellte Methode könnte in Zukunft dabei helfen, die chirurgische und strahlentherapeutische Behandlung von Glioblastomen zu verbessern, indem sie die Lokalisation von späteren Tumorrezidiven schon von den ersten präoperativen MRT-Bildern vorherzusagen vermag.

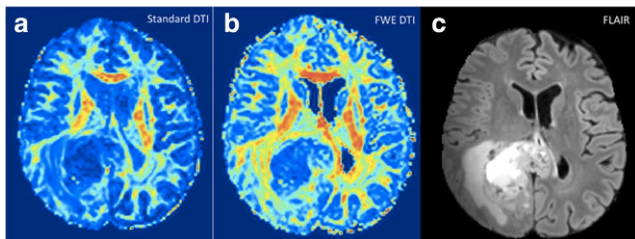
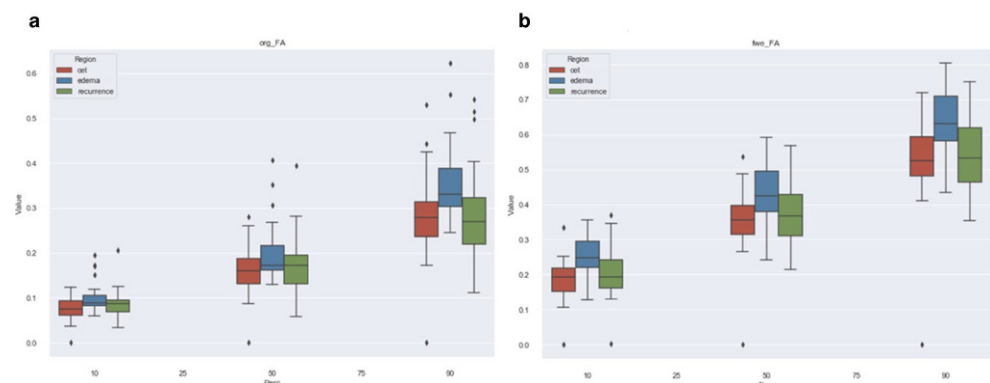


**Abb. 1 | 98** Vergleich der DTI-Daten eines Glioblastom-Patienten. Das Standard-Bild (a) zeigt ein reduziertes Signal im den Tumor umgebenden Ödem, wohingegen nach Elimination des Signals des freien Wasseranteils das Signal wiederhergestellt ist (b) und Informationen über eine Tumor-Infiltration des FLAIR-hyperintensiven Areals um den Tumor herum (c) liefert

**Fig. 2 | 98** a) Standard FA-Werte; b) FA-Werte nach Korrektur des freien Wasseranteils



176

## GLINT: GLUCOCEST IN NEOPLASTIC TUMORS BEI 3 TESLA—ERSTE KLINISCHE ERGEBNISSE VON GLUCOCEST BEI HIRNTUMOREN

Tobias Lindig<sup>\*1,2</sup>, Moritz Zaiss<sup>2</sup>, Kai Herz<sup>2</sup>, Anagha Deshmane<sup>2</sup>, Marco Skardelly<sup>3</sup>, Jens Schittenhelm<sup>4</sup>, Xavier Golay<sup>5</sup>, Klaus Scheffler<sup>2</sup>, Ulrike Ernemann<sup>1</sup>, Benjamin Bender<sup>1</sup>

<sup>1</sup>Universitätsklinikum Tübingen, Radiologische Klinik, Neuroradiologie, Tübingen, Deutschland

<sup>2</sup>Max-Planck-Institut für biologische Kybernetik, Hochfeld-Magnetresonanz, Tübingen, Deutschland

<sup>3</sup>Universitätsklinikum Tübingen, Neurochirurgie, Tübingen, Deutschland

<sup>4</sup>Universitätsklinikum Tübingen, Neuropathologie, Tübingen, Deutschland

<sup>5</sup>Queen Square Institute of Neurology, Department of Brain Repair & Rehabilitation, London, England

**Hintergrund:** Die dynamische, glukoseverstärkte (DGE) CEST-Bildgebung wurde aufgrund der geringen Effektgröße fast ausschließlich im Ultra-Hochfeld (UHF) gezeigt. Erste Ergebnisse bei Hirntumorpatienten einer DGE CEST-Methode mit schneller 3D-Bildgebung, die für die klinische Feldstärke bei 3T entwickelt wurde, werden hier vorgestellt.

**Methoden:** CEST gesättigte Bilder mit unterschiedlichen Frequenzabweichungen wurden mit einer zeitlichen Auflösung von 6,3 s (gesamt: 16:45 min) zu 160 Zeitpunkten vor, während und nach der intravenösen Gabe von Glukose (0,3 mg/kg) aufgenommen, um eine Akkumulation der Glukose im Gehirn zu detektieren. Zwei Glioblastompatienten (IDH Wildtyp, MGMT-Promotor unmethyliert; 1: männlich, 70 Jahre; 2: weiblich, 75 Jahre) und 3 gesunde Kontrollen wurden an einem klinischen 3T MRT (MAGNETOM Prisma fit, Siemens) untersucht. DGE-Kontrastaufnahmen wurden analysiert, indem jedes Bild von einem Basisbild vor Glukosegabe subtrahiert wurde:  $\Delta DGE_{(t)} = DGE_{\text{baseline}} - DGE_{(t)}$ .

**Ergebnisse:** Im hochgradigen Gliom (1) konnte die Glukose-Aufnahme innerhalb der Gadolinium-aufnehmenden Region etwa 4 Minuten nach Injektion mit einem maximalen Anstieg von  $\Delta DGE = 0,51 \pm 0,078$  nachgewiesen werden, während eine kontroll-ROI des kontralateralen Marklagers keinen gleichzeitigen Anstieg zeigte ( $\Delta DGE = 0,07 \pm 0,085$ ). Das zweite Gliom (2), mit gleicher Histologie und Graduierung, zeigte nur sehr wenig Gadolinium-Aufnahme und keinen signifikant nachweisbaren DGE-Effekt. Gesunde Kontrollen zeigten keinen signifikanten DGE-Kontrast.

**Fazit:** Wir konnten zeigen, dass eine stabile dynamische, glukoseverstärkte Bildgebung bei klinischer Feldstärke, unter Verwendung optimierter Sättigungs- und Ausleseparameter, erreicht werden kann. Erste

Ergebnisse sind vielversprechend und deuten darauf hin, dass Gluco-CEST eher einer Störung der Blut-Hirnschranke mit Gadolinium-Aufnahme entspricht als dem molekularen Tumorprofil oder der Graduierung des Tumors.

189

**MR SPECTROSCOPY-BASED RADIOGENOMIC ANALYSIS OF BRAIN TUMOR PATIENTS**

Urs Würtemberger\*<sup>1</sup>, Horst Urbach<sup>1</sup>, Irene Hübschle<sup>2</sup>, Pamela Heiland<sup>2</sup>, Dieter Henrik Heiland<sup>2</sup>

<sup>1</sup>Uniklinik Freiburg—Klinik für Neuroradiologie, Freiburg im Breisgau, Deutschland

<sup>2</sup>Uniklinik Freiburg—Klinik für Neurochirurgie, Freiburg im Breisgau, Deutschland

**Background:** The 2016 revision of the WHO brain tumor classification incorporates for the first time genetic and molecular parameters, and thereby challenges the tasks of MR-imaging. We report a prospective imaging study evaluating MR spectroscopy in brain tumor imaging. The study aim was a precise preoperative molecular prediction of brain tumors. We mapped the landscape of metabolic patterns and its heterogenic distribution in health and disease.

**Methods:** 105 patients received anatomical MRI and multivoxel MR spectroscopy using a semiLASER-sequence with 5×5×20 mm voxel size. Tumor regions were segmented and registered to equivalent spectroscopic voxels. We extracted the metabolic pattern of 15760 single-voxel and mapped the distribution of metabolic pattern. Clinical data were collected and used for further validation of our computational model.

**Result:** Cluster analysis identified 15 distinct clusters based on gap-statistic algorithm (5 main clusters C1-5 and 2–3 subclusters). C1 consist-

ed primarily of spectra corresponding to the normal appearing matter. C2 was composed of spectra associated with the ventricles and subventricular regions. C3-5 represent various voxels in pathological lesions and brain tumors. Within clusters C3-5 an accurate separation of all glioma subgroups in 59.2% of the voxels was determined. The conventionally used metabolites which were used to classify tumor-spectra showed a subordinate role.

**Discussion:** Radiomic studies focus on structural imaging, but no association between radiomic features and genetic alterations can be demonstrated so far. MR spectroscopy allows the detection of metabolic changes and provides insights into the molecular properties of the tumour. We demonstrate strong metabolic heterogeneity of brain tumors complicating sufficient prediction of genetic subgroups. However, a large part of the tumor localized spectra can be distinctly assigned to their underlying genetic alterations.

**Conclusion:** MR-spectroscopy based radiogenomic prediction of genetic and molecular subtypes in brain tumor patients shows to be a robust tool in preoperative non-invasive imaging work-up. MR-spectroscopy has the potential to include the need of “personalized medicine” by improving neurooncologic imaging and could influence in the future the clinical and surgical management of brain tumor patients.

**References**

1. Diamandis E, et al. MR-spectroscopic imaging of glial tumors in the spotlight of the 2016 WHO classification. *J Neurooncol.* 2018;139(2):431–40. Sep.

Fig. 1 | 189

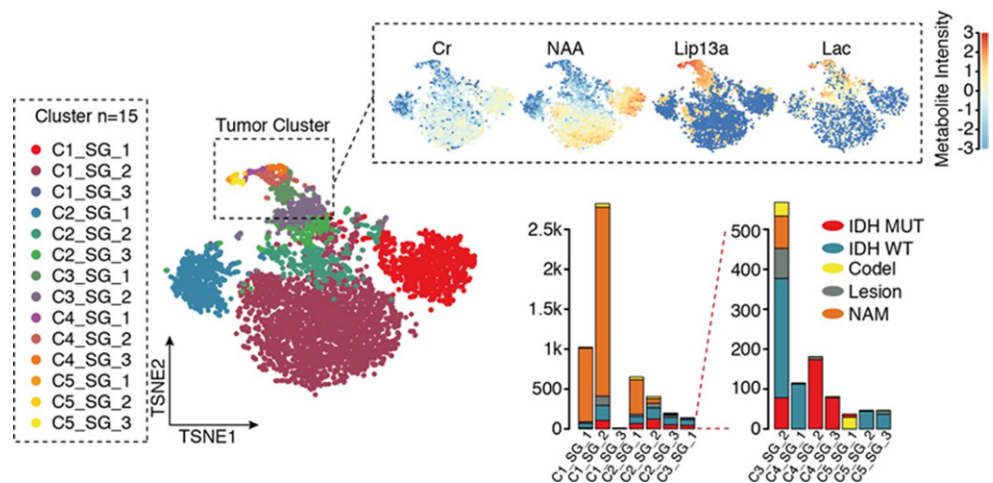
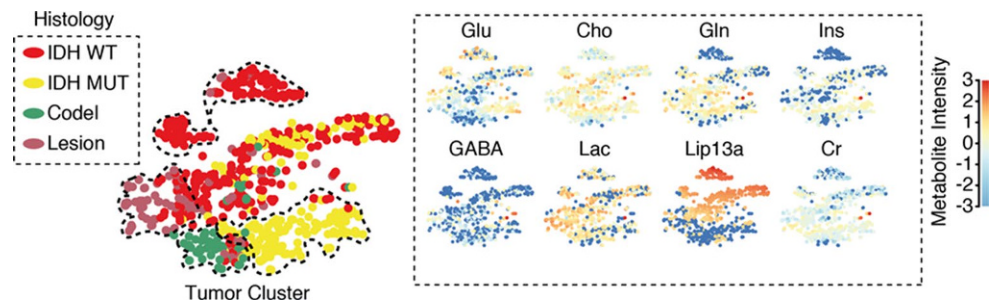


Fig. 2 | 189



### PSEUDOPROGRESSION IN PEDIATRIC LOW-GRADE GLIOMA FOLLOWING PRIMARY RADIOTHERAPY—FIRST RESULTS FROM THE GERMAN LGG—STUDY COHORT

Annika Stock\*<sup>1</sup>, Caroline-Victoria Hancken<sup>1</sup>, Daniela Kandels<sup>2</sup>, Astrid K. Gnekow<sup>2</sup>, Rolf-Dieter Kortmann<sup>3</sup>, Beate Timmermann<sup>4</sup>, Torsten Pietsch<sup>5</sup>, Brigitte Bison<sup>1</sup>, Mirko Pham<sup>1</sup>, Monika Warmuth-Metz<sup>1</sup>

<sup>1</sup>Universitätsklinikum Würzburg, Institut für Diagnostische und Interventionelle Neuroradiologie, Würzburg, Deutschland

<sup>2</sup>SIOP-LGG-Studienzentrale, Universitätsklinikum Augsburg, Augsburg, Deutschland

<sup>3</sup>Klinik für Strahlentherapie und Radioonkologie, Universitätsklinikum Leipzig, Leipzig, Deutschland

<sup>4</sup>Klinik für Partikeltherapie (WPE), Universitätsklinikum Essen, Essen, Deutschland

<sup>5</sup>Institut für Neuropathologie, Universitätsklinikum Bonn, Bonn, Deutschland

**Background:** Early expansion of tumor volume and/or edema following radiotherapy may indicate pseudoprogression (PsPD). The differentiation between true progression (PD) and PsPD is frequently difficult but nevertheless of utmost importance because PD usually calls for a change in treatment. The aim of this study was to examine the incidence of PsPD in pediatric low-grade gliomas (LGG) with regard to the individual radiation modalities.

**Methods:** 74 pediatric patients of the SIOP-LGG 2004 study cohort and LGG-registry cohort after primary radiotherapy (RT) were included, representing nearly half of all documented patients with sufficient image data sets). MRI controls at 3, 6, 12, 18 and 24 months post-treatment were evaluated. PsPD was considered upon significant increase in tumor size, increasing perifocal edema or increase of contrast medium enhancement. PsPD was determined when these changes decreased on further follow-up MRIs or a reduction in tumor size was noted despite progressive edema or contrast enhancement.

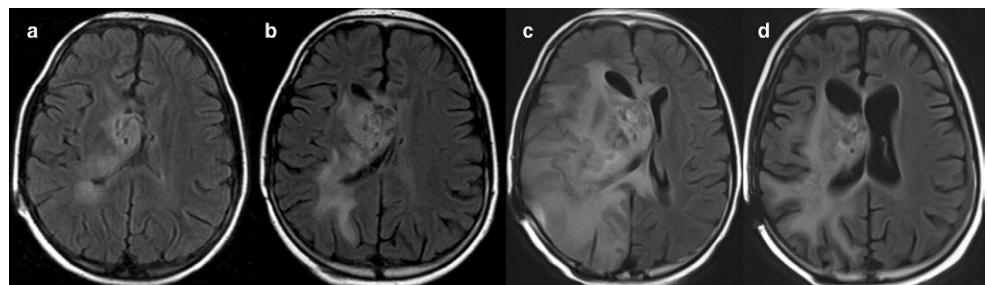
**Result:** Treatment modalities were iodine seeds in 27/74 patients (36.5%), photon-therapy in 35/74 (47.3%) and proton-therapy in 12/74 (16.2%). PsPD most often started at month 3 and 6 and was characterized by progressive edema in most cases. We found a total of 34/74 (45.9%) PsPD (iodine seeds 12/27 [44.4%], photon-therapy 17/35 [48.6%] and proton-therapy 5/12 [41.7%]). PsPD did not correlate to the mode of RT applied (Chi-square test).

**Conclusion:** PsPD is a frequent phenomenon and much more common in LGG than in high-grade glioma<sup>1</sup>. PsPD frequency does not seem to differ significantly between iodine seed-, proton- and photon-therapy.

#### References

1. Carceller F. *et al.* Pseudoprogression in children, adolescents and young adults with non-brainstem high grade glioma and diffuse intrinsic pontine glioma. *J Neurooncol.* 2016;129:109–21.

**Fig. 1 | 220** Massive PsPD after photon-therapy. **a)** Initially the tumor showed no perifocal edema. **b)** Edema grew from little at 6 months to **c)** massive at 8 months post-therapy. **d)** At 12 months post-therapy perifocal edema regressed



### LONGITUDINAL, LEAKAGE CORRECTED AND UNCORRECTED RCBV DURING THE FIRST-LINE TREATMENT OF GLIOBLASTOMA: A PROSPECTIVE STUDY.

Eike Steidl\*<sup>1</sup>, Mathias Müller<sup>2</sup>, Andreas Müller<sup>2</sup>, Ulrich Herrlinger<sup>3</sup>, Elke Hattingen<sup>1</sup>

<sup>1</sup>Institut für Neuroradiologie, Universitätsklinikum Frankfurt, Frankfurt, Deutschland

<sup>2</sup>Radiologische Klinik, Universitätsklinikum Bonn, Bonn, Deutschland

<sup>3</sup>Klinik und Poliklinik für Neurologie, Universitätsklinikum Bonn, Sektion Klinische Neuroonkologie, Bonn, Deutschland

**Hintergrund:** Dynamic susceptibility contrast (DSC) MR-perfusion is becoming a standard of care for the monitoring of glioblastoma. Yet, technical standards are lacking and measurements without leakage correction are still common [1]. Also, data on leakage corrected measurements during stable disease is scarce. In this study we hypothesized that basic leakage correction would significantly enhance data quality during stable disease and improve progress detection. We furthermore investigated whether longitudinal data could increase diagnostic performance.

**Methoden:** Patients with histologically proven glioblastoma undergoing first-line therapy were prospectively recruited. We conducted DSC perfusion measurements without prebolus administration in 6-week intervals from the end of radiotherapy until progression. Maximum relative cerebral volume values (rCBVmax) with and without leakage correction were calculated using Philips IntelliSpace®.

**Ergebnisse:** We recruited 16 patients and conducted 82 MRI scans with a mean follow up of 7.2 month. During stable disease, corrected rCBVmax was significantly more stable than uncorrected rCBVmax. Detection of progression with a rCBVmax cutoff was better for corrected (specificity 86%) than for uncorrected rCBVmax (specificity 41%). Interestingly, the increase of corrected rCBVmax upon progression also had a good diagnostic performance with a combination of both cutoffs delivering the best result (sensitivity/specificity 89%/93%).

**Diskussion:** In our prospective study we demonstrated, that even an easy approach to leakage correction significantly improves data quality and diagnostic performance in detecting glioblastoma progression. Corrected rCBVmax supports the imaging finding of a stable disease and large increases during longitudinal observation support the diagnosis of tumor progression.

**Fazit:** Further studies to investigate the value of longitudinal rCBV dynamics for the differentiation of real tumor progression from pseudoprogression are warranted.

#### Literatur

1. Welker K, Boxerman J, Kalnin A, Kaufmann T, Shiroishi M, Wintermark M. ASFN recommendations for clinical performance of MR dynamic susceptibility contrast perfusion imaging of the brain. *Ajnr Am J Neuroradiol.* 2015;36:E41–51. <https://doi.org/10.3174/ajnr.A4341>.

### RESTRICTED KETOGENIC DIET AND FASTING IN COMBINATION WITH RE-IRRADIATION IN GLIOBLASTOMA IMPACT INTRACELLULAR pH AND INTRACEREBRAL METABOLISM AS DETERMINED BY <sup>1</sup>H/<sup>31</sup>P MR-SPECTROSCOPY

Katharina Wenger-Alakmech<sup>\*1</sup>, Marlies Wagner<sup>1</sup>, Nina von Mettenheim<sup>2</sup>, Patrick Harter<sup>3</sup>, Kea Franz<sup>4</sup>, Jörg Bojunga<sup>5</sup>, Elke Hattingen<sup>1</sup>, Joachim Steinbach<sup>2</sup>, Oliver Bähr<sup>2</sup>, Emmanouil Fokas<sup>6</sup>, Detlef Imhoff<sup>6</sup>, Claus Rödel<sup>6</sup>, Johannes Rieger<sup>7</sup>, Ulrich Pilatus<sup>1</sup>, Martin Voss<sup>2</sup>

<sup>1</sup>Department of Neuroradiology, University Hospital Frankfurt, Frankfurt, Deutschland

<sup>2</sup>Dr. Senckenberg Institute of Neurooncology, University Hospital Frankfurt, Frankfurt, Deutschland

<sup>3</sup>Institute of Neuropathology (Edinger-Institute), University Hospital Frankfurt, Frankfurt, Deutschland

<sup>4</sup>Department of Neurosurgery, University Hospital Frankfurt, Frankfurt, Deutschland

<sup>5</sup>Department of Medicine 1, University Hospital Frankfurt, Frankfurt, Deutschland

<sup>6</sup>Department of Radiation Oncology, University Hospital Frankfurt, Frankfurt, Deutschland

<sup>7</sup>Department of Neurology, University Hospital Tuebingen, Frankfurt, Deutschland

**Background:** Some Glioblastoma (GBM) cells show increased glycolysis even in the presence of oxygen and may lack metabolic flexibility to oxidize ketone bodies (KB). This could result in a glucose dependent tumor being starved during fasting and unable to maintain a reversed pH gradient. The aim of this study was to explore metabolic effects of combining a calorie restricted ketogenic diet (CRKD)/fasting (CR) with re-irradiation therapy (RT) in patients with recurrent GBM using MR-Spectroscopy. **Methods:** The prospective multicentric, randomized study included an extended MRS protocol with 3D FID <sup>31</sup>P CSI and a 2D <sup>1</sup>H PRESS sequence. 50 patients with recurrent GBM and indication for RT were randomized (1:1) in 2 groups: Group A keeping a CRKD/CR for 9 days and group B keeping a balanced diet. RT was performed on day 4–8. 32 patients received MRS at baseline (day –1) and 23/32 on day 6. Voxels were selected from the area of recurrent tumor and the contralateral hemisphere (control). A basis set for LCModel including 3-hydroxybutyrate (BOHB), acetone (Acn) and acetoacetate (AcAc) was simulated and metabolites were quantified.

**Results:** 20 patients in Group A and 22 patients in Group B completed dietary intervention. 17/25 patients in group A had a serum ketone level of >0.5 mmol/l at day 6 during CRKD/CR. There was a significant difference at day 6 between groups ( $p < 0.01$ ). An Acn signal at 2.22 ppm was detected in 4 patients at day 6 (Group A). In one patient Acn signal was fitted within tumor tissue and NAWM, in all other patients within NAWM only (concentration range 0.12–0.28 mmol/l). Group A showed a significant increase in pH<sub>i</sub> in tumor voxels comparing baseline levels to day 6 ( $p = 0.028$ ); there was no significant change for Group B. ATP levels were stable in tumor or control voxels in both groups.

**Discussion:** With no significant decrease in ATP levels during CRKD/CR and maintenance of an alkaline pH<sub>i</sub>, our study suggests a metabolic flexibility of GBM cells with a possible breakdown of KB and shift towards oxidative phosphorylation. Correspondingly, metabolic inflexibility of tumor cells has been recently contradicted in rat glioma models with upregulation of monocarboxylate transporter 1 (MCT-1), facilitating uptake and oxidation of KB.<sup>1</sup> Acn is freely diffusible across the BBB and might be detected earlier intracerebrally than AcAc and BOHB, which depend on MCT upregulation.

#### References

- de Feyter HM, Behar KL, Rao JU, et al. A ketogenic diet increases transport and oxidation of ketone bodies in RG2 and 9L gliomas without affecting tumor growth. *Neuro-oncology*. 2016.

### 3. Entzündliche ZNS-Erkrankungen

#### SHORT-TERM REORGANIZATION OF CORTICAL INFORMATION FLOW IN MULTIPLE SCLEROSIS: A LONGITUDINAL FMRI EFFECTIVE CONNECTIVITY STUDY

Vinzenz Fleischer<sup>\*1</sup>, Muthuraman Muthuraman<sup>1</sup>, Abdul Rauf Anwar<sup>2</sup>, Gabriel Gonzalez-Escamilla<sup>1</sup>, Angela Radetz<sup>1</sup>, René-Maxime Gracien<sup>3</sup>, Stefan Bittner<sup>1</sup>, Felix Luessi<sup>1</sup>, Sven G. Meuth<sup>4</sup>, Frauke Zipp<sup>1</sup>, Sergiu Groppa<sup>1</sup>

<sup>1</sup>Department of Neurology, Focus Program Translational Neuroscience (FTN), University Medical Center of the Johannes Gutenberg University, Mainz, Germany, Mainz, Deutschland

<sup>2</sup>Bio-medical Engineering Department, University of Engineering & Technology, Lahore, Pakistan, Lahore, Pakistan

<sup>3</sup>Department of Neurology and Brain Imaging Center, Goethe University, Frankfurt (Main), Germany, Frankfurt, Deutschland

<sup>4</sup>Department of Neurology with Institute of Translational Neurology, University of Muenster, Germany, Muenster, Deutschland

**Hintergrund:** Effective connectivity (EC) as derived from functional MRI is able to explore causal effects between brain areas and can be traced longitudinally to depict reorganization processes in brain diseases like Multiple Sclerosis (MS). Thus, the application of EC analysis in MS may provide an imaging biomarker for disease progression. Here, we examined EC dynamics in MS patients and healthy controls (HC) at short-term intervals and in relation to clinical impairment.

**Methoden:** Serial longitudinal 3-Tesla resting-state functional MRI was performed every 12-weeks over one year in twelve MS patients (mean age  $41.7 \pm 11.5$  years). Twelve healthy subjects served as controls (mean age  $33.5 \pm 9.6$  years). Two recently established approaches for EC quantification were used: Causal Bayesian Network (CBN) and Time-resolved Partial Directed Coherence (TPDC). EC was determined between frontal, prefrontal, temporal, occipital, and parietal lobes, the cerebellum and deep grey matter nuclei. The EC strength was correlated with the Expanded Disability Status Scale (EDSS) and the Fatigue Scale for Motor and Cognitive functions (FSMC).

**Ergebnisse:** Our findings demonstrated a longitudinal increase in EC between specific brain regions, detected in both the CBN and the TPDC analysis in MS patients. EC from the deep grey matter, frontal, prefrontal and temporal regions showed a continuous increase over the study period, whereas the EC from the remaining regions did not change over one year. No longitudinal changes in EC were attested in HC over the same period of time in either method. Furthermore, we observed an association between clinical performance and EC strength. In particular, the EC increase in fronto-cerebellar connections showed an inverse correlation with the EDSS and patients' fatigue score.

**Diskussion:** Our data depict continuous functional reorganization between specific brain regions indicated by increasing EC over time in MS, which is not detectable in healthy controls. In particular, fronto-cerebellar connections, which are closely related to clinical performance, may provide a marker of brain plasticity and functional reserve in MS.

**Fazit:** Our longitudinal EC data provide novel insights into the recruitment of directed connections in MS patients over time, by showing for the first time where and when functional reorganization processes occur in clinically stable patients (neither inflammatory activity nor disease progression).

## PITFALLS IN DIAGNOSIS OF PSEUDOTUMORS OF THE CENTRAL NERVOUS SYSTEM—A TUMEFACTIVE MULTIPLE SCLEROSIS LESION MIMICKING A GLIOBLASTOMA

Anna Schrum\*<sup>1</sup>, Roland Coras<sup>2</sup>, Reimer Andresen<sup>1</sup>

<sup>1</sup>Institut für Diagnostische und Interventionelle Radiologie/  
Neuroradiologie, Westküstenklinikum Heide, Heide, Deutschland

<sup>2</sup>Institut für Neuropathologie, Friedrich-Alexander Universität,  
Erlangen, Deutschland

**Background:** Pseudotumors of the central nervous system are rare lesions. Patients often present symptoms suggesting a space-occupying tumor or an ischemia. On imaging they can mimic a broad range of underlying diseases like ischemia, tumor lesions, inflammatory and demyelinating ailments. We intend to highlight such a case and the redundant pitfalls in the diagnosis of such cases.

**Methods:** Case report about a 34y old female patient that was hospitalized under the suspicion of having a stroke.

**Result:** All radiological criteria of the initial cCT and cMRI (Sequences: T2, T1-/+ contrast, FLAIR, DWI, ADC, TOF) strengthened the diagnosis of a fresh ischemia of the right frontoparietal region. In combination with results from a liquoranalysis the stroke was deemed post-infectious. Because of a clinical deterioration a follow-up MRI was conducted 6 weeks later. What had previously been described as an ischemic area now showed the characteristics of a tumorous lesion with signs of malignancy. Furthermore a new lesion was found in the frontal region which was then biopsied. The lesion showed areas of demyelination. Consequently the diagnosis was Multiple Sclerosis (MS). After a cortisone treatment the clinical symptoms decreased and there was an improvement of the radiological findings. A maintenance therapy with Interferon- $\beta$  followed.

**Discussion:** In some cases MS-lesions can mimic radiographic and histologically neoplasia like high-grade gliomas. The lesions can show a rapid enlargement, a surrounding edema and a marginal contrast-enhancement. Such lesions lead to the term: Tumefactive multiple sclerosis (1). A special entity of such tumor-like MS-lesions is the concentric sclerosis baló (2). The pathologically and radiologically criterias are concentric rings of demyelination and myelin-preserved regions of the white matter with a corresponding concentric contrast-enhancement. The parietal lesion, found in this case, showed such radiographic criteria.

**Conclusion:** The initial diagnosis and also the subsequent management of a Pseudotumor, as shown in this case, can be difficult.

### References

1. Lucchinetti CF, et al. Clinical and radiographic spectrum of pathologically confirmed tumefactive multiple sclerosis. *Brain*. 2008;131:1759–75.
2. Baló J. Encephalitis periaxialis concentrica. *Arch Neurol Psychiatry*. 1928;19:242–64.

### 101

#### MR-DARSTELLUNG DER AKUTEN OPTIKUSNEURITIS MIT HILFE DER 3D T1-W BLACK-BLOOD SEQUENZ

Isabelle Riederer\*<sup>1</sup>, Nico Sollmann<sup>1</sup>, Mark Mühlau<sup>2</sup>, Claus Zimmer<sup>1</sup>, Jan S Kirschke<sup>1</sup>

<sup>1</sup>Neuroradiologie, Klinikum rechts der Isar, TU München, München, Deutschland

<sup>2</sup>Neurologie, Klinikum rechts der Isar, TU München, München, Deutschland

**Hintergrund:** Kürzlich konnte gezeigt werden, dass sich mit Hilfe der 3D T1w TSE BlackBlood (BB) Sequenz mehr zerebrale kontrastmit-

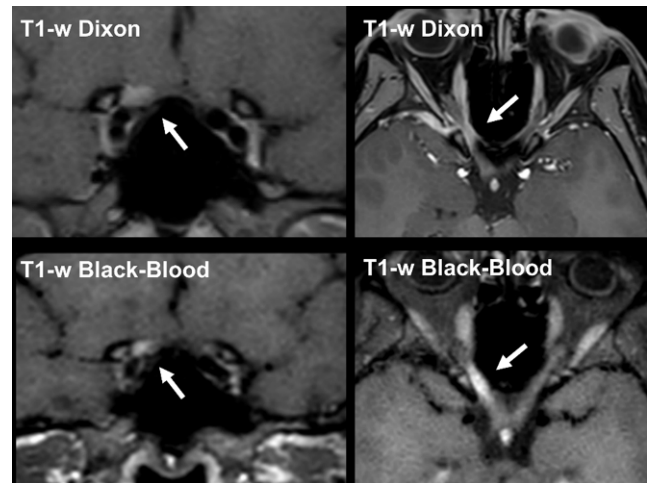


**Abb. 1 | 101** Kontrastmittellaffine Läsion im rechten N. opticus in T1-w Dixon (oben) und T1-w Black-Blood (unten) in koronaler (link) und axialer (rechts) Orientierung

telaffine Läsionen in MSPatienten darstellen lassen als mit der StandardT1w MPRAGEsequenz (1). Ziel unserer Studie ist, T1w BB mit speziellen fettgesättigten T1w Bildern bei Patienten mit einer akuten Neuritis nervi optici (NNO) zu vergleichen.

**Methoden:** MRDaten (inklusive 3D T1w TSE BB, 3D T1w MPRAGE und 3D T1w Dixon oder koronale 2D T1w TSE Dixon nach i. v. KM) von 29 Patienten mit Symptomen einer akuten NNO wurden retrospektiv untersucht. Das KontrastRauschVerhältnis (CNR) wurde in einer kontrastmittellaffinen Läsion im Sehnerv berechnet. Zusätzlich wurden die Daten von zwei Neuroradiologen hinsichtlich der Bildqualität, Artefakte, diagnostischen Sicherheit und visuellen Kontrastmittelanreicherung auf einer 5 bzw. 4Punkte Skala bewertet.

**Ergebnisse:** Die Diagnose einer akuten NNO konnte bei 20 Patienten klinisch bestätigt werden, 16 von ihnen zeigten eine kontrastmittellaffine Läsion im N. opticus; alle 9 Patienten mit anderen Diagnosen zeigten keine Kontrastmittelanreicherung. Keine der Kontrastmittelanreicherungen wurde in der T1-w BB übersehen, jedoch wurden in der MP-RAGE insgesamt 5 Läsionen von einem der beiden Radiologen nicht erkannt. Das CNR war signifikant ( $p < 0.05$ ) höher in T1-w BB ( $1.8 \pm 1.0$ ) und T1-w Dixon ( $1.7 \pm 1.1$ ) im Vergleich zur MP-RAGE ( $0.7 \pm 0.7$ ). Die Bildqualität wurde in der T1-w TSE BB ( $4.1 \pm 0.6$ ) und T1-w Dixon ( $4.1 \pm 0.7$ ) besser bewertet als in der MP-RAGE ( $2.7 \pm 0.5$ ,  $p < 0.05$ ), mit ebenfalls höherer diagnostischer Sicherheit in der T1-w TSE BB ( $4.4 \pm 0.7$ ) und T1-w Dixon ( $4.1 \pm 0.7$ ) verglichen mit der T1-w MP-RAGE ( $2.6 \pm 0.7$ ,  $p < 0.05$ ).

**Diskussion:** Unsere Ergebnisse sollten durch prospektive Studien weiter validiert werden; bei konsistenten Ergebnissen könnte ggfs. das MR-Protokoll um spezielle Orbitasequenzen gekürzt werden, falls eine 3D T1-w TSE BB zur sensitiveren Darstellung von aktiven Hirnläsionen ohnehin akquiriert wird.

**Fazit:** 3D T1-w TSE BB zeigt ähnlich hohe qualitative und quantitative Charakteristiken wie T1-w Dixon und scheint der MP-RAGE Sequenz bezüglich der Darstellung einer akuten NNO überlegen zu sein.

### Literatur

1. Sommer NN, Saam T, Coppnath E, et al. Multiple Sclerosis: Improved Detection of Active Cerebral Lesions With 3-Dimensional T1 Black-Blood Magnetic Resonance Imaging Compared With Conventional 3-Dimensional T1 GRE Imaging. *Invest Radiol*. 2018;53(1):13–9.

**SIMPLE MR PLANIMETRIC MEASUREMENTS FOR DIAGNOSIS AND OUTCOME PREDICTION OF MULTIPLE SCLEROSIS**

Stephanie Mangesius\*<sup>1,2</sup>, Sergiy Pereverzyev Jr.<sup>1,2</sup>, Lukas Lamplmayr<sup>1</sup>, Lukas Lenhart<sup>1,2</sup>, Gabriel Bsteh<sup>3,4</sup>, Sebastian Wurth<sup>3</sup>, Florian Deisenhammer<sup>3</sup>, Elke Gizewski<sup>1,2</sup>

<sup>1</sup>Medical University Innsbruck, Department of Neuroradiology, Innsbruck, Österreich

<sup>2</sup>Medical University Innsbruck, Neuroimaging Core Facility, Innsbruck, Österreich

<sup>3</sup>Medical University Innsbruck, Department of Neurology, Innsbruck, Österreich

<sup>4</sup>Medical University Vienna, Department of Neurology, Wien, Österreich

**Hintergrund:** Brain volume change has been suggested as a reliable MRI predictor of disability in different stages of multiple sclerosis (MS). However, the measurement of volume change is not being used in daily clinical practice neither as a prognostic factor nor to monitor treatment effects, as no accepted methodology for routine clinical use exists to date. In this pilot study, the main objective was to investigate whether a number of easily applicable planimetric measurements proposed for different neurologic disease entities can predict the more complex volumetric measurements in patients with MS.

**Methoden:** For estimating the volumetric characteristics (gray matter [GM], white matter [WM], cerebrospinal fluid [CSF]) using planimetric characteristics in 10 MS patients, we first employed a planimetric characteristic selection based on Spearman’s correlation coefficient (SC). For constructing volumetric characteristics estimators using the selected planimetric characteristics, we then used neural networks (NNs) functions.

**Ergebnisse:** Planimetric characteristics with a high correlation with volumetric characteristics are listed in Table 1. In the considered patient set, we constructed the NNs that predict the volumes of GM, WM, and CSF using the corresponding planimetric characteristics, given in Table 1. The relative prediction errors of these NNs were below 11% for GM, 5% for WM and 15% for CSF (Fig. 1).

**Diskussion:** Even in this low patient number, we observed a high correlation between MR planimetric and volumetric measurements and a low prediction error, which makes the proposed approach very promising.

**Fazit:** Further studies in larger patient cohorts are needed to test MR planimetry as an easy to apply and robust imaging biomarker to evaluate cerebral and ventricular volume in patients with MS with similar accuracy and strong correlations with volumetric measurements.

**MEAN KURTOSIS WITHIN THE CORPUS CALLOSUM IS ASSOCIATED WITH CLINICAL IMPAIRMENT IN MULTIPLE SCLEROSIS**

Christian Thaler\*<sup>1</sup>, Tobias D. Faizy<sup>1</sup>, Anna Kyselyova<sup>1</sup>, Maxim Bester<sup>1</sup>, Sune Jespersen<sup>2</sup>, Brian Hansen<sup>2</sup>, Jan-Patrick Stellmann<sup>3</sup>, Christoph Heesen<sup>3</sup>, Jens Fiehler<sup>1</sup>, Susanne Siemonsen<sup>1</sup>

<sup>1</sup>Universitätsklinikum Hamburg-Eppendorf, Klinik für neuroradiologische Diagnostik und Intervention, Hamburg, Deutschland

<sup>2</sup>Universität Aarhus, Department of Clinical Medicine, Center of Functionally Integrative Neuroscience, Aarhus, Dänemark

<sup>3</sup>Universitätsklinikum Hamburg-Eppendorf, Klinik für Neurologie, Hamburg, Deutschland

**Hintergrund:** Clinical-radiological correlations are in general low in Multiple Sclerosis (MS). Recent studies, that focused on diffusional kurtosis imaging (DKI), have shown that mean kurtosis (MK) is sensitive to diffuse white and gray matter injury in MS and might improve clinical-radiological correlations.[1]

**Methoden:** Fourteen patients with relapsing-remitting MS received brain imaging on a 3T MR scanner at baseline and again after 12 months. Scan protocols included a sagittal 3-dimensional FLAIR sequence and a fast DKI sequence, recently introduced by Hansen et al. [2] Subsequently, MK was measured within the corpus callosum (CC), which was automatically segmented using FreeSurfer, and within a FLAIR lesion mask which was manually outlined for each patient. Additionally, imaging results were correlated with clinical impairment

**Table 1 | 106** Planimetric characteristics with high correlation with volumetric characteristics

volume	correlation	planimetric characteristics
GM	SC >0.85	Frontooccipital diameter, Midbrain diameter, Pontine area, Midbrain-to-pontine diameter ratio
WM	SC >0.80	transverse skull diameter, Frontooccipital diameter, Midbrain diameter, Pontine area
CSF	SC >0.80	Third ventricle width unaligned, Anterior segment of corpus callosum/genu, corpus callosum index (CCI), regional anterior CCI

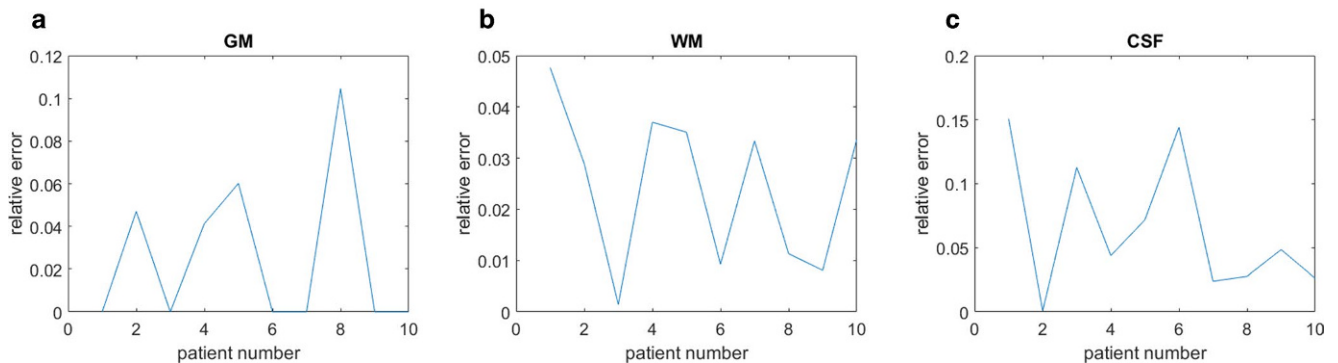


**Fig. 1 | 106** Relative prediction errors of the constructed NNs for predicting the volumes of GM, WM, CSF

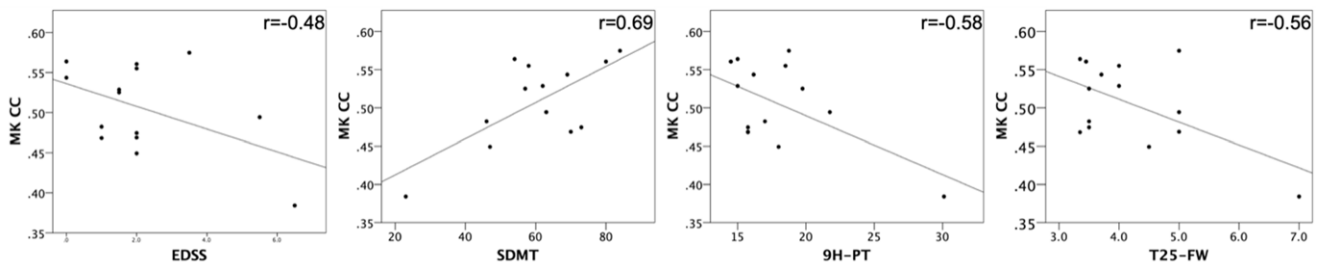


**Fig. 1 | 110** Correlation between mean kurtosis (MK) within the corpus callosum (CC) and clinical parameters, including Expanded Disability Status Scale (EDSS), Symbol Digit Modalities Test (SDMT), 9-Hole Peg Test (9H-PT) and Timed 25-foot Walk (T25-FW) (for all  $p < 0.05$ )

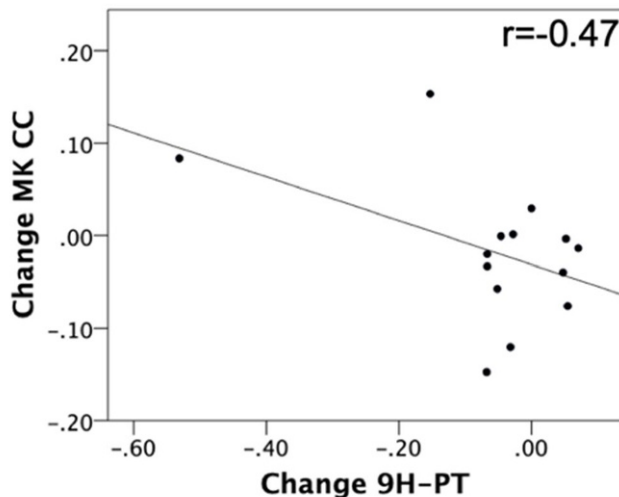


**Fig. 2 | 110** Correlation between relative change in mean kurtosis (MK) within the corpus callosum (CC) and 9-Hole Peg Test (9H-PT) ( $p < 0.05$ )

using the Expanded Disability Status Scale (EDSS), the 9-Hole Peg Test (9H-PT), the Symbol Digit Modalities Test (SDMT) and Timed 25-foot Walk (T25-FW).

**Ergebnisse:** At baseline, significant correlations were obtained between MK within the CC and all obtained clinical test scores (see Fig. 1). No correlations were found for MK within the FLAIR lesion mask and any clinical test score. Comparing the baseline and follow-up data, we found a significant correlation between relative changes in MK within the CC and relative changes in the 9H-PT (see Fig. 2).

**Diskussion:** MK within the CC correlates well with clinical impairment in MS patients and might improve the detection and evaluation of diffuse white matter injury. The fast DKI sequence used in our study can be easily integrated in clinical routine and provides a novel imaging biomarker that might close the clinical-radiological gap. At the time of abstract submission, further regions of interests were investigated.

**Fazit:** MK within the CC is a potential biomarker that provides further information about the progression of cognitive and motor impairment in MS patient.

#### Literatur

1. Bester, et al. *Mult Scler.* 2015.
2. Hansen, et al. *Magn Reson Med.* 2016.

#### 142

#### DETECTION OF OPTIC NERVE LESIONS IN PATIENTS WITH ED AND VISUAL SYMPTOMS: COMPARISON OF 2D STIR AND 3D DIR SEQUENCES

Justus Cordt\*<sup>1</sup>, Sönke Peters<sup>1</sup>, Christian Riedel<sup>1</sup>, Olav Jansen<sup>1</sup>

<sup>1</sup>UKSH Campus Kiel, Klinik für Radiologie und Neuroradiologie, Kiel, Deutschland

**Background:** As T2-hyperintense optic nerve (ON) lesions no longer define “dissemination in space” in the 2017 revised McDonald Criteria<sup>1</sup>, other recommendations (e. g. MAGNIMS) still use them. Vision problems, like onset of blurred vision, are one of the first and most common clinical presentations in patients suffering from ED (*encephalomyelitis disseminata*, ED). Previously, detection of these lesions required coronal 2D short tau inversion recovery sequences (STIR). As 3D double inversion recovery (DIR) sequences being used increasingly to determine cortical lesions, we wondered if they also detect ON lesions.

**Methods:** Simultaneously acquired STIR and DIR images of 47 ED-patients were assessed by two experienced radiologists. Both of them had to quantify the likelihood of signal alterations of ON in a typical five-level Likert scale. The detection of ON lesions in patients with reported visual symptoms and/or vision loss were considered as “true positives”.

**Result:** DIR sequences showed superior interrater reliability and general capability of detecting ON lesions, as shown:

**Discussion:** DIR sequences are superior to STIR sequences in detecting optic nerve lesions in ED-patients. These findings support former studies, which also showed a good performance with a high a sensitivity (95%) and specificity (94%) in detecting optic neuritis<sup>2</sup>.

**Conclusion:** 3D DIR sequences are capable of detecting ON lesions in patients with ED. They are even superior to 2D STIR sequences. These findings could result in short but all-embracing protocols. Further studies need to evaluate the diagnostic value of detecting ON lesions, especially regarding signal alterations in visually asymptomatic ED-patients and the recently revised McDonald criteria.

#### References

1. Thomsen, et al. Diagnosis of multiple sclerosis: 2017 revisions of the McDonald criteria. *Lancet Neurol.* 2018;2018:.
2. Hodel, et al. Comparison of 3 D double inversion recovery and 2D STIR FLAIR MR sequences for the imaging of optic neuritis: pilot study. *Eur Radiol.* 2014;:.
3. Sartoretti, et al. How Common Is Signal-Intensity Increase in Optic Nerve Segments on 3D Double Inversion Recovery Sequences in Visually Asymptomatic Patients with Multiple Sclerosis? *Ajn Am J Neuroradiol.* 2017;:.

Fig. 1 | 142

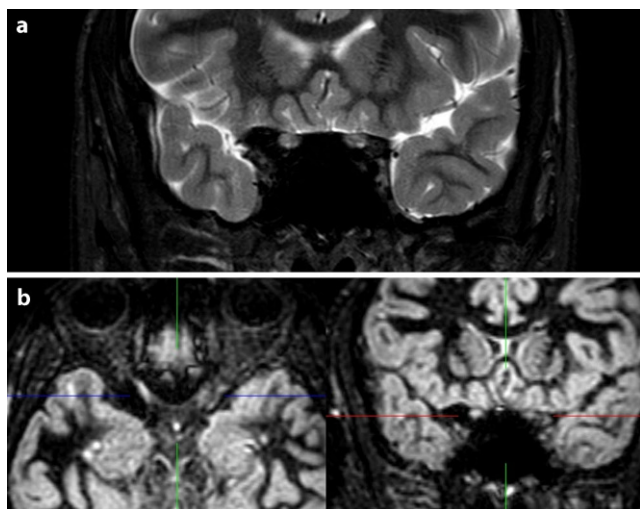
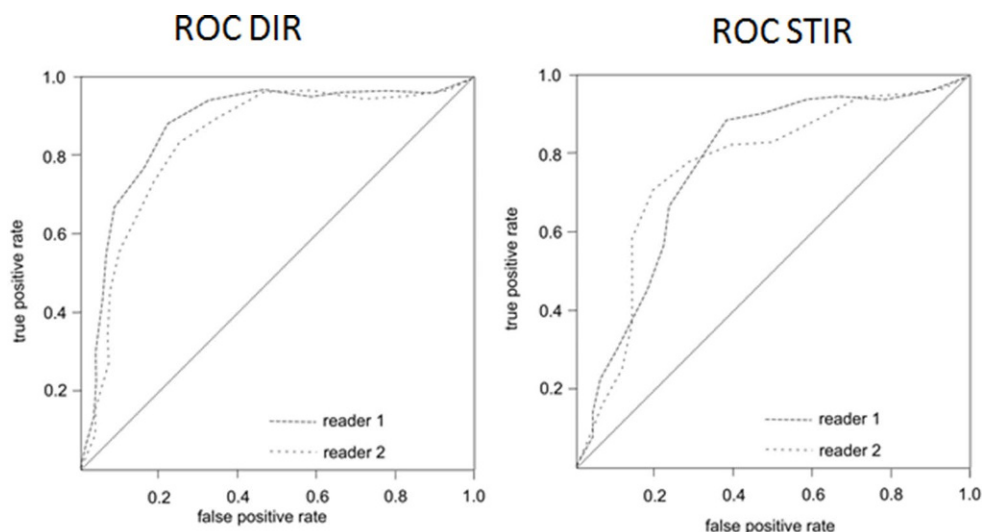


Fig. 2 | 142 Example of two corresponding sequences of the same patient: **a)** 2D STIR sequence with uncertain signal alteration of the right optic nerve, **b)** corresponding 3D DIR sequence with striking hyperintensity in the right optic nerve [transverse slice orientation (*left*), coronal slice orientation (*right*)]

166

**DIFFUSIONAL KURTOSIS IMAGING HELPS TO DIFFERENTIATE MS LESION TYPES**

Christian Thaler\*<sup>1</sup>, Anna Kyselyova<sup>1</sup>, Tobias D. Faizy<sup>1</sup>, Maxim Bester<sup>1</sup>, Christoph Heesen<sup>2</sup>, Jan-Patrick Stellmann<sup>2</sup>, Sune Jespersen<sup>3</sup>, Brian Hansen<sup>3</sup>, Maria Stark<sup>4</sup>, Jens Fiehler<sup>1</sup>, Susanne Siemonsen<sup>1</sup>

<sup>1</sup>Universitätsklinikum Hamburg-Eppendorf, Klinik für neuro-radiologische Diagnostik und Intervention, Hamburg, Deutschland

<sup>2</sup>Universitätsklinikum Hamburg-Eppendorf, Klinik für Neurologie, Hamburg, Deutschland

<sup>3</sup>Universität Aarhus, Department of Clinical Medicine, Center of Functionally Integrative Neuroscience, Aarhus, Dänemark

<sup>4</sup>Universitätsklinikum Hamburg-Eppendorf, Zentrum für Experimentelle Medizin, Institut für Medizinische Biometrie und Epidemiologie, Hamburg, Deutschland

**Hintergrund:** Diffusional kurtosis imaging (DKI) is novel MRI technique measuring the leading deviation from Gaussian diffusion. Mean kurtosis (MK), one of the parameters derived from MKI, has shown increased sensitivity to tissue microstructure in several neurological disorders, including Multiple Sclerosis.

**Methoden:** Thirty-four patients with relapsing-remitting MS and eleven healthy controls (HC) were enrolled in this study and received brain imaging on a 3T MR scanner. The MR protocol included a sagittal 3-dimensional FLAIR sequence, a T1w MPRAGE sequence before and after Gadolinium injection and a fast DKI sequence, recently introduced by Hansen et al. [1] Subsequently, MK and MD were measured in white matter of HC, normal-appearing white matter and three different lesion types, namely contrast enhancing lesion (CEL), FLAIR lesion (FLAIR-L) and black holes (BH).

**Ergebnisse:** Overall 1501 lesions were analyzed, including 30 CEL, 835 FLAIR-L and 636 BH. The results for MK and MD within the white matter ROIs and MS lesions are summarized in Fig. 1. Furthermore, we used multinomial logistic regression to investigate the prognostic value of MK and MD. The results for MK are displayed in Table 1. No significant correlation was found for MD.

**Diskussion:** The fast DKI sequence used in our study can be easily integrated in clinical routine and provides further information about diffuse white matter injury, lesion microstructure and damage. Furthermore, MK showed good prognostic value to differentiate between the different lesion categories without the use of gadolinium.

**Fazit:** DKI helps to evaluate diffuse white matter and lesional injury in MS.

**Literatur**

1. Hansen, et al. Magn Reson Med. 2016;:

**Table 1 | 166** Odds Ratios including lower and upper confidence intervals for mean kurtosis (MK) in normal-appearing white matter (NAWM), contrast enhancing lesions (CEL) and black holes (BH) compared to FLAIR lesions as control group. Multinomial regression also included age, sex, disease duration, EDSS and lesion size

MK	Odds Ratio	Lower CI	Upper CI	p
NAWM	1.17*10 <sup>5</sup>	1.68*10 <sup>4</sup>	8.15*10 <sup>5</sup>	<0.001
CEL	5.03*10 <sup>1</sup>	1.82*10 <sup>0</sup>	1.52*10 <sup>3</sup>	<0.05
BH	1.91*10 <sup>-1</sup>	6.71*10 <sup>-2</sup>	5.4*10 <sup>-1</sup>	<0.01

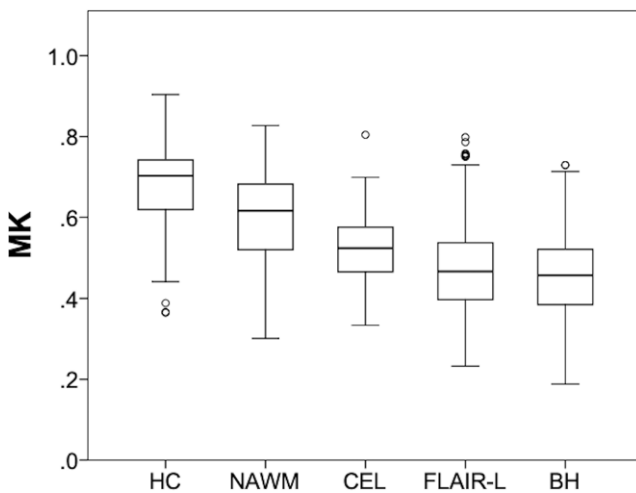


Fig. 1 | 166 Mean kurtosis (MK) in different lesion categories

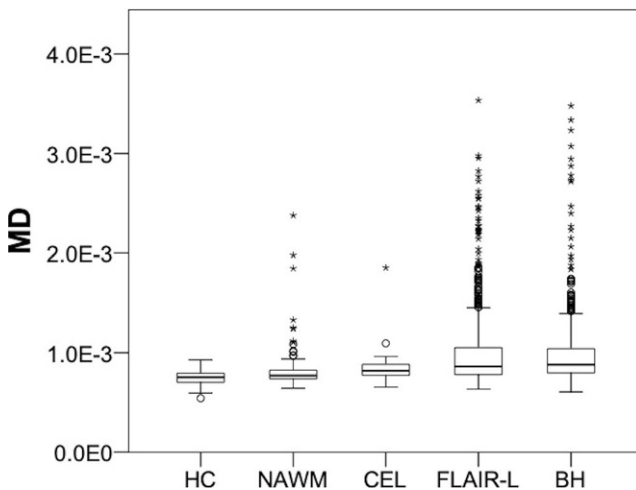


Fig. 2 | 166 Mean diffusion (MD) in different lesion categories

194

### THE CORRELATION OF LESIONS TO THE CENTRAL AND PERIPHERAL NERVOUS SYSTEM IN MULTIPLE SCLEROSIS: AN IN-PATIENT STUDY USING MAGNETIC RESONANCE NEUROGRAPHY

Johann Jende<sup>\*1</sup>, Markus Weiler<sup>2</sup>, Martin Bendszus<sup>1</sup>, Sabine Heiland<sup>1</sup>, Wolfgang Wick<sup>2</sup>, Brigitte Wildemann<sup>2</sup>, Jennifer Kollmer<sup>1</sup>

<sup>1</sup>Universitätsklinikum Heidelberg, Abteilung Neuroradiologie, Heidelberg, Deutschland

<sup>2</sup>Universitätsklinikum Heidelberg, Abteilung Neurologie, Heidelberg, Deutschland

**Background:** Multiple sclerosis (MS) is generally assumed to be restricted to the central nervous system (CNS). Recent studies have shown, however, that lesions can also be detected in the peripheral nervous system (PNS) even at very early stages of the disease. (1) The aim of this study was to investigate a potential connection between CNS and PNS lesions in patients with relapsing-remitting MS.

**Methods:** Seventy MS patients underwent high resolution magnetic resonance neurography (MRN) of the sciatic nerve at 3 Tesla and

detailed neurological and electrophysiological testing. CNS MRI was available or additionally acquired in all patients. T2w lesion count of the brain and spinal cord as well as T2w-hyperintense fascicular lesions to the sciatic nerve were assessed by two independent, neuroradiologists blinded to clinical data.

**Result:** There was an inverse correlation of sciatic nerve T2w-lesions and total CNS T2w-lesions ( $r=-0.432$ ;  $p=0.0002$ ). Specifically, an inverse correlation between sciatic nerve T2w-lesions and supratentorial ( $r=-0.411$ ;  $p=0.0005$ ), infratentorial ( $r=-0.300$ ;  $p=0.0129$ ), and total (supratentorial+infratentorial) brain T2w lesions ( $r=-0.417$ ;  $p=0.0004$ ) was identified. The only other parameter that correlated with PNS lesion numbers was patients' body weight ( $r=0.295$ ;  $p=0.0146$ ). No correlation was found between PNS T2w lesion numbers and electrophysiological parameters.

**Discussion:** Our results might help to elucidate the underlying pathomechanism in MS by indicating that PNS lesions in MS do not seem to occur as a consequence of CNS lesions in the sense of Wallerian degeneration, and that the immunological processes causing higher T2w lesion numbers in the PNS are different from those leading to demyelination in the CNS.

**Fazit:** T2w-hyperintense PNS and CNS lesions are inversely correlated in relapsing-remitting MS.

### References

- Jende JME, Hauck GH, Diem R, Weiler M, Heiland S, Wildemann B, et al. Peripheral nerve involvement in multiple sclerosis: Demonstration by magnetic resonance neurography. *Ann Neurol*. 2017;82(5):.

214

### BRAIN AND MEDULLARY ATROPHY IN MULTIPLE SCLEROSIS AND CLINICALLY ISOLATED SYNDROMES: A 30-YEAR FOLLOW-UP

Lukas Haider<sup>\*1 2 2</sup>, Karen Chung<sup>1</sup>, Giselle Birch<sup>1</sup>, Arman Eshaghi<sup>1 3</sup>, Stephanie Mangesius<sup>4</sup>, Ferran Prados<sup>1 3 5</sup>, Olga Ciccarelli<sup>1 6</sup>, Frederik Barkhof<sup>1 3 6 7</sup>, Declan Chard<sup>1 6</sup>

<sup>1</sup>NMR Research Unit, Queens Square MS Centre, Department of Neuroinflammation, UCL Queen Square Institute of Neurology, Faculty of Brain Science, University College London, London, England

<sup>2</sup>Department of Biomedical Imaging and Image Guided Therapy, Medical University of Vienna, Vienna, Österreich

<sup>3</sup>Centre for Medical Image Computing (CMIC), Department of Medical Physics and Biomedical Engineering, University College London, London, England

<sup>4</sup>Department of Neuroradiology, Medical University Innsbruck, Innsbruck, Österreich

<sup>5</sup>Universitat Oberta de Catalunya, de Barcelona, Barcelona, Spanien

<sup>6</sup>National Institute for Health Research (NIHR), University College London Hospitals (UCLH) Biomedical Research Centre, London, England

<sup>7</sup>Department of Radiology and Nuclear Medicine, VU University Medical Centre, Amsterdam, Niederlande

**Hintergrund:** Brain atrophy, and the neurodegeneration underlying it, starts early in multiple sclerosis (MS), however the long-term clinical relevance of early atrophy and its relation to subsequent atrophy is not known. We aimed to assess brain atrophy rates following clinically isolated syndromes (CIS) suggestive of MS, and their relationship with long-term clinical and MRI outcomes

**Methoden:** 132 age- matched people presenting with a CIS were recruited between 1984–87 and followed up clinically and with magnetic resonance imaging (MRI) one, five, ten, 14, 20 and now 30 years later.

Of those with MS, only 14% were treated with a disease modifying therapy, with the earliest treatment starting 10 years after the initial diagnosis. Using the MRI scans, third ventricular width and medullary width were measured. Clinical outcomes (CIS, relapsing remitting (RR) and secondary progressive (SP) MS, and death due to MS (MSRD)) and Expanded Disability Status Scale scores were determined at 30 years.

**Ergebnisse:** The change in medullary width from baseline to five years, and third ventricular width baseline to ten years, differed significantly between CIS and SPMS (medullary width 0–5:  $p=0.000$ ; third ventricular width, 0–10:  $p=0.048$ ), and CIS and those who had an MS related death, as defined by 30 year outcome (medullary width 0–5:  $p=0.005$ ; third ventricular width, 0–10:  $p=0.043$ ).

The change in medullary width from 10 to 30 years was associated with the early medullary width change over the first five years ( $\beta=0.400$  (0.194)  $P=0.039$ ), but not WM lesions accrual over the first five years ( $\beta=0.045$  (0.313)  $P=0.886$ ). In contrast, third ventricular width change from 10 to 30 years, was not associated with early TVW change ( $\beta=0.055$  (0.150)  $P=0.715$ ), but was associated with early WM lesion accrual ( $\beta=0.698$ (0.288)  $P=0.015$ ).

The change from 0–5 in medullary width and white matter lesions were associated with an  $R^2$  of 0.413,  $p=0.000$  with the Expanded Disability Status Scale at 30 years, correcting for the total intracranial volume and gender.

**Diskussion:** Medullary atrophy measurements within 5 years of a CIS, and third ventricular width within 10 years, are related to clinical outcomes over the next 20 to 25 years.

**Fazit:** Our data suggests that the processes underlying brain atrophy, and ultimately less favourable clinical outcomes, are already active at, or soon after, the clinical onset of MS.

296

**ACQUIRED CEREBRAL ANGIOMATOSIS AND ITS DIFFERENTIAL DIAGNOSES. A CASE REPORT ON CEREBRAL MANIFESTATIONS IN A PATIENT WITH FOLIC ACID SHORTAGE.**

Lucas Ivo Emanuel Becker\*<sup>1</sup>, Peter Schramm<sup>1</sup>, Hannes Schwenke<sup>1</sup>

<sup>1</sup>Institut für Neuroradiologie, Universitätsklinikum Schleswig-Holstein, Campus Lübeck, Lübeck, Deutschland

**Hintergrund:** Acquired cerebral angiomas are unusual intracranial manifestations of different origins, most commonly caused by Celiac Disease in Western Europe. In Neuroimaging, acquired angiomas share many features with Sturge-Weber-Angiomas (SWA) and, as such, are prone to initial misdiagnosis. We present a 61-year old female patient with a history of Rheumatoid Arthritis and long-term Methotrexate therapy and insufficient folic acid supplementation with recurrent episodes of blurry vision and suspected intracranial tumor.

**Methoden:** Intracranial computer tomography (CT) was performed to exclude intracranial hemorrhage or bland intracranial malignancies. As CT rendered no clear diagnosis, we performed MRI and MR spectroscopy, diagnostic Digital Subtraction Angiography (dDSA) and surgical biopsy in close succession to clarify the diagnosis.

**Ergebnisse:** CT showed no intracranial hemorrhage, however a hypodense area with laminar calcifications in both occipital lobes were detected (a). Cerebral MRI showed T2w hypointense calcifications in bilateral occipital and right parietal lobes with adjacent leptomeningeal enhancement and cerebral edema (b). Perfusion imaging revealed relative Cerebral Blood Volume (rCBV) to be elevated by thrice the value of surrounding unscathed brain parenchyma (c). To confirm our hypothesized diagnosis, we advised MR spectroscopy, which revealed

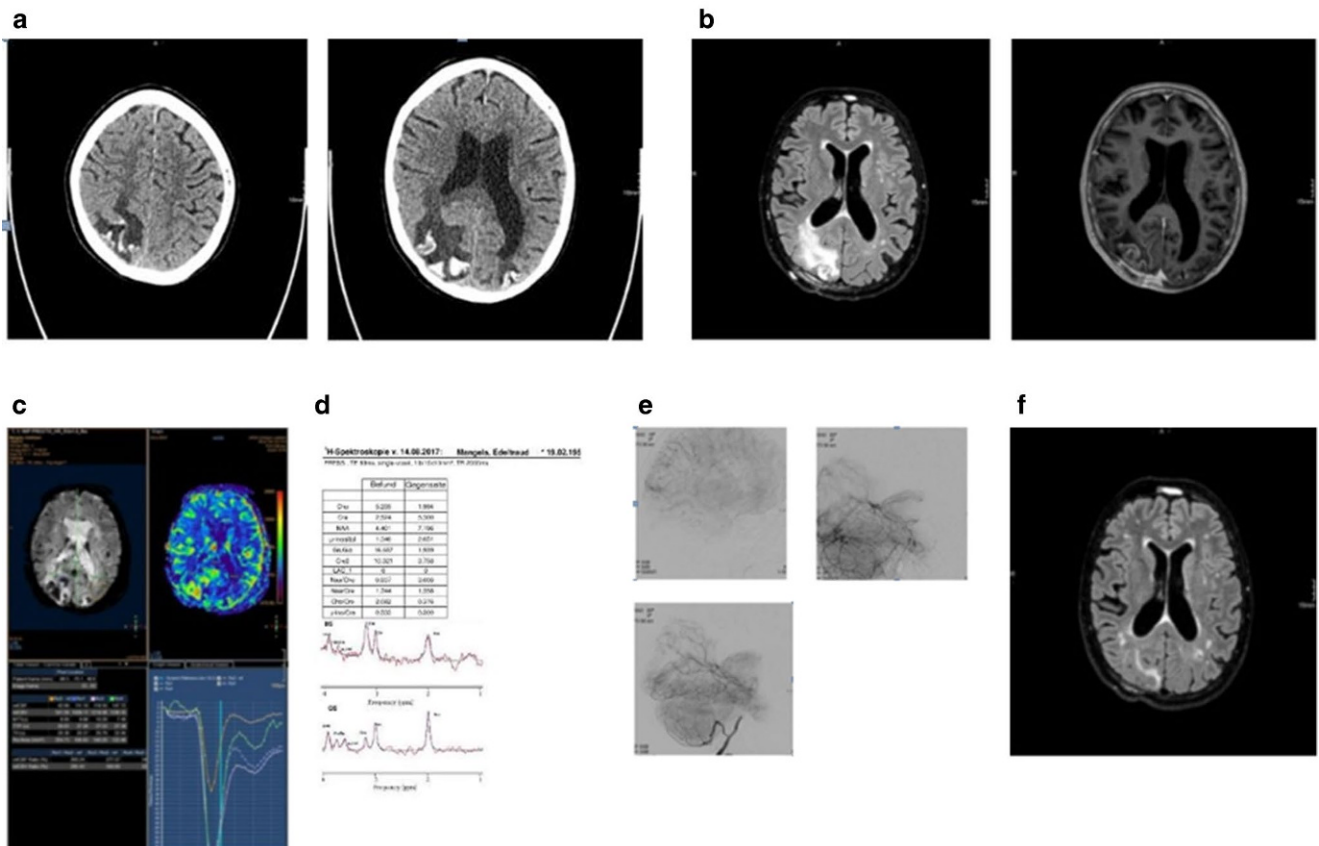


Fig. 1 | 296

an unusual intralesional choline peak (d). dDSA revealed bilateral occipital blush (e). A follow-up MRI after 3 months revealed a regressive cerebral edema and constant leptomeningeal enhancement under folic acid supplementation (f). No more neurological deficit was seen after folic acid levels were replenished.

**Fazit:** Other than in most publications, all possible imaging modalities (CT, MRI, MR Perfusion Imaging, MR Spectroscopy, dDSA) have been carried out in this case. MRI undoubtedly renders most information. Leptomeningeal calcifications with angiomas are rare and often expressions of SWA. Gobbi-Syndrome should be considered when a history of Celiac Disease or a history of Methotrexate therapy with insufficient folic acid supplementation is present.

#### Literatur

1. Wyllie E, Gupta A, Lachhwani DK. The treatment of epilepsy, principles & practice. Lippincott Williams & Wilkins. (2006) ISBN:0781749956.

### 303

#### EXPLORATION OF MYELINATION DIFFERENCES IN INDIVIDUAL MULTIPLE SCLEROSIS LESIONS WITH MYELIN WATER IMAGING

Hagen H. Kitzler<sup>1</sup>, Hannes Wahl<sup>1</sup>, Paul Kuntke<sup>1</sup>, Tjalf Ziemssen<sup>2</sup>, Jennifer Linn<sup>1</sup>, Caroline Koehler<sup>1</sup>

<sup>1</sup>Institut für Diagnostische und Interventionelle Neuroradiologie, Medizinische Fakultät Carl Gustav Carus, Technische Universität Dresden, Dresden, Deutschland

<sup>2</sup>Klinik und Poliklinik für Neurologie, Medizinische Fakultät Carl Gustav Carus, Technische Universität Dresden, Dresden, Deutschland

**Background:** Multiple sclerosis (MS) is an inflammatory disease of the central nervous system characterized by demyelinated lesions. Conventional magnetic resonance imaging (MRI) detects various pathological changes in the tissue but is non-specific for myelin. The in vivo MRI technique Multi-Component Driven Equilibrium Single Pulse Observation of T1 and T2 (mcDESPOT) [1], which allows the determination of relative myelination by measuring the myelin water fraction (MWF) [2], can enable the quantification of demyelination in lesions. The aim of this study was to assess the intra- and interindividual variability of MWF in lesions to analyze differences in focal myelin loss in an RRMS cohort.

**Methoden:** FLAIR images and mcDESPOT data were measured from  $n = 112$  relapsing remitting patients. A 1.5T MR scanner and an 8-channel head coil was used to obtain the multi-component T1 and T2 information from sets of Fast Low Angle SHot (FLASH) and True Fast Imaging with Steady State Precession (TrueFISP) sequences over a range of flip angles measured at constant TR [1]. The co-registration of the MR data was done with Statistical Parametric Mapping (SPM) [3]. The MWF maps were calculated according to the established method from the mcDESPOT sequences [1]. The lesions were segmented into binary masks. An algorithm was developed to automate the reading of the MWF of individual lesions for analysis of myelination differences. To compare two groups, the two-sided Wilcoxon rank sum test was used (significance level 5%).

**Results:** The median MWF in the white matter (WM) of healthy controls showed a significant difference ( $p = 0.0011$ ) to RRMS patients. 2787 WM FLAIR lesions were examined. The median MWF loss within the lesions varies from 6% to 70% for different patients compared to control white matter MWF levels. In a group comparison it could be shown that patients with a higher degree of disability of EDSS  $\geq 4$  significantly ( $p = 0.00026$ ) have lower MWF values than patients with EDSS  $\leq 2$ .

**Discussion:** Significant reduction and heterogeneity of MWF in NAWM and MS lesions has been identified, reflecting varying degrees of demyelination.

**Conclusion:** This technique may be helpful to differentiate patients with early onset of strong myelin loss from those with low myelin loss.

#### References

1. Deoni, et al. Gleaning multicomponent T1 and T2 information from steady-state imaging data. *Magn Reson Med*. 2008; 6:1372–87
2. Laule, et al. Magnetic resonance imaging of myelin. *Neurotherapeutics*. 2007;4(3):460–84.
3. <https://www.fil.ion.ucl.ac.uk/spm/software>

### 4. Neurodegeneration

157

#### EFFECT OF MRI ACQUISITION ACCELERATION VIA COMPRESSED SENSING AND PARALLEL IMAGING ON BRAIN VOLUMETRY

Michael Dieckmeyer\*<sup>1</sup>, Jörg Döpfert<sup>2</sup>, Pere Ferrera Bertran<sup>2</sup>, Andreas Lemke<sup>3</sup>, Claus Zimmer<sup>1</sup>, Dennis Hedderich<sup>1</sup>

<sup>1</sup>Abteilung für Diagnostische und Interventionelle Neuroradiologie, Klinikum rechts der Isar, Technische Universität München, München, Deutschland

<sup>2</sup>Mediaire GmbH, Berlin, Deutschland

**Background:** Quantitative MRI-based brain volumetry<sup>1</sup> is increasingly used in the clinical setting<sup>2</sup>, e.g. in the workup of neurodegenerative disorders. Also, new advancements in parallel imaging techniques, namely Compressed Sensing<sup>3,4</sup> (CS), have substantially shortened ac-

quisition times of brain MRI. In the present work, we investigate the effect of brain MRI data undersampling on brain volumetry.

**Methods:** Nine datasets were acquired (three repetitions of a 3D-T1-weighted brain scan with repositioning in between on each of three days within one week) in each of two healthy male subjects (age=27y & 31y). Each dataset was acquired at increasing CS factors of 4, 8, 12, 16, 20 and 32 (Fig. 2) representing a gradual increase of undersampling. For volumetric calculations the commercially available and CE-certified software-tool md.brain v1.1.1 (mediaire GmbH) was used. The software performs an atlas-based segmentation of different brain regions and then determines their volumes. The following brain volumes were analyzed: total gray matter (TGM), total white matter (TWM), combined total gray and white matter (TGWM), cortical gray matter (CGM), and cerebrospinal fluid (CSF). Mean (M) and coefficients of variation (CV) were calculated. All statistical analyses were performed using MATLAB.

**Results:** Except for TWM, brain volumetry measurements decrease with increasingly undersampled MRI data, resulting in significant ( $p < 0.05$ ) volume reductions for CS factors >8. The CV is relatively

**Fig. 1 | 157** Absolute (a, d) and relative (normalized to the mean volume at CS factor=4; b, e) mean volumes as well as CV (c, f) of the five analyzed brain regions

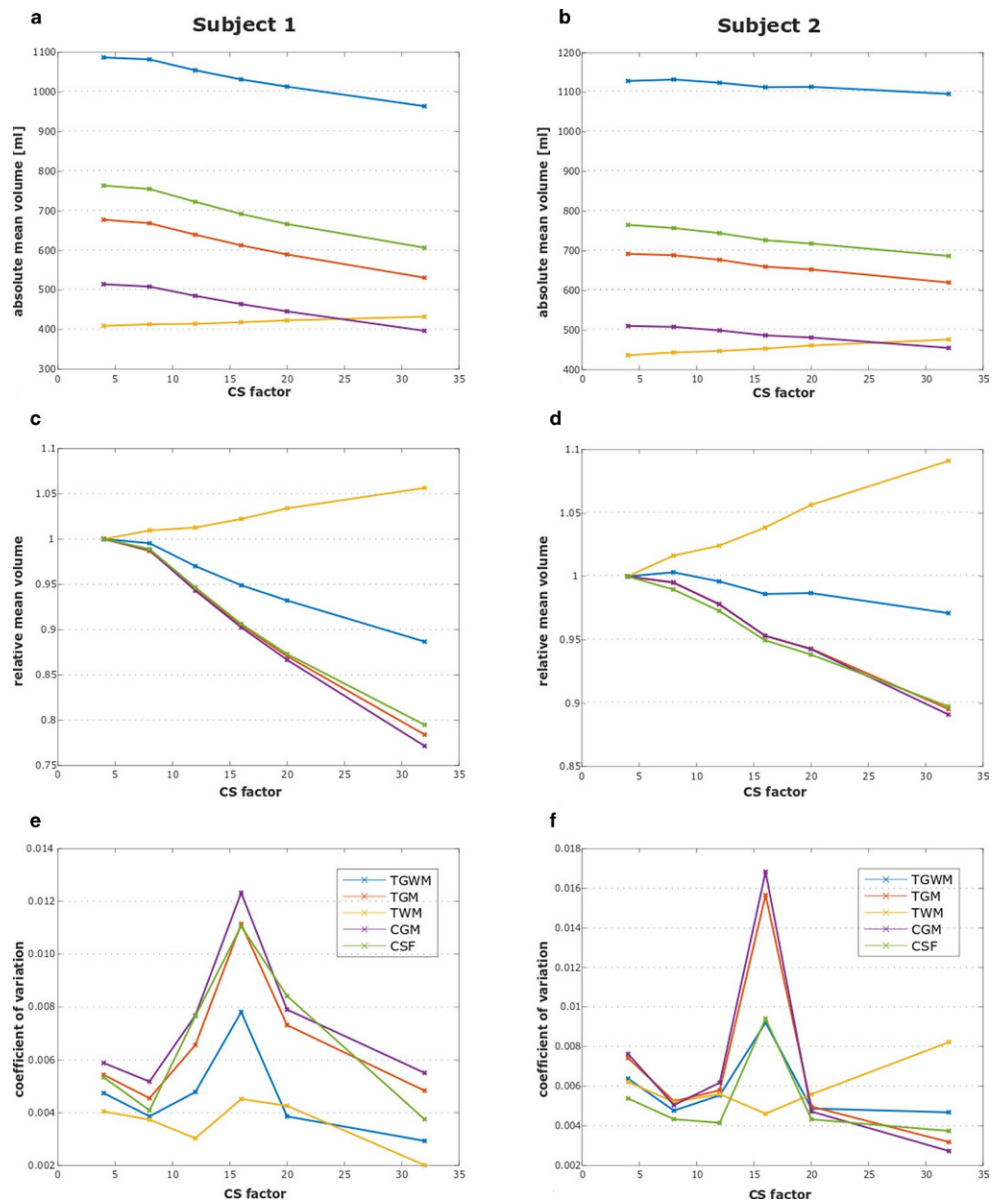
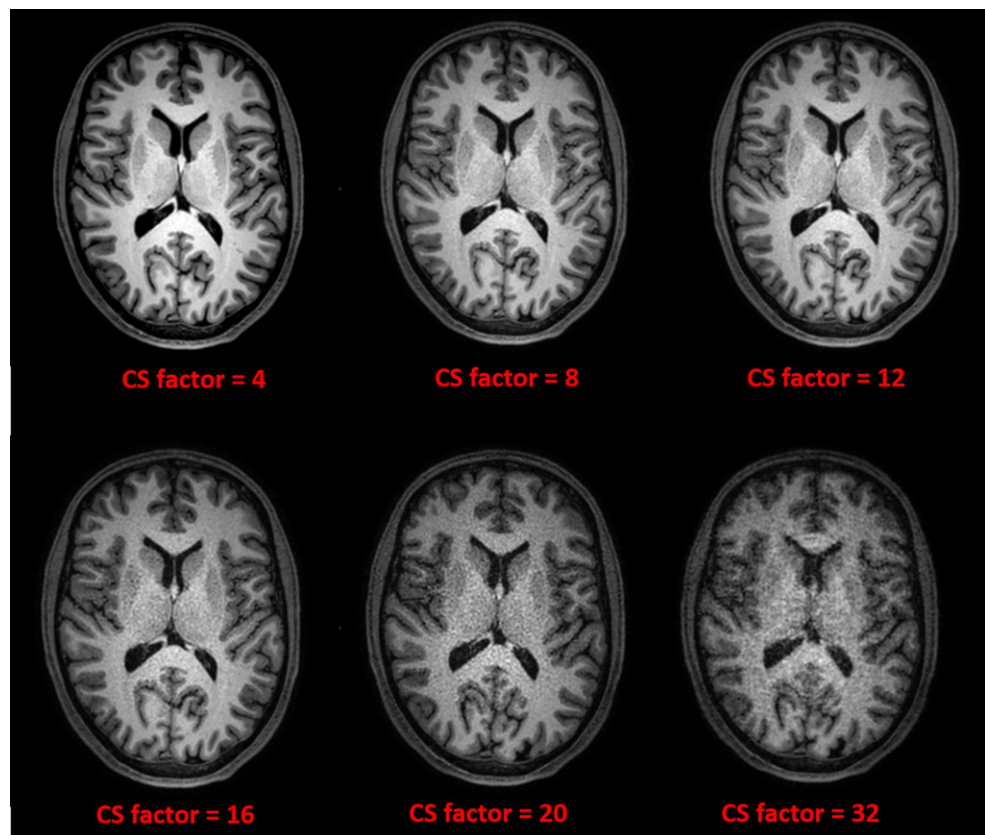


**Fig. 2 | 157** Sample axial reconstructions of the acquired 3D T1-weighted brain images at increasing CS factors of one of the subjects



low for CS factors 4, 8, 20 and 32 and thus suggests a high precision whereas for CS factors 12 and 16 the CV.

**Discussion/Conclusion:** We have shown that the deployment of parallel imaging for brain MRI has a systematic biasing effect on volumetric measurements of the brain that scales linearly with the degree of acceleration. Acceptable precision is reached for CS factors 4 and 8 which translates into acquisition times as low as 2 min 30sec for a whole brain volumetric dataset. Further research is needed to investigate the cause of the observed systematic bias and to analyze the effect on smaller brain subregions.

#### References

1. Ashburner J. . 2000;:
2. Giorgio A. . 2013;:
3. Donoho, D. (2006)
4. Candes, E. J. (2006)

171

#### DECREASE OF BRAIN REGIONAL CORTICAL THICKNESS IN AMYOTROPHIC LATERAL SCLEROSIS PATIENTS

Tong Fu\*<sup>1</sup>, Kobeleva Xenia<sup>2</sup>, Birte Schmitz<sup>1</sup>, Paul Bronzlik<sup>1</sup>, Patric Nösel<sup>1</sup>, Mete Dadak<sup>1</sup>, Heinrich Lanfermann<sup>1</sup>, Susanne Petri<sup>2</sup>, Xiao-Qi Ding<sup>1</sup>

<sup>1</sup>Institute of Diagnostic and Interventional Neuroradiology, Hannover Medical School, Hannover, Deutschland

<sup>2</sup>Clinics for Neurology, Hannover Medical School, Hannover, Deutschland

**Hintergrund:** Amyotrophic lateral sclerosis (ALS) is a fatal neurodegenerative disease with heterogeneous motor and non-motor defi-

cits. This cross-section study aimed to assess the brain regional cortical thickness (rCTh) change in ALS in vivo by using quantitative MRI analysis.

**Methoden:** 18 ALS patients (39–78 years, 58.22 ± 12.20 years, female: male = 4: 14) diagnosed according to EI Escorial criteria<sup>1</sup> and 19 healthy control (HC) (39–70 years, 53.63 ± 7.50 years, female: male = 7: 12) underwent MRI examination. Surface based morphology were performed with CAT12 toolbox implanted in SPM12 to obtain global cortical thickness (gCTh), estimated total intracranial volume (eTIV), gray matter volume (GMV), and white matter volume (WMV); as well as rCTh defined based on DK\_40 atlas<sup>2</sup>. The two-sided t-tests in general linear model were performed for the comparison between ALS patients and HC. The threshold-free cluster enhancement<sup>3</sup> was performed for multiple comparison correction (FDR,  $p < 0.05$ ).

**Ergebnisse:** In comparison to HC, significant lower GMV ( $p = 0.005$ ) in ALS patients was found, as well as significant decreases of rCTh overlaid 20 of 34 ROIs (FDR,  $p = 0.016–0.042$ ) in left hemisphere, and 15 of 34 ROIs (FDR,  $p = 0.016–0.046$ ) in right hemisphere. These ROIs located in frontal (13 ROIs), temporal (11 ROIs), parietal (8 ROIs), occipital (1 ROI) lobes and insula.

**Diskussion:** Thinning of regional cortical thickness with a frontal-temporal-parietal lobes distribution pattern seems to be major morphological alterations associated with ALS, which may be responsible to the motor and non-motor deficits in patients.

**Fazit:** The decreases of rCTh may be used to fully understand and monitor pathological progress of ALS.

#### Literatur

1. World Federation of Neurology Research Group on Neuromuscular Diseases E1.. E1 Escorial World Federation of Neurology Criteria for the Diagnosis of Amyotrophic Lateral Sclerosis. J Neurol Sci. 1994;124:96–107.

2. Desikan RS, Ségonne F, Fischl B, et al. An automated labeling system for subdividing the human cerebral cortex on MRI scans into gyral based regions of interest. *Neuroimage*. 2006;31:968–80.
3. Smith SM, Nichols TE. Threshold-free cluster enhancement: Addressing problems of smoothing, threshold dependence and localization in cluster inference. *Neuroimage*. 2009;44:83–98.

184

### RHEOLOGICALLY ESSENTIAL SURFACTANT PROTEINS OF THE CSF INTERACTING WITH PERIVENTRICULAR WHITE MATTER CHANGES IN HYDROCEPHALUS PATIENTS—IMPLICATIONS FOR CSF DYNAMICS AND THE GLYMPHATIC SYSTEM

Alexander Weiß<sup>\*1</sup>, Stefan Schob<sup>2</sup>, Matthias Krause<sup>3</sup>, Wolfgang Härtig<sup>4</sup>, Karl-Titus Hoffmann<sup>2</sup>, Ulf Quäschling<sup>2</sup>, Anika Stockert<sup>5</sup>, Cindy Richter<sup>2</sup>, Joana Puchta<sup>2,4</sup>, Pervinder Bhogal<sup>6</sup>, Alexander Emmer<sup>7</sup>, Cordula Scherlach<sup>2</sup>

<sup>1</sup>Klinik für Radiologie und Nuklearmedizin, Universitätsklinikum Magdeburg, Magdeburg, Deutschland

<sup>2</sup>Abteilung für Neuroradiologie, Universitätsklinikum Leipzig, Leipzig, Deutschland

<sup>3</sup>Klinik für Neurochirurgie, Universitätsklinikum Leipzig, Leipzig, Deutschland

<sup>4</sup>Paul-Flechsig-Institut für Hirnforschung, Universität Leipzig, Leipzig, Deutschland

<sup>5</sup>Klinik für Neurologie, Universitätsklinikum Leipzig, Leipzig, Deutschland

<sup>6</sup>Klinik für Interventionelle Neuroradiologie, Royal London Hospital, London, England

<sup>7</sup>Klinik für Neurologie, Universitätsklinikum Halle-Wittenberg, Halle (Saale), Deutschland

Surfactant proteins (SP) are multi-systemic proteins playing crucial roles in the regulation of rheological properties of physiological fluids, host defense, and the clearance of potentially harmful metabolites. Hydrocephalus patients suffer from disturbed cerebrospinal fluid (CSF) homeostasis and remarkably altered SP concentrations within it. A connection between CSF-SPs, CSF flow, and ventricular dilatation, a morphological hallmark of hydrocephalus, has been reported previously. Currently, there are no studies investigating the link between SPs and periventricular white matter changes caused by impaired CSF microcirculation in hydrocephalic conditions.

The present study included 47 individuals. CSF specimens were analyzed for concentrations of SP-A, SP-C, and SP-D by using ELISAs. Axial T2w TIRM MR imaging was employed in all cases. Using a MATLAB-based tool for quantification of MR signal intensities (SI) in the brain, parameters related to disturbed deep white matter CSF microcirculation were estimated (TIRM SI—mean, min, max, median, mode, std, percentiles p10th, p25th, p75th, p90th, and kurtosis, skewness, entropy of the SI distribution). Statistical analysis was performed to identify differences between hydrocephalic patients and healthy individuals and to investigate the connections between CSF-SP changes and deep white matter SI.

SP-A and SP-C differed between healthy controls and hydrocephalus patients in a significant manner. Corresponding quantification of white matter SI revealed differences between hydrocephalus patients and controls: SImean, SImax, SImedian, SImode, SIstd, all percentiles, skewness, and entropy. There were no differences for SP-D levels in both groups. In the acute hydrocephalic subgroup, SP-A showed a significant correlation with SImax, SIstd, SIp90, and inverse correlation with entropy. SP-C correlated inversely with entropy. For the chronic hydrocephalus subgroup, SP-A only correlated with kurtosis. SP-C correlated with SImean, SImax, SImedian, SImode, SIstd, SIp25, SIp75, and SIp90.

SP-A and SP-C are involved in different aspects of CSF physiology. SP-A appears to play an essential compensatory role in acute hydrocephalus. In contrary, SP-C and white matter changes are remarkably connected in CSF of chronic hydrocephalus patients. Considering the association between CSF flow phenomena, white matter changes, and SP-C profiles, the latter may especially contribute to the regulation of glymphatic physiology. SP-D apparently does not play a major role in CSF homeostasis.

204

### AUTOMATED AGE-SPECIFIC VOLUMETRIC ESTIMATION OF REGIONAL BRAIN ATROPHY: WORKFLOW AND FEASIBILITY

Julian Caspers<sup>\*1</sup>, Adrian Heeger<sup>1</sup>, Bernd Turowski<sup>1</sup>, Christian Rubbert<sup>1</sup>

<sup>1</sup>Düsseldorf, Universitätsklinikum Düsseldorf, Institut für Diagnostische und Interventionelle Radiologie, Düsseldorf, Deutschland

**Background:** Estimating regional brain volume relative to the patient's age norm from structural MRI is challenging and entails immense variations across readers. An automated framework for age-specific estimation of brain volume changes relative to a standard population is presented and evaluated.

**Methods:** The proposed workflow uses age- and sex-specific grey-matter (GM) templates derived from a large population-based cohort to estimate GM deviations in single subjects.

T1w MRIs of 693 healthy subjects aged between 16 and 77 years from the publicly available enhanced Nathan Kline Institute Rockland Sample were preprocessed in a standardized way comprising GM segmentation, normalization to MNI152 and 8 mm smoothing as implemented in CAT12 for SPM12. For each sex and age between 18 and 75, voxel-wise mean and standard deviation (SD) maps were generated across subjects aged two years under to two years over the respective age.

To estimate volume changes of a specific individual, his or her 3D T1w scan is preprocessed in the same way as for template generation. Then, voxel-wise z-values are generated from the resulting subject's normalized GM map and the respective mean and SD template for his or her age and sex. The z-map is transformed into subject space, color coded and fused with the structural MRI.

The workflow was evaluated on T1w brain images of 205 subjects (age-range 55–75y, mean age 70y 67% females; 80 Alzheimer's disease patients, 76 mild cognitively impaired patients, 49 healthy controls) from the Alzheimer's Dementia Neuroimaging Initiative (ADNI) by assessing the rate of technical success in atrophy map generation.

**Result:** Atrophy map generation with the proposed workflow was successful in all 205 ADNI subjects (100%). A parieto-temporal atrophy pattern was clearly visible in most AD patients. Processing time for each subject was less than 10 min on a state-of-the-art server.

**Discussion:** The atrophy maps have high potential to improve radiologic evaluation of brain MRI by semi-quantitative assessment of atrophy. The workflow will be made publicly available as open source with an integrated Picture Archiving and Communication System (PACS) interface.

**Conclusion:** Automated brain volume change estimation with the proposed workflow is feasible and technically reliable.

**Fig. 1 | 204** Processing pipeline for generation of atrophy maps illustrated for a 68 year old male from the Alzheimer's Disease Neuroimaging Initiative (ADNI). Standardized preprocessing (yellow box) comprises normalization to MNI152, grey matter segmentation and spatial smoothing. A Z-score map (red box) is generated from the preprocessed image and the template maps for the specific sex and age (green box), and then color-coded and fused with the original T1w image

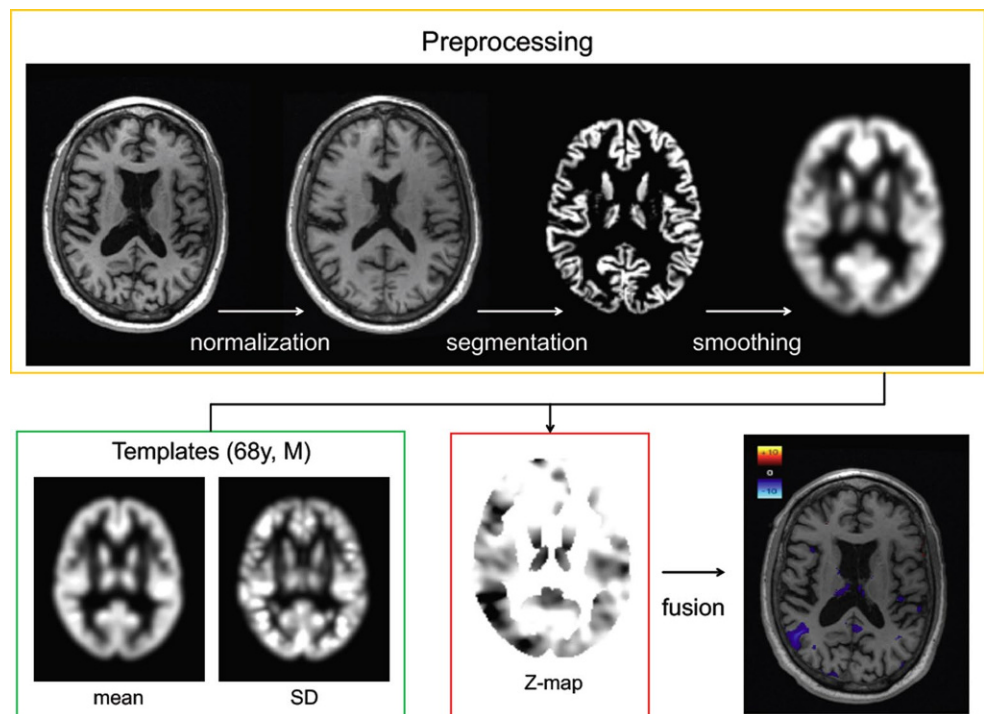
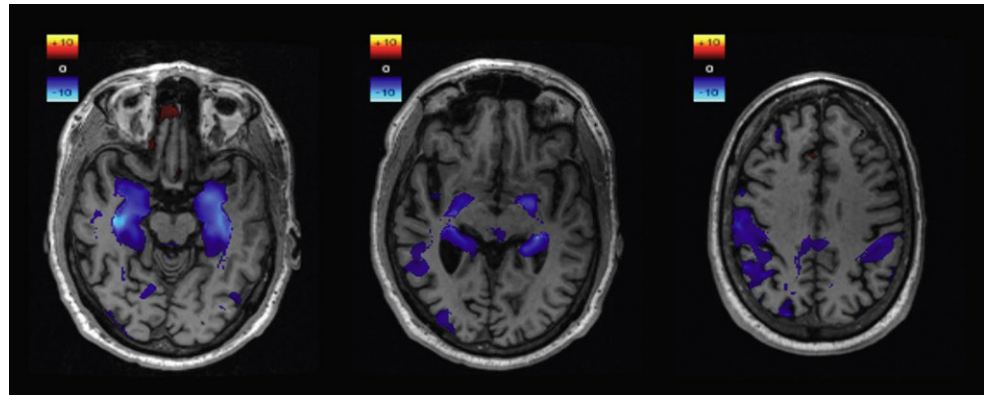


**Fig. 2 | 204** Atrophy map of 68 year old male from the Alzheimer's Disease Neuroimaging Initiative (ADNI) showing several parietal, medial temporal and hippocampal atrophy relative to his age-norm. Three representative axial slices are shown



211

### STATINS AND DIABETIC NEUROPATHY

Johann Jende<sup>1</sup>, Jan Gröner<sup>2</sup>, Christian Rother<sup>1</sup>, Stefan Kopf<sup>2</sup>, Zoltan Kender<sup>2</sup>, Peter Nawroth<sup>2</sup>, Sabine Heiland<sup>1</sup>, Arthur Hahn<sup>1</sup>, Fabian Preisner<sup>1</sup>, Tim Hilgenfeld<sup>1</sup>, Alexander Juerchott<sup>1</sup>, Martin Bendszus<sup>1</sup>, Felix Tobias Kurz<sup>\*1</sup>

<sup>1</sup>Universitätsklinikum Heidelberg, Abteilung Neuroradiologie, Heidelberg, Deutschland

<sup>2</sup>Universitätsklinikum Heidelberg, Innere Medizin I, Endokrinologie, Heidelberg, Deutschland

**Background:** Lowering serum cholesterol is an established treatment for dyslipidemia in type 2 diabetes (T2D). A recent study found that nerve lesions in T2D increase with low serum cholesterol levels, indicating that lowering serum cholesterol levels may contribute to diabetic neuropathy (DN) in T2D. (1) The objective of this study was to investigate whether there is a correlation between statin doses and peripheral nerve lesions in T2D patients with and without DN.

**Methods:** 100 participants (52 under statin treatment, 48 without statin treatment) underwent magnetic resonance neurography (MRN) of the right leg at 3 Tesla and clinical, serological, and electrophysiological assessment. Three-dimensional reconstruction of the sciatic nerve was performed to quantify the nerve's diameter and lipid equivalent lesion load (LEL) with a subsequent correlation-analysis of all acquired clinical and serological data.

**Result:** LEL correlated negatively with nerve conduction velocities and amplitudes of the tibial ( $r=-0.33;p=0.014$  and  $r=-0.31;p=0.020$ , respectively) and peroneal nerve ( $r=-0.51;p<0.001$  and  $r=-0.28;p=0.034$ , respectively). The statin dose, calculated as the equivalent of Simvastatin, correlated positively with the nerve's LEL ( $r=0.39;p=0.005$ ) and the nerve's mean cross-sectional area ( $r=0.40;p=0.005$ ). All correlations remained significant after multivariate analysis for patients' sex, age, disease duration, body-mass-index, HbA1c levels, triglycerides, Cystatin C and glomerular filtration rate.

**Discussion:** Our findings indicate that the intake of statins in T2D DN is associated with a higher amount of nerve lesions and nerve swelling.

These findings are relevant with regards to emerging therapies that promote an aggressive lowering of serum cholesterol in T2D.

**Conclusion:** Our results indicate that lowering cholesterol with statins is potentially harmful in diabetic neuropathy. Further longitudinal studies on the impact of lipid lowering therapies on the course of DN are required.

## References

- Jende JME, Groener JB, Rother C, Kender Z, Hahn A, Hilgenfeld T, et al. Association of Serum Cholesterol Levels With Peripheral Nerve Damage in Patients With Type 2 Diabetes. *JAMA*. 2019;2(5):e194798. <https://doi.org/10.1001/jamanetworkopen.2019.4798>.

256

## INTRA-NETWORK FUNCTIONAL CONNECTIVITY CHANGES OF THE FRONTO-PARIETAL NETWORK IN PARKINSON'S DISEASE

Nikolas Teichert<sup>\*1</sup>, Christian Rubbert<sup>1</sup>, Benjamin Sigl<sup>2</sup>, Christian Mathys<sup>3</sup>, Simon Eickhoff<sup>4,5</sup>, Felix Hoffstaedter<sup>4,5</sup>, Martin Südmeyer<sup>6</sup>, Christian Hartmann<sup>7,8</sup>, Bernd Turowski<sup>1</sup>, Alfons Schnitzler<sup>7,8</sup>, Julian Caspers<sup>1</sup>

<sup>1</sup>Department of Diagnostic and Interventional Radiology, University Dusseldorf, Medical Faculty, Düsseldorf, Deutschland

<sup>2</sup>Department of Biomedical Imaging and Image-guided Therapy, Medical University of Vienna, Wien, Österreich

<sup>3</sup>Institute of Radiology and Neuroradiology, Evangelisches Krankenhaus, University of Oldenburg, Oldenburg, Deutschland

<sup>4</sup>Institute of Neuroscience and Medicine (INM-7), Research Centre Juelich, Jülich, Deutschland

<sup>5</sup>Institute for Systems Neuroscience, Medical Faculty, Heinrich-Heine University, Düsseldorf, Deutschland

<sup>6</sup>Department of Neurology, Ernst-von-Bergmann Klinikum, Potsdam, Deutschland

<sup>7</sup>Institute of Clinical Neuroscience and Medical Psychology, Medical Faculty, Heinrich-Heine-University, Düsseldorf, Deutschland

<sup>8</sup>Department of Neurology, Center for Movement Disorders and Neuromodulation, Medical Faculty, Heinrich Heine University, Düsseldorf, Deutschland

**Background:** The frontoparietal network (FPN) is a major intrinsic brain network that is typically hemispherically lateralized. It is involved in cognitive action control as a mediator between the Dorsal Attention Network (DAN) and Default Mode Network (DMN). While neuroimaging studies have shown network alterations of the DMN and DAN in Parkinson's disease (PD), the role of the FPN in PD is still unclear. Hence, we investigated functional connectivity changes of the FPN in PD.

**Methods:** Resting-state functional magnetic resonance imaging (3T, EPI, TR=2.2s TE=30 ms, 3.1mm<sup>3</sup>, 11 min) was assessed in 38 PD patients and 43 healthy controls (HC, matched for age, gender, movement). Patients were scanned under dopaminergic medication (ON) and after >12 h withdrawal (OFF). The preprocessed fMRI time series were split into 20 intrinsic brain networks using independent component analysis. For both FPN, voxel-wise functional connectivity group differences were determined using a dual regression approach.

**Result:** There was increased connectivity with right FPN in ipsilateral sensorimotor, inferior parietal, parietal opercular, and extrastriate visual areas in PD OFF compared to HC. For left FPN, PD OFF showed increased connectivity in the ipsilateral postcentral gyrus, inferior parietal, intraparietal sulcus, extrastriate visual, and frontopolar regions. In PD ON vs. HC, there was decreased connectivity with right FPN in the contralateral pre- and postcentral gyri, supplementary motor area, inferior parietal and inferior frontal regions. For left FPN, PD ON showed increased connectivity with ipsilateral postcentral, inferior parietal, inferior frontal, parietal opercular, thalamic, frontopolar and ventral visual areas. At the same time, there was decreased connectivity in the contralateral primary sensorimotor cortex in PD ON vs HC.

**Conclusion:** Both FPNs show increased ipsilateral intra-network connectivity in PD, especially with sensorimotor and inferior parietal regions, while alterations of right FPN are more severe. As the FPN primarily facilitates motor control, increased FPN connectivity probably resembles a compensatory mechanism for motor deficits in PD by increased motor control. The connectivity decreases with contralateral sensorimotor areas in PD ON may hint to a dopamine-induced protective decoupling to shield the ipsilateral motor control system from disturbing interferences of the contralateral hemisphere.

**Fig. 1 | 256** Left and right frontoparietal networks

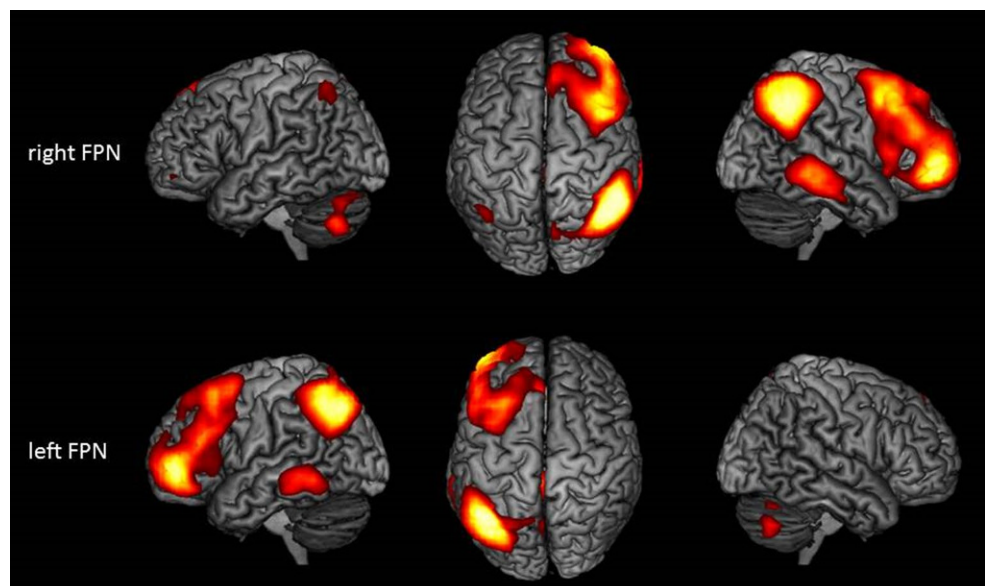
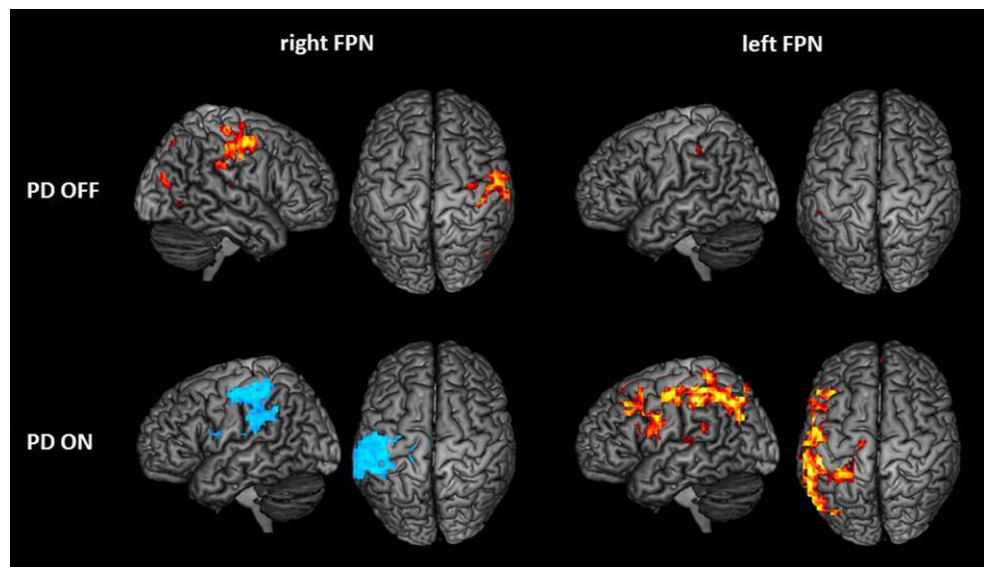


**Fig. 2 | 256** Functional connectivity increases (hot colors) and decreases (cool colors) of PD patients OFF and ON medication within right and left FPN



289

### IMPLICIT MOTOR LEARNING MODULATES FUNCTIONAL CONNECTIVITY OF DBS THERAPEUTIC TARGET FOR TREMOR.

Amr Farahat<sup>\*1,2</sup>, Hermann Hinrichs<sup>3,4,5,6</sup>, Hans-Jochen Heinze<sup>3,4,5</sup>, Catherine Sweeney-Reed<sup>1</sup>

<sup>1</sup>Universitätsklinikum Magdeburg, Neurokybernetik und Rehabilitation Arbeitsgruppe, Abteilung Neurologie, Magdeburg, Deutschland

<sup>2</sup>Universitätsklinikum Magdeburg, Neuroradiologie, Magdeburg, Deutschland

<sup>3</sup>Universitätsklinikum Magdeburg, Abteilung Neurologie, Magdeburg, Deutschland

<sup>4</sup>Leibniz-Institut für Neurobiologie, Abteilung Verhaltensneurologie, Magdeburg, Deutschland

<sup>5</sup>Deutsches Zentrum für Neurodegenerative Erkrankungen e. V. (DZNE), Magdeburg, Deutschland

<sup>6</sup>Forschungscampus STIMULATE, Magdeburg, Deutschland

**Hintergrund:** The ventral intermediate nucleus of the thalamus (VIM) is the therapeutic target of deep brain stimulation (DBS) for pharmacoresistant essential tremor (ET) and tremor-dominant Parkinson's disease (tPD). VIM-DBS effectiveness in tremor control is attributed to VIM involvement in the cerebello-thalamo-cortical circuit. Striato-cerebello-thalamo-cortical circuits are also thought to underlie motor learning. Even though the VIM involvement in these circuits are not proven, motor learning side-effects of VIM DBS were reported. Here we investigated whether the VIM is part of motor learning circuits by examining task-related VIM functional connectivity (FC) modulations in 30 right-handed healthy participants during 7T fMRI scanning. **Methoden:** A multiband GE-EPI sequence with parallel imaging was recorded during 4 runs of a serial reaction time task, which involves implicit motor learning. Each run comprised 6 alternating random (R) and learned (L) blocks to ensure implicit learning. Each L block comprised 4 repetitions of a 12-trial sequence.

**Ergebnisse:** Using the difference in the change in average reaction times (RTs) between R and L blocks across runs to indicate motor learning, we observed a significant reduction in the RTs between the first and the second, third, and fourth runs only during L blocks. A psychophysiological interactions (PPI) analysis of the fMRI data using the left VIM as a seed ROI was applied to examine change in VIM-FC from the first to fourth run. FC increased between the VIM and right

and left putamen, globus pallidus, amygdala and supplementary motor area (SMA), left precentral gyrus and superior and middle frontal gyri, suggesting VIM involvement in motor learning and a functional relationship between VIM and basal ganglia.

**Diskussion:** Structural connectivity has previously been identified between intraoperatively electrophysiologically-defined tremor-suppressive VIM-DBS sites and the pallidum. Moreover, resting state FC between VIM and the right putamen, SMAs and parietal lobe areas was also recently shown to correlate with ET severity. We provide evidence for VIM involvement also in implicit motor learning through the putamen and motor cortical areas, which are also involved in tremor generation.

**Fazit:** These findings could explain VIM-DBS motor learning side-effects and suggest a potential role for preoperative fMRI in DBS planning to avoid potential side-effects.

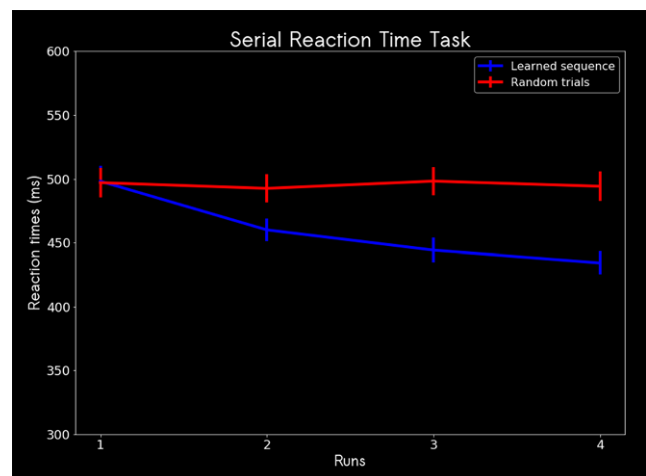


**Fig. 1 | 289**

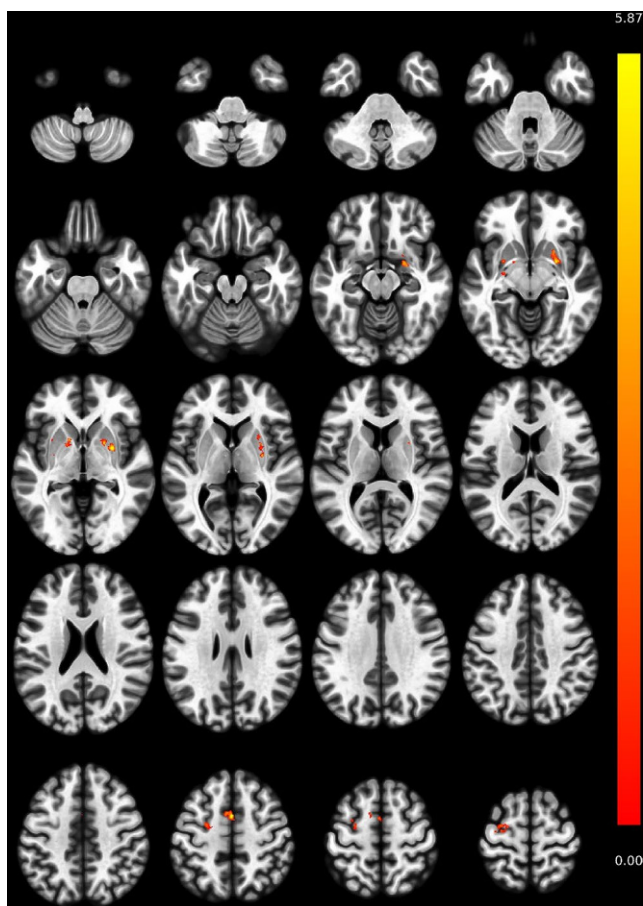


Fig. 2 | 289

310

**AMYOTROPHIC LATERAL SCLEROSIS SELECTIVE CORTICOSPINAL TRACT MYELIN IMAGING AND DIFFUSION MRI**

Hagen H. Kitzler\*<sup>1</sup>, Paul Kuntke<sup>1</sup>, Carolin Schwamborn<sup>1</sup>, Hannes Wahl<sup>1</sup>, René Günther<sup>2</sup>, Jennifer Linn<sup>1</sup>

<sup>1</sup>Institut und Poliklinik für Diagnostische und Interventionelle Neuroradiologie, Universitätsklinikum Carl Gustav Carus, Technische Universität Dresden, Dresden, Deutschland

<sup>2</sup>Institut und Poliklinik für Neurologie, Universitätsklinikum Carl Gustav Carus, Technische Universität Dresden, Dresden, Deutschland

**Background:** Selective neurodegeneration in Amyotrophic Lateral Sclerosis (ALS) affects the primary motor system. We aimed to understand the relationship between cortical degeneration and the disintegration of the related motor corticospinal tract (CST) by applying both Diffusion Tensor Imaging (DTI) and the *multi-component driven equilibrium single pulse observation of T1 and T2* (mcDESPOT).

**Methods:** ALS patients ( $n=27$ ) were recruited for the NiSALS (*Neuroimaging Society in Amyotrophic Lateral Sclerosis*) registry and underwent cerebral neuroimaging and quantitative MRI. Age/range matched healthy control subjects ( $n=21$ ) provided a comparative dataset.

Data was acquired on a SIEMENS Verio 3T scanner. DTI: EPI sequence, diffusion scheme with two b/values (0/100), 64 diffusion directions and a resolution of 2 mm<sup>3</sup>. Mean diffusivity (MD), axial (AD) and radial diffusivity (RD) and fractional anisotropy (FA) measures were calculated. mcDESPOT: isotropic 1.7 mm<sup>3</sup> whole-brain data; FLASH (TR= 5.9 ms, FA=[4, 5.3, 6.6, 8, 9.3, 12, 17.3, 24]°),

trueFISP (TR 5.6 ms; FA = [9.8, 13.1, 16.4, 19.7, 22.9, 29.5, 42.6, 59]°) and inversion prepared FLASH (TR 5.7 ms, FA = 5°, TI [450, 700] ms, PE 72). The relaxation measures T1 time and T2 time, myelin water fraction (MWF) and residence time (MRT) were retrieved.

The corticospinal tract (CST) was generated as region-of-interest (ROI) by tractographic reconstruction (DSIstudio) and diffusion measures were acquired. The multicomponent relaxation characteristics and myelin water measures were retrieved (Deoni et al.) including T1/T2 time, MWF and MRT of individual tracts.

**Results:** Higher MD ( $p<0.01$ ) and lower FA ( $p<0.01$ ) were found in ALS CST. Notably, RD revealed highly significant lower values in ALS CST ( $p=0.0013$ ). Whereas the CST MWF in ALS patients was non-significantly lower than in controls we found significantly higher values in CST MRT in ALS ( $p<0.01$ ).

**Discussion:** Motor system degeneration in ALS effects CST integrity reflected by changes MD, RD and FA. Whereas significant differences in MRT also reveals early alteration of myelin integrity, the relative myelin content measured by MWF was assumably not significantly different in ALS given the early observation at the time of disease diagnosis.

**Conclusion:** Secondary WM tract degeneration occurs early in disease. Besides the loss of structural integrity early alterations of the myelin characteristics indicate changes of its composition.

**References**

1. Verde, et al. Arch Ital Biol. 2017.
2. Deoni, et al. Magn Reson Med. 2008.
3. Kitzler, et al. Neuroimage. 2012.

358

**MIDSAGITTALE MITTELHIRNFLÄCHE UND MITTELHIRN/PONS-RATIO IM T1-GEWICHTETEN MRT ZUR DIFFERENZIERUNG ZWISCHEN TAUOPATHIEN (PSP) UND TDP-43 PROTEINOPATHIEN (ALS)**

Daniel Cantré\*<sup>1</sup>, Martin Dyrba<sup>2</sup>, Caroline Koch<sup>3</sup>, Johannes Prudlo<sup>3</sup>

<sup>1</sup>Institut für Diagnostische und Interventionelle Radiologie, Kinder- und Neuroradiologie, Universitätsmedizin Rostock, Rostock, Deutschland

<sup>2</sup>Deutsches Zentrum für Neurodegenerative Erkrankungen (DZNE) Rostock/Greifswald, Rostock, Deutschland

<sup>3</sup>Klinik und Poliklinik für Neurologie, Universitätsmedizin Rostock, Rostock, Deutschland

**Hintergrund:** Die PSP ist eine Tauopathie, die ALS eine TDP-43 Proteinopathie. Beide können mit einer frontotemporalen Demenz assoziiert sein. Bei Überlappungssyndromen mit prominentem oberem Motoneuronsyndrom kann die Vorhersage der zugrundeliegenden Histopathologie nach klinischen Kriterien schwierig bis unmöglich sein [1–2], ist jedoch die Voraussetzung für eine gezielte Therapie. Ziel dieser Untersuchung ist es zu prüfen, ob MRT-Kriterien in Form der midsagittalen Mittelhirnfläche (MHF) und der Mittelhirn/Pons-Ratio (MH/Pons-Ratio) geeignet sind, zwischen den histopathologischen Entitäten zu unterscheiden.

**Methoden:** Mit einem 3 Tesla Siemens MAGNETOM Verio Scanner wurden T1-gewichtete MPRAGE-Sequenzen mit 1 mm isotropen Voxeln von insgesamt 179 Probanden erfasst, darunter 71 ALS-Patienten, 36 PSP-Patienten und 72 gesunde Kontrollen (HC), jeweils gematcht nach Alter und Geschlecht. MHF und midsagittale Pons-Fläche wurden von zwei verblindeten Auswertern planimetrisch bestimmt und die MH/Pons-Ratio berechnet [3].

**Ergebnisse:** Die Messergebnisse wiesen eine starke Interrater-Reliabilität auf, der Pearson-Korrelationskoeffizient für die MHF betrug  $r=0,98$  und für die MH/Pons-Ratio  $r=0,96$ . Die mittlere MHF lag bei den ALS-Patienten bei  $136 \pm 21,4$  mm<sup>2</sup>, bei den HC bei  $139 \pm 20,2$  mm<sup>2</sup>

und bei den PSP-Patienten bei  $94.3 \pm 19.2 \text{ mm}^2$  (ALS vs. HC  $p=0.77$ ; ALS vs. PSP  $p<0.0001$ ). Die MH/Pons-Ratio betrug bei den ALS-Patienten  $0.246 \pm 0.039$ , bei den HC  $0.250 \pm 0.036$  und bei den PSP-Patienten  $0.185 \pm 0.034$  (ALS vs. HC  $p=0.67$ ; ALS vs. PSP  $p<0.0001$ ).

**Diskussion:** MHF und MH/Pons-Ratio der ALS-Patienten liegen signifikant oberhalb der Werte der PSP-Patienten und weisen keinen Unterschied gegenüber gesunden Kontrollen auf. Beide Parameter eignen sich daher zur Differenzierung von ALS und PSP.

**Fazit:** Die Messung der MHF ist ein geeigneter Surrogatmarker, um TPD 43-Proteinopathien (ALS) von Tauopathien (PSP) zu differenzieren. Als Einzel-Parameter ist sie in der klinischen Routine einfach zu bestimmen. Die MH/Pons-Ratio ist ebenfalls geeignet, aber aufwendiger zu bestimmen.

#### Literatur

1. McCluskey LF, et al. Amyotrophic lateral sclerosis-plus syndrome with TAR DNA-binding protein-43 pathology. Arch Neurol. 2009;66(1):121–4. Jan.
2. Nagao S, et al. Progressive supranuclear palsy presenting as primary lateral sclerosis but lacking parkinsonism, gaze palsy, aphasia, or dementia. J Neurol Sci. 2012;15;323(1–2):147–53. Dec.
3. al Möller L. Manual MRI morphometry in Parkinsonian syndromes. Mov Disord. 2017;32(5):778–82. May.

## 5. Wirbelsäule

96

### STATISTICAL PARAMETRIC MAPPING OF REGIONAL BONE DENSITY AT THE THORACOLUMBAR SPINE FOR OPPORTUNISTIC OSTEOPOROSIS SCREENING

Maximilian T. Löffler<sup>\*1</sup>, Alexander Valentinitzsch<sup>1</sup>, Alina Jacob<sup>1</sup>, Benita Schmitz-Koep<sup>1</sup>, Thomas Baum<sup>1</sup>, Claus Zimmer<sup>1</sup>, Yu-MI Ryang<sup>2,3</sup>, Jan Kirschke<sup>1</sup>

<sup>1</sup>Department of Diagnostic and Interventional Neuroradiology, School of Medicine, Klinikum rechts der Isar, Technical University of Munich, München, Deutschland

<sup>2</sup>Department of Neurosurgery, School of Medicine, Klinikum rechts der Isar, Technical University of Munich, München, Deutschland

<sup>3</sup>Department of Neurosurgery, Helios Klinikum Berlin-Buch, Berlin, Deutschland

**Background:** Osteoporosis is a major risk factor for procedure related complications in neurosurgical operations at the spine [1]. With statistical parametric mapping (SPM) regional bone loss at the thoracolumbar spine can be analyzed using routine CT data [2]. The aim of this study was to compare regional trabecular bone mineral density (BMD) between patients with normal, low, and osteoporotic bone mass as defined by dual energy X-ray absorptiometry (DXA).

**Methods:** In this retrospective study, 252 patients with lumbar DXA and a CT scan within 12 months were included. Clinical CT scans were performed for reasons other than densitometry on four different CT scanners each asynchronously calibrated to yield volumetric BMD. SPM of thoracolumbar vertebral bodies were calculated by registration, normalization and voxel-wise statistics (gender-adjusted ANOVA and t-test,  $p=0.05$  corrected for multiple testing). Patients with spinal metastasis and vertebrae with compression fractures or degenerative sclerosis were excluded from the analysis.

**Result:** According to DXA, 84 patients had osteoporosis, 91 had low bone mass, and 77 were healthy with normal bone mass. In healthy patients, mean BMD was lowest at L3 with  $129.0 \pm 54.3 \text{ mg/cm}^3$  and highest at T1 with  $208.7 \pm 54.8 \text{ mg/cm}^3$  (Fig. 1). Compared to healthy patients, statistically significant decreases in BMD were observed in

**Fig. 1 | 96** Characteristics of the reference group (normal bone mass: DXA T-score  $> -1$ ) and comparison groups (low bones mass:  $-2.5 < T \leq -1$  and osteoporosis:  $T \leq -2.5$ ) stratified by vertebral level with the number of included vertebrae ( $n$ ). BMD, volumetric bone mineral density;  $SD$  standard deviation, DXA dual energy X-ray absorptiometry

Vertebral level	Normal (reference)		Low bone mass		Osteoporosis	
	n	BMD, mean $\pm$ SD	n	BMD, mean $\pm$ SD	n	BMD, mean $\pm$ SD
<b>T1</b>	23	208.7 $\pm$ 54.8	26	176.3 $\pm$ 50.7	27	164.4 $\pm$ 48.9
<b>T2</b>	27	192.4 $\pm$ 42.4	31	154.8 $\pm$ 33.7	26	139.1 $\pm$ 34.8
<b>T3</b>	27	186.4 $\pm$ 41.5	32	150.1 $\pm$ 33.3	31	128.9 $\pm$ 33.6
<b>T4</b>	28	175.3 $\pm$ 40.3	34	143.5 $\pm$ 31.0	30	116.7 $\pm$ 29.4
<b>T5</b>	27	173.1 $\pm$ 36.6	32	138.3 $\pm$ 32.6	32	118.3 $\pm$ 31.9
<b>T6</b>	31	163.4 $\pm$ 37.6	31	136.0 $\pm$ 33.7	29	124.3 $\pm$ 40.2
<b>T7</b>	25	158.3 $\pm$ 37.0	29	138.4 $\pm$ 34.1	25	123.3 $\pm$ 38.2
<b>T8</b>	34	154.6 $\pm$ 41.8	36	128.0 $\pm$ 33.4	31	142.0 $\pm$ 53.3
<b>T9</b>	37	159.3 $\pm$ 45.5	40	131.1 $\pm$ 37.1	35	130.0 $\pm$ 48.7
<b>T10</b>	40	159.7 $\pm$ 44.6	48	129.9 $\pm$ 37.4	42	114.8 $\pm$ 42.7
<b>T11</b>	44	152.7 $\pm$ 44.7	51	119.3 $\pm$ 35.7	43	113.9 $\pm$ 44.2
<b>T12</b>	42	141.6 $\pm$ 39.5	56	112.7 $\pm$ 32.0	44	99.6 $\pm$ 41.9
<b>L1</b>	50	132.9 $\pm$ 45.7	57	109.3 $\pm$ 36.7	51	86.6 $\pm$ 33.9
<b>L2</b>	53	135.1 $\pm$ 52.6	57	106.8 $\pm$ 44.0	57	87.3 $\pm$ 40.1
<b>L3</b>	50	129.0 $\pm$ 54.3	62	135.0 $\pm$ 64.7	54	98.3 $\pm$ 54.3
<b>L4</b>	54	135.6 $\pm$ 61.3	58	149.5 $\pm$ 73.3	48	92.7 $\pm$ 45.5
<b>L5</b>	44	159.7 $\pm$ 68.3	60	136.8 $\pm$ 71.6	53	109.8 $\pm$ 58.2

osteoporotic patients at all vertebral levels with an emphasis on the upper thoracic (minimum at T4 with T-score=-3.2 and 91% affected volume) and on the thoracolumbar junction/upper lumbar spine (min-

Vertebral level	Low bone mass		Osteoporosis	
	T-score	ADR	T-score	ADR
T1	-2.3	0%	-3.1	21%
T2	-0.5	6%	-1.0	49%
T3	-2.3	11%	-3.2	80%
T4	-0.6	4%	-1.1	91%
T5	-2.1	29%	-3.0	85%
T6	-0.5	1%	-0.7	36%
T7	-0.7	0%	-1.1	11%
T8	-0.5	2%	-0.1	7%
T9	-0.5	5%	-0.4	13%
T10	-0.5	6%	-0.8	43%
T11	-0.6	30%	-0.7	38%

Fig. 2 | 96 Gender-adjusted T-score of patients with low bone mass and osteoporosis compared to the reference group and affected density regions (ADR), defined as proportion of significant voxel on P-maps with decreased bone mineral density

imum at L2 with T-score=-0.94 and 83% affected volume; Fig. 2, Fig. 3). Similar trends were observed for patients with low bone mass. **Discussion:** SPM revealed reduced trabecular BMD in osteoporotic patients pronounced at the upper thoracic spine and thoracolumbar junction. The mid-thoracic spine (T6–T10) with the least overall motion range due to ribcage stiffness seems to be less prone to osteoporosis-related deterioration of trabecular BMD.

**Conclusion:** SPM can quantify and visualize regional bone loss at the spine for opportunistic osteoporosis screening and may impact neurosurgical planning.

**References**

1. Zaidi Q, Danisa OA, Cheng W. Measurement Techniques and Utility of Hounsfield Unit Values for Assessment of Bone Quality Prior to Spinal Instrumentation: A Review of Current Literature. Spine. 2019;.
2. Valentinitich A, Trebeschi S, Alarcón E, et al. Regional analysis of age-related local bone loss in the spine of a healthy population using 3D voxel-based modeling. Bone. 2017;.

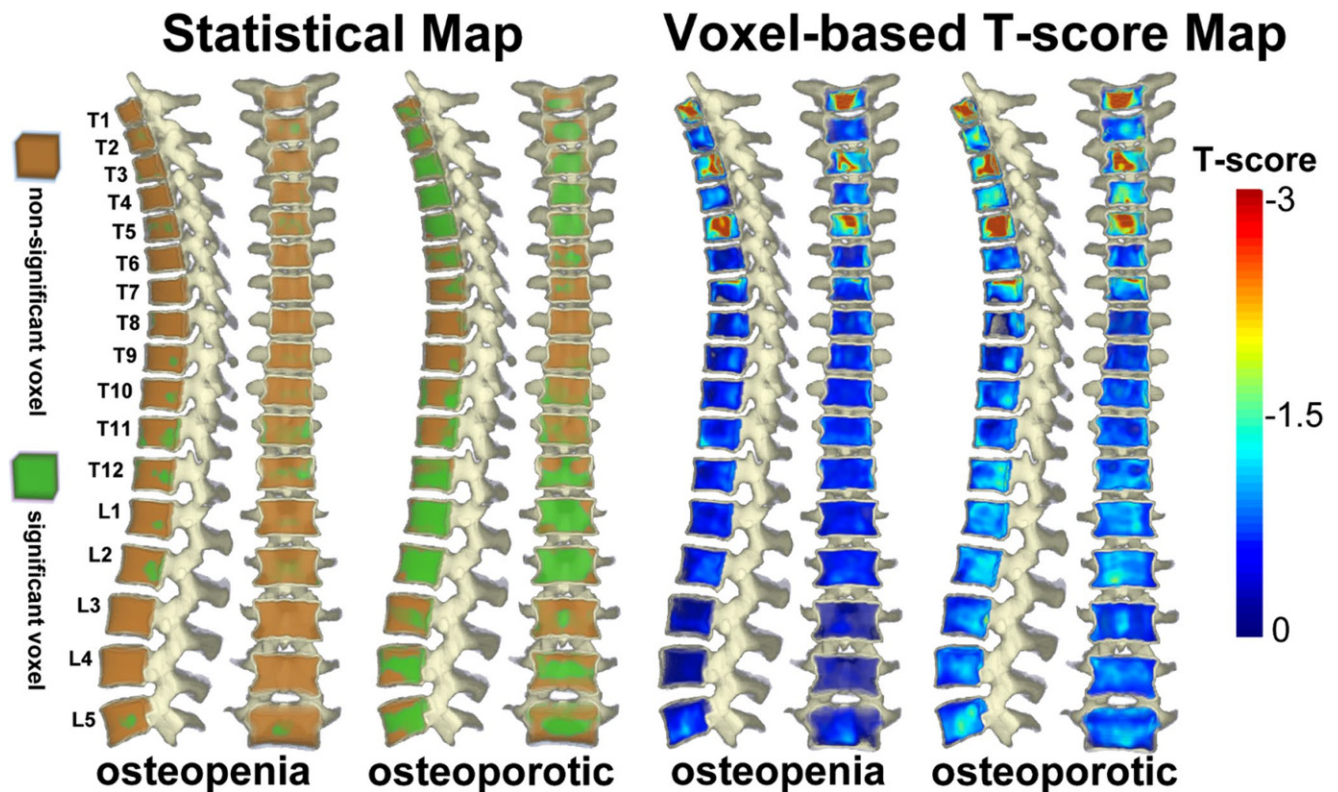


Fig. 3 | 96 Statistical parametric maps of volumetric trabecular BMD at the thoracolumbar spine calculated between patients with normal bone mass (reference group, not shown) and low bone mass (osteopenia) or osteoporosis. Diagnostic categories of osteoporosis ( $T \leq -2.5$ ) and low bone mass ( $-2.5 < T \leq -1$ ) are defined by DXA reference standard. Gender-adjusted ANOVA yielded P-maps illustrating in green color regions of statistically significant differences in BMD between the reference group and patients with low bone mass or osteoporosis ( $p = 0.05$  corr.). Corresponding T-maps visualize the magnitude of regional BMD loss between the reference group and patients with low bone mass or osteoporosis ( $p = 0.05$  corr.). BMD bone mineral density; ANOVA analysis of variance, DXA dual energy X-ray absorptiometry; corr. corrected for multiple comparisons per vertebra

111

### THE IMPACT OF SPARSE SAMPLING AND VIRTUAL TUBE CURRENT REDUCTION ON DETECTION OF VERTEBRAL FRACTURES

Nico Sollmann<sup>1</sup>, Kai Mei<sup>2</sup>, Dennis M. Hedderich<sup>1</sup>, Christian Maegerlein<sup>1</sup>, Felix K. Kopp<sup>2</sup>, Maximilian T. Löffler<sup>1</sup>, Ernst J. Rummeny<sup>2</sup>, Jan S. Kirschke<sup>1</sup>, Claus Zimmer<sup>1</sup>, Peter B. Noel<sup>2</sup>, Thomas Baum<sup>1</sup>

<sup>1</sup>Abteilung für Diagnostische und Interventionelle Neuroradiologie, Klinikum rechts der Isar, Technische Universität München, München, Deutschland

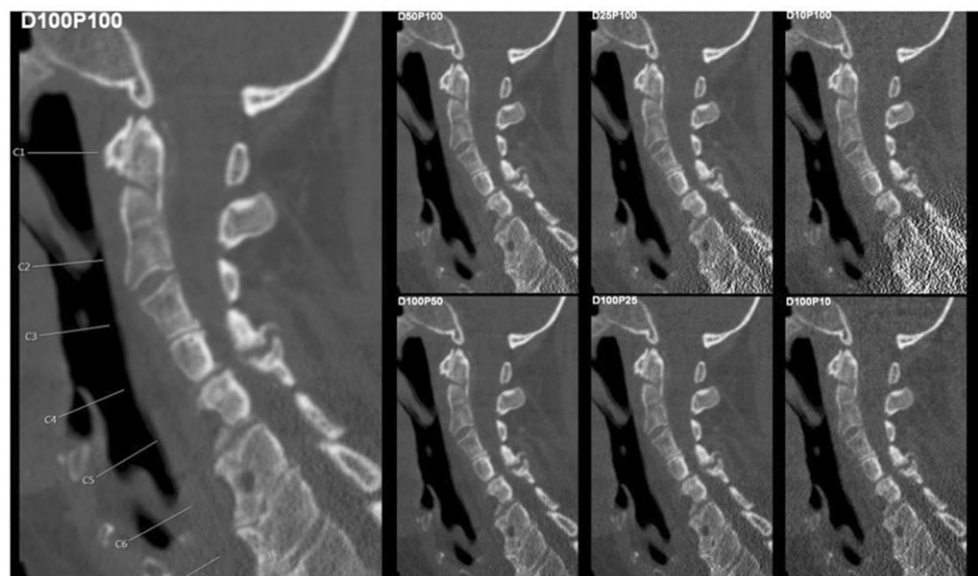
<sup>2</sup>Abteilung für Diagnostische und Interventionelle Radiologie, Klinikum rechts der Isar, Technische Universität München, München, Deutschland

**Hintergrund:** Multi-detector computed tomography (MDCT) is frequently used in clinical routine to identify vertebral fractures. However, the application of MDCT for vertebral fracture diagnostics comes at cost of considerable radiation exposure for the patients. The purpose of this study is to investigate the effects of sparse sampling and virtual tube current reduction on image quality and vertebral fracture diagnostics in MDCT.

**Methoden:** In routine MDCT scans of 35 patients (age:  $70.6 \pm 14.2$  years, 65.7% showing vertebral fractures), reduced radiation doses were retrospectively simulated by virtually lowering tube currents and applying sparse sampling, considering 50%, 25%, and 10% of the original tube current and projections, respectively. Two readers evaluated items of image quality and presence of vertebral fractures. Readout between the evaluations in the original images and those with virtually lowered tube currents or sparse sampling were compared.

**Ergebnisse:** A significant difference was revealed between the evaluations of image quality between MDCT with virtually lowered tube current and sparse-sampled MDCT ( $p < 0.001$ ). Sparse-sampled data with only 25% of original projections still showed good to very good overall image quality and contrast of vertebrae as well as minimal artifacts according to both readers. There were no missed fractures in sparse-sampled MDCT with 50% reduction of projections, and clinically acceptable determination of fracture age was possible in MDCT with 75% reduction of projections, in contrast to MDCT with 50% or 75% virtual tube current reduction, respectively.

**Fig. 1 | 111** Virtual tube current reduction and sparse sampling in multi-detector CT (MDCT) of the cervical spine. Sagittal slices derived from full-dose MDCT (D100 P100), MDCT with virtually lowered tube current (D50 P100, D25 P100, and D10 P100), and MDCT with sparse sampling (D100 P50, D100 P25, and D100 P10) in a patient with a cervical fracture (C2, dens fracture)



**Fazit:** Sparse-sampled MDCT provides adequate image quality and diagnostic accuracy for vertebral fracture detection with 50% of original projections in contrast to corresponding MDCT with lowered tube current. Sparse sampling is a promising technique for dose reductions in MDCT that could be introduced in future generations of commercially available MDCT scanners.

128

### CT-GESTÜTZTE LUMBALPUNKTION BEI PATIENTEN MIT SPINALER MUSKELATROPHIE

Omar Abu-Fares\*<sup>1</sup>, Paul Bronzlik<sup>1,2,3</sup>, Alma Osmanovic<sup>4</sup>, Olivia Schreiber-Katz<sup>4</sup>, Susanne Petri<sup>4</sup>, Heinrich Lanfermann<sup>1</sup>, Friedrich Götz<sup>1</sup>

<sup>1</sup>Medizinische Hochschule Hannover, Neuroradiologie, Hannover, Deutschland

<sup>2</sup>Hannover, Deutschland

<sup>3</sup>Medizinische Hochschule Hannover, Hannover, Deutschland

<sup>4</sup>Medizinische Hochschule Hannover, Neurologie, Hannover, Deutschland

**Hintergrund:** Bei spinaler Muskelatrophie (SMA) stellt die intrathekale Injektion von Nusinersen derzeit die einzige zugelassene Therapie dar. Wir haben bei unserem Kollektiv mit SMA die durchgeführten Lumbalpunktionen analysiert.

**Methoden:** Retrospektive Auswertung des prospektiv erfassten Patientenkollektiv von Erwachsenen mit SMA. Bei allen CT-geführten Punktionen wurden Scanparameter, CTDI und DLP, Scanlänge und Zahl der für die Punktion verwendeten Sequenzen erfasst.

**Ergebnisse:** Seit 11/17 wurden bei 27 Patienten (10 SMA Typ II, 16 SMA Typ III, 1 SMA Typ IV) im Alter von 18 bis 65 Jahren mit einer Erkrankungsdauer zwischen zwei und 61 Jahren regelmäßig Lumbalpunktionen zur Liquordiagnostik und intrathekalen Nusinersen-Therapie durchgeführt. Bei 15 Patienten war die Lumbalpunktion problemlos durch die Stationsärzte möglich. Bei 12 Patienten, 4 Frauen und 8 Männern, waren 11 Durchleuchtungs- und 53 CT-gestützte Punktion des lumbalen Wirbelkanals wegen ausgeprägten Wirbelsäulendeformitäten erforderlich. Gemäß Behandlungsschema wurden zwischen 2 und 7 bildgestützte Lumbalpunktionen, alle waren erfolgreich. Überwiegend war eine interlaminäre Punktion möglich; gelegentlich musste wegen der vom Patientenzustand vorgegebenen Lagerungsmöglichkei-

**Fig. 2 | 111** Virtual tube current reduction and sparse sampling in multi-detector CT (MDCT) of the thoracic and lumbar spine. Sagittal slices derived from full-dose MDCT (D100 P100), MDCT with virtually lowered tube current (D50 P100, D25 P100, and D10 P100), and MDCT with sparse sampling (D100 P50, D100 P25, and D100 P10) are shown in a patient with five thoracic fractures (T3, T6, T8, T10 and T11)



ten ein transforaminaler Zugang gewählt werden. Die Strahlenexposition resultiert aus dem Spiraldatensatz zur Wirbelsäulendarstellung und den erforderlichen Kontrollen während der Punktion. Die durchschnittlichen Werte betragen für CTDI 7,2 mGy, DLP 156 mGy-cm, Scanlänge 10,3 cm und Zahl der für die Punktion verwendeten Sequenzen 4. Komplikationen traten bei keiner der durchgeführten Punktionen auf. **Diskussion:** Wegen schweren krankheitsbedingten Wirbelsäulendeformitäten ist bei etwa der Hälfte der Erwachsenen mit SMA eine CT-gestützte Punktion des lumbalen Wirbelkanals erforderlich. Sowohl interlaminaire als auch transforaminale Zugänge können erfolgreich und komplikationslos durchgeführt werden.

**Fazit:** Bei Anwendung von low dose CT-Technik ist diese Maßnahme mit einer relativ geringen Strahlenexposition durchführbar

164

#### SYSTEMATIC EVALUATION OF LOW-DOSE IMAGING FOR CT-GUIDED PERIRADICULAR INFILTRATIONS

Simon Schön<sup>\*1</sup>, Kai Mei<sup>2</sup>, Isabelle Riederer<sup>1</sup>, Felix K. Kopp<sup>2</sup>, Claus Zimmer<sup>1</sup>, Jan Kirschke<sup>1,3</sup>, Peter Noel<sup>2,4</sup>, Thomas Baum<sup>1</sup>, Nico Sollmann<sup>3,5</sup>

<sup>1</sup>Department of Diagnostic and Interventional Neuroradiology, Klinikum rechts der Isar, Technische Universität München, Munich, Germany, München, Deutschland

<sup>2</sup>Department of Diagnostic and Interventional Radiology, Klinikum rechts der Isar, Technische Universität München, Munich, Germany, München, Deutschland

<sup>3</sup>TUM-Neuroimaging Center, Klinikum rechts der Isar, Technische Universität München, München, Deutschland

<sup>4</sup>Department of Radiology, Perelman School of Medicine, University of Pennsylvania, Philadelphia, United States

<sup>5</sup>Department of Diagnostic and Interventional Neuroradiology, Klinikum rechts der Isar, Technische Universität München, München, Deutschland

**Background:** Periradicular infiltrations are frequently performed in neuroradiological routine and are planned and guided by multi-detector computed tomography (MDCT). The objective of this study was to evaluate image quality and confidence for planning of periradicular infiltrations using virtually lowered tube currents and iterative reconstruction (IR).

**Methods:** Twenty patients (age: 54.9±13.1 years) underwent MDCT for planning purposes of periradicular infiltrations at the level of the lumbosacral spine using a standard imaging protocol provided by the MDCT vendor. Planning scans were simulated as if they were made at 50% (D50), 10% (D10), 5% (D5), and 1% (D1) of the original tube current. Image reconstruction was achieved with two levels of IR (A: similar to clinical reconstructions, B: ten times stronger regularization). Two readers (R1 and R2) performed qualitative image evaluation considering overall image quality and artifacts, image contrast, deter-

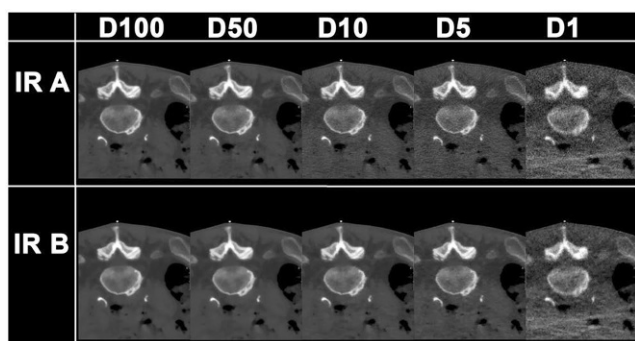


**Fig. 1 | 164** Virtual tube current reduction and sparse sampling in multi-detector CT (MDCT) performed for planning of periradicular infiltrations. Tube currents were lowered down to 50% (D50), 10% (D10), 5% (D5) and 1% (D1) compared to original imaging (D100). Two levels of iterative reconstruction (IR; A and B) were used

mination of nerve roots (scoring: 1—possible, 2—unclear, and 3—not possible), and confidence for intervention planning (scoring: 1—high, 2—medium, and 3—low confidence).

**Result:** Level A of IR was favorable regarding overall image quality, artifacts, and image contrast according to both readers, with preserved very good to excellent scores for D10. Similarly, level A of IR led to better scores for determination of nerve roots, with D10 still allowing for clear nerve root depiction in the majority of patients (D10 A: R1:  $1.4 \pm 0.5$  vs. R2:  $1.5 \pm 0.5$ ,  $p > 0.05$ ). The confidence for intervention planning remained high for tube currents virtually lowered down to 5% of the original dose (D5 A:  $1.4 \pm 0.5$  vs. R2:  $1.4 \pm 0.5$ ,  $p > 0.05$ ). Inter-reader agreement of confidence for intervention planning was good to excellent (weighted Cohen's kappa  $> 0.60$ ).

**Conclusion:** MDCT for planning purposes of lumbosacral periradicular infiltrations may be conducted with tube currents lowered down to 5% of standard imaging without restrictions in intervention planning confidence. Thus, radiation exposure could be decreased considerably.

199

#### PRÄOPERATIVE EMBOLISATION UND CHIRURGISCHE RESEKTION MIT SPONDYLODESE: THERAPIEREGIME FÜR AGGRESSIV WACHSENDE SPINALE HÄMANGIOME UND IHRE REZIDIVE

Christiane Pöckler-Schöniger<sup>\*1</sup>, Jörg Drumm<sup>2</sup>, Christoph Berthold<sup>2</sup>, Tobias Pitzen<sup>2</sup>, Michael Ruf<sup>2</sup>

<sup>1</sup>Diagnostische Radiologie/Neuroradiologie, SRH Klinikum Karlsbad-Langensteinbach, Karlsbad, Deutschland

<sup>2</sup>Zentrum für Wirbelsäulenchirurgie, Orthopädie und Traumatologie, SRH Klinikum Karlsbad-Langensteinbach, Karlsbad, Deutschland

**Hintergrund:** Spinale Hämangiome sind meist gutartige, vaskuläre Tumoren mit einem Anteil von 11 % der benignen Tumore der Wirbelsäule. In 0,9–1,2 % können sogenannte aggressive Hämangiome große Anteile des Wirbelkörpers aushöhlen und durch intraspinale Wachstum oder Frakturen Schmerzen und neurologische Defizite verursachen. Behandlungsoptionen sind transarterielle Embolisation, Radio, Vertebroplastie/Kyphoplastie auch in Kombination mit Radiatio und chirurgische Resektion mit Fixation. Allerdings sehen wir unter dieser Therapie eine relevante Anzahl von lokalen Rezidiven, ebenso primär lokal aggressiv wachsende Tumore mit Invasion des Spinalkanals und Kompression des Rückenmarks oder der Nervenwurzeln.

Wir präsentieren unsere Erfahrungen mit präoperativer Embolisation und chirurgischer Resektion der aggressiv wachsenden Hämangiome

**Methoden:** Die Daten stammen aus dem klinikeigenen Register eines großen deutschen Wirbelsäulenzentrums von 1/1997–10/2018. Ausgewertet wurden demografische Daten, klinische Symptomatik, Tumorklassifikation, vorausgegangene Therapien, endgültige Versorgung des Rezidivs bzw. primäre Tumorthherapie in unserer Klinik mit präoperativer Bildgebung und Tumorembolisation mittels Mikrospiralen und PVA-Partikeln.

**Ergebnisse:** 24 Patienten, Alter  $55 \pm 17$  Jahre, Follow up 1 Monat–19 Jahre, 14F und 10M. 75 % der Patienten gaben lokale Schmerzen an, 25 % zeigten neurologische Defizite. Hauptlokalisierung war die BWS (62 %), immer war der Wirbelkorpus betroffen mit epiduraler Tumorausdehnung. 33 % der Patienten waren vorbehandelt, 3 × Vertebroplastie, 5 × Dekompression und Spondylodese. Die endgültige Versorgung in unserer Klinik erfolgte mit präoperativer Embolisation in 19/24 Fällen, die chirurgische Therapie erfolgte überwiegend mit en bloc Resektion und Spondylodese (83 %). Bislang keine Rezidive im FU.

**Fazit:** Für aggressiv wachsende Hämangiome, die zu lokalen Schmerzen oder neurologischen Defiziten führen, ist unserer Erfahrung nach eine Dekompression mit Instrumentation bzw. Vertebroplastie nicht ausreichend. Sowohl bei Rezidiven als auch bei primär aggressivem intraspinalem Wachstum scheint die präoperative Embolisation mit radikaler Resektion und Spondylodese sinnvoll.

205

#### ASSOCIATION OF THIGH AND PARASPINAL MUSCLE COMPOSITION IN HEALTHY ADULTS USING CHEMICAL SHIFT ENCODING-BASED WATER-FAT MRI

Egon Burian<sup>\*1</sup>, Stephanie Inhuber<sup>2</sup>, Sarah Schlaeger<sup>3</sup>, Michael Dieckmeyer<sup>4</sup>, Elisabeth Klupp<sup>4</sup>, Daniela Franz<sup>3</sup>, Nico Sollmann<sup>4</sup>, Maximilian Löffler<sup>4</sup>, Ansgar Schwirtz<sup>2</sup>, Ernst Rummeny<sup>3</sup>, Claus Zimmer<sup>4</sup>, Jan Kirschke<sup>4</sup>, Dimitrios Karampinos<sup>3</sup>, Thomas Baum<sup>4</sup>

<sup>1</sup>Department of Diagnostic and Interventional Neuroradiology, Klinikum rechts der Isar, Technical University of Munich, München, Deutschland

<sup>2</sup>Department of Sport and Health Sciences, Technical University of Munich, München, Deutschland

<sup>3</sup>Department of Diagnostic and Interventional Radiology, Klinikum rechts der Isar, Technical University of Munich, München, Deutschland

<sup>4</sup>Department of Diagnostic and Interventional Neuroradiology, Klinikum rechts der Isar, Technical University of Munich, München, Deutschland

**Background:** Paraspinal and thigh muscles comprise the major muscle groups of the human body. Their function is essential for stability and mobility and is affected by various diseases including degenerative changes, metabolic disorders, sarcopenia and cachexia. We investigated the composition of the psoas, erector spinae, quadriceps femoris and hamstring muscle groups and their association to each other using chemical shift encoding-based water-fat magnetic resonance imaging (MRI) in young, healthy adults.

**Methods:** 25 healthy subjects (14 males, age:  $30.3 \pm 5.0$  years, body mass index [BMI]:  $27.6 \pm 3.0$  kg/m<sup>2</sup> and 11 females, age:  $30.2 \pm 7.0$  years, BMI:  $26.0 \pm 1.8$  kg/m<sup>2</sup>) were recruited for this study. Proton density fat fraction (PDFF) of the psoas, erector spinae, quadriceps femoris and hamstring muscle groups were determined (Fig. 1 and 2). For the quadriceps and the hamstring muscle group the intramuscular PDFF for each dedicated muscle was assessed separately (Fig. 2).

**Results:** After consideration of age and BMI as control variables, PDFF values of the erector spinae correlated significantly with those

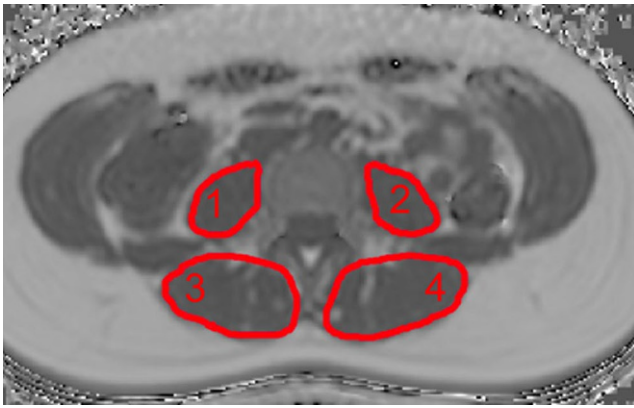


Fig. 1 | 205

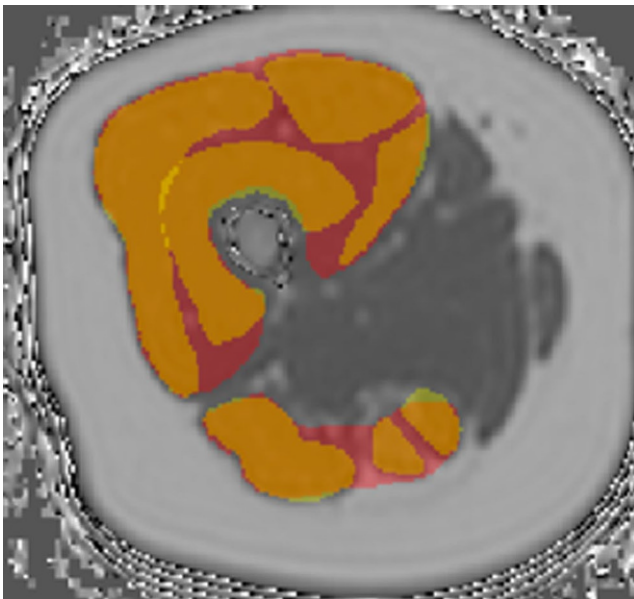


Fig. 2 | 205

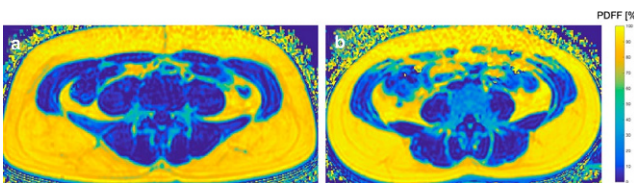


Fig. 3 | 205

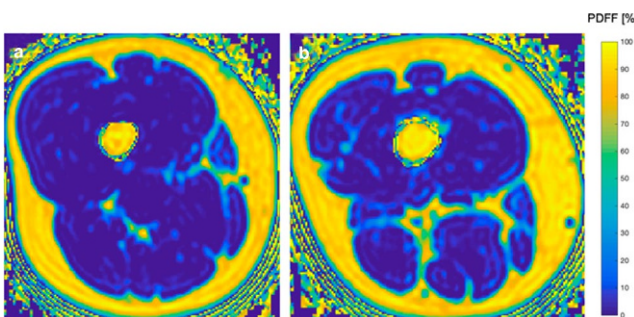


Fig. 4 | 205

of the entire quadriceps muscle ( $r=0.466$ ,  $p=0.044$ ) and the rectus femoris muscle ( $r=0.542$ ,  $p=0.017$ ) (Fig. 3 and 4). The PDFF of the psoas muscle was not significantly associated with any of the other muscle groups ( $p>0.05$ ).

**Discussion:** PDFF of the erector spinae, entire quadriceps and rectus femoris muscles were significantly associated with each other. In the light of expensive MRI scan time and time-consuming muscle segmentation, each of them may serve as an independent biomarker allowing for assessment of overall muscular fatty infiltration patterns and for quantification of the muscle tissue alterations due to muscular diseases.

**Conclusion:** The findings may indicate a high suitability of these muscle groups as target muscles to assess overall fatty infiltration patterns in musculature.

314

**MR-DERIVED CT-LIKE IMAGES IN COMPARISON TO CONVENTIONAL CT FOR THE ASSESSMENT OF VERTEBRAL FRACTURES AND OSSEOUS DEGENERATIVE CHANGES IN THE THORACOLUMBAR SPINE**

Benedikt J. Schwaiger<sup>\*1</sup>, Charlotte Schneider<sup>1</sup>, Sophia Kronthaler<sup>1</sup>, Christoph Böhm<sup>1</sup>, Christoph Zöllner<sup>1</sup>, Stefan Ruschke<sup>1</sup>, Julian Zapf<sup>2</sup>, Thomas Baum<sup>3</sup>, Jan S. Kirschke<sup>3</sup>, Ernst J. Rummeny<sup>1</sup>, Klaus Wörtler<sup>1</sup>, Dimitrios C. Karampinos<sup>1</sup>, Markus Wurm<sup>2</sup>, Alexandra S. Gersing<sup>1</sup>

<sup>1</sup>Institut für Radiologie, Klinikum rechts der Isar, München, Deutschland

<sup>2</sup>Klinik und Poliklinik für Unfallchirurgie, Klinikum rechts der Isar, München, Deutschland

<sup>3</sup>Abteilung für Neuroradiologie, Klinikum rechts der Isar, München, Deutschland

**Background:** CT-like datasets derived from a dedicated MR imaging sequence may add diagnostic value to the assessment of vertebral fractures and osseous degenerative changes in the thoracolumbar spine without an additional CT examination.

**Methods:** Morphologies of vertebral fractures ( $n=27$ ) as well as osseous degenerative changes in non-fractured levels ( $n=32$ ) were evaluated in 16 patients ( $65 \pm 17$  years, 11 females) examined with conventional CT and 3T MR imaging, including a high-resolution 3D T1w gradient-echo sequence. From MR data, intensity-inverted CT-like



Fig. 1 | 314 48-year-old male with an acute vertebral fracture of L2 with a condensation zone (arrow) and degenerative changes at L3/4 and L5/S1 (arrowheads), clearly depicted in sagittal reformations of both, MR-derived CT images (left) and conventional CT (right)

images were calculated. The evaluation was performed separately in MR-derived CT-like images and conventional CT independently by two radiologists, and agreement between the two modalities as well as inter- and intrareader reproducibility was assessed using weighted Cohen's  $\kappa$  (for ordinal data) and intraclass correlation coefficients (ICC; for ratio data).

**Results:** Quantitative measurements showed an almost perfect to perfect agreement among both modalities, with ICCs ranging between 0.90 [95% confidence interval, 0.72–0.96] for intervertebral foramen AP diameter and 0.99 [0.98–0.99] for vertebral body and disc height measurements. Analogously, ordinal scaled parameters such as Genant and AO fracture classifications (each,  $\kappa$  1.0) as well as the extent of osteophytes ( $\kappa$  1.0), diffuse sclerosis ( $\kappa$  0.76) and facet joint degeneration ( $\kappa$  0.95) showed a substantial to perfect agreement among modalities. Both, inter- and intrareader ICCs as well as  $\kappa$  were substantial to excellent (>0.90), respectively. Average acquisition time for the sequence was  $5.12 \pm 0.17$  minutes.

**Discussion:** MR-derived CT-like images showed a high agreement with conventional CT as well as a high inter- and intrareader reproducibility.

**Conclusion:** Results suggest that for the assessment of vertebral fractures and osseous degenerative changes, MR-derived CT-like images are on par with conventional CT. Including the sequence in MR imaging protocols could spare patients additional examinations and radiation doses.

### 330

#### A COMPLEX SPINAL ANATOMY IS NOT AN OBSTACLE FOR INTRATHECAL NUSINERSEN ADMINISTRATION IN ADULT SPINAL MUSCULAR ATROPHY PATIENTS

Christian Maegerlein\*<sup>1</sup>, Benjamin Friedrich<sup>1</sup>, Paul Lingor<sup>2</sup>, Bernhard Hemmer<sup>2</sup>, Claus Zimmer<sup>1</sup>, Marcus Deschauer<sup>2</sup>, Isabell Cordts<sup>2</sup>

<sup>1</sup>Klinikum rechts der Isar, TU München, Abteilung für Neuroradiologie, München, Deutschland

<sup>2</sup>Klinikum rechts der Isar, TU München, Klinik für Neurologie, München, Deutschland

**Background:** Intrathecal administration of nusinersen in adult spinal muscular atrophy (SMA) patients presents challenges due to severe scoliosis and preceding spinal surgery. In patients with a complex spinal situation, the expense and potential risks of the intrathecal application often lead to a delayed treatment initiation.

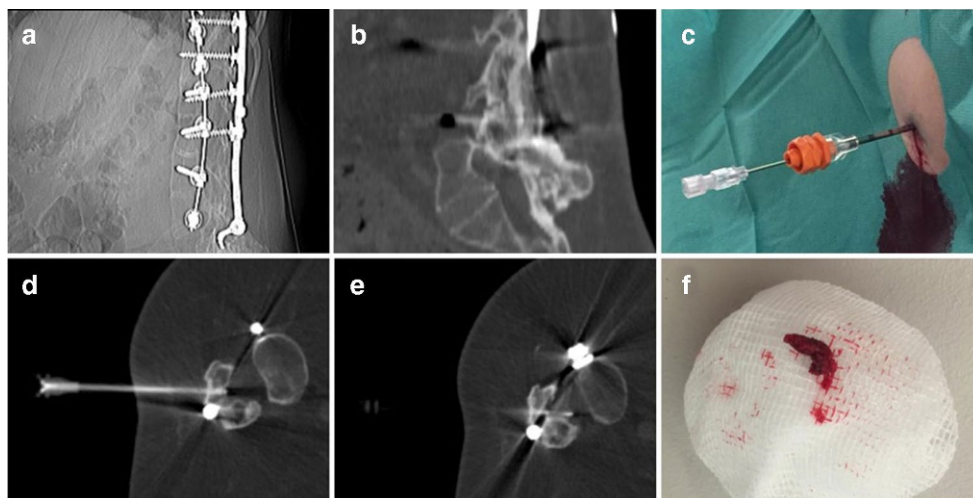
**Methods:** In this study, we analyzed 53 CT-guided lumbar punctures of 11 non-ambulatory SMA type 2 and 3 patients with known scoliosis.

**Result:** Drug administration was successful in 100% patients and no patient stopped the treatment. Complete osseous interlaminar fusion precluded conventional access in 8 lumbar punctures of 4 patients, necessitating alternative routes including transforaminal lumbar punctures and transpedicular drilling. Mean duration of lumbar punctures was 11 minutes and mean dose length product of radiation exposure was 112 mGy cm. No major complications occurred during the interventions.

**Discussion:** Our data suggest that nusinersen can be successfully, safely and rapidly administered in adult SMA patients with complex spinal conditions, transpedicular drill being a new, alternative approach.

**Conclusion:** We hereby illustrate intrathecal nusinersen treatment should not be limited to patients without severe spine deformities but emphasize the need for further studies investigating the drug's efficacy in adult SMA patients.

**Fig. 1 | 330** 45-year-old patient with SMA II and complete dorsal fusion of the body spine after dorsal stabilization (a, b). As access to the spinal canal a bone canal at level L3/4 (c–e) was drilled in the first session, through which a spinal needle could be inserted during the first as well as the subsequent interventions. (f) shows the bone cylinder removed during the first procedure



## 6. Zerebrovaskuläre Erkrankungen

39

### ENDOVASCULAR MECHANICAL THROMBECTOMY FOR CEREBRAL VENOUS SINUS THROMBOSIS: A SINGLE CENTER EXPERIENCE

Hanna Styczen\*<sup>1</sup>, Ioannis Tsogkas<sup>1</sup>, Jan Liman<sup>1</sup>, Volker Maus<sup>1</sup>, Marios-Nikos Psychogios<sup>1</sup>

<sup>1</sup>Göttingen, Universitätsmedizin Göttingen, Abteilung für Diagnostische und Interventionelle Neuroradiologie, Göttingen, Deutschland

**Background:** Cerebral venous thrombosis (CVT) is a rare entity with a potentially fatal outcome. Especially patients who do not respond to standard medical therapy alone may benefit from endovascular treatment options. We evaluate the angiographic and clinical results of mechanical thrombectomy (MT) in patients with severe CVT.

**Methods:** Endovascular procedures were performed in 13 patients with CVT additionally to standard anticoagulation therapy between 2011 and 2018. Clinical and radiological parameters, procedure details, angiographic and clinical outcomes were reviewed retrospectively.



Fig. 1 | 39

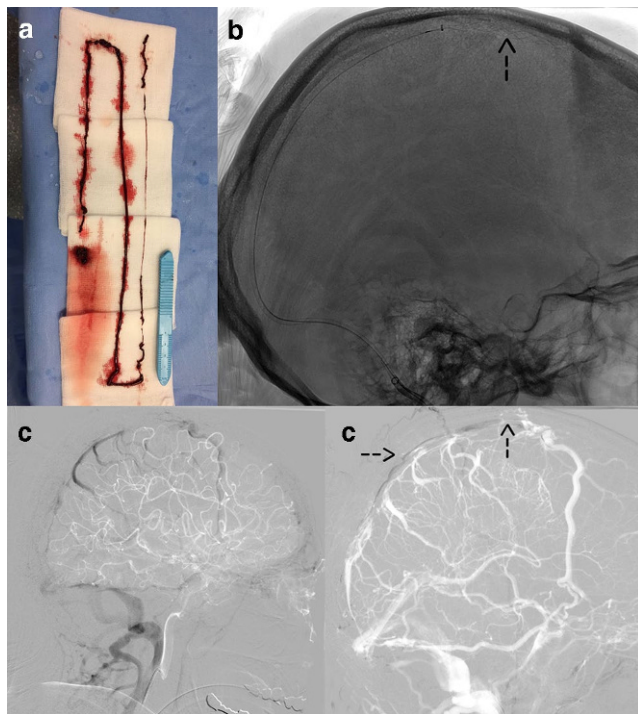


Fig. 2 | 39

**Result:** In total, 14 thrombectomy procedures were executed. Successful recanalization of the occluded sinus was achieved in 86% of cases (12/14); of those, 29% were recanalized completely. Procedural complications included perforation of the transverse sinus in one case (7%). Worsening of intracranial hemorrhage occurred in 14% (2/14) of cases. Favorable clinical outcome (modified Rankin Scale 0–2) was achieved in 12/13 patients (92%).

**Discussion:** The recanalization rate at final angiogram was slightly lower with 86% than described in recent systemic reviews [1,2]. In correlation to our results, recent studies reported mortality rates in patients undergoing MT due to severe CVT between 4–14% (8% in our study) with excellent (mRS 0–1) and favorable (mRS 0–2) outcomes of 72% and 84%, respectively [1,2,3]. This is comparable to our results with 77% excellent and 92% favorable outcome despite of lower rate of complete recanalization.

**Conclusion:** Transvenous MT is feasible, safe and effective leading to high degree of successful recanalization rate of occluded dural sinus. It may be a salvage treatment for selected patients with severe CVT refractory to standard medical treatment.

### References

1. Ilyas A, Chen CJ, Raper DM, et al. Endovascular mechanical thrombectomy for cerebral venous sinus thrombosis: a systematic review. *J Neurointerv Surg.* 2017;9:1086–92. <https://doi.org/10.1136/neurintsurg-2016-012938>.
2. Siddiqui FM, Dandapat S, Banerjee C, et al. Mechanical thrombectomy in cerebral venous thrombosis: systematic review of 185 cases. *Stroke.* 2015;46(5):1263–8. <https://doi.org/10.1161/STROKEAHA.114.007465>.
3. Konakondla S, Schirmer CM, Li F, et al. New Developments in the Pathophysiology, Workup, and Diagnosis of Dural Venous Sinus Thrombosis (DVST) and a Systematic Review of Endovascular Treatments. *Aging Dis.* 2017;8:136–48. <https://doi.org/10.14336/AD.2016.0915>.

42

### PREDICTORS OF PERIPHERAL EMBOLI AFTER MECHANICAL THROMBECTOMY: A PROSPECTIVE STUDY USING HIGH RESOLUTION DWI

Michael Schönfeld\*<sup>1</sup>, Reza Kabiri<sup>1</sup>, Helge Kniep<sup>1</sup>, Gabriel Brooks<sup>1</sup>, Marielle Sophie Ernst<sup>1</sup>, Lukas Meyer<sup>1</sup>, Jens Fiehler<sup>1</sup>, Uta Hanning<sup>1</sup>

<sup>1</sup>Klinik und Poliklinik für Neuroradiologische Diagnostik und Intervention, Universitätsklinikum Hamburg-Eppendorf, Hamburg, Deutschland

**Background:** To analyze the factors influencing the incidence of peripheral emboli after mechanical thrombectomy (MT) of intracranial large vessel occlusions (LVO).

**Methods:** We performed a prospective analysis of patients successfully treated with MT for an LVO of the anterior circulation that received a 1.5T MRI with diffusion-weighted imaging (DWI) in high resolution on the day following the intervention. Recanalization success was assessed on post-thrombectomy digital subtraction angiography (DSA) using the extended thrombolysis in cerebral infarction (eTICI) scale. Punctuate DWI lesions distant to the DWI core lesion were classified as peripheral emboli. Thrombus properties (location, length, density, density ratio) were measured on pre-interventional CT imaging. Procedural details of medical management (iv alteplase treatment) and mechanical thrombectomy (primary aspiration or stent retrieval with or without balloon occlusion, number of passes) were collected. The influence of thrombus properties and procedural details on the number of peripheral emboli was analyzed using univariate and multivariate linear regression models.

**Result:** 37 patients undergoing successful MT met the inclusion criteria. In 35/37 (94.6%) patients a total of 411 peripheral emboli were seen on DWI. The number of emboli correlated with eTICI score (Spearman's rho 0.605;  $p < 0.001$ ). Use of a balloon guide catheter was associated with a reduced number of peripheral emboli with a median number of peripheral DWI lesions of 5 (IQR 1.25–8.25) with and 12 (IQR 4–19) without the use of a balloon-guide catheter. Use of a balloon-guide catheter and recanalization success were the only factors that independently contributed to the number and volume of peripheral emboli (odds ratio –0.355 95% CI –15.746—0.798;  $p = 0.031$ ).

**Conclusion:** Together with a more complete recanalization the use of a balloon-guide catheter may reduce peripheral emboli leading to peripheral ischemias after mechanical thrombectomy. Proximal flow-arrest with a balloon guided catheter therefore should be the standard of practice whenever possible.

Intravenous alteplase treatment pre-MT does not appear to influence the number of peripheral ischemias later seen on DWI

### 53

#### UNTERSUCHUNG DES FMRT-BOLD-SIGNALVERLAUFS WÄHREND KURZER ATEMPAUSEN ZUR BEURTEILUNG DER ZEREBROVASKULÄREN REAKTIVITÄT

Leonie Zerweck<sup>\*1</sup>, Till-Karsten Hauser<sup>2</sup>, Constantin Roder<sup>3</sup>, Uwe Klose<sup>2</sup>

<sup>1</sup>Universitätsklinikum Tübingen, Radiologische Klinik, Abteilung für Diagnostische und Interventionelle Neuroradiologie, Tübingen, Deutschland

<sup>2</sup>Universitätsklinikum Tübingen, Radiologische Klinik, Abteilung für Diagnostische und Interventionelle Neuroradiologie, Tübingen, Deutschland

<sup>3</sup>Universitätsklinikum Tübingen, Klinik für Neurochirurgie, Tübingen, Deutschland

**Hintergrund:** CO<sub>2</sub>-stimulierte fMRT-Messungen können zur Beurteilung der zerebrovaskulären Reaktivität (CVR) von Moyamoya-Patienten, bei denen die CVR gegenüber Hyperkapnie vermindert ist, dienen [1,2]. Im gesunden Gewebe führt durch Atempausen hervorgerufene Hyperkapnie zu gesteigertem zerebralen Blutfluss und BOLD (Blood-Oxygen-Level-Dependent)-Signalanstieg [3]. Ziel dieser Arbeit war die Ermittlung der notwendigen Dauer der Atempausen für replizierbare Signalanstiege.

**Methoden:** Bei 14 gesunden Probanden wurden prospektiv fMRT-Messungen (3T) während abwechselnd endexpiratorischer Atempausen jeweils unterschiedlicher Dauer (3s, 6s, 9s, 12s) und Phasen normaler Atmung durchgeführt.

Um die Befolgung der Atempausen zu überprüfen, wurden die Atmungsbewegungen der Probanden aufgezeichnet.

Der im Kortex gemessene Signalverlauf wurde über alle Probanden gemittelt (Abb. 1).

Das Integral des Signalverlaufs über ein Zeitfenster von 12s während des maximalen Signalanstiegs wurde über alle Probanden gemittelt und nach Normalisierung räumlich dargestellt (Abb. 2).

**Ergebnisse:** Atempausen von 12s, 9s und 6s führten zu Signalanstiegen von 0,9 %, 0,8 % und 0,3 % (Abb. 1). Nach Atempausen von 3s waren keine vergleichbaren Signalanstiege messbar.

Zusätzlich zu den erwarteten Signalanstiegen waren initial kleinere Signalanstiege zu beobachten. Diese zeigten sich besonders, wenn die Probanden vor den endexpiratorischen Atempausen auffällig tief einatmeten.

**Diskussion:** Für replizierbare Signalanstiege wurden Atempausen von mindestens 9s benötigt. Eine weitere Verlängerung der Atempausen führte nur zu geringfügigem Signalzuwachs.

Den initialen Signalanstieg erklären wir durch tiefe Inhalation vor der Atempause.

Die wie erwartet [3] höhere Aktivierung in der grauen Substanz deutet auf die Differenzierungsfähigkeit des Verfahrens von Hirnregionen unterschiedlicher CVR hin.

**Fazit:** In der klinischen Routine eignen sich endexpiratorische Atempausen von 9s, da diese im gesunden Gewebe zu deutlichen BOLD-Signalanstiegen führen und leicht durchzuführen sind.

#### Literatur

1. Neuroimage Clin. 2019;22:101713.
2. AJNR Am J Neuroradiol. 2010;31(5):862–7.
3. Stroke. 1998;29(12):2641–5.

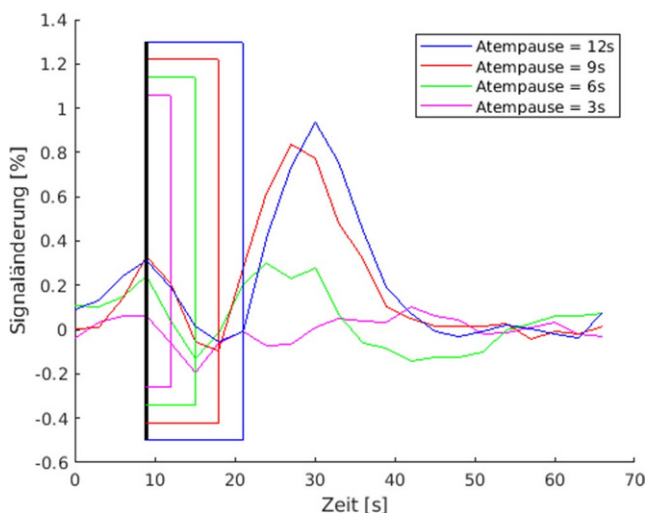


**Fig. 1 | 53** Relative Signaländerungen nach Atempausen unterschiedlicher Dauer. Die farbigen Rechtecke stellen die entsprechenden Atempausen dar. Es zeigten sich höhere BOLD-Signalanstiege in der grauen als in der weißen Substanz (Abb

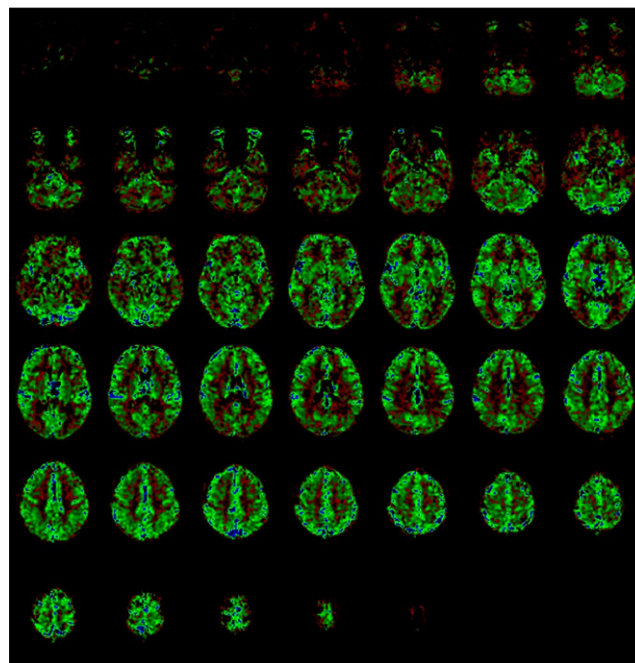


**Fig. 2 | 53** Farbcodiertes Aktivierungsmuster (blau > grün > rot > schwarz)

63

### HIGH RESOLUTION VESSEL WALL IMAGING INVOLVING 3T COMPRESSED SENSING (CS) TIME-OF-FLIGHT MRA IN A CASE OF ACUTE INTRACRANIAL ANTERIOR CIRCULATION DISSECTION

Theo Demerath\*<sup>1</sup>, Leo Bonati<sup>2</sup>, Tilman Schubert<sup>3</sup>

<sup>1</sup>Klinik für Neuroradiologie, Universitätsklinikum Freiburg, Freiburg, Deutschland

<sup>2</sup>Klinik für Neurologie, Universitätsspital Basel, Basel, Schweiz

<sup>3</sup>Klinik für Neuroradiologie, Universitätsspital Zürich, Zürich, Schweiz

**Hintergrund:** Acute, isolated intracranial dissection (ICDs) represents a generally rare and clinically challenging cause of acute stroke[1,2]. Current MRA-techniques may be insufficient in demonstrating a vessel wall hematoma and intimal flap, as being commonly seen in extracranial artery dissections. We compared common 0.5 mm parallel imaging (PI) TOF MRA (3T, 20 Channel Head Coil=Ch HC) with a 0.3 mm compressed sensing (CS) TOF MRA sequence (3T, 64 Ch HC) in a young patient suffering from acute ICA/M1 dissection.

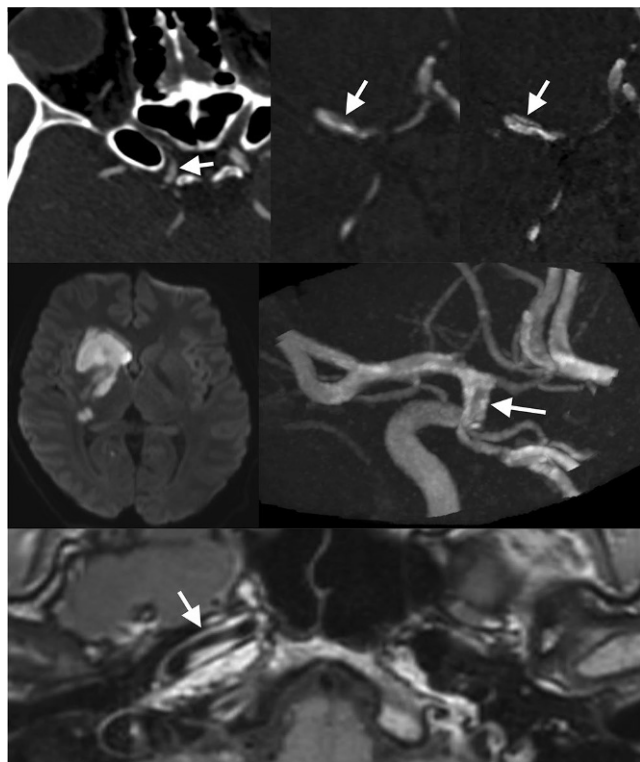


**Fig. 1 | 63** Acute right ICA/MCA dissection, perforator artery stroke and upstream concentric vessel wall enhancement. (A) Initial CTA demonstrates subtle narrowing of the right ICA terminus (*arrow*). Comparison of 0.5 mm PI TOF MRA (B) and 0.3 mm compressed-sensing Time-of-Flight MRA (C), revealing in (C) a thin dissecting flap extending from the ophthalmic ICA to the right M1 segment (*arrows*) causing (E) extensive flow signal alterations. (D) DWI-MRI shows extensive right basal ganglia perforator artery infarctions involving the anterior choroideal artery territory. High resolution black-blood post-contrast 3D T1 vessel wall imaging demonstrates a non-specific smooth concentric wall thickening and enhancement in the (F) petrous and (not shown) cavernous ICA segments (*arrows*). No vessel wall hematoma was detected on native T1w Sequences

**Methoden:** TOF MRA with an in plane resolution of 0.5 mm (Siemens Skyra 3T, 20 Channel Head Coil), compressed sensing (CS) TOF MRA sequence with an in plane resolution 0.3 mm (Siemens Prisma 3T, 64 Channel Head Coil) and high-resolution 3D black-blood T1 vessel wall imaging (pre- and post Gd) were performed.

**Ergebnisse:** Apart from non-specific lumen narrowing, both 0.7 mm CTA and 0.5 mm TOF MRA (Skyra 3T, 20 Ch HC) were insufficient in demonstrating specific signs of clinically highly suspected dissection. Instead, 0.3 mm compressed sensing (CS) TOF MRA clearly demonstrated an extensive dissection flap originating from the paraophthalmic ICA to the mid-M1-Segment. Beyond that, extensive concentric enhancement of the terminal and upstream ICA vessel wall was noted.

**Diskussion:** High resolution CS-TOF MRA may prove helpful acute isolated intracranial dissections and may render more invasive DSA unnecessary. Concentric vessel wall enhancement constitutes a non-specific finding and may also be found in focal inflammatory arteriopathy, CNS vasculitis or reversible vasoconstriction syndrome (RCVS)[3] but may cause confusion in the acute/subacute diagnostic stroke setting.

**Fazit:** 0.3 mm CS TOF MRA (3T, 64 Ch HC) was in this single case of an isolated intracranial anterior circulation dissection clearly superior to 0.5 mm PI TOF MRA (3T, 20 Ch HC).

#### References

1. Chaves C, Estol C, Esnaola MM, Gorson K, O'Donoghue M, De Witt LDCL. Spontaneous intracranial internal carotid artery dissection: report of 10 patients. *Arch Neurol.* 2002;59:977–81.
2. Caplan LR. Dissections of brain-supplying arteries. *Nat Clin Pract Neurol.* 2008;4:34–42.
3. Mandell DM, Mossa-Basha M, Qiao Y, Hess CP, Hui F, Matouk C, et al. Intracranial vessel wall MRI: Principles and expert consensus recommendations of the American society of neuroradiology. *Am J Neuroradiol.* 2017;38:218–29.

64

### ESTIMATION OF LESION AGE IN WAKE-UP STROKE PATIENTS – MAY CT-BASED LESION WATER UPTAKE IMAGING REPLACE MRI?

Gabriel Brooks\*<sup>1</sup>, Andre Kemmling<sup>2</sup>, Uta Hanning<sup>1</sup>, Gerhard Schoen<sup>3</sup>, Götz Thomalla<sup>4</sup>, Jens Fiehler<sup>1</sup>, Hannes Leischner<sup>1</sup>

<sup>1</sup>Universitätsklinikum Hamburg-Eppendorf, Neuroradiologie, Hamburg, Deutschland

<sup>2</sup>UKM, Neurologie, Münster, Deutschland

<sup>3</sup>Universitätsklinikum Hamburg-Eppendorf, Epidemiologie und Biometrie, Hamburg, Deutschland

<sup>4</sup>Universitätsklinikum Hamburg-Eppendorf, Neurologie, Hamburg, Deutschland

**Background:** Magnetic resonance imaging (MRI) may be used to estimate lesion age in patients with wake-up stroke to enable thrombolytic therapy. However, MRI has a limited availability and feasibility, and is more time-consuming in the acute situation. The purpose of this study was to directly compare computed tomography (CT) based quantification of lesion water uptake with MRI in identifying patients with lesion age <4.5 hours from symptom onset.

**Methods:** 50 patients with acute anterior circulation stroke were analyzed who received both imaging modalities at admission. Mismatch between diffusion-weighted MRI (DWI) and fluid-attenuated inversion recovery (FLAIR) was diagnosed by consensus reading according to established criteria and quantitative lesion water uptake (NWU) was calculated in admission CT. An established cut-off for NWU was applied to distinguish patients within and beyond 4.5 hours in a blinded approach.

**Result:** In 32 patients, the time from symptom onset to CT imaging was <4.5 h and 18 patients presented >4.5 h (range: 0.5–7.8 h). The median time from CT to MRI was 36 minutes (IQR: 24–55). DWI-

FLAIR mismatch correctly assigned 34/50 patients (68%) with a sensitivity of 70% (95%CI: 51–85%) and specificity of 72% (95%CI: 47–90%). CT-based NWU correctly assigned 43/50 (86%) with a sensitivity of 91% (95%CI: 75–98%) and specificity of 78% (95%CI: 75–94%) using 11.5% as established threshold.

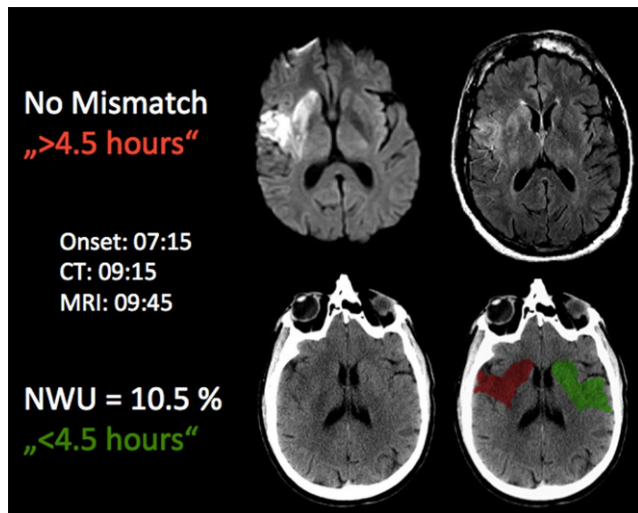


Fig. 1 | 64

Fig. 2 | 64 Stratification of lesion age <4.5 hours according to DWI-FLAIR mismatch

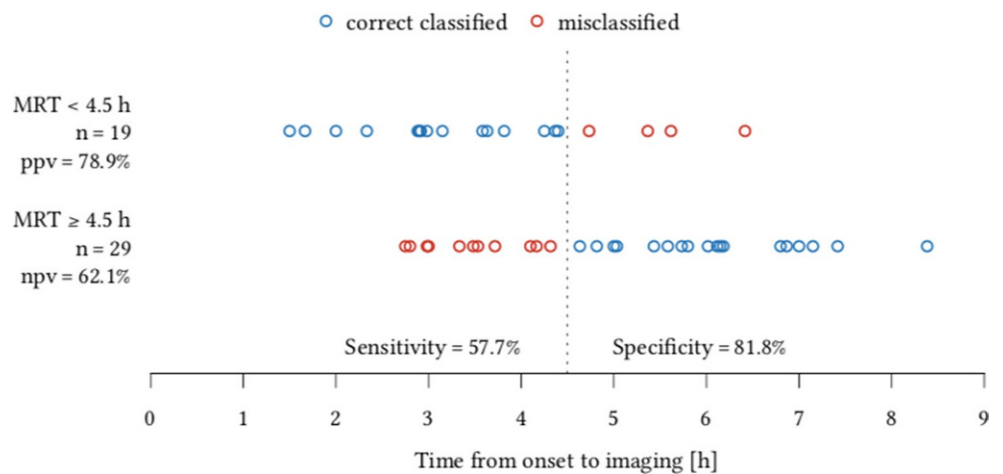
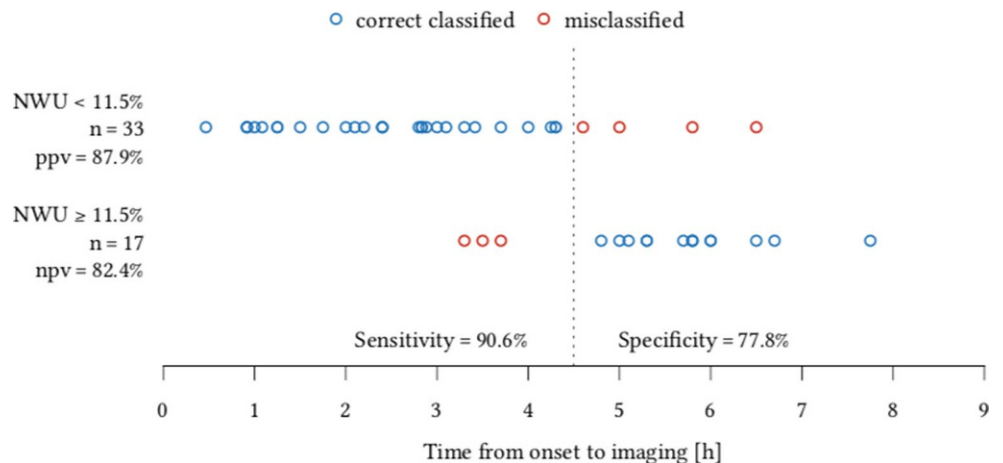


Fig. 3 | 64 Stratification of lesion age <4.5 hours according to CT based NWU 11.5 %



**Conclusion:** In this cohort, CT-based quantitative NWU was superior to visual assessment of DWI-FLAIR mismatch in identifying patients within the thrombolysis time window. Future trials could use quantitative NWU as imaging biomarker to stratify unknown onset stroke patients.

**References**

1. Minnerup J, Broocks G, Kalkoffen J, Langner S, Knauth M, Psychogios MN, et al. Computed tomography-based quantification of lesion water uptake identifies patients within 4.5 hours of stroke onset: A multicenter observational study. *Ann Neurol*. 2016;80:924–34.
2. Thomalla G, Cheng B, Ebinger M, Hao Q, Tourdias T, Wu O, et al. DWI-FLAIR mismatch for the identification of patients with acute ischaemic stroke within 4.5 h of symptom onset (PRE-FLAIR): a multicentre observational study. *Lancet Neurol*. 2011;10:978–86.

**65**

**STRALENEXPOSITION BEI DER ENDOVASKULÄREN SCHLAGANFALLTHERAPIE – REFERENZLEVEL FÜR ISCHÄMISCHE SCHLAGANFÄLLE DER VORDEREN ZIRKULATION**

Charlotte Weyland\*<sup>1</sup>, Johannes Pfaff<sup>1</sup>, Felix Hemmerich<sup>1</sup>, Markus Möhlenbruch<sup>1</sup>, Martin Bendszus<sup>1</sup>

<sup>1</sup>Klinik für Neurologie, Universitätsklinikum Heidelberg, Abteilung für Neuroradiologie, Heidelberg, Deutschland

**Hintergrund:** Aufgrund der weltweiten Etablierung der mechanischen Rekanalisation als Schlaganfall-Standardtherapie ist die Strahlenexpo-

sition (SE) der endovaskulären Schlaganfalltherapie (EST) von steigender Signifikanz. Mit der hier vorliegenden Analyse wurde erstmals die SE abhängig von der Anzahl der interventionellen Manöver für unkomplizierte Interventionen untersucht, um Dosis-Referenzlevel (DRL) für die EST der vorderen Zirkulation zu ermitteln.

**Methoden:** In dieser monozentrischen Analyse der SE (gemäß Dosisflächenprodukt (DFP) in  $\mu\text{Gy}\cdot\text{cm}^2$ ) wurden alle Patienten, die eine EST der vorderen Zirkulation zwischen 04/2016 und 04/2018 erhielten, eingeschlossen.

Komplizierte ESTs wurden von der Analyse ausgeschlossen (intraprozeduralen Komplikationen, Ballonangioplastie, eingeschränkte Erfahrung des Interventionalisten (<25 Prozeduren), DYNA-CT).

**Ergebnisse:** Insgesamt wurden 356 Fälle (männl.:  $n = 149$  (41.9 %), Alter: Mittelwert (SD): 74 (13), NIHSS (Median (IQR)) von 15 (10–20), TICI 2b-3 87,4 %) analysiert. Am häufigsten waren Verschlüsse der A. cerebri media im M1- ( $n = 177$  (49.7 %)) oder M2- Segment ( $n = 99$  (27.8 %)), gefolgt von Carotis-T-Verschlüssen ( $n = 77$  (21.6 %)).

Für alle analysierten Fälle belief sich das Dosisflächenprodukt (DFP) im Median (IQR) auf 10752 (6852–15402) mit 2 Interventionsmanövern im Median (IQR: 1–3). Der Vergleich der ESTs nach Manöveranzahl zeigt einen signifikanten Anstieg der SE zwischen Fällen mit einem Manöver (DFP: 6846 (5102–9962)) und zwei Manövern (DFP: 10724 (7853–15015);  $p$ -Wert: <0.0001) sowie bei Fällen mit zwei Manövern und drei Manövern (DFP: 13927 (10851–18454);  $p$ -Wert: 0.011).

**Diskussion:** Erwartungsgemäß steigt die SE der EST mit steigender Manöveranzahl signifikant an. Mit dieser Analyse konnten erstmalig DRL für unkomplizierte Interventionen der vorderen Zirkulation ermittelt werden.

**Fazit:** Die hiermit mögliche Etablierung von DRL kann maßgeblich zum Strahlenschutz für Patienten und Interventionalisten im Rahmen der immer häufiger werdenden Schlaganfallinterventionen beitragen und damit das stochastische Risiko für Strahlenfolgen minimieren sowie deterministische Strahlenfolgen vermeiden.

## Literatur

1. Farah, et al. Dose reference levels and clinical determinants in stroke neuroradiology interventions. *Eur Radiol.* 2019;29:645–53.
2. Alexander, et al. Patient radiation exposure during diagnostic and therapeutic interventional neuroradiology procedures. *J Neurointerv Surg.* 2010;2:6–10.

68

## CEREBRAL VASOSPASM AFTER SPONTANEOUS SUBARACHNOID HEMORRHAGE: VALIDATION OF RISK FACTORS FOR RECURRENCE AND RELATED INFARCTION SUBSEQUENT TO TRANSLUMINAL BALLOON ANGIOPLASTY

Alexander Neumann<sup>\*1</sup>, Jan Küchler<sup>2</sup>, Claudia Ditz<sup>2</sup>, Linda Aulmann<sup>1</sup>, Peter Schramm<sup>1</sup>, Hannes Schacht<sup>1</sup>

<sup>1</sup>Institut für Neuroradiologie, UKSH, Campus Lübeck, Lübeck, Deutschland

<sup>2</sup>Klinik für Neurochirurgie, UKSH, Campus Lübeck, Lübeck, Deutschland

**Background:** After spontaneous subarachnoid hemorrhage (sSAH), cerebral vasospasm (CVS) is common and potentially resulting in delayed cerebral ischemia and related cerebral infarction mainly responsible for an unfavorable outcome. Besides the local therapy with calcium channel blockers (in particular nimodipine), transluminal balloon angioplasty (TBA) is also widely used, but exact principles of its use and impact are still unknown. We aimed to identify risk factors of recurrent CVS and related infarction following treatment with TBA.

**Methods:** We analyzed 35 patients with sSAH (initial treatment modality: 6 clipping and 28 endovascular, 1 angiogram-negative) and consecutive CVS who received TBA after previous intra-arterial nimodipine infusion with 41 procedures in a total of 99 vessel segments. All were characterized for the point of time after admission, localization and precise technique (compliant/non-compliant) of TBA. Furthermore, the angiographic response, the recurrence of CVS and the onset of related infarction in computed tomography within 48 h after TBA were described. Also depending on demographic characteristics and clinical grading, the localization of the aneurysm, the initially chosen treatment modality and previous infarction, univariate and multivariate logistic regression analysis for recurrence of CVS and related infarction were evaluated. Statistical significance was accepted at  $p < 0.05$ .

**Results:** TBA was carried out all in one with only one artery dissection as a complication and averagely in two vessel segments at day 9 after admission, based on diverse localizations of CVS. In 16 of 99 vessel segments (16%), who were former treated with TBA, we documented recurrent CVS. The angiographic response after TBA was mostly classified as good (87%), it was negatively associated with recurrence of CVS ( $p = 0.004$ ) and related infarction ( $p = 0.001$ ). Furthermore, male gender was associated with a higher incidence of CVS-related infarction ( $p = 0.040$ ).

**Discussion/Conclusion:** Our data support TBA as a safe and, if implemented successfully, effective therapy for CVS. Our results will augment the still sparse evidence concerning risk factors for recurrence and CVS-related infarction subsequent to TBA and provide new information for individual considerations. Further precise analyses with large collectives are necessary.

69

## TITEL: MECHANISCHE THROMBEKTOMIE BEI PATIENTEN MIT ZEREBRALEM GROßGEFÄßVERSCHLUSS DER VORDEREN ZIRKULATION: ZUSAMMENHANG DER SCHLAGANFALLÄTIOLOGIE MIT DEM KOLLATERALSTATUS

Eva Hassler<sup>\*1</sup>, Markus Kneihls<sup>2</sup>, Hannes Deutschmann<sup>1</sup>, Nicole Hinteregger<sup>1</sup>, Kurt Niederkorn<sup>2</sup>, Christian Enzinger<sup>1,2</sup>, Simon Fandler<sup>2</sup>, Sebastian Eppinger<sup>2</sup>, Franz Fazekas<sup>2</sup>, Thomas Gattringer<sup>2</sup>

<sup>1</sup>Medizinische Universität Graz, Universitätsklinik für Radiologie, Klinische Abteilung für Neuroradiologie, Vaskuläre und Interventionelle Radiologie, Graz, Österreich

<sup>2</sup>Medizinische Universität Graz, Universitätsklinik für Neurologie, Klinische Abteilung für Allgemeine Neurologie, Graz, Österreich

**Hintergrund:** Der zerebrale Kollateralstatus ist bedeutend für das klinische Outcome beim akuten intrakraniellen Großgefäßverschluss. Über den Zusammenhang zwischen der Schlaganfallätiologie und Ausprägung der zerebralen Kollateralen ist noch wenig bekannt. In dieser retrospektiven Studie haben wir untersucht, ob ein besserer zerebraler Kollateralstatus im Kontext einer vorbestehenden zervikalen Karotisstenose im Vergleich zu Patienten ohne Makroangiopathie mit einem besseren klinischen Outcome korreliert ist.

**Methoden:** Es wurden alle Schlaganfallpatienten, die zwischen 2010 und 2017 am LKH-Universitätsklinikum Graz aufgrund eines Großgefäßverschlusses der vorderen Zirkulation mittels mechanischer Thrombektomie behandelt worden waren, eingeschlossen und in eine „atherothrombotische“ ( $\geq 50$  %ige ipsilaterale Karotisstenose) und eine „nicht-atherothrombotische“ Gruppe unterteilt. Ausgeschlossen wurden Patienten mit einem extrakraniellen Karotisverschluss oder einer Dissektion. Der zerebrale Kollateralstatus wurde in der präinterventionellen MR- oder CT-Angiographie nach dem *Tan Score* ausgewertet und in fehlende/schlechte und moderate/gute Kollateralen eingeteilt. Weiters wurde die finale Infarktgröße, postinterventionelle Komplikationen (symptomatische Hirnblutung/Gefäßreokklusion) und der mRS nach 90 Tagen evaluiert.

**Ergebnisse:** 281 Patienten wurden eingeschlossen. Davon wiesen 46 (16 %) eine atherothrombotische und 235 (84 %) eine nicht-atherothrombotische Schlaganfallgenese auf. Die Patienten der atherothrombotischen Gruppe hatten einen geringeren initialen Schlaganfallschweregrad (medianer NIHSS: 14 vs. 15,  $p=0,068$ ) und in der präinterventionellen Bildgebung häufiger einen guten Kollateralstatus (76 % vs. 46 %,  $p<0,001$ ).

Die Reperusionsrate, der mRS nach 90 Tagen und die postinterventionelle Infarktgröße waren vergleichbar ( $p>0,1$ ). In der „atherothrombotischen“ Gruppe konnten häufiger Komplikationen im Rahmen der Thrombektomie beobachtet werden (20 % vs. 6 %,  $p=0,007$ ).

**Diskussion:** Patienten mit atherothrombotischer Schlaganfallätiologie, die auf Grund eines Großgefäßverschlusses im vorderen Kreislauf thrombektomiert wurden, zeigten eine bessere zerebrale Kollateralisierung als jene mit nicht-atherothrombotischer Genese. Dieser Befund war jedoch nicht mit einem besseren klinischen Outcome assoziiert, was auf die höhere Rate an postinterventionellen Komplikationen in dieser Gruppe zurückzuführen sein könnte.

## 70

### COLLATERAL SCORING IN ACUTE STROKE PATIENTS WITH LOW ASPECTS – AN UNNECESSARY OR UNDERESTIMATED TOOL FOR TREATMENT SELECTION?

Gabriel Broocks\*<sup>1</sup>, Helge Knipf<sup>1</sup>, Peter Schramm<sup>2</sup>, Uta Hanning<sup>1</sup>, Lukas Meyer<sup>1</sup>, Fabian Flottmann<sup>1</sup>, Hannes Leischner<sup>1</sup>, Jens Fiehler<sup>1</sup>, Andre Kemmling<sup>3</sup>

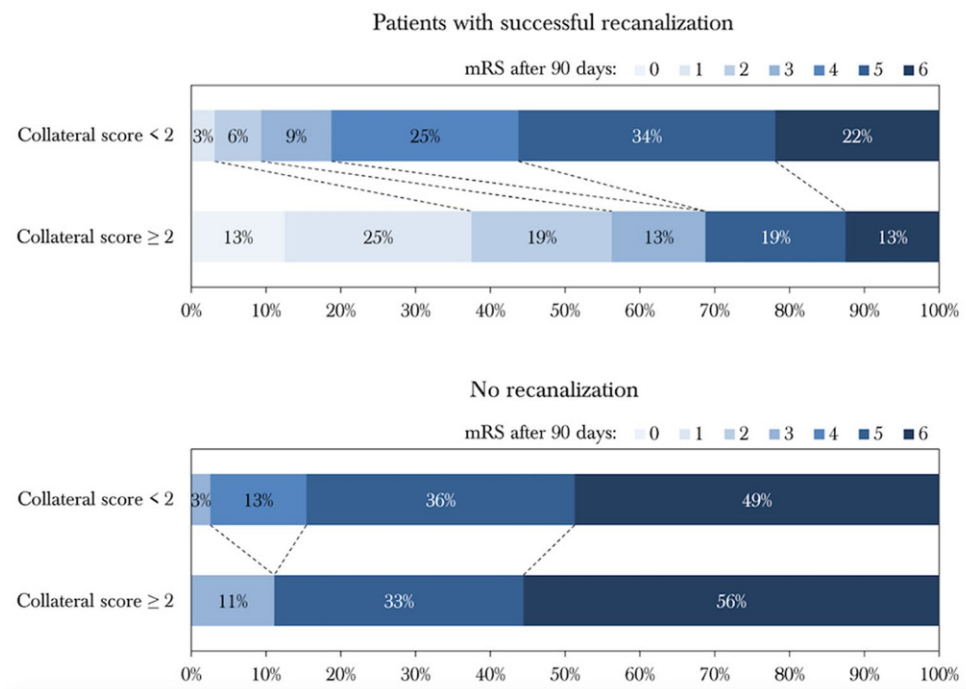
<sup>1</sup>Universitätsklinikum Hamburg-Eppendorf, Neuroradiologie, Hamburg, Deutschland

<sup>2</sup>Universitätsklinikum Schleswig-Holstein, Campus Lübeck, Neuroradiologie, Lübeck, Deutschland

<sup>3</sup>Westfälische Wilhelms-Universität Münster, Münster, Deutschland

**Background:** Benefit of thrombectomy in patients with a low initial Alberta Stroke Program Early CT score (ASPECTS) is still uncertain. We hypothesized that, despite low ASPECTS, patients may benefit from endovascular recanalization if good collaterals are present.

**Fig. 1 | 70** Modified Rankin scale scores at 90 days in the study cohort



**Methods:** Ischemic stroke patients with large vessel occlusion in the anterior circulation and an ASPECTS of  $\leq 5$  were analyzed. Collateral status (CS) was assessed using a 5-point-scoring system in CT-angiography with poor CS defined as CS=0–1. Clinical outcome was determined using modified Rankin Scale (mRS) score after 90 days. Edema formation was measured in admission and follow-up CT by net water uptake.

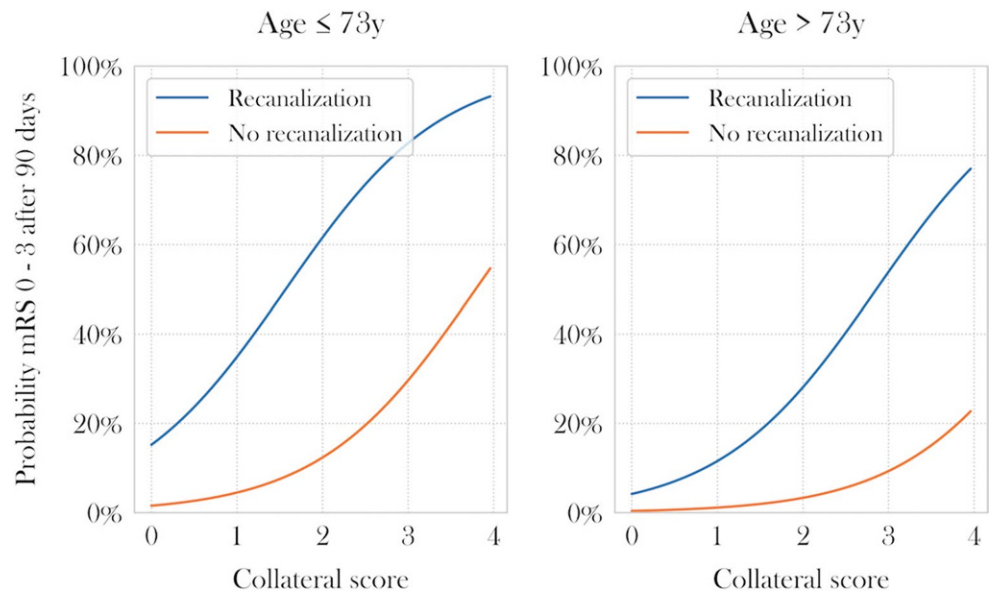
**Result:** 27/100 (27%) patients exhibited a CS of 2–4. 50 patients underwent successful vessel recanalization and 50 patients had a persistent vessel occlusion. In multivariable logistic regression analysis, collateral status (odds ratio [OR] 3.0;  $p=0.003$ ) and vessel recanalization (OR 12.2;  $p=0.009$ ) significantly increased likelihood of a good outcome (mRS 0–3). A 1-point increase in CS was associated with 1.9% lowered lesion water uptake in follow-up CT (95%CI: 0.2–3.7%).

**Conclusion:** Endovascular recanalization in patients with ASPECTS of  $\leq 5$  but good collaterals was linked to improved clinical outcome and attenuated edema formation. Collateral status may serve as selection criterion for thrombectomy in low ASPECTS patients.

## References

- Broocks G, Hanning U, Flottmann F, Schoenfeld M, Faizy T, Sporns P, et al. Clinical Benefit of Thrombectomy in Stroke Patients with Low ASPECTS is Mediated by Edema Reduction. *Brain*. 2019;142:1399–407.
- Tan BY, Wan-Yee K, Paliwal P, Gopinathan A, Nadarajah M, Ting E, et al. Good Intracranial Collaterals Trump Poor ASPECTS (Alberta Stroke Program Early CT Score) for Intravenous Thrombolysis in Anterior Circulation Acute Ischemic Stroke. *Stroke*. 2016;47:2292–8.

**Fig. 2 | 70** Impact of recanalization, age, and collateral score on functional outcome in multivariable logistic regression analysis



**75**

**ESTIMATION OF „TISSUE CLOCK“ USING CT BASED QUANTITATIVE LESION WATER UPTAKE – A SUITABLE METHOD TO SELECT PATIENTS FOR THROMBECTOMY IN THE EXTENDED TIME WINDOW?**

Gabriel Broocks<sup>1</sup>, Svenja Tessarek<sup>\*1</sup>, Helge Kniep<sup>1</sup>, Fabian Flottmann<sup>1</sup>, Götz Thomalla<sup>2</sup>, Jens Fiehler<sup>1</sup>, Uta Hanning<sup>1</sup>

<sup>1</sup>Universitätsklinikum Hamburg-Eppendorf, Neuroradiologie, Hamburg, Deutschland

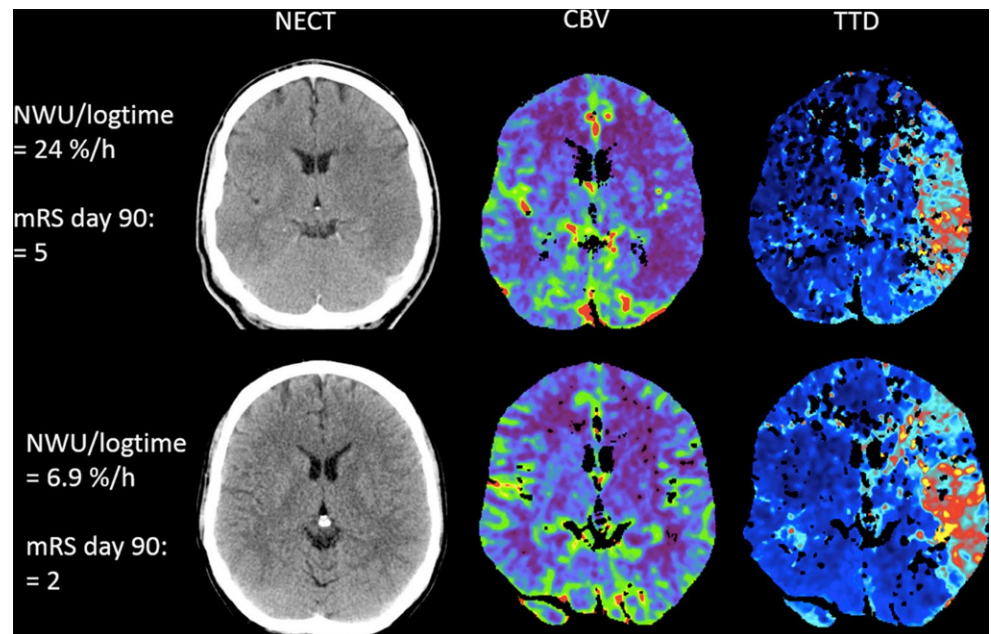
<sup>2</sup>Universitätsklinikum Hamburg-Eppendorf, Neurologie, Hamburg, Deutschland

**Background:** Patients presenting in the extended time window may benefit from endovascular treatment (ET) according to recent trials; however, selection for ET in this patient group has only been per-

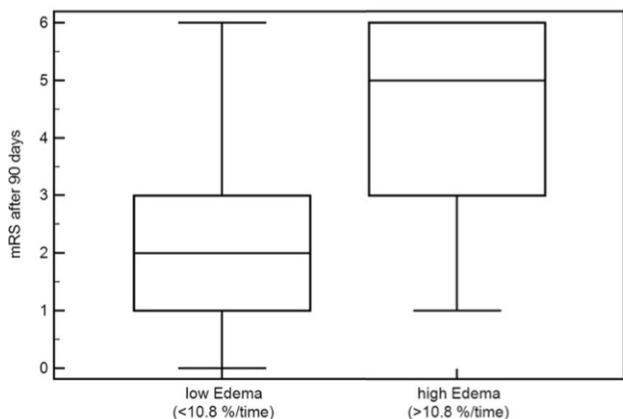
formed using imaging platforms such as RAPID, which is not comprehensively available and may overestimate ischemic core volume leading to exclusion of patients from ET. We hypothesized that quantitative lesion water uptake per time may serve as imaging biomarker of “tissue clock” and predicts clinical outcome in extended time window patients undergoing ET.

**Methods:** In this pilot study, 46 acute middle cerebral artery stroke patients presenting 4.5–24 hours after symptom onset, who received initial multimodal CT and underwent ET were analyzed. Quantitative lesion net water uptake (NWU) was calculated in admission CT and NWU per time was determined after dividing NWU by the logarithm of time from onset (NWU/time). Prediction of clinical outcome was performed using univariable receiver operating curve (ROC) analysis and multivariable logistic regression analysis. Clinical outcome was assessed using modified Rankin Scale scores (mRS) after 90 days.

**Fig. 1 | 75** Two patients presenting 6 hours after onset who which subsequent successful thrombectomy



Box plots comparing patients with low and high early edema formation per time and their median modified Rankin Scale score after 90 days.



Patients in the extended time window distinguished into two groups based on their median net water uptake per logarithm of time.

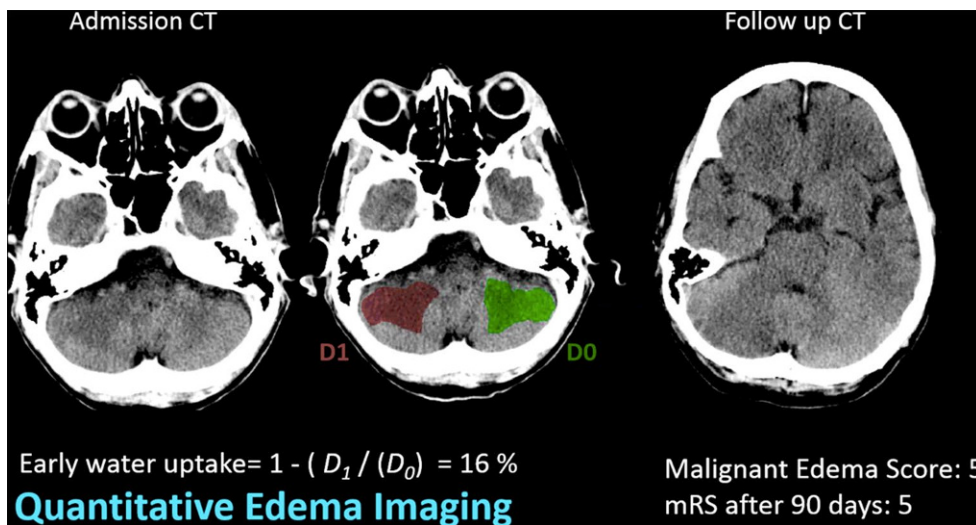
Fig. 2 | 75

**Result:** The mean (range) time from onset to imaging was 6.5 hours (4.5–15.5 h) and the mean (SD) NWU/time was 11.8%/h (6.8). Based on ROC analysis, NWU/time above 8.9% identified patients with functional independence (mRS 0–2) with high discriminative power (area under curve [AUC]: 0.86, 95%CI: 0.67–0.96,  $p < 0.0001$ ). In multivariable logistic regression, the probability of poor outcome (mRS 5–6) was significantly associated with NWU/time (odds ratio: 1.32, 95%CI: 1.06–1.64,  $p = 0.01$ ), adjusted for recanalization status and ASPECTS. **Conclusion:** Quantitative lesion water uptake per time could serve as imaging biomarker of “tissue clock” and may predict clinical outcome in patients undergoing ET in the extended time window. This method might be tested to select patients for late time window ET compared to CT perfusion based ischemic core assessments.

**References**

- Broocks G, et al. Quantitative Lesion Water Uptake in Acute Stroke Computed Tomography Is a Predictor of Malignant Infarction. Stroke. 2018;49:1906:1912.

Fig. 1 | 79 Example of early lesion water uptake quantification



**PREDICTION OF MALIGNANT POSTERIOR CIRCULATION STROKES USING CT BASED QUANTITATIVE LESION WATER UPTAKE**

Gabriel Broocks<sup>1</sup>, Sarah Elsayed<sup>\*1</sup>, Helge Kniep<sup>1</sup>, Andre Kemmling<sup>2</sup>, Peter Sporns<sup>3</sup>, Thilo Rusche<sup>3</sup>, Jens Fiehler<sup>1</sup>, Uta Hanning<sup>1</sup>

<sup>1</sup>Universitätsklinikum Hamburg-Eppendorf, Neuroradiologie, Hamburg, Deutschland

<sup>2</sup>Universitätsklinikum Münster, Neurologie, Münster, Deutschland

<sup>3</sup>Universitätsklinikum Münster, Radiologie, Münster, Deutschland

**Background:** In posterior circulation ischemic stroke, malignant cerebellar edema (MCE) is a life-threatening complication that requires timely diagnosis and management. Yet, there is no established imaging biomarker available that may serve as predictor of MCE. Early edematous water uptake can be determined using quantitative lesion net water uptake (NWU), but this biomarker has only been applied in anterior circulation strokes. We hypothesized that NWU in early posterior circulation stroke lesions predicts MCE with poor clinical outcome.

**Methods:** 179 patients with acute vessel occlusion in the posterior circulation and multimodal CT imaging at admission were included. 35 (19.5%) patients developed MCE defined by using an established 10-point scale in follow-up CT, of which >3 are considered malignant. NWU was quantified in admission and follow-up CT based on CT-densitometry and compared with posterior circulation Alberta Stroke Program Early CT Score (pc-ASPECTS) as predictor of MCE using univariable receiver operating curve (ROC) analysis and multivariable logistic regression analysis.

**Result:** Edematous tissue expansion by NWU within the early infarct lesion was 24.6% (± 8.4) for malignant and 7.2% (± 7.4) for non-malignant infarctions, respectively ( $p < 0.0001$ ). Based on ROC analysis, NWU above 14.9% identified MCE with high discriminative power (AUC: 0.94, 95%CI: 0.89–0.97) and was superior to pc-ASPECTS (AUC: 0.81, 95%CI: 0.75–0.87). In multivariable logistic regression analysis, early NWU (odds ratio [OR]: 1.28; 95%CI: 1.15–1.42,  $p < 0.0001$ ) and pc-ASPECTS (OR: 0.71, 95%CI: 0.53–0.95,  $p = 0.02$ ) were significantly associated with MCE adjusted for age and recanalization status.

**Conclusion:** Quantitative NWU in early posterior circulation stroke is an important surrogate marker for developing MCE. Besides pc-ASPECTS, the measurement of lesion water uptake may further support identifying patients at risk for MCE at an early stage indicating stricter monitoring and consideration for decompressive surgery.

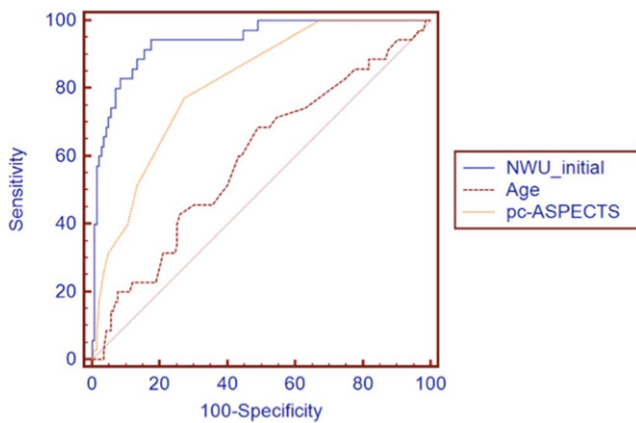


**Fig. 2 | 79** ROC curve analysis to display the impact of early lesion water uptake, age, and pc-ASPECTS score on the development of MCE

#### References

1. Fabritius MP, et al. Early Imaging Prediction of Malignant Cerebellar Edema Development in Acute Ischemic Stroke. *Stroke*. 2017;48:2597–600.
2. Broocks G, et al. Quantitative Lesion Water Uptake in Acute Stroke Computed Tomography Is a Predictor of Malignant Infarction. *Stroke*. 2018;49:1906–12.

81

#### QUANTITATIVE MRI PERFUSION-DIFFUSION MISMATCH: THE ROLE OF USER-INDEPENDENT SOFTWARE

nicole hinteregger\*<sup>1</sup>, Ulrike Wießpeiner<sup>1</sup>, Markus Kneihls<sup>2</sup>, Simon Fandler-Höfler<sup>2</sup>, Hannes Deutschmann<sup>1</sup>, Franz Fazekas<sup>2</sup>, Gernot Reishofer<sup>1</sup>

<sup>1</sup>Medizinische Universität Graz, Universitätsklinik für Radiologie, Klinische Abteilung für Neuroradiologie, vaskuläre und interventionelle Radiologie, Graz, Österreich

<sup>2</sup>Medizinische Universität Graz, Universitätsklinik für Neurologie, Graz, Österreich

**Background:** Mechanical thrombectomy (MT) is considered as the standard therapy in patients with acute stroke caused by large vessel occlusion of the anterior circulation. When performing MT in an extended time window up to 24 hours after onset of clinical symptoms, advanced imaging is needed. Therefore, software applications for quantitative MRI perfusion–diffusion mismatch calculations have been developed to support decision making. The aim of our study was to compare two established software applications (RAPID® and Olea Sphere®) in terms of apparent diffusion coefficient (ADC) lesions volumes, volume of hypoperfused brain tissue and calculated mismatch volumes.

**Methods:** MRI examinations of 86 patients with a large vessel occlusion of the anterior circulation were analyzed. Perfusion-diffusion mismatch was calculated automatically with RAPID® software and recalculated with Olea Sphere® software. For both software applications, the results included the automatically calculated ADC values, the volume of hypoperfused brain tissue and the mismatch volume (all given in ml). The calculated parameters from both methods were compared quantitatively using statistical methods.

**Result:** Both software applications showed a good mean concordance for the volume of hypoperfused brain tissue and ADC lesions volume with no significant differences. However, a statistically significant difference of perfusion-diffusion mismatch volume could be observed.

For individual patients, the differences of all evaluated parameters were found to be dramatically large.

**Conclusion:** Despite the undoubted benefits of automated imaging software to support clinical decisions, proposed limits, such as the volume of the perfusion-diffusion mismatch, are only partially transferable to a variety of software platforms. We observed that volume segmentation plays a crucial role for the evaluation of perfusion-diffusion mismatch. Therefore, decision-relevant parameters should be determined individually for each software system

#### References

1. Campbell BCV, Majoie CBLM, Albers GW. Penumbra imaging and functional outcome in patients with anterior circulation ischaemic stroke treated with endovascular thrombectomy versus medical therapy: a meta-analysis of individual patient-level data (vol 18, pg 46, 2019). *Lancet Neurol*. 2019;18(3):E2–E2.
2. Tsvigoulis G, Katsanos AH, Schellinger PD, et al. Advanced Neuroimaging in Stroke Patient Selection for Mechanical Thrombectomy A Systematic Review and Meta-Analysis. *Stroke*. 2018;49(12):3067–70.

82

#### EFFECT OF CONSCIOUS SEDATION VS. GENERAL ANESTHESIA ON RADIATION EXPOSURE, PROCEDURE TIME AND FLUOROSCOPY TIME IN PATIENTS TREATED FOR THROMBOEMBOLIC BASILAR ARTERY OCCLUSIONS – A RETROSPECTIVE SINGLE-CENTER ANALYSIS

Felix Hemmerich\*<sup>1</sup>, Charlotte Weyland<sup>1</sup>, Markus Möhlenbruch<sup>1</sup>, Martin Bendszus<sup>1</sup>, Johannes Pfaff<sup>1</sup>

<sup>1</sup>Universitätsklinikum Heidelberg Neurologische Klinik: Neuroradiologie, Neurologische Klinik, Neuroradiologie, Heidelberg, Deutschland

**Background:** To quantify the effect of conscious sedation (CS) vs. general anesthesia (GA) on radiation exposure, procedure time and fluoroscopy time in patients treated for thromboembolic basilar artery occlusions (BAO) using mechanical thrombectomy (MT).

**Methods:** Retrospective analysis of an institutional review board–approved stroke database of a comprehensive stroke center focusing on radiation exposure (as per dose area product in  $\mu\text{Gy}\cdot\text{m}^2$ , median [IQR]), procedure and fluoroscopy time (in minutes, median [IQR]) in patients receiving MT for thromboembolic basilar artery occlusions according to the mode of sedation.

**Result:** Overall 119 patients (GA:  $n=84$  (70.6%), CS:  $n=35$  (29.4%)) have been included in this analysis. Patients who received MT under GA had a more severe initial severity of stroke symptoms (as per National Institutes of Health Stroke Scale; GA: 27 (15–36); CA: 11 (7–19),  $p$ -value:  $<0.0001$ ) and were treated more often using stent-retrievers only (GA:  $n=71/84$  (84.5); CS:  $n=17/35$  (48.6),  $p$ -value:  $<0.0001$ ). There was no statistical significant difference regarding procedure time (GA: 74 (45–111); CS: 65 (44–91);  $p$ -value: 0.318), fluoroscopy time (GA: 33 (21–55); CS: 28 (18–51),  $p$ -value: 0.932), and dose area product (GA: 14514 (9584–22574); CS: 10767 (7506–19212),  $p$ -value: 0.104). Procedure time, fluoroscopy time and dose area product remained comparable in a subgroup analysis of patients receiving only MT using Stent-Retrievers.

**Conclusion:** This retrospective analysis showed no effect of the mode of sedation during mechanical thrombectomy for thromboembolic basilar artery occlusions on radiation exposure, procedure time and fluoroscopy time. This circumstance suggests that dose reference levels could be established without a particular need to regard a specific type on anesthesia during MT.

86

### ADDITIONAL RADIATION EXPOSURE AND FLUOROSCOPY TIME IN PATIENTS TREATED FOR TANDEM OCCLUSIONS IN THE ANTERIOR CIRCULATION – A MATCHED-PAIR ANALYSIS

Charlotte Weyland<sup>1</sup>, Felix Hemmerich<sup>\*1</sup>, Markus Möhlenbruch<sup>1</sup>, Martin Bendszus<sup>1</sup>, Johannes Pfaff<sup>1</sup>

<sup>1</sup>Klinik für Neurologie, Abteilung für Neuroradiologie, Heidelberg, Deutschland

**Background:** Since radiation exposure in interventional radiology is of growing interest and the number of performed endovascular stroke treatments (EST), i. e. mechanical thrombectomy (MT)—is increasing, the demand of dose reference levels (DRL) is growing. This study was performed to quantify the additional radiation exposure (RE) and fluoroscopy time (FT) needed in patients treated for a tandem occlusion in the anterior circulation compared to patients without a preceding carotid artery occlusion or stenosis receiving EST.

**Methods:** Retrospective analysis of a prospectively maintained stroke database of a comprehensive stroke center focusing on the RE (as per dose area product in  $\mu\text{Gy}\cdot\text{m}^2$ , median [IQR]), procedure and FT (in minutes, median [IQR]) in patients receiving carotid artery stenting (CAS) and MT in the anterior circulation ischemic stroke. Patients who received CAS and MT were matched with patients needing only MT according to number of thrombectomy maneuvers, location of intracranial occlusion, mode of anesthesia, gender and age (order of decreasing priority).

**Ergebnisse:** Overall 236 patients ( $n=118$  in each group) have been included in this analysis. Additionally to matching criteria, there was no significant difference in patient's pre-morbid degree of disability (as per modified Rankin Scale), initial severity of stroke symptoms (as per National Institutes of Health Stroke Scale), and administration of i. v. rtPA or time from stroke onset to groin puncture in patients with known symptom onset. Procedure times (CAS+: 121 [80–176]; CAS-: 66 [45–106]), fluoroscopy times (CAS+: 57 [37–88]; CAS-: 32 [20–53]) as well as radiation exposure (CAS+: 19042 [13603–28722]; CAS-: 12379 [9307–18969]) were significantly higher in patients receiving CAS (all  $p$ -values:  $<0.0001$ ). This is a relative median increase of radiation exposure of 53.8% and a relative increase of 78.2% of fluoroscopy time.

**Conclusion:** As expected, patients treated for tandem occlusions receiving carotid artery stenting and intracranial mechanical thrombectomy have a massive increase of radiation exposure and fluoroscopy time compared to patients treated for intracranial large vessel occlusion only. This circumstance should be considered, when dose reference levels are compared.

89

### RADIATION EXPOSURE AND FLUOROSCOPY TIME IN MECHANICAL THROMBECTOMY OF ANTERIOR CIRCULATION ISCHEMIC STROKE DEPENDING ON THE INTERVENTIONALIST'S EXPERIENCE – A RETROSPECTIVE SINGLE CENTER EXPERIENCE

Charlotte Weyland<sup>\*1</sup>, Felix Hemmerich<sup>1</sup>, Markus Möhlenbruch<sup>1</sup>, Martin Bendszus<sup>1</sup>, Johannes Pfaff<sup>1</sup>

<sup>1</sup>Klinik für Neurologie, Abteilung für Neuroradiologie, Heidelberg, Deutschland

**Background:** Dose reference levels (DRL) for the radiation exposure (RE) endovascular stroke treatment (EST) have been suggested recently. (1, 2) These DRL, however, might be confounded as they originate from a dataset including EST in the anterior and posterior circulation, more complex procedures and do not consider the interventionalist's

experience. We hypothesized, that the interventionalist's learning curve influences the RE during EST.

**Methods:** Retrospective analysis of a prospectively maintained stroke database of a comprehensive stroke center focusing on the radiation exposure (as per dose area product in  $\mu\text{Gy}\cdot\text{m}^2$ , median [IQR]), procedure and fluoroscopy time (in minutes, median [IQR]) in patients receiving EST in anterior circulation ischemic stroke. Patients receiving cervical or intracranial angioplasty were excluded. Procedures have been assigned according to the interventionalist's experience in EST into three groups: A =  $<25$  procedures; B = 26–50 procedures; C =  $\geq 50$  procedures.

**Result:** Overall 696 patients have been included in this analysis, treated by 18 different interventionalists (number of their procedures: median [IQR]: 14 [9–18]). Procedure times (A: 86 [54–131]; B: 67 [48–103],  $p$ -value: 0.006), fluoroscopy times (A: 39 [25–72]; B: 32 [20–53],  $p$ -value: 0.001) as well as RE (A: 14813 [8958–24337]; B: 11160 [7049–18057],  $p$ -value: 0.001) was significantly lower in group B ( $n=151$ ) than in group A ( $n=152$ ). Procedure times (C: 59 [36–99]), fluoroscopy times (C: 31 [16–53]) and RE (C: 11391 [6848–18288]) in group C ( $n=393$ ) were also significantly lower than in group A (all  $p$ -values:  $<0.0001$ ), but comparable to group B ( $p$ -values: 0.071, 0.809 and 0.934).

**Discussion:** There is a learning curve of interventionalists, who perform EST, regarding the RE in EST. When DRLs are established for a better monitoring of RE in EST this should not be neglected. Furthermore the established of DRLs depending on the experience level can be used as a feedback for the interventionalist in training leading to an individually higher awareness of radiation applied in EST.

**Conclusion:** DRLs of RE in EST are significantly influenced by the interventionalist's learning curve.

### References

1. Farah J, Rouchaud A, Henry T, Regen C, Mihalea C, Moret J, et al. Dose reference levels and clinical determinants in stroke neuroradiology interventions. *Eur Radiol.* 2019;29(2):645–53.
2. Cai X, et al. Radiation Outcome in Mechanical Thrombectomy of Acute Ischemic Stroke. *Transl Neurosci.* 2019;10:10–3.

94

### ONE-STOP MANAGEMENT WITH PERFUSION FOR TRANSFER STROKE PATIENTS DUE TO A LARGE-VESSEL OCCLUSION – FEASIBILITY AND EFFECTS ON IN-HOSPITAL TIMES

Alex Brehm<sup>\*1,2</sup>, Ilko Maier<sup>3</sup>, Ioannis Tsogkas<sup>1,2</sup>, Hanna Josephin Eisenberger<sup>3</sup>, Pengfei Yang<sup>4</sup>, Jian-Min Liu<sup>4</sup>, Jan Liman<sup>3</sup>, Marios-Nikos Psychogios<sup>1,2</sup>

<sup>1</sup>Diagnostische und interventionelle Neuroradiologie, Unispital Basel, Basel, Schweiz

<sup>2</sup>Diagnostische und interventionelle Neuroradiologie, Universitätsmedizin Göttingen, Göttingen, Deutschland

<sup>3</sup>Neurologie, Universitätsmedizin Göttingen, Göttingen, Deutschland

<sup>4</sup>Department of Neurosurgery, Second Military Medical University, Shanghai, China

**Background:** In-hospital time delays lead to a significant deterioration of neurological outcomes in stroke patients with large-vessel occlusions (LVO). At the moment, CT perfusion is relevant in the triage of late-window stroke patients. We conducted this study to determine, whether one-stop management with perfusion is feasible and leads to a reduction of in-hospital times.

**Methods:** In this observational study, we report the first fifteen consecutive transfer stroke patients with an externally confirmed LVO, who received flat-detector CT (FDCT) perfusion and thrombectomy in the same room. Preinterventional imaging consisted of noncontrast FDCT

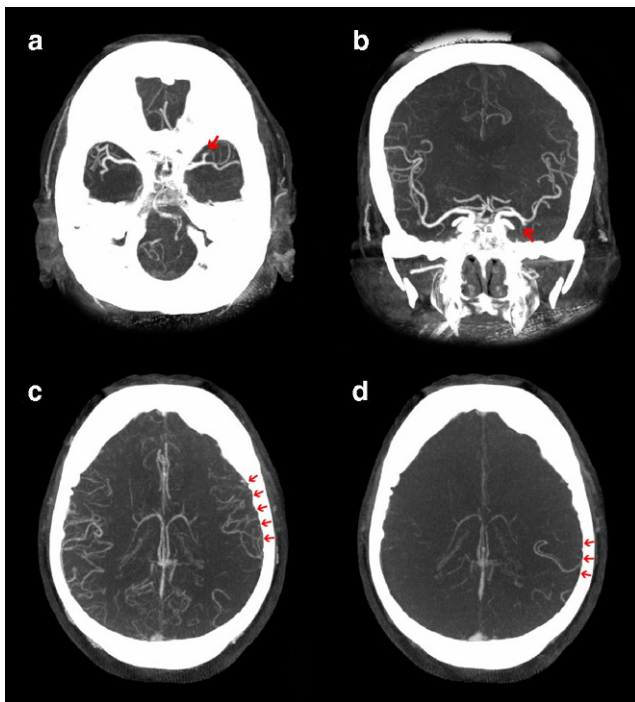


**Fig. 1 | 94** FDCT angiography for the identification of an LVO on a transversal FDCT angiography (a); on a coronal FDCT angiography (b); early phase (c) and late phase (d) collaterals

and FDCT perfusion, acquired with a biplane angio system. The FDCT perfusion was used to reconstruct an FDCT angiography to confirm the LVO. After confirmation of the LVO the patient underwent mechanical thrombectomy. We recorded time metrics and safety parameters prospectively and compared them with transfer patients, which we treated before the introduction of one-stop management with perfusion.

**Results:** Fifteen transfer patients received FDCT perfusion and were treated with mechanical thrombectomy in the time-period from June 2017 to January 2019. The median time from symptom onset to admission was 241 minutes. Median door to groin time was 24 minutes. Compared to 23 transfer patients imaged with MDCT it was reduced significantly (24 minutes (95% CI: 19–37) vs. 53 (95% CI: 44–66);  $p < 0.001$ ). Safety parameters were comparable between both groups.

**Conclusion:** In this small series, one-stop management with perfusion led to a significant reduction of in-hospital times compared to our previous workflow.

**Table 1 | 94** Baseline characteristics and time-metrics

	OneStop Perfusion (n=15)	MDCT Perfusion (n=23)	p-Value
Baseline characteristics			
Female	7	9	1
Age	78 (68–88)	68 (61–78)	0.048
NIHSS_a	15 (12–19)	18 (14–24)	0.117
Symptom to door	241 (204–282)	248 (175–327)	0.784
Time-metrics			
Door to CT	11 (8–25)	15 (11–25)	0.129
Door to groin	24 (19–34)	53 (41–69)	<0.001
CT to groin	14 (10–22)	34 (22–43)	<0.001
Door to reperfusion	76 (59–95)	97 (81–122)	0.078
CT to reperfusion	55 (47–85)	80 (63–106)	0.083
NIHSS_a	admission National Institutes of Health Stroke Scale		

**99**

**BLUTUNGSRISIKO UND KLINISCHES OUTCOME VON PATIENTEN MIT TANDEMLÄSION NACH ENDOVASKULÄRE THROMBEKTOMIE: EINE „PROPSITY SCORE MATCHING“-ANALYSE**

Dominik Sepp\*<sup>1</sup>, Claus Zimmer<sup>1</sup>, Maria Berndt<sup>1</sup>, Sebastian Mönch<sup>1</sup>, Silke Wunderlich<sup>2</sup>, Christian Maegerlein<sup>1</sup>, Tobias Boeckh-Behrens<sup>1</sup>, Benjamin Friedrich<sup>1</sup>

<sup>1</sup>Klinikum rechts der Isar, Technische Universität München, Abteilung für Diagnostische und Interventionelle Neuroradiologie, München, Deutschland

<sup>2</sup>Klinikum rechts der Isar, Technische Universität München, Neurologische Klinik und Poliklinik, München, Deutschland

**Hintergrund:** Die mechanische Thrombektomie ist mittlerweile bei akuten Schlaganfallpatienten mit einem Gefäßverschluss im vorderen Kreislauf gut etabliert. Allerdings stellen Tandemläsionen weiterhin eine Herausforderung dar mit mutmaßlich höherem Blutungsrisiko aufgrund häufig erforderlicher aggressiverer Thrombozytenaggregationshemmung (TAH).

Diese Studie untersucht das klinische Outcome und das Blutungsrisiko nach mechanischer Thrombektomie von akuten Schlaganfallpatienten mit einer Tandemläsion im Vergleich zu Patienten mit isoliertem intrakraniellen Gefäßverschluss.

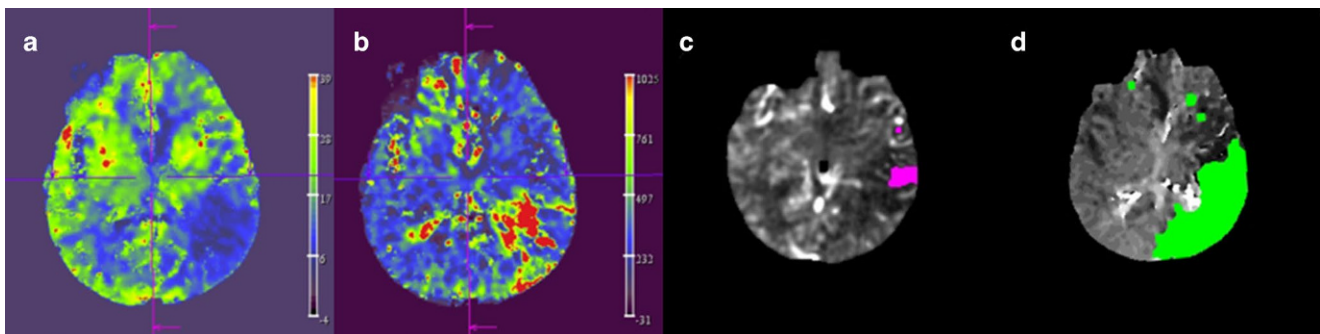


**Fig. 2 | 94** Reconstruction of the CBF (a) and MTT (b) map by the Syngo workstation and visualization of the 10 ml infarct core (c) and the 225 ml mismatch volume (d) by the RAPID Angio software solution

**Methoden:** Eingeschlossen wurden 63 konsekutive Schlaganfallpatienten mit einer Tandemläsion (proximaler Gefäßverschluss im vorderen Kreislauf sowie der ipsilateralen A. carotis interna), die in den Jahren 2014–2018 mechanisch rekanalisiert wurden. Als Kontrollen wurden 111 Schlaganfallpatienten mit einem isolierten intrakraniellen Gefäßverschluss ausgewählt nach „propensity score matching“-Analyse in einem 1:2 Verhältnis (Kovariate: Geschlecht, Alter, Einordnung als „wake-up stroke“, rtPA-Gabe und NIHSS).

**Ergebnisse:** Die Quote der erfolgreichen Rekanalisierungen (TICI 2b/3) unterschied sich in den Gruppen nicht (93 % vs 87 %,  $p=0,19$ ). Periprozedurale Komplikationen traten bei Tandemläsionen nicht häufiger auf. Obwohl Patienten mit Tandemläsion häufiger mit aggressiverer TAH behandelt wurden, ergab sich in dieser Gruppe kein schlechteres klinisches Outcome und keine erhöhte Inzidenz von symptomatischen intrakraniellen Blutungen (7,9 % vs 5,4 %,  $p=0,51$ ).

Unter den Patienten mit einer Tandemläsion war eine aggressivere TAH (Tirofiban oder doppelte TAH) nicht mit einem höheren Risiko für eine symptomatische intrakranielle Blutung assoziiert (5,6 % vs 11,1 %,  $p=0,42$ ).

**Diskussion:** Der Therapieerfolg und das Risiko einer symptomatischen intrakraniellen Blutung nach mechanischer Rekanalisation waren bei akuten Schlaganfallpatienten mit einer Tandemläsion vergleichbar mit Patienten mit einem isolierten intrakraniellen Gefäßverschluss. Die häufig notwendige aggressivere TAH bei Tandemläsionen war nicht mit einem erhöhten Risiko einer symptomatischen Blutung assoziiert.

**Fazit:** Die komplexeren technischen Anforderungen einer mechanischen Thrombektomie bei Tandemläsionen und das befürchtete höhere Blutungsrisiko durch die häufig notwendige Gabe von TAH sollten nicht zu einer zurückhaltenderen Therapie von Tandemläsionen führen, die die Chance auf ein gutes klinisches Outcome verringern könnte.

100

#### INITIAL EXPERIENCE WITH TRANSRADIAL ACCESS FOR CEREBROVASCULAR PROCEDURES: IS IT FEASIBLE AND SAFE?

Hanna Styczen<sup>\*1,2</sup>, Volker Maus<sup>3</sup>, Ioannis Tsogkas<sup>1,4</sup>, Dan Meila<sup>5</sup>, Jan-Hendrik Buhk<sup>6</sup>, Marios-Nikos Psychogios<sup>1,4</sup>

<sup>1</sup>Institut für Diagnostische und Interventionelle Neuroradiologie, Universitätsmedizin Göttingen, Göttingen, Deutschland

<sup>2</sup>Institut für Diagnostische und Interventionelle Radiologie und Neuroradiologie, Universitätsklinikum Essen, Essen, Deutschland

<sup>3</sup>Institut für Diagnostische und Interventionelle Radiologie, Neuroradiologie und Nuklearmedizin, Universitätsklinikum Knappschaftskrankenhaus Bochum, Bochum, Deutschland

<sup>4</sup>Abteilung für Neuroradiologie, Universitätsspital Basel, Basel, Schweiz

<sup>5</sup>Abteilung für Interventionelle Neuroradiologie, Johanna Etienne Krankenhaus, Neuss, Deutschland

<sup>6</sup>Abteilung für Diagnostische und Interventionelle Neuroradiologie, Universitätsklinikum Hamburg-Eppendorf, Hamburg, Deutschland

**Background:** Despite the exceptional benefit of transradial access over transfemoral access in cardiac procedures, the transition for cerebrovascular procedures has been reluctant. Here we present our experience with transradial access in cerebral diagnostic angiographies and neurointerventional procedures.

**Methods:** We performed a retrospective analysis of patients who underwent transradial access for cerebrovascular procedures in 3 German centers between February 2017 and May 2019. Demographics, technical features and complications were evaluated.

**Result:** Transradial access was successful in 40 endovascular procedures, resulting in a success rate of 89% (40/45). Selected catheterization of the intended vessels was obtained in 95% (40/42) of cases. The rate of procedure-related vascular complications was 2% (1/45).

**Discussion:** Various recent studies documented a 92.2–98.6% success rate of transradial cerebral angiography [1–4]. In the present analysis the success rate with 89% (including neurointerventional and diagnostic procedures) was slightly lower mostly due to puncture and cannulation failures. Catheterization of the intended supra-aortic vessels succeeded in 95% (40/42) patients and is comparable to rates reported in previous studies [1, 3–5].

**Conclusion:** During the initial experience with transradial access, the alternative approach proved to be safe and efficient, although a certain learning curve existed. Follow-up one-vessel cerebral angiographies via transradial access in particular could be performed on ambulatory basis prospectively.

#### References

1. Jo KW, Park SM, Kim SD, et al. Is transradial cerebral angiography feasible and safe? A single center's experience. *J Korean Neurosurg Soc.* 2010;47:332–7. <https://doi.org/10.3340/jkns.2010.47.5.332>.
2. Snelling BM, Sur S, Shah SS, et al. Transradial cerebral angiography: techniques and outcomes. *J Neurointervent Surg.* 2018;10:874–81. <https://doi.org/10.1136/neurintsurg-2017-013584>.
3. Matsumoto Y, Hongo K, Toriyama T, et al. Transradial approach for diagnostic selective cerebral angiography: results of a consecutive series of 166 cases. *Ajnr Am J Neuroradiol.* 2001;22:704–8.
4. Park JH, Kim DY, Kim JW, et al. Efficacy of transradial cerebral angiography in the elderly. *J Korean Neurosurg Soc.* 2013;53:213–7. <https://doi.org/10.3340/jkns.2013.53.4.213>.
5. Goland J, Doroszuk GF, Garbugino SL, et al. Transradial approach to treating endovascular cerebral aneurysms: Case series and technical note. *Surg Neurol Int.* 2017;8:73. [https://doi.org/10.4103/sni.sni\\_393\\_16](https://doi.org/10.4103/sni.sni_393_16).

103

#### BASILAR ARTERY OCCLUSIONS WITH WORSE OUTCOME: EARLY IDENTIFICATION OF UNDERLYING STENOSIS

Maria Berndt<sup>\*1</sup>, David Pree<sup>1</sup>, Fabian Mück<sup>2</sup>, Dominik Sepp<sup>1</sup>, Silke Wunderlich<sup>3</sup>, Claus Zimmer<sup>1</sup>, Stefan Wirth<sup>2</sup>, Christian Maegerlein<sup>1</sup>, Benjamin Friedrich<sup>1</sup>, Johannes Kaesmacher<sup>4</sup>, Tobias Boeckh-Behrens<sup>1</sup>

<sup>1</sup>Technische Universität München, Fakultät für Medizin, Klinikum rechts der Isar, Neuroradiologie, München, Deutschland

<sup>2</sup>DONAUISAR Klinikum Deggendorf, Radiologie, Deggendorf, Deutschland

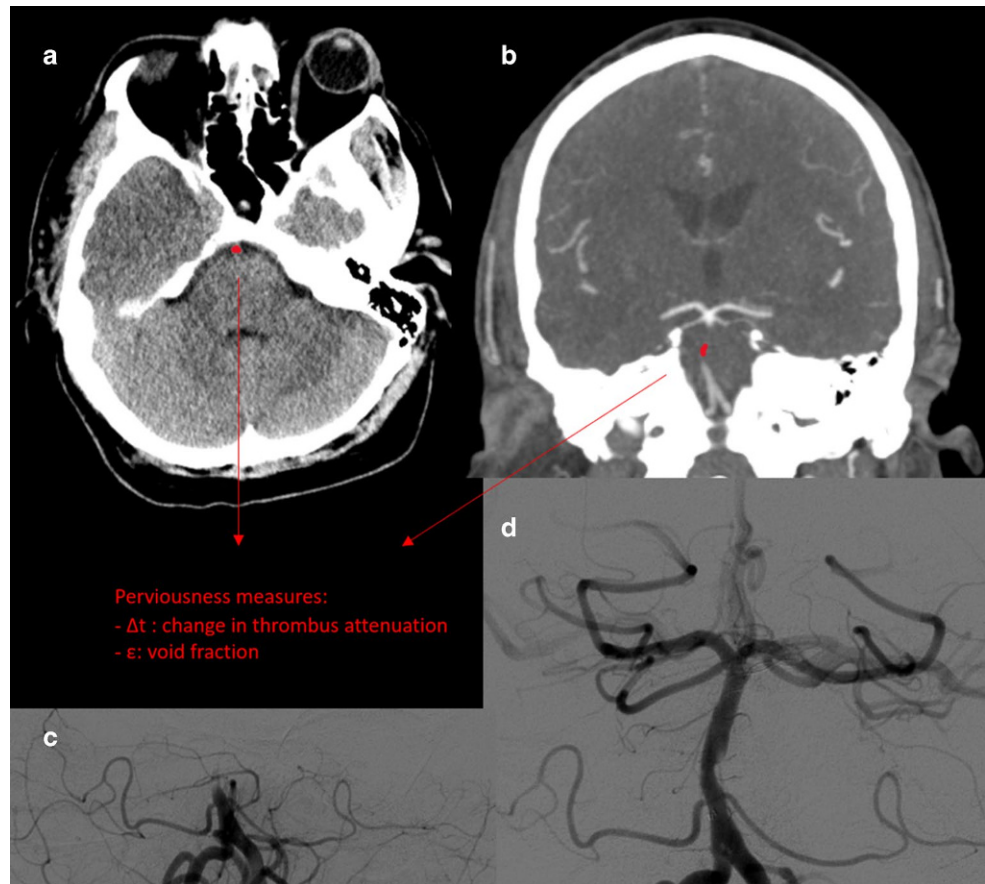
<sup>3</sup>Technische Universität München, Fakultät für Medizin, Klinikum rechts der Isar, Neurologie, München, Deutschland

<sup>4</sup>University Hospital Bern, Inselspital, Neuroradiologie, Bern, Deutschland

**Background:** Recent studies show that mechanical thrombectomy of acute basilar artery occlusions (BAO) results in high successful recanalization and good outcomes. However, the impact of pathogenesis, especially the presence of an underlying basilar stenosis (BS) is not fully understood. Aim of the study was to investigate angiographic and clinical outcome parameter for this entity and test the potential of known perviousness measures for an early identification.

**Methods:** All consecutive patients with acute BAO, treated with second-generation thrombectomy devices at a single-center between March 2008 and August 2017 ( $n=134$ ), were included. Underlying pathogenesis (basilar stenosis) was examined in respect of angiographic (complete reperfusion TICI 3) and clinical (NIHSS/MRS) outcome parameters, that were existing for  $n=115$  patients. Thrombus permeability measures (change in thrombus attenuation  $\Delta t$  and corrected void fraction  $\epsilon$ ,  $n=58$ ) were assessed in admission CT imaging and correlated to different etiological subgroups and clinical outcome (see Fig. 1).

**Fig. 1 | 103** Example of an acute basilar occlusion with underlying basilar stenosis. Assessment of perviousness measures  $\Delta t$  and  $\varepsilon$  after coalignment of native CT scan (a) and CT-angiography (b). Corresponding pre- (c) and post-thrombectomy (d) angiography in anteroposterior view



**Results:** For the BS-group, less patients were successfully recanalized (86% vs. 93% for BAO without BS) and higher NIHSS/MRS values were obtained ( $p=0.001/0.002$ ). The group of BS turned out to have significant lower native density values ( $39.9 \pm 16.1$  HU) and higher perviousness measures  $\Delta t$  ( $32.8 \pm 36.7$ ) and  $\varepsilon$  ( $0.21 \pm 0.21$ ) than thrombi without an underlying BS ( $54.8 \pm 15.2/12.8 \pm 16.7/0.07 \pm 0.10$ ,  $p=0.003/0.007/0.001$ ).

**Discussion:** Concordant to previous studies, outcome of mechanical thrombectomy of BAO depends on pathogenesis. For the subgroup of underlying basilar stenosis worse recanalization success and clinical presentation was found, that raise the need for an early identification. It was further shown, that perviousness has the potential to differentiate BAO with and without BS in admission imaging.

**Conclusion:** Perviousness may be valuable as an early imaging marker for identifying underlying basilar stenosis in acute BAO, that presents with worse angiographic and clinical performance. This could be relevant for timely therapeutic and rehabilitative decisions.

108

#### WEB + STENT ZUR BEHANDLUNG INTRAKRANIELLER ANEURYSMEN: SUPPORTIVES STENTING BEHANDELT WEB-PROTRUSIONEN IN DAS TRÄGERGEFÄß EFFEKTIV

Christin Clajus<sup>\*1</sup>, Donald Lobsien<sup>1</sup>, Joachim Klisch<sup>1</sup>

<sup>1</sup>Institut für diagnostische und interventionelle Radiologie und Neuroradiologie, Helios Klinikum Erfurt, Erfurt, Deutschland

**Hintergrund:** Zur Prävention von Aneurysmaresten und -rezidiven ist die optimale Größenauswahl eines WEB Device essenziell. Gelegent-

lich tritt eine leichte Protrusion des WEB Device an der Basis des Aneurysmas in das Trägergefäß auf, teils durch moderates Oversizing des Device bedingt. Zur Vermeidung flussrelevanter Stenosen am Trägergefäß wurde die supportive Implantation eines Stents im Rahmen der WEB-Implantation beurteilt.

**Methoden:** Von insgesamt 240 WEB Device-Implantationen (10/2010–04/2019) erforderten WEB-Protrusionen bei 14 Aneurysmapatienten (5,8 %) die zusätzliche Implantation eines Stents. In 11 Fällen (78,6 %) erfolgte die Behandlung elektiv, bei 3 Patienten (21,4 %) im Rahmen einer akuten SAB. Die behandelten intrakraniellen Aneurysmen befanden sich vor allem in der vorderen Zirkulation ( $n=9$ , 64,3 %), zu einem geringen Anteil in der hinteren Zirkulation ( $n=5$ , 35,7 %). Für diese kombinierte Technik wurden 13 Solitaire-Stents (92,9 %) und 1 LVIS jr. Stent (7,1 %) verwendet.

**Ergebnisse:** Die kombinierte Behandlung konnte in 100 % der Fälle technisch komplikationslos durchgeführt werden. Ein SAB-Patient erlitt dennoch eine frühe Re-Blutung aus einem Aneurysmarest. Dieser Patient wurde mittels Coiling nachbehandelt und zeigte ein gutes klinisches Outcome. Ein SAB-Patient (7,1 %) erlitt kleine Infarkte der hinteren Zirkulation, 1 weiterer Patient (7,1 %) ein inguinales Aneurysma. DSA-Kontrollen bei 9 Patienten (64,3 %) durchschnittlich 15 Monate nach Intervention zeigten bei 8 Aneurysmen (85,7 %) einen vollständigen Verschluss, 1 weiteres Aneurysma (11,1 %) bedurfte einer Re-Intervention aufgrund eines Rezidiv-Aneurysmas.

**Diskussion:** Die Verschlussraten der Aneurysmen in den Follow-ups liegen in dieser kleinen Fallserie über dem Durchschnitt unserer allein mit WEB Device versorgten Aneurysmen<sup>1</sup>. Nachteilig gegenüber der vorgenannten Patientengruppe erscheint die Notwendigkeit der Thrombozytenaggregation nach intrakraniell Stenting.

**Fazit:** Supportives Stenting mit WEB Device versorgter Aneurysmen ist eine technisch gut durchführbare und sichere Behandlungsmethode.

Die beschriebene Methode erweitert so das Spektrum mit WEB behandelbarer Aneurysmen.

## Literatur

- Clajus C, Strasilla C, Fiebig T, Sychra V, Fiorella D, Klisch J. Initial and mid-term results from 108 consecutive patients with cerebral aneurysms treated with the WEB device. *J Neurointerv Surg.* 2017;9(4):411–7. <https://doi.org/10.1136/neurintsurg-2016-012276>.

112

## GADOLINIUM LEAKAGE IN OCULAR STRUCTURES IN ACUTE ISCHEMIC STROKE

Alex Förster<sup>\*1</sup>, Mansour Al-Zghloul<sup>1</sup>, Holger Wenz<sup>1</sup>, Johannes Böhme<sup>1</sup>, Christoph Groden<sup>1</sup>, Angelika Alonso<sup>2</sup>

<sup>1</sup>Abteilung für Neuroradiologie, Universitätsmedizin Mannheim, Mannheim, Deutschland

<sup>2</sup>Neurologische Klinik, Universitätsmedizin Mannheim, Mannheim, Deutschland

**Hintergrund:** Gadolinium leakage in ocular structures (GLOS) on fluid attenuated inversion recovery images (FLAIR) is a novel imaging marker in acute ischemic stroke.<sup>1,2</sup> In the present study, we investigated the frequency and pattern of blood-brain barrier as well as blood-retina barrier impairment in acute ischemic stroke as demonstrated by hyperintense acute reperfusion marker (HARM) and GLOS respectively on FLAIR.

**Methoden:** From an MRI report database we identified patients with acute ischemic stroke who underwent repeated MRI with intravenous contrast agent administration. On FLAIR, the presence of HARM was assessed. Furthermore, the presence of GLOS was noted in the anterior chamber and vitreous body.

**Ergebnisse:** Overall 144 patients (mean age  $64.4 \pm 17.5$  years, 89 (61.8 %) male) were included. Of these, 120 (83.3 %) had a territorial infarction, and 24 (16.7 %) a lacunar infarction. Intravenous thrombolysis was performed in 68 (47.2 %) patients. Follow-up MRI was performed within  $33.2 \pm 21.0$  hours after the first MRI. On DWI, acute ischemic lesions were observed in the ACA (8.3 %), MCA (72.9 %), PCA (22.2 %) territory, in the brainstem (5.6 %), and the cerebellum (6.3 %). Mean ischemic lesion size was  $25.9 \pm 47.4$  ml. On contrast-enhanced FLAIR, GLOS was observed in 66 (45.8 %) patients: in 12 (8.3 %) in the anterior chamber only, and in 54 (37.5 %) in the anterior chamber and vitreous body (see Fig. 1). HARM was observed in 34 (23.6 %) patients. Presence of GLOS was significantly associated with older age ( $p=0.01$ ), and detection of HARM ( $p<0.001$ ). No significant relationship with ischemic lesion size ( $p=0.6$ ), intravenous thrombolysis ( $p=0.7$ ), or recanalization ( $p=0.2$ ) was found.

**Diskussion:** In patients with acute ischemic stroke, GLOS is a frequent finding and associated with presence of HARM, and older age. As GLOS seems to share its pathophysiology at least to some extent with HARM, it might be used as surrogate marker for blood-brain barrier impairment in acute ischemic stroke.

## References

- Förster A, Wenz H, Böhme J, Groden C, Alonso A. Asymmetrical Gadolinium Leakage in Ocular Structures in Stroke Due to Internal Carotid Artery Stenosis or Occlusion. *Clin Neuroradiol.* 2018; <https://doi.org/10.1007/s00062-018-0754-5>. Epub ahead of print.
- Förster A, Al-Zghloul M, Wenz H, Böhme J, Groden C, Alonso A. Gadolinium Leakage in Ocular Structures Is Common in Lacunar Infarction. *Stroke.* 2018; <https://doi.org/10.1161/STROKEAHA.118.023573>.

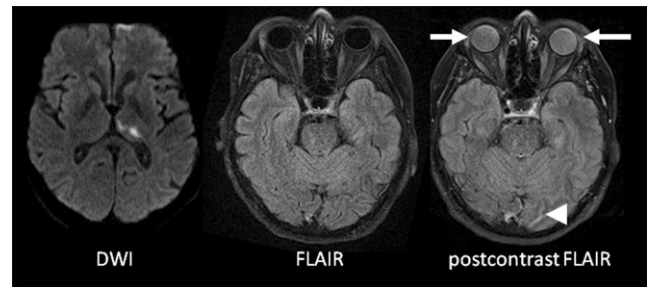


Fig. 1 | 112

115

## BESCHLEUNIGTE TIME-OF-FLIGHT MAGNETRESONANZANGIOGRAPHIE DURCH VERWENDUNG VON SPIRAL BILDAKQUISITION MIT 3 TESLA

Tobias Greve<sup>\*1</sup>, Nico Sollmann<sup>1,2</sup>, Andreas Hock<sup>3</sup>, Silke Hey<sup>3</sup>, Velmurugan Gnanaprakasam<sup>3</sup>, Marco Nijenhuis<sup>3</sup>, Claus Zimmer<sup>1</sup>, Jan Kirschke<sup>1,2</sup>

<sup>1</sup>Abteilung für Diagnostische und Interventionelle Neuroradiologie, Klinikum rechts der Isar, Technische Universität München, München, Deutschland

<sup>2</sup>TUM-Neuroimaging Center, Klinikum rechts der Isar, Technische Universität München, München, Deutschland

<sup>3</sup>Health Systems Philips Switzerland, Horgen, Schweiz

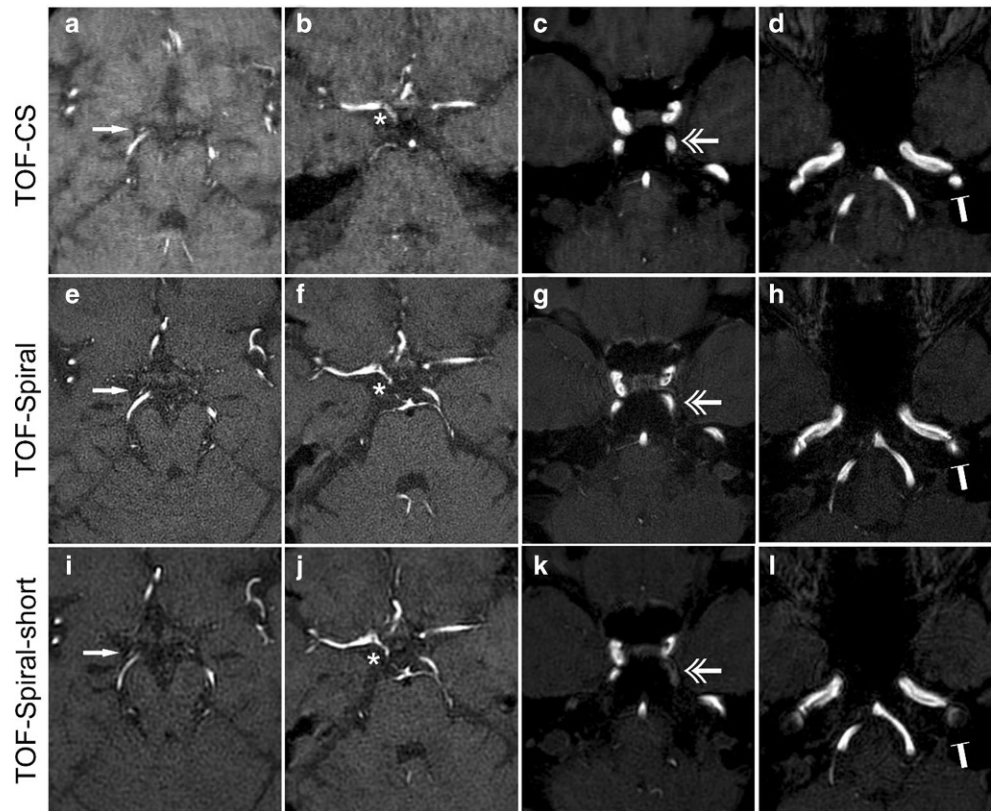
**Hintergrund:** Ziel war die systematische Bewertung der Bildqualität intra- und extrakranieller hirnversorgender Gefäße und der diagnostischen Sicherheit bei der Beurteilung von Gefäßpathologien zwischen drei Time-of-Flight Magnetresonanztomographie Sequenzen (TOF-MRA), welche auf Compressed SENSE (TOF-CS) und auf Spiral-Akquisition (TOF-Spiral) zurückgreifen.

**Methoden:** Retrospektiv wurden Patienten eingeschlossen, welche innerhalb von 8 Wochen nach Implementierung einer neuen MRT-Software, welche Spiral-Akquisition erlaubt, ein 3-Tesla MRT mit Gefäßdarstellung erhielten. Es wurden 3 TOF-MRA Sequenzen akquiriert: TOF-CS (4 min), TOF-Spiral (3 min) sowie eine schnellere „TOF-Spiral-short“ (1 min) mit eingeschränktem Field-of-View. Zwei Rater werteten verblindet zu Patienten und Sequenz die Bildqualität der Gefäße und die Erkennbarkeit von Pathologien aus.

**Ergebnisse:** In der TOF-CS waren die extrakraniellen (Fig 1., flacher Pfeil) und intraossären (Fig 1., doppelköpfiger Pfeil) Gefäßabschnitte des vorderen Kreislaufs mit weniger Artefakten dargestellt. TOF-Spiral konnte hingegen kleine intrakranielle Gefäße wie die A. choroidea anterior (Fig 1., Pfeile) und die A. communicans posterior (Fig 1., Stern) deutlicher darstellen. Die diagnostische Sicherheit zur Erkennung von Gefäßpathologien unterschied sich in TOF-Spiral und TOF-CS nicht. TOF-Spiral-short zeigte deutlich mehr Artefakte der extra- und intrakraniellen Gefäße. Insgesamt konnten jedoch alle Gefäßpathologien in allen 3 Sequenzen identifiziert werden. Die Inter-rater-Reliabilität war hoch.

**Diskussion:** TOF-CS und TOF-Spiral zeigten eine gute Bildqualität, wobei TOF-CS geringere Artefakte an der Schädelbasis aufwies und TOF-Spiral kleine intrakranielle Gefäße klarer darstellt und 25 % schneller akquiriert wird. TOF-Spiral-short ist 75 % schneller als TOF-CS, zeigte aber eine deutlich reduzierte Bildqualität im Vergleich zu TOF-CS und TOF-Spiral. Diese Sequenz bleibt jedoch nach weiterer Optimierung eine vielversprechende Methode zum schnellen Screening von Gefäßpathologien. Eine Kombination von TOF-Spiral und TOF-CS könnte in Zukunft die Nachteile beider Techniken ausgleichen und so die Akquisitionszeit weiter reduzieren.

**Abb. 1 | 115** Axiale Schichten der akquirierten TOF-MRA Sequenzen Kacheln **a, e, i** zeigen Schichten auf Höhe der A. choroidea anterior und der A. cerebelli superior. Kacheln **b, f, j** zeigen Schichten auf der Höhe des Circulus Willisii. Kacheln **c, g, k** zeigen Schichten auf Höhe des cavernösen Segments der A. carotis interna. Kacheln **d, h, l** zeigen Schichten auf der Höhe des extra-intrakraniellen Überganges am Carotiskanal



**Fazit:** TOF-CS und TOF-Spiral weisen eine hohe Bildqualität auf, wobei jede Sequenz andere Schwächen und Stärken in der Darstellung hat. Ultra-kurze TOF-Spiral Sequenzen eignen sich zum schnellen Screening von Gefäßpathologien.

117

**COMPARISON OF ENDOVASCULAR TREATMENT OF RUPTURED AND UNRUPTURED INTRACRANIAL ANEURYSMS USING THE WEB 17 (WOVEN ENDOBRIDGE) AND THE WEB 21 SYSTEM: A TWO-CENTER RETROSPECTIVE STUDY**

Isabell König<sup>\*1</sup>, Christoph Maurer<sup>2</sup>, Ansgar Berlis<sup>2</sup>, Werner Weber<sup>1</sup>, Sebastian Fischer<sup>1</sup>

<sup>1</sup>Universitätsklinikum Knappschafts-Krankenhaus Bochum, Bochum, Deutschland

<sup>2</sup>Universitätsklinikum Augsburg, Augsburg, Deutschland

**Hintergrund:** Many studies already verified the safety and effectiveness of the older generation Woven Endobridge (WEB) which need the VIA 21 microcatheter. Single studies reported about the newest generation of WEB 17, a smaller device with less and finer wires [1–3].

**Methoden:** Between August 2014 and May 2019 70 intracranial aneurysms in 69 patients were treated with the WEB 21 system and 137 intracranial aneurysms in 126 patients were treated with the WEB 17 system in two German centers. We retrospectively compared the safety and angiographic outcomes of the WEB 21 system and the new WEB 17 system.

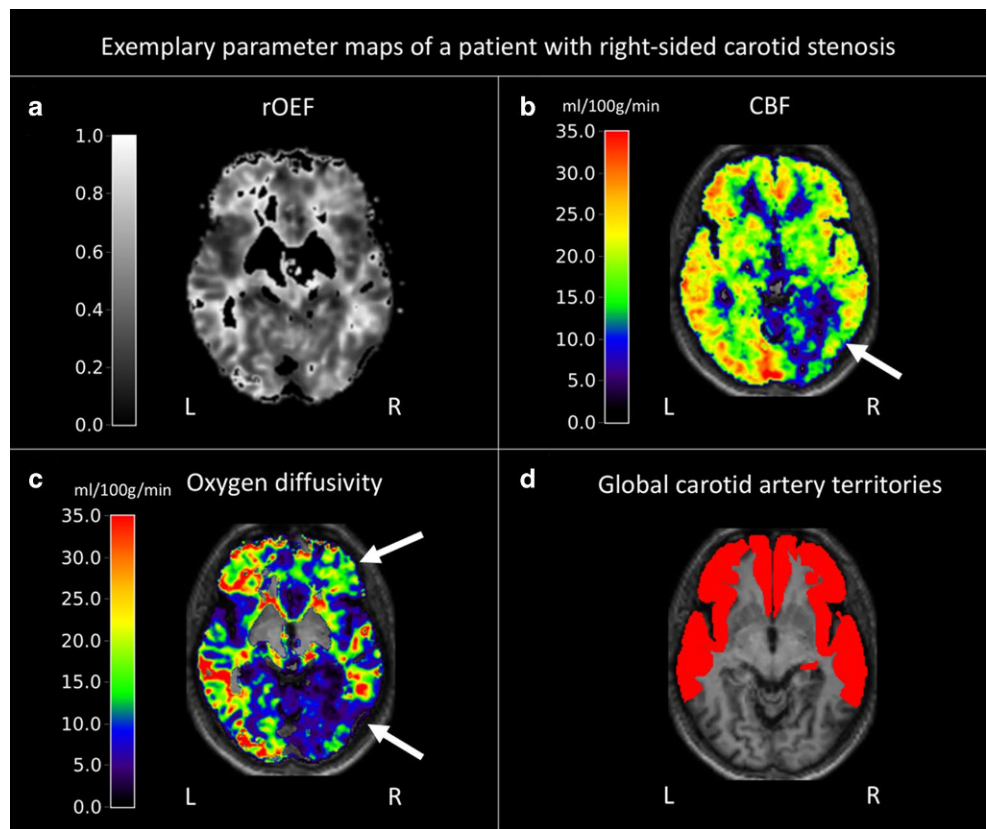
**Ergebnisse:** In 66 of 70 cases the Implantation of WEB 21 system and in 134 of 137 cases of WEB 17 system was successfully. Additional devices were necessary in 9 cases (13,6%) of WEB 21 group and in 16 cases (11,9%) of WEB 17 group. 5 (7,6%) thromboembolic complications were counted at WEB 21 and 7 (5,2%) at WEB 17. To date

the angiographic outcome shows a complete/adequate occlusion rate of 68,5%/87,0% in the WEB 21 and 74,2%/88,8% of the WEB 17 group. **Fazit:** In summary the WEB 17 is at least as safe and effectively as the WEB 21. The most important advantage of WEB 17 is the possibility to treat smaller and more distal located intracranial aneurysms with less complications and promising occlusion rates. The results support the positive development of the WEB device and demonstrate the possibility to treat successfully even more aneurysms in the future.

**References**

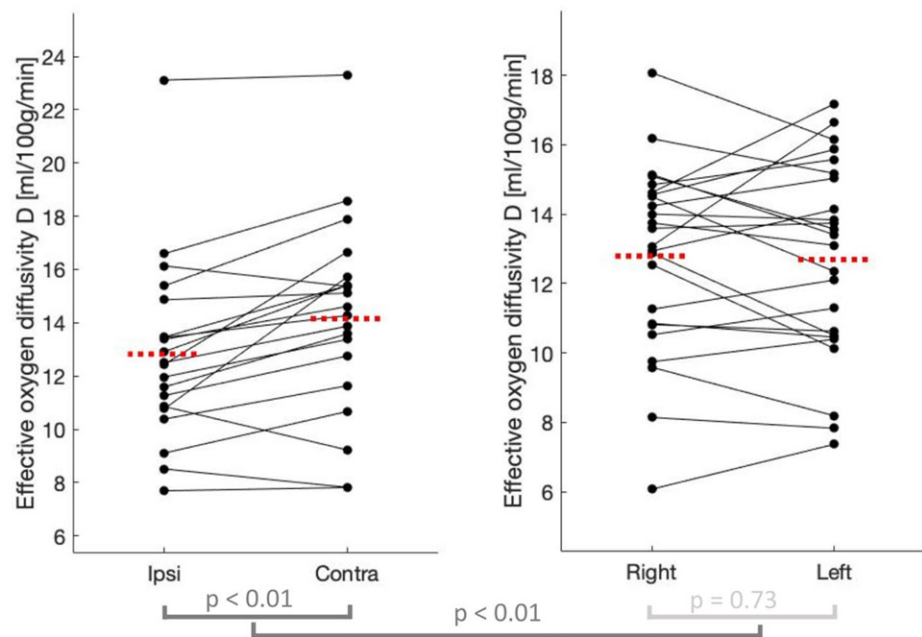
1. Arthur AS, Molyneux A, Coon AL, Saatci I, Szikora I, Baltacioglu F, et al. The safety and effectiveness of the Woven EndoBridge (WEB) system for the treatment of wide-necked bifurcation aneurysms: Final 12-month results of the pivotal WEB Intracranial Therapy (WEB-IT) Study. *J Neurointerv Surg.* 2019; <https://doi.org/10.1136/neurintsurg-2019-014815>.
2. Popielski J, Berlis A, Weber W, Fischer S. Two-Center Experience in the Endovascular Treatment of Ruptured and Unruptured Intracranial Aneurysms Using the WEB Device: A Retrospective Analysis. *AJNR Am J Neuroradiol.* 2018;39(1):111–7. <https://doi.org/10.3174/ajnr.A5413>.
3. van Rooij SBT, Peluso JP, Sluzewski M, Kortman HG, van Rooij WJ. The New Low-Profile WEB 17 System for Treatment of Intracranial Aneurysms: First Clinical Experiences. *AJNR Am J Neuroradiol.* 2018;39(5):859–63. <https://doi.org/10.3174/ajnr.A5608>.

**Fig. 1 | 121 a-d: Exemplary parameter maps of a patient with right-sided carotid stenosis** Oxygen extraction fraction (rOEF, a), cerebral blood flow (CBF, b), oxygen diffusivity (d, c) and carotid artery territories used for group-level analysis (d). CBF and diffusivity are ipsilaterally decreased (arrows). **e-f: Paired scatterplot of oxygen diffusivity lateralization.** Diffusivity is ipsilaterally decreased in ICAS (t-test,  $p < 0.01$ ) and symmetrical in HC ( $p = 0.73$ ). Lateralization is also significantly different between ICAS and HC (two-sample-test,  $p < 0.01$ )



**Lateralization of oxygen diffusivity within the carotid arteries' territories in GM**

**e ICAS patients** **f Healthy controls**



121

**MRI-BASED ASSESSMENT OF IMPAIRED OXYGEN DIFFUSIVITY IN ASYMPTOMATIC INTERNAL CAROTID ARTERY STENOSIS**

Jan Kufer\*<sup>1</sup>, Jens Göttler<sup>1,2,3</sup>, Claus Zimmer<sup>1</sup>, Fahmeed Hyder<sup>2</sup>, Christine Preibisch<sup>1,4</sup>, Stephan Kaczmarz<sup>1,2</sup>

<sup>1</sup>Klinikum rechts der Isar, Technische Universität München, Abteilung für Diagnostische und Interventionelle Neuroradiologie, München, Deutschland

<sup>2</sup>MRRC, Yale University, New Haven, CT, United States

<sup>3</sup>Klinikum rechts der Isar, Technische Universität München, Institut für Diagnostische und Interventionelle Radiologie, München, Deutschland

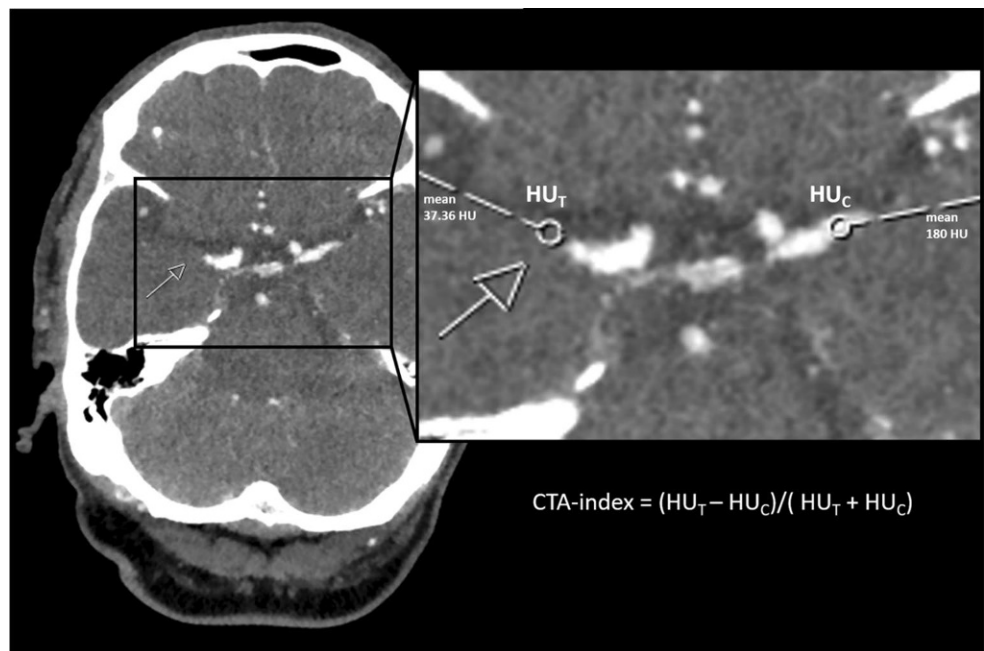
<sup>4</sup>Klinikum rechts der Isar, Technische Universität München, Neurologische Klinik und Poliklinik, München, Deutschland

**Background:** Even supposedly ‘asymptomatic’ internal carotid artery stenosis (ICAS) patients without stroke signs have been shown to suffer from cognitive<sup>1</sup> and hemodynamic impairments,<sup>2-4</sup> which may be associated with microvascular dysfunction. A highly promising biomarker of microvascular integrity is the oxygen diffusivity of the capillary bed,<sup>5,6</sup> which may help to select patients who benefit from revascularization treatment in order to delay cognitive decline. Here we apply a novel MR-based approach to assess oxygen diffusivity in asymptomatic ICAS patients and healthy controls (HC).

**Methods:** We performed MRI in 59 participants (29 asymptomatic, unilateral ICAS patients, age = 70.1 ± 4.8 y, and 30 age-matched HC, age = 70.3 ± 7.3 y) on a Philips 3T Ingenia. Normalized maps of relative oxygen extraction fraction (rOEF) were obtained following the mqBOLD approach,<sup>7</sup> while pCASL yielded cerebral blood flow (CBF). Maps of relative oxygen diffusivity (D) were calculated voxel-wisely following the Hyder-model<sup>5</sup> with  $D = -CBF \times \ln(1 - rOEF)$ . Lateralization of rOEF, CBF and D between both hemispheres was investigated in GM within the carotid arteries’ perfusion territories<sup>8</sup> in ICAS and HC.

**Results:** Fig. 1a-d shows exemplary parameter maps of an ICAS patient. While rOEF was not significantly lateralized in the patient group (t-test,  $p = 0.81$ ), both CBF and diffusivity were significantly decreased ipsilateral to the stenosis (t-test,  $p < 0.01$ , Fig. 1e). For HC, all parameters were symmetrically distributed (Fig. 1 f).

**Fig. 1 | 125** Example of CTA-index assessment for a patient that underwent admission CTA imaging of an acute occlusion of the right middle cerebral artery within the M1 segment. The ROIs for measurements of mean HU were placed 1.5 mm behind the occlusion site (T) and at a corresponding position of the contralateral, not occluded vessel (C)



**Discussion:** We successfully obtained oxygen diffusivity maps. Significantly decreased oxygen diffusivity and CBF was found in ICAS patients. Notably, diffusivity decreases were distributed more diffusely than hemodynamic reductions. This apparent diffusivity-perfusion mismatch points to oxygen permeability disturbances at the microvasculature level, providing novel insights into disease mechanisms.

**Conclusion:** Our proposed MR-based diffusivity mapping approach is sensitive to microvascular impairments in ICAS and facilitates new pathophysiological insights with high clinical potential to evaluate impairments before treatment, as well as their recovery after revascularization treatment.

**References**

1. Göttler, JCBFM(2018a)
2. Kaczmarz, ISMRM(2019)
3. Göttler, JCBFM(2018b)
4. Bouvier, HBM(2015)
5. Hyder, JApplPhysiol(1998)
6. Germuska, Neuroimage(2019)
7. Hirsch, NMR Biomed(2014)
8. Tatu, Neurology(1998)

125

**CT-MEASURING OF THROMBUS PERVIOUSNESS IN ACUTE STROKE PATIENTS**

Maria Berndt\*<sup>1</sup>, Fabian Mück<sup>2</sup>, Johannes Kaesmacher<sup>3</sup>, Sebastian Mönch<sup>1</sup>, Claus Zimmer<sup>1</sup>, Silke Wunderlich<sup>4</sup>, Stefan Wirth<sup>2</sup>, Christian Maegerlein<sup>1</sup>, Benjamin Friedrich<sup>1</sup>, Tobias Boeckh-Behrens<sup>1</sup>

<sup>1</sup>Technische Universität München, Fakultät für Medizin, Klinikum rechts der Isar, Neuroradiologie, München, Deutschland

<sup>2</sup>DONAUISAR Klinikum Deggendorf, Radiologie, Deggendorf, Deutschland

<sup>3</sup>University Hospital Bern, Inselspital, Neuroradiologie, Bern, Schweiz

<sup>4</sup>Technische Universität München, Fakultät für Medizin, Klinikum rechts der Isar, Neurologie, München, Deutschland

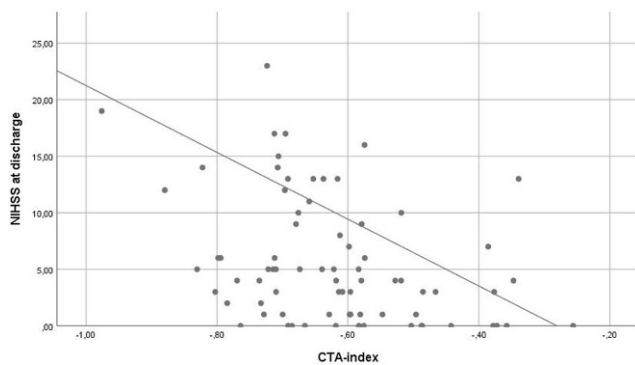


**Fig. 2 | 125** Graph show the association of CTA-index to clinical outcome (NIHSS at discharge) within the validation cohort: CTA-index (lower values mean lower relative thrombus attenuation as surrogate for lower perviousness) is negatively correlated to NIHSS at discharge. NIHSS National Institute of Health Stroke Scale

**Background:** Thrombus features in admission CT imaging are useful imaging markers for clot characterization, stroke pathogenesis and outcome prediction. In this context, thrombus perviousness is a promising parameter, but assessment in daily clinical practice is demanding. Aim of the present study is to evaluate an easy to assess measuring method at the time of admission for utilization in clinical practice.

**Methods:** CTA-index, measuring relative thrombus attenuation in CTA admission imaging (see Fig. 1), was compared to the known perviousness parameter ‘void fraction’ in a collective of 101 patients with large-vessel occlusions (LVO) of the middle cerebral artery (MCA) and correlated to clinical outcome (MRS after 90 days). For validation, an association between CTA-index and outcome measurements (NIHSS/MRS) was assessed in a second, independent cohort ( $n=87$ ).

**Results:** In the first cohort, a coherence between void fraction and CTA-index was shown ( $r=0.3$ ,  $p=0.005$ ) and CTA-index differed significantly between favorable (MRS after 90 days  $\leq 2$ ,  $-0.55 \pm 0.16$ ) and non-favorable outcome (MRS after 90 days  $> 2$ ,  $-0.64 \pm 0.14$ ,  $p=0.01$ ). In the validation cohort, this result could be independently reproduced ( $-0.52 \pm 0.13$ – $-0.70 \pm 0.09$ ,  $p<0.01$ ) by two independent raters. CTA-index is negatively correlated to NIHSS at discharge ( $r=-0.29$ ,  $p=0.007$ , see Fig. 2) and significantly predicts favorable MRS after 90 day in a logistic regression model ( $\beta=20.46$ ,  $p<0.001$ ).

**Discussion:** CTA-index is an easy to assess imaging parameter in admission imaging at the acute stroke phase for daily clinical practice and is useful as predictor of clinical outcome. It can be considered as equivalent measuring method for thrombus perviousness that is known to provide useful information for further stroke progress and clinical course as well as therapeutic and rehabilitative decisions.

**Conclusion:** CTA-index is introduced as a new imaging parameter and simplified measurement to perviousness within acute stroke admission imaging, that has the potential to serve as additional prediction marker for clinical outcome.

127

### MECHANICAL RECANALIZATION OF ACUTE ISCHEMIC STROKE: A CONSECUTIVE SINGLE-CENTER STUDY ON THE IMPACT OF BALLOON GUIDE CATHETER USAGE ON MICROSTRUCTURAL PENUMBRA INTEGRITY

Maria Berndt<sup>\*1</sup>, Christian Maegerlein<sup>1</sup>, Tobias Boeckh-Behrens<sup>1</sup>, Silke Wunderlich<sup>2</sup>, Claus Zimmer<sup>1</sup>, Sebastian Mönch<sup>1</sup>, Fabian Mück<sup>3</sup>, Stefan Wirth<sup>3</sup>, Johannes Kaesmacher<sup>4</sup>, Benjamin Friedrich<sup>1</sup>

<sup>1</sup>Technische Universität München, Fakultät für Medizin, Klinikum rechts der Isar, Neuroradiologie, München, Deutschland

<sup>2</sup>Technische Universität München, Fakultät für Medizin, Klinikum rechts der Isar, Neurologie, München, Deutschland

<sup>3</sup>DONAUISAR Klinikum Deggendorf, Radiologie, Deggendorf, Deutschland

<sup>4</sup>University Hospital Bern, Inselspital, Neuroradiologie, Bern, Schweiz

**Background:** While the association between reperfusion success, applied interventional technique, macrostructural ischemia and clinical outcome after mechanical recanalization of acute ischemic stroke is clear, the impact of microstructural ischemic processes within the salvaged penumbra was not studied yet.

Aim of the study was to analyze possible microstructural penumbra alterations in respect of reperfusion success, BGC (balloon guide catheter)-application utilizing its proximal flow arrest and clinical outcome.

**Methods:** All patients that underwent mechanical recanalization of a large intracranial vessel occlusion of the anterior circulation between April 2016 and December 2018 ( $n=439$ ) were included. Usage of BGC, angiographic as well as the clinical outcome was recorded. For the final study cohort with existing admission CT-perfusion and MRI within three days ( $n=65$ ), microstructural integrity was assessed by diffusion tensor imaging (Fig. 1). DTI data were used to determine MD (mean diffusivity)-index within the salvaged grey matter of the formerly penumbra. Finally, MD-index was correlated to reperfusion success, usage of BGC and clinical outcome.

**Results:** MD-index was higher for completely recanalized patients as well as for the BGC group ( $0.010 \pm 0.035$  vs. nBGC:  $-0.015 \pm 0.027$ ,  $p=0.04$ ). The Spearman correlation coefficient between MD-index and NIHSS/NIHSS-improvement was  $r=-0.33/0.41$  ( $p=0.04/0.01$ ). MD-index was associated with MRS after 90 days in a linear regression model ( $\beta=18.58$ ,  $p=0.04$ ). Considering the whole study group, both the MD-index and volume of infarction mediated the relationship between recanalization success and clinical outcome (Fig. 2).

**Discussion:** Differences in the microstructural integrity of the salvaged penumbra were found early after mechanical recanalization dependent on reperfusion success. Furthermore, a higher MD-index within the salvaged penumbra was observed with the use of BGC, that means less microstructural ischemia.

**Conclusion:** Thus, the interventional technique impacts the occurrence of microstructural ischemia, that is associated with neurological and functional deficits, underlining their potential clinical importance.

129

### FIBER INTEGRITY AND CLINICAL OUTCOME AFTER THROMBECTOMY IN PATIENTS WITH DIFFERENT MEDIA INFARCTS

Maria Berndt<sup>\*1</sup>, Dominik Pürner<sup>2</sup>, Claus Zimmer<sup>1</sup>, Silke Wunderlich<sup>2</sup>, Sebastian Mönch<sup>1</sup>, Stefan Wirth<sup>3</sup>, Fabian Mück<sup>3</sup>, Johannes Kaesmacher<sup>4</sup>, Christian Maegerlein<sup>1</sup>, Benjamin Friedrich<sup>1</sup>, Tobias Boeckh-Behrens<sup>1</sup>

<sup>1</sup>Technische Universität München, Fakultät für Medizin, Klinikum rechts der Isar, Neuroradiologie, München, Deutschland

<sup>2</sup>Technische Universität München, Fakultät für Medizin, Klinikum rechts der Isar, Neurologie, München, Deutschland

<sup>3</sup>DONAUISAR Klinikum Deggendorf, Radiologie, Deggendorf, Deutschland

<sup>4</sup>University Hospital Bern, Inselspital, Neuroradiologie, Bern, Deutschland

**Background:** Impairment of fiber integrity of the corticospinal tract (CST) after ischemic stroke has been described, predominantly in the subacute and chronic phase showing an association with poor motor outcome. However, outcome predictions are especially valuable in the acute stroke phase, and the impact of acute CST alterations on clinical course is not clarified yet, especially regarding the increasing occurrence of basal ganglia infarction (BGI).

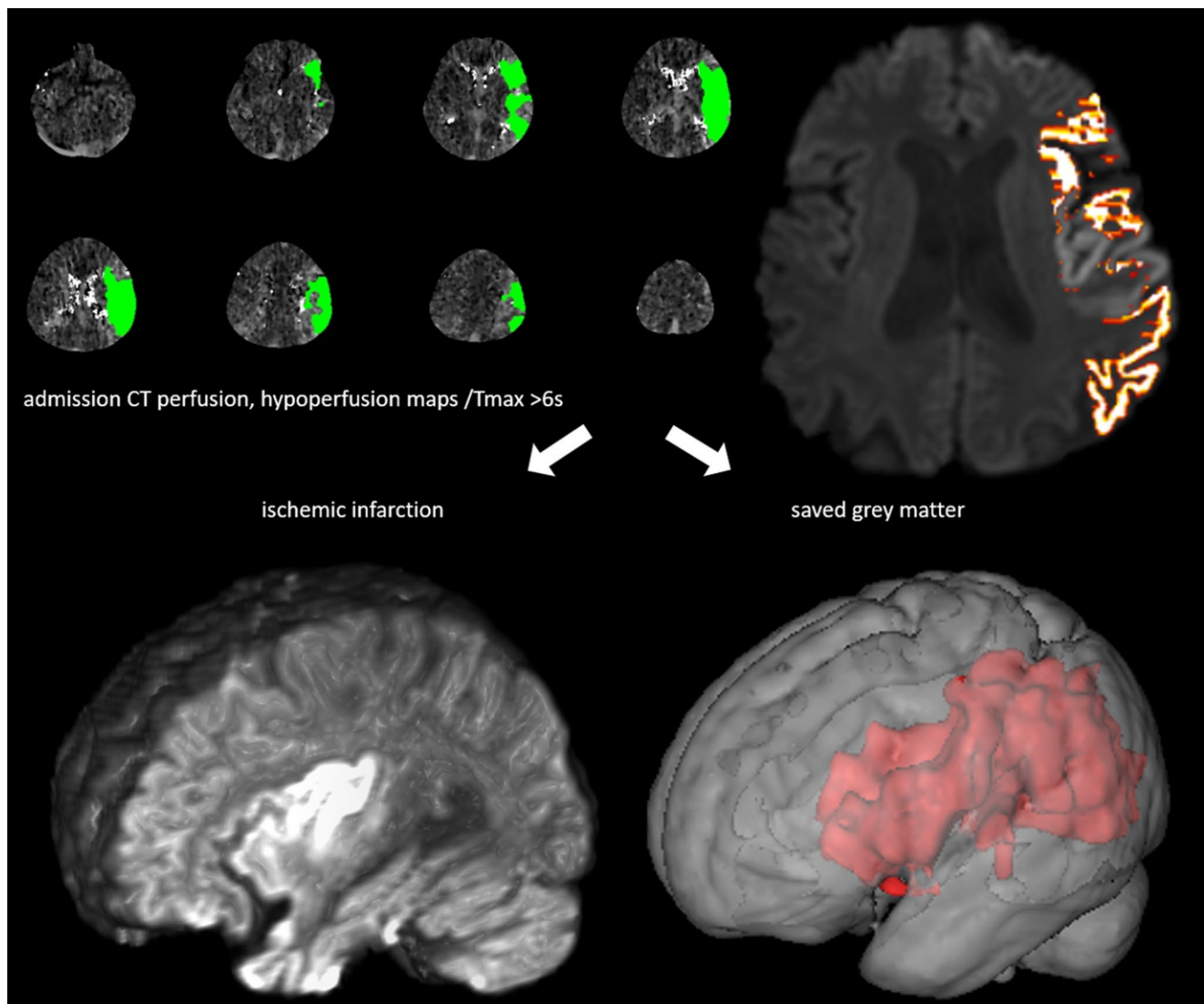


**Fig. 1 | 127** The tissue at risk (penumbra) in admission CT perfusion imaging (maps generated by RAPID software) was co-registered to MRI scan, including DTI sequence, within three days after mechanical thrombectomy of acute occlusions of the anterior circulation. Penumbra was classified in ischemic infarction, segmented in diffusion weighted imaging, and saved grey matter; that was further analyzed in respect of microstructural changes by calculation of MD-index in DTI images

**Methods:** In the acute phase (day 3) after mechanical recanalization of a large intracranial vessel of the anterior circulation 165 patients were examined with diffusion tensor imaging and the CST was reconstructed by probabilistic fibertracking (Fig. 1). FA-index within the posterior limb of the Capsula interna (CIP) was calculated and correlated to clinical parameters (NIHSS/MRS-Score). Subgroup analyses focused on BGI ( $n=59$ ) versus peripheral infarcts ( $n=106$ ).

**Results:** FA-index of the CST within CIP is reduced in the acute stroke phase (Fig. 2) and correlated to clinical presentation (e. g. NIHSS-motor subscore ( $r=-0.28$ ,  $p<0.001$ )). FA-index can significantly predict MRS (at 90 days,  $\beta=0.33$ ,  $p<0.001$ ), moderated by stroke subtype with significant effects for peripheral infarcts ( $-11.0$ ,  $p<0.0001$ ), but not for BGI ( $-0.9$ ,  $p=0.61$ ). Within the group of peripheral infarcts, FA-index mediates the association between infarction severity and clinical outcome after 90 days (Fig. 3).

**Discussion:** In large intracranial vessel occlusions of the anterior circulation the previously described predictive value of structural CST abnormalities is already observable even in an early stage after me-

chanical recanalization, increasing its clinical value for further therapeutic and rehabilitative strategies. This association seems to be only true for peripheral infarcts, but not for the increasingly occurring BGI after thrombectomy.

**Conclusion:** Early CST alterations can predict outcome for peripheral media infarcts, underlining their potential clinical importance. This prediction capacity is absent for BGI, that requires further and longitudinal exploration of fiber integrities with respect to reversibility and processes of neuroplasticity.

**Fig. 2 | 127** Imaging parameters such as volume of infarction and grey matter integrity of the saved tissue (measured by MD-index of DTI imaging within three days after mechanical thrombectomy of acute occlusions of the anterior circulation) significantly mediate the effect of reperfusion success (measured by TICI) on the clinical presentation (measured by percental improvement of NIHSS); the covariates age/sex and time between recanalization and MRI scan showed no significant influence in the analysis

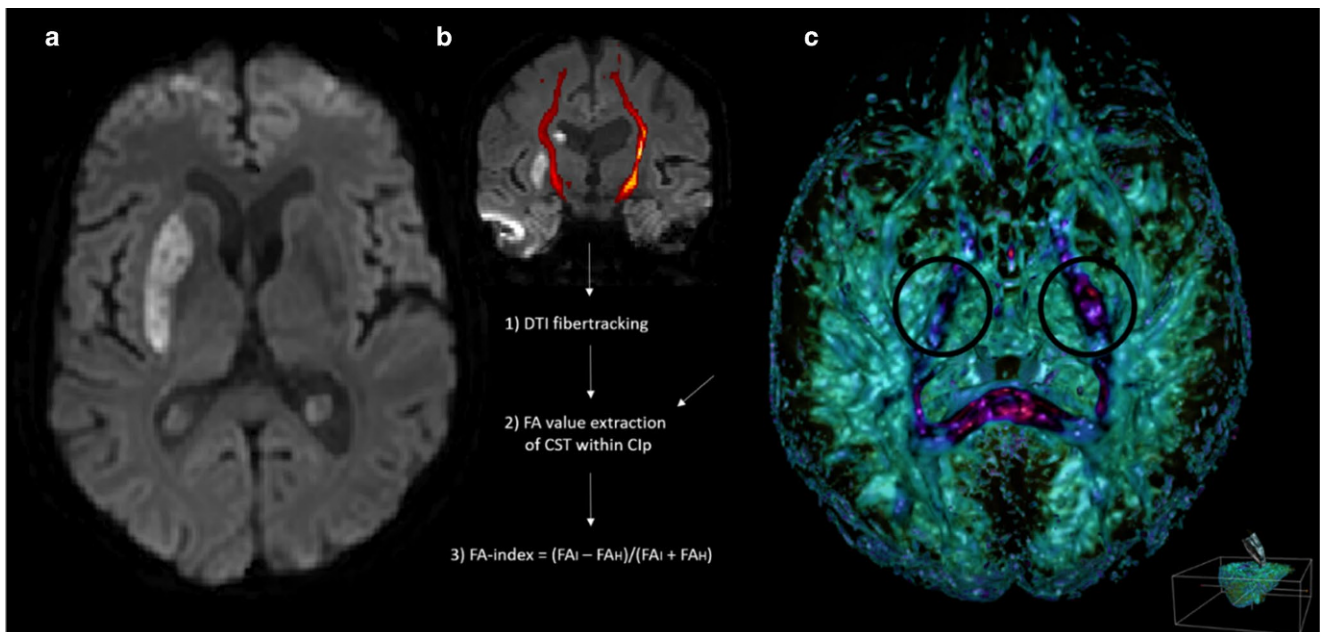
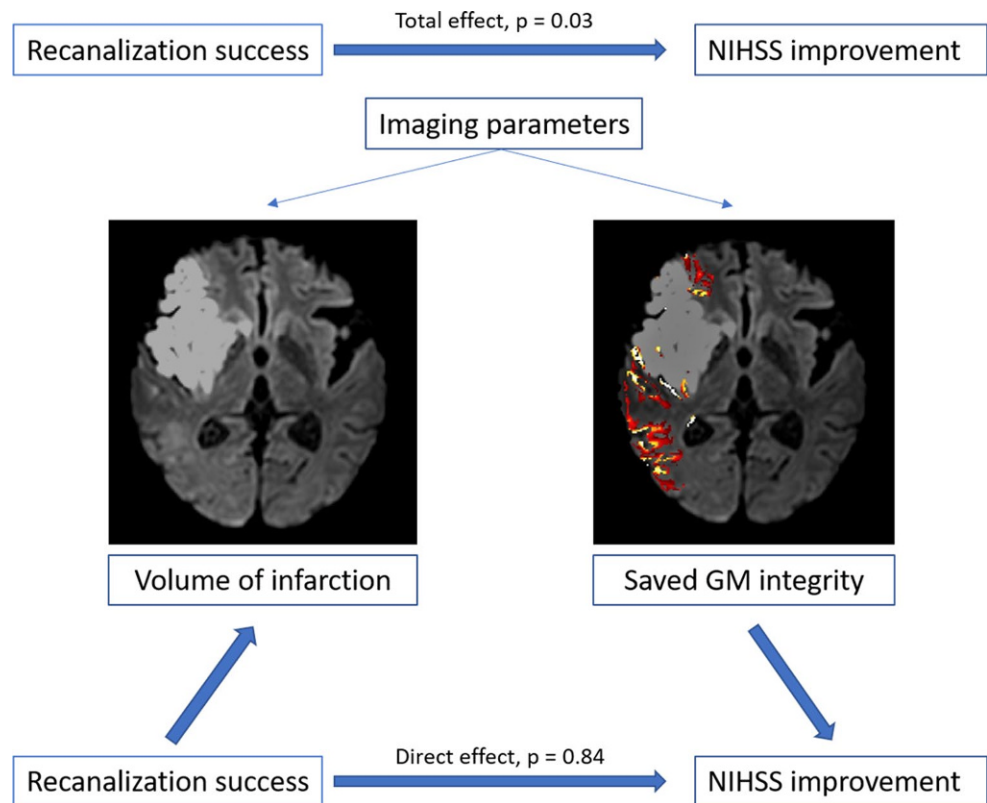


**Fig. 1 | 129** An example of a patient three days after mechanical recanalization of a right MCA occlusion and basal ganglia infarct (a) The tracked corticospinal tract (CST), overlaid on the reconstructed DWI trace picture, shows higher connectivity values (yellow) on the healthy side (left) than on the affected right side (b), increasing connectivity values from red to yellow). Higher FA-values of the CST within the posterior limb of the internal capsule (Clp) are found for the infarcted (I) in comparison to the healthy, non-affected side (H), see c

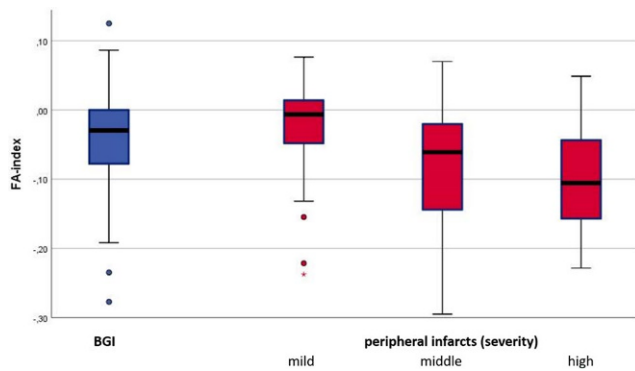


**Fig. 2 | 129** Boxplots of FA-index of the CST within the posterior limb of the internal capsule (Cpi) for the different stroke subtypes (basal ganglia infarction [BGI], peripheral infarction further divided into infarction severity [mild: below 1/3, middle: between 1/3 and 2/3, high: above 2/3 of the media territory])

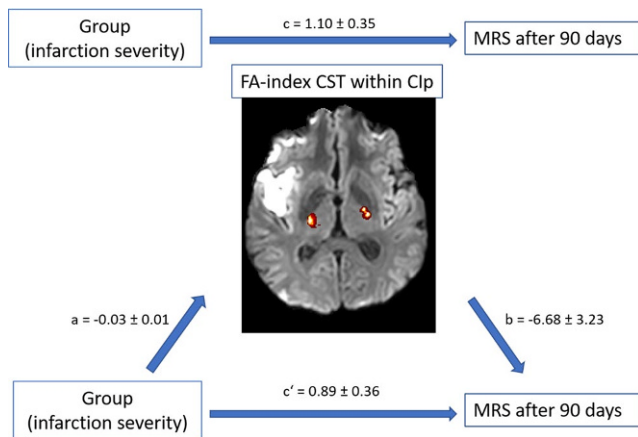


**Fig. 3 | 129** For the subgroup of peripheral infarcts, FA-index of the corticospinal tract (CST) within the posterior limb of the internal capsule (Cip) significantly mediates the effect of infarction severity (measured by ischemic demarcation) on the clinical outcome (measured by MRS after 90 days)

**130**

**STROKE LESION TOPOGRAPHY AND ITS RELATION TO SEVERITY OF NIHSS AND EARLY RECOVERY POTENTIAL IN ACUTE LEFT MCA ISCHEMIA**

Jessica Jesser<sup>\*1</sup>, Bianca Dinse<sup>1</sup>, Martin Bendszus<sup>1</sup>

<sup>1</sup>Universitätsklinikum Heidelberg, Neuroradiologie, Heidelberg, Deutschland

Stroke lesion topography and its relation to severity of NIHSS and early recovery potential in acute left MCA ischemia

**Background:** It has been shown that stroke lesion size alone only poorly predicts the clinical situation and recovery potential of acute stroke patients. This study aims to improve predictions on severity of neurological symptoms and early recovery potential by taking lesion topography into account.

**Methods:** Patients were included when suffering from acute left-sided media infarction without DWI (diffusion weighted imaging)—PWI (perfusion weighted imaging)—mismatch. Furthermore NIHSS-Scores at admission and two days after stroke were assessed.

DWI lesions were manually segmented. Recovery Score was defined as “0” if there was no improvement of the NIHSS at admission and at 48 hours after admission, as “1” if there was only minor improvement and as “2” if there was more than 5 points improvement for initial NIHSS > 10, more than 2 points improvement for initial NIHSS of 5–10 and at least 1 point improvement for initial NIHSS of < 5.

**Results:** 75 patients were included into the analysis of acute NIHSS scores. 49 patients were analyzed for early recovery potential. Voxel-based lesion symptom (VLSM) analysis revealed five critical regions associated with high NIHSS Scores: two of them cortically situated—in the left pars triangularis of the frontal inferior gyrus and in the left supramarginal gyrus, three of them subcortically—in the anterior and dorsal centrum semiovale and in the corona radiata. Patients with no lesions in critical brain areas showed the best early recovery potential followed by patients with only cortical lesions, even if situated in the predefined critical regions. Patients with both subcortical and cortical lesions or only subcortical lesions showed a significantly worse early recovery than the groups aforementioned.

**Discussion:** Our results indicate that especially lesions in integrative white matter regions cause high NIHSS Scores in the acute stage of the disease and limit early recovery potential. Cortical lesions in the Pars triangularis and in the supramarginal gyrus cause high NIHSS scores in the acute stage, but if not associated with white matter lesions show a very high recovery potential, probably via early cortical reorganization mechanisms.

**Conclusion:** Lesion location is most relevant when correlating image information with acute NIHSS and when predicting early recovery potential.

**132**

**THROMBOZYPENIE UND ABFALL DER THROMBOZYTENZAHL – PRÄDIKTOREN FÜR MORTALITÄT UND KLINISCHES OUTCOME NACH MECHANISCHER REKANALISATION**

Sebastian Mönch<sup>\*1</sup>, Tobias Boeckh-Behrens<sup>1</sup>, Kornelia Kreiser<sup>1</sup>, Philipp Blüm<sup>2</sup>, Dennis Hedderich<sup>1</sup>, Christian Maegerlein<sup>1</sup>, Maria Berndt<sup>1</sup>, Silke Wunderlich<sup>3</sup>, Claus Zimmer<sup>1</sup>, Benjamin Friedrich<sup>1</sup>

<sup>1</sup>Abteilung für diagnostische und interventionelle Neuroradiologie, Klinikum rechts der Isar, Technische Universität München, München, Deutschland

<sup>2</sup>Klinik für Hämatonkologie, Klinikum rechts der Isar, Technische Universität München, München, Deutschland

<sup>3</sup>Klinik für Neurologie, Klinikum rechts der Isar, Technische Universität München, München, Deutschland

**Hintergrund:** Der akute ischämische Schlaganfall hat gutuntersuchte Risikofaktoren. Die Bedeutung der Thrombozyten bei Patienten, die mittels mechanischer Thrombektomie behandelt wurden, ist jedoch bisher nicht untersucht worden. Das Ziel dieser Studie war zu untersuchen, ob eine Assoziation zwischen einer vorbestehenden Thrombozytopenie bei Aufnahme oder einem Abfall der Thrombozytenzahl im Verlauf der Hospitalisierung mit dem klinischem Outcome, der Mortalität oder von intrakraniellen Blutungen bei akuten Schlaganfallpatienten, die mittels mechanischer Thrombektomie behandelt wurden, besteht.

**Methoden:** In einer Fall-Kontroll-Studie wurden konsekutive mechanisch rekanalisierte Patienten analysiert. Eine multivariate logistische Regressionsanalyse wurde verwendet, um gutes klinisches Outcome (mRS 90 Tage  $\leq 2$ ) und Mortalität adjustiert für Alter, NIHSS bei Aufnahme, Vorbehandlung mit intravenöser Lyse/Statinen/Thrombozyteninhibitoren, Okklusionsstelle, Zeit vom Symptombeginn bis zur Rekanalisation, vorbestehender Thrombozytopenie bei Aufnahme ( $< 150 \times 10^9/L$ ) und einem deutlichen Abfall der Thrombozytenzahl ( $> 26\%$ ) zu untersuchen. Zudem wurden die Raten von intrakraniellen Blutungen verglichen.

**Ergebnisse:** Von 294 eingeschlossenen Patienten hatten 9.6 % eine vorbestehende Thrombozytopenie bei Aufnahme und 23.8 % einen Abfall der Thrombozytenzahl im Verlauf von >26 %. Die Mortalitätsrate bei Patienten mit normwertigen Thrombozytenzahlen bei Aufnahme war 26.1 % vs. 48.3 % ( $p=0.002$ ) bei Patienten mit einer vorbestehenden Thrombozytopenie bei Aufnahme mit einer aOR of 3.47 (CI 1.28–9.4,  $p=0.005$ ), wohingegen keine Unterschiede bei gutem klinischen Outcome ( $p=0.204$ ) und den Raten von intrakraniellen Blutungen ( $p=0.180$ ) vorlagen. Ein deutlicher Abfall der Thrombozytenzahl von mehr als 26 % in den ersten fünf Tagen der Hospitalisierung prognostizierte die Mortalitätsrate (aOR 2.4 CI 1.14–5.04,  $p=0.021$ ) sowie die Chance für gutes klinisches Outcome (aOR 0.291 CI 0.128–0.666,  $p=0.003$ ) ohne signifikante Unterschiede in den Raten von intrakraniellen Blutungen ( $p=0.735$ ).

**Fazit:** Bei Patienten mit akutem ischämischen Schlaganfall, welche mittels mechanischer Rekanalisation behandelt wurden, war eine vorbestehende Thrombozytopenie bei Aufnahme ein unabhängiger Prädiktor für eine erhöhte Mortalität und ein deutlicher Abfall der Thrombozyten im Verlauf ein unabhängiger Prädiktor für erhöhte Mortalitätsraten und ungünstigeres klinisches Outcome.

134

### TIME METRICS TO ENDOVASCULAR THROMBECTOMY IN THREE TRIAGE CONCEPTS: A PROSPECTIVE, OBSERVATIONAL STUDY (NEUROSQUAD TRIAL)

Fatih Seker<sup>\*1</sup>, Jens Fiehler<sup>2</sup>, Markus Möhlenbruch<sup>1</sup>, Friederike Heimann<sup>1</sup>, Fabian Flottmann<sup>2</sup>, Peter Arthur Ringleb<sup>3</sup>, Götz Thomalla<sup>4</sup>, Thorsten Steiner<sup>5</sup>, Christoffer Kraemer<sup>6</sup>, Caspar Brekenfeld<sup>2</sup>, Martin Bendszus<sup>3</sup>

<sup>1</sup>Universitätsklinikum Heidelberg, Neuroradiologie, Heidelberg, Deutschland

<sup>2</sup>Universitätsklinikum Hamburg-Eppendorf, Neuroradiologie, Hamburg, Deutschland

<sup>3</sup>Universitätsklinikum Heidelberg, Neurologie, Heidelberg, Deutschland

<sup>4</sup>Universitätsklinikum Hamburg-Eppendorf, Neurologie, Hamburg, Deutschland

<sup>5</sup>Klinikum Frankfurt Höchst, Neurologie, Frankfurt am Main, Deutschland

<sup>6</sup>Klinikum Lüneburg, Neurologie, Lüneburg, Deutschland

**Background:** NEUROSQUAD is a prospective, observational, bi-center trial comparing three triage pathways in endovascular stroke treatment: Mothership (MS), drip and ship (DS) and transferring a neurointerventionalist to a remote hospital for thrombectomy (drive the doctor, DD).

**Methods:** Between February and October 2018, all stroke patients undergoing thrombectomy at two university hospitals and two associated remote hospitals were included. Primary outcome measures were time from onset to groin puncture and time from imaging to groin puncture. Secondary outcome measures were time from onset to imaging and time from onset to thrombolysis.

**Results:** In total, 447 patients were included of which 145 (32.4%) were in the MS group, 250 (55.9%) in the DS group and 52 (11.6%) in the DD group. Median time from onset to groin puncture (170 min) and time from imaging to groin puncture (52 min) were the shortest in the MS group. Time from onset to groin puncture (DD median 225 min vs. DS median 301 min,  $P=0.001$ ) and time from imaging to groin puncture (DD median 118 min vs. DS median 172 min,  $P<0.001$ ) were shorter in the DD group compared to DS. Time from onset to imaging was similar among MS, DS and DD ( $P=0.332$ ). In patients receiving thrombolysis, time from onset to needle was similar among the three groups as well ( $P=0.619$ ).

**Conclusion:** The NEUROSQUAD study adds evidence that DD may be a feasible alternative to DS, leading to shorter delay between symptom onset and groin puncture. Both are time-wise inferior compared to MS, though.

135

### DIAGNOSTIC PERFORMANCE OF FIVE COLLATERAL SCORES IN THE PREDICTION OF CLINICAL OUTCOME AFTER ENDOVASCULAR THROMBECTOMY IN ISCHEMIC STROKE

Fatih Seker<sup>\*1</sup>, Benjamin Pereira-Zimmermann<sup>2</sup>, Johannes Pfaff<sup>1</sup>, Jan Purrucker<sup>3</sup>, Christoph Gumbinger<sup>3</sup>, Silvia Schönenberger<sup>3</sup>, Martin Bendszus<sup>1</sup>, Markus Möhlenbruch<sup>3</sup>

<sup>1</sup>Universitätsklinikum Heidelberg, Neuroradiologie, Heidelberg, Deutschland

<sup>2</sup>University of Valparaiso, Radiology, Valparaiso, Chile

<sup>3</sup>Universitätsklinikum Heidelberg, Neurologie, Heidelberg, Deutschland

**Background:** Several collateral scores have been published for stroke in the middle cerebral artery territory, each considering different aspects of cerebral collateralization. This retrospective study aimed at comparing five collateral scores regarding their prediction of clinical outcome.

**Methods:** Inclusion criteria were M1 occlusion, premorbid modified Rankin Scale of 0–2, treatment with endovascular thrombectomy, groin puncture within 6 hours after stroke onset, and Thrombolysis In Cerebral Infarction score of 2b–3. Maas, Miteff, Tan, ASITN/SIR and mCTA collateral scores were assessed in multiphase CTA images and correlated with 90 day modified Rankin Scale (90d-mRS). Good outcome was defined as 90d-mRS 0–2.

**Results:** In total, 69 patients were included of which 49.3% achieved a good outcome. Area Under the Curve values of Receiver Operating Characteristic curve analysis for Maas, Miteff, Tan, ASITN/SIR and mCTA scores were 0.64 (0.53–0.76), 0.62 (0.53–0.71), 0.65 (0.53–0.76), 0.65 (0.53–0.78) and 0.66 (0.54–0.79), respectively. Correlation between 90d-mRS and Maas ( $r=-0.39$ ,  $P<0.001$ ), Miteff ( $r=-0.40$ ,  $P<0.001$ ), Tan ( $r=-0.42$ ,  $P<0.001$ ), ASITN/SIR ( $r=-0.44$ ,  $P<0.001$ ) and mCTA ( $r=-0.44$ ,  $P<0.001$ ) scores was moderate.

**Conclusion:** Maas, Miteff, Tan, ASITN/SIR and mCTA collateral scores show similarly moderate diagnostic performance in the prediction of clinical outcome when assessed in multiphase CTA.

136

### MOTHERSHIP VERSUS DRIP AND SHIP – A RETROSPECTIVE ANALYSIS OF A REGIONAL STROKE REGISTRY WITH 2797 PATIENTS

Fatih Seker<sup>\*1</sup>, Susanne Bonekamp<sup>1</sup>, Susanne Rode<sup>2</sup>, Sonja Hyrenbach<sup>2</sup>, Martin Bendszus<sup>1</sup>, Markus Möhlenbruch<sup>1</sup>

<sup>1</sup>Universitätsklinikum Heidelberg, Neuroradiologie, Heidelberg, Deutschland

<sup>2</sup>Qualitätssicherung im Gesundheitswesen Baden-Württemberg GmbH, Stuttgart, Deutschland

**Background:** This study aims at comparing short-term clinical outcome after thrombectomy in patients directly admitted to a comprehensive stroke center (mothership, MS) with patients secondarily transferred from a primary stroke center (drip and ship, DS).

**Methods:** In a prospective regional stroke registry, all stroke patients with premorbid modified Rankin Scale (mRS) 0–2 who were admitted within 24 hours after stroke onset and treated with thrombectomy between 2014 and 2017 were analyzed retrospectively. MS and DS were

compared regarding the proportion of good outcome (discharge mRS 0–2), median discharge mRS, mRS shift (difference between pre-morbid mRS and mRS on discharge) and occurrence of symptomatic intracranial hemorrhage.

**Results:** Of 2797 patients, 1051 (37.6%) achieved good clinical outcome. In the MS group ( $n=1657$ ), proportion of good outcome was higher (MS 42.2% vs. DS 30.9%,  $P<0.001$ ) and median discharge mRS (MS 3 vs. DS 4,  $P<0.001$ ) and median mRS shift (MS 3 vs. DS 4,  $P<0.001$ ) were lower. The rate of symptomatic intracranial hemorrhage was similar in both groups (MS 9.3% vs. DS 7.5%,  $P=0.101$ ). Multivariate analysis revealed that direct admission (MS) was an independent predictor of good clinical outcome (adjusted OR 1.32, CI 1.09–1.60,  $P=0.004$ ).

**Conclusion:** These results confirm prior studies stating that direct admission to a comprehensive stroke center (MS) leads to better outcome compared to DS in stroke patients undergoing thrombectomy.

137

### IMPACT OF BRIDGING THROMBOLYSIS ON CLINICAL OUTCOME IN STROKE PATIENTS UNDERGOING THROMBECTOMY

Fatih Seker\*<sup>1</sup>, Susanne Bonekamp<sup>1</sup>, Susanne Rode<sup>2</sup>, Sonja Hyrenbach<sup>2</sup>, Martin Bendszus<sup>1</sup>, Markus Möhlenbruch<sup>1</sup>

<sup>1</sup>Universitätsklinikum Heidelberg, Neuroradiologie, Heidelberg, Deutschland

<sup>2</sup>Qualitätssicherung im Gesundheitswesen Baden-Württemberg GmbH, Stuttgart, Deutschland

**Background:** It is unclear whether stroke patients should receive intravenous thrombolysis (IVT) prior to endovascular thrombectomy (EVT). This study aims at analyzing the impact of bridging IVT on short-term clinical outcome.

**Methods:** In a prospective regional stroke registry, all stroke patients with pre-morbid modified Rankin Scale (mRS) 0–2 who were admitted within 4.5 hours after onset and treated with EVT were analyzed retrospectively. Patients receiving IVT prior to EVT (IVEVT) were compared to those undergoing EVT only regarding the proportion of good outcome (discharge mRS 0–2), discharge mRS, mRS shift (difference between pre-morbid mRS and mRS on discharge), hospital mortality and occurrence of symptomatic intracranial hemorrhage.

**Results:** In total, 2022 patients were included of which 816 patients (40.4%) achieved good clinical outcome. 1293 patients (63.9%) received bridging IVT. There was no significant difference between both groups regarding the proportion of good outcome (IVEVT 41.4% vs. EVT 38.5%,  $P=0.231$ ), discharge mRS (median, IVEVT 3 vs. EVT 3,  $P=0.178$ ) and mRS shift (median, IVEVT 3 vs. EVT 3,  $P=0.960$ ). Hospital mortality was non-significantly higher in IVEVT (IVEVT 19.3% vs. 11.0%,  $P=0.984$ ). Bridging IVT was not associated with clinical outcome ( $P=0.231$ ). Symptomatic intracranial hemorrhage was significantly more frequent in IVEVT (9.3% vs. 5.2%,  $P=0.001$ ).

**Conclusion:** According to this analysis of a regional stroke registry with 2022 patients, bridging thrombolysis does not lead to better clinical outcome. However, it is associated with a higher rate of symptomatic intracranial hemorrhage.

138

### ACUTE OCCLUSIONS AND THROMBOSES OF DUAL-LAYER CAROTID STENTS IN ENDOVASCULAR STROKE TREATMENT OF TANDEM OCCLUSIONS – A RETROSPECTIVE MULTICENTER EXPERIENCE

Johannes Pfaff\*<sup>1</sup>, Christoph Maurer<sup>2</sup>, Erasmia Müller-Thies-Broussalis<sup>3</sup>, Hendrik Janssen<sup>4,5</sup>, Raphael Blanc<sup>6</sup>, Cyril Dargazanli<sup>7</sup>,

Vincent Costalat<sup>7</sup>, Michel Pötin<sup>6</sup>, Frank Runck<sup>2</sup>, Ansgar Berlis<sup>2</sup>, Monika Killer<sup>3</sup>, Johannes Hensler<sup>8</sup>, Martin Bendszus<sup>1</sup>, Fritz Wodarg<sup>8</sup>, Markus Möhlenbruch<sup>1</sup>

<sup>1</sup>Universitätsklinikum Heidelberg, Abteilung für Neuroradiologie, Heidelberg, Deutschland

<sup>2</sup>Augsburg, Deutschland

<sup>3</sup>Salzburg, Österreich

<sup>4</sup>Ingolstadt, Deutschland

<sup>5</sup>Nürnberg, Deutschland

<sup>6</sup>Paris, Frankreich

<sup>7</sup>Montpellier, Frankreich

<sup>8</sup>Kiel, Deutschland

**Hintergrund:** A recent retrospective single center study showed a rate of 45% of thrombotic occlusion of dual-layer carotid stents within 72 hours after emergent CAS during treatment of a tandem occlusion. (1) As the sample size in this study is small and this study appear to show a higher-than-anticipated occlusion rate, we hypothesize that the rate of occlusion is lower and rather comparable to previously reported occlusion rates in single layer stents and propose a retrospective multi-center evaluation to increase the power to assess this.

**Methoden:** Multicentric retrospective data collection and analysis of stroke databases of 7 comprehensive stroke centers from 3 European countries.

**Ergebnisse:** Overall 160 patients (age: mean (SD)=66 (12); male:  $n=104$  (65%); median baseline NIHSS (IQR): 14 (9–18), IV lysis:  $n=97$  (60.6%) were treated for a cervical carotid artery occlusion or stenosis using a CASPER Stent (CASPER Stent, Carotid Artery Stent designed to Prevent Embolic Release, MicroVention, Aliso Viejo, CA) and received mechanical thrombectomy for an intracranial occlusion between April 2014 and November 2018. During the procedure or within 72 h, formation of thrombus and complete occlusion of the CASPER-Stent was observed in 33/160 patients (20.8%), respectively in 12/160 patients (7.5%). In 25/33 (75.8%), respectively in 9/12 patients (75%) this occurred during the procedure. No statistical significant difference was observed between patients with and without thrombus formation with regard to a pre-existing long-term medication with anticoagulants or intraprocedural administration of either heparin, ASA or heparin and ASA. Favorable early neurological outcome was similar in patients with ( $n=15$ ; 45.5%) and without ( $n=63$ ; 49.6%) thrombus formation at the CASPER-Stent.

**Diskussion:**

**Fazit:** Acute thrombosis or occlusion of CASPER-stents in thrombectomy patients receiving emergent extracranial internal carotid artery stenting for tandem occlusions can be observed more often during the procedure rather than within 72 h follow-up, were less frequent than previously reported and showed no impact on early neurological outcome.

### References

1. Yilmaz U, Korner H, Muhl-Benninghaus R, Simgen A, Kraus C, Walter S, et al. Acute Occlusions of Dual-Layer Carotid Stents After Endovascular Emergency Treatment of Tandem Lesions. *Stroke*. 2017;48(8):2171–5

139

### PRÄDIKTIVER WERT DER PERFUSIONS-BILDGEBUNG AUF DIE VORHERSAGE DER HÄMORRHAGISCHEN TRANSFORMATION NACH ENDOVASKULÄRER SCHLAGANFALLS-THERAPIE

Antonia Carlotta Fischer, Olav Jansen, Patrick Langguth, Fritz Wodarg, Naomi Larsen, Friederike Austein

Department of Radiology and Neuroradiology, University Hospital Schleswig-Holstein, Campus Kiel, Kiel, Deutschland

**Hintergrund:** Das Ziel dieser retrospektiven monozentrischen Studie war die Identifizierung von prädiktiven Parametern aus der Perfusions-Bildgebung für eine hämorrhagische Transformation bei Patienten mit akutem ischämischen Schlaganfall (AIS) nach endovaskulärer Therapie (EVT).

**Methoden:** Patienten mit einem akuten Gefäßverschluss im vorderen Stromgebiet im Zeitraum von 2010–2017, die eine prä-interventionelle multimodale CT Bildgebung (Non-Contrast-CT (NCCT), CT-Angiographie (CTA) und CT-Perfusion (CTP)) erhielten, anschließend mittels EVT therapiert wurden und eine Verlaufsbildgebung erhielten wurden analysiert. Eine hämorrhagische Transformation wurde in der Follow-up-Bildgebung diagnostiziert und gemäß den ECASS II-Kriterien klassifiziert und nach betroffenen Regionen bezüglich des Alberta Stroke Program Early CT Scores (ASPECTS) aufgeschlüsselt. Neben den Auswirkungen ausgewählter demografischer Merkmale, klinischer und therapieassoziierter Faktoren, wurden insbesondere die unterschiedlichen Perfusionsparameter für die Vorhersage einer ICB in univariablen und multivariablen logistischen Regressionsmodellen einbezogen. Die Korrelation zum funktionellen Ergebnis nach 90 Tagen wurde ebenfalls bewertet.

**Ergebnisse:** 397 Patienten erfüllten die Einschlusskriterien von denen 170 Patienten eine zusätzliche i. v. Lyse erhielten. Eine parenchymatöse Blutung Typ 2 (PH 2) wurde in 23 Fällen diagnostiziert, parenchymatöse Blutung Typ 1 in 18 Fällen, ein hämorrhagischer Infarkt Typ 2 in 56 Fällen und ein hämorrhagischer Infarkt Typ 1 in 20 Fällen. (Die Daten der multivariablen und univariablen Regressionsanalysen liegen noch nicht abschließend vor).

**Fazit:** Perfusionsparameter sind neben einem niedrigen ASPECTS unabhängige zuverlässige Prädiktoren für eine ICB nach erfolgreicher EVT. Dieser Befund ist von klinischer Relevanz, da das ICB-Risiko nach EVT bei AIS in der realen klinischen Praxis signifikant höher ist als in randomisierten-klinischen Studien. Weitere prospektive Studien sind erforderlich.

144

## KLINISCHE UND RADIOLOGISCHE UNTERSCHIEDE VON PATIENTEN MIT VERSCHIEDENEN HÄMORRHAGISIERENDEN

### MIKROANGIOPATHIEN

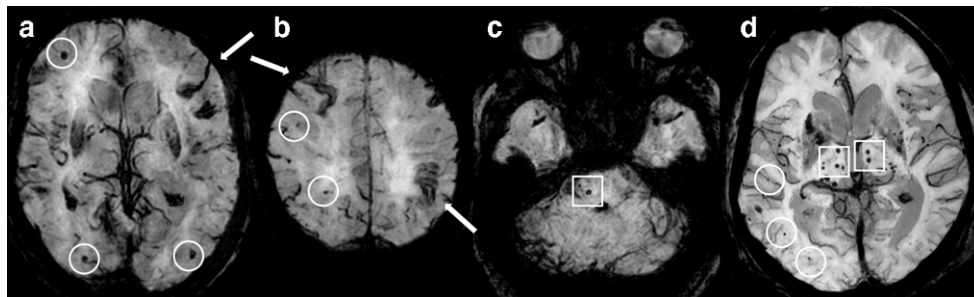
Ulf Jensen-Kondering<sup>\*1</sup>, Caroline Weiler<sup>2</sup>, Patrick Langguth<sup>1</sup>, Gregor Kühlenbäumer<sup>2</sup>, Olav Jansen<sup>1</sup>, Nils Margraf<sup>2</sup>

<sup>1</sup>Klinik für Radiologie und Neuroradiologie, Kiel, Deutschland

<sup>2</sup>Klinik für Neurologie, Kiel, Deutschland

**Hintergrund:** Die cerebrale Amyloidangiopathie ist gekennzeichnet durch kortexnahe Mikroblutungen, kortikale Siderosen und lobäre intracraniale Blutungen (ICB). Die Diagnose erfolgt anhand der modifizierten Boston Kriterien<sup>1</sup>. Differentialdiagnostisch muss eine hypertensive Enzephalopathie (HTE) abgegrenzt werden, bei der es zu Mikroblutungen in tief gelegenen Hirnabschnitten kommt. Weiterhin

**Abb. 1 | 144** Suszeptibilitäts-gewichtete Bildgebung (SWI) von Patienten mit CAA (a und b) und MLH (c und d). Lobäre Mikroblutungen (a Kreise) und superfizielle kortikale Siderose (a und b Pfeile). Mikroblutung im Hirnstamm (c Kasten) und in der tiefen grauen Substanz (d Kästen) neben lobären Mikroblutungen (Kreise)



gibt es eine Mischform (mixed location hemorrhage, MLH<sup>2</sup>), bei der Merkmale beider Erkrankungen zu finden sind (Abb. 1). In dieser Arbeit sollen klinische und radiologische Merkmale dieser beiden Erkrankungen (CAA und MLH) vor dem Auftreten einer ICB verglichen werden.

**Methoden:** Retrospektive Identifizierung von Patienten mit CAA (mindestens „wahrscheinlich“ nach den modifizierten Boston Kriterien) und Patienten mit MLH ohne vorausgegangene ICB. Erfassung multipler klinischer und radiologischer Parameter. Berechnung der absoluten und relativen Häufigkeiten dieser Parameter und Gruppenvergleiche mit Hilfe des  $\chi^2$ -Tests, Mann-Whitney-Tests bzw. t-Tests. Das Signifikanzniveau wurde auf  $p < 0.05$  festgelegt.

**Ergebnisse:** Es konnten insgesamt 91 Patienten (CAA = 51, MLH = 40) eingeschlossen werden. Hinsichtlich folgender Parameter ergab sich ein signifikanter Unterschied: Lakunen (49 % vs 70 %,  $n = 25/28$ ,  $p = 0.04$ ), superfizielle kortikale Siderose (20 % vs 5 %,  $n = 10/2$ ,  $p = 0.04$ ). Alle anderen Vergleiche waren nicht signifikant ( $p > 0.05$ ), hinsichtlich folgender Parameter ergab sich ein allerdings ein Trend ( $p < 0.10$ ): Alter ( $78 \pm 7.5$  vs  $75 \pm 9$  Jahre,  $p = 0.06$ ), arterielle Hypertension (73 % vs 90 %,  $n = 38/36$ ,  $p = 0.06$ ), >10 Mikroblutungen (46 % vs 65 %,  $n = 24/26$ ,  $p = 0.09$ ).

**Diskussion und Fazit:** Schon bevor Patienten mit CAA oder MLH eine ICB erleiden, unterscheiden sich diese beiden Patientengruppen. Unklar bleibt, ob es sich bei der MLH um eine ausgeprägte Form der HTE handelt, oder ob ein Mischbild aus CAA und HTE vorliegt. Dies muss in der Risikoabschätzung bei einer notwendigen Antikoagulation berücksichtigt werden.

### Literatur

1. Linn J, et al. Baillieres Clin Neurol. 2010;74:1346–50.
2. Pasi M, et al. Baillieres Clin Neurol. 2018;90:e119–26.

147

## CONTINUOUS INTRA-ARTERIAL NIMODIPINE INFUSION AS A TREATMENT OF DELAYED CEREBRAL ISCHEMIA AFTER ANEURYSMAL SUBARACHNOID HEMORRHAGE

Moritz Selbach<sup>\*1</sup>, Andreas Kramer<sup>2</sup>, Thomas Kerz<sup>2</sup>, Florian Ringel<sup>2</sup>, Marc A. Brockmann<sup>1</sup>, Carolin Brockmann<sup>1</sup>

<sup>1</sup>Universitätsmedizin der Johannes Gutenberg-Universität Mainz, Klinik und Poliklinik für Neuroradiologie, Mainz, Deutschland

<sup>2</sup>Universitätsmedizin der Johannes Gutenberg-Universität Mainz, Neurochirurgische Klinik und Poliklinik, Mainz, Deutschland

**Background:** Delayed cerebral ischemia (DCI)<sup>1</sup> is a frequently occurring complication in patients with aneurysmal subarachnoid hemorrhage (aSAH), that may lead to disabling neurological deficits or death. Multiple factors may contribute to DCI with vasospasm of large intracranial vessels being the most widely recognized<sup>2</sup>. Continuous intra-arterial nimodipine infusion (CIAN) is a promising endovascular thera-

peutic option in severe cases of DCI, which are refractory to standard therapy (hemodynamic therapy and oral NDP).

**Methods:** CIAN was initiated and ended based on an individual interdisciplinary evaluation of the clinical and diagnostic course of the patient using transcranial Doppler (TCD), CT angiography (CTA), CT perfusion (CTP) and digital subtraction angiography (DSA). One or two microcatheters were placed into the internal carotid or vertebral artery according to the site of suspected DCI. Nimodipine (NDP) was administered continuously in a rate of 0.5–2 mg/h. During CIAN, intensive care was conducted. The outcome measures were the Glasgow Outcome Scale (GOS) at discharge and within 1 year after aSAH and the occurrence of cerebral infarction in subsequent CT-scans.

**Results:** In the period of May 2016 to January 2018, 17 patients received CIAN. The median duration was 5 (1–13) days. Favorable outcome (GOS 4 or 5) was achieved in 9 patients (53%) at discharge and in 13 patients within 1 year (76%). Follow-up imaging showed minor infarction in 5 and major infarction in 3 patients. One patient developed a localized cerebral edema as a possible side effect. One patient died due to malignant posthemorrhagic edema. Normalization of CTP-parameters within 2 days was observed in 9/17 patients. The remaining 6 patients showed clinical response and thus did not receive short-term CTP imaging.

**Discussion:** Our results concerning the outcome within one year are in line with previously published retrospective studies<sup>3,4</sup>. The study is limited by its retrospective character, the lack of a control group and the small number of patients.

**Conclusion:** CIAN is a feasible, safe and effective therapeutic option for patients with severe therapy-refractory delayed cerebral ischemia. A prospective randomized clinical trial is needed to confirm the positive retrospective results of this study and previously published studies.

**References**

1. Vergouwen M, Vermeulen M, Gijn J, et al. 2010.
2. Budohoski KP, Guilfoyle M, Helmy A, et al. 2014.
3. Bele, S., Proescholdt, M. A., Hochreiter, A. et al. 2015.
4. Hockel K, Diedler J, Steiner J, et al. 2016.

148

**STABLE LOCALIZATION OF WATERSHED AREAS AFTER REVASCULARIZATION THERAPY IN PATIENTS WITH ASYMPTOMATIC INTERNAL CAROTID ARTERY**

**STENOSIS**

Lena Schmitzer\*<sup>1</sup>, Stephan Kaczmarz<sup>1</sup>, Nico Sollmann<sup>1</sup>, Claus Zimmer<sup>1</sup>, Christine Preibisch<sup>1</sup>, Jens Götter<sup>1</sup>

<sup>1</sup>Klinikum Rechts der Isar der Technischen Universität München, Abteilung für diagnostische und interventionelle Neuroradiologie, München, Deutschland

**Hintergrund:** Watershed areas (WSA) are located between vascular territories and thus especially vulnerable to hypoperfusion.<sup>1</sup> This can be caused by internal carotid artery stenosis (ICAS), a disease accounting for approx. 10% of all strokes.<sup>2,3</sup>

While stenosis treatment is known to alter cerebral hemodynamics,<sup>4</sup> it remains unclear how WSA localization is affected. We addressed this issue in a follow up study in ICAS patients after revascularization treatment.

**Methoden:** Sixteen patients (age 73.0±6.1y, five females) and 17 healthy elderly (age 72.3±5.5y, eleven females) were examined on a clinical 3T Philips Ingenia after patients had undergone carotid endarterectomy or stenting.

WSAs were defined semi-automatically based on Time-to-Peak-maps<sup>5</sup> (Fig. 1). Every subject's WSAs mask was normalized to MNI-space and probability maps were calculated for each group. Spatial overlap of each subject's WSA mask of both scans was assessed by the Dice coefficient (DC) and compared between groups.

TTP values were extracted within each individual WSA and compared between hemispheres.

**Ergebnisse:** WSAs could be reliably segmented in both groups (Fig. 2). The mean DC for the WSA comparison between scans 1 and 2 was similar (DC≈0.6) in controls and patients (non-significant difference, two-sample t-test, *p*=0.287). In patients, relative TTP (rTTP) in WSAs was significantly reduced in the affected vs. the unaffected hemisphere pre-interventionally (*p*<0.001), whereas no sig significant difference was observed post-interventionally (*p*=0.446, Fig. 3).

**Diskussion:** Similar DCs in patients and controls (≈0.6) suggest that the spatial extent of WSAs was not changed by revascularization ther-

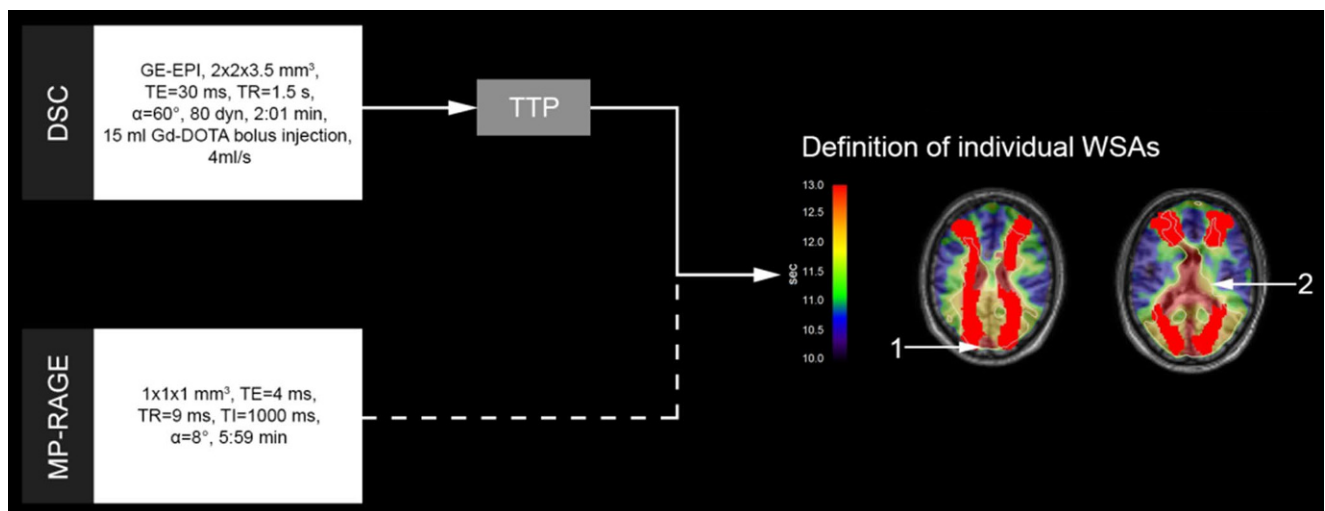


**Fig. 1 | 148** Defining WSAs (marked red) semi-automatically based on TTP derived from dynamic susceptibility contrast (DSC) and adaption them to the individual's anatomy by omitting sinuses (1) and the ventricular system (2)

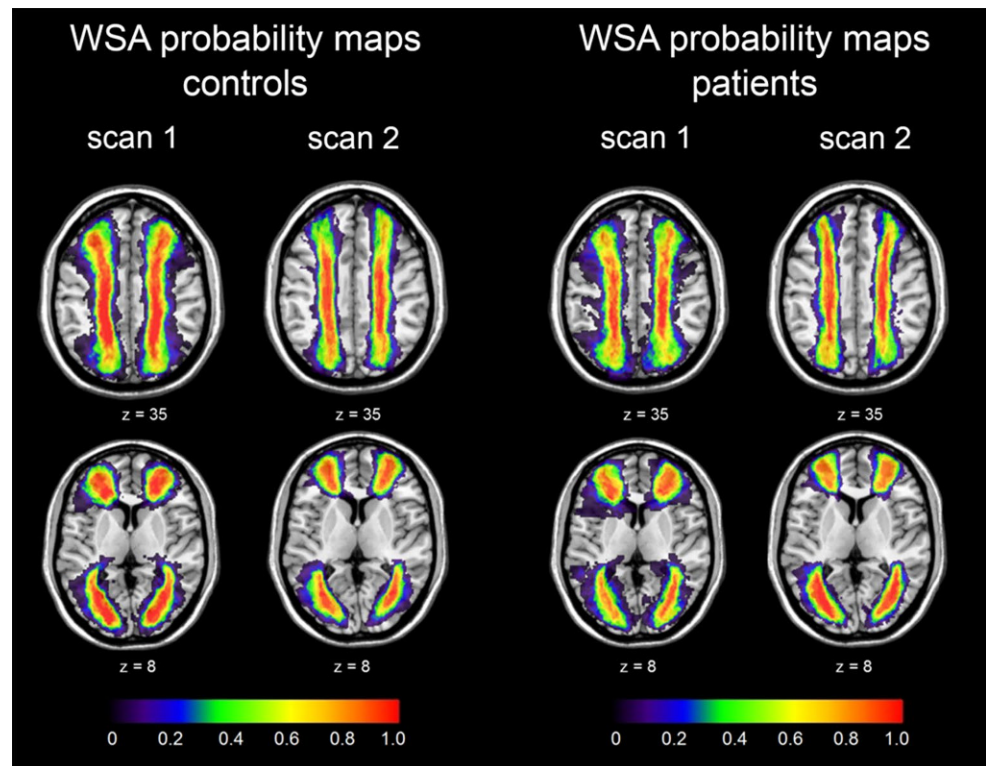


**Fig. 2 | 148** Probability maps depict the likelihood for each voxel to belong to WSAs across subjects and were calculated for each group for scan 1 (pre-interventional) and 2 (post-interventional). Accessed by the Dice Coefficient no significant difference of WSA's location between scans 1 and 2 was observed

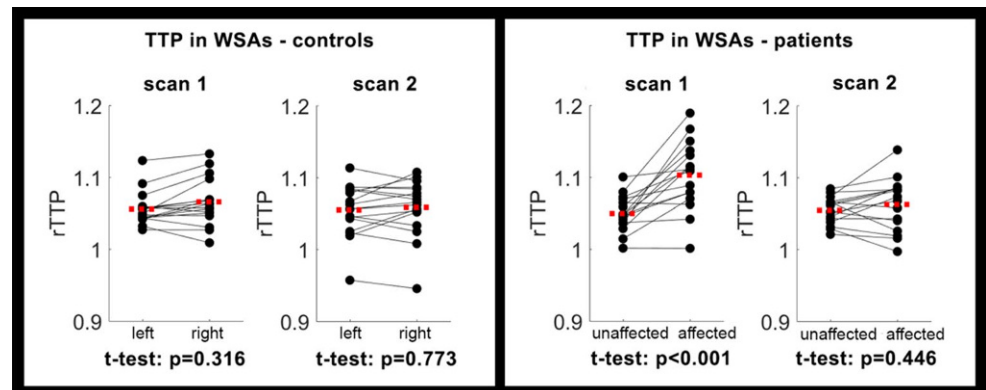


**Fig. 3 | 148** TTP values were normalized by the mean individual white matter relative TTP (rTTP) and extracted within individual WSA. The comparison of rTTP between hemispheres in scan 1 (pre-intervention) and 2 (post-intervention) revealed recovery of rTTP in patients after stenosis treatment

apy (Fig. 2), whereas altered hemodynamics, as expected and indicated by rTTP asymmetries, significantly improved post-interventionally (Fig. 3). As shifts of vascular territories have been reported after treatment of ICAS patients,<sup>6</sup> our finding demonstrates that WSAs—as regions at higher risk for ischemia—remain unchanged.

**Fazit:** Despite changing hemodynamics, revascularization therapy does not change the spatial extent of WSAs in patients with asymptomatic ICAS.

#### References

1. Momjian-Mayor, et al. Stroke. 2005.
2. D'Amore, et al. FrontNeurolNeurosci. 2012.
3. Jorgensen, et al. NeurolSci. 1969.
4. Kawai, et al. JStrokeCVDisease. 2014;::
5. Kaczmarz, et al. Neuroradiology. 2018;::
6. VanLaar et al., VascSurg et al., 2007

#### 158

#### SIZE AND LOCATION OF THE EARLY INFARCT: HOW ACCURATE IS NON-CONTRAST-ENHANCED CT?

Ikram Eda Duman<sup>\*1</sup>, Elias Kellner<sup>1</sup>, Karl Egger<sup>1</sup>, Horst Urbach<sup>1</sup>

<sup>1</sup>Universitätsklinikum Freiburg, Abteilung Neuroradiologie, Freiburg, Deutschland

**Hintergrund:** Infarct volume on non-contrast-enhanced CT or MRI is used as auxiliary outcome measure in therapeutic trials for acute ischemic stroke (1–2). The goal of this study was to evaluate its reliability in patients with acute ischemic stroke by comparing the volumes of CT and CT-Perfusion based infarct cores.

**Methoden:** Patient data were retrieved from the Freiburg stroke data bank. The early ischemic infarct area on CT was semiautomatically drawn by board-certified radiologist using the ROI tool of the post-processing software „NORA“ (3) (Fig. 1). This mask was overlaid on

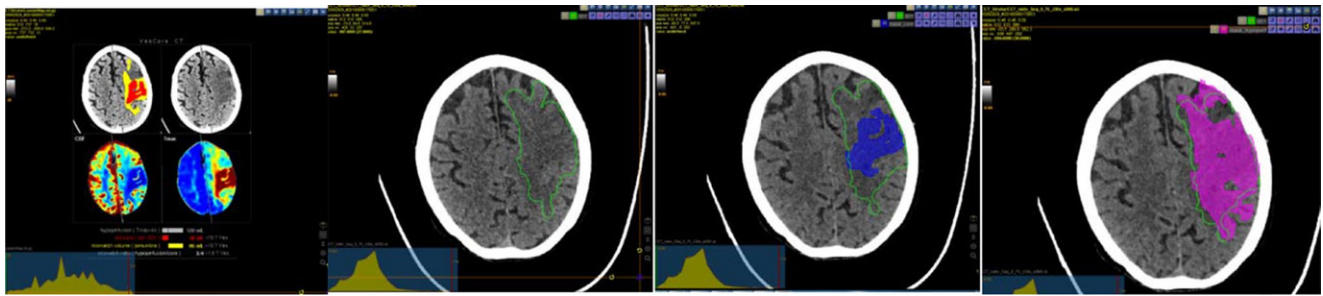


Fig. 1 | 158

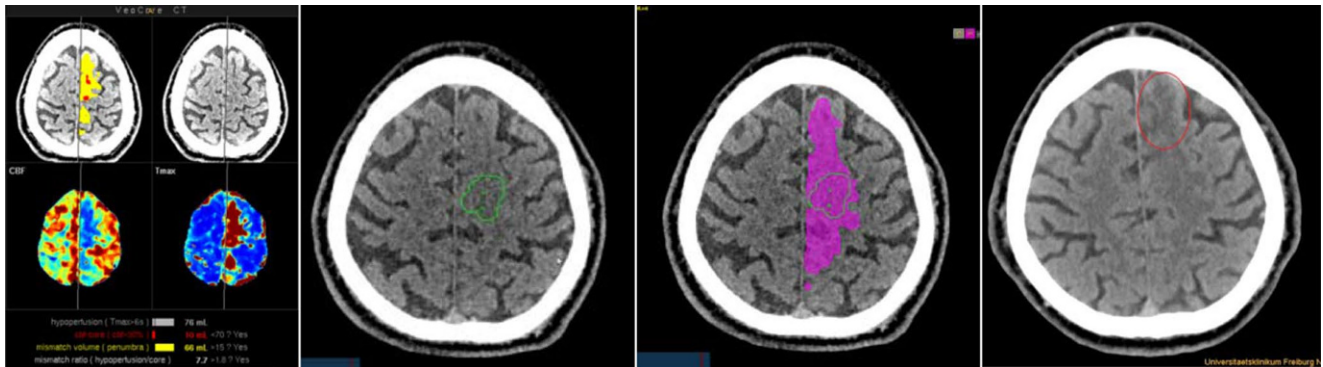


Fig. 2 | 158

the CT-P-based infarct core generated by the processing software „VeoCore“. Volumetry was compared by calculating DICE coefficients. Follow-up CT or MRI was performed to prove infarct demarcations. **Ergebnisse:** 45 patients (age 76 (51–92), NIHSS 14 (2–23)) were included in the analysis. A total of 38 patients showed early infarct signs. In 2 patients, the early ischemic infarcts were overlooked (false negatives). In 6 patients, ischemic infarcts were falsely drawn on CT (false positives) (Fig 2.). Mean early infarct volumes on non-contrast CT was 32.3 (0–248) mL and 31.7 (0–158) mL on CT-P. Mean DICE coefficient between non-contrast-enhanced CT and CT-P infarct core maps was 0.203, and between non-contrast-enhanced CT and CT-P hypoperfusion maps 0.198. Correlation coefficients were 0.30 and 0.36, respectively. **Fazit:** Low DICE coefficients indicate a low accuracy of non-contrast-enhanced CT to depict the early ischemic infarct.

**References**

1. Song D, Yoo J, Baek JH, et al. Infarct Core Expansion on Computed Tomography before and after Intravenous Thrombolysis. *Yonsei Med J.* 2018;59(2):310–6. <https://doi.org/10.3349/ymj.2018.59.2.310>.
2. Han M, Choi JW, Rim NJ, et al. Cerebral infarct volume measurements to improve patient selection for endovascular treatment. *Medicine (Baltimore).* 95(35):e4702. <https://doi.org/10.1097/MD.0000000000004702>.
3. Kellner E, Reisert M, Kiselev VG, Maurer CJ, Beume LA, Urbach H, et al. Automated Infarct Core Volumetry Within the Hypoperfused Tissue: Technical Implementation and Evaluation. *J Comput Assist Tomogr.* 2017;41(4):515–20.

162

**TRANSKRANIELLE MOTORISCH EVOZIERTE POTENZIALE IN DER ENDOVASKULÄREN**

**REVASKULARISATIONSTHERAPIE ISCHÄMISCHER SCHLAGANFÄLLE – WORK IN PROGRESS.**

Tobias Greve\*<sup>1</sup>, Arthur Wagner<sup>2</sup>, Bernhard Meyer<sup>3</sup>, Claus Zimmer<sup>1</sup>, Silke Wunderlich<sup>3</sup>, Ehab Shiban<sup>2</sup>, Kornelia Kreiser<sup>1</sup>

<sup>1</sup>Abteilung für Diagnostische und Interventionelle Neuroradiologie, Klinikum rechts der Isar der Technischen Universität München, München, Deutschland

<sup>2</sup>Neurochirurgische Klinik und Poliklinik, Klinikum rechts der Isar der Technischen Universität München, München, Deutschland

<sup>3</sup>Neurologische Klinik und Poliklinik, Klinikum rechts der Isar der Technischen Universität München, München, Deutschland

**Hintergrund:** Die Aussagekraft motorisch evozierter Potenziale (MEPs) bei der endovaskulären mechanischen Rekanalisation (EMK) ischämischer Schlaganfälle unter Allgemeinanästhesie ist bisher wenig untersucht. Wir korrelierten die Amplituden (AMPs) von MEPs der oberen Extremitäten vor und nach EMK mit Symptombesserung (SYM\_D7) und Infarktmarkierung in der cMRT (DEMARK\_D7) an Tag 7.

**Methoden:** Prospektiv wurden bis 05/2019 Patienten mit Hemisyndrom und Verschluss der A. carotis interna/media (ICA/MCA) bzw. A. basilaris (BA) eingeschlossen, bei denen das MEP-Setup die EMK nicht verzögerte. mRS- und NIHSS wurden am Behandlungstag (D0) und Tag 7 (D7) erfasst. MEPs wurden an C3/C4 transkraniell elektrisch stimuliert und die AMPs am Abductor pollicis brevis (APB) bilateral vor und nach der EMK abgeleitet.

**Ergebnisse:** 26 Patienten (12w; 73,1 ± 12,2J; 4 ICA-/18 MCA-/4 BA-Verschlüsse) wurden bislang eingeschlossen. Zwischen Symptombesserung

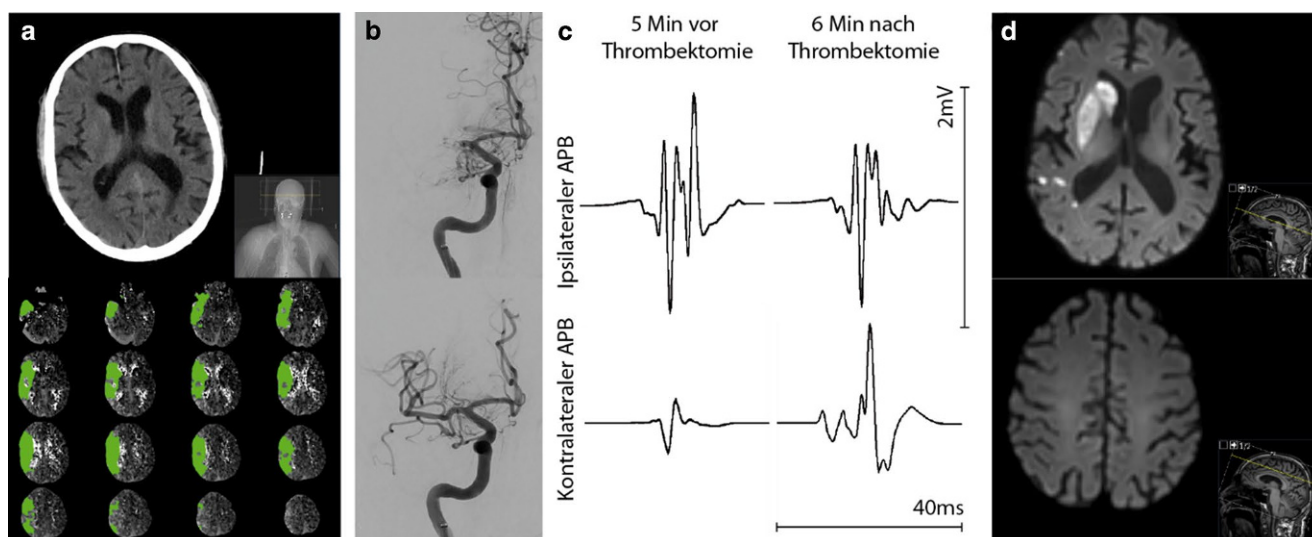


**Abb. 1 | 162** Falldarstellung; **a** Präinterventionelles natives cCT ohne Demarkation und Perfusionsdarstellung mit großem Tissue-at-Risk; **b** Subtraktionsangiographie (a.p.) des M1-Segmentes vor und nach Thrombektomie; **c** MEPs des APB vor und nach Thrombektomie mit Erholung der Amplitude kontralateral zum Gefäßverschluss; **d** Postinterventionelles cMRT (Diffusionssequenz) mit Darstellung einer Ischämie der Stammganglien ohne Einbezug der motorischen Bahnen

ginn und EMK lagen 4 h [1,75–12 h]. Der mRS an D0 war 4,6 [1–5] (NIHSS 13,9 [7–20]). Vor EMK waren AMPs kontralateral in 3 Fällen ( $308 \pm 89 \mu\text{V}$ ), und ipsilateral in allen Fällen ( $760 \pm 686 \mu\text{V}$ ) sichtbar. Nach EMK erholten sich die MEPs kontralateral in 16 Fällen nach  $5,8 \pm 3,3$  min ( $655 \pm 330 \mu\text{V}$ ). Der mTICI lag postinterventionell bei 3 (1x), 2c (2x), 2b (10x), 2a (1x) und 0 (2x). SYM\_D7 trat in 17 Fällen ein. DEMARK\_D7 im cMRT zeigte sich bei allen Patienten, 11 hiervon mit Einbezug motorischer Bahnen. In 9 dieser Fälle erholte sich das MEP nicht. Der mRS an D7 war 3,3 [1–6] (NIHSS 7 [0–24]). MEPs wiesen (stratifiziert nach SYM\_D7) eine Sensitivität (Spezifität) von 67 % (76 %) auf. Eine erfolgreiche EMK (mTICI  $\geq 2b$ ) hatte eine Sensitivität (Spezifität) von 33 % (100 %). Stratifiziert nach DEMARK\_D7 mit Beteiligung motorischer Bahnen lag die Sensitivität (Spezifität) der MEPs bei 82 % (93 %). Die erfolgreiche EMK hatte hierfür eine Sensitivität (Spezifität) von 27 % (100 %).

**Diskussion:** Eine MEP-Erholung tritt früh nach Reperfusion motorischer Bahnen ein. Sie scheint in unserer ersten Serie dem mTICI-Status in der Vorhersagekraft des Outcomes überlegen. Zur Vorhersage von Infarkten mit Beteiligung motorischer Bahnen war die MEP-Erholung dem mTICI-Status deutlich überlegen. Die mögliche klinische Bedeutung dieser Ergebnisse wird diskutiert.

**Fazit:** Die Ableitung von MEPs der oberen Extremitäten stellt eine wertvolle Zusatzinformation für den Interventionalisten dar und kann Infarkte motorischer Bahnen besser vorhersagen als der mTICI-Status.

## 172

### LONGITUDINAL IN VIVO EVALUATION OF LARGE VESSEL VASOSPASM IN MICE USING A MICRO-CT

Vanessa Weyer<sup>1</sup>, Máté Maros<sup>1</sup>, Stefanie Kirschner<sup>1</sup>, Christoph Groden<sup>1</sup>, Clemens Sommer<sup>2</sup>, Andrea Kronfeld<sup>2</sup>, Yasemin Tanyildizi<sup>2</sup>, Martin Kramer<sup>3</sup>, Marc A. Brockmann<sup>2</sup>

<sup>1</sup>Mannheim, Deutschland

<sup>2</sup>Mainz, Deutschland

<sup>3</sup>Gießen, Deutschland

**Background:** To date, no data exist regarding longitudinal *in vivo* imaging of subarachnoid hemorrhage (SAH)-induced cerebral vasospasm in mice. Aims of this study were to longitudinally evaluate SAH-in-

duced vasospasm using digital subtraction angiography (DSA) and to develop a novel prognostic scoring system for SAH severity in mice.

**Methods:** In 30 C57Bl/6J-mice (7 sham and 23 SAH) the right jugular vein was catheterized and a mini-port for repetitive administration of contrast agent was placed subcutaneously. DSA was performed using a  $\mu\text{CT}$  (80 kV, 75  $\mu\text{As}$ , 30fps). DSA was acquired pre-SAH and directly after inducing SAH by filament perforation (day 0). The amount and distribution of SAH were quantified by  $\mu\text{CT}$  using a novel scoring system (Fig 1). Longitudinal evaluation of large vessel vasospasm was assessed by DSA.

**Result:** Mice with SAH had a significantly shorter median survival time than the sham group ( $p=0.0016$ ,  $n=27$ ). Vasospasm peaked on days 2 and 4 after induction of SAH (Fig 2) and normalized between days 6 and 14. Vessel diameters decreased up to 30%, which was most pronounced in the basilar ( $\Delta_{\text{max}}=23.49\%$ ,  $p<0.001$ ), intracranial carotid ( $\Delta_{\text{max}}=30.5\%$ ,  $p<0.001$ ) and anterior cerebral artery ( $\Delta_{\text{max}}=21.2\%$ ,  $p=0.014$ ). Using our newly developed SAH-scoring system, all animals in the sham group scored 0 points (grade 0,  $n=6$ ), whereas mice in the SAH group had a significantly higher median score of 6 points ( $n=21$ ;  $p<0.01$ ). Longitudinal data analyses revealed significant correlations between the extent of vasospasms, neuroscore and our novel SAH-score. Especially the latter two on day 1 showed highly significant positive correlation ( $r_{\text{sp}}=0.835$ ,  $p<0.001$ ,  $n=27$ ). In three mice we were able to capture growing pseudoaneurysms at the perforation site by DSA and confirmed them histologically.

**Conclusion:** For the first time, we demonstrated that it is feasible to longitudinally monitor SAH-induced cerebral vasospasms with DSA and to detect the development of growing pseudoaneurysm in living mice. Further, we introduced and validated a novel prognostic scoring system of SAH severity for murine models.

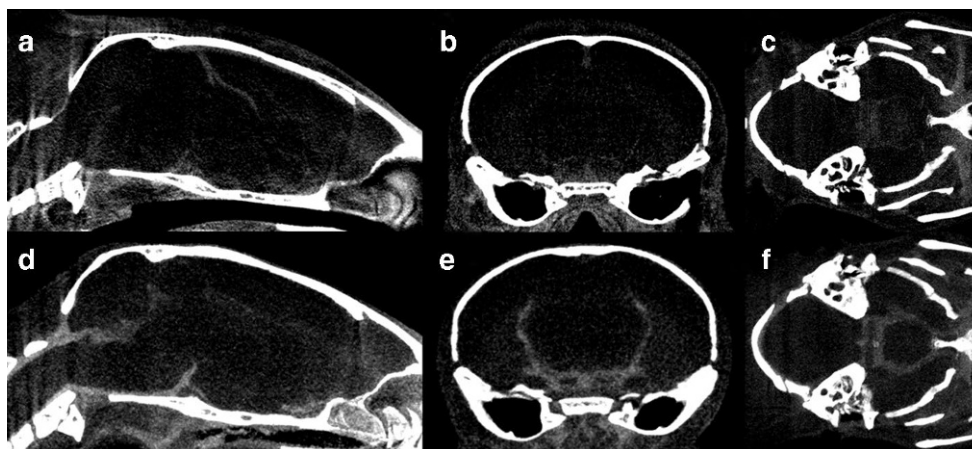


**Fig. 1 | 172** Micro-CT of a sham operated mouse without SAH (SAH grade 0; **a–c**) and a mouse with pronounced SAH after filament perforation (SAH grade 3; **d–f**). All micro-CT images were evaluated in the sagittal (**a, d**), coronal (**b, e**) and transversal planes (**c, f**) to establish a newly developed SAHscoring system. Depending on the blood distribution in the subarachnoid space each animal scored between 0 and 8 points and based on the total score they were stratified into four grades (grade 0=0 points, grade 1=1–3 points, grade 2=4–6 points, grade 3=7–8 points)

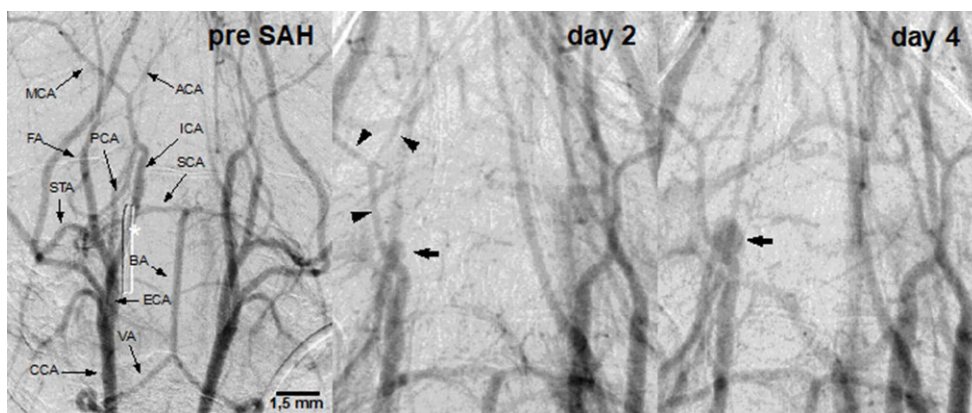


**Fig. 2 | 172** DSA of a mouse (dorsoventral beam path) before induction of SAH (pre SAH) and on days 2 and 4 (picture detail of the Circle of Willis) after SAH. On days 2 and 4 DSA showed vasospasms sinistral (black arrowhead) at A. basilaris (BA), A. carotis interna (ICA), A. cerebri media (MCA) and A. cerebri anterior (ACA) as well as growing pseudoaneurysms at the filament perforation site (black arrow). A 27G-cannula was placed as benchmark for calibration into the field-of-view (asterisk)

174

**EFFECT OF „DIRECT TRANSFER TO ANGIO-SUITE“ VS. „CT-SUITE“ FOR STROKE IMAGING ON WORKFLOW METRICS IN PATIENTS RECEIVING MECHANICAL THROMBECTOMY – A PROSPECTIVE, RANDOMIZED SINGLE CENTER TRIAL**

Johannes Pfaff\*<sup>1</sup>, Silvia Schönenberger<sup>2</sup>, Christian Herweh<sup>1</sup>, Christian Ulfert<sup>1</sup>, Simon Nagel<sup>2</sup>, Peter Arthur Ringleb<sup>2</sup>, Martin Bendszus<sup>1</sup>, Markus Möhlenbruch<sup>1</sup>

<sup>1</sup>Universitätsklinikum Heidelberg, Abteilung für Neuroradiologie, Heidelberg, Deutschland

<sup>2</sup>Universitätsklinikum Heidelberg, Abteilung für Neurologie, Heidelberg, Deutschland

**Hintergrund:** To quantify workflow metrics in patients undergoing mechanical thrombectomy (MT) after receiving stroke imaging in either a computed-tomography scanner suite (CTSS) or an angio-suite (“direct transfer to angio-suite”—DTAS—using cone-beam CT).

**Methoden:** Prospective, cluster randomized controlled, single-center institutional review board–approved trial in a comprehensive stroke center focusing on time from imaging to groin-puncture (primary endpoint) and time from imaging to final angiographic result (secondary endpoint) in patients receiving MT for anterior circulation large vessel occlusion after being randomized to receive stroke imaging (non-contrast-enhanced CT and CT-angiography) using either a CTSS or DTAS workflow before groin puncture.

**Ergebnisse:** Overall 62 patients (CTSS:  $n=34/62$  (54.8%); DTAS:  $n=28/62$  (45.2%)) were included in this trial. No significant difference in patient’s baseline characteristics, with the exception of more severe initial severity of stroke symptoms (as per National Institutes

of Health Stroke Scale; median (IQR): CTSS: 18 (13–20); DTAS: 15 (8–19),  $p$ -value: 0.046) in CTSS-patients was observed. Time from imaging to groin-puncture was shorter in DTAS-patients (in minutes, median (IQR): CTSS: 26 (23–32), DTAS: 19 (15–24);  $p$ -value: 0.001). Time from imaging to final angiographic result was comparable between the patient groups (CTSS: 59 (51–78), DTAS: 56 (46–89),  $p$ -value: 0.437).

**Fazit:** This prospective, randomized trial showed a significant reduction in time from imaging to groin-puncture when patients are transferred directly to the angio-suite to use cone-beam CT for advanced stroke-imaging compared to receiving imaging in a computed-tomography scanner suite. This initial timesaving however could not translate into a shorter time to final angiographic reperfusion in this trial.

181

**A COMPARISON OF PUNCTUATE HIPPOCAMPAL INFARCTION IN ISOLATION AND AS PART OF MULTIFOCAL POSTERIOR CEREBRAL ARTERY INFARCTION**

Alex Förster\*<sup>1</sup>, Mansour Al-Zghloul<sup>1</sup>, Angelika Alonso<sup>2</sup>, Holger Wenz<sup>1</sup>, Johannes Böhme<sup>1</sup>, Christoph Groden<sup>1</sup>

<sup>1</sup>Abteilung für Neuroradiologie, Universitätsmedizin Mannheim, Mannheim, Deutschland

<sup>2</sup>Neurologische Klinik, Universitätsmedizin Mannheim, Mannheim, Deutschland

**Hintergrund:** Punctuate hippocampal infarction (PHI) in isolation is rare and usually not associated with a clinical presentation characteristic for transient global amnesia (TGA).<sup>1</sup> Nevertheless, some authors

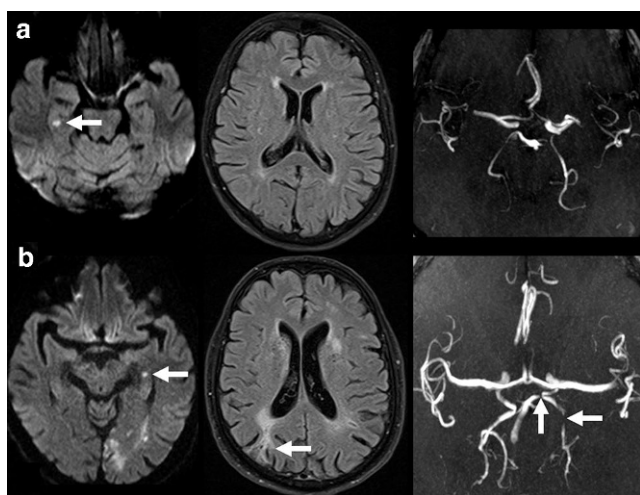


Fig. 1 | 181

suggested that it might rather be an atypical form of TGA than ischemic infarction. In the present study, we present a detailed comparison of PHI in isolation and as part of multifocal posterior cerebral artery (PCA) infarction.

**Methoden:** From an MRI database we identified 270 patients with hippocampal infarction. Of these, 14 patients (median age 67 years, 8 male) had PHI in isolation and 23 patients (median age 68 years, 15 male) as part of multifocal PCA infarction and were compared with regard to risk factors, clinical symptoms, and MRI findings.

**Ergebnisse:** Regarding clinical presentation, none of the patients showed TGA typical symptoms. Nausea was more common in isolated PHI ( $p=0.02$ ), while hemiparesis was more common in patients with PHI as part of multifocal PCA infarction ( $p<0.001$ ). On DWI, no significant differences between both groups were found regarding lesion distribution, size, or relative ADC. On FLAIR, isolated PHI (see Fig. 1a) was less frequently associated with chronic ischemic stroke lesions ( $p=0.02$ ) and more extensive (Fazekas score 2/3) age related white matter lesions (ARWML,  $p=0.03$ ) compared to PHI as part of multifocal PCA infarction (see Fig. 1B). On MR angiography a vascular pathology of the basilar artery or PCA was more frequent in PHI as part of multifocal PCA infarction ( $p=0.04$ ).

**Diskussion:** Since PHI in isolation lacks clinical symptoms typical for TGA and shares cerebrovascular risk factors with PHI as part of multifocal PCA infarction, it should be treated as acute ischemic stroke. However, subtle differences in clinical presentation, underlying vessel

pathologies, as well as associated chronic vascular lesions could indicate a different aetiology of PHI in isolation and as part of multifocal PCA infarction and should provide an incentive for future studies to reveal the true nature of PHI in isolation.

## References

1. Förster A, Al-Zghloul M, Wenz H, Böhme J, Groden C, Neumaier-Probst E. Isolated punctuate hippocampal infarction and transient global amnesia are indistinguishable by means of MRI. *Int J Stroke*. 2017;12(3):292–6. <https://doi.org/10.1177/1747493016676613>.

## 183

### ONE-STOP CARDIAC-STROKE CT IN ACUTE STROKE FOR EARLY DETECTION OF MAJOR SOURCES OF CARDIOEMBOLIC STROKE MAY OFFER A RELEVANT OPTION TO IMPROVE PATIENT CARE

Patrick Langguth<sup>\*1</sup>, Naomi Larsen<sup>1</sup>, Mona Salehi Ravesh<sup>1</sup>, Hannes Gottschalk<sup>1</sup>, Johannes Meyne<sup>2</sup>, Thomas Lindner<sup>1</sup>, Annett Lebenatus<sup>1</sup>, Jakob Engel<sup>1</sup>, Tim-Christian Piesch<sup>1</sup>, Olav Jansen<sup>1</sup>, Friederike Austein<sup>1</sup>

<sup>1</sup>Department of Radiology and Neuroradiology, University Hospital Schleswig-Holstein, Campus Kiel, Kiel, Deutschland

<sup>2</sup>Department of Neurology, University Hospital Schleswig-Holstein, Campus Kiel, Kiel, Deutschland

**Background:** Currently, transesophageal (TEE) and transthoracic echocardiography (TTE) are considered as standard work-up for identifying sources of cardioembolic stroke (CES). This approach is time-consuming if performing TEE, semi-invasive, and not always feasible in patients with acute ischemic stroke (AIS), potentially delaying secondary stroke prevention. We assessed a one-stop cardiac-stroke CT (CS-CT) protocol including delayed-phase cardiac acquisition compared to standard work-up.

**Methods:** Patients with AIS verified by conventional stroke CT and subsequently examined by CS-CT were included in this study. Accuracy of CS-CT were compared to standard-of-care echocardiography.

**Result:** In this ongoing-trial currently 51 AIS patients were included; 37 of them received echocardiography in follow-up. Median time interval between stroke and echocardiography was 4 (IQR 2–6) days. Regarding the major sources of CES, three cases of intracardiac thrombus were observed with CS-CT but not detected with echocardiography (Fig. 1). Four patients with cardiac thrombus in the CS-CT received no echocardiography during their clinical stay. In total, CS-CT compared to echocardiography demonstrated a higher rate in detection of major sources of CES.

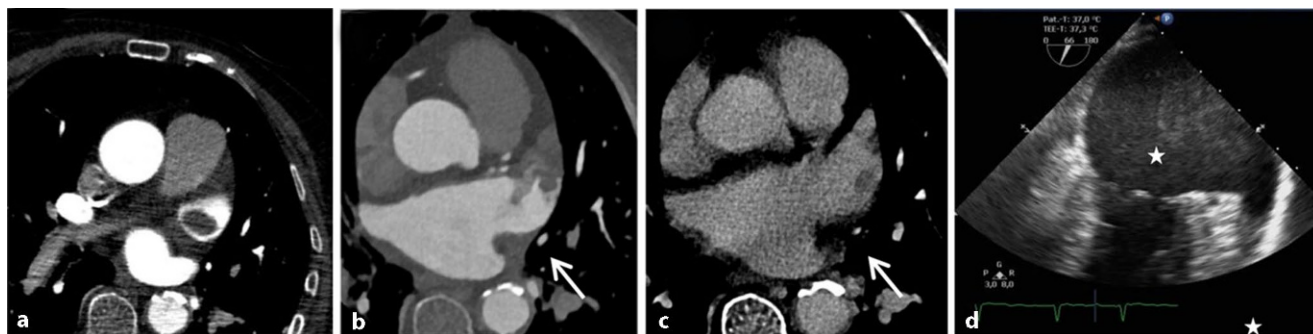


Fig. 1 | 183 This case presents a patient in whom a thrombus decreased over time, even without administration of therapeutic lysis therapy due to early cerebral infarct bleeding. In the initial CTA, an oval contrast agent recess with a diameter of 24 mm in the sense of a thrombus can be seen (a, white arrow). In cardiac CT examination on the following day (b, c), 17 hours after initial imaging, in the arterial (b) and venous phase (c) a smaller thrombus (10 mm, white dotted arrows) could be detected. Note the LAA circulatory disorder with triangular contrast agent sparing in the arterial phase (b). The TEE on day 7 shows spontaneous echo contrast (SEC) or „smoke-like“ echo (white stars), without solid thrombus detection (d)

**Discussion:** CS-CT, as an almost always feasible clinical test, has the potential to improve patient care, particularly concerning therapeutic decision-making to prevent secondary stroke when echocardiography alone cannot be performed at all or is greatly delayed.

**Conclusion:** With excellent accuracy in identifying major CES sources, CS-CT has the potential to improve early diagnosis and accelerates decision-making to prevent secondary stroke and, moreover, might reduce preliminary assessment as cryptogenic stroke by ensuring early, definite diagnosis.

190

### ENDOVASCULAR EMBOLIZATION OF 108 CRANIAL DURAL ARTERIOVENOUS FISTULAS WITH ONYX

Dominik Vollherbst<sup>\*1</sup>, Christian Herweh<sup>1</sup>, Silvia Schönenberger<sup>2</sup>, Fatih Seker<sup>1</sup>, Simon Nagel<sup>2</sup>, Peter Ringleb<sup>2</sup>, Martin Bendszus<sup>1</sup>, Markus Möhlenbruch<sup>1</sup>

<sup>1</sup>Universitätsklinikum Heidelberg, Abteilung Neuroradiologie, Heidelberg, Deutschland

<sup>2</sup>Universitätsklinikum Heidelberg, Abteilung Neurologie, Heidelberg, Deutschland

**Hintergrund:** Endovascular embolization can be an effective treatment for dural arteriovenous fistulas (DAVF). The purpose of this study was to report our single-center experience of endovascular embolization of DAVFs with Onyx.

**Methoden:** Clinical data, angiographic features, complications, treatment success (defined as complete symptom remission for low-grade DAVFs and complete occlusion for high-grade DAVFs), occlusion and recurrence rates were assessed.

**Ergebnisse:** 102 patients with 108 DAVFs were treated in 128 treatment procedures. Twenty-eight patients (27.5 %) presented with intracerebral hemorrhage and 20 patients (19.6 %) with cerebral venous congestion. Most of the DAVFs were located at the transverse and/or sigmoid sinus (40.7 %), followed by tentorial/petrosal location (23.1 %) and the superior sagittal sinus (18.5 %). The majority of DAVFs were high-grade fistulas (Cognard III-IV/Borden III; 73.1 %). Overall treatment success and complete occlusion rates were 82.4 % and 90.7 %, respectively. The median follow-up period was 16.5 months (1st quartile: 5.7 months, 3rd quartile: 36.5 months). Sixty-one patients (59.8 %) had a follow-up >12 months with a treatment success and complete occlusion rate of 82.0 % and 91.8 %, respectively. Forty-one patients (40.2 %) had a follow-up >24 months with a treatment success and complete occlusion rate of 82.9 % and 90.2 %, respectively. At the latest follow-up, 95.4 % of the patients showed complete symptom remission or symptom relief. Overall complication rate was 8.6 % (4.7 % asymptomatic, 2.3 % transient and 1.6 % permanent complications with fatal outcome). Recurrence was observed in 4 cases (3.7 %), of which 3 DAVFs were successfully re-treated with endovascular Onyx embolization and 1 DAVF was successfully treated by neurosurgical ligation of the fistula.

**Fazit:** Endovascular embolization of cranial DAVFs with Onyx is safe and offers high rates of long-term occlusion and symptom remission.

193

### TRANSARTERIAL BALLOON-ASSISTED LIQUID EMBOLIZATION OF DURAL ARTERIOVENOUS FISTULAS USING A DUAL-LUMEN MICRO-BALLOON CATHETER

Dominik Vollherbst<sup>\*1</sup>, Christian Herweh<sup>1</sup>, Silvia Schönenberger<sup>2</sup>, Fatih Seker<sup>1</sup>, Simon Nagel<sup>2</sup>, Peter Ringleb<sup>2</sup>, Martin Bendszus<sup>1</sup>, Markus Möhlenbruch<sup>1</sup>

<sup>1</sup>Universitätsklinikum Heidelberg, Abteilung Neuroradiologie, Heidelberg, Deutschland

<sup>2</sup>Universitätsklinikum Heidelberg, Abteilung Neurologie, Heidelberg, Deutschland

**Hintergrund:** Transarterial balloon-assisted liquid embolization can be an effective technique for the treatment of dural arteriovenous fistulas (DAVFs). The currently available data reporting on this treatment technique is rare. The purpose of this study is to report our single-center experience of patients with DAVFs who were treated with transarterial balloon-assisted liquid embolization using a dual-lumen micro-balloon catheter.

**Methoden:** A retrospective analysis of a prospectively collected database was performed. Demographic data, clinical data, angiographic features, procedural parameters, complications, occlusion rates, follow-up imaging and clinical outcome were assessed.

**Ergebnisse:** Twenty patients were treated in 26 treatment procedures. All but two patients were symptomatic (90.0%). Five patients (25.0%) initially presented with intracerebral hemorrhage. Four patients (20.0%) suffered from cerebral venous congestion. Most DAVFs (95.0%) were high-grade fistulas (presence of cortical venous reflux). Direct cortical venous drainage was present in 85.0% of the DAVFs. The most frequent localization was the transverse and/or sigmoid sinus (50.0%), followed by the tentorial localization (25.0%). In three procedures (11.5%) transarterial balloon-assisted liquid embolization was combined with transvenous balloon-assisted protection of the affected venous sinus. Complete angiographic occlusion was achieved in 90.0% of the patients (75.0% initial angiographic occlusion, 15.0% complete angiographic occlusion during follow-up after initial subtotal embolization). There was one complication (vessel perforation with a subsequent small, transiently symptomatic intracerebral hemorrhage), resulting in a complication rate of 4.0%. There were no permanent complications and no procedure-related deaths. After a mean follow-up period of 17.1 months, 14 patients (70.0%) achieved complete symptom remission, while the remaining 6 patients (30.0%) showed symptom relief.

**Fazit:** Transarterial balloon-assisted liquid embolization using a dual-lumen micro-balloon catheter is an effective and safe technique for the treatment of dural arteriovenous fistulas.

195

### MICROVASCULAR DECOMPRESSION IN TRIGEMINAL NEURALGIA: ENHANCEMENT OF CLINICAL OUTCOME ESTIMATION BY IMAGE COMBINATION OF MR-SPACE WITH MR-ANGIOGRAPHY

Sebastian Müller<sup>\*1</sup>, Eya Khadhraoui<sup>1</sup>, Ali Khanafer<sup>1</sup>, Marios-Nikos Psychogios<sup>1</sup>, Veit Rohde<sup>2</sup>, Levent Tanrikulu<sup>2</sup>

<sup>1</sup>Neuroradiologie, Göttingen, Deutschland

<sup>2</sup>Neurochirurgie, Göttingen, Deutschland

**Background:** Detailed imaging of cranial nerves at the surface of the brainstem is recommended for the visualization of causative neurovascular compression (NVC) in patients with trigeminal neuralgia (TN). High-resolution MRI enables the differentiation between causative arteries and veins. The goal of this study is to analyze the impact of the combination of highly-resolved MRI techniques on the clinical post-operative outcome estimation of microvascular decompression (MVD).

**Methods:** 62 patients (m/f:37/25) with classical TN were analyzed. 14 patients were excluded. 48 patients underwent MVD of the REZ of the trigeminal nerve. 38 out of 48 operated patients received preoperative highly-resolved imaging by T2-SPACE sequences in combination with time of flight (TOF) MR-angiography. 10 patients had preoperative T2-CISS imaging. The patients were categorized into four subgroups: 1) NVC negative, 2) venous NVC, 3) arterial NVC, 4) combined arterial and venous NVC. The preoperative MRI findings were compared to the intraoperative morphological parameters. Outcome parameters were quantified by the Barrow Neurological Institute pain score.

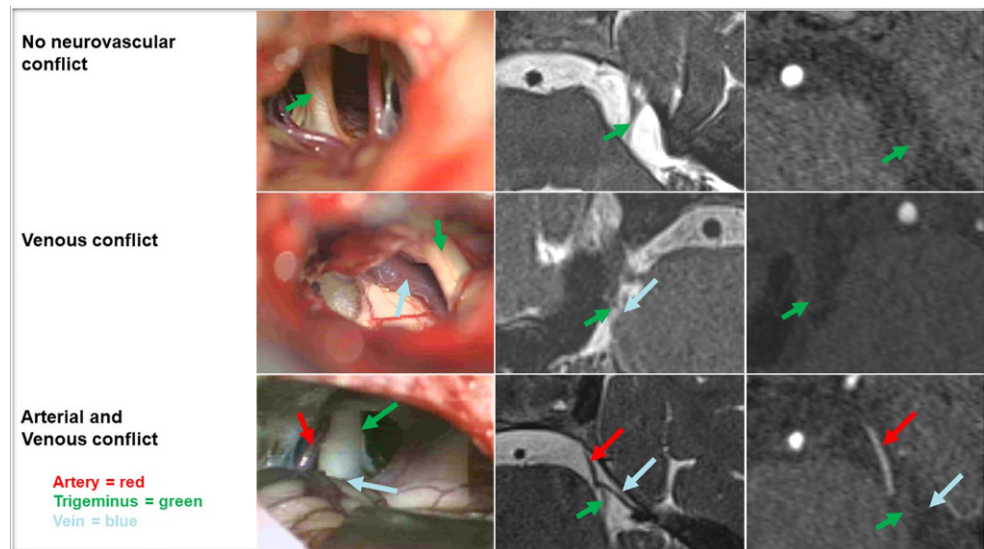


**Fig. 1 | 195** Comparison of operation pictures, MRI and MR-A

**Results:** 29 pure arterial NVC (SCA: 27, AICA: 2), 8 venous NVC and 3 combined NVC (SCA+vein) were detected. In 8 cases no NVC was noticed during MVD. The neurovascular findings from the MRI correlated in 91.7 % of the treated patients with the intraoperative findings. In the examined cases with a combined image analysis of T2-SPACE/CISS with MR-TOF the correlation was enhanced to 94.7 % of the examined subjects. The clinical outcome was significantly higher in the patients with arterial NVC compared to venous NVC.

**Discussion:** Comparing our study with the other literature a standard preoperative imaging workup by highly-resoluted T2-SPACE and MR-angiography should be performed in all patients with trigeminal neuralgia. A detailed multidisciplinary analysis of the patients should be performed by the neurologist, neuroradiologist and the neurosurgeon in order to optimize the surgical result for pain-freedom.

**Conclusion:** Combined imaging of T2-SPACE/CISS with MR-TOF enables an optimized delineation of arterial and venous neurovascular conflicts and may allow a better prediction of clinical outcome compared to T2 imaging data alone.

## 196

### EFFECT OF DIRECT THROMBOASPIRATION VS. STENT-RETRIEVER-THROMBECTOMY ON RADIATION EXPOSURE, PROCEDURE TIME AND FLUOROSCOPY TIME IN PATIENTS TREATED FOR ANTERIOR CIRCULATION ISCHEMIC STROKE – A MATCHED-PAIR ANALYSIS

Charlotte Weyland<sup>\*1</sup>, Felix Hemmerich<sup>1</sup>, Markus Möhlenbruch<sup>1</sup>, Martin Bendszus<sup>1</sup>, Johannes Pfaff<sup>1</sup>

<sup>1</sup>Klinik für Neurologie, Abteilung für Neuroradiologie, Heidelberg, Deutschland

**Background:** To quantify the effect of stent-retriever thrombectomy vs. direct thromboaspiration on radiation exposure (RE), procedure time (PT) and fluoroscopy time (FT) in patients with endovascular stroke treatment (EST) for anterior circulation ischemic stroke.

**Methods:** Retrospective analysis of an institutional review board-approved stroke database of a comprehensive stroke center focusing on RE (as per dose area product in  $\mu\text{Gy}\cdot\text{m}^2$ , median [IQR]), procedure and fluoroscopy time (in minutes, median [IQR]) in patients receiving EST in anterior circulation ischemic stroke. Patients who received EST using direct thromboaspiration (DT) were matched with patients treated using stent-retriever thrombectomy (SR) according to location of

intracranial occlusion, mode of anesthesia, number of thrombectomy maneuvers and gender (order of decreasing priority).

**Result:** Overall 136 patients ( $n=68$  in each group) have been included in this analysis. Apart from patient age (in years, mean (SD): DT=74 (13); SR=79 (11),  $p$ -value: 0.023), there is no significant difference in patient's baseline characteristics. PT (DT: 26 (21–38); SR: 49 (37–77);  $p$ -value: <0.0001) and FT (DT: 12 (7–18); SR: 26 (14–43),  $p$ -value: <0.0001) are shorter in patients who received direct thromboaspiration. RE (DT: 6255 (4170–8944); SR: 8984 (5367–13.168),  $p$ -value: 0.034) is significantly lower in patients who received EST using direct thromboaspiration. This is a relative median increase of RE of 43.6%, a relative increase of 116.6% of FT and of 88.5% of PT in patients who received stent-retriever assisted thrombectomy.

**Discussion:** In this retrospective analysis EST using direct thromboaspiration was associated with lower RE, FT and PT compared to matched patients who received stent-retriever thrombectomy. This result is contradictory to the RE – analysis of Farah et. al [1] who showed no difference in RE concerning the EST maneuvers in their evaluation of dose reference level for EST.

**Conclusion:** Our analysis shows a difference in RE between maneuvers in endovascular stroke treatment with a higher RE in stent-retriever thrombectomy compared with direct thromboaspiration.

### References

- Farah J, Rouchaud A, Henry T, Regen C, Mihalea C, Moret J, et al. Dose reference levels and clinical determinants in stroke neuroradiology interventions. *Eur Radiol.* 2019;29(2):645–53.

## 197

### RADIATION EXPOSURE, PROCEDURE TIME AND FLUOROSCOPY TIME IN PATIENTS

#### TREATED FOR ACUTE BASILAR ARTERY OCCLUSION – A MATCHED-PAIR ANALYSIS

Charlotte Weyland<sup>\*1</sup>, Felix Hemmerich<sup>1</sup>, Markus Möhlenbruch<sup>1</sup>, Martin Bendszus<sup>1</sup>, Johannes Pfaff<sup>1</sup>

<sup>1</sup>Klinik für Neurologie, Universitätsklinik Heidelberg, Abteilung für Neuroradiologie, Heidelberg, Deutschland

**Background:** Since the establishment of dose reference levels (DRLs) for radiation exposure (RE) in endovascular stroke treatment (EST) of

anterior circulation ischemic stroke has recently begun [1] we sought to quantify RE, procedure time (PT) and fluoroscopy time (FT) in patients receiving EST for acute basilar artery occlusions (BAO).

**Methods:** Retrospective analysis of an institutional review board–approved stroke database of a comprehensive stroke center focusing on RE (as per dose area product in  $\mu\text{Gy}\cdot\text{m}^2$ , median [IQR]), PT and FT (in minutes, median [IQR]) in patients receiving EST for acute BAO. Patients who received EST for BAO were matched with patients who received EST for middle cerebral artery occlusions (MCAO) according to mode of anesthesia, number of maneuvers and gender (order of decreasing priority).

**Result:** 184 patients ( $n=92$  in each group) have been included in this analysis. No significant difference in patient’s baseline characteristics, with the exception of a more severe initial severity of stroke symptoms (as per National Institutes of Health Stroke Scale; BAO: 21 (9–34); MCAO: 17 (14–21),  $p$ -value: 0.025) and a trend towards a longer time from stroke onset to groin puncture (BAO: 302 (171–602); MCAO: 247 (156–403),  $p$ -value: 0.053) in patients treated for BAO was observed. PT (BAO: 60 (44–102); MCAO: 50 (34–99);  $p$ -value: 0.397) and FT (BAO: 28 (21–52); MCAO: 26 (17–45),  $p$ -value: 0.640) were comparable. RE (BAO: 12.494 (8401–20.211); MCAO: 9577 (6369–15.337),  $p$ -value: 0.01) was significantly higher in patients who received EST for BAO. This reflects a relative increase of 30.5% of RE in patients who received EST for BAO.

**Discussion:** In this retrospective analysis EST for acute BAO was associated with a significantly higher RE compared to matched patients who received EST for MCAO. Thus contradicting comparable studies as Farah et. al [1], who primarily investigated DRLs for EST in ischemic stroke of the anterior circulation, but also included cases of EST for the posterior circulation in their analysis. We consider our results as methodically more accurate also due to a significantly larger sample size (Farah et. al:  $n=16$ , 5.1% of the overall sample size of).

**Conclusion:** This study shows that RE is significantly higher in EST for acute BAO than in EST for MCAO, which should be considered in the establishment of DRLs for EST.

**References**

1. Farah J, Rouchaud A, Henry T, Regen C, Mihalea C, Moret J, et al. Dose reference levels and clinical determinants in stroke neuroradiology interventions. *Eur Radiol.* 2019;29(2):645–53.

**203**

**ENDOVASCULAR THERAPY FOR ISCHEMIC STROKE: MORE THAN THREE RETRIEVAL ATTEMPTS IMPROVE THE RATE OF FLOW RESTORATION BUT NOT CLINICAL OUTCOME**

Fabian Flottmann\*<sup>1</sup>, Hannes Leischner<sup>1</sup>, Milani Deb-Chatterji<sup>2</sup>, Götz Thomalla<sup>2</sup>, Jens Fiehler<sup>1</sup>, Caspar Brekenfeld<sup>1</sup>

<sup>1</sup>Klinik und Poliklinik für Neuroradiologische Diagnostik und Intervention, Universitätsklinikum Hamburg-Eppendorf, Hamburg, Deutschland

<sup>2</sup>Klinik für Neurologie, Universitätsklinikum Hamburg-Eppendorf, Hamburg, Deutschland

**Background:** In acute ischemic stroke due to large-vessel occlusion, endovascular therapy (EVT) allows flow restoration in a majority of cases. Often more than one retrieval attempt is required to achieve reperfusion. A single-center study<sup>1</sup> observed that more than three retrieval attempts lead to increased rates of successful reperfusion, but might not further improve clinical outcome. This study aimed at testing this hypothesis in a large multi-center patient cohort.

**Methods:** In this retrospective multi-center analysis, 1852 patients who underwent EVT with at least one retrieval attempt were included. Successful recanalization was defined as TICI 2b/3, and good clinical

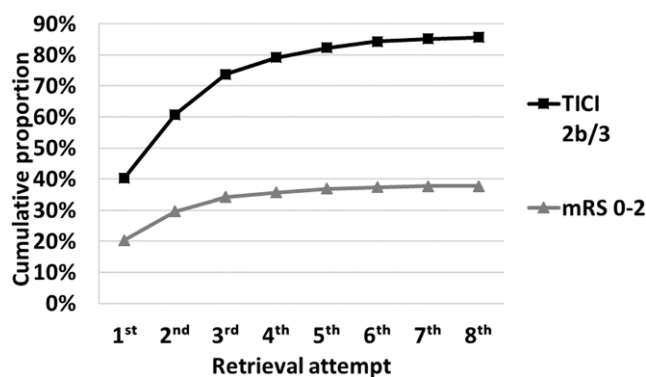


Fig. 1 | 203 Cumulative proportion of TICI 2b/3 reperfusion and good clinical outcome after a certain number of retrieval attempts ( $n=1852$ )

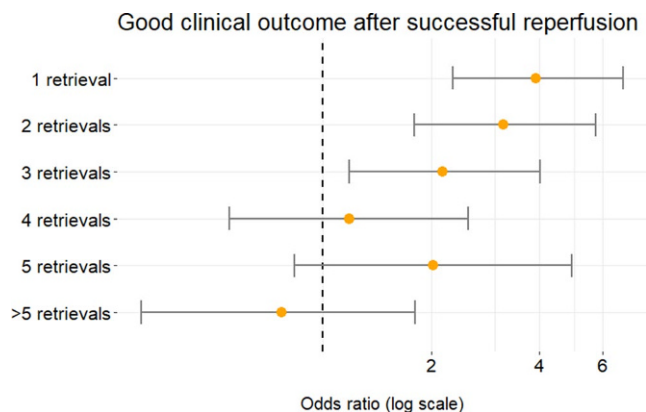


Fig. 2 | 203 Logistic regression of good clinical outcome, adjusted for confounders (time to reperfusion, age, sex, admission NIHSS, location of occlusion)

outcome was defined as mRS at 90 days of  $\leq 2$ . Logistic regression was used to model the occurrence of good clinical outcome after adjusting for confounders.

**Result:** After 3 retrieval attempts, 73.8% of all patients showed successful reperfusion, which increased to 85.1% percent after 6 retrievals. Conversely, after 3 retrieval attempts, 34.2% showed good clinical outcome, and this number only increased slightly to 37.3% after 6 attempts.

In multivariate logistic regression, successful reperfusion after 1–3 attempts was associated with good clinical outcome, but this association was lost after subsequent retrieval attempts (adjusted OR after one retrieval: 3.9 (95% CI 2.3–6.8) vs. 4 retrievals: 1.2 (95% CI 0.5–2.54)).

**Discussion:** Using logistic regression in a large multi-center cohort, we were able to support the hypothesis that there is an apparent contradiction between improved rates of successful reperfusion but not clinical outcome after >3 retrieval attempts.

**Conclusion:** More than 3 retrievals improve rates of successful reperfusion, but not so much the rate of good clinical outcome.

**References**

1. Flottmann, et al. Recanalization Rate per Retrieval Attempt in Mechanical Thrombectomy for Acute Ischemic. *Stroke Stroke.* 2018.

### TRUE FIRST-PASS EFFECT FOR THE POSTERIOR CIRCULATION: FIRST-PASS COMPLETE REPERFUSION IMPROVES CLINICAL OUTCOME IN STROKE THROMBECTOMY PATIENTS

Nuran Abdullayev\*<sup>1</sup>, Volker Maus<sup>2</sup>, Daniel Behme<sup>3</sup>, Jan Borggrefe<sup>1</sup>, Marc Schlamann<sup>1</sup>, Thomas Liebig<sup>4</sup>, Christoph Kabbasch<sup>1</sup>, Anastasios Mpotsaris<sup>5</sup>

<sup>1</sup>Department of Radiology, University Hospital of Cologne, Köln, Deutschland

<sup>2</sup>Institute of Diagnostic and Interventional Radiology, Neuroradiology and Nuclear Medicine, Knappschaftskrankenhaus Bochum, Ruhr University Bochum<sup>4</sup> Bochum, Deutschland

<sup>3</sup>Department of Neuroradiology, University Medical Center Goettingen, Goettingen, Deutschland

<sup>4</sup>Institute of Neuroradiology, University Hospital Munich (LMU), München, Deutschland

<sup>5</sup>Department of Neuroradiology, RWTH Aachen, Aachen, Deutschland

**Background:** Complete reperfusion (mTICI 3) in stroke patients after a single mechanical thrombectomy (MT) pass has been hypothesized as a predictor for favorable outcome (mRS 0–2) and a true first-pass effect defined as improved clinical outcome after complete reperfusion in the anterior circulation with one pass has been already scientifically proven. But a true first-pass effect with complete reperfusion in the posterior circulation with one vs. multiple passes has not yet been specifically addressed in the literature.

**Methods:** Patients with occlusions in the posterior circulation (carried out between 2010 and 2017) were analyzed and clinical outcome of basilar artery occlusions (BAO) patients with complete reperfusion and known symptom onset were compared. After adjustment for multiple confounding factors such as demographics, time intervals, stroke severity (NIHSS), early stroke signs (PC ASPECTS) and comorbidity, we compared outcome at 90 days between matched cohorts of firstpass complete reperfusion vs. multipass complete reperfusion.

**Result:** A total of 90 MTs of BAO were analyzed. We compared clinical outcome of 56 patients with BAO and known symptom onset, in whom we achieved complete reperfusion (mTICI 3), depending on whether complete reperfusion was achieved after a single thrombectomy pass ( $n=28$ ) or multiple thrombectomy passes ( $n=28$ ). Multivariable analysis of our cohort of 56 nonmatched patients revealed that there was a highly significant association between first-pass complete reperfusion and favorable clinical outcome ( $p<0.0001$ ). In our matched cohorts ( $n=7$  vs.  $n=7$ ), favorable clinical outcome was only seen if complete reperfusion was achieved after one pass (86% vs. 0%).

**Discussion:** Rapid and complete reperfusion is widely accepted to be crucial for favorable outcome<sup>1,2</sup>. Our results imply that the first thrombectomy maneuver should be undertaken with the technique with the highest first-pass complete reperfusion rates, but our study cannot address the question how to best achieve first-pass complete reperfusion.

**Conclusion:** First-pass complete reperfusion in the posterior circulation is an independent predictor of favorable outcome. Achieving complete reperfusion after multiple passes might simply not be good enough in the posterior circulation.

#### References

1. Khatri P, et al. Good clinical outcome after ischemic stroke with successful revascularization is timedependent. *Neurology*.
2. Zaidat OO, et al. First pass effect: A new measure for stroke thrombectomy devices. *Stroke*.

### TUBING-TUNING: EINFLUSS DES TUBINGS AUF DIE ASPIRATIONSRATE GÄNGIGER ASPIRATIONSUMPEN

Hannes Schwenke\*<sup>1</sup>, Astrid Aumann<sup>1</sup>, Peter Schramm<sup>1</sup>

<sup>1</sup>Institut für Neuroradiologie, UKSH, Campus Lübeck, Lübeck, Deutschland

**Hintergrund:** Zu den Einflussgrößen auf die Thrombusaspiration zählt neben dem Innendurchmesser des Aspirationskatheters auch die Leistung des mechanischen Aspirationssystems, bestehend aus einer Aspirationspumpe und dem dazugehörigen Tubing. Im Rahmen der vorliegenden Arbeit wurde in vitro untersucht, welche Kombinationen von verschiedenen Aspirationspumpe und Tubings den optimalen Einfluss auf eine Steigerung der maximalen Aspirationsrate der Aspirationskatheter hat. Insbesondere wurde untersucht, ob sich die Aspirationsrate der Pumpen unabhängig vom Tubing unterscheidet.

**Methoden:** In  $n=280$  Messungen á 20 Sek. Messdauer wurde die Aspirationsrate verschiedener Aspirationskatheter (Penumbra: ACE 64, ACE 68, 5 MAX, 4 MAX, 3 MAX, 5 MAX ACE; Stryker: Catalyst 6) über eine Messung im Messzylinder ermittelt. Hierbei wurde Glycerin-Wasser-Gemisch aspiriert und die Aspirationsmenge pro Zeit mit einer Hochpräzisionswaage (A&D EK-2000i, 10 Datenpunkte pro Sek.) erfasst. Die Pumpen (Penumbra MAX; Medela Dominant Flex) und die Tubings (jeweils zugehöriges Penumbra-Tubing; Medela-Tubing) wurden systematisch variiert. Die Datenanalyse erfolgte über ANOVAs mittels Matlab 2018b.

**Ergebnisse:** Die mittlere Aspirationsrate beider Pumpen unabhängig vom Tubing unterschied sich in unserem Experiment nicht signifikant voneinander (Abb. 1). Die Anwendung des Medela-Tubings führte zu einer signifikant höheren Aspirationsrate als das Penumbra-Tubing (Abb. 2), unabhängig von der angewendeten Pumpe. Die Aspirationsrate der mit einem Medela-Tubing ausgestatteten Medela-Pumpe war signifikant höher als die mit einem Penumbra-Tubing ausgestattete Penumbra-Pumpe (Abb. 2).

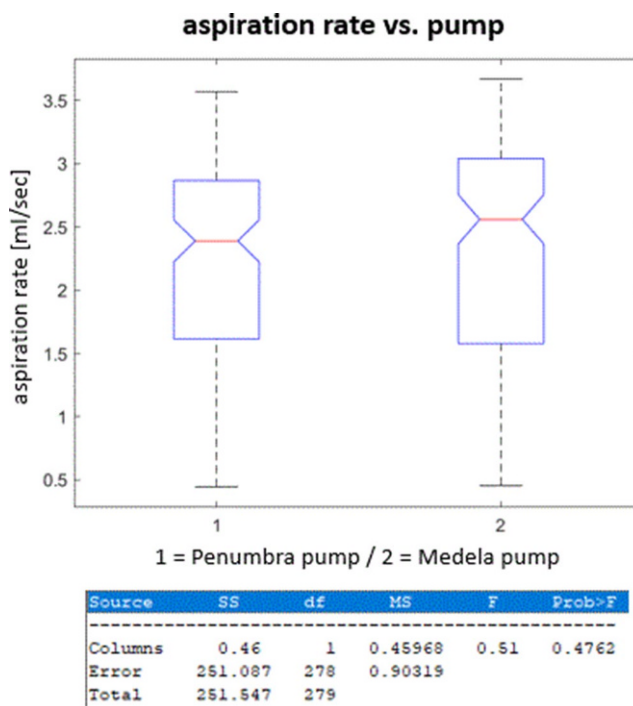


Abb. 1 | 222

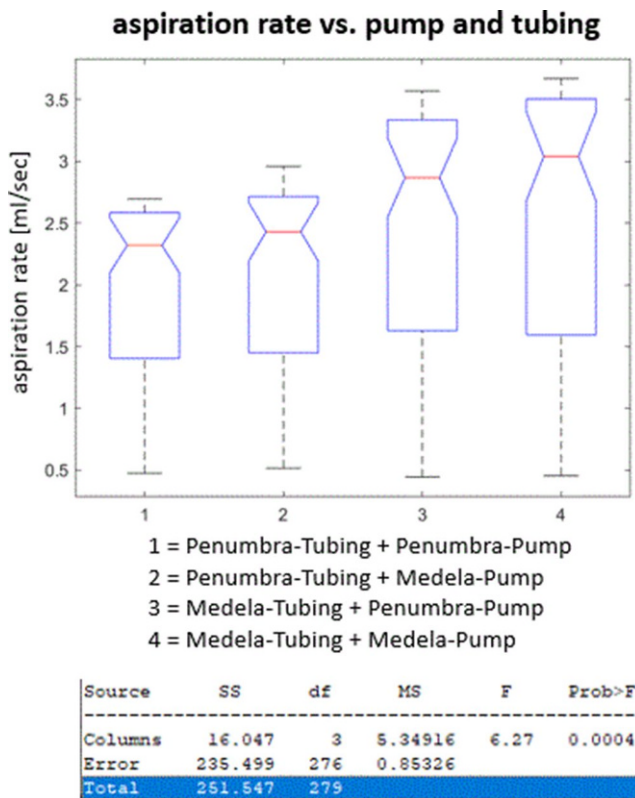


Abb. 2 | 222

**Diskussion:** Die maximale Aspirationsrate kann mittels Wechsel auf ein Tubing mit großem Innendurchmesser gesteigert werden („Tubing-Tuning“). In unserem Experiment führte ein Wechsel auf das größlumigere Tubing ohne integrierte On-Off-Adapter zu einer Verbesserung der Aspirationsrate um ca. 20 %. Die Aspirationsrate verringerte sich dementsprechend bei beiden Pumpen mit Anwendung des Tubings, welches den eingebauten, flussreduzierenden On-Off-Konnektor aufweist. **Fazit:** Insbesondere das Tubing und weniger die Pumpen stellen einen Einflussfaktor auf die Aspirationsraten der Aspirationssysteme dar. Lumenreduzierende Adapter innerhalb der Tubings können im Direktvergleich die Aspirationsrate in vitro signifikant reduzieren.

223

**TREATMENT OF INTRACRANIAL ANEURYSMS WITH THE NEW-GENERATION LOW-PROFILE ACANDIS ACCLINO MICROSTENT: LONG-TERM SAFETY AND EFFICACY IN A MULTICENTER STUDY**

Lukas Görtz<sup>\*1</sup>, Michael Smyk<sup>2</sup>, Anastasios Mpotsaris<sup>3</sup>, Jan Borggrefe<sup>1</sup>, Franziska Dorn<sup>4</sup>, Thomas Liebig<sup>4</sup>, Marc Schlamann<sup>1</sup>, Bernd Turowski<sup>2</sup>, Christoph Kabbasch<sup>1</sup>

<sup>1</sup>Köln, Deutschland  
<sup>2</sup>Düsseldorf, Deutschland  
<sup>3</sup>Aachen, Deutschland  
<sup>4</sup>München, Deutschland

**Background:** Stent-assisted coiling (SAC) represents an established treatment option for complex intracranial aneurysms. The Acandis Acclino is a novel self-expandable closed-cell nitinol microstent which complies with a 0.0165” or 0.017” microcatheter. We report long-term clinical and angiographic outcome in a multicenter setting. **Methods:** The Acclino micro-stent was used in 98 consecutive patients (55.4±13.5 years) for treatment of 98 aneurysms (28 unruptured, 20

recurrent, 50 ruptured) at three German tertiary care centers within a 6-year period. We retrospectively analyzed technical success, complication rates, clinical outcome and angiographic results.

**Result:** Stent implantation was technically successful in all aneurysms achieving immediate complete occlusion in 89.8%. Among 65 patients (66.3%) with 6-month angiographic follow-up, complete and near-complete occlusion was obtained in 92.3% and 98.5%, respectively. At long-term follow-up (38 patients, mean: 21 months), the complete and near-complete occlusion rates were 81.2% and 89.5%, respectively. Aneurysm recurrence between mid- and long-term follow-up was observed in 14.3%. Retreatment was performed in 11.3%. The overall complication rate was 8.2% (8/98), including three thromboembolic events (3.1%) and five hemorrhagic events (5.1%). Neurological complications occurred in three patients, of which one was device-related (one ischemic stroke in a patient with subarachnoid hemorrhage). Among scheduled patients, procedural and device-related morbidity rates were 2.1% (1/48) and 0% (0/48), respectively.

**Discussion:** To date, robust data on long-term angiographic outcome is available for the Enterprise stent system, achieving 59% and 81% complete or near-complete occlusion rates in a study by Fargen et al. [1]. The results of the current study compare favourably and may indicate a more durable long-term aneurysm occlusion of the low-profile Acclino stent with minimal complication and morbidity rates.

**Conclusion:** The present study demonstrates a high safety profile of the Acclino microstent, with an ischemic stroke rate of 1.0%. Long-term aneurysm rates compare favorably to first-generation stents and justify further investigation of this device.

References

1. Fargen KM, Mocco J, Neal D, Dewan MC, Reavey-Cantwell J, Woo HH, et al. A multicenter study of stent-assisted coiling of cerebral aneurysms with a Y configuration. Neurosurgery. 2013;73:466–72.

224

**LOW-PROFILE WEB 17 VERSUS PREDECESSOR WEB 21 SYSTEM FOR TREATMENT OF SMALL INTRACRANIAL ANEURYSMS: COMPARATIVE ANALYSIS OF PROCEDURAL SAFETY AND FEASIBILITY**

Lukas Görtz<sup>\*1</sup>, Thomas Liebig<sup>2</sup>, Eberhard Siebert<sup>3</sup>, Moritz Herzberg<sup>2</sup>, Marc Schlamann<sup>1</sup>, Jan Borggrefe<sup>1</sup>, Franziska Dorn<sup>2</sup>, Christoph Kabbasch<sup>1</sup>

<sup>1</sup>Köln, Deutschland  
<sup>2</sup>München, Deutschland  
<sup>3</sup>Berlin, Deutschland

**Background:** Woven EndoBridge (WEB) represents an efficient technique for endovascular treatment of wide-necked and bifurcation aneurysms. The WEB 17 system has been recently introduced for facilitated endovascular treatment of small bifurcation aneurysms (≤7 mm) with low profile microcatheters. We compared the WEB 17 with its predecessor versions in terms of procedural safety and feasibility.

**Methods:** This is a multicenter review of aneurysms ranging from 3 to 7 mm treated with the WEB between 2011 and 2019. Aneurysm characteristics, procedural parameters and complications were retrospectively compared between treatment with the WEB 17 and a control group that was treated with its predecessor 21-version using inverse probability of treatment weighting (IPTW).

**Results:** The study cohort consisted of 38 patients treated with a WEB 17 (mean size: 4.9±1.5 mm) and 70 with a WEB 21 (mean size: 5.6±1.4 mm). The 21 system had a higher failure rate (10.3%) than WEB 17 (0%, p=0.05). Additional stenting was performed more often with WEB 21 (10%) than with WEB 17 (2.6%, adjusted p=0.005).

Thromboembolic events occurred more often in the WEB 21 group (14.3%) than in the WEB 17 group (5.3%, adjusted  $p=0.002$ ). Neurological complications (WEB 17: 2.6%, WEB 21: 2.9%, adjusted  $p=1.0$ ) and immediate complete aneurysm occlusion rates (WEB 17: 57.9%, WEB 21: 54.3%, adjusted  $p=0.21$ ) did not differ significantly between both groups.

**Discussion:** Small wide-necked aneurysms are generally difficult to treat by endovascular means. The WEB 17 system consists of fewer and thinner nitinol wires than the predecessor WEB 21 and is therefore compatible with a 0.017" low-profile microcatheter. This system aims to increase flexibility of the device and to facilitate deployment in small aneurysms. In our study, the WEB 17 was associated with a higher success rate and a significantly reduced thromboembolic compared to the WEB 21 in the adjusted analysis. Long-term angiographic outcome data will be necessary to investigate the efficacy of the new WEB 17 system.

**Conclusion:** The low-profile WEB 17 provides a feasible and safe approach for endovascular treatment of small wide-necked aneurysms. Long-term outcome analysis will be necessary to draw a definite conclusion.

## 225

### DOES THE SIZE MATTER? 6F ADAPT ONLY VS 5F ADAPT AND PROXIMAL FLOW ARREST IN A M1 OCCLUSION MODEL

Jawid Madjidyar\*, Lars Nerkada, Olav Jansen

Klinik für Radiologie und Neuroradiologie, Universitätsklinikum Schleswig-Holstein, Campus Kiel, Kiel, Deutschland

**Hintergrund:** A direct aspiration first pass technique (ADAPT) has proven to be a highly effective thrombectomy option in patients with stroke due to large vessel occlusion. Simultaneously, balloon guide catheters seem to lead to better results in mechanical recanalization, mostly in combination with stent retrievers. At the moment the 6F aspiration devices do not fit through a balloon guide catheter on the market. In this experimental study the efficacy of ADAPT only via 6F aspiration device and ADAPT combined with BGC using a 5F aspiration device were compared.

**Methoden:** Two different clot models were used: A fibrin rich (white) clot and a RBC rich (red) clot. Each clot was placed into the M1 segment of a transparent silicon phantom of the anterior circulation. Physiological hemodynamic conditions were maintained by a programmable piston pump. Thrombectomy was performed with 1) SOFIA 6 F via 6F Neuron MAX Long Sheath and 2) SOFIA 5F via 8F FlowGate Balloon Guide Catheter. The thrombectomy was performed under direct visual control. Primary endpoints were the number of passes and the occurrence/number of distal emboli.

**Ergebnisse:** 10 experiments were made with each clot model and thrombectomy setup (total of  $n=40$ ). First pass full recanalization could be achieved by the 6F ADAPT only technique in 80 % of the cases in red clots and 90 % in white clots. However, the catheter was clogged by the white clots in every experiment, though it had to be pulled back into the long sheath and distal emboli were caused in 20 % of the experiment (10 % in red clots).

Using 5F ADAPT combined with BGC a first pass full recanalization rate of 90% could be achieved in red clots and 100% in white clots. In both clot models a 10% rate of distal emboli occurred. In 85% of the experiments the thrombi clogged the catheter and had to be pulled back into the BGC.

**Diskussion:** In this experimental setting the smaller inner diameter of the aspiration catheter is more than compensated by the additional use of the BGC, but there is no statistical significance. Both 6F ADAPT and 5F ADAPT combined with BGC show a high first pass efficacy and a low distal emboli rate. As soon as the aspiration catheter was clogged

the proximal aspiration via the long sheath or BGC was crucial to guarantee the thrombectomy.

**Fazit:** The size depends on the setting: ADAPT via a 6F aspiration catheter was equal to ADAPT via a 5F aspiration catheter combined with BGC. Both techniques were highly effective, though a cost analysis could be made to decide which technique to choose.

## 234

### RESULTS AFTER CAROTID STENTING WITH THE CGUARD STENT AS PART OF INTRACRANIAL AND EXTRACRANIAL THROMBECTOMY

Teodor Catalin Sabou\*, Reimer Andresen, Christian Wissgott, Christoph Kopetsch, Fabian Scheer

Institute of Diagnostic and Interventional Radiology/Neuroradiology, Westküstenklinikum Heide, Academic Teaching Hospital of the Universities of Kiel, Luebeck and Hamburg, Heide, Deutschland

**Background:** The purpose of the study was to evaluate the MicroNet coated CGuard Nitinol stent for safety and efficacy in the treatment of acute occlusions of the cerebral arteries.

**Methods:** In our department for interventional neuroradiology in the period between 01.01.2016 and 03.03.2019, a total of 20 patients underwent aspiration thrombectomy after acute occlusion of the cerebral arteries due to a high-grade stenosis or occlusion at the origin of the internal carotid artery with concomitant occlusion of the middle cerebral artery. During the same intervention, the internal carotid artery lesion was treated with the double-layered CGuard nitinol stent. Postinterventionally, 18 patients underwent a Therapy with aspirin (100 mg daily) and clopidogrel (75 mg daily)(11 patients only aspirin, 2 patients only clopidogrel, 8 patients combined and 2 patients only heparin). The stent patency was performed using dopple ultrasonography.

**Result:** The stent was successfully placed in all 20 patients. Postinterventional dopple ultrasound was performed in the neurological department in 17 patients after a mean time of 4,18 days (MIN 1; MAX 9). No in-stent stenosis and no stent thrombosis were detected. Postinterventionally, dual platelet aggregation inhibition was administered after 2,9 days (STDEV  $\pm$  2,3; MIN 0; MAX 9). Preinterventional systemic lysis was administered in 9 patients. Intracranial hemorrhage in the infarct area was detected in 11 patients. Two patients have died due to intracranial hemorrhage.

**Discussion:** The recommendations of the European Society for Vascular Surgery regarding the endovascular treatment of the carotid artery stenosis are a premedication with aspirin (300 mg initially for up to 14 days followed by 75 mg daily if not already taking aspirin) and clopidogrel (75 mg daily) 3 days prior to carotid artery stenting (1). In our cases the intervention was performed without a premedication. No in-stent stenosis or thrombosis were observed in the follow-up.

**Conclusion:** The use of the CGuard stent for the treatment of internal carotid artery stenosis or occlusion in acute stroke treatment is a safe and effective method. No in-stent occlusions or stenosis were detected despite late administration of platelet aggregation inhibitors and lack of premedication.

## References

1. Naylor AR, et al. Editor's Choice – Management of Atherosclerotic Carotid and Vertebral Artery Disease: 2017 Clinical Practice Guidelines of the European Society for Vascular Surgery (ESVS). Eur J Vasc Endovasc Surg. 2018;55(1):3–81.

### ENDOVASCULAR TREATMENT OF VERY ELDERLY PATIENTS AGED 90+ WITH ACUTE ISCHEMIC STROKE

Lukas Meyer\*<sup>1</sup>, Maria Alexandrou<sup>2</sup>, Fabian Flottmann<sup>1</sup>, Milani Deb-Chatterji<sup>3</sup>, Nuran Abdullayev<sup>4</sup>, Volker Maus<sup>5</sup>, Maria Politi<sup>2</sup>, Christian Roth<sup>2</sup>, Andreas Kastrup<sup>6</sup>, Caspar Brekenfeld<sup>1</sup>, Götz Thomalla<sup>3</sup>, Christian Gerloff<sup>3</sup>, Anastasios Mpotsaris<sup>7</sup>, Panagiotis Papanagiotou<sup>2</sup>, Jens Fiehler<sup>1</sup>, Hannes Leischner<sup>1</sup>

<sup>1</sup>Universitätsklinikum Hamburg-Eppendorf, Diagnostische und Interventionelle Neuroradiologie, Hamburg, Deutschland

<sup>2</sup>Klinikum Bremen-Mitte, Diagnostische und Interventionelle Neuroradiologie, Bremen, Deutschland

<sup>3</sup>Universitätsklinikum Hamburg-Eppendorf, Neurologie, Hamburg, Deutschland

<sup>4</sup>Universitätsklinikum Köln, Diagnostische und Interventionelle Radiologie, Köln, Deutschland

<sup>5</sup>Ruhr-Universität Bochum- Universitätsklinikum Knappschafts-Krankenhaus, Diagnostische und Interventionelle Neuroradiologie, Bochum, Deutschland

<sup>6</sup>Klinikum Bremen-Mitte, Neurologie, Bremen, Deutschland

<sup>7</sup>Universitätsklinikum Aachen, Diagnostische und Interventionelle Neuroradiologie, Aachen, Deutschland

**Background:** Patients aged 90+ were excluded or underrepresented in past thrombectomy trials<sup>1</sup>; thus, uncertainty remains if treatment benefits can be expected regardless of age. This study aims to analyze outcome and safety of thrombectomy in very elderly patients to improve decision-making in a real world setting.

**Methods:** All currently available data of patients aged 90+ enrolled in the German Stroke Registry-Endovascular Treatment were combined with a smaller cohort from three tertiary stroke centers. Baseline characteristics, procedural (TICI) and functional outcome (NIHSS, mRS) parameter as well as complications (sICH, SAEs) were analyzed for all patients. Good functional outcome was defined with regard to a very elderly population as mRS≤3 at 90-days.

**Results:** 203 patients with anterior circulation stroke and pre-mRS≤3 were included. The rate of successful recanalization (TICI ≥2 b) was 75.9% (154/203). Good functional outcome was observed in 21.6% (41/193) of patients at 90-days. In-hospital mortality was 27.1% (55/203) and increased significantly at 90-days to 48.9% (93/190;  $p < 0.001$ ). sICH occurred in 3% (6/203) of patients. Logistic regression analysis identified NIHSS (adjusted OR 0.88; 95CI 0.81–0.96;  $p = 0.006$ ) and ASPECTS (adjusted OR 1.58; 95CI 1.03–2.42;  $p = 0.036$ ) as independent predictors for good outcome at 90-days. Patients with successful recanalization had a significant ( $p = 0.001$ ) shift of mRS distribution with higher rates of good functional outcomes (23.8%, 34/143 vs. 14.9% 7/47) and lower mortality at 90-days (46.8%, 67/143 vs. 55.3%, 26/47).

**Conclusion:** While higher mortality and less frequent good outcome can be expected in nonagenarians compared to younger patients, our data suggest that the procedure is probably still efficacious. Individual decision-making for thrombectomy in patients aged 90+ should be based on initial NIHSS and ASPECTS.

#### References

- Goyal M, Menon BK, van Zwam WH, Dippel DW, Mitchell PJ, Demchuk AM, et al. Endovascular thrombectomy after large-vessel ischaemic stroke: a meta-analysis of individual patient data from five randomised trials. *Lancet*. 2016;387:1723–31.

### STENTING WITH THE ACCLINO® -FLEX FOR INTERCRANIAL STENOSIS AS SECONDARY STROKE PREVENTION

Lukas Meyer\*<sup>1</sup>, Hannes Leischner<sup>1</sup>, Götz Thomalla<sup>2</sup>, Lars Udo Krause<sup>3</sup>, Stephan Lowens<sup>4</sup>, Jan Rothaupt<sup>4</sup>, Uta Hanning<sup>1</sup>, Jens Fiehler<sup>1</sup>, Rene Chapot<sup>5</sup>, Christian Paul Stracke<sup>5</sup>, Maxim Bester<sup>1</sup>

<sup>1</sup>Universitätsklinikum Hamburg-Eppendorf, Diagnostische und Interventionelle Neuroradiologie, Hamburg, Deutschland

<sup>2</sup>Universitätsklinikum Hamburg-Eppendorf, Neurologie, Hamburg, Deutschland

<sup>3</sup>Klinikum Osnabrück GmbH, Neurologie, Osnabrück, Deutschland

<sup>4</sup>Klinikum Osnabrück GmbH, Diagnostische und Interventionelle Radiologie, Osnabrück, Deutschland

<sup>5</sup>Alfried Krupp Krankenhaus in Rüttenscheid, Interventionelle Neuroradiologie, Essen, Deutschland

**Background:** Though recurrence rates of stroke are high in patients with symptomatic intracranial stenosis despite best medical treatment, elective intracranial stenting (eICS) as an endovascular therapy option has remained unpopular. This study aims to reevaluate the feasibility, safety and outcome of eICS with a new device combination.

**Methods:** We retrospectively reviewed data of three high-volume stroke centers and analyzed all patients that were treated with eICS for symptomatic intracranial stenosis using exclusively the Acclino® (Flex)—Stent and the NeuroSpeed® Balloon Catheter. Study endpoints were defined with regard to the SAMMPRIS Study[1] at the time of follow-up: transient ischemic attacks (TIA), stroke, death and stent-patency. Interventional safety evaluation included symptomatic intracranial hemorrhage (sICH), mortality and intervention related serious adverse events (SAEs).

**Result:** 77 patients with a median age of 69 years met the inclusion criteria and 54.5% (42/77) of the target vessels were located within the anterior circulation. In 76.6% (59/77) the Neuroseed® Catheter was used for stent-deployment. The rate of in-hospital mortality was 6.4% (5/77). In 5 patients intracerebral bleedings occurred postinterventionally, including one symptomatic intracerebral hemorrhage. There was no intervention-related serious adverse event. During one- and three-month follow-up 10 cases showed in-stent stenosis of which 3 had to be treated with re-percutaneous transluminal angioplasty. Within the time of follow-up occurrence rates of TIA were 2.9% (2/68), stroke 1.4 (1/68) and further mortality 7.3% (5/68).

**Conclusion:** This study on elective stenting for symptomatic intracranial stenosis with the Acclino® (Flex)—Stent/the NeuroSpeed® Balloon Catheter demonstrates feasibility, safety and low mortality rates and therefore, re-encourages eICS as an endovascular therapy-option.

#### References

- Chimowitz MI, Lynn MJ, Derdeyn CP, Turan TN, Fiorella D, Lane BF et al. Stenting versus Aggressive Medical Therapy for Intracranial Arterial Stenosis. *New Engl J Med*. 2011;365(11):993–1003.

### STANDARDIZED TIME FRAMES IN MANAGEMENT OF ACUTE ISCHEMIC STROKE PATIENTS

Hanna Styczen\*<sup>1,2</sup>, Imke Sahlmann<sup>1</sup>, Volker Maus<sup>3</sup>, Antonia Zapf<sup>4</sup>, Leonie Schmitz<sup>4</sup>, Jan Liman<sup>5</sup>, Marios-Nikos Psychogios<sup>1,6</sup>

<sup>1</sup>Institut für Diagnostische und Interventionelle Neuroradiologie, Universitätsmedizin Göttingen, Göttingen, Deutschland

<sup>2</sup>Institut für Diagnostische und Interventionelle Radiologie und Neuroradiologie, Universitätsklinikum Essen, Essen, Deutschland

<sup>3</sup>Institut für Diagnostische und Interventionelle Radiologie, Neuroradiologie und Nuklearmedizin, Universitätsklinikum Knappschaftskrankenhaus Bochum, Bochum, Deutschland

<sup>4</sup>Institut für Medizinische Biometrie und Epidemiologie, Universitätsklinikum Hamburg-Eppendorf, Hamburg, Deutschland

<sup>5</sup>Klinik für Neurologie, Universitätsmedizin Göttingen, Göttingen, Deutschland

<sup>6</sup>Abteilung für Neuroradiologie, Universitätsspital Basel, Basel, Schweiz

**Background:** Outcome studies in acute ischemic stroke have focused on time from onset of stroke symptoms to reperfusion. Definitions of other relevant key points such as “door”, “imaging”, “groin” and “reperfusion” were partly different or missing completely. The aim of this study was to analyze and define standard time frames in management of acute stroke patients and investigate whether they affect outcome or predict treatment response.

**Methods:** Five interval times from patients treated by mechanical thrombectomy were analyzed: door to imaging, imaging to groin, door to groin, groin to reperfusion and door to reperfusion. Various types of definitions for “door”, “groin” and “reperfusion” were elaborated derived from international trials and publications [1–3], divided into three different timing paradigms and compared using ANOVA. Association between patient characteristics and time intervals, outcome and successful reperfusion (mTICI  $\geq$  2b) were modeled by using negative binominal regression.

**Result:** One of the described paradigms had significantly lower median groin to reperfusion time compared to the other groups (17 min vs. 40 and 44.5 min, respectively;  $p < 0.001$ ). Outcome was predicted differently by the individual groups. Age, mRS and NIHSS at admission, anesthesia, intravenous thrombolysis and groin to reperfusion time had a relevant impact on mRS at discharge.

**Discussion:** Time intervals between the three groups were significantly different with a 18 min difference between A and B (image to groin), 31 min between B and C (image to reperfusion) and 27.5 min between C and A (groin to reperfusion). Outcome was predicted differently by using the various groups.

**Conclusion:** Standard definitions of “groin” and especially “reperfusion” are needed to ensure comparability between future studies.

## References

1. Goyal M, Demchuk AM, Menon BK, et al. Randomized Assessment of Rapid Endovascular Treatment of Ischemic Stroke. *N Engl J Med*. 2015;372(11):1019–30.
2. Velasco A, Buerke B, Stracke CP, et al. Comparison of a balloon guide catheter and a non-balloon guide catheter for mechanical thrombectomy. *Radiology*. 2016;280:169–76.
3. Psychogios MN, Behme D, Schregel K, et al. One-stop management of acute stroke patients: minimizing door-to-reperfusion times. *Stroke*. 2017;48:3152–5.

251

## EARLY NEUROLOGICAL RECOVERY AFTER THROMBECTOMY FOR ANTERIOR CIRCULATION STROKE: WHAT SERVES BEST AS A SURROGATE FOR FAVORABLE OUTCOME AT 90-DAYS? A SUBANALYSIS OF THE GERMAN STROKE REGISTRY

Lukas Meyer<sup>\*1</sup>, Gabriel Brooks<sup>1</sup>, Fabian Flottmann<sup>1</sup>, Hannes Leischner<sup>1</sup>, Bastian Cheng<sup>2</sup>, Milani Deb-Chatterji<sup>2</sup>, Christian Gerloff<sup>2</sup>, Götz Thomalla<sup>2</sup>, Caspar Brekenfeld<sup>1</sup>, Jens Fiehler<sup>1</sup>, Uta Hanning<sup>1</sup>

<sup>1</sup>Universitätsklinikum Hamburg-Eppendorf, Diagnostische und Interventionelle Neuroradiologie, Hamburg, Deutschland

<sup>2</sup>Universitätsklinikum Hamburg-Eppendorf, Neurologie, Hamburg, Deutschland

**Background:** Most large thrombectomy studies<sup>1</sup> set their primary functional outcome endpoint at 90-days defining favorable outcome as modified Rankin Scale (mRS) 0–2. Early neurological recovery (ENR) is known to be associated with a long-term favorable outcome but definitions have been used inconsistently. This study aims to investigate the reliability of ENR scores as predictors for favorable outcome at 90-days.

**Methods:** All patients from the German Stroke Registry that received thrombectomy for anterior circulation were included. Functional outcome data, including Neurological Institute of Helath Stroke Scale (NIHSS) at 24 h and discharge, as well as mRS at 24 h and discharge were analyzed as predictors for favorable long-term outcome (mRS0–2 at 90-days) according to definitions of ENR from past publications: Dramatic neurological improvement ( $\geq 10$  NIHSS points), major early neurological recovery (NIHSS  $\geq 8$  points or 0–1), mRS0–2 at 24 h, mRS 0–2 at discharge.

**Result:** 1229 patients with anterior circulation stroke were included. Favorable functional outcome (mRS0–2) at 90-days was observed in 45.2% (557/1229). In univariable analysis all definitions of ENR were significantly associated with long-term favorable outcome. Multivariable analysis confirmed mRS0–2 at discharge as the most significant predictor (adjusted OR13.01; 95CI 8.91–19.01;  $p < 0.001$ ). Patients with neurological deterioration (worsening of  $\geq 4$ -NIHSS points) at discharge had a significant (adjusted OR1.58; 95CI 0.11–0.64;  $p = 0.003$ ) lower chance of reaching favorable long-term outcome.

**Conclusion:** Long-term favorable outcome (defined as mRS 0–2) at 90-days after thrombectomy for anterior circulation stroke is most significantly predicted by mRS 0–2 at discharge. This surrogate could serve as reliable study endpoint for future stroke trials.

## References

1. Goyal M, Menon BK, van Zwam WH, Dippel DW, Mitchell PJ, Demchuk AM, et al. Endovascular thrombectomy after large-vessel ischaemic stroke: a meta-analysis of individual patient data from five randomised trials. *Lancet*. 2016;387:1723–31.

255

## FACTORS ASSOCIATED WITH FAILURE OF ENDOVASCULAR THERAPY IN ACUTE ISCHEMIC STROKE: A MULTICENTER ANALYSIS

Fabian Flottmann<sup>\*1</sup>, Hannes Leischner<sup>1</sup>, Milani Deb-Chatterji<sup>2</sup>, Götz Thomalla<sup>2</sup>, Jens Fiehler<sup>1</sup>, Caspar Brekenfeld<sup>2</sup>

<sup>1</sup>Klinik und Poliklinik für Neuroradiologische Diagnostik und Intervention, Universitätsklinikum Hamburg-Eppendorf, Hamburg, Deutschland

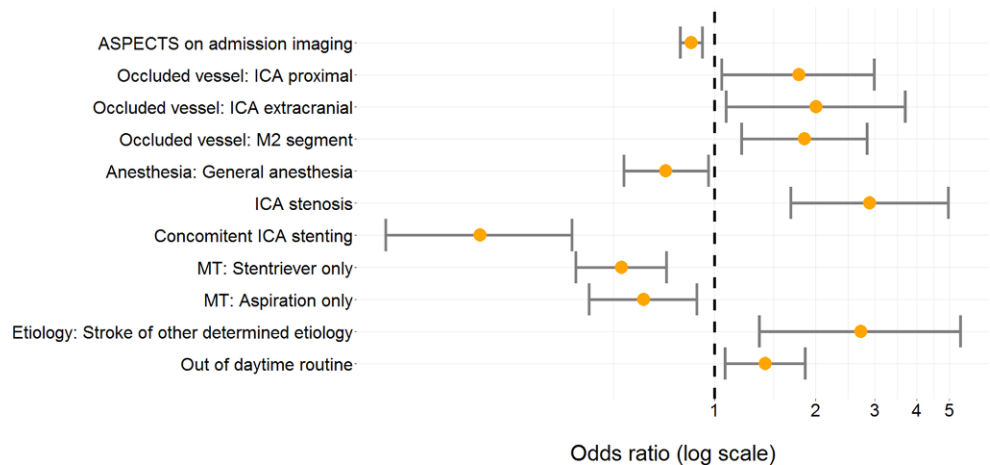
<sup>2</sup>Klinik und für Neurologie, Universitätsklinikum Hamburg-Eppendorf, Hamburg, Deutschland

**Background:** In acute ischemic stroke, endovascular therapy (EVT) fails to achieve successful reperfusion in up to 41% of cases. We aimed at identifying predictors of failed reperfusion in a large multi-center patient cohort.

**Methods:** In this multicenter study we retrospectively analyzed 2211 ischemic stroke patients who received EVT for anterior circulation strokes. Failure of reperfusion was defined as no, minimal or partly reperfusion (defined by TICI 0/1/2a), as opposed to complete reperfusion (TICI 2b–3). In 1674 patients with complete datasets, associations between failure of recanalization and baseline clinical data, comorbidities, location of occlusion, iv-thrombolysis, and type of anesthesia were assessed with logistic regression.

**Result:** Failure of reperfusion occurred in 371 patients (13.5%). Failure was associated with the following locations of occlusion: extracranial ICA (adjusted OR 2.01, 95% CI 1.08–3.69), proximal (non-CTO)

**Fig. 1 | 255** Logistic regression analysis of failure of reperfusion (TICI 0-2a) in 1674 patients with complete datasets, adjusted for multiple confounders



ICA (adjusted OR 1.79, 95% CI 1.05–2.98) and M2 segment (adjusted OR 1.86, 95% CI 1.21–2.84). Furthermore, it was associated with proximal ICA stenosis (adjusted OR 2.90, 95% CI 1.69–4.97), stroke of other determined etiology (adjusted OR 2.73, 95% CI 1.36–5.39) and treatment out of daytime routine (adjusted OR 1.41, 95% CI 1.07–1.86).

Successful reperfusion (i.e. negative correlation with failure) was associated with ASPECTS (adjusted OR 0.85, 95% CI 0.79–0.92), general anesthesia (adjusted OR 0.72, 95% CI 0.54–0.96), and concomitant stenting of ICA stenosis (adjusted OR 0.20, 95% CI 0.11–0.38). Furthermore, it occurred more often when more than one EVT technique (stentriever or aspiration devices) was used.

**Discussion:** Failure of reperfusion occurs more often when vessels other than CTO or M1 are affected. Proximal ICA stenosis is a risk factor, which can be successfully treated when concomitant ICA stenting is possible. EVT is less successful in strokes that are not of cardioembolic or atherosclerotic etiology. Obviously, whenever the EVT technique had to be switched, successful reperfusion was less likely.

Higher ASPECTS on admission, general anesthesia and treatment during daytime routine were associated with improved odds of successful reperfusion after EVT.

**Conclusion:** The “non-standard” EVT patient (e.g. proximal ICA occlusion with low ASPECTS treated in the middle of the night) has a higher risk of unsuccessful reperfusion.

**259**

**HÄMOSIDERINABLAGERUNGEN IM SPLENIUM DES CORPUS CALLOSUM BEI SCHWEREM ARDS NACH PULMONALEM BEFALL EINES ANAPLASTISCH-GROßZELBIGEM LYMPHOMS**

Michael Schnitzbauer\*<sup>1</sup>, Marius Hartmann<sup>1</sup>

<sup>1</sup>Institut für Neuroradiologie, HELIOS Klinikum Berlin-Buch, Berlin, Deutschland

**Hintergrund:** Hämosiderinablagerungen im Splenium des Corpus callosum wurden bei intakter intracerebraler Perfusion mit Hypoxämie bisher bei Bergsteigern, die ein höhenassoziertes Hirnödem (HACE) mit schwerer ARDS überlebt haben und bei Intensivpatienten unter ECMO-Therapie beobachtet.

**Fallbeschreibung/Case Report:** Ein 17-jähriger Patient stellte sich in der Rettungsstelle mit einer cervikalen Lymphadenopathie und B-Symptomatik vor. Im PET-CT zeigten sich flächenhafte pulmonale Konsolidierungen im apikalen Unterlappen links, progrediente Pleuraergüsse bds., Aszites bei Hepatosplenomegalie und eine deutliche Lymphadenopathie cervikal, paraaortal/iliacal und inguinal. Nach

bioptischer Sicherung wurde die Diagnose eines anaplastisch-großzellig-ALK-NPM positiven Lymphoms (ALCL) gestellt.

Unter Chemotherapie (nach NHL-BFM-Register 2012) zeigte sich eine kardiopulmonale Dekompensation, interkurrenter Knochenmarkaplasie und Neutropenie bei schwerem ARDS mit Sepsis bei ausgeprägtem pulmonalem Lymphombefall. Unter fortgeführter Intensivtherapie mit Antibiose kam es zuerst zu einer Besserung der Symptomatik. Im Verlauf entwickelt der Patient während des Intensivaufenthalts starke Kopfschmerzen und zum Ausschluss einer Sinusvenenthrombose wurde ein MRT des Schädels durchgeführt. Hier sah man auf den SWI-Aufnahmen multiple Hämosiderinablagerungen im Splenium des Corpus callosum.

Nach Fortführung der Chemotherapie wurde ein Frührezidiv des Lymphoms festgestellt mit Nachweis einer Meningeosis supra- und infratentoriell. Die weitere Therapie erfolgte eskalierter Chemotherapie und kraniospinaler Bestrahlung, die bei starker Neutropenie des Patienten abgebrochen wurde. Der Patient verstarb mit einer schweren Kachexie an den Folgen des Lymphoms auf der Intensivstation.

**Diskussion/Discussion:** Der pulmonale Befall durch ein anaplastisch-großzelliges Lymphom mit schwerem ARDS kann zu intrakranieller Hypoxämie bei erhaltener Perfusion unter CPAP-Therapie führen. Dadurch resultiert eine temporäre fokale Störung der Blut-Hirn-Schranke mit erhöhter Permeabilität und Einwanderung von Erythrozyten mit Hämosiderinablagerung bevorzugt im Splenium des Corpus callosum. Der aktuelle Fall zeigt, dass auch durch den Abfall des Pao<sub>2</sub>/F<sub>iO<sub>2</sub></sub> unter CPAP-Therapie eine Hypoxämie bei erhaltener Perfusion induziert werden kann, die wie beim HACE zu Hämosiderinablagerungen im Splenium des Corpus callosums führen.

**260**

**PRÄVALENZ NEUROVASKULÄRER KOMPRESSION DER ROSTRALEN VENTROLATERALEN MEDULLA OBLONGATA IN EINER POPULATIONSBASIERTEN MRT-STUDIE**

Daniel Cantrés\*<sup>1</sup>, Friederike Groth<sup>2</sup>, Sascha Groth<sup>2</sup>, Steffen Fleck<sup>3</sup>, Eiko Rathmann<sup>2</sup>, Sönke Langner<sup>1</sup>

<sup>1</sup>Institut für Diagnostische und Interventionelle Radiologie, Kinder- und Neuroradiologie, Universitätsmedizin Rostock, Rostock, Deutschland

<sup>2</sup>Institut für Diagnostische Radiologie und Neuroradiologie, Universitätsmedizin Greifswald, Greifswald, Deutschland

<sup>3</sup>Klinik für Neurochirurgie, Universitätsmedizin Greifswald, Greifswald, Deutschland

**Hintergrund:** Die Kompression der rostralen ventrolateralen Medulla oblongata (RVLM) durch elongierte vertebrobasiläre Arterien wird zu den neurovaskulären Kompressionssyndromen gerechnet [1], da ihr eine blutdrucksteigernde Wirkung zugeschrieben wird [2]. Ihre Bedeutung als Ursache für die essentielle arterielle Hypertonie (aHT) wird kontrovers diskutiert [2, 3]. Die Prävalenz dieser neurovaskulären Kompression (NVK) wurde bisher nur an kleinen Studienkollektiven untersucht [4, 5]. Ziel dieser Arbeit war es, Prävalenz und Ausmaß der NVK der RVLM bei gesunden Probanden einer populationsbasierten MRT-Studie zu untersuchen.

**Methoden:** Im Rahmen der SHIP (Study of Health in Pomerania)-Studie erhielten 3079 gesunde freiwillige Probanden eine Ganzkörper-MRT mit 1,5 T, die eine cerebrale Bildgebung mit T1-gewichteter MPR-Sequenz mit 1 mm isotropen Voxeln und eine TOF-Angiografie beinhaltete. Auftreten und Schweregrad der NVK wurde auf einer 3-Punkt-Skala bewertet und das betreffende Gefäß wurde identifiziert.

**Ergebnisse:** Bei 249 Probanden konnte ein neurovaskulärer Kontakt und bei 138 Probanden eine NVK der RVLM gefunden werden. Dabei zeigten 70 Probanden (50,7 %) eine geringe und 12 Probanden (8,7 %) eine hochgradige Kompression. Ursache der NVK waren am häufigsten die A. vertebralis (43,6 %) und die A. cerebelli posterior inferior (29,2 %) oder eine Kombination beider Arterien (25,3 %).

**Diskussion/Fazit:** Die Prävalenz der NVK der RVLM erweist sich in einer populationsbasierten MRT-Studie mit 12,6 % höher als bislang berichtet. Zur Einschätzung der klinischen Relevanz als mögliche Ursache einer aHT ist neben der Korrelation mit weiteren klinischen Daten eine prospektive Untersuchung erforderlich.

#### Literatur

1. Jannetta PJ. Neurovascular compression in cranial nerve and systemic disease. *Ann Surg.* 1980;192(4):518–25.
2. Naraghi R, et al. Arterial hypertension and neurovascular compression at the ventrolateral medulla. A comparative microanatomical and pathological study. *J Neurosurg.* 1992;77(1):103–12. Jul.
3. Solar M, et al. Neurovascular compression: sympathetic activity in severe arterial hypertension. *Physiol Res.* 2009;58(6):913–6.
4. Boogaarts HD, et al. Primary hypertension and neurovascular compression: a meta-analysis of magnetic resonance imaging studies. *J Neurosurg.* 2012;116(1):147–56. Jan.
5. Sandell T, et al. Hypertension in patients with cranial nerve vascular compression syndromes and comparison with a population-based cohort. *J Neurosurg.* 2013;119(5):1302–8. Nov.

#### 263

##### A SINGLE CENTER EXPERIENCE OF ACUTE SETTING ENDOVASCULAR TREATMENT FOR SYMPTOMATIC INTRACRANIAL STENOSIS

Marie-Sophie Schüngel\*<sup>1</sup>, Ulf Quäsching<sup>1</sup>, Cindy Richter<sup>1</sup>, Karl-Titus Hoffmann<sup>1</sup>, Stefan Schob<sup>1</sup>

<sup>1</sup>Universitätsklinikum Leipzig, Neuroradiologie, Leipzig, Deutschland

**Hintergrund:** Stenosis within the circle of Willis remains an important cause for stroke. Sudden thrombotic occlusion, frequently mimicking a distal thromboembolic event, or severe hemodynamic insufficiency causing fluctuating neurological deficits are probable manifestations of the condition. We aim to report our single center experience with stenting of symptomatic intracranial stenosis in the acute setting.

**Methoden:** We retrospectively reviewed 58 interventions in 56 patients who underwent stent-PTA for treatment of progressive stroke in the acute setting. Enterprise, Solitaire, Wingspan and Leo+Baby as well as Liberté, Pharos, Rebel and Coroflex were used for endovascular treatment. A total of 72 stents were employed, but only 64 were

finally implanted. The distinct majority of implanted devices were Rebel-stents (35; 54.69%).

**Ergebnisse:** 34 patients were treated using balloon-expandable stents (BES, 58.62%), 17 with self-expanding stents (SES, 29.31%) and two with BES&SES (3.45%). In 5 cases stenting was technically impossible (8.62%). In those, 2 were treated by balloon-PTA alone, 3 were treated conservatively to improvement of the hemodynamic situation.

14 of 56 patients (25%) died despite the intervention. 67% of deaths occurred in the context of an acutely thrombosed basilar artery stenosis, 33% as a consequence of a malignant MCA syndrome. 75% gained functional independence after 90 days (mRS<3).

**Diskussion:** In our experience, off label use of BES yields a good risk-benefit ratio, however, they exhibit a comparatively high stiffness and large profile, which in some cases impede successful treatment. SES+PTA should be considered an alternative in this context. However, complication rates remain high in this challenging patients collective, especially in case of basilar artery involvement.

**Fazit:** Decompensated, clinically symptomatic intracranial stenosis require immediate endovascular treatment to prevent death or severely disabling stroke—in our experience balloon-expandable coronary stents are the most promising approach.

#### 271

##### EARLY PREDICTION OF FINAL INFARCT VOLUME WITH MATERIAL DECOMPOSITION IMAGES OF DUAL-ENERGY CT AFTER MECHANICAL THROMBECTOMY

Silke Hopf-Jensen\*<sup>1</sup>, Max Anraths<sup>2</sup>, Stephanie Lehrke<sup>2</sup>, Silke Szymczak<sup>3</sup>, Mario Hasler<sup>4</sup>, Stefan Müller-Hülsbeck<sup>2</sup>

<sup>1</sup>Department of Diagnostic and Interventional Radiology and Neuroradiology, Diakonissenhospital Flensburg, Germany, Flensburg, Deutschland

<sup>2</sup>Department of Diagnostic and Interventional Radiology and Neuroradiology, Diakonissenhospital Flensburg, Germany, Flensburg, Deutschland

<sup>3</sup>Institute of Medical Informatics and Statistics, Kiel University, University Hospital Schleswig-Holstein, Campus Kiel, Germany, Kiel, Deutschland

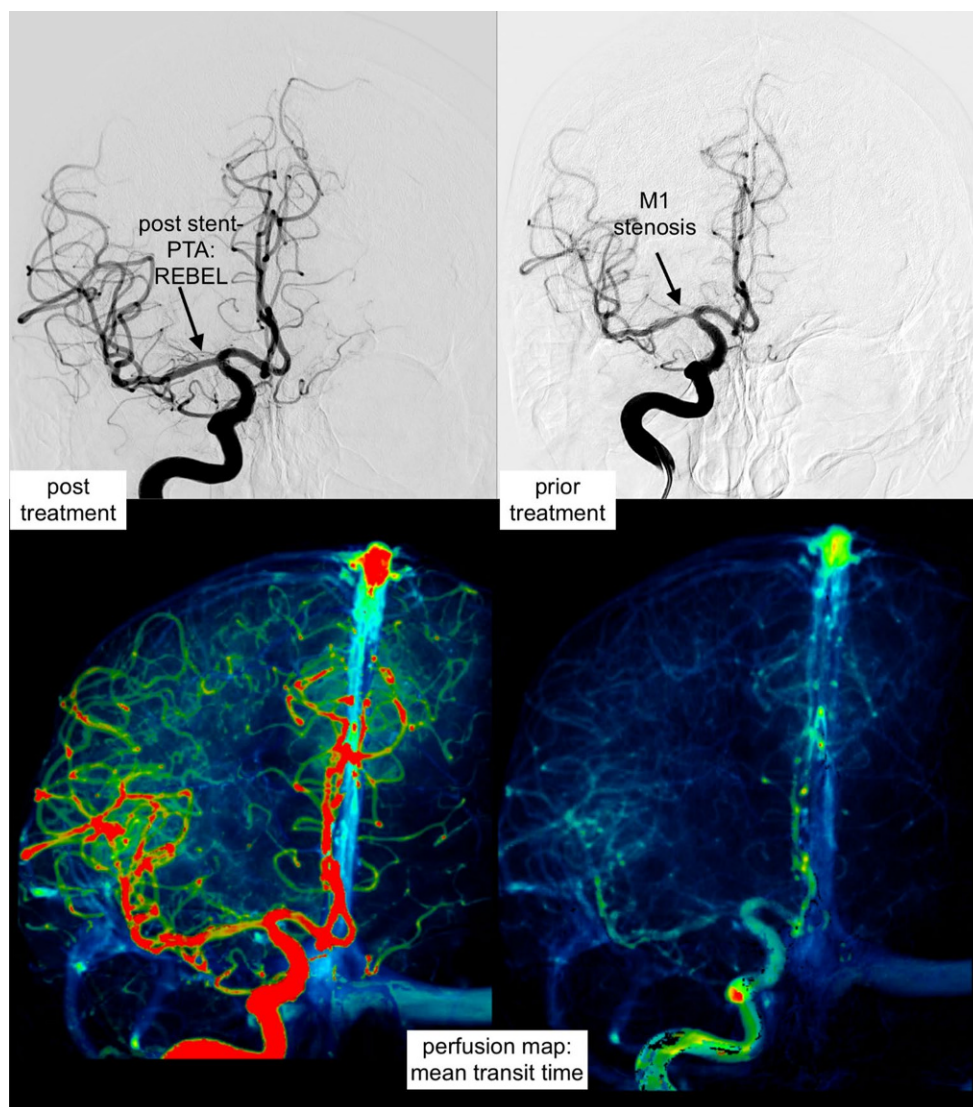
<sup>4</sup>Faculty of Agricultural and Nutritional Sciences, Kiel University“ Kiel, Deutschland

**Purpose:** Evaluation of water material density images (wMDIm) of single source Dual-Energy CT (DECT) for early prediction of final infarct volume (fiV) and correlation with clinical outcome after mechanical thrombectomy (MT).

**Methods:** 50 patients (mean age: 69 yrs (± 12.1 yrs, range 40–90 yrs), 50% female) with middle cerebral artery (MCA) occlusion were included (M1: 86%, M2: 14%). 16–24 h after MT early infarct volumes were analyzed in monoenergetic images (MonoIm) and wMDIm at 60 keV in DECT and compared with the fiV in single energy CT (SECT) after 4.9 days on average (± 4, 1–22). Association between infarct volume in wMDIm and functional outcome at time of discharge and 90 days after MT was tested by linear regression analysis.

**Results:** TICI 3 was achieved in 46 patients (92%). wMDIm shows a prior visible infarct demarcation (60.7 ml, ± 74.9 ml) compared to the MonoIm (37.57 ml, ± 76.7 ml). Linear regression analysis, Bland-Altman plots and Pearson correlation coefficients show a close correlation of infarct volume in wMDIm to the fiV in SECT (r=0.86; 95 CI: 0.76–0.92), compared to MonoIm and follow-up SECT (r=0.81; 95% CI: 0.69–0.89). The agreement with follow-up CT is substantially higher in patients with infarct volumes <70 ml (n=33; 66%). Coefficients were smaller with r=0.59 (95% CI: 0.31; 0.78) for MonoIm and follow-up CT compared to r=0.77 (95% CI: 0.57; 0.88) for wMDIm and follow-up CT. At admission mean NIHSS score and mRS were 17.02 (± 4.7) and 4.9 (± 0.2), respectively. Good functional outcome (mRS ≤2)

Fig. 1 | 263



was achieved in 28 patients (56%) at 90 days with mean mRS of 2.5 ( $\pm 0.8$ ) at discharge.

**Conclusion:** Material decomposition of DECT allows an earlier visualization of the final infarct volume. This promises a more precise evaluation of dimension and severity of infarction and may lead to a more targeted/directed therapy.

274

#### EFFEKT VON ULTRACLOSED CELL STENTS FÜR DIE BEHANDLUNG VON KAROTISSTENOSEN – EIN RETROSPEKTIVER VERGLEICH MIT ETABLIERTEN CLOSED CELL STENTS AN PATIENTENDATEN

Zarlasht Aludin\*<sup>1</sup>, Schekeb Aludin<sup>1</sup>, Naomi Larsen<sup>1</sup>, Olav Jansen<sup>1</sup>, Fritz Wodarg<sup>1</sup>

<sup>1</sup>Klinik für Radiologie und Neuroradiologie, Universitätsklinikum Schleswig-Holstein, Campus Kiel, Kiel, Deutschland

**Hintergrund:** Die Karotis-Stentangioplastie (CAS) stellt ein etabliertes Verfahren zur Therapie der Karotisstenose dar. Es kommen verschiedene Stenttypen zum Einsatz, die sich unter anderem anhand ihrer

Maschenweite unterscheiden. Stents mit engeren Maschen scheinen dabei eine höhere Behandlungssicherheit zu gewährleisten. In unserem Zentrum wurde bis 2014 der closed-cell Wallstent (WS) und ab 2014 der ultraclosed-cell Casper-Stent (CS) eingesetzt. Das übrige technische Vorgehen blieb unverändert. Ziel dieser Arbeit ist der Vergleich der beiden Stenttypen hinsichtlich Sicherheit und klinischer Parameter. **Methoden:** In einem retrospektiven Ansatz wurden Daten von 597 Patienten, welche zwischen 01/2011 und 03/2018 mittels CAS therapiert wurden, entsprechend des verwendeten Stenttyps in 2 Gruppen kategorisiert (CS = 343; WS = 254). Als Testparameter wurden die Re-Stenoserate, die periprozedurale Komplikationsrate und die postinterventionelle Infarktrate in 30 Tagen erfasst. Zur Beurteilung des Effekts auf die Strömungsverhältnisse in der meist überstenoteten A. carotis externa (ACE) wurden dopplersonografisch erhobene Flussgeschwindigkeiten prä- und postinterventionell analysiert. Zusätzlich erfolgte eine Subgruppenanalyse zwischen symptomatischen, asymptomatischen und akuten Fällen. **Ergebnisse:** In der Gruppe der mit dem CS behandelten Patienten traten signifikant seltener Restenosen auf (6,1 % vs 15,7 %;  $p < 0.05$ ). Bei der periprozeduralen Komplikationsrate, der Infarktrate sowie der ACE-Perfusion zeigten sich keine signifikanten Unterschiede zwischen den Gruppen. In der Subgruppenanalyse ließen sich bei symptomatischen und asymptomatischen Patienten konsistent signifikante Unterschiede

bezüglich der Restenoserate feststellen. Bei akuten Fällen zeigten sich keine signifikanten Unterschiede zwischen den Gruppen.

**Diskussion:** Anhand unserer Daten scheint die Verwendung von ultraclosed-cell Stents im Vergleich zu closed-cell Stents eine geringere Restenoserate zu gewährleisten. Trotz der engeren Maschen scheint der Fluss in der ACE nicht relevant beeinflusst zu werden. Bezüglich der Komplikations- und Infarkttraten ergaben sich keine Unterschiede zwischen den Gruppen.

276

### TREATMENT OF IN-STENT RESTENOSIS OF DUAL-LAYER MICROMESH CAROTID ARTERY STENTS

Silke Hopf-Jensen<sup>\*1</sup>, Michael Preiß<sup>1</sup>, Stefan Müller-Hülsbeck<sup>1</sup>

<sup>1</sup>Department of Diagnostic and Interventional Radiology and Neuroradiology, Diakonissenhospital Flensburg, Flensburg, Deutschland

**Purpose:** To analyse the incidence and treatment options of restenosis in patients treated with super-closed dual-layer carotid artery stents.

**Methods:** Between 02/2014–05/2019 208 pts were treated with 213 dual-layer stents (191 Roadsaver<sup>TM</sup> stents, Terumo, Tokyo, Japan: 89.7% and 22 CGuard stents<sup>TM</sup>, Inspire MD, Tel Aviv, Israel: 10.3%). Stent patency was evaluated by ultrasound before discharge, after 3 months and then every 6 months during follow up. Stenosis degree >60% for asymptomatic and >50% for symptomatic stenosis (NAS-CET) are indicated for re-treatment.

**Results:** During mid-term follow up (mean 3.4 years, range 4 weeks–5.2 years) 7 pts with asymptomatic restenosis (3%) and 3 pts with asymptomatic stent occlusions (1.4%) were detected. All restenosis were characterized as neointimal hyperplasia. In cases with stent occlusion 2 cases with progressive atherosclerotic plaques and one case with soft thrombo-embolic material were recorded.

In Roadsaver<sup>TM</sup> stents 7 restenosis were treated as follows: 2 re-PTA (with drug-coated balloon) with new, but asymptomatic DWI lesion in MRI, 4 re-stenting of the distal flair ends with 2 single-layer stents (Wallstent<sup>TM</sup>, Natick, MA, USA) with technical and clinical success and 2 dual-layer stents (1 Roadsaver<sup>TM</sup> and 1 CGuard<sup>TM</sup>, latter with following symptomatic occlusion). 3 asymptomatic stent occlusion after CAS with Roadsaver<sup>TM</sup> stents were detected: 1 case 12 month after treatment of a tandem lesion with simultaneous intracranial thrombectomy, 1 case 4 days after acute stenting with thrombectomy in a setting without given ASA in the acute situation and 1 case 6 month after emergency stenting within 12 hours after symptoms onset.

One CGuard<sup>TM</sup> restenosis was treated with re-stenting with single-layer stent (Xact<sup>TM</sup> Abbott Vascular, Santa Clara, CA, USA) with good technical and clinical success.

**Conclusions:** The restenosis rate of dual-layer stents seems to be low compared to conventional single-layer stents, but treatment of restenosis of the dual-layer cell design differ fundamentally. Re-PTA can increase intracranial thromboembolic complications due to the small cell design. Re-stenting with single-layer stents seems to be superior to dual-layer stents again to preserve the blood vessel diameter.

277

### NEUROPHYSIOLOGICAL MONITORING IN THE ENDOVASCULAR THERAPY OF NEURYSMS

Silke Hopf-Jensen<sup>\*1</sup>, Michael Preiß<sup>1</sup>, Gisa Andresen<sup>2</sup>, Wolfgang Börm<sup>3</sup>, Ulf Linstedt<sup>2</sup>, Stefan Müller-Hülsbeck<sup>1</sup>

<sup>1</sup>Department of Diagnostic and Interventional Radiology and Neuroradiology, Diakonissenhospital Flensburg, Flensburg, Deutschland

<sup>2</sup>Department of Anesthesiology and Intensive Care Therapy, Diakonissenhospital Flensburg, Flensburg, Deutschland

<sup>3</sup>Department of Neurosurgery, Diakonissenhospital Flensburg, Flensburg, Deutschland

**Purpose:** To evaluate the relevancy of neurophysiological monitoring techniques with somatosensory evoked potentials (SSEP) during endovascular treatment of cerebral aneurysms.

**Methods:** Embolization of 20 aneurysms (ACom: 5 ICA: 9, Carotid-T: 2, MCA: 4) were monitored by SSEPs using bilateral median or posterior tibial nerve stimulation. Critical SSEP changes were defined as an amplitude reduction of >50% or a latency delay (N19/P24). The techniques included coil embolization (14), balloon-remodelling coiling (3) and stent-assisted coiling (3).

**Results:** 20 patients (female: 16 patients, mean 58 years<sup>”</sup> range: 42–86 years) with 12 ruptured (60%) and 8 incidental (40%) aneurysms were treated. There were transient SSEP changes in 5 patients (25%) during embolization, with 2 of these 5 events occurring during balloon-remodelling technique without visible embolus or delayed perfusion. The remaining 3 cases were associated with thrombus formation at the aneurysm basis, in one case within an underlying stent. SSEP changes lead to an immediate closer inspection of the whole angiological status, especially the peripheral angiogram, and initiation of thrombolysis therapy, i. e. Glycoprotein IIb/IIIa inhibitors. No neurological changes were found in all cases postprocedural after successful thrombus clearing.

**Conclusion:** Somatosensory evoked potential monitoring is sensitive for the early detection of subcortical ischemia during aneurysm embolization. Neuromonitoring provides additional safety tool during technical complex endovascular treatment of cerebral aneurysms.

278

### CEREBRO-VASCULAR REACTIVITY MAPPING (CVRM) – PROMISES AND PITFALLS

Andreas Bartsch<sup>\*1,2</sup>

<sup>1</sup>Radiologie Bamberg, Bamberg, Deutschland

<sup>2</sup>WIN (FMRI) Oxford, JR Hospital, Oxford, England

**Hintergrund:** CVRM has been promoted to assess the cerebrovascular reserve capacity (CVRC) in steno-occlusive arteriopathies such as moyamoya. CVRM promises to detect „neurovascular uncoupling“ (NVU): Insufficient perfusion and collateralization is presumed to lead to vasodilation irresponsive to hypercapnic challenges requiring revascularization such as bypass surgery [1].

**Methoden:** We performed BOLD-CVRM (3T, TR = 3s/TE = 30 ms) by 10 endexpiratory breath-hold (BH) maneuvers for 21s, alternating with 10 episodes of normal breathing for 42s, in 2 moyamoya-patients: 1 primary (50 year-old female) and 1 secondary due to neurofibromatosis type 1 (23 year-old male; Fig. 1A). In addition, dynamic susceptibility contrast (DSC-)perfusion imaging (TR = 1.17s/same TE) and vasomotor reserve (VMR) testing with transcranial duplex (TCD) under Carbogen inhalation were performed. BH-CVRM and DSC-perfusion were analyzed using a model- (i. e., respiratory response = RRF [2] and arterial input = AIF function-based) and data-driven (ICA-based) approach in FSL ([www.fmrib.ox.ac.uk/fsl](http://www.fmrib.ox.ac.uk/fsl)).

**Ergebnisse:** Model-driven CVRM by a single Gaussian RRF-predictor (explanatory variable EV), which is conventionally used for general linear modelling (GLM), suggested absent CVR in the affected media-territory of both cases (Fig. 1B). However, VMR was intact (45 and 33 % velocity increase under Carbogen) and time-to-peak (TTP) delays of DSC-perfusion matched exactly data-driven CVRM delays of the measured BOLD signal in both cases (7 and 11s; Fig. 1D for patient 2), which is remarkable in that the two modalities based on exo- (DSC) and endogenous (BH-CVRM) T2\*-weighted contrast converged precisely.

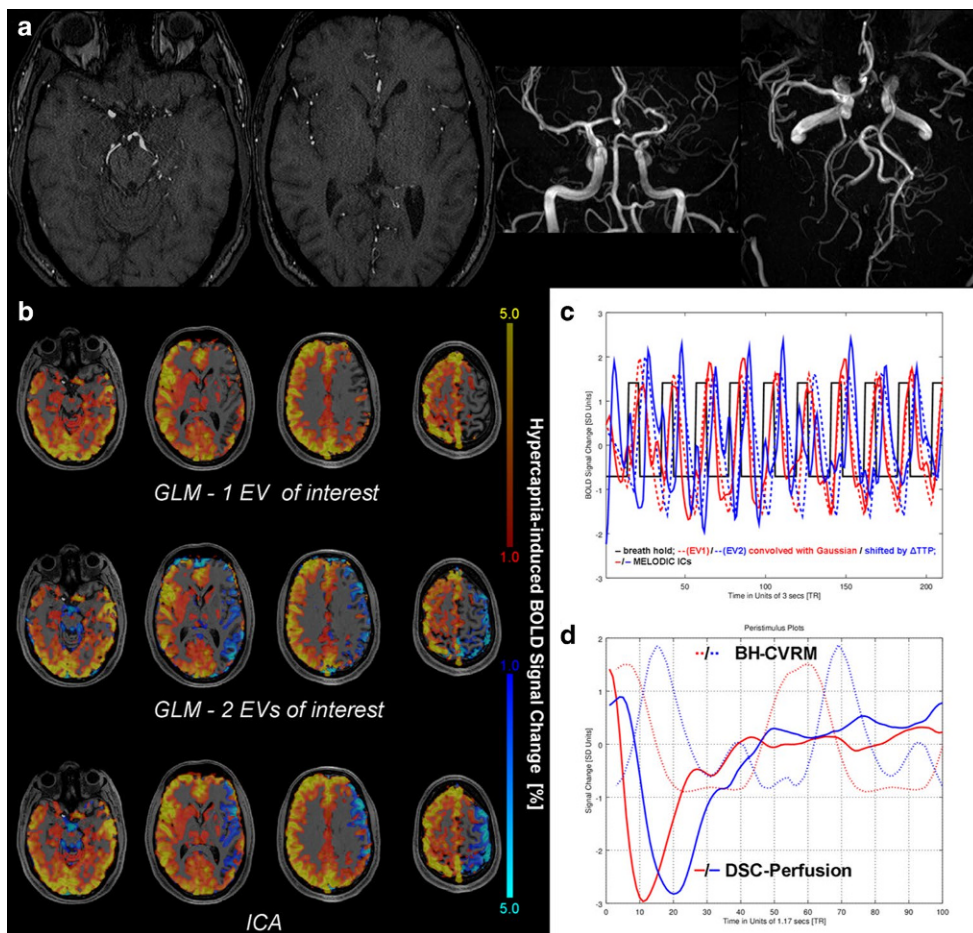


Fig.. 1 | 278

**Diskussion:** Incomplete/incorrect modelling in the temporal domain by a single predictor is shown to cause false-negatives of CVRM (modelling pitfall). Model-free analysis by ICA can overcome this fallacy. Confirming NVU or an abolished CVRC by CVRM requires to demonstrate a lack of activation, i. e. failing to reject the null hypothesis, which is statistically challenging (inferential pitfall).

**Fazit:** TTP differences in DSC perfusion propagate into and may mimic NVU in CVRM while CVRC (and neurovascular coupling) is actually preserved (Fig. 1B-D). Clinical utility of CVRM to accurately predict the need for revascularization critically depends on avoiding modelling and inferential pitfalls.

**References**

1. Stroke 2013, 44: S55–S57
2. Neuroimage 2008, 40: 644–654

281

**THE CONTOUR INTRASACULAR FLOW-DIVERSION DEVICE – SAFETY AND EFFICACY REPORT FROM INITIAL CLINICAL EXPERIENCES**

Fritz Wodarg<sup>\*1</sup>, Jawid Madjidyar<sup>1</sup>, Naomi Larsen<sup>1</sup>, Olav Jansen<sup>1</sup>

<sup>1</sup>Klinik für Radiologie und Neuroradiologie, Universitätsklinikum Schleswig-Holstein, Campus Kiel, Kiel, Deutschland

**Background:** The CONTOUR-Device was designed as an intrasacral flow-diverting implant for the treatment of cerebral aneurysms.

Compared with other devices it offers a new design by covering only the neck of the aneurysm with a tight mesh in an inverted umbrella shape. Here we present our first clinical cases including pre and post-procedural MRI and CT imaging, as well as the results of the follow up DSA after 6 months.

**Methods:** Eight patients were treated within the CERUS Study following standard of care praxis in our center. Pre-implantation imaging was done by MRI and DSA in all cases. Follow-up imaging was done the day after the procedure by MRI or CTA. Six months follow up was done with DSA and MRI or CTA for 2 of 8 Patients by the time of abstract submission and will be done for 7 of 8 Patients by the time of the presentation.

**Result:** In all cases treatment was technically easy, without complications and an immediate intrasaccular stasis effect was observed. In one of eight cases a little dog-ear remained at the aneurysm base. The two existing 6 months follow ups showed a stable aneurysm occlusion. In the post procedural MRI images metal artifacts from the proximal device marker lead to a limited assessability of the aneurysm. Thin T2 weighted slices or CTA offered the best visualization of the treated aneurysm sac and base.

**Discussion:** From our initial experiences the CONTOUR-Device offers a technically easy, safe and fast option for intrasaccular aneurysm treatment. The selection of proper aneurysm-shapes as well as the sizing of the device for an optimal angiographic result still needs to be clarified. First 6 month follow ups showed good results but the long-term efficacy has still to be proven. The present device-design causes severe MRI artifact which consecutively lead to limited assessability during follow-up.

285

**REAL COMPLICATION RATE OF CAROTID ARTERY STENTING IN A NEURORADIOLOGY HIGH-VOLUME-CENTER**

Ali Khanafer\*<sup>1</sup>, Sebastian Müller<sup>1</sup>, Volker Maus<sup>2</sup>, Marios-Nikos Psychogios<sup>1</sup>

<sup>1</sup>Göttingen, Deutschland  
<sup>2</sup>bochum, Deutschland

**Hintergrund:** Carotid artery stenting (CAS) is a reliable alternative treatment to carotid endarterectomy (CEA). However, the reported randomized studies showed higher incidences of periprocedural mortality and stroke than for CEA. In these studies, performing by neuroradiologists in a neuroradiology high-volume center was not a main criterion. The aim of this study was to evaluate adverse events periprocedural and 90-day after CAS performed only by neuroradiologists in our department.

**Methoden:** We retrospectively analyzed the clinical outcomes of all patients with carotid artery stenosis who underwent CAS therapy in our Neuroradiology department in Göttingen from June 2016 to August 2018. The decision for the interventional treatment was determined in our online interdisciplinary carotid-conference from senior neuroradiologists, neurologists and vascular surgeons. Patients were followed up with neurological examination and with serial duplex ultrasound scanning. Clinical complication included amaurosis fugax, transient ischemic attack or stroke.

**Ergebnisse:** A total of 161 cases were identified in our prospective observational study. The average age was 65 years (IQR 74,5–56), and females constituted 27,09%. The indication for the CAS was the presence of asymptomatic (17.17% n=28) carotid stenosis (>65%) or of symptomatic (50.92% n=83) carotid stenosis of at least 50% or patients with acute TANDEM occlusions of ICA (31.9% n=50). Success rate was 98,75%; whereas, the peri-procedural complication rate of patients with symptomatic and asymptomatic severe carotid artery sten-

oses was 0,91% and 0% death (0–30 days). Follow up was planned 90 days after the CAS and showed 1,16% clinical complications and 0% mortality. The median duration of follow up was 184 (IQR 63–354).

**Diskussion/Discussion:** Prospective studies need to show, if our results are transferable.

**Fazit/Conclusion:** The CAS treatment of ICA stenosis and the implementation of treatment in the hands of experienced neuroradiologists in a high-volume center showed a very low postoperative risk compared to the literature CAS and CEA results.

We suppose to include interdisciplinary decision for the best possible treatment and the application of CAS only by experienced neuroradiologists as criteria in future studies.

288

**HEMODYNAMIC IMPAIRMENTS IN ASYMPTOMATIC UNILATERAL CAROTID ARTERY STENOSIS ARE MOST PRONOUNCED WITHIN INDIVIDUAL WATERSHED AREAS**

Stephan Kaczmarz<sup>1</sup>, Jan Petr<sup>2</sup>, Mikkel Bo Hansen<sup>3</sup>, Andreas Hock<sup>4</sup>, Jan Kufer<sup>1</sup>, Kim Mouridsen<sup>3</sup>, Claus Zimmer<sup>1</sup>, Fahmeed Hyder<sup>5</sup>, Christine Preibisch<sup>1</sup>, Jens Götter\*<sup>1,6</sup>

<sup>1</sup>Dept. of Neuroradiology, TUM, München, Deutschland  
<sup>2</sup>Helmholtz-Zentrum Dresden-Rossendorf, Dresden, Deutschland  
<sup>3</sup>Aarhus University, Aarhus, Dänemark  
<sup>4</sup>Philips Healthcare, Hamburg, Deutschland  
<sup>5</sup>Yale University, New Haven, CT, United States  
<sup>6</sup>Dept. of Radiology, TUM, München, Deutschland

**Background:** Watershed areas are most susceptible for ischemia in patients with high-grade internal carotid artery stenosis (ICAS) [1]. Thorough investigation of the currently not well understood hemodynamic impairments is important to improve treatment guidelines. [2] Here, we propose a multimodal-MRI protocol to better characterise hemod-

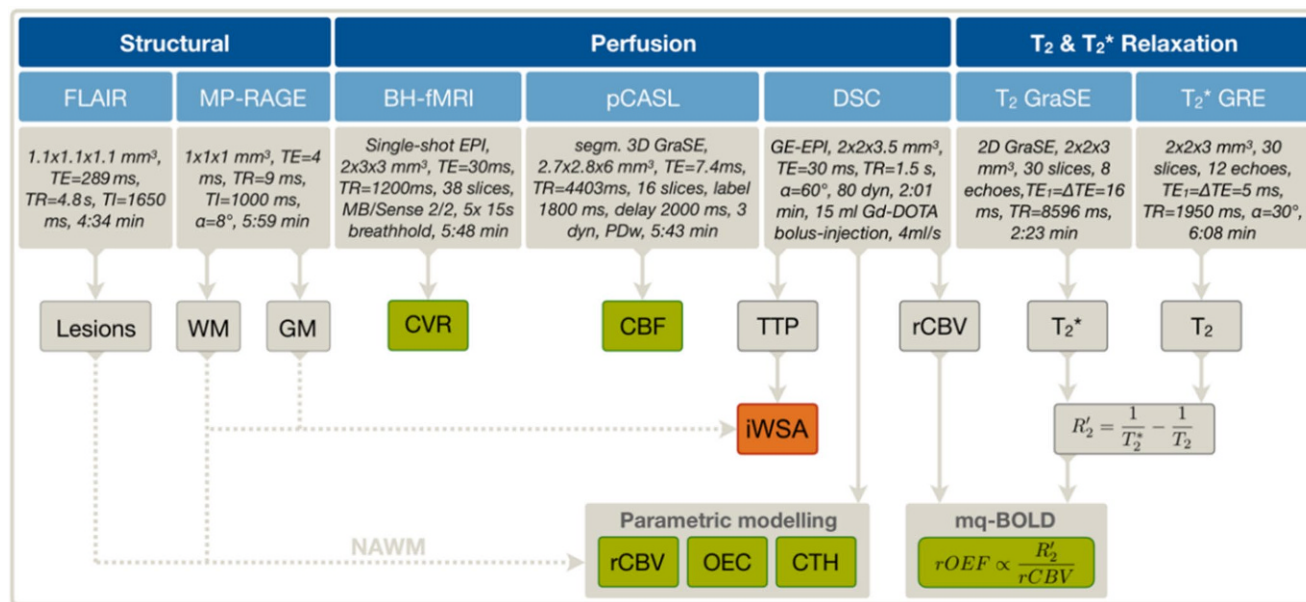


**Fig. 1 | 288** Overview of MRI protocol and derived parameters. FLAIR was applied for lesion detection and MP-RAGE for white matter (WM) and grey matter (GM) masks. Breathhold-fMRI (BH-fMRI) was performed to measure cerebral vascular reactivity (CVR)<sup>3</sup> and pseudo-continuous arterial spin labelling (pCASL) for cerebral blood flow (CBF)<sup>4</sup>. By dynamic susceptibility contrast (DSC), individual watershed areas (iWSA) of each subject were generated<sup>7</sup> and additionally GM/WM masked. By parametric modelling, relative cerebral blood volume (rCBV), normalised by NAWM=2.5%,<sup>5</sup> oxygen extraction Capacity (OEC) and capillary transit-time heterogeneity (CTH) maps were generated.<sup>6</sup> By mq-BOLD, rOEF was calculated based on rCBV, T<sub>2</sub>\* and T<sub>2</sub>.<sup>5</sup>

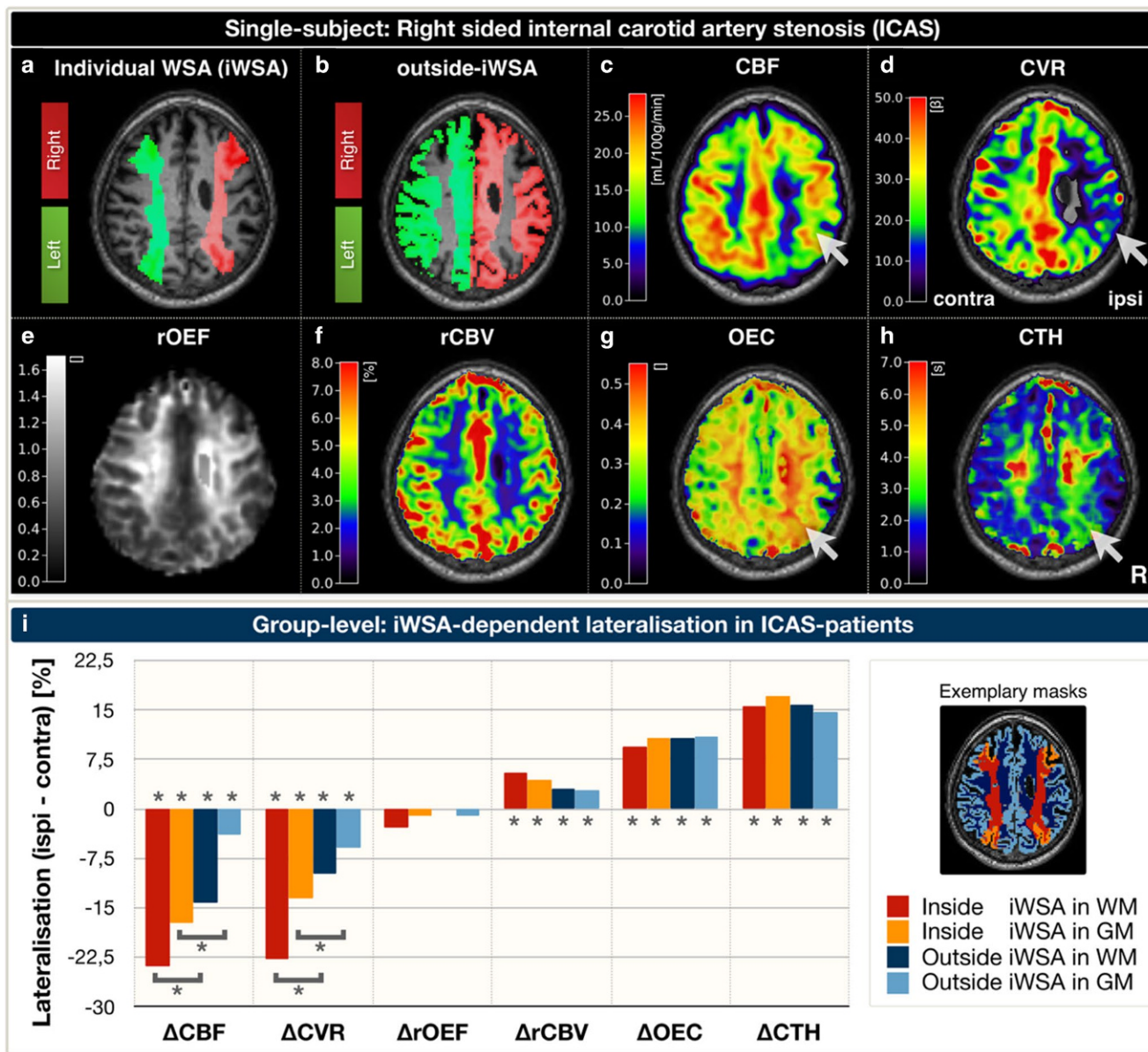


**Fig. 2 | 288** Exemplary data of iWSA (a) and haemodynamics (c–h) with impairments ipsilateral to the stenosis (arrows). On group level, lateralisation between ipsilateral and contralateral hemispheres was evaluated for all parameters (i). Four VOI’s were compared (see inset): inside iWSA in WM (red) & GM (orange) and outside iWSA in WM (dark blue) & GM (light blue). Asterisks indicate statistically significant differences (T-test,  $p < 0.05$ )

dynamic impairments in asymptomatic ICAS with increased sensitivity within individual watershed areas (iWSA).

**Methods:** Twenty-nine asymptomatic, unilateral ICAS patients (age =  $70.1 \pm 4.8$ y), and 30 age-matched healthy controls (age =  $70.3 \pm 7.3$ y) underwent 3T-MRI. Imaging yielded maps of cerebrovascular reactivity (CVR) [3], cerebral blood flow (CBF) [4], relative oxygen extraction fraction (rOEF), [5] relative cerebral blood volume (rCBV), capillary transit-time heterogeneity (CTH), and oxygen extraction capacity (OEC) [6] (Fig. 1). Based on DSC-derived time-to-peak (TTP) maps, iWSAs were defined for each participant (Fig. 2a) [7]. Mean hemodynamic parameter values within each hemisphere were compared between ICAS-patients vs. HC and inside vs. outside iWSAs (Fig. 2a, b) within GM and WM.

**Result:** We found significant lateralisation of CBF, CVR, rCBV, CTH, and OEC for ICAS-patients (all  $p < 0.05$ ), whereas no significant rOEF

lateralisation was found (Fig. 2). Inside iWSAs, lateralisation was enhanced for CBF and CVR ( $p < 0.05$ ), with a strong trend for rCBV. Overall, lateralisation was stronger within WM than GM (Fig. 2i). Contrary, OEC and CTH were indeed lateralised, but comparable inside vs. outside iWSAs (Fig. 2i). For HC, all parameters were symmetrical between hemispheres (data not shown).

**Discussion:** Observed impairments of CBF, CVR, and CBV are in line with recent studies [8]. As proposed, CBF and CVR impairments are specifically pronounced within iWSAs (Fig. 2i). Interestingly, CTH and OEC were lateralized, however not specifically changed within iWSAs, indicating an independently impaired hemodynamic mechanism.

**Conclusion:** CBF and CVR reductions may be indicative of the severity of hemodynamic changes within iWSAs, and thus future stroke risk. CTH and OEC impairments are independent of iWSA locations.

## References

1. Momjian-Mayor, et al. *Stroke*. 2005;36(3):567–77.
2. Jalbert, et al. *JAMA Neurol*. 2015;72(3):276–86.
3. Pillai, et al. *Am J Neurorad*. 2014;36(1):7–13.
4. Alsop, et al. *MRM*. 2015;73(1):102–16.
5. Hirsch, et al. *NMR Biomed*. 2014;27(7):853–62.
6. Jespersen, et al. *JCBFM*. 2012;32(2):264–77.
7. Kaczmarz, et al. *Neurorad*. 2018;60(3):311–23.
8. Bouvier, et al. *HBM*. 2015;36:695–706.

## 290

### RECOVERY OF CEREBROVASCULAR REACTIVITY AFTER TREATMENT OF ASYMPTOMATIC CAROTID ARTERY STENOSIS IS ASSESSABLE BY NON-INVASIVE BREATH-HOLD FMRI WITHIN GLOBAL WATERSHED AREAS

Stephan Kaczmarz<sup>1</sup>, Jan Petr<sup>2</sup>, Nico Sollmann<sup>1</sup>, Andreas Hock<sup>3</sup>, Claus Zimmer<sup>1</sup>, Fahmeed Hyder<sup>4</sup>, Christine Preibisch<sup>1</sup>, Jens Göttinger<sup>1,5</sup>

<sup>1</sup>Dept. of Neuroradiology, TUM, München, Deutschland

<sup>2</sup>Helmholtz-Zentrum Dresden-Rossendorf, Dresden, Deutschland

<sup>3</sup>Philips Healthcare, Hamburg, Deutschland

<sup>4</sup>Yale University, New Haven, CT, Deutschland

<sup>5</sup>Dept. of Radiology, TUM, München, Deutschland

**Background:** Treatment of asymptomatic internal carotid artery stenosis (ICAS) patients remains still controversial [1]. Hemodynamic biomarkers such as the cerebrovascular reactivity (CVR) are promising to identify patients who benefit from revascularization procedures [2–4]. However, commonly employed methods are invasive acetazolamide or complicated gas applications [2–6]. The aim of our study was therefore to measure CVR recovery in ICAS-patients after treatment by easily-applicable breath-hold fMRI (BH-fMRI) with increased sensitivity by evaluation within global watershed areas (gWSAs) [7].

**Methods:** Thirty-three participants (16 asymptomatic, unilateral ICAS-patients, age = 71.4 ± 5.8y, and 17 healthy controls [HC], age = 70.8 ± 5.3y, see Fig. 1) underwent MRI on a 3T Philips Ingenia. All participants were scanned twice, patients before and at least three months after treatment, HC at similar follow-up delays. BH-fMRI comprised five breath-holds à 15s each; CVR-maps were calculated by data-driven analysis [8] (Fig. 2a, b). Lateralization of CVR was calculated in GM of gWSAs between hemispheres for each participant (Fig. 2c).

**Result:** Exemplary ICAS-patient's data shows impaired CVR before treatment, which recovered after treatment (Fig. 1A,B). On group level, CVR was significantly impaired ipsilateral to the stenosis before treatment (Fig. 3a, t-test,  $p=0.0038$ ). After treatment, CVR significantly recovered (2-sample t-test,  $p=0.0495$ ) resulting in symmetrical CVR between hemispheres (t-test,  $p=0.25$ ). HC data was symmetrical between hemispheres (Fig. 3b,  $p>0.60$ ).

**Discussion:** BH-fMRI based evaluation within gWSAs was sensitive to CVR impairments in asymptomatic ICAS, indicating chronic vasodilation [5]. Specificity was affirmed by symmetrical HC results. Consistent with current literature, CVR recovered after ICAS-treatment [4–7], demonstrating improved hemodynamic status.

**Conclusion:** We successfully analyzed CVR recovery after ICAS treatment by easily applicable, tolerable and non-invasive BH-fMRI within clinically feasible scan times. This technique could potentially improve future treatment decisions.

## References

1. Alberts, et al. *JAMA Neurol*. 2015;72(3):263–4.
2. Pillai, et al. *Am J Neurorad*. 2014;36(1):7–13.
3. Mandell, et al. *AJNR*. 2011;32(4):721–7.
4. Vagal, et al. *AJNR*. 2009;30(5):876–88.
5. Sam, et al. *BMJ Open*. 2015;5(2):e6014.

6. Han, et al. *Stroke*. 2011;42(11):3047–54.

7. Momjian-Mayor, et al. *Stroke*. 2005;36(3):567–77.

8. Vondráčková, et al. *ISMRM*. 2016;24:3801.

## 291

### KONTRAINDIKATIONEN FÜR DIE ENDOVASKULÄRE THERAPIE (EVT) BEI SCHLAGANFALLPATIENTEN, DIE AN EIN ZENTRUM

#### VERLEGT WERDEN

Kevin Hädrich<sup>\*1</sup>, Johannes Gerber<sup>1</sup>, Kay Engelland<sup>1</sup>, Angela Müller<sup>1</sup>, Jessica Barlinn<sup>2</sup>, Volker Puetz<sup>2</sup>, Jennifer Linn<sup>1</sup>

<sup>1</sup>Institut für Neuroradiologie, Universitätsklinikum Carl Gustav Dresden, Dresden, Deutschland

<sup>2</sup>Klinik für Neurologie, Universitätsklinikum Carl Gustav Dresden, Dresden, Deutschland

**Hintergrund:** Ziel eines Netzwerks ist, die Abläufe so zu optimieren, dass zur EVT verlegte Schlaganfallpatienten auch interventionell behandelt werden können. Gelegentlich werden aus Netzwerk-Krankenhäusern transferierte Schlaganfallpatienten, trotz dort festgestellter Indikation zur EVT, am Zentrum nicht interventionell behandelt. Wir untersuchen die Kontraindikationen.

**Methoden:** Wir schlossen alle Schlaganfallpatienten ein, die zwischen 01/2016 und 12/2018 aus Netzwerk-Krankenhäusern an das Zentrum verlegt wurden. Wir analysierten die EVT-Kontraindikationen dieser Patientengruppe. Datenquelle war die prospektiv geführte Netzwerkdatenbank.

**Ergebnisse:** Im untersuchten Zeitraum wurden 487 Patienten aus Netzwerk-Krankenhäusern an das Zentrum verlegt (316 [65 %] hatten eine IVT erhalten). Einen Gefäßverschluss (LVO) im vorderen Kreislauf hatten 422 Patienten (209 Männer, medianes Alter 74 Jahre [IQR 28–93], medianer NIHSS 17 [IQR 5–32]), von denen 237 [56 %] eine EVT erhielten. Die Zeit von Symptombeginn bis Aufnahme am Zentrum (onset to door) betrug im Median 207 min (IQR 174–254), bis zur Leistenpunktion vergingen 275 min (IQR 243–325 min) und bis zur Rekanalisation 351 min (IQR 310–414).

Gründe die EVT insgesamt 185 Patienten vorzuenthalten, war bei 109 [59 %] ein großer Infarkt (ASPECTS 0–5), keine LVO in der CTA bei 56 [30 %] (davon 52 [88 %] mit i. v. rtPA vorbehandelt), kein Mismatch in der CT-Perfusion bei 8 [4 %], keine oder geringe Symptomatik nach Verlegung bei 7 [4 %] sowie sonstige Ausschlusskriterien bei 6 Patienten [3 %] (limitierende Nebenerkrankungen etc.).

**Diskussion und Fazit:** Der ausgedehnte Infarkt war die häufigste EVT-Kontraindikation bei sekundär verlegten Patienten. Ein Infarktwachstum über die Zeit ist anzunehmen. Die Prozeduren-Zeiten müssen daher monitort und optimiert werden: vom Symptombeginn bis zur Aufnahme in der Netzwerk-Klinik, von der Ankunft im Zentrum bis zur Reperfusion. Es ist zu diskutieren, welche Strukturen geschaffen werden können, um EVT-geeignete Schlaganfallpatienten aus dem Netzwerk direkt am Zentrum aufzunehmen.

## 292

### IMPACT OF CASCADE ON FURTHER COURSE OF ARTERIOPATHY AND RECURRENCE OF CHILDHOOD STROKE

Maik Böhmer<sup>\*1</sup>, Thomas Niederstadt<sup>2</sup>, Walter Heindel<sup>1</sup>, Moritz Wildgruber<sup>1</sup>, Ronald Sträter<sup>3</sup>, Uta Hanning<sup>4</sup>, André Kemmling<sup>5</sup>, Peter Sporns<sup>1</sup>

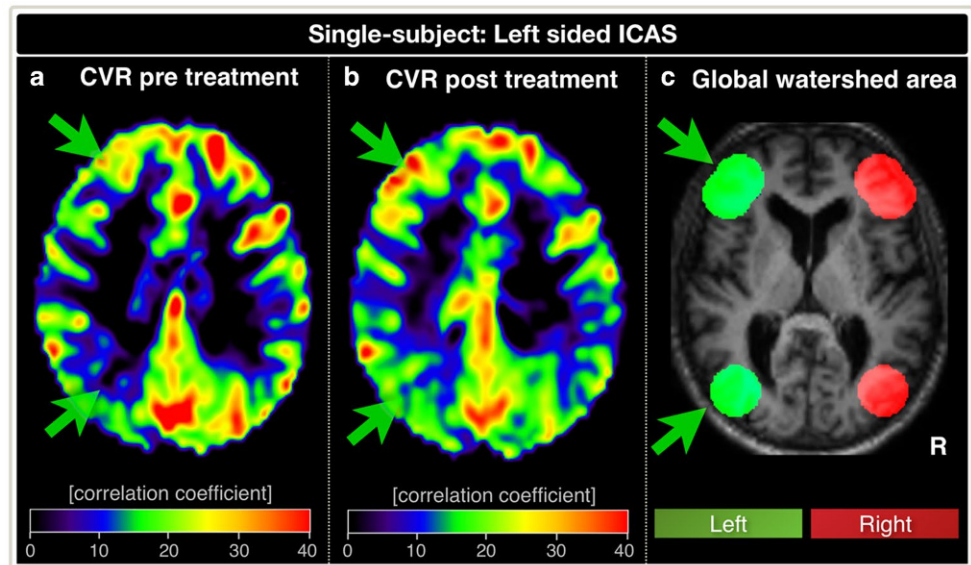
<sup>1</sup>Institut für Klinische Radiologie, Universitätsklinik Münster, Münster, Deutschland

<sup>2</sup>Klinik für Neuroradiologie, Clemenshospital Münster, Münster, Deutschland

**Fig. 1 | 290** Study participants overview. Presented are the status, healthy control (HC) or ICAS-patient; the side of the stenosis; gender; age at the pre treatment scan in years; type of treatment, carotid endarterectomy (CEA) or carotid artery stenting (CAS); the delay between treatment and the second post treatment scan in months; and the inclusion or exclusion to the study based on visual ratings (CP, JG, SK). After exclusion, related to low CVR image quality in pre and/or post treatment scans, 20 participants remained for the analysis

Subject number	Status	Stenosis	Gender	Age at first scan [y]	Treatment type	Time interval between treatment and second scan [months]	Inclusion / good imaging quality
1	ICAS	left	f	72	CEA	21	✓
2	ICAS	left	m	75	CAS	20	✓
3	HC	-	m	64	-	-	✓
4	HC	-	m	73	-	-	✓
5	HC	-	m	76	-	-	✓
6	ICAS	left	m	70	CEA	18	✗
7	ICAS	right	m	72	CAS	not verified	✗
8	ICAS	right	f	72	CEA	not verified	✗
9	HC	-	f	69	-	-	✗
10	HC	-	f	61	-	-	✗
11	HC	-	f	62	-	-	✗
12	HC	-	f	75	-	-	✓
13	HC	-	m	74	-	-	✓
14	HC	-	f	70	a <sup>-</sup> b <sup>-</sup> c <sup>-</sup>	-	✗
15	ICAS	right	m	76	CAS	13	✗
16	ICAS	right	m	65	CAS	12	✗
17	HC	-	f	75	-	-	✓
18	HC	-	f	65	-	-	✗
19	HC	-	f	75	-	-	✓
20	HC	-	m	66	-	-	✗
21	HC	-	f	73	-	-	✗
22	HC	-	m	76	-	-	✓
23	ICAS	right	m	65	CAS	10	✓
24	HC	-	f	77	-	-	✓
25	HC	-	f	73	-	-	✓
26	ICAS	right	m	67	CAS	9	✓
27	ICAS	left	m	74	CEA	10	✓
28	ICAS	right	f	71	CEA	6	✗
29	ICAS	right	f	59	CEA	5	✓
30	ICAS	right	f	84	CEA	6	✓
31	ICAS	right	m	74	CAS	5	✓
32	ICAS	left	m	77	CAS	3	✓
33	ICAS	left	f	70	CEA	not verified	✓

**Fig. 2 | 290** Exemplary maps from a left-sided ICAS-patient of CVR before and after treatment (A,B) and global watershed area (gWSA, C). Initially impaired CVR ipsilateral to the stenosis (A) recovered after treatment at gWSA-locations (8, arrows).



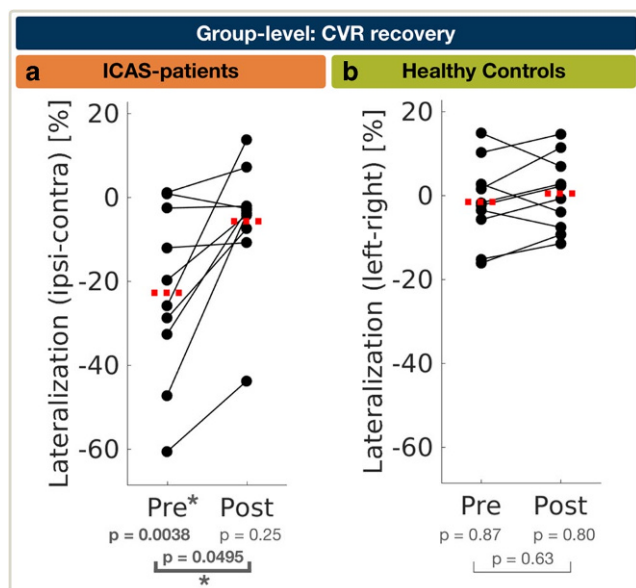


**Fig. 3 | 290** Lateralisation of CVR within GM of gWSA between both hemispheres in both scans for ICAS-patients and healthy controls. Each data point depicts the CVR lateralisation of one participant, lines connect both sessions of the same participant. CVR was significantly lateralised before treatment (a, t-test,  $p=0.0038$ ). After treatment, the lateralisation significantly improved (a, 2-sample t-test,  $p=0.0495$ ) and shows no CVR difference between the hemispheres anymore (a, t-test,  $p=0.25$ ). Asterisks indicate statistically significant differences. Both HC scans were symmetrical (b)

<sup>3</sup>Klinik für Kinder- und Jugendmedizin – Pädiatrische Hämatologie und Onkologie, Universitätsklinik Münster, Münster, Deutschland

<sup>4</sup>Klinik und Poliklinik für Neuroradiologische Diagnostik und Intervention, Universitätsklinikum Hamburg-Eppendorf, Hamburg, Deutschland

<sup>5</sup>Klinik für Neurologie mit Institut für Translationale Neurologie, Universitätsklinik Münster, Münster, Deutschland

**Background:** Arterial ischemic stroke (AIS) in childhood is a severe disease with potentially lifelong restrictions. Apart from cardiac or prothrombotic embolism, arteriopathy has been identified as a major cause and significant target of secondary stroke prevention. The Childhood Arterial Ischemic Stroke Standardized Classification and Diagnostic Evaluation (CASCADE) criteria facilitate a structured tool for categorizing and reporting childhood strokes according to the underlying cause. Our study aims to identify the prognostic value of CASCADE classification on admission for further course of arteriopathy and risk of stroke recurrence.

**Methods:** Between 2004 and 2017, we identified 86 children with an acute arterial ischemic stroke classified in the 7-basic and 19-expanded subgroups of the acute CASCADE criteria. All included children were diagnosed and followed-up by magnetic resonance imaging. All arteriopathic strokes were further categorized into the chronic CASCADE criteria, including progressive, stable, reversible, and indeterminate course. Outcomes were defined as stroke recurrence and course of arteriopathy according to chronic CASCADE criteria. Associations were assessed by Fisher exact test and Mann-Whitney *U* test.

**Result:** A total of 86 children were included; of these, 57 presented with arteriopathic stroke (CASCADE 1–4) and 29 as nonarteriopathic. Unilateral cerebral arteriopathy (CASCADE 2;  $P=0.036$ ) and bilateral cerebral arteriopathy (CASCADE 3;  $P=0.016$ ) significantly correlated with stroke recurrence, and progressive arteriopathy significantly correlated with unilateral focal cerebral arteriopathy ( $P<0.001$ ). Time

points of progress of arteriopathy differed; whereas patients with unilateral focal cerebral arteriopathy presented with early median progress after 11 days, patients with bilateral cerebral arteriopathy had a significantly later median progress after 124 days ( $P=0.005$ ).

**Discussion:** Our results are limited by small patient numbers, as well as the retrospective and single-center design. However, for pediatric stroke populations, we present a comparably large consecutive cohort of pediatric stroke patients with a homogenous MRI-based imaging work up and with frequent and long follow-ups.

**Conclusion:** Initial CASCADE classification is associated with risk of recurrent strokes and progress of arteriopathy. Moreover, time points of arteriopathic progress vary according to the underlying cause.

293

### IDENTIFICATION OF ACUTE LARGE VESSEL STROKE PATIENTS WITH POINT-OF-CARE ULTRASOUND

Ivaylo Dimitrov<sup>1</sup>, Kolja Schürmann<sup>1</sup>, Jan Philipp Bach<sup>1</sup>, Arno Reich<sup>1</sup>, Martin Wiesmann<sup>2</sup>, Omid Nikoubashmann<sup>2\*</sup>

<sup>1</sup>Neurologie, UKA, Aachen, Deutschland

<sup>2</sup>Neuroradiologie, UKA, Aachen, Deutschland

**Hintergrund:** We investigated the feasibility of ultrasound for the detection of large-vessel-occlusion acute stroke.

**Methoden:** Two neurologists (one experienced and one junior reader) retrospectively analyzed point-of-care ultrasound exams of the common carotid arteries of 30 patients with and without large-vessel-occlusion.

**Ergebnisse:** Ultrasound of the carotid arteries allows detecting large-vessel-occlusion with a sensitivity and positive predictive value of 73.3% and 95.7%, respectively. Inter-rater reliability was excellent (Cohen's Kappa, .813;  $p<.001$ ). Positive predictive value of ultrasound for the detection of LVO was higher than all clinical scores and sensitivity was higher than all clinical scores except for the NIHSS-cutoff at 7 points. Without clinical information, agreement between predicted and actual value was moderate/substantial for the experienced reader (Cohen's Kappa, .568;  $p<.001$ ) and the junior reader (Cohen's Kappa, .644;  $p<.001$ ). Agreement between the junior reader and the experienced reader was moderate (Cohen's Kappa, .581;  $p<.001$ ). With clinical information, agreement between predicted and actual value was moderate/substantial for the experienced reader (Cohen's Kappa, .717;  $p<.001$ ) and the junior reader (Cohen's Kappa, .769;  $p<.001$ ). Agreement between the junior reader and the experienced reader was excellent (Cohen's Kappa, .813;  $p<.001$ ).

**Diskussion/Discussion:** Ultrasound of the carotid arteries allows detecting large-vessel-occlusion with a high sensitivity and positive predictive value.

**Fazit/Conclusion:** Point-of-care ultrasound in the acute stroke setting is feasible and may serve as a complementary tool for the detection of proximal large-vessel-occlusion that may be missed otherwise.

297

### EMERGENCY EVERSION CAROTID ENDARTERECTOMY VERSUS CAROTID ARTERY STENTING IN ENDOVASCULAR ACUTE STROKE TREATMENT.

Raveena Singh<sup>1</sup>, Nora Schäferhenrich<sup>1</sup>, Hani Ridwan<sup>1</sup>, Anastasios Mpotsaris<sup>1</sup>, Arno Reich<sup>2</sup>, Johannes Kalder<sup>3</sup>, Ahmend E Othman<sup>4</sup>, Martin Wiesmann<sup>1</sup>, Omid Nikoubashmann<sup>2\*</sup>

<sup>1</sup>Neuroradiologie, UKA, Aachen, Deutschland

<sup>2</sup>Neurologie, UKA, Aachen, Deutschland

<sup>3</sup>Gefäßchirurgie, UKA, Aachen, Deutschland

<sup>4</sup>Radiologie, UK Tübingen, Tübingen, Deutschland

**Hintergrund:** Data in the literature suggest that thrombectomy with emergency carotid artery stenting (CAS) in acute stroke is associated with an increased hemorrhage rate. As we perform thrombectomy under general anesthesia, we avoid emergency CAS and perform emergency eversion carotid endarterectomy (eCEA) in the same anesthesia session in our angiography suite. We perform eCEA 1) before thrombectomy whenever necessary and 2) after thrombectomy whenever possible. In this analysis we focus on hemorrhage rates in patients who receive thrombectomy and emergency CAS vs. eCEA.

**Methoden:** We retrospectively analyzed data from our prospectively maintained stroke registry and included 27 thrombectomy patients who received emergency eCEA and 63 patients who received emergency CAS with GP2b/3a-inhibitors or dual antiplatelet therapy in the same time span.

**Ergebnisse:** Baseline characteristics (NIHSS, age, sex, rate of IV and IA thrombolysis, patients with unknown time window) were comparable ( $p > .070$ ). Symptomatic hemorrhage rate was 0 % (0/27) in the eCEA group and 10 % (6/63) in the CAS group ( $p = .173$ ). Parenchymal hemorrhage rate (PH2) was 7 % (2/27) in the eCEA group and 16 % (10/63) in the CAS group ( $p = .499$ ). Both parenchymal hemorrhages in the eCEA group occurred during the intervention and were diagnosed on immediate postinterventional imaging, whereas 2 parenchymal hemorrhages in the CAS group occurred during the intervention and the remaining 8 hemorrhages occurred within three days after the intervention ( $p = .091$ ). There were no delayed hemorrhages in the eCEA group. Clinical outcome upon 90 days was comparable with 39 % of eCEA and 50 % of CAS patients achieving good clinical outcome (mRS 0–2) ( $p = .384$ ).

**Diskussion:** Parenchymal hemorrhage rate was half as high in the eCEA group, albeit this difference did not reach statistical significance. All hemorrhages in the eCEA group occurred during the intervention, implying that hemorrhage in this group was likely to be caused by reperfusion injury, whereas delayed hemorrhage is likely to be caused by dual antiplatelet therapy.

**Fazit:** eCEA is a feasible alternative for CAS in acute stroke patients and has the advantage that dual antiplatelet therapy is not needed.

## 298

### INCREASED HEMORRHAGE RATE IN ACUTE STROKE PATIENTS WITH CAROTID ARTERY STENTING AND DUAL ANTIPLATELET THERAPY

Omid Nikoubashmann<sup>\*1</sup>, Felix Hadler<sup>2</sup>, Arno Reich<sup>2</sup>, Ahmend E Othman<sup>3</sup>, Hani Ridwan<sup>1</sup>, Alexander Riabikin<sup>1</sup>, Martin Wiesmann<sup>1</sup>

<sup>1</sup>Neuroradiologie, UKA, Aachen, Deutschland

<sup>2</sup>Neurologie, UKA, Aachen, Deutschland

<sup>3</sup>Radiologie, UK Tübingen, Tübingen, Deutschland

**Hintergrund:** Hemorrhage rates in the literature after thrombectomy with emergency carotid artery stenting (CAS) vary considerably, ranging from 0–43% for parenchymal hemorrhage. We analyzed parenchymal hemorrhage rates (ECASS-PH2) in a homogeneous patient cohort of thrombectomy patients with additional CAS and identified risk factors for hemorrhage, hypothesizing that intravenous thrombolysis and high blood pressure during the intervention are risk factors for hemorrhage.

**Methoden:** We identified 122 consecutive patients who received thrombectomy and emergency CAS. We focused our analysis on parenchymal hemorrhage rates in 117 patients, who received CAS with GP2b/3a-inhibitors or dual antiplatelet therapy, which is the standard in our institution. One patient was excluded from further analysis, because hemorrhage was due to vessel perforation during the intervention, which left 116 to be included.

**Ergebnisse:** Symptomatic hemorrhage rate was 5% (6/116) and parenchymal hemorrhage rate was 14% (16/116). 5 (4%) of these parenchymal hemorrhages occurred during the intervention and were diagnosed

on immediate postinterventional CT, whereas 8 hemorrhages occurred on the first day after intervention and the remaining 3 hemorrhages occurred on the second ( $n=1$ ) and third ( $n=2$ ) days. All hemorrhages occurred under either GP2b/3a-inhibitor or dual antiplatelet therapy. There was re-hemorrhage in 7 (44%) cases. All but one hemorrhage, which occurred two days after the intervention and was located atypically, were located within the infarcted area, with 13 of 16 (81%) hemorrhages being mainly located in the basal ganglia. Older age was a risk factor for hemorrhage ( $p = .03$ ), whereas IV thrombolysis ( $p = .782$ ), IA thrombolysis ( $p = .357$ ), the occurrence of contrast extravasation ( $p = .759$ ), unknown time window ( $p = .772$ ), NIHSS ( $p = .090$ ), initial infarction size ( $p = .926$ ), and blood pressure ( $p \geq .266$ ) were not.

**Diskussion/Discussion:** There is an increased hemorrhage risk in thrombectomy patients who receive emergency stenting with dual antiplatelet therapy. IV thrombolysis and high blood pressure are no risk factors for hemorrhage, whereas older age is.

**Fazit/Conclusion:** CAS with dual antiplatelet therapy in acute large-vessel stroke is associated with an increased hemorrhage rate.

## 300

### RECRUITMENT OF LEPTOMENINGEAL COLLATERALS DOES NOT PREVENT MICROSTRUCTURAL CORTICAL TISSUE DAMAGE IN CEREBRAL LARGE-ARTERY STENO-OCLUSIVE DISEASE: A DSC PERFUSION AND QUANTITATIVE MRI STUDY

Alexander Seiler<sup>\*1,2</sup>, Annemarie Brandhofe<sup>1</sup>, René-Maxime Gracien<sup>1</sup>, Waltraud Pfeilschifter<sup>1</sup>, Ulrike Nöth<sup>3</sup>, Ralf Decihmann<sup>3</sup>, Elke Hattingen<sup>2</sup>, Marlies Wagner<sup>2</sup>

<sup>1</sup>Klinik für Neurologie, Universitätsklinikum Frankfurt (Goethe-Universität), Frankfurt am Main, Deutschland

<sup>2</sup>Institut für Neurodiagnostik, Goethe-Universität Frankfurt, Frankfurt am Main, Deutschland

<sup>3</sup>Brain Imaging Center, Goethe-Universität Frankfurt, Frankfurt am Main, Deutschland

**Background:** Collateral blood flow is believed to be pivotal in large-artery steno-occlusive disease to prevent ischemic tissue damage, which may involve the cerebral cortex and not be detected on conventional magnetic resonance imaging (MRI). The aim of this study was to investigate whether a higher abundance of leptomeningeal collaterals may be protective regarding cortical microstructural damage.

**Methods:** 30 patients with high-grade unilateral internal carotid artery (ICA) or middle cerebral artery (MCA) stenosis/occlusion were included. High-resolution quantitative (q)T2 mapping was used to estimate microstructural damage of normal-appearing cortex within the dependent vascular territory. The volumetric abundance of leptomeningeal collaterals was assessed based on perfusion-weighted imaging (PWI) raw data as described earlier<sup>1</sup>. The ratio relative cerebral blood flow/relative cerebral blood volume (rCBF/rCBV) as a surrogate of relative cerebral perfusion pressure (rCPP) was used to investigate the intravascular hemodynamic competency of pial collateral vessels and the hemodynamic state of brain parenchyma in the dependent vascular territory.

**Results:** Cortical qT2 values were significantly increased within the dependent vascular territory compared to the contralateral side ( $p = 0.0001$ ). While volumetric abundance of adjacent leptomeningeal collaterals was significantly increased ( $p < 0.01$ ), there was a significant decline in pial intravascular ( $p < 0.01$ ) and parenchymal ( $p = 0.0001$ ) rCPP on the affected side. Relative increase of cortical qT2 was significantly correlated with relative reduction of parenchymal rCPP ( $p < 0.05$ ).

**Conclusions:** In unilateral large-artery steno-occlusive disease, microstructural cortical damage is closely related to hemodynamic impairment. Increasing pial collateral recruitment is associated with decreasing perfusion pressure and should therefore rather be deemed a warning sign than a sign of effective compensation in this condition.

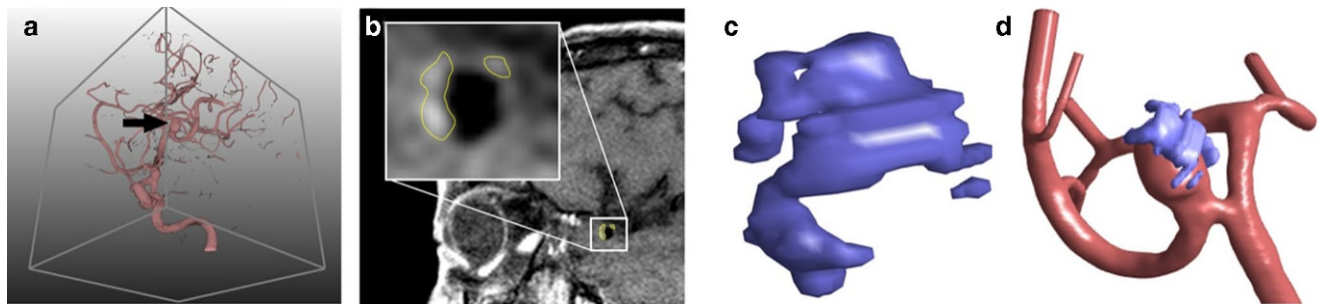


**Fig. 1 | 301** a) Illustration of the 3D DSA data with an MCA aneurysm (arrow). b) Corresponding MR-VWI dataset with yellow contours masking the enhanced regions. c) 3D model of the enhancement. d) Co-registered 3D DSA aneurysm surface mesh and 3D MR-VWI enhancement surface mesh

301

### COMBINING HIGH-RESOLUTION VESSEL WALL IMAGING WITH IMAGE-BASED FLOW EVALUATION IN UNRUPTURED MIDDLE CEREBRAL ANEURYSMS

Philipp Berg<sup>\*1</sup>, Naomi Larsen<sup>2</sup>, Charlotte Flüh<sup>3</sup>, Samuel Voss<sup>1</sup>, Sylvia Saalfeld<sup>1</sup>

<sup>1</sup>Forschungscampus STIMULATE, Otto-von-Guericke Universität Magdeburg, Magdeburg, Deutschland

<sup>2</sup>Institut für Neurochirurgie, Universitätsklinikum Schleswig-Holstein Campus Kiel, Kiel, Deutschland <sup>3</sup>Institut für Radiologie und Neuroradiologie, Universitätsklinikum Schleswig-Holstein Campus Kiel, Kiel, Deutschland

**Hintergrund:** The assessment of intracranial aneurysm rupture risk remains challenging due to a highly individual appearance in size and shape, as well as an unpredictable course of the disease. However, high-resolution magnetic resonance vessel wall imaging (MR-VWI) was recently used to associate wall enhancement with inflammatory cell invasion in intracranial aneurysms.

**Methoden:** Within this study twenty-five unruptured saccular middle cerebral artery (MCA) aneurysms who underwent pre-operative high-resolution MR-VWI showing wall enhancement, digital subtraction angiography, microsurgical aneurysm clipping, and histologic analysis of the resected aneurysm wall were investigated using image-based blood flow simulations.

**Ergebnisse:** The computational results reveal that vessel wall enhancement in MCA aneurysms is associated with lower cycle-averaged wall shear stresses, decreased oscillatory shear, and increased low shear areas compared to the overall aneurysm surfaces. Furthermore, flow structures perpendicular to the main flow occur in the region of enhancement.

**Diskussion/Discussion:** These findings highlight that a correlation between local hemodynamics and measurable processes occurring within the aneurysmal vessel wall exists. Hence, patient-specific flow conditions can be assessed using image-based modeling to identify potentially endangered aneurysm wall regions.

**Fazit/Conclusion:** Overall, MR-VWI may be beneficial in the evaluation of unruptured aneurysms regarding rupture risk assessment.

#### References

1. Matouk CC, et al. Vessel wall magnetic resonance imaging identifies the site of rupture in patients with multiple intracranial aneurysms: Proof of principle. *Neurosurgery*. 2013;72(3):492–6.
2. Larsen N, et al. Vessel wall enhancement in unruptured intracranial aneurysms: An indicator for higher risk of rupture? High-resolution MR imaging and correlated histologic findings. *AJNR Am J Neuroradiol*. 2018;39(9):1617–21.

304

### DIRECT ASPIRATION THROMBECTOMY IN DISTAL VESSEL OCCLUSIONS EITHER WITH 5F SOFIA CATHETER OR WITH HEADWAY 27 MICROCATHETER

Dan Meila<sup>\*1</sup>, Ingmar Born<sup>1</sup>, Ralf Rulands<sup>1</sup>, Gebhard Schmid<sup>1</sup>

<sup>1</sup>Johanna Etienne Krankenhaus, Neuss, Deutschland

**Hintergrund:** Recent studies suggest that the proven benefits of thrombectomy for the treatment of large vessel occlusions are transferable to more peripheral distal vessel occlusions (DVO). Safely accessing and extracting these thrombi however remains challenging, particularly in more tortuous peripheral arteries. For such cases we have utilized either 5F Sofia catheter or Headway 27 microcatheter thrombectomy, with the aim of reducing potential trauma associated with negotiating stent retrievers into the peripheral intracranial vasculature. We describe our technique as well as present angiographic and clinical outcomes.

**Methoden:** Retrospective review of our institution's prospectively collected thrombectomy registry for the 12 months spanning June 2018 to May 2019. Data on all cases of distal vessel occlusions were collected and analyzed.

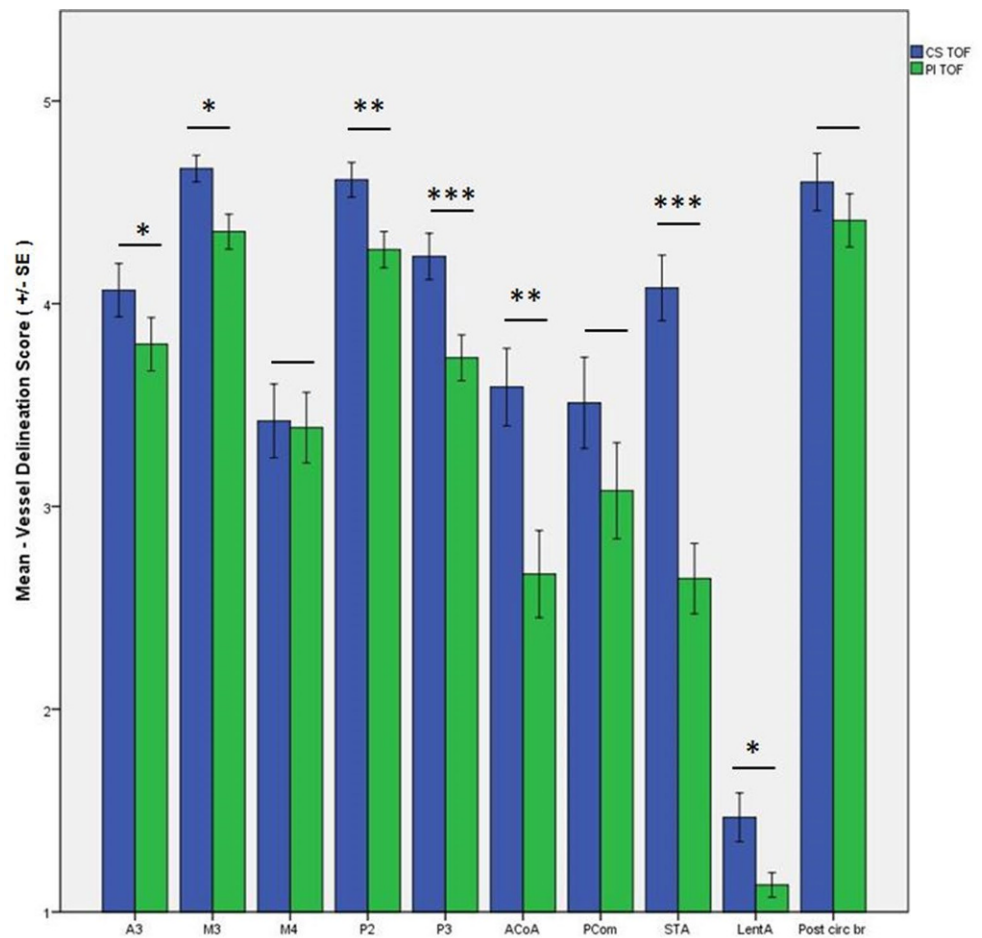
**Ergebnisse:** Direct aspiration thrombectomy in distal vessel occlusions was performed 13 times over the study period, with a recanalization rate of 92 %. DVO strokes in multiple locations were treated, including the A3, M3 and P2 segments. No complications relating to the technique were recorded. No perforation, no dissection, no bleeding and no vasospasm was noted

**Fazit/Conclusion:** The aspiration technique either with 5F Sofia or with Headway 27 microcatheter is an atraumatic technique that enlarges the range of TICI 2c/3 thrombectomies even in far distal occlusions. Due to certain limitations sole aspiration is not always feasible. Further development of material is crucial.

#### References

1. Grieb D, Schlunz-Hendann M, Brinjikji W, Melber K, Greling B, Lanfermann H, et al. Mechanical thrombectomy of M2 occlusions with distal access catheters using ADAPT. *J Neuroradiol*. 2019;46(4):231–7. Jul.
2. Crockett MT, Phillips TJ, Chiu AHY. Dual suction Headway27 microcatheter thrombectomy for the treatment of distal intracranial arterial occlusion strokes: initial experience with the micro-ADAPT technique. *J Neurointerv Surg*. 2018;24.

**Fig. 1 | 309** Mean vessel delineation scores in intracranial and extracranial (STA) segments rated on a 1–5 point scale



**309**

**COMPRESSED-SENSING (CS) 3D TOF MRA IN A CLINICAL SETTING: A QUALITATIVE COMPARISON STUDY IN 45 PATIENTS.**

Theo Demerath<sup>\*1</sup>, Grzegorz Karwacki<sup>2</sup>, Tilman Schubert<sup>3</sup>

<sup>1</sup>Klinik für Neuroradiologie, Universitätsklinikum Freiburg, Freiburg, Deutschland

<sup>2</sup>Klinik für Radiologie und Nuklearmedizin, Universitätsspital Basel, Basel, Schweiz

<sup>3</sup>Klinik für Neuroradiologie, Universitätsspital Zürich, Zürich, Schweiz

**Hintergrund:** Compressed-sensing (CS) techniques can be used to improve spatial resolution in TOF MRA while keeping acquisition time constant. Our aim was to compare image quality in CS TOF MRA to „conventional“ (con) TOF MRA in a non-selected clinical population of 45 patients.

**Methoden:** CS TOF MRA with a voxel size of 0.14 mm<sup>3</sup> (0.6×0.6×0.4 mm) was compared to con TOF MRA with a voxel size of 0.49 mm<sup>3</sup> (0.78×1.05×0.6 mm) in a 3T (Siemens Skyra/Skyra fit, 20 CH Head coil) MRI, giving a 70 % decrease in voxel size from con TOF to CS TOF MRA. General image quality and vessel delineation (A3, M3, M4, P2, P3, ACoA, PCom Segments and superficial temporal arteries (STA)) were blindly assessed by 2 board-certified neuroradiologists by using a 1–4 point (gen. image quality) and 1–5 (vessel delineation) point scale. Mean Scales were compared by using Mann-Whitney-U-Test; interrater agreement κ-statistics were moderate to low.

**Ergebnisse:** Mean general image quality (1.59 vs. 1.84 SE 0.093/0.079) and vessel delineation scales were rated higher in A3, M3, P2, P3, ACoA and STA Segments in CS TOF MRA compared to con TOF MRA.

**Diskussion:** General image quality was rated slightly lower in CS TOF MRA, which might be attributable to intrinsic image noise. Vessel delineation in most intracranial and STA segments were rated higher in CS TOF MRA compared to con TOF MRA while keeping acquisition time constant, which is conformable with sparse available data [2].

**Fazit:** Besides being used to reduce acquisition time, Compressed-sensing (CS) techniques can lead to improved spatial resolution while keeping acquisition time constant, which may improve peripheral vessel delineation.

**References**

1. Fushimi Y, et al. Clinical evaluation of time-of-flight MR angiography with sparse undersampling and iterative reconstruction for cerebral aneurysms. *Nmr Biomed.* 2017;30(11).
2. Lin Z, et al. Clinical feasibility study of 3D intracranial magnetic resonance angiography using compressed sensing. *J Magn Reson Imaging.* 2019.

## 313

### INTRAKRANIELLES STENTING IN DER ZEIT NACH SAMMPRIS: “LETZTER RETTUNGSVERSUCH FÜR HOFFNUNGSLOSE FÄLLE” ODER “EFFEKTIVE BEHANDLUNGSOPTION”?

Dimah Hasan<sup>1,2</sup>, Annemarie Brandhofe<sup>3</sup>, Joachim Berkefeld<sup>1</sup>, Fee Keil<sup>\*1</sup>

<sup>1</sup>Neuroradiologie, Universitätsklinikum JWG Universität Frankfurt, Frankfurt, Deutschland

<sup>2</sup>Neuroradiologie, Uniklinikum Aachen, Aachen, Deutschland

<sup>3</sup>Universitätsklinikum JWG Universität Frankfurt, Neurologie, Frankfurt, Deutschland

**Hintergrund:** Nach den für das Stenting intrakranieller Stenosen negativen Ergebnissen der SAMMPRIS-Studie<sup>1</sup> wurden die Indikationsstellung auf Patienten mit unter optimierter medikamentöser Therapie rezidivierenden Symptomen und Infarkten und auf Fälle mit einem akuten Schlaganfall und Gefäßobstruktionen auf dem Boden einer Stenose beschränkt. Ziel dieser Studie war es, bei den in einem einzelnen Zentrum verbliebenen Fällen Rekanalisationsergebnisse und klinische Behandlungsergebnisse zu analysieren.

**Methoden:** Im Zeitraum zwischen 2011 und 2018 wurden im neurologischen Institut des Frankfurter Universitätsklinikums insgesamt 45 Patienten mit intrakraniellen Stenosen mit Stents behandelt. In 28 Fällen wurde die Intervention zusätzlich zur Thrombektomie bei akuten Schlaganfällen mit atherothrombotischem Gefäßverschluss durchgeführt, die übrigen 17 Patienten kamen überwiegend mit subakuten, meist hämodynamisch bedingten rezidivierenden Symptomen und Infarkten. Die interventionelle Behandlung erfolgte mit ballonexpandierenden oder selbstexpandierenden Stents.

**Ergebnisse:** Ein technisch erfolgreiches Stenting mit einer mehr als 50% igen Lumenerweiterung gelang bei allen 45 Patienten. Beim Stenting plus Thrombektomie kam es in 2 von 28 Fällen zu einer raschen Rethrombose. Eine erfolgreiche Rekanalisation TICI IIb/III konnte bei den übrigen Patienten erreicht werden. Die Rate an guten klinischen Ergebnissen, mRS 0–2 nach 3 Monaten lag bei den Thrombektomiepatienten bei 44%. Symptomatische Blutungen traten in zwei Fällen auf.

**Diskussion:** Unter Berücksichtigung der Komplikationsrate kann ein großzügiger Einsatz des intrakraniellen Stentings bei frustranen Thrombektomieversuchen gerechtfertigt sein. Bei Patienten mit rezidivierender Symptomatik unter optimierter medikamentöser Therapie kann auch eine prologierte Indikationsstellung zum Stenting negative Auswirkungen auf das outcome haben.

**Fazit:** In einem erfahrenen Zentrum ist das intrakranielle Stenting von Patienten mit atherothrombotischen Gefäßobstruktionen mit akzeptablen Komplikationsraten durchführbar. Bei im Rahmen der Schlaganfallbehandlungen durchgeführten Interventionen sind die Rekanalisationsergebnisse und klinische Behandlungsergebnisse ähnlich wie bei Thrombektomien embolischer Gefäßverschlüsse.

#### Literatur

1. Chimowitz, et al. Stenting vs aggressive medical therapy for intracranial arterial stenosis. *N Eng J Med.* 2011.

## 320

### EARLY VERSUS LATE ESTABLISHMENT OF FULL DUAL ANTIPLATELET THERAPY AFTER EMERGENCY CAROTID ARTERY STENTING IN TANDEM OCCLUSIONS

Alena Haußmann<sup>\*1</sup>, Ruben Mühl-Benninghaus<sup>1</sup>, Andreas Simgen<sup>1</sup>, Wolfgang Reith<sup>1</sup>, Umut Yilmaz<sup>1</sup>

<sup>1</sup>Universitätsklinikum des Saarlandes, Diagnostische und Interventionelle Neuroradiologie, Homburg, Deutschland

**Hintergrund:** Currently emergency carotid artery stenting is having a renaissance since a series of randomized trials demonstrated the benefit of mechanical thrombectomy in acute large vessel occlusions of the anterior circulation and 30% of those are accompanied by an additional occlusion or high grade stenosis of the extracranial ICA that requires PTA and/or stenting in order to gain access to the intracranial clot. However emergency stenting bears the risk of acute stent occlusions due to the emergency setting with an insufficient preparation with antiplatelet medication and on the other hand the risk of hemorrhagic complications due to the application of antiplatelet medication in combination with iv-thrombolysis.

The purpose of this study was to compare occlusion rates and hemorrhagic complications when dual antiplatelet therapy is started within 24 hours after endovascular treatment or thereafter.

**Methoden:** Patients with acute tandem occlusions of the anterior circulation who were endovascularly treated at our institution were identified from our registry of neuroendovascular interventions.

Clinical, angiographic and neuroimaging data was analyzed. Endpoints included acute occlusions of the carotid stents and symptomatic ICH.

**Ergebnisse:** 36 patients were included. Full dual antiplatelet therapy was established within 24 hours after intervention in 18 patients. Rates of acute stent occlusions did not differ between patients who received antiplatelet therapy within 24 h and those who did not ( $n=2$  in either group).

**Fazit:** Late establishment of full dual antiplatelet therapy after emergency carotid artery stenting in tandem occlusions did not have a higher risk of acute stent occlusion in this retrospective analysis.

#### References

1. Yilmaz U, Körner H, Mühl-Benninghaus R, et al. Acute Occlusions of Dual-Layer Carotid Stents After Endovascular Emergency Treatment of Tandem Lesions. *Stroke.* 2017;4:.

## 322

### SIMULTANEOUS TREATMENT OF ATHEROSCLEROTIC TANDEM OCCLUSIONS IN ACUTE ISCHEMIC STROKE USING RETRIEVER WIRE SUPPORTED CAROTID ARTERY REVASCLARIZATION (REWISED CARE).

Volker Maus<sup>\*1</sup>, Daniel Behme<sup>2</sup>, Christoph Maurer<sup>3</sup>, Andrei Tropine<sup>4</sup>, Stephanie Tritt<sup>4</sup>, Ansgar Berlis<sup>3</sup>, Marios Psychogios<sup>2</sup>

<sup>1</sup>Bochum, Deutschland

<sup>2</sup>Göttingen, Deutschland

<sup>3</sup>Augsburg, Deutschland

<sup>4</sup>Wiesbaden, Deutschland

**Background:** Endovascular treatment of cerebral large vessel occlusions and concomitant atherosclerotic lesions of the ipsilateral internal carotid artery (ICA) are matter of debate. We report a multi-center experience using the “Retriever wire supported carotid artery revascularization” (ReWised CARE) technique allowing simultaneous therapy of both lesions.

**Methods:** We retrospectively analyzed 23 patients with acute tandem occlusions (TO) undergoing ReWised CARE at 3 German centers. Clinical (including demographics and NIHSS) and procedural (including angiographic evaluation of recanalization) data were evaluated. Favorable clinical outcome was defined as modified Rankin Scale (mRS)  $\leq 2$  at 90 days.

**Result:** Median age was 70 years (IQR 65–80) and 70% were male. Median baseline NIHSS was 15 (IQR 11–17). Out of 23 patients, 22 (96%) had an intracranial occlusion of the anterior circulation. Successful stent retriever deployment with subsequent carotid artery treatment was feasible in all cases without dislocation of the stent retriever during the procedure. Overall, successful reperfusion (mTICI  $\geq 2b$ ) was achieved in 22/23 (96%) patients with 10/23 (44%) individuals com-

pletely reperfused (mTICI 3). Median groin puncture to stent retriever deployment was 29 minutes (IQR 23–46) and groin puncture to final revascularization was 63 minutes (IQR 56–78). Median NIHSS at discharge was 5 (IQR 3–12) with favorable clinical outcome at 90 days in 11 out of 20 patients (55%).

**Discussion:** The results of this study show that ReWiSed CARE is a technical feasible approach for the treatment of atherosclerotic TO with 100% successful distal stent retriever placement and subsequent carotid artery treatment utilizing the stent retriever wire. The technique is not associated with higher rates of ENT compared to what has been reported when an ante- or retrograde approach has been utilized. Another aspect is the long dwell time of the stent retriever during the procedure, which might result in a better angiographic outcome.

**Conclusion:** Endovascular treatment using ReWiSed CARE is safe, fast and efficient in TO patients with underlying atherosclerotic lesion of the extracranial ICA.

323

**INTRACRANIAL MECHANICAL THROMBECTOMY OF LARGE VESSEL OCCLUSIONS IN THE POSTERIOR CIRCULATION USING SAVE**

Volker Maus\*<sup>1</sup>, Hanna Styczen<sup>2</sup>, Jan Liman<sup>2</sup>, Ilko Maier<sup>2</sup>, Alex Brehm<sup>2</sup>, Ioannis Tsogkas<sup>2</sup>, Marios Psychogios<sup>2</sup>

<sup>1</sup>Bochum, Deutschland  
<sup>2</sup>Göttingen, Deutschland

**Background:** Mechanical thrombectomy (MT) using stent retriever assisted vacuum-locked extraction (SAVE) is a promising method for anterior circulation strokes. We present our experience with SAVE for large vessel occlusions (LVO) of the posterior circulation.

**Methods:** We retrospectively analyzed 66 consecutive MT patients suffering from LVO of the posterior circulation. Primary endpoints were first-pass and overall complete/near complete reperfusion, defined as a modified thrombolysis in cerebral infarction (mTICI) score of 2c and 3. Secondary endpoints contained number of passes, time interval from groin puncture to reperfusion and rate of postinterventional symptomatic intracranial hemorrhage (sICH).

**Result:** Median age was 75 years (interquartile range (IQR) 54–81 years). Baseline median National Institutes of Health stroke scale (NIHSS) was 13 (IQR 8–21). Fifty-five (83%) patients had LVO of the basilar artery and 11 (17%) of the posterior cerebral artery. Eighteen (27%) patients were treated with SAVE and 21 (32%) with aspiration only. First pass mTICI2c or 3 and overall mTICI2c or 3 were documented in 11/18 (61%) and 14/18 (78%) with SAVE and in 4/21 (19%) and 13/21 (33%) with aspiration only. Median attempt was 1 (IQR 1–2) with SAVE and 2 (IQR 1–4) with aspiration ( $p=0.0249$ ). Median groin to reperfusion time did not differ significantly between groups. The rate of sICH was 5% without any complications in the SAVE cohort.

**Discussion:** Similar to our previous results, we observed SAVE to be an effective and safe thrombectomy method in patients suffering from LVO in the posterior circulation.<sup>1</sup> Although the procedure times by using SAVE tended to be longer compared to aspiration only, no differences in clinical outcome at discharge were observed, which might possibly be explained by the better reperfusion results.

**Conclusion:** Mechanical thrombectomy of posterior large vessel occlusions with SAVE is feasible, safe, and effective with high rates of near-complete and complete reperfusion.

**References**

1. Maus V, et al. The SAVE Technique: Large-Scale Experience for Treatment of Intracranial Large Vessel Occlusions. Clin Neuroradiol. 2018; <https://doi.org/10.1007/s00062-018-0702-4>.

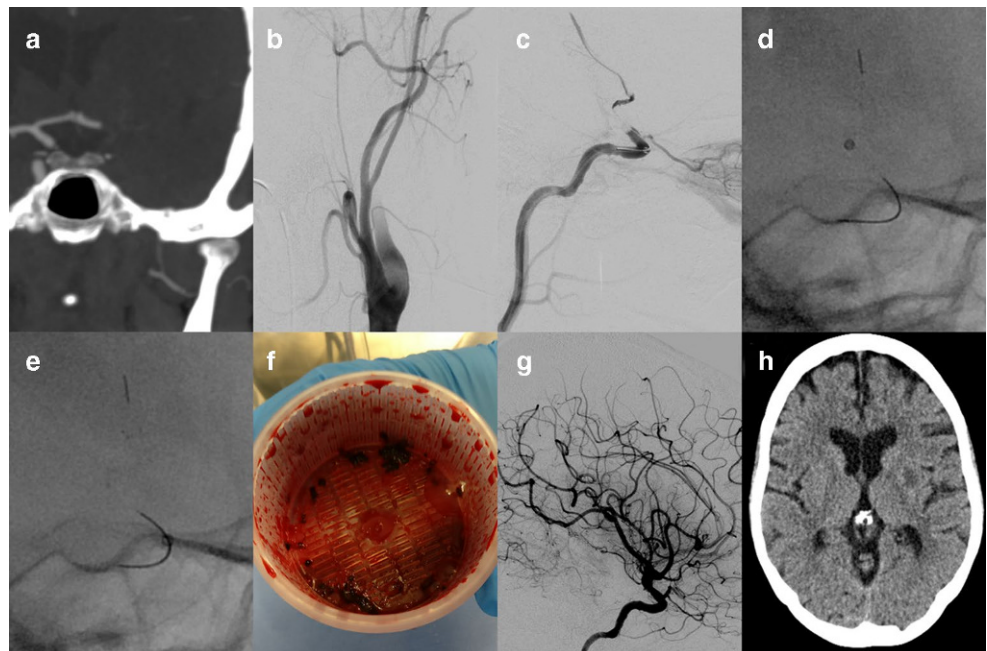
324

**CLOT REDUCTION PRIOR TO EMBOLECTOMY: MSAVE AS A FIRST-LINE TECHNIQUE FOR LARGE CLOTS**

Marios Psychogios<sup>1</sup>, Ioannis Tsogkas<sup>1</sup>, Alex Brehm<sup>1</sup>, Amelie Hesse<sup>1</sup>, Ryan Mctaggart<sup>2</sup>, Mayank Goyal<sup>3</sup>, Ilko Maier<sup>1</sup>, Marlena Schnieder<sup>1</sup>, Daniel Behme<sup>1</sup>, Volker Maus\*<sup>4</sup>

<sup>1</sup>Göttingen, Deutschland  
<sup>2</sup>Rhode Island, United States  
<sup>3</sup>Calgary, Kanada  
<sup>4</sup>Bochum, Deutschland

Fig.1 | 324



**Background:** The “Stent retriever Assisted Vacuum-locked Extraction” (SAVE) technique is a promising embolectomy method for intracranial large vessel occlusion (LVO).<sup>1</sup> We report our experience using a modified SAVE (mSAVE) approach for clot reduction prior to embolectomy in acute ischemic stroke patients with large clots.

**Methods:** We retrospectively analyzed 20 consecutive patients undergoing mSAVE in our center due to intracranial LVO. Angiographic data (including first-pass and overall complete reperfusion, defined as an eTICI score of 3, rate of successful reperfusion (eTICI  $\geq 2c$ ), number of passes, time from groin puncture to reperfusion) and clinical data (favorable outcome at 90 days, defined as modified Rankin Scale (mRS)  $\leq 2$ ) were assessed.

**Result:** First-pass and overall eTICI 3 reperfusion was reached in 13/20 (65%) and 14/20 (70%), respectively. The rate of successful reperfusion (eTICI  $\geq 2c$ ) after one pass was 85% and on final angiogram 90% with an average number of  $1.1 \pm 0.3$  attempts. Eight out of 11 (73%) ICA occlusions were reperfused successfully and 5 (46%) completely after a single pass. Median groin to reperfusion time was 33 minutes (IQR 25–46). A favorable clinical outcome was achieved in 9/20 (45%) patients at discharge and after 90 days, respectively.

**Discussion:** The pivotal idea of mSAVE is reducing the amount of clot (Fig 1) by repeatedly retrieving and advancing the aspiration catheter in an alternating fashion, while the catheter is connected with an activated pump and without movement of the stent retriever. The idea is to perform an aspiration maneuver with distal embolus protection, due to the distally placed stent retriever and the remaining distal part of the clot. Especially for patients with ICA occlusions mSAVE seems to be a promising approach as the rate of complete and successful reperfusion after a single pass was 46% and 73%, respectively. It is to point out that in this study the thrombus amount was large throughout our cohort with a median CBS of 4 and a median clot length of 18 mm. A potential drawback might be a trauma of the inner vessel wall by the repeated movement of the large-bore aspiration catheter. However, we did not observe any vessel injuries such as arterial dissections.

**Conclusion:** Clot reduction followed by embolectomy (mSAVE) is feasible and may be an important tool in the treatment of large clots.

## References

1. Maus V, et al. The SAVE Technique: Large-Scale Experience for Treatment of Intracranial Large Vessel Occlusions. Clin Neuroradiol. 2018; <https://doi.org/10.1007/s00062-018-0702-4>.

329

## DO MY VESSEL IMPLANTS WORK? AN ANSWER ATTEMPTED WITH MRI

Mariya Pravdivtseva<sup>\*1,2,3</sup>, Eva Peschke<sup>1,2,3</sup>, Prasanth Velvaluri<sup>3,4</sup>, Olav Jansen<sup>1</sup>, Jan-Bernd Hövener<sup>1,2,3</sup>

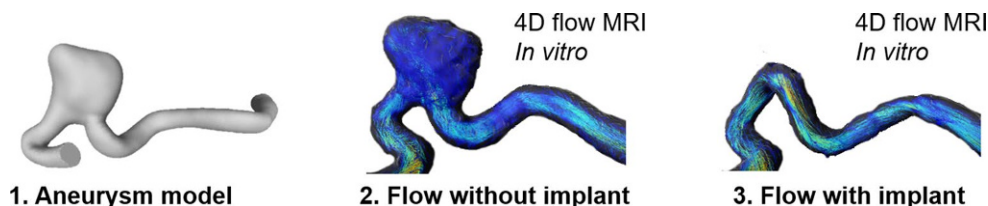
<sup>1</sup>UKSH, Department of Radiology and Neuroradiology, Kiel, Deutschland

<sup>2</sup>Molecular Imaging North Competence Center, Section Biomedical Imaging, Kiel, Deutschland

<sup>3</sup>Kiel Universität, Kiel, Deutschland

<sup>4</sup>Institute of Material Science and Engineering, Kiel, Deutschland

Fig. 1 | 329



**Background:** Intracranial aneurysms can cause life-threatening bleeding. Flow diverter stents (FDS) are a new and minimally invasive option for their treatment. Despite an outcome that is often positive, complications such as delayed aneurysm rupture or partial occlusion arise. The goal of this work was to evaluate the treatment efficacy of different FDS after the placement using modern imaging techniques.

**Methods:** Based on 3D digital subtraction angiography (DSA) of the intracranial aneurysm, vascular models were produced (Mevislab, Autodesk fusion, Meshmixer) using 3D printing (Form 2, Formlabs). Three different FDS were deployed into the models (FD1: P64, Phenox; FD2: Derivo, Acandis; FD3: Silk, Balt Extrusion), and a glycerin-water mixture was pumped through the model (CompuFlow 1000, Schelley Medical). Magnetic resonance imaging (MRI, time-of-flight, 3D phase-contrast, 3 T, 32-channel volume coil, Philips) and 2D DSA (Aneurysm Flow; Angio Suit, Philips) was acquired of the model with and without FDS.

**Result:** Reduced flow into an aneurysm was observed by MRI and DSA for all devices. In general, FD1 exhibited the greatest effect on the considered hemodynamic parameters (flow, velocity, pressure, vorticity). For example, mean velocity spatially averaged in the aneurysm was reduced on 62% (FD1), 39% (FD2) and 23% (FD3). No changes in flow parameters were found at a distance to any FDS.

**Discussion:** Despite apparent metal artefacts on MRI, hemodynamic parameters were measured. However, it remains unclear, how reliable these values were in the presence of artefacts. DSA showed reduced flow in to the aneurysm, but, due to its 2D nature, the accuracy of the measurements is influenced by the vessel orientation.

**Conclusion:** For all stens, a reduced flow into the aneurysm was observed by flow-sensitive MRI, although metal artefacts with unknown effect were present. The hemodynamic parameters provided by MRI are promising for the evaluation of flow-diversion efficiency of different FDS designs, but further investigation with an increased number of stents and patient geometries is needed. In particular, the effect of artefacts has to be elucidated. DSA showed reduced flow into the aneurysm, but further investigation of the impact of vessel orientation on flow measurements is required.

331

## THROMBECTOMY IN RECURRENT ISCHEMIC STROKE DUE TO LARGE VESSEL OCCLUSION—AN APPROACH TO ITS ETIOLOGY

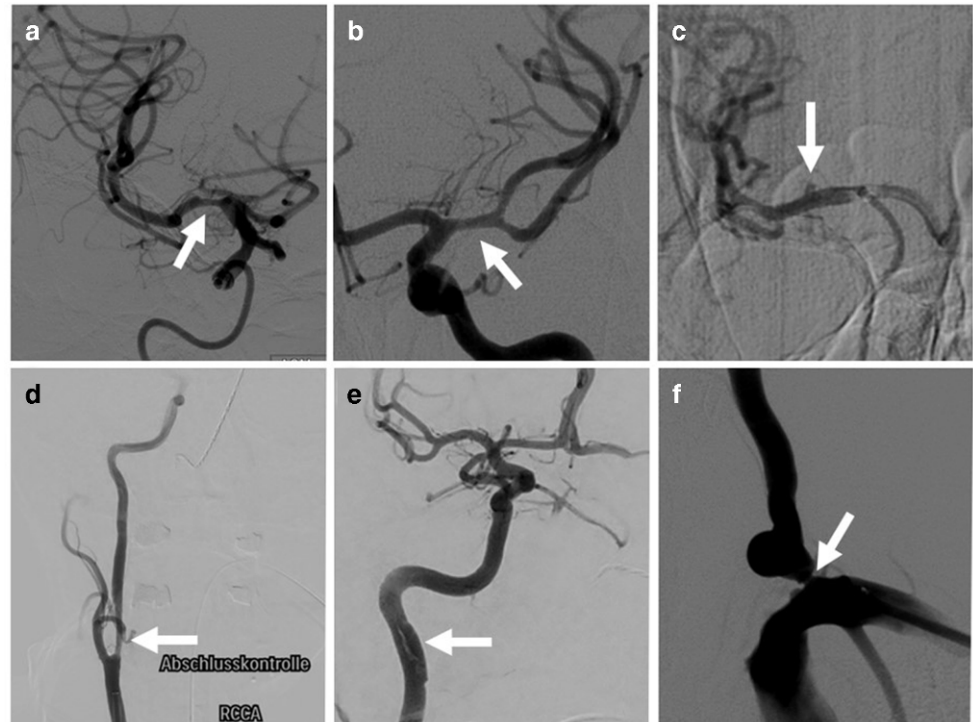
Christian Maegerlein<sup>\*1</sup>, Claus Zimmer<sup>1</sup>, Jennifer Roesler<sup>2</sup>, Benno Ikenberg<sup>2</sup>

<sup>1</sup>Klinikum rechts der Isar, TU München, Abteilung für Neuroradiologie, München, Deutschland

<sup>2</sup>Klinikum rechts der Isar, TU München, Klinik für Neurologie, München, Deutschland

**Background:** Recurrent mechanical thrombectomy for acute stroke treatment in individual patients has been proved feasible. However, less is known about the etiology of such recurrent large vessel occlusions following prior mechanical thrombectomy. In order to better understand if the etiology of recurrent events differ from the index stroke and which patients are at higher risk for another large vessel occlusion, we analyzed stroke etiologies of such patients.

**Fig. 1| 331** Local arterial pathologies after mechanical thrombectomy (MT) in six different patients (A-F), potentially causative for short-term recurrent large vessel occlusion strokes. The corresponding findings are marked by white arrows: Local stenosis and opacification of the M1 segments of the middle cerebral artery after stent retriever based MT in two different patients (**a, b**) either due to incomplete removal of the clot or local dissections; **c**) local endothelial lesion with pseudo-aneurysmatic presentation after manipulation with an aspiration catheter in the MCA (arrow); **d**) Local extracranial dissection due to over-inflation of the balloon-guide catheter in the proximal internal carotid artery; **e**) Local dissection of the right internal carotid artery shortly before entering the base of the skull; **f**): Atherosclerotic lesion of the proximal left vertebral artery.



**Methods:** Retrospectively we identified all patients at our center who received a recurrent mechanical thrombectomy between 2007 and 2019 for acute stroke treatment. Clinical data were retrieved from medical records. Presumed etiology of stroke was evaluated retrospectively and angiographic studies were revisited.

**Result:** In total 23 patients (1.5%) were identified with a recurrent thrombectomy, with 20 patients receiving a thrombectomy twice, and 3 patients receiving a thrombectomy three times. Median age was 68 years (IQR 56–77). 15 patients (65.2%) were female. Mean NIHSS score at first admission was 11 points (IQR 5–15). In 16 patients (69.6%) the etiology of the index stroke event and its recurrence was considered as likely being same, i.e. mostly (13 patients; 56.5%) of cardioembolic or unknown origin. In the 7 remaining patients (30.4%) the cause of stroke was considered to differ possibly from the index event, with 5 patients (21.7%) having a retrospectively detected postinterventional endothelial intracranial lesion as potential cause of stroke. Among the entire study population 5 (21.7%) cases showed a remarkable extracranial pathology causative linked stroke.

**Discussion:** The need for recurrent thrombectomy was low, in line with prior reports. The high number of patients with known (cardio-embolic) origin of their underlying stroke etiology raises the question how monitoring of such patients may be optimized.

**Conclusion:** The number of patients with remarkable extracranial pathologies or intracranial endothelial lesions suggests paying special attention to the final angiographic series.

340

#### A PROSPECTIVE MULTICENTRE REGISTRY OF PATIENTS TREATED FOR UNRUPTURED INTRACRANIAL ANEURYSMS WITH THE DERIVO FLOW DIVERTER: PROCEDURAL SAFETY AND CORE-LAB ADJUDICATED ANGIOGRAPHIC BASELINE RESULTS

Christian Taschner<sup>\*1</sup>, Paul Stracke<sup>2</sup>, Franziska Dorn<sup>3</sup>, Krzysztof Kadziolka<sup>4</sup>, Kornelia Kreiser<sup>5</sup>, Mirko Pham<sup>6</sup>, Jan-Hendrik Buhk<sup>7</sup>, Bernd Turowski<sup>8</sup>, Wolfgang Reith<sup>9</sup>, Hendrik Janssen<sup>10</sup>, Oliver Beuing<sup>11</sup>, René Chapot<sup>2</sup>

<sup>1</sup>Uniklinik Freiburg, Freiburg, Deutschland

<sup>2</sup>Alfried Krupp Krankenhaus, Essen, Deutschland

<sup>3</sup>Uniklinik München (LMU), München, Deutschland

<sup>4</sup>Grodszick Mazowiecki, Warschau, Poland

<sup>5</sup>Uniklinik München (TU), München, Deutschland

<sup>6</sup>Uniklinik Würzburg, Würzburg, Deutschland

<sup>7</sup>Uniklinik Hamburg Eppendorf, Hamburg, Deutschland

<sup>8</sup>Uniklinik Düsseldorf, Düsseldorf, Deutschland

<sup>9</sup>Uniklinik Homburg/Saar, Homburg/Saar, Deutschland

<sup>10</sup>Klinikum Ingolstadt, Ingolstadt, Deutschland

<sup>11</sup>Uniklinik Magdeburg, Magdeburg, Deutschland

**Hintergrund:** The study objective is to examine the safety and efficacy of the Derivo flow-diverter (Acandis, Germany) for the treatment of unruptured intracranial aneurysms.

**Methoden:** A prospective multicentre, observational, single arm, uncontrolled registry trial was conducted at 12 centres in Germany and Poland. Patients aged 18 to 75 years with untreated unruptured intracranial aneurysms were eligible. Additional coiling was allowed as clinically required. Angiographic images at baseline were reviewed by an independent imaging core laboratory. Primary end point is clinical outcome at 18 months follow-up.

**Ergebnisse:** Patient inclusion was started in April, 2013, and was stopped in January, 2018, after enrolment of 104 patients. Seven patients were excluded for missing data. Ninety-seven patients were analysed on an intention-to-treat basis. Mean age was 54.1 (range 18–86), 73 (75%) were female. Modified Rankin score at presentation was 0 in 74 (75%), and 1 in 24 (25%). Eighty-three (86%) of aneurysms were located in the anterior circulation, 12 (12%) in the posterior circulation. Seventy-seven (79%) of aneurysms treated were saccular, 21 (21%) were fusiform. Median diameter was 9.0 mm (5.4–13.5). All flow-diverter (FD) treatments were performed under dual anti-platelet therapy. Additional coiling occurred in 51 (52%). On average 1.2 FD were placed per patient. Technical complications were observed in 9 (9%) patients. Clinical complications were reported in 10 (10%) cases. Modified Rankin scores at discharge were 0 in 81 (83%), 1 in 14 (14%), 2 in 2 (2%), and 4 in 1 (1%), respectively.

**Diskussion:** With a morbidity rate of 3% and a mortality rate of 0, the results of our observational trial compare favourably with FD treatment reported in the literature. Brinjikji reported results from a metaanalysis ( $n = 1451$ ) with a morbidity rate of 5% and a mortality rate of 4% for FD treatment of intracranial aneurysms (1). In a prospective registry on FD treatment with the Pipeline device ( $n = 108$ ) Becske et al. observed morbidity and mortality rates of 5.6% and 2.7% respectively.

**Fazit:** Our data suggests that aneurysm treatment with the Derivo FD has a safety profile comparable to other FD available on the market.

#### References

1. Brinjikji W, et al. Endovascular treatment of intracranial aneurysms with flow diverters: a meta-analysis. *Stroke*. 2013;44(2):442–7.
2. Becske T, et al. Pipeline for uncoilable or failed aneurysms: 3-year follow-up results. *J Neurosurg*. 2017;127(1):81–8.

#### 341

### MECHANICAL THROMBECTOMY FOR ACUTE DISTAL POSTERIOR CEREBRAL ARTERY OCCLUSIONS -PROCEDURAL OUTCOMES, SAFETY AND TECHNICAL ASPECTS

Eberhard Siebert<sup>\*1</sup>, Justus Kleine<sup>1</sup>, Hans-Christian Bauknecht<sup>1</sup>, Simon Fuchs<sup>1</sup>, Georg Bohner<sup>1</sup>

<sup>1</sup>Neuroradiologie, Charité Berlin, Berlin, Deutschland

**Background:** MTE in emergent proximal large vessel occlusion has been shown to be highly effective in several randomized controlled trials (RCTs). However, for acute distal posterior cerebral artery (PCA) occlusions evidence from RCTs is lacking although resultant infarctions can portend a significant neurologic morbidity. We describe our experience in this specific MTE setting.

**Methods:** Consecutive acute ischemic stroke patients from April 2013 until May 2019 undergoing MTE for distal PCA occlusion (P2 segment and further distal) were identified in our prospectively maintained stroke database. Demographic patient information, location of arterial occlusion, MTE strategy and materials employed, number of recanalization attempts and results (TICI) as well as complications and infarct development were recorded.

**Result:** 17 patients were included into the study (10 female, mean age 68,3 years, range 36–89 years). Occlusion site was P2 segment in 13 and P3 in 4. Techniques employed were ADAPT technique in 4 and Solumbra technique in 13 cases. Several types of stent retrievers and aspiration catheters were used. Mean number of MTE attempts was 1,8 (range 1–5). Successful recanalization (TICI 2b/3) was achieved in 13 patients (76,4%). 4 patients developed no infarct on follow-up imaging, 7 patients had infarcts <50% and 7 had infarcts >50% of PCA territory. We encountered no symptomatic complications.

**Discussion:** MTE for acute distal posterior cerebral artery appears both feasible and safe with high successful recanalization rates (76,4%)

similar to other locations. Common MTE techniques developed for carotid, MCA or BA MTE can be applied to distal PCA MTE.

**Conclusion:** MTE for acute distal posterior cerebral artery occlusions appears to be both technically feasible and safe. However, clinical benefit has yet to be demonstrated in RCTs.

#### 347

### PREDICTORS OF GOOD CLINICAL OUTCOME AFTER TICI3 RECANALIZATIONS IN ACUTE ISCHEMIC STROKE PATIENTS

Noel van Horn<sup>\*1</sup>, Uta Hanning<sup>1</sup>, Hannes Leischner<sup>1</sup>, Götz Thomalla<sup>2</sup>, Milani Deb-Chatterji<sup>2</sup>, Caspar Brekenfeld<sup>1</sup>, Jens Fiehler<sup>1</sup>, Fabian Flottmann<sup>1</sup>

<sup>1</sup>Institut für Diagnostische und Interventionelle Neuroradiologie, Universitätsklinikum Hamburg-Eppendorf, Hamburg, Deutschland

<sup>2</sup>Klinik und Poliklinik für Neurologie, Universitätsklinikum Hamburg-Eppendorf, Hamburg, Deutschland

**Background:** In acute ischemic stroke, endovascular thrombectomy (EVT) leads to successful reperfusion in up to 71% after anterior circulation large vessel occlusion (LVO). However, of these patients, only 55% show a favourable clinical outcome. We aim to determine prognostic factors associated with good outcome after successful EVT.

**Methods:** In this retrospective study we analyzed 452 consecutive acute ischemic stroke patients from July 2015 until November 2018 at a single center treated with EVT after LVO of the anterior circulation. Full recanalization was defined as complete reperfusion (TICI 3) and primary outcome of disability was measured on the modified ranking scale after 90 days (mRS 90), where mRS 90 of 0–2 was defined as “good outcome”. Logistic regression analysis was performed with good outcome as dependant variable and baseline clinical data, admission NIHSS and pre-stroke mRS, comorbidities, location of occlusion and ASPECTS on admission as independent variables.

**Result:** 159/452 (35.2%) showed complete reperfusion (TICI 3). In 68/159 patients, outcome on mRS 90 was “good” (42.7%). Good outcome was significantly associated with the following parameters after adjusting for confounders: Age (adjusted OR 0.92, 95% CI 0.87–0.97), NIHSS (adjusted OR 0.86, 95% CI 0.78–0.94), ASPECTS (adjusted OR 1.50, 95% CI 1.12–2.09) and proximal M1-segment occlusion (adjusted OR 5.29, 95% CI 1.34–23.56).

**Conclusion:** After TICI3 reperfusion for LVO, patients’ outcome is heterogeneous. Good clinical outcome is more likely in younger patients with less severe strokes and occlusions of the proximal M1 segment.

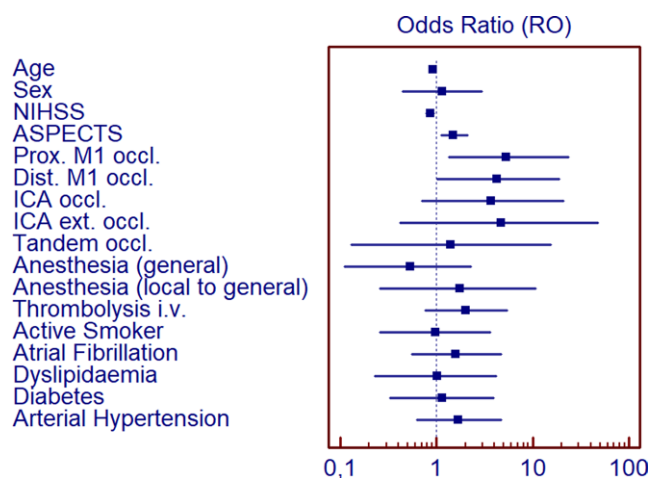


Fig. 1 | 347 Logistic analysis for good clinical outcome

**References**

1. Byung Moon K. Causes and Solutions of Endovascular Treatment Failure. *J Stroke*. 2017;19(2):131–42.
2. Kaesmacher J, Dobrocky T, Heldneret MR, et al. Systematic review and meta-analysis on outcome differences among patients with TICI2b versus TICI3 reperfusions: success revisited. *J Neurol Neurosurg Psychiatr*. 2018;89(9):910–7.

348

**EVALUATION OF THE STANDARD DEVIATION OF THE MEAN TRANSIT TIME WITH REGARD TO FUNCTIONAL OUTCOME AFTER ANEURYSMAL SUBARACHNOID HAEMORRHAGE**

Kai Jannusch<sup>1</sup>, Kerim Beseoglu<sup>2</sup>, Marius Kaschner<sup>1</sup>, Nikolas Teichert<sup>1</sup>, Indradeo Hemraj<sup>1</sup>, Hadi Nasri<sup>1</sup>, Athanasios K. Petridis<sup>2</sup>, Bernd Turowski<sup>1</sup>, Julian Caspers<sup>1</sup>, Christian Rubbert\*<sup>1</sup>

<sup>1</sup>Department of Diagnostic and Interventional Radiology, University Dusseldorf, Medical Faculty, Düsseldorf, Deutschland  
<sup>2</sup>Department of Neurosurgery, Medical Faculty, Heinrich-Heine-University, Düsseldorf, Deutschland

**Background:** The pathogenesis leading to poor functional outcome after aneurysmal subarachnoid haemorrhage (aSAH) is multifactorial

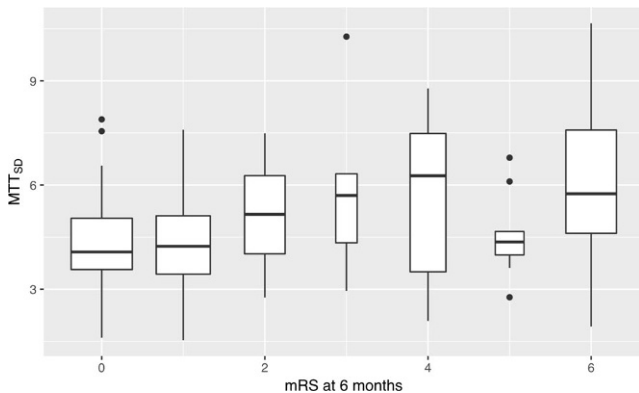


Fig. 1 | 348

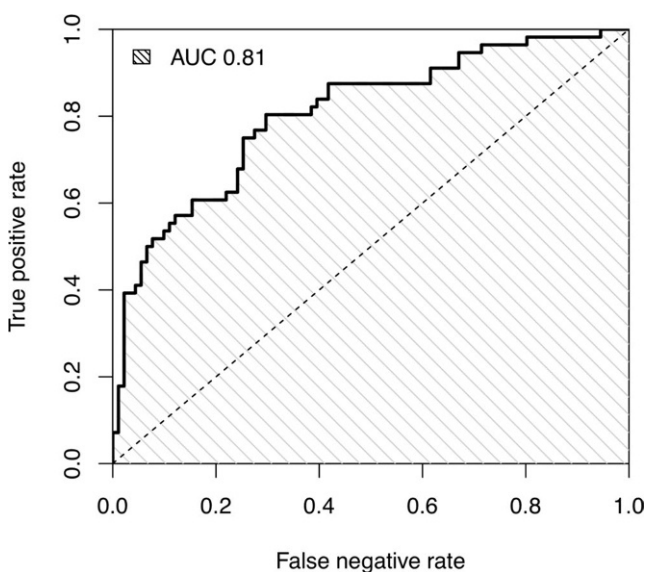


Fig. 2 | 348

and not fully understood. CT perfusion imaging (CTP), especially the mean transit time (MTT), is increasingly used in the care of aSAH patients to monitor for delayed cerebral ischemia. We evaluated patient age, sex and MTT with regard to the functional outcome six months after ictus. The hypothesis of the current work is, that a large amount of variation in early MTT measurements after patient admission is predictive of functional outcome. We therefore focused on the standard deviation (SD) of the MTT, which has so far not been systemically evaluated.

**Methods:** Out of 630 consecutive subarachnoid haemorrhage patients (2008–2015), 147 were retrospectively analysed (mean age 54.5, 66.7% female. Inclusion: aSAH, admission within 24 h of ictus, CTP within 24 h of admission, documented functional outcome after six months (modified Rankin scale grades; mRS). Exclusion: previous aSAH, CTP not evaluable).

Bihemispheric MTT was recorded over 360° along a 10 mm wide, ribbon-like region of interest (ROI) along the cortex of the brain using a sliding window approach spanning 10° in 2° increments. Mean, maximum and SD of the MTT were computed.

A t-Test was used to compare MTT<sub>SD</sub> between patient groups dichotomized by mRS (≤2; >2). Furthermore, a logistic regression model with stepwise regression was evaluated, initially using MTT<sub>mean</sub>, MTT<sub>max</sub>, MTT<sub>SD</sub>, patient age, sex, World Federation of Neurosurgical Societies and modified Fisher score, to assess dichotomized mRS (≤2; >2).

**Result:** A boxplot of MTT<sub>SD</sub> vs. functional outcome at 6 months (mRS) is shown in Fig 1. There was a statistically significant difference between MTT<sub>SD</sub> of patients with an mRS ≤2 vs. >2 (p<0.001). After stepwise regression of the variables, the logistic regression model retained MTT<sub>SD</sub> (p=0.021), age (p=0.003) and modified Fisher score (p=0.0004). McFadden R<sup>2</sup> was 0.22, indicating a good to excellent model fit.<sup>1</sup> The model yielded an area under the Receiver Operating Characteristics curve of 0.81 (Fig 2).

**Discussion/Conclusion:** MTT<sub>SD</sub> as a measurement of the amount of variation of the MTT, might be a marker for regional inhomogeneities in cerebral perfusion. Together with the modified Fisher score and patient age, the MTT<sub>SD</sub> can be of use to predict functional outcome 6 month after aSAH ictus. MTT<sub>SD</sub> should be further evaluated for monitoring efforts and prognostic assessments of aSAH patients.

**References**

1. Behavioural Travel Modelling. Taylor & Francis; 1979.

349

**MR VESSEL WALL IMAGING INTRAKRANIELLER ANEURYSMEN NACH ENDOVASKULÄRER THERAPIE**

Johannes Hensler\*<sup>1</sup>, Jawid Madjidyar<sup>1</sup>, Olav Jansen<sup>1</sup>, Fritz Wodarg<sup>1</sup>, Naomi Larsen<sup>1</sup>

<sup>1</sup>Universitätsklinikum Schleswig-Holstein, Campus Kiel, Klinik für Radiologie und Neuroradiologie, Kiel, Deutschland

**Hintergrund:** Eine Kontrastmittelaufnahme der Wand intrakranieller Aneurysmen im MR vessel wall imaging ist ein möglicher Biomarker einer erhöhten Rupturgefahr. Die klinische Relevanz der Kontrastmittelaufnahme von Aneurysmen nach endovaskulärer Therapie ist nicht bekannt. Wir beschreiben die Muster der Kontrastmittelaufnahme intrakranieller Aneurysmen nach endovaskulärer Therapie.

**Methoden:** Es wurden Patienten eingeschlossen, bei denen eine endovaskuläre Therapie eines intraduralen Aneurysmas und ein posttherapeutisches kontrastmittelverstärktes MR vessel wall imaging durchgeführt wurde. Die Kontrastmittelaufnahme des Aneurysmas wurde in folgenden Lokalisationen beurteilt: a) Aneurysmawand, b) innerhalb des Aneurysmasackes. Anhand von TOF-Angiographien oder DSA

Verlaufsuntersuchungen wurde bewertet, ob eine Reperfusion des Aneurysmas aufgetreten war.

**Ergebnisse:** Es wurden 40 Patienten mit 44 Aneurysmen eingeschlossen. Innerhalb der ersten 6 Monate nach Therapie wurde signifikant häufiger ein Enhancement der Aneurysmwand als in Verlaufskontrollen nach mehr als 6 Monaten beobachtet.

Eine Kontrastmittelaufnahme innerhalb des Aneurysmasackes wurde nur bei stabilen Aneurysmen, die keine Reperfusion im Verlauf aufwiesen, beobachtet.

**Diskussion:** Eine Kontrastmittelaufnahme der Aneurysmwand im posttherapeutischen Vessel wall imaging stellt womöglich eine physiologische Reaktion der Gefäßwand auf die posttherapeutisch veränderte Hämodynamik und Thrombusbildung dar, und nimmt im Verlauf ab. Eine Kontrastmittelaufnahme innerhalb des gewickelten Aneurysmalumens entspricht möglicherweise einer Neovaskularisation im chronisch thrombosierte und fibrosierte Lumen, und könnte einen potentiellen Surrogatmarker einer fortgeschrittenen Aneurysmaheilung darstellen.

**Fazit:** MR vessel wall imaging kann ein wichtiges Instrument zur Prognoseabschätzung nach interventioneller Aneurysmabehandlung darstellen. Weitere Untersuchungen hierzu sind notwendig. Außerdem leistet das Vessel wall imaging einen wichtigen Beitrag zum pathophysiologischen Verständnis intrakranieller Aneurysmen.

355

### RADIATION DOSE IN ENDOVASCULAR TREATMENT OF INTRACRANIAL ANEURYSMS

Robert Forbrig<sup>\*1</sup>, Thomas Liebig<sup>1</sup>, Franziska Dorn<sup>1</sup>, Christoph Trumm<sup>1</sup>

<sup>1</sup>Institut für Neuroradiologie, LMU München, München, Deutschland

**Hintergrund:** In the field of endovascular treatment of intracranial aneurysms, several modern techniques have been introduced recently. In this context, peri-interventional radiation dose gains broad attention regarding recently updated diagnostic reference levels (1). This analysis focuses on radiation dose of the three following techniques: coiling, flow-diverter (FD) stenting, and Woven EndoBridge (WEB) device implantation.

**Methoden:** In this retrospective single-center study, we report data of 60 patients with an intracranial aneurysm successfully treated with coiling, FD or WEB between 2015 and 2019. Re-interventions, combined or other techniques, and patients with several aneurysms were excluded. Aneurysm location, kind of intervention, time of intervention and fluoroscopy, acquisition count, and the dose area product were recorded for each intervention, and compared between techniques.

**Ergebnisse:** Aneurysms were mainly located at the supra-optic segment of the internal carotid artery (21/60 patients, 35%), the anterior

or communicating artery (16, 27%), and the basilar tip (8, 13%). Most common kind of intervention was coiling (22/60 patients, 37%) followed by FD (20, 33%) and WEB (18, 30%). Time of intervention and fluoroscopy as well as acquisition count was lowest for WEB ( $p < 0.05$ , each). Median overall dose area product was 11.452 cGy x cm<sup>2</sup>. In detail, no significant difference was found between groups ( $p > 0.05$ ).

**Diskussion:** According to our data, radiation dose of neurointerventional aneurysm therapy is reasonable independent from the applied technique. Though implantation of a WEB device is commonly quick, the choice of the dedicated technique is dependent on several variables such as difficulty of anatomical approach, aneurysm location, aneurysm size, and aneurysm morphology.

**Fazit:** Modern endovascular treatment of intracranial aneurysms is feasible without radiation dose penalty.

### References

1. [http://www.bfs.de/DE/themen/ion/anwendung-medizin/diagnostik/referenzwerte/referenzwerte\\_node.html](http://www.bfs.de/DE/themen/ion/anwendung-medizin/diagnostik/referenzwerte/referenzwerte_node.html)

356

### EFFECT OF PRE- AND IN-HOSPITAL DELAY ON REPERFUSION IN MECHANICAL THROMBECTOMY: DOES DAWDLING DIMINISH REPERFUSION?

Johannes Kaesmacher<sup>\*1</sup>, Jan Gralla<sup>1</sup>, Urs Fischer<sup>2</sup>, On Behalf of the Beyond-Swift Investigators<sup>2</sup>

<sup>1</sup>Bern, University Hospital Bern, Neuroradiology, Bern, Schweiz

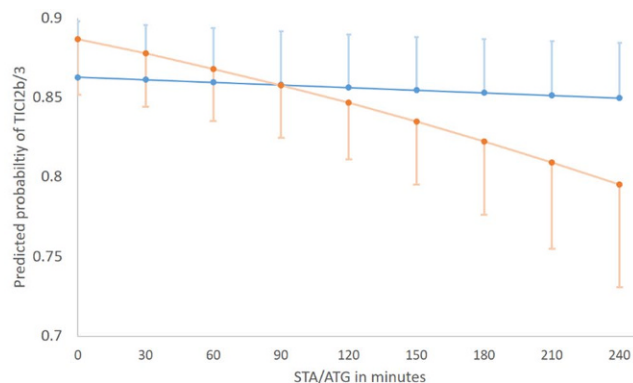
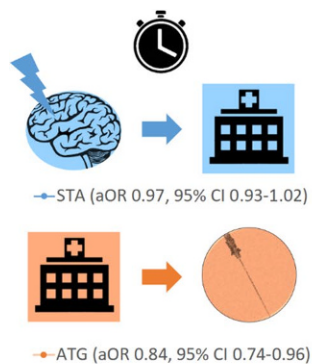
<sup>2</sup>Bern, University Hospital Bern, Neurology, Bern, Schweiz

**Background:** Post-hoc analyses of randomized-controlled clinical trials evaluating mechanical thrombectomy (MT) have suggested that in-hospital delay is associated with reduced reperfusion rates. Objective of this analysis was to estimate the effect size of admission-to-groin-puncture (ATG) delay on reperfusion in a large, real-world cohort of patients undergoing mechanical thrombectomy (MT) for anterior circulation strokes at comprehensive stroke centers.

**Methods:** Patients included into the BEYOND-SWIFT cohort (ClinicalTrials.gov identifier: NCT03496064) were analyzed (N=1272). Association between baseline characteristics and ATG was evaluated using mixed linear regression analysis. The effect of increasing symptom-onset-to-admission (STA), and ATG intervals on successful reperfusion (defined as Thrombolysis in Cerebral Infarction, TIC12b/3) was evaluated using logistic regression analysis adjusting for potential confounders.

**Results:** Prolonged ATG intervals were associated with direct admissions ( $\beta = +39.8$  min,  $P < .001$ ), general anesthesia ( $\beta = +21.3$  min,  $P < .001$ ) and borderline selection criteria, such as lower NIHSS, late presentations or distal occlusions. There was a 16% relative odds reduction for TIC12b/3 per hour ATG delay (aOR 0.84, 95%-CI 0.74–

**Fig. 1 | 356** No association between symptom-onset-to-admission and the likelihood of achieving successful reperfusion (Thrombolysis in Cerebral Infarction score 2b/3) was found (blue). In contrast, a significant association between admission-to-groin-puncture (ATG) intervals and reduced rates of successful reperfusion (Thrombolysis in Cerebral Infarction score 2b/3) was found (orange)



0.95), without a significant association between STA and rate of TIC12b/3 (aOR 0.97, 95%-CI 0.93–1.02). Sensitivity analyses did not change the primary observations.

**Discussion/Conclusion:** The association between in-hospital delay and reduced reperfusion rates is tangible in real world clinical data, stressing the need to optimize in-hospital workflows. Given the lack of an association between STA and reperfusion, the causal relationship of this finding warrants further research, because mere pathophysiological considerations (i.e. changing thrombus characteristics over time) seem unlikely to fully explain the effect observed.

357

**SAFETY AND EFFICACY OF INTRA-ARTERIAL UROKINASE AFTER FAILED, UNSUCCESSFUL OR INCOMPLETE MECHANICAL THROMBECTOMY IN ANTERIOR CIRCULATION LARGE-VESSEL OCCLUSION STROKE.**

Johannes Kaesmacher\*<sup>1</sup>, Sebastian Bellwald<sup>2</sup>, Tomas Dobrocky<sup>1</sup>, Thomas Meinel<sup>2</sup>, Eike Immo Piechowiak<sup>1</sup>, Martina Goeldlin<sup>2</sup>, Christoph Kurmann<sup>1</sup>, Mirjam Rachel Heldner<sup>2</sup>, Simon Jung<sup>2</sup>,

Pasquale Mordasini<sup>1</sup>, Marcel Arnold<sup>2</sup>, Pascal Mosimann<sup>1</sup>, Gerhart Schroth<sup>1</sup>, Heinrich Mattle<sup>2</sup>, Jan Gralla<sup>1</sup>, Urs Fischer<sup>2</sup>

<sup>1</sup>Bern, University Hospital Bern, Neuroradiology, Bern, Schweiz

<sup>2</sup>Bern, University Hospital Bern, Neurology, Bern, Schweiz

**Background:** Administration of intra-arterial (IA) thrombolysis may help to improve reperfusion during or after incomplete mechanical thrombectomy (MT) in large-vessel occlusions (LVO) stroke patients. However, data on its safety and efficacy is scarce.

**Methods:** Consecutive acute ischemic stroke patients of a prospective registry presenting with anterior circulation LVO stroke were analyzed (N=1017). Patients who received additional IA Urokinase during or after MT (+/- intravenous tPA) were compared to those treated with MT (+/- intravenous tPA) only. Primary safety measures included asymptomatic and symptomatic intracranial hemorrhage (aICH and sICH) according to PROACT-II criteria, and all-cause mortality. Primary efficacy endpoints were angiographic reperfusion and Thrombolysis in Cerebral Infarction (TICI) improvement, together with functional independence at day 90 (defined as modified Rankin Scale ≤2). Endpoints were assessed using multivariate logistic regression analyses adjusting for confounders underlying case selection.

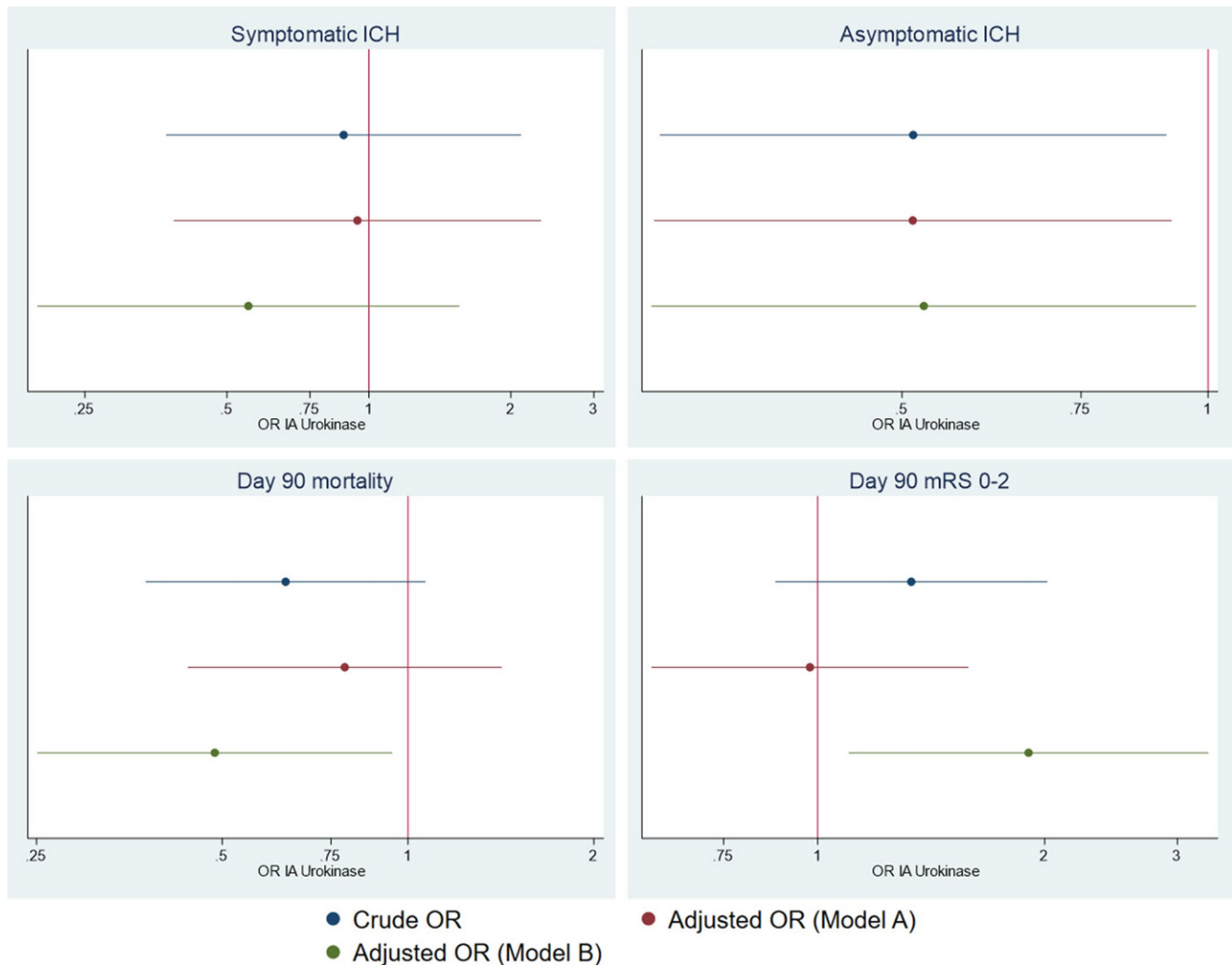


**Fig. 1 | 357** Crude/Adjusted Odds Ratios (OR) and corresponding 95% confidence intervals for outcomes. Adjustments for baseline characteristics tended to shift the point estimates in favor of the group without IA Urokinase (Model A), while additional adjustments for e.g. poor reperfusion grade cases revealed a potential benefit of IA Urokinase (Model B)

**Results:** Additional IA Urokinase was administered in 102 of 1017 patients (10.0%). The most common reason for administering IA Urokinase was incomplete reperfusion (TICI<3) after MT (52.9%). After adjusting for baseline characteristics underlying case selection, IA Urokinase did not increase the risk of aICH (0.51, 95%-CI 0.29–0.92), sICH (aOR 0.95, 95%-CI 0.39–2.32) or 3-month mortality (0.71, 95%-CI 0.40–1.26). In approximately two-thirds of patients treated with IA Urokinase, early reperfusion improvement was observed, with around one-third being TICI-grade tangible. Correspondingly, patients treated with IA Urokinase had higher rates of functional independence after adjusting for the selection bias favoring poor TICI cases in the IA Urokinase group (aOR 1.90, 95%-CI 1.10–3.30).

**Discussion/Conclusion:** In selected patients, adjunctive treatment with IA Urokinase during or after MT seems to be safe, without an increased risk of intracranial bleedings. Additionally, IA Urokinase harbors the potential to improve the reperfusion status of patients undergoing endovascular interventions and may thus improve outcomes.

### 364

#### GADOLINIUM LEAKAGE IN OCULAR STRUCTURES IN TRANSIENT ISCHEMIC ATTACK

Alex Förster<sup>\*1</sup>, Johannes Böhme<sup>1</sup>, Holger Wenz<sup>1</sup>, Christoph Groden<sup>1</sup>, Angelika Alonso<sup>2</sup>

<sup>1</sup>Abteilung für Neuroradiologie, Universitätsmedizin Mannheim, Mannheim, Deutschland

<sup>2</sup>Neurologische Klinik, Universitätsmedizin Mannheim, Mannheim, Deutschland

**Hintergrund:** Gadolinium leakage in ocular structures (GLOS) on fluid attenuated inversion recovery images (FLAIR) is a novel imaging marker in acute ischemic stroke.<sup>1,2</sup> In the present study, we investigated the frequency and pattern of blood-brain barrier as well as blood-retina barrier impairment in patients with transient ischemic attack (TIA) as demonstrated by hyperintense acute reperfusion marker (HARM) and GLOS respectively on FLAIR.

**Methoden:** From an MRI report database we identified patients with TIA who underwent repeated MRI with intravenous contrast agent administration. On FLAIR, the presence of HARM was assessed. Furthermore, the presence of GLOS was noted in the anterior chamber and vitreous body.

**Ergebnisse:** Overall 28 TIA patients (mean age  $66.5 \pm 17.2$  years, 17 (51.5%) male) were included. Follow-up MRI was performed within  $34.4 \pm 18.8$  hours after the first MRI. On DWI, acute ischemic lesions were observed in 21 (75%), while the remainder was DWI negative. On contrast-enhanced FLAIR, GLOS was observed in 11 (39.3%) patients: in 1 (3.6%) in the anterior chamber only, and in 10 (35.7%) in the anterior chamber and vitreous body. HARM was observed in 3 (10.7%) patients. In one TIA patient without ischemic lesion on DWI or HARM on FLAIR, GLOS was observed in the anterior chamber and vitreous body (see Fig. 1). Presence of GLOS was significantly associated with detection of HARM ( $p=0.023$ ) whereas no significant relationship with older age ( $p=0.06$ ), or presence of an ischemic lesion on DWI ( $p=0.12$ ) was found.

**Diskussion:** In patients with TIA, GLOS is a frequent finding and associated with presence of HARM on contrast-enhanced FLAIR. As GLOS was observed in one TIA patient without presence of an ischemic lesion or HARM, it might be useful as an additional imaging marker of transient cerebral ischemia in TIA patients.

#### References

1. Förster A, Wenz H, Böhme J, Groden C, Alonso A. Asymmetrical Gadolinium Leakage in Ocular Structures in Stroke Due to Internal Carotid Artery Stenosis or Occlusion. Clin Neuroradiol. 2018; <https://doi.org/10.1007/s00062-018-0754-5>. Epub ahead of print.

2. Förster A, Al-Zghloul M, Wenz H, Böhme J, Groden C, Alonso A. Gadolinium Leakage in Ocular Structures Is Common in Lacunar Infarction. Stroke. 2018; <https://doi.org/10.1161/STROKEAHA.118.023573>. STROKEAHA118023573.

### 365

#### MIDTERM TREATMENT RESULTS USING THE FRED FLOWDIVERTER

Christian Ulfert<sup>\*1</sup>, Christian Herweh<sup>1</sup>, Martin Bendszus<sup>1</sup>, Markus Möhlenbruch<sup>1</sup>

<sup>1</sup>Heidelberg University Hospital, Heidelberg, Deutschland

**Hintergrund:** Flow diverter have become an essential alternative or addition to conventional coiling in the endovascular treatment of intracranial aneurysms.

For the newer generation of flow diverters that have been introduced in the last 5 years there is sufficient data covering immediate and short term outcomes but little covering the mid to long term results.

We report a series of 70 patients that were treated with the Flow-Redirection Intraluminal Device (FRED) flow diverter and in whom there is at least 2 years of follow up imaging available.

**Methoden:** We retrospectively selected all endovascular procedures from our aneurysm database that were treated with a FRED flowdiverter and have obtained at least 24 months of follow up imaging.

All patients received regular follow ups as well as clinical examinations. Clinical outcome was assessed using the mRs. Aneurysm occlusion was measured using the 3 point modified Raymond Roy Occlusion classification. Imaging was performed in a 3T MRI acquiring unenhanced and contrast enhanced time of flight angiography.

All base characteristics of the patients were obtained, including age, gender, intervention date and base mRs.

**Ergebnisse:** Overall 70 patients harbouring 70 aneurysms were included. 48 (68.6%) were female 22 (31.4%) were male. Four of the patients (5.7%) had suffered an SAH directly prior to treatment.

Mean age of the patients was 54 years (15–80). Aneurysm dimensions were on average  $9.1 \times 5.7 \times 5.8$  mm (width x depth x height).

All patients were successfully treated with a FRED flowdiverter. The median follow up time was 34 months ranging from 24 to 68 months.

In their last available follow up 57 (81.4%) of the aneurysms were completely occluded (ROC 1), 12 (17.1%) aneurysms had a neck remnant and 1 (1.4%) showed persisting aneurysm perfusion.

**Diskussion:** Most of the available publications on mid to long term flowdiverter follow up data show ‘adequate’ occlusion rates around 90%. In this series ‘adequate’ occlusion was achieved in 98.5% of the patients after a median follow up time of 34 months showing good long term efficacy of the FRED flowdiverter.

**Fazit:** Intracranial aneurysms treated with the FRED flowdiverter show stable mid term results with an adequate aneurysms occlusion rate of 98,5%.

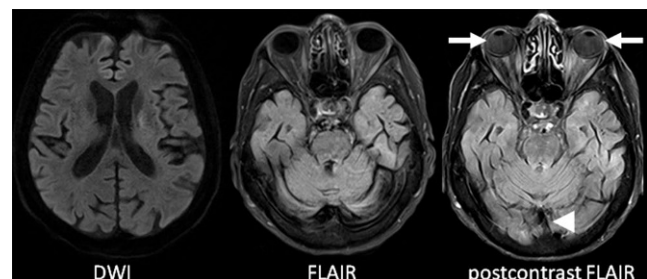


Fig. 1 | 365

370

**AGE PLAYS AN IMPORTANT ROLE IN EDEMA FORMATION AFTER THROMBECTOMY FOR ANTERIOR CIRCULATION STROKE.**

Lukas Meyer<sup>\*1</sup>, Michael Schönfeld<sup>1</sup>, Götz Thomalla<sup>2</sup>, Uta Hanning<sup>1</sup>, Jens Fiehler<sup>1</sup>, Andre Kemmling<sup>3</sup>, Gabriel Broocks<sup>1</sup>

<sup>1</sup>Universitätsklinikum Hamburg-Eppendorf, Diagnostische und Interventionelle Neuroradiologie, Hamburg, Deutschland

<sup>2</sup>Universitätsklinikum Hamburg-Eppendorf, Neurologie, Hamburg, Deutschland

<sup>3</sup>Universitätsklinikum Münster, Diagnostische und Interventionelle Neuroradiologie, Münster, Deutschland

**Background and Purpose:** Subgroups of very low and high age were excluded or underrepresented in past mechanical thrombectomy (MT) landmark trials. Although younger age is linked to better outcome it is also an established risk factor for malignant infarction with poor outcome. Yet, the effect of age on lesion pathophysiology on the context of MT has been poorly investigated. This study aims to investigate the impact of age on ischemic lesion water homeostasis, which is the pathophysiological hallmark of brain infarction.

**Methods:** A prospectively collected data set of patients receiving MT for LVO within the anterior circulation was retrospectively analyzed. Lesion-NWU was quantified in multimodal admission CT and follow-up CT, and Δ-NWU was calculated as difference. Consequently NWU edema formation was analyzed and compared in different age groups (<74 vs. >74). Moreover, the effect of edema formation was analyzed with regard to the final recanalization status.

**Results:** Baseline characteristics showed no significant differences in NIHSS, NWU and time from onset to imaging between age groups on admission. At follow-up imaging, Δ -NWU was significantly higher in younger patients. In multivariate linear regression analysis there was an independent significant association ( $p=0.0116$ ) for final delta NWU showing a development of higher edema formation in younger patients (95CI:  $-0.184 -2.54$ ). Further independent significance ( $p<0.001$ ) was observed for status of vessel recanalization with less edema formation after successful recanalization (TICI  $\geq 2b$ ).

**Conclusion:** Younger age was significantly associated with higher edema formation independent of treatment, which might have an im-

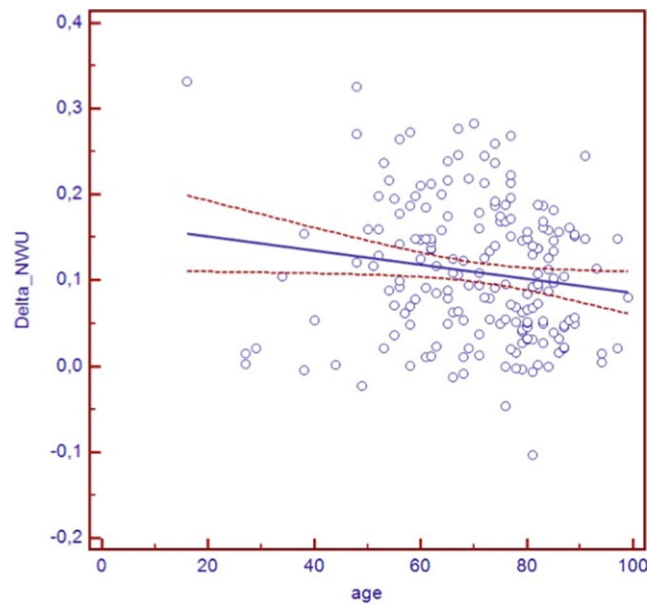


**Fig. 2 | 370** Relation between age and final edema formation at follow-up imaging

portant impact on clinical outcome. Younger patients with LVO might especially benefit from adjuvant treatment with anti-edematous drugs such as glyburide.

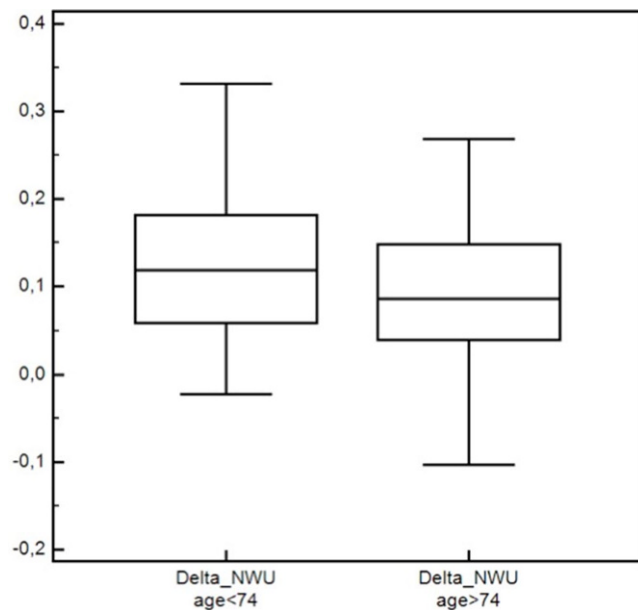


**Fig. 1 | 370** Comparison of NIHSS on admission between age groups

## 7. Sonstiges

51

### FULLY AUTOMATED ALIGNMENT OF CRANIAL CT SCANS TO THE ANTERIOR COMMISSURE—POSTERIOR COMMISSURE LINE

Christian Rubbert<sup>\*1</sup>, Bernd Turowski<sup>1</sup>, Julian Caspers<sup>1</sup><sup>1</sup>Department of Diagnostic and Interventional Radiology, University Dusseldorf, Medical Faculty, Düsseldorf, Deutschland

**Background:** Standardized alignment of cranial CT scans to a common reference plane is important for sufficient orientation and accurate follow-up evaluations of intracranial findings, but often requires manual reformation, especially in cases of incoherent patients or non-tiltable gantries. We developed a fully automated, PACS-integrated system to align cranial CT scans with the established anterior commissure-posterior commissure (ACPC) line to generate easily interpretable and comparable brain scans and released it as open source.

**Methods:** A fully automated workflow was created, using the publicly available software-tools DCMTK, parallel, dcm2niix, FSL, fslypy, and

nifti2dicom. It accepts DICOM storage requests and processes scans in parallel. Eligible scans are aligned to an ACPC-aligned atlas from the Clinical Toolbox for SPM using FMRIB's Linear Image Registration Tool by linear transformation in X, Y and Z direction (Fig 1). Five mm mean slabs are generated with the top non-air slice as the starting point. DICOM header information of the ACPC-aligned scans are updated, which are then sent to the PACS.

For testing, clinical cranial trauma CT scans with a slice thickness  $\leq 2.5$  mm, window center=40, and "SOFT" or "STANDARD" kernel from the public CQ500 dataset<sup>1</sup> were processed ( $n=263$  patients, 301 scans).

**Result:** Out of 301 series, 295 (98%) were successfully aligned with the ACPC line. Examples are shown in Fig 2]. Average rotation to achieve alignment was  $|X|=5.01^\circ$  (SD 4.32,  $0^\circ-25.85^\circ$ ),  $|Y|=1.90^\circ$  (SD 1.57,  $0^\circ-8.30^\circ$ ), and  $|Z|=3.08^\circ$  (SD 2.36,  $0.02^\circ-15.57^\circ$ ). Processing failed in 2 scans, not yielding axial scans, while 4 scans were not well-aligned to the ACPC line.

**Discussion:** The proposed workflow can robustly and automatically align cranial CT scans to the ACPC line without any end-user interaction. Overall processing was found to be robust, even in presence of large mass effect pathologies or atrophy (Fig 3).

Fig. 1 | 51

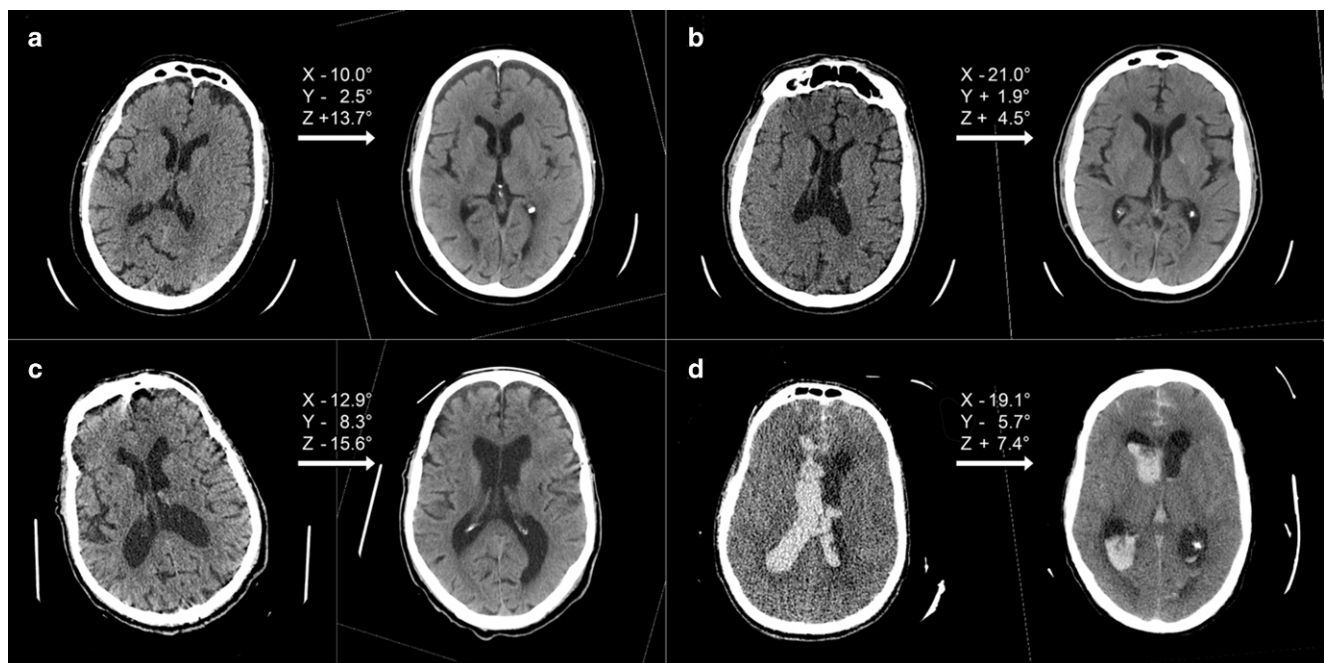
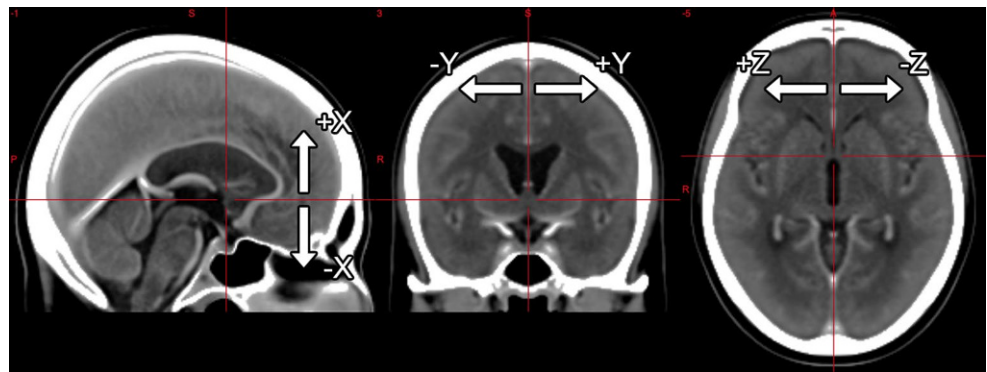


Fig. 2 | 51

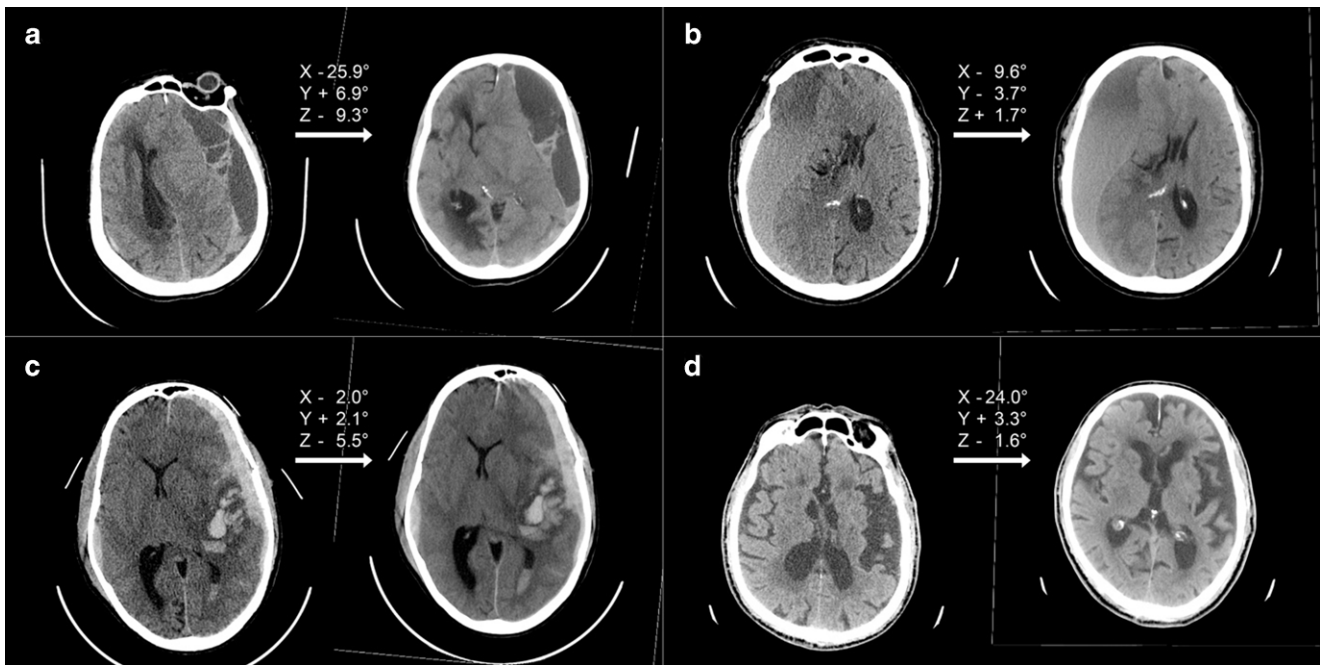


Fig. 3 | 51

## References

1. <http://headctstudy.qure.ai/dataset>; Chilamkurthy S, Ghosh R, Tamamala S, et al. Deep learning algorithms for detection of critical findings in head CT scans: a retrospective study. The Lancet. Elsevier. 2018

57

### VERWENDUNG DES KLEINEN CT-RÖHRENFOKUS ERHÖHT DIE ORTSAUFLÖSUNG IN DER KOPF-HALS-CTA

Johannes Roßkopf<sup>\*1</sup>, Michael Braun<sup>2</sup>, Bernd Schmitz<sup>3</sup>

<sup>1</sup>Universitätsklinikum Ulm, Diagnostische und Interventionelle Radiologie, Ulm, Deutschland

<sup>2</sup>BKH Günzburg, Neuroradiologie, Günzburg, Deutschland

<sup>3</sup>Universitätsklinikum Ulm, Diagnostische und Interventionelle Radiologie, Ulm, Deutschland

**Hintergrund:** Zur Detektion von Gefäßpathologien in der Kopf-Hals-CTA ist eine verbesserte Ortsauflösung hilfreich. Wie aus der konventionellen Röntgendiagnostik bekannt, in CT-Systemen aber bisher wenig beachtet, hängt die Zeichenschärfe in der CTA vom Röhrenfokus ab. Ziel war es, den Einfluss des kleinen Röhrenfokus in der CTA auf die Zeichenschärfe der Kopf-Hals-Gefäße zu quantifizieren.

**Methode:** Kopf-Hals-CTA Datensätze (Philips 40 Zeiler Brilliance CT) wurden an 22 Patienten mit großem und kleinem Röhrenfokus akquiriert. Mittels eines semi-automatischen Prozesses konnte der HU Dichteanstieg an der Gefäßkante von insgesamt 544 Kopf-Hals-Gefäßsegmenten in Winkelgrad quantifiziert werden. Da der Übergang vom hochkontrastierten Gefäßlumen zur Gefäßwand eine scharfe Grenze darstellt, müsste bei idealer Abbildung hier ein Winkel von 90° auftreten. Niedrigere Winkel sind daher ein quantitatives Maß für die geometrische Unschärfe des Abbildungssystems.

**Ergebnisse:** Der HU Dichteanstieg an der Gefäßkante war durch Verwendung des kleinen Röhrenfokus in der CTA signifikant steiler, im Schnitt von 75° auf 82° Winkelgrad ( $p < 0.05$ ).

**Fazit:** Ein kleiner Röhrenfokus kann durch eine verbesserte Zeichenschärfe der Kopf-Hals-Gefäße in der CTA dazu beitragen Gefäßpathologien zu erkennen.

62

### CT-GUIDED THORACIC SYMPATHICOLYSIS (CTS) VERSUS ENDOSCOPIC TRANSTHORACIC SYMPATHECTOMY (ETS) IN PATIENTS WITH SEVERE PRIMARY PALMAR HYPERHIDROSIS

Julian Ramin Andresen<sup>\*1</sup>, Fabian Scheer<sup>2</sup>, Erik Schlöricke<sup>3</sup>, Aria Sallakhi<sup>1</sup>, Marc Olaf Liedke<sup>4</sup>, Reimer Andresen<sup>5</sup>

<sup>1</sup>Medical School, Sigmund Freud University, Vienna, Austria, Vienna, Österreich

<sup>2</sup>Westkuestenklinikum Heide, Academic Teaching Hospital of the Universities of Kiel, Luebeck and Hamburg, Heide, Germany, Institute of Diagnostic and Interventional Radiology/Neuroradiology, Heide, Deutschland

<sup>3</sup>Westkuestenklinikum Heide, Academic Teaching Hospital of the Universities of Kiel, Luebeck and Hamburg, Heide, Germany, Department of Visceral, Thoracic and Vascular Surgery, Heide, Deutschland

<sup>4</sup>Westkuestenklinikum Heide, Academic Teaching Hospital of the Universities of Kiel, Luebeck and Hamburg, Heide, Germany, Department of Visceral, Thoracic and Vascular Surgery, Heide, Deutschland

<sup>5</sup>Westkuestenklinikum Heide, Academic Teaching Hospital of the Universities of Kiel, Luebeck and Hamburg, Heide, Germany, Institute of Diagnostic and Interventional Radiology/Neuroradiology, Heide, Deutschland

**Background:** The aim of the present study was to compare the methods CTSy and ETS with regard to their clinical success and to determine minor and major complications.

**Methods:** Retrospectively, 68 patients (mean age 37.2  $\pm$  15 years) who had been treated using CTSy and 64 patients (mean age 34.6  $\pm$  11 years) who had been treated using ETS were included. The indication for treatment was primary focal palmar hyperhidrosis after ex-

haustion of all conservative treatment options and a continued high level of suffering. All patients evaluated their sense of discomfort within the context of a quality control before the start of treatment, two days postinterventionally/postoperatively, and six and twelve months after treatment, on the basis of a Dermatology Quality of Life Index (DLQI) as well as the side effects that occurred. As statistical test procedures, the Wilcoxon rank-sum test was applied to test the differences in DLQI values over the course and the Mann-Whitney U test to compare the different methods.

**Results:** Both methods were technically feasible in all patients. Both treatments led to a marked reduction in the preinterventional sense of discomfort two days postinterventionally/postoperatively as well as six and twelve months after treatment ( $p < 0.001$ ), whereby mild recurrent sweating occurred over the further course, which was significantly higher in the patients who had undergone CTSy. Temporary miosis and ptosis was found in 8 of 68 (11.8%) patients after CTSy and in 6 of 64 (9.4%) patients after ETS. As the most common side effect, temporary compensatory sweating, predominantly on the trunk, was reported by 16 of 68 (23.5%) patients after CTSy and 18 of 64 (28.1%) patients after ETS. Pneumothoraces developed during the surgical intervention in 26.6%, which were treated adequately by inserting a drain.

**Conclusion:** For patients with severe palmar hyperhidrosis, CTSy and ETS represented a minimally invasive treatment option that provided a high and largely equivalent level of benefit. Recurrent sweating is slightly more common and more pronounced after CTSy than after ETS. However, a higher rate of major complications is seen in the case of ETS.

67

#### MECHANICAL THROMBECTOMY IN ACUTE MIDDLE CEREBRAL ARTERY M2 SEGMENT OCCLUSION WITH REGARD TO VESSEL INVOLVEMENT

Vivien Lorena Ivan\*<sup>1</sup>, Christian Rubbert<sup>1</sup>, Julian Caspers<sup>1</sup>, John-II Lee<sup>2</sup>, Michael Gliem<sup>2</sup>, Sebastian Jander<sup>2</sup>, Bernd Turowski<sup>1</sup>, Marius Kaschner<sup>1</sup>

<sup>1</sup>Department of Diagnostic and Interventional Radiology, University Dusseldorf, Medical faculty, Duesseldorf, Deutschland

<sup>2</sup>Department of Neurology, University Dusseldorf, Medical faculty, Duesseldorf, Deutschland

**Background:** Mechanical thrombectomy (MTE) is an established procedure in patients with acute ischemic stroke due to occlusion of the proximal (M1) segment of the middle cerebral artery. However, the effectiveness of MTE in acute M2-segment occlusions has so far not been systematically evaluated.

**Methods:** All patients with M2-segment-occlusions treated by MTE in the local department (01/2012–12/2017) were included ( $n = 57$ , mean National Institutes of Health Stroke Scale of 11, range 0 to 20). Patients were grouped according to the localization of the M2-occlusion (Cohort A ( $n = 14$ ): central region only, B ( $n = 24$ ): central region and involvement of frontal vessels, C ( $n = 19$ ): parietal, occipital and/or temporal vessels). Differences in proximal (M2-trunk,  $n = 34$ ) and distal (M2-branches,  $n = 23$ ) occlusions were also examined. Reperfusion (Thrombolysis in Cerebral Infarction (TICI)), early clinical outcome at discharge (modified Rankin Scale, mRS) and complications (hemorrhage, emboli to new territories) were noted. Mann-Whitney-U, Kruskal-Wallis-, Fisher's-Exact-Tests and one-way ANOVA were performed, as needed.

**Result:** Successful reperfusion (TICI 2b–3) was found in 49 patients (86.0%). Favorable early clinical outcome (mRS 0–2) was achieved in  $n = 19$  (37.7%). Compared to admission, mRS at discharge improved significantly (median mRS at admission 5 vs. median mRS at discharge 4,  $p < 0.001$ , Mann-Whitney-U). Early clinical outcome was more favorable in patients with better reperfusion (mean mRS of  $4.43 \pm 1.40$ ,

median 4, for TICI 0–2a vs. mean mRS of  $3.00 \pm 1.68$ , median 4, for TICI 2b–3;  $p = 0.043$ , unpaired Mann-Whitney-U). Symptomatic intracranial hemorrhage (sICH) was observed in only 6 patients (10.5%). Four patients died (7.0%).

No significant differences in favorable clinical outcome (mRS at discharge  $\leq 2$ : cohort A 42.9% vs. B 50.0% vs. C 16.7%,  $p = 0.14$ , Fisher's Exact) were found with regard to the vessel involvement. Early clinical outcome did not differ in proximal and distal occlusions.

**Discussion/Conclusion:** MTE in patients with acute M2-occlusion is efficient and leads to a significant clinical improvement at discharge. No significant differences in clinical outcome or complications were found with regard to the localization of the M2-occlusion.

#### References

- Dorn F, et al. Mechanical Thrombectomy of M2-Occlusion. J Stroke Cerebrovasc Dis. 2015;24(7):1465–70.

80

#### EINFLUSS DER NARKOSEFÜHRUNG AUF DIE STRAHLEN-EXPOSITION UND DURCHLEUCHTUNGSZEIT WÄHREND DER ENDOVASKULÄREN SCHLAGANFALLTHERAPIE

Felix Hemmerich\*<sup>1</sup>, Charlotte Weyland<sup>1</sup>, Markus Möhlenbruch<sup>1</sup>, Martin Bendszus<sup>1</sup>, Johannes Pfaff<sup>1</sup>

<sup>1</sup>Universitätsklinikum Heidelberg, Neurologische Klinik, Neuroradiologie, Heidelberg, Deutschland

**Hintergrund:** Die steigenden Behandlungszahlen in der endovaskulären Schlaganfalltherapie (EST) lässt eine Standardisierung zur Sicherung der Behandlungsqualität notwendig werden. Hierunter zählt unseres Erachtens auch eine Berücksichtigung der Strahlenexposition. Zur Strahlenexposition bestehen jedoch keine systematischen Daten.

Unsere Hypothese ist, dass – im Vergleich zu einer Behandlung in Vollnarkose – die vermehrte Bewegung der Patienten, die in Wachnarkose behandelt werden, und der damit mutmaßlich verbundenen erhöhten Schwierigkeit der Navigation von (Mikro-)Kathetern, (Mikro-)Drähten und Stent-Retrievern während der endovaskulären Schlaganfalltherapie, zu einer höheren Strahlenexposition sowie zu längeren Durchleuchtungszeiten führt.

**Methoden:** In diese klinisch-retrospektive Analyse wurden alle Patienten mit akutem ischämischen Schlaganfall in der vorderen Strombahn eingeschlossen, die in der Zeit von Jan. 2013 bis April 2018 eine EST mittels moderner Stent-Retriever-Thrombektomie und/oder direkter Aspirationstherapie, zu einer höheren Strahlenexposition sowie zu längeren Durchleuchtungszeiten führt.

**Ergebnisse:** In der Gesamtpopulation dieser Studien ( $n = 679$ ) besteht zwischen den Patienten, die in Intubationsnarkose (GA,  $n = 196$ ) behandelt wurden, und den Patienten, die in Wachnarkose behandelt wurden (CS,  $n = 483$ ) mit Hinblick auf das Patientenalter, die initiale Schwere des Schlaganfalls und der Verschlusslokalisation ein signifikanter Unterschied (siehe Tabelle). Das Dosisflächenprodukt DFP (in  $\mu\text{Gy} \cdot \text{cm}^2$ , Median (IQR): GA: 11747; CS: 11352;  $p$ -Wert: 0.419) und die Durchleuchtungszeit (in Minuten, Median (IQR): GA: 35 (21–59); CS: 31 (17–54);  $p$ -Wert: 0.095) sind hingegen vergleichbar.

Bei einer isolierten Betrachtung der Patienten mit einem Mediahauptstammverschluss (GA:  $n = 89$ , CS:  $n = 219$ ), bei der sich mit Ausnahme der initialen Schwere der Symptomatik keine signifikanten Unterschiede der Patientencharakteristika ergeben, sind das DFP (GA: 10643; CS: 9582;  $p$ -Wert: 0.68) und die Durchleuchtungszeit (GA: 33; CS: 25;  $p$ -Wert: 0.19) ebenfalls nicht signifikant unterschiedlich.

**Fazit:** Das Ergebnis der Analyse der Thrombektomie-Datenbank zeigt, dass es keinen signifikanten Einfluss der Narkoseführung auf die Durchleuchtungszeit und die Strahlenexposition während der endovas-

**Fig. 1 | 80** Gesamtes Patienten-Kollektiv 01/2013–04/2019

	<b>GA Patienten</b> (n= 196)	<b>CS Patienten</b> (n= 483)	<b>p-Wert</b>
Alter (in Jahren), Mittelwert (SD)	70.1 (14.3)	73.8 (12.7)	0.001
<u>Männlich</u> (%)	95 (48.5)	222 (46)	0.554
<u>Initialer NIHSS</u> , Median (IQR)	19 (15 – 22)	15 (10 – 19)	<0.0001
<u>Verschlusslokalisation</u>			
<u>Carotis T</u> (%)	60 (30.6)	71 (14.7)	
M1 (%)	106 (54.1)	253 (52.4)	
M2 (%)	22 (11.2)	144 (29.8)	
M3 (%)	4 (2)	10 (2.1)	
ACA (%)	4 (2)	5 (1)	<0.0001
Dosisflächenprodukt (μGy*m <sup>2</sup> ), Median (IQR)	11747 (7329 – 19453)	11352 (6846 – 18508)	0.419
<u>Durchleuchtungszeit</u> (Minuten), Median (IQR)	35 (21 – 59)	31 (17 – 54)	0.095

GA = General Anesthesia (Vollnarkose), CS = Conscious Sedation (Wachnarkose)  
 NIHSS = National Institutes of Health Stroke Scale

**Fig. 2 | 80** Patienten mit isoliertem Mediahauptstammverschluss

	<b>GA Patienten</b> (n= 89)	<b>CS Patienten</b> (n= 219)	<b>p-Wert</b>
Alter (in Jahren), Mittelwert (SD)	72.3 (13.6)	74.4 (12.8)	0.207
<u>Männlich</u> (%)	32 (36)	86 (39,3)	0.588
<u>Initialer NIHSS</u> , Median (IQR)	19 (15 – 22)	16 (11 – 20)	<0.0001
Dosisflächenprodukt (μGy*m <sup>2</sup> ), Median (IQR)	10643 (6617 – 16588)	9582 (6161 – 16464)	0.677
<u>Durchleuchtungszeit</u> (Minuten), Median (IQR)	33 (19 – 54)	25 (14 – 45)	0.195

GA = General Anesthesia (Vollnarkose), CS = Conscious Sedation (Wachnarkose)  
 NIHSS = National Institutes of Health Stroke Scale

kulären Schlaganfalltherapie gibt. Die erhobenen Werte zur Strahlenexposition und Durchleuchtungszeit könnten zukünftig als Orientierung im Sinne von Dosis-Referenz-Werten dienen.

92

**NUCLEUS ACCUMBENS PROJECTIONS: VALIDITY AND RELIABILITY OF FIBER RECONSTRUCTIONS BASED ON HIGH-RESOLUTION DIFFUSION-WEIGHTED MRI**

Thilo Rusche\*<sup>1</sup>, Jörn Kaufmann<sup>2</sup>, Jürgen Voges<sup>3</sup>

<sup>1</sup>Institut für Klinische Radiologie, Universitätsklinikum Münster, Münster, Deutschland

<sup>2</sup>Klinik für Neurologie, Universitätsklinikum Magdeburg, Otto-von-Guericke Universität, Magdeburg, Deutschland

<sup>3</sup>Klinik für Stereotaktische Neurochirurgie, Universitätsklinikum Magdeburg, Otto-von-Guericke Universität, Magdeburg, Deutschland

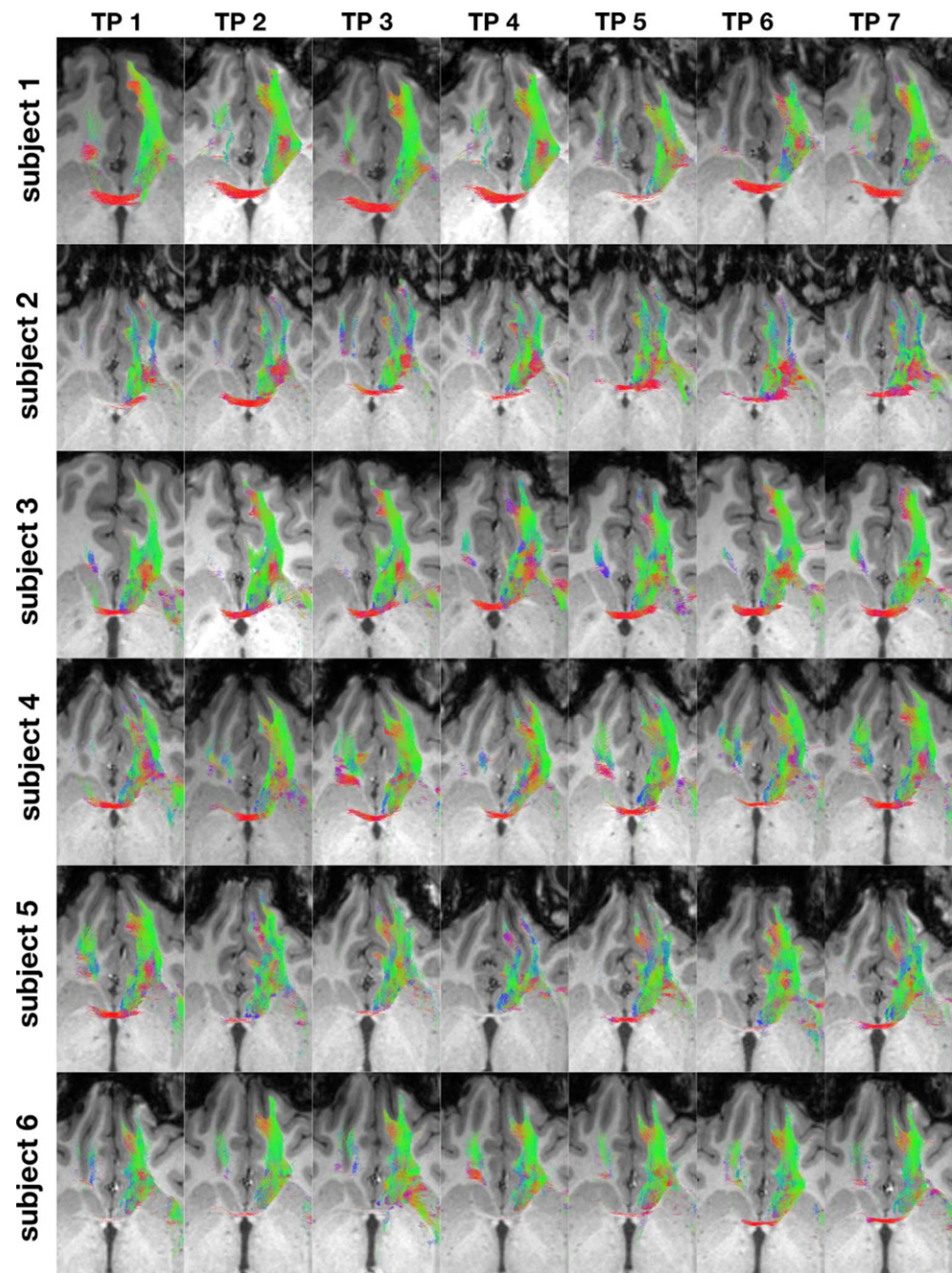
**Background:** The N. accumbens (NAc) is a key relay in the mesolimbic dopaminergic reward system. As such, it is a promising target for deep brain stimulation (DBS) in patients with psychiatric diseases. In the present study, we aimed to reconstruct the neural projections con-

necting the NAc with the medial prefrontal cortex (mPFC), the anterior cingulate cortex (ACC), the amygdala, the hippocampus, the dorsomedial thalamus (dmT) and the ventral tegmental area (VTA) using probabilistic fiber tractography based on diffusion-weighted MR-imaging (dMRI).

**Methods:** MR-data (T1-MPRAGE; FLAIR; DWI: 1.6 mm isotropic resolution, 60 gradient directions) for 11 healthy subjects were acquired in seven sessions on a *Siemens MAGNETOM Prisma 3T* MRI-scanner. For each subject, the bilateral NAc, mPFC, ACC, amygdala, hippocampus, dmT and VTA were manually/automated segmented based on the T1 and FLAIR data and transformed to the session-specific DWI space for probabilistic fiber tractography. The results were subject to detailed visual inspection to assess their validity in terms of anatomical plausibility by comparing them with the relevant literature. To quantitatively assess the reliability of the reconstructions, exemplarily the individual fiber-tracts between the NAc and mPFC for each session and subject were clustered and transformed to a main-tract before performing an intra-subject comparison.

**Results:** Using MRI data from 11 healthy subjects, we were able to reconstruct neural projections connecting the NAc with the mPFC (see figure 1/2), ACC, amygdala, hippocampus, dmT and VTA.

**Fig. 1 | 92** Fiber-reconstruction of the NAc-mPFC-pathway of subject 1–11 for the point 1–7 and the left hemisphere



**Discussion:** The connectivity patterns formed by the obtained fibers were in good concordance with the literature (anatomical tracer/fiber-dissection studies). Furthermore, the reliability assessment of the NAc ↔ mPFC fiber-tracts yielded to high correlations between the obtained main-tracts.

**Conclusion:** We assessed the feasibility and reliability of the *in vivo* reconstruction of neural fibers connecting the human NAc with the abovementioned target regions from high-resolution dMRI data using probabilistic fiber-tractography. In clinical practice, the presented procedure may guide selective electrical stimulation of the mesolimbic fibers using directional lead technology. Compared to undirected neuromodulation of the entire NAc, this could improve for example the efficacy of DBS for the treatment of mental disorders.

105

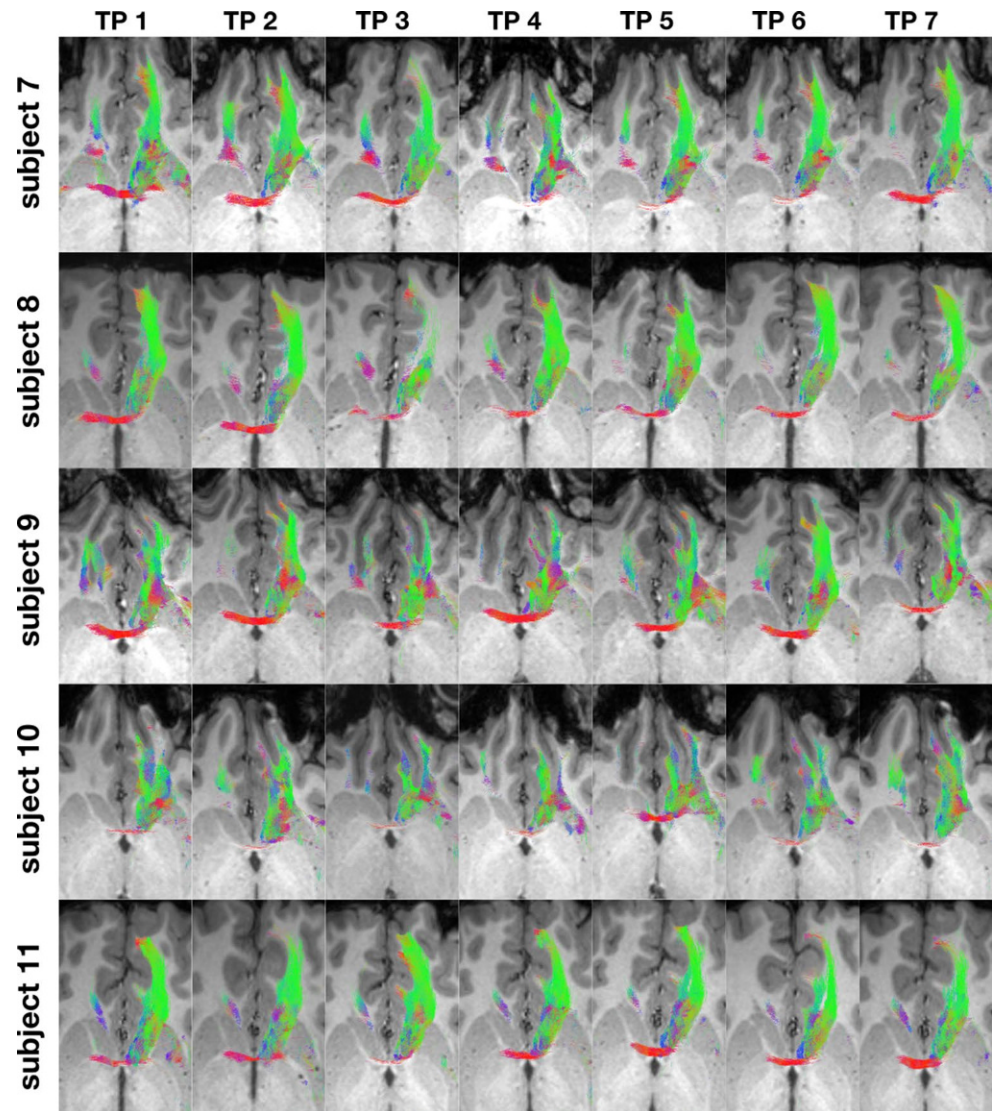
#### ALTERED CORTICO-STRIATAL FUNCTIONAL CONNECTIVITY DURING RESTING STATE IN OBSESSIVE-COMPULSIVE DISORDER

Benita Schmitz-Koep<sup>\*1</sup>, Jessica Calzà<sup>1,2</sup>, Deniz A. Gürsel<sup>1,2</sup>, Benno Bremer<sup>1</sup>, Lena Reinholz<sup>3</sup>, Götz Berberich<sup>4</sup>, Kathrin Koch<sup>1,2,5</sup>

<sup>1</sup>Department of Diagnostic and Interventional Neuroradiology, Klinikum rechts der Isar, Technische Universität München, München, Deutschland

<sup>2</sup>TUM-Neuroimaging Center, Klinikum rechts der Isar, Technische Universität München, München, Deutschland

**Fig. 2 | 92** Fiber-reconstruction of the NAc-mPFC-pathway of subject 1–11 for the point 1–7 and the left hemisphere



<sup>3</sup>Department of Psychology, Ludwig-Maximilians-Universität, München, Deutschland

<sup>4</sup>Windach Institute and Hospital of Neurobehavioural Research and Therapy (WINTR), Windach, Deutschland

<sup>5</sup>Graduate School of Systemic Neurosciences, Ludwig-Maximilians-Universität, München, Deutschland

**Hintergrund:** Neuroimaging studies show that obsessive-compulsive disorder (OCD) is characterized by an alteration of the cortico-striato-thalamo-cortical (CSTC) system [1]. As resting-state functional connectivity (FC) studies investigated only specific parts of the CSTC in patients with OCD up to now, the present study aimed at exploring FC in the CSTC as a whole.

**Methoden:** We investigated potential alterations in resting-state FC within the CSTC system in 44 OCD patients and 40 healthy controls by taking into consideration all relevant nodes of the direct and indirect CSTC loop.

**Ergebnisse:** Compared to healthy controls, OCD patients showed an increased FC between the left subthalamic nucleus (STN) and the left external globus pallidus (GPe), as well as an increased FC between the left GPe and the left internal globus pallidus (GPi).

**Diskussion:** The results further support CSTC involvement in OCD pathology. However, our findings showing increased FC between rele-

vant structures of the indirect pathway contradict the current hypothesis. The results highlight the role of the STN which is a relevant target region of deep brain stimulation (DBS) in patients with treatment-refractory OCD [2]. Hence, our findings could contribute a neurobiological framework to a better comprehension of the fundamental processes underlying DBS.

**Fazit:** Our findings highlight the importance of the indirect pathway, especially of the STN, in OCD pathology and could introduce an altered interpretation of the classical model of the CSTC. Furthermore, the results may improve insight on DBS as a treatment for severe OCD. They could provide a basis for future investigations improving the accurate choice of DBS targets and thus increasing clinical outcome for patients as well as reducing the probability of adverse events.

## References

1. Saxena S, Rauch SL. Functional neuroimaging and the neuroanatomy of obsessive-compulsive disorder. *Psychiatric Clinics of North America*. 2000;23(3):563–86.
2. Mulders AEP, Plantinga BR, Schruers K, Duits A, Janssen MLF, Ackermans L, et al. Deep brain stimulation of the subthalamic nucleus in obsessive-compulsive disorder: Neuroanatomical and pathophysiological considerations. *Eur Neuropsychopharmacol*. 2016;26(12):1909–19.

109

### TUBE CURRENT REDUCTION IN COMPUTED TOMOGRAPHY ANGIOGRAPHY—HOW LOW CAN WE GO IN PATIENTS WITH SUSPECTED ACUTE STROKE?

Nico Sollmann<sup>1</sup>, Kai Mei<sup>2</sup>, Isabelle Riederer<sup>1</sup>, Simon Schön<sup>1</sup>, Felix K. Kopp<sup>2</sup>, Maximilian T. Löffler<sup>1</sup>, Jan S. Kirschke<sup>1</sup>, Ernst J. Rummeny<sup>2</sup>, Claus Zimmer<sup>1</sup>, Peter B. Noel<sup>2</sup>, Thomas Baum<sup>1</sup>

<sup>1</sup>Abteilung für Diagnostische und Interventionelle Neuroradiologie, Klinikum rechts der Isar, Technische Universität München, München, Deutschland

<sup>2</sup>Abteilung für Diagnostische und Interventionelle Radiologie, Klinikum rechts der Isar, Technische Universität München, München, Deutschland

**Hintergrund:** Computed tomography angiography (CTA) as part of first-line stroke imaging protocols entails considerable radiation exposure. However, research on dose reductions for head and neck CTA is scarce. The aim of this study is to evaluate image quality, detectability of large vessel occlusion (LVO) or dissection, and diagnostic confidence in CTA with virtually lowered tube current and iterative reconstruction (IR) in patients with suspected acute stroke.

**Methoden:** Thirty patients (age:  $79.0 \pm 10.4$  years, 50% with LVO or dissection) underwent CTA of the supraaortal up to the intracranial arterial vessels. CTA scans were simulated as if they were made at 50% (D50), 25% (D25), and 10% (D10) of the original tube current. Image

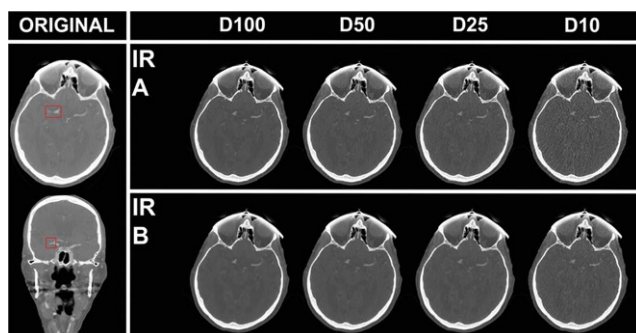


**Fig. 1 | 109** 84-year-old man with right-sided thrombotic occlusion of the middle cerebral artery (M1 segment). CT angiograms were processed with two iterative reconstruction (IR) algorithms (A and B) and simulated with 50% (D50), 25% (D25), and 10% (D10) of original tube current (D100)

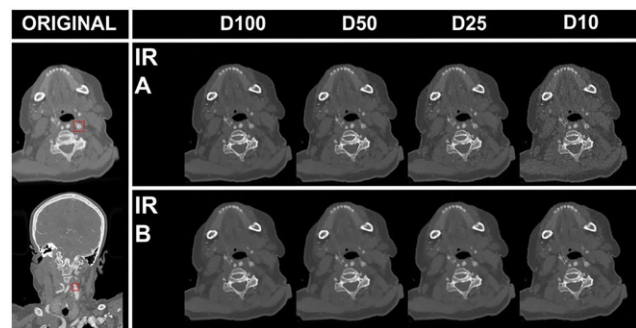


**Fig. 2 | 109** 81-year-old woman with left-sided dissection of the extracranial internal carotid artery. CT angiograms were processed with two iterative reconstruction (IR) algorithms (A and B) and simulated with 50% (D50), 25% (D25), and 10% (D10) of original tube current (D100)

reconstruction was achieved with two levels of IR (A: similar to clinical reconstructions, B: two times stronger regularization). Two readers (R1 and R2) performed qualitative image evaluation considering overall image quality and artifacts, vessel contrast, detection of vessel pathology, and diagnostic confidence (scoring: 1—low, 2—medium, and 3—high confidence).

**Ergebnisse:** Level B of IR was favorable regarding overall image quality and artifacts for D10, while level A was favorable for D100 and D50. CTA scans with D25 and both levels of IR still showed good vessel contrast, with even peripheral arterial branches of the anterior, middle, and posterior cerebral artery being clearly detectable. Further, CTA scans with D25 using level A of IR showed an adequate level of diagnostic confidence without any missed LVO or dissection according to evaluations of both readers (D25 A: R1:  $2.5 \pm 0.6$  vs. R2:  $2.6 \pm 0.6$ ,  $p > 0.05$ ). Inter-reader agreement was high for all items of evaluations, particularly when level A of IR was used.

**Fazit:** CTA using IR and tube currents lowered down to 25% of original imaging is feasible without drawbacks regarding vessel contrast or detection of vessel pathology in patients with suspected acute stroke. Our approach enables reductions in radiation exposure for head and neck CTA, with an average decrease from  $8.5 \pm 1.5$  mGy to 2.1 mGy in our patients.

126

### BRAIN METABOLISM OF PATIENTS UNDER IMMUNOSUPPRESSION WITH TACROLIMUS AFTER KIDNEY TRANSPLANTATION—A SINGLE VOXEL 1H-MR SPECTROSCOPY STUDY

Patrick Nösel\*<sup>1</sup>, Henning Pflugrad<sup>2,3</sup>, Birte Schmitz<sup>1</sup>, Heinrich Lanfermann<sup>1</sup>, Hannelore Barg-Hock<sup>4</sup>, Jürgen Klempnauer<sup>3,4</sup>, Mario Schiffer<sup>3,5</sup>, Karin Weissenborn<sup>2,3</sup>, Xiao-Qi Ding<sup>1</sup>

<sup>1</sup>Institute of Diagnostic and Interventional Neuroradiology, Hannover Medical School, Hannover, Deutschland

<sup>2</sup>Department of Neurology, Hannover Medical School, Hannover, Deutschland

<sup>3</sup>Integrated Research and Treatment Centre Transplantation, Hannover, Deutschland

<sup>4</sup>Clinic for Visceral and Transplant Surgery, Hannover Medical School, Hannover, Deutschland

<sup>5</sup>Clinic for Nephrology, Hannover Medical School, Hannover, Deutschland

**Hintergrund:** While the immunosuppression therapy with tacrolimus has remarkably improved the survival of patients after organ transplantation, long-term side effects of tacrolimus medication become an important research topic with respect to improvement of patient care. This work aimed to assess possible alterations of brain metabolism in patients under long-term tacrolimus medication after kidney transplantation (KTx-patients) by using single voxel 1H-MR spectroscopy (1H-MRS).

**Methoden:** 40 KTx-patients (age:  $55.57 \pm 8.34$  years, standard tacrolimus dose:  $7.19 \pm 0.9$  µg/l, years after KTx:  $7.24 \pm 4.03$ ) and 16 age-, sex- and education- adjusted healthy controls underwent MR examinations at 3T (Verio, Siemens, Erlangen), which included a single voxel spectroscopy (SVS) of 4 ml brain tissue in parieto-occipital white matter. SVS data were analyzed by using software LCModel to determine concentrations of brain metabolites N-acetylaspartate (NAA), Choline (Cho), Creatine (Cr), Glutamate and Glutamine (Glx), and Myo-Inositol (ml) in reference to internal water and as ratio to Cr. The Battery for the Assessment of Neuro-psychological Status (RBANS) was used to assess the cognitive functions of the subjects. The results were compared between patients and controls by using nonparametric median test with post hoc Bonferroni pairwise comparison. For data quality assurance, only metabolite values with a Cramer-Rao lower

bound (CRLB) of max. 20% were considered for the analysis. The statistical analysis was done with SPSS 25.

**Diskussion:** We found that, in comparison to the healthy controls, the KTx-patients showed a significantly lower Cr concentration ( $p=0.041$ ), which is considered as an indication of altered brain energy metabolism, and lowered RBANS total scores ( $p=0.005$ ) that reflect impaired cognitive function. NAA, Cho, Glx and ml showed no significant alterations in patients.

**Fazit:** In conclusion, the present study revealed altered brain metabolism associated with impaired cognitive function in KTx-patients under long-term tacrolimus treatment. Further longitudinal studies are needed to clarify if these alterations are possibly due to neurotoxic-side-effect of tacrolimus.

143

**COMPARING SWI SEQUENCES AND QSM RECONSTRUCTION METHODS FOR CLINICAL MEASUREMENT OF VENOUS SUSCEPTIBILITY**

Ronja Berg<sup>\*1</sup>, Jakob Meineke<sup>2</sup>, Andreas Hock<sup>3</sup>, Claus Zimmer<sup>1</sup>, Christine Preibisch<sup>1</sup>

<sup>1</sup>Klinikum rechts der Isar der Technischen Universität München, Abteilung für Neuroradiologie, München, Deutschland

<sup>2</sup>Philips Research, Hamburg, Deutschland

<sup>3</sup>Philips Healthcare, Hamburg, Deutschland

**Hintergrund:** Many neuro-degenerative diseases such as stroke and tumor but also Alzheimer’s disease or multiple sclerosis<sup>1-2</sup> may affect

the oxygen metabolism. Quantitative Susceptibility Mapping (QSM) is a non-invasive alternative<sup>1-2</sup> to the gold standard 15O PET for measuring changes in the oxygenation and thus for studying such diseases in more detail. We compared QSM parameter maps, measured with different SWI sequences and reconstructed with different techniques, with respect to clinical applicability.

**Methoden:** 7 healthy subjects (22–48y) were scanned on a 3T Philips Elition using 3 different 3D multi-echo GE SWI sequences: 1) standard sequence with first-echo flow compensation (FC), 2) modified sequence with full multi-echo FC (both SENSE=2), 3) multi-echo FC with Compressed SENSE (CS=3).

QSM maps were calculated using: 1) FANSI (Fast Algorithm for Nonlinear Susceptibility Inversion)<sup>3</sup>; 2) MEDI (Morphology Enabled Dipole Inversion)<sup>4</sup>; 3) iLSQR<sup>5</sup> and STAR<sup>6</sup> reconstructions from STI Suite with 2 parameter settings each (Fig. 1). For whole volume vessel segmentation we used automatic multi-scale vessel filtering from JIST-LayoutTool of MIPAV.

**Ergebnisse:** From all QSM parameter maps, MEDI provides highest contrast while FANSI appears slightly blurred. The most homogeneous vessel representation is provided by STI Suite while FANSI and MEDI yield more inhomogeneous structures (Fig. 3c). Mean susceptibility values of automatically segmented voxels depend mostly on reconstruction algorithms (Fig. 2).

**Diskussion:** Our results suggest that SWI sequences with higher acceleration (CS=3) than regular SENSE can be applied without loss of fidelity. Generally, reconstructions with STI Suite are most homogeneous and the venous susceptibility values vary least.

**Fazit:** QSM parameter maps obtained with STI Suite are most reliable for studying changes of venous oxygenation in neurological diseases.

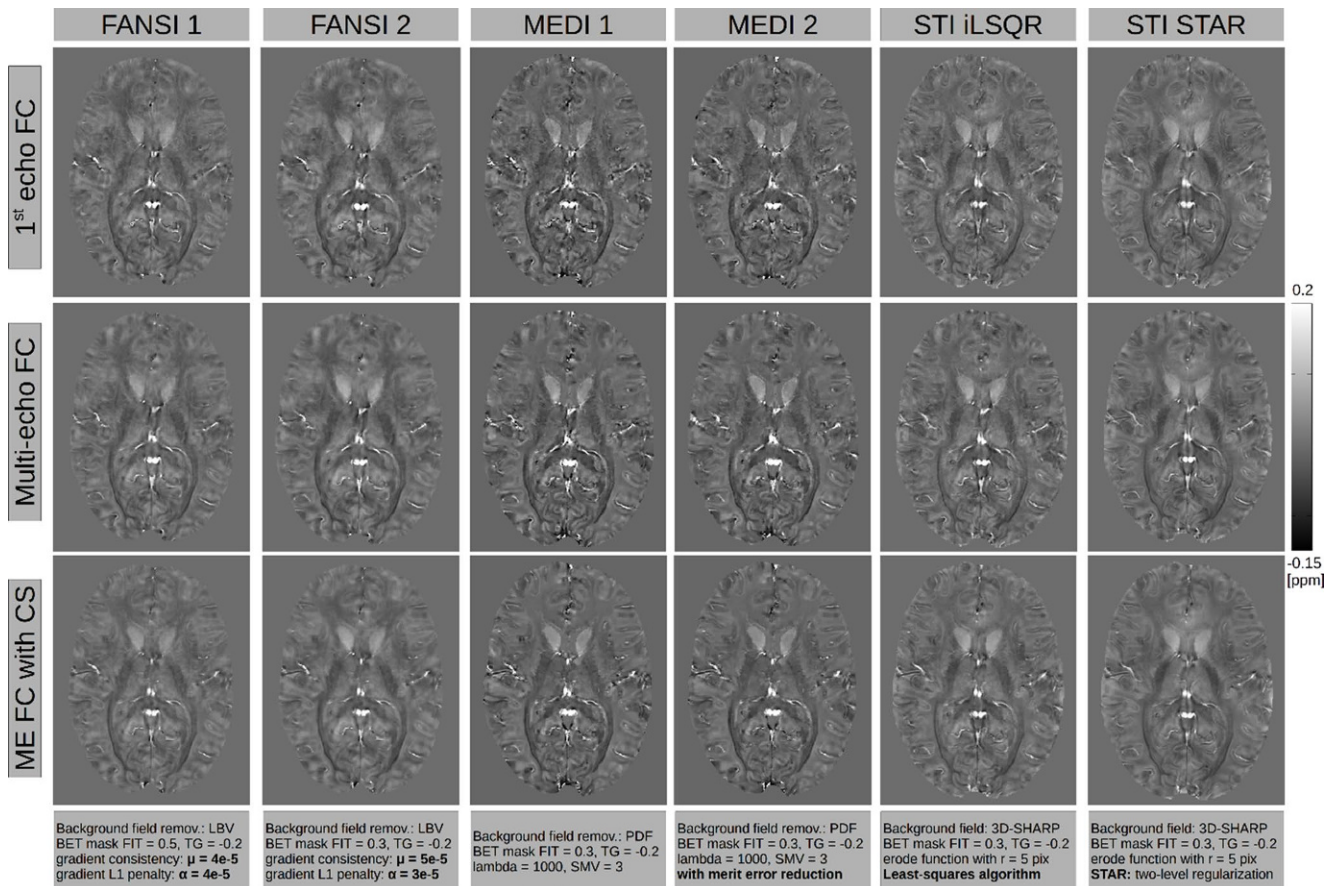
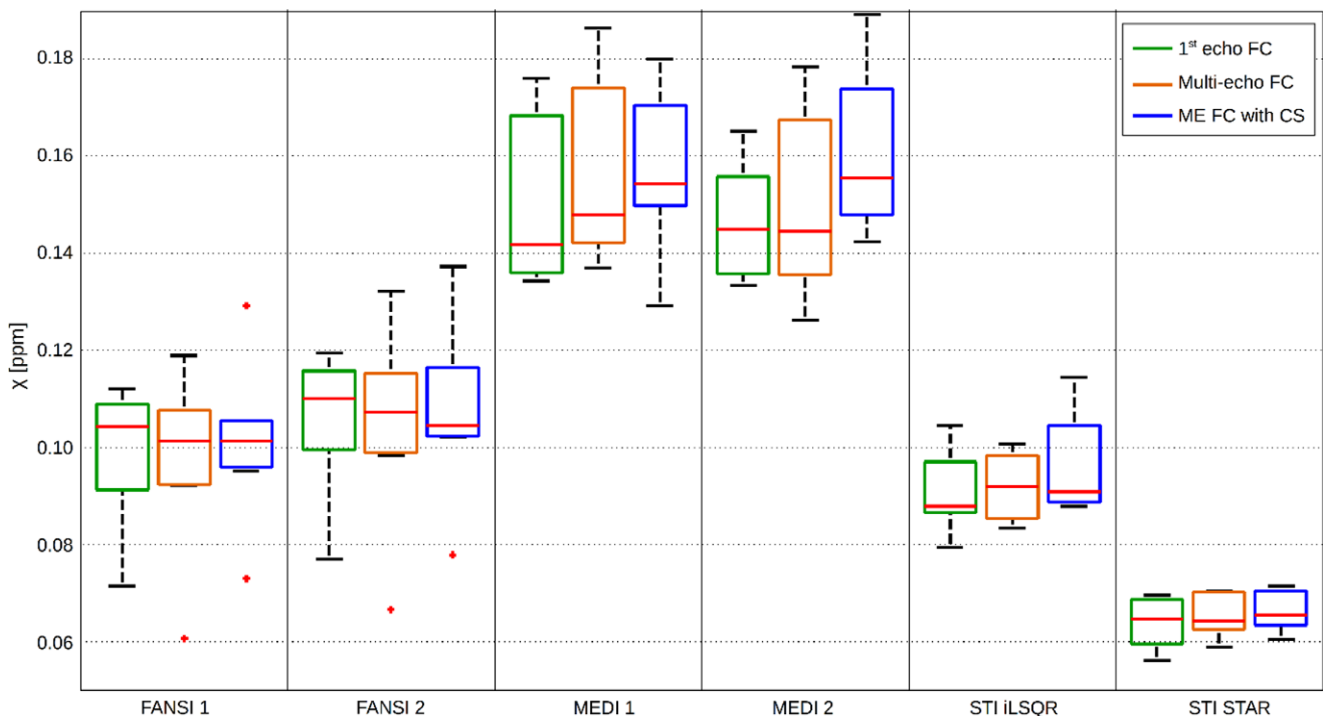
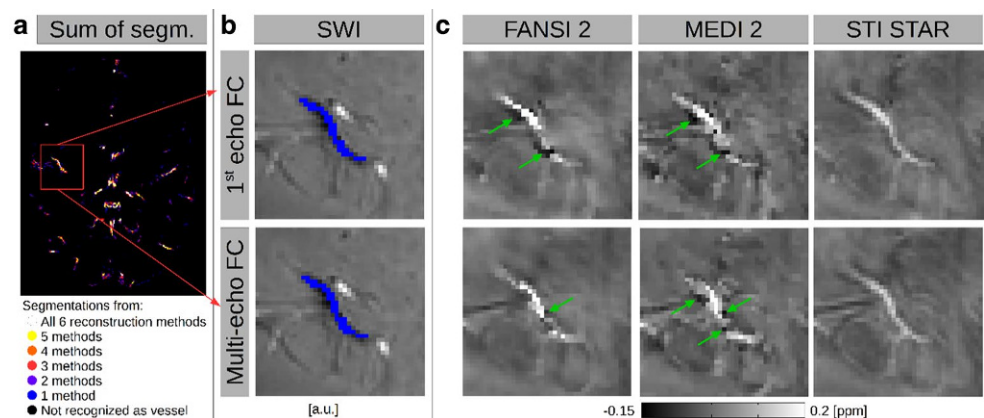


Fig. 1 | 143 1 QSM parameter maps from 3 SWI sequences and 6 QSM reconstruction methods



**Fig. 2 | 143** Mean susceptibility values obtained from automatically segmented QSM voxels for all sequences and reconstruction methods

**Fig. 3 | 143** Exemplary manual segmentation of a vessel, for different reconstruction methods



## References

1. Fan, et al. JCBFM. 2015.
2. Fan, et al. MRM. 2014.
3. Bilgic, et al. MRM. 2014.
4. Liu J, et al. Neuroimage. 2012.
5. Wei H, et al. MRM. 2017.
6. Wei H, et al. Nmr Biomed. 2015.

145

## QUANTITATIVE FUNCTIONAL MRI OF HUMAN VISUAL CORTEX ACTIVATION USING MULTI-PARAMETRIC QUANTITATIVE BOLD

Christine Preibisch<sup>\*1,2,3</sup>, Samira Epp<sup>1,2</sup>, Stephan Kaczmarz<sup>1,2</sup>, Valentin Riedl<sup>1,2</sup>

<sup>1</sup>Technische Universität München, Klinikum rechts der Isar, Abteilung für Diagnostische und Interventionelle Neuroradiologie, München, Deutschland

<sup>2</sup>Technische Universität München, Klinikum rechts der Isar, TUM Neuroimaging Center (TUM-NIC), München, Deutschland

<sup>3</sup>Technische Universität München, Klinikum rechts der Isar, Klinik für Neurologie, München, Deutschland

**Hintergrund:** Cerebral metabolic rate of oxygen (CMRO<sub>2</sub>) can be assessed by combining multi-parametric quantitative blood oxygenation level dependent (mq-BOLD) and arterial spin labeling (ASL) MRI. We tested the sensitivity of mq-BOLD for task-related changes in tissue oxygenation in visual cortex during different stimulation states by performing quantitative multi-echo gradient echo (multi-GE) and multi-echo spin echo (multi-SE) measurements of intrinsic susceptibility-related transverse relaxation rates R<sub>2</sub>'.

**Methoden:** We performed whole-brain fMRI in 12 healthy subjects (30.8 ± 6.8y; five men) during eyes closed, eyes open, and visual stimulation (8 Hz checkerboard) on 3T Elition MR scanner (Philips). We acquired T2-w multi-SE, T2\*w multi-GE and pseudo-continuous arterial spin labeling (pCASL) (≈7 min per modality and condition). Task-fMRI (30sec block-design) was used for VOI definition. We obtained in-

**Fig. 1 | 145** Single slice of exemplary quantitative parameter maps (T2, T2\*, R2', CBF)

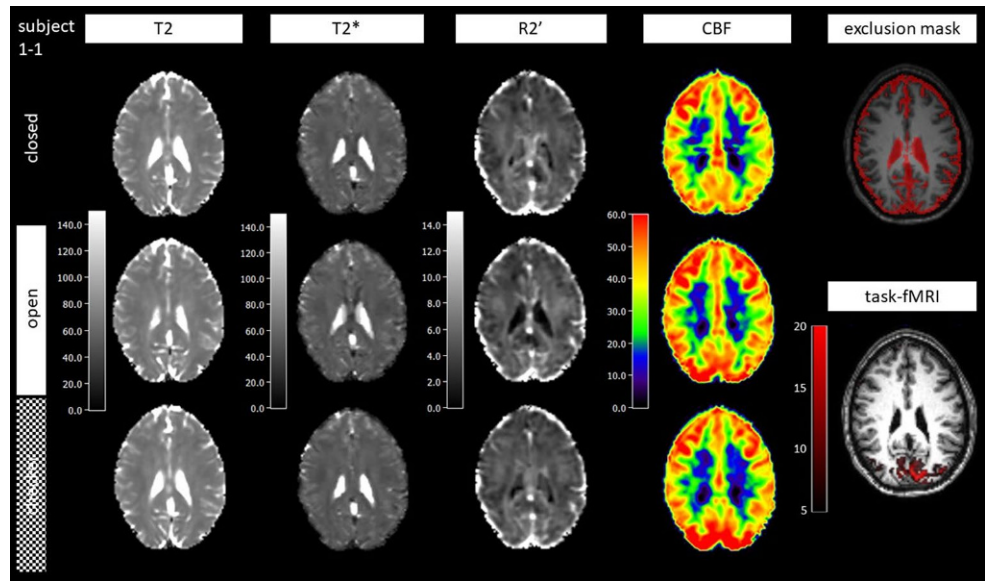


**Fig. 2 | 145** Mean values of VOI average quantitative parameter values (CBF, R2, R2\*, R2')

VOI	t-map (open>closed), t > 10.0			t-map (checker>open), t > 10.0		
	eyes closed	eyes open	8Hz checker	eyes closed	eyes open	8Hz checker
CBF [ml/100g/min]	36.3 ± 9.6	39.5 ± 10.6	42.7 ± 11.9	36.1 ± 9.2	35.8 ± 8.8	47.4 ± 11.8
ΔCBF [ml/100g/min]	3.20 ± 3.55 (p = 0.048)		3.18 ± 4.36 (p = 0.095)	-0.33 ± 2.60 (p = 0.679)		11.64 ± 4.26 (p < 0.001)
R2' [sec <sup>-1</sup> ]	6.7 ± 0.8	6.6 ± 1.1	6.7 ± 0.6	6.9 ± 0.8	6.9 ± 0.7	6.6 ± 0.7
ΔR2' [sec <sup>-1</sup> ]	-0.15 ± 0.42 (p = 0.373)		0.14 ± 0.48 (p = 0.464)	0.08 ± 0.35 (p = 0.473)		-0.29 ± 0.29 (p = 0.007)
R2 [sec <sup>-1</sup> ]	14.1 ± 0.9	14.2 ± 0.7	14.2 ± 0.8	14.0 ± 0.3	14.0 ± 0.3	14.0 ± 0.3
ΔR2 [sec <sup>-1</sup> ]	0.09 ± 0.18 (p = 0.236)		-0.06 ± 0.10 (p = 0.153)	0.02 ± 0.11 (p = 0.627)		-0.05 ± 0.18 (p = 0.339)
R2* [sec <sup>-1</sup> ]	20.5 ± 1.7	20.4 ± 1.9	20.4 ± 1.5	20.4 ± 0.9	20.5 ± 0.9	20.2 ± 0.9
ΔR2* [sec <sup>-1</sup> ]	-0.10 ± 0.40 (p = 0.529)		-0.00 ± 0.61 (p = 0.984)	0.08 ± 0.34 (p = 0.456)		-0.35 ± 0.22 (p < 0.001)
ΔR2* [sec <sup>-1</sup> ] (BOLD-TC)	-1.29 ± 0.23 (p < 0.001)		∅	∅		-0.89 ± 0.12 (p < 0.001)
nvoxel	111 ± 109			567 ± 267		

trinsic R2 (=1/T2), effective R2\* (=1/T2\*) and susceptibility related R2' (=R2\*-R2) from multi-SE and multi-GE data by mono-exponential fits and corrected T2\* for macroscopic background gradients<sup>1</sup> and motion.<sup>2</sup> CBF maps were calculated from pCASL data.<sup>3</sup>

**Ergebnisse/Results:** Fig. 1 shows an exemplary slice of all imaging modalities with comparable data quality across conditions. Visual inspection suggests higher CBF in visual cortex for 'open' and 'checker'. VOI analysis of quantitative mq-BOLD parameters (Fig. 2) yielded a significant increase of CBF in both contrasts, though weaker for 'open>closed'. We also found significantly decreased R2' upon checkerboard stimulation, but not for 'open>closed'.

**Diskussion:** Our results demonstrate that mq-BOLD measurements of activation-related changes are well feasible for standard visual stimulation experiments. However, subject motion and transient states of brain activation might impact on data quality due to prolonged measurement times. These challenges need to be addressed by study design and improved head immobilization.

**References**

1. Preibisch, et al. MRM. 2008;60(4):908–16.
2. Noth, et al. NI. 2014;92:106–19.
3. Alsop, et al. MRM. 2015;73:102–16.

150

**JUDGEMENT OF AND EMPATHY WITH OTHER PEOPLE'S FACIAL EXPRESSIONS: A PSYCHOPHYSICAL AND FMRI STUDY**

Carola Widmann<sup>1</sup>, Sibylle Wimmer<sup>1</sup>, Denise Potthoff<sup>2</sup>, Rüdiger Seitz<sup>2</sup>, Johannes Trenkler<sup>1</sup>, Raimund Kleiser<sup>\*1</sup>

<sup>1</sup>Neuromed Campus, Kepler University Hospital, Neuroradiology, Linz, Österreich

<sup>2</sup>LVR-Klinikum, Heinrich-Heine-University Düsseldorf, Department of Neurology, Düsseldorf, Deutschland

**Hintergrund:** Empathy is a key element in interpersonal relationships and varies from weak to strong in its manifestation. Many neuropsychi-

atric disorders are accompanied by impaired recognition of emotions and poor empathic processing.

**Methoden:** To explore the neural structures involved in empathic processes we performed a fMRI-study on 16 healthy volunteers in a 3T MRI scanner. The emotional stimuli consisted of black and white pictures depicting anger, sadness, happiness and fear in males and females (Averaged Karolinska directed emotional faces AKDEF<sup>1</sup>). The stimuli started with a neutral expression and changed continuously within 30 pictures presented for 750 ms each to one of the strongest emotional expressions. Functional data were recorded with EPI sequences with a repetition time of TR=1,5 sec and 38 slices with a slice thickness of 3 mm covering the whole brain. The quality and response times of emotion recognition and empathizing with them were measured by a response grip. The volunteers had to press the right button when they recognized the emotion in the stimuli. Furthermore the left button, if they were able to empathize the emotion.

**Ergebnisse:** FMRI revealed a network involving occipital, parietal and frontal cortical areas. Moreover, strong activity in the amygdala—a central neural component in emotion processing—was found.

**Diskussion:** Thus, judging and reasoning with other people's emotion involves different cortico-subcortical neural circuits. Happiness was recognized and empathized faster and more intense than the other emotions, showing especially a subcortical activation. Moreover we measured the strongest activation when recognizing the mood in important subcortical areas.

## References

1. Lundqvist & Litton, 1998

178

## DARSTELLUNG PERIPHERER HIRNNERVEN UND IHRER PATHOLOGIE IM EXTRACRANIEN VERLAUF MITTELS NEUER HOCHAUFLÖSENDER SEQUENZEN

Monika Probst<sup>\*1</sup>, Lisa Maier<sup>2</sup>, Teresa Robl<sup>2</sup>, Claus Zimmer<sup>2</sup>, Egon Burian<sup>2</sup>

<sup>1</sup>Klinikum rechts der Isar, Abteilung für Diagnostische und Interventionelle Neuroradiologie, München, Deutschland

**Hintergrund:** Die Darstellbarkeit peripherer Hirnnerven im extracraniellen Verlauf gestaltet sich aufgrund der anatomischen Verhältnisse im Gesicht und Hals oft als schwierig. Dabei können im Rahmen der bislang etablierten Sequenzen wegweisende Pathologien übersehen werden.

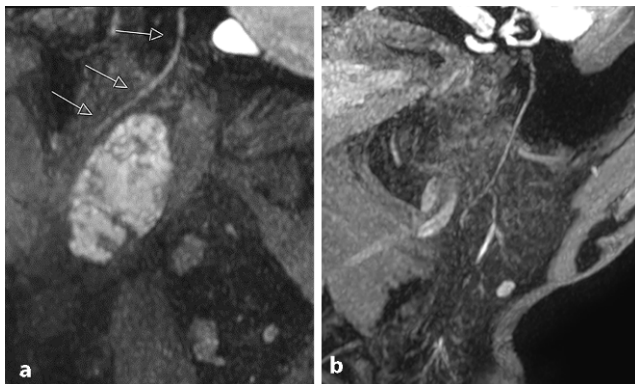


**Abb. 1 | 178 a)** N. facialis in unmittelbarer Nähe zu einem Tumor in der Glandula parotis. **b)** Abgrenzbarkeit des N. facialis vom Austritt aus dem Foramen stylomastoideum bis in seine Aufzweigungen

**Methoden:** Es wurden im Rahmen einer Studie 43 Probanden (28–80 Jahre) und 17 Patienten mittels hochauflösender (0,55 mm Voxel) 3D STIR (Short tau inversion recovery) und 3D WATS (Water selective excitation) Sequenzen untersucht. Diese wurden im Vorfeld an die Gegebenheiten der Mund-, Kiefer- und Gesichtsregion angepasst. Bei Probanden und Patienten wurde durch zwei Radiologen erfasst, inwiefern sich die Hirnnerven (insb. N. facialis und N. trigeminus) im extracraniellen Verlauf darstellen lassen.

**Ergebnisse:** In der STIR Sequenz weisen periphere Nerven ein hohes Signal zu Muskel Verhältnis auf (aNMCCNR=Apparent nerve-muscle contrast to noise ratio). In der WATS Sequenz gelang die beste Abgrenzbarkeit im Verlauf durch einen hohen Gesamtcontrast zum umliegenden Gewebe mit niedrigem Gefäßsignal, wodurch die Nerven weniger stark maskiert wurden. Am besten ließen sich die Trigeminusäste (V2 und V3) bei hoher Übereinstimmung beider Rater darstellen. Wilcoxon matched-pairs two-tailed Test (significantly different  $p < 0,05$ ): WATS aNMCCNR: V3 proximal  $p = 0,76$ , STIR aNMCCNR: V3 proximal  $p = 0,33$ . Die Darstellbarkeit des N. facialis hängt stark von dem Grad der Verfettung der Glandula parotis ab.

**Fazit:** Bei der Diagnostik von Pathologien im Verlauf peripherer Gesichtsnerven liefern die hochauflösenden WATS und STIR Sequenzen wertvolle Zusatzinformationen sowohl präoperativ bei enger Lagebeziehung von Parotistumoren zum N. facialis sowie im Rahmen der Diagnostik der idiopathischen Trigeminusneuralgie.

## Literatur

1. Zuniga JR, Mistry C, Tikhonov I, Dessouky R, Chhabra A. Magnetic Resonance Neurography of Traumatic and Nontraumatic Peripheral Trigeminal Neuropathies. *J Oral Maxillofac Surg.* 2018;76(4):725–36.

186

## TRANSIENTES HIRNÖDEM UNTER ERHALTUNGSDIALYSE—UNTERSUCHUNGEN MIT STRUKTURELLER UND FUNKTIONELLER MRT

Matthias Schaefer<sup>1</sup>, Robert Christian Wolf<sup>2</sup>, Katharina Kubera<sup>2</sup>, Simon Nagel<sup>3</sup>, Andreas Bartsch<sup>4</sup>, Martin Zeier<sup>1</sup>, Martin Bendszus<sup>4</sup>, Christian Herweh<sup>\*4</sup>

<sup>1</sup>Medizinische Universitätsklinik, Universität Heidelberg, Nephrologie, Heidelberg, Deutschland

<sup>2</sup>Zentrum für Psychosoziale Medizin, Universität Heidelberg, Allgemeine Psychiatrie, Heidelberg, Deutschland

<sup>3</sup>Neurologische Universitätsklinik, Universität Heidelberg, Neurologie, Heidelberg, Deutschland

<sup>4</sup>Neurologische Universitätsklinik, Universität Heidelberg, Neuroradiologie, Heidelberg, Deutschland

**Hintergrund:** Hämodialyse kann, insbesondere initial, zu neurologischen Symptomen wie Kopfschmerzen und Schwindel bis hin zu einem Delir führen, dem sog. Hämodialyse-Dysequilibrium-Syndrom. Hierfür wird ein transientes, vasogenes Hirnödem verantwortlich gemacht. Dieses konnte unter solchen Bedingungen auch mit Diffusions-gew. MRT (DWI) nachgewiesen werden. Inwieweit es auch unter Erhaltungsdialyse bei neurologisch unauffälligen Patienten zu einem Hirnödem kommt, ist bislang ungeklärt.

**Methoden:** Acht Patienten mit chronischer Niereninsuffizienz (CNI) unter Erhaltungsdialyse (EHD) seit mindestens 6 Wochen wurden unmittelbar vor und nach einer Dialyse-Behandlung mit MRT incl. Diffusionstensor-Bildgebung (DTI) und struktureller T1-gew. Sequenzen untersucht. Es wurde eine TBSS (tract based spatial statistics)—Analyse sowie eine Voxel-basierte Morphometrie (VBM) durchgeführt. Außerdem wurden 8 gesunde Kontrollpersonen mit entsprechendem Alter und Geschlecht untersucht.

**Ergebnisse:** Bereits vor EHD waren die FA (fraktionale Anisotropie)- und AD (axiale Diffusivität)-Werte der Patienten signifikant reduziert. Nach Dialyse fiel die FA weiter ab, während axiale, radiale und mittlere Diffusivität (AD, RD & MD) im gesamten Marklager signifikant anstiegen ( $p < 0.025$ ). Gleichzeitig nahm das Marklager-Volumen zentral in der rechten Hemisphäre und im Splenium signifikant zu. Das Volumen der grauen Substanz war initial bei den Patienten im Vergleich zu den Kontrollen bds. insulär reduziert. Nach EHD kam es im anterioren mediofrontalen Kortex und im rostralen Cingulum bds. ( $p < 0.05$ ). Keiner der Patienten zeigte nach EHD neurologische Auffälligkeiten.

**Diskussion:** Wie aus früheren Studien bekannt, bestehen bei CNI-Patienten Zeichen einer chronischen axonalen Schädigung. Gleichzeitig kommt es unter der Erhaltungs-Dialyse zu einem reversiblen vasogenem Hirnödem auch ohne das Auftreten neurologischer Symptome, was bislang nicht gezeigt worden war. Dies zeigt die Relevanz des Untersuchungszeitpunktes solcher Studien. Die vorliegenden Ergebnisse sind vorläufig und in weiteren Studien sollten insbesondere mögliche neuropsychologische sowie langfristige Auswirkungen untersucht werden.

188

**EVALUATION DER STENT-RÖNTGENSICHTBARKEIT IN ABHÄNGIGKEIT DER MARKERSTRUKTUR**

Samuel Voß<sup>1</sup>, Andreas Ding<sup>2</sup>, Philipp Berg<sup>1</sup>, Cindy Lübeck<sup>1</sup>, Giorgio Cattaneo<sup>2</sup>, Robert Fryscht<sup>1</sup>, Oliver Beuing<sup>3</sup>

<sup>1</sup>Forschungscampus STIMULATE, Magdeburg, Deutschland

<sup>2</sup>Acandis GmbH—Engineering Stroke Solutions, Pforzheim, Deutschland

<sup>3</sup>Institut für Neuroradiologie, Universitätsklinikum Magdeburg, Magdeburg, Deutschland

**Hintergrund:** Die Röntgensichtbarkeit ist für die sichere Freisetzung von Stents zur Behandlung intrakranieller Aneurysmen wesentlich. Die üblichen punktförmigen Röntgenmarker an den Stent-Enden (Endmarker) werden zunehmend durch Marker über die gesamte Stentlänge (Längsmarker) ersetzt. Trotzdem bleibt die klare Differenzierung von proximalem und distalem Stent-Ende für die Positionierung entscheidend.

**Methoden:** Im Rahmen dieser Studie wurden ein DERIVO-Stent 3.5×20 mm (Acandis GmbH & Co KG) mit Endmarkern und eine Neuentwicklung mit Längsmarker (nicht für klinischen Einsatz, nicht käuflich erhältlich) hinsichtlich Röntgensichtbarkeit verglichen. Die Aufnahmen der Stents erfolgte mithilfe des C-Arm-CTs Artis Zeego (Siemens Healthineers AG), wobei diese in einem Schädelphantom platziert wurden. Die Variation des Aufnahmewinkels (7 Winkel) sowie der Bildauflösung (4 Stufen) resultieren in 28 2D-Aufnahmen pro Stent. Die Sichtbarkeit wurde durch einen in vaskulärer Bildgebung und Therapie langjährig erfahrenen Neuroradiologen bewertet.

**Ergebnisse:** Bei vorliegenden Endmarkern wurde das proximale und distale Stent-Ende jeweils zu 93% erfolgreich differenziert. Die Verwendung von Längsmarkern führt zu einer richtigen Differenzierung von 89% bzw. 82%. Zudem steigert die Sichtbarkeit des Stent-Korpus durch Längsmarker die Bewertung des Auffaltverhaltens.

**Diskussion:** Die Optimierung von Materialzusammensetzung und strukturellem Aufbau ermöglicht eine verbesserte Röntgensichtbarkeit

für eine sichere Aneurysma-Behandlung. In weiteren Schritten wird die Erkennung von Komplikationen bei der Freisetzung systematisch untersucht.

**Fazit:** Längsmarker unterstützen die Röntgensichtbarkeit bei der Freisetzung zerebraler Stents zur Behandlung von intrakraniellen Aneurysmen.

200

**MR-NEUROGRAPHIE ZUR CHARAKTERISIERUNG PERIPHERER NERVENLÄSIONEN BEI ALKOHOLINDUZIRTER POLYNEUROPATHIE IN KORRELATION MIT KLINISCHEN UND ELEKTROPHYSIOLOGISCHEN KRITERIEN**

Christian Rother\*<sup>1</sup>

<sup>1</sup>Klinik für Neuroradiologie, Universitätsklinikum Heidelberg, Heidelberg, Deutschland

**Hintergrund:** Ziel unserer Studie ist, mit Hilfe MR-neurographischer, klinischer und elektrophysiologischer Untersuchungsmethoden das Ausmaß, das Muster sowie die Lokalisation der Nervenschädigung bei Patienten mit alkoholinduzierter Polyneuropathie (ALN) zu identifizieren und zu quantifizieren. Dazu wurden 10 Patienten mit gesicherter ALN untersucht, als Kontrollgruppen dienten uns 10 alkoholranke Patienten ohne Polyneuropathie sowie 10 gesunde Probanden analogen Alters und Geschlechts.

**Methoden:** In den letzten Jahren konnte gezeigt werden, dass mit der Magnetresonanztomographie (MRT) als nicht-invasives Untersuchungsverfahren wertvolle Zusatzinformationen zur klinischen Untersuchung sowie den elektrophysiologischen Verfahren gewonnen werden können. Die diagnostische Wertigkeit und Validität der MRT konnte in umfassenden experimentellen und klinischen Studien belegt werden [1, 2].

**Ergebnisse:** Alle der 10 untersuchten Patienten mit elektrophysiologisch und klinisch gesicherter alkoholinduzierter Polyneuropathie zeigten in der MR-Neurographie ein polyneuropathietypisches Läsionsmuster mit Signalsteigerungen mehrerer Faszikel der Nervi ischiadicus, tibialis und peroneus. Wie in anderen Studien zur MR-Neurographie bei Polyneuropathien, zeigte sich ein proximales Verteilungsmuster der Nervenläsionen [3].

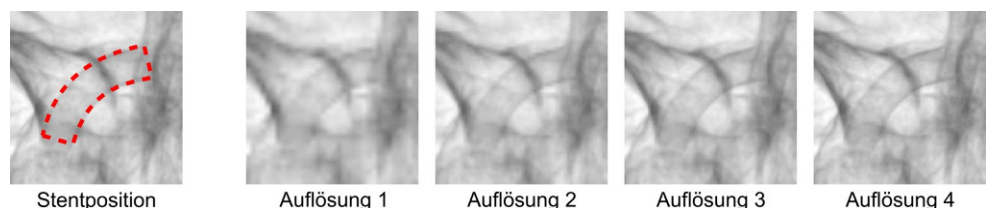
**Diskussion:** Mit Hilfe der MR-Neurographie könnte eine ALN in Zukunft schneller und zuverlässiger diagnostiziert werden. Weitergehende Studien mit größeren Fallzahlen sind notwendig, um die MR-morphologischen Veränderungen mit den klinischen und laborparametrischen Daten zu korrelieren.

**Fazit:** Unsere Studie zeigt, dass Nervenläsionen bei Patienten mit alkoholinduzierter Polyneuropathie mit Hilfe hochauflösender MR-Neurographie sichtbar gemacht werden können.

**Literatur**

1. Pham M, Oikonomou D, Hornung B, et al. Magnetic resonance neurography detects diabetic neuropathy early and with Proximal Predominance. *ann Neurol*. 2015;78(6):939–48. <https://doi.org/10.1002/ana.24524>.

**Abb. 1 | 188:** Bildausschnitt mit Markierung der Stentposition und Variation der Auflösung.



- Kollmer J, Sahn F, Hegenbart U, et al. Sural nerve injury in familial amyloid polyneuropathy. *Baillieres Clin Neurol*. 2017;89(5):475–84. <https://doi.org/10.1212/WNL.0000000000004178>.
- Kollmer J, Hund E, Hornung B, et al. In vivo detection of nerve injury in familial amyloid polyneuropathy by magnetic resonance neurography. 2015;201(4):549–62. <https://doi.org/10.1093/awu396>.

207

### CLINICAL IMPLEMENTATION OF MRI FOR DETECTION OF INFERIOR ALVEOLAR NERVE INVOLVEMENT IN COURSE OF MANDIBLE FRACTURE—A FEASIBILITY STUDY

Egon Burian\*<sup>1</sup>, Florian Probst<sup>2</sup>, Lisa Maier<sup>1</sup>, Claus Zimmer<sup>1</sup>, Lucas Ritschl<sup>3</sup>, Monika Probst<sup>1</sup>

<sup>1</sup>Department of Diagnostic and Interventional Neuroradiology, Klinikum rechts der Isar, Technische Universität München, München, Deutschland

<sup>2</sup>Department of Oral and Maxillofacial Surgery and Facial Plastic Surgery, LMU München, München, Deutschland

<sup>3</sup>Department of Oral and Maxillofacial Surgery and Facial Plastic Surgery, Klinikum rechts der Isar, Technical University of Munich, München, Deutschland

**Background:** Computed tomography (CT) or cone beam computed tomography (CBCT) are the gold standard in clinical traumatology imaging when structures of the head and neck region are involved. However, CT and CBCT harbor inherent limitations in regard of soft tissue visualization. In course of mandible fractures particularly the inferior alveolar nerve (IAN) is at risk for damage. The aim of this study was to assess the IAN pre- and postoperatively and correlate elevated signal-to-noise-ratios (SNR) with potential sensitivity impairment.

**Methods:** 10 patients suffering from a mandible fracture were examined on a 3T scanner. The conducted sequence protocol consisted of a 3D STIR, 3D WATS and a 3D T1 FFE “black bone”-sequence (15 min scan time). Nerve function was assessed as: normal, hypesthesia, anesthesia or allodynia.

**Results:** The 3D T1 FFE sequences allowed for fracture detection in all patients. The 3D STIR sequence showed the highest SNR with re-

gard to potential nerve damage ( $p < 0.05$ ). Besides same diagnostic accuracy in fracture detection like CT the direct visualization of neural structures was possible (Fig. 1). Positive clinical nerve testing correlated with physiological SNR.

**Discussion:** The study highlights the feasibility of MRI for fracture detection and affection of IAN. The applied sequence protocol showed comparable diagnostic power in detection mandible fractures as CT. Additionally, a reliable assessment of potential IAN damage with good correlation to clinical sensory testing could be achieved.

**Conclusion:** Applying the described sequence protocol allowed for precise fracture detection as well as reliable nerve damage assessment.

226

### MRI OF THE INFERIOR ALVEOLAR NERVE AND LINGUAL NERVE—BENCHMARK VALUES AND ANATOMICAL VARIETY IN HEALTHY SUBJECTS

Egon Burian\*<sup>1</sup>, Florian Probst<sup>2</sup>, Teresa Robl<sup>1</sup>, Claus Zimmer<sup>1</sup>, Lucas Ritschl<sup>3</sup>, Monika Probst<sup>1</sup>

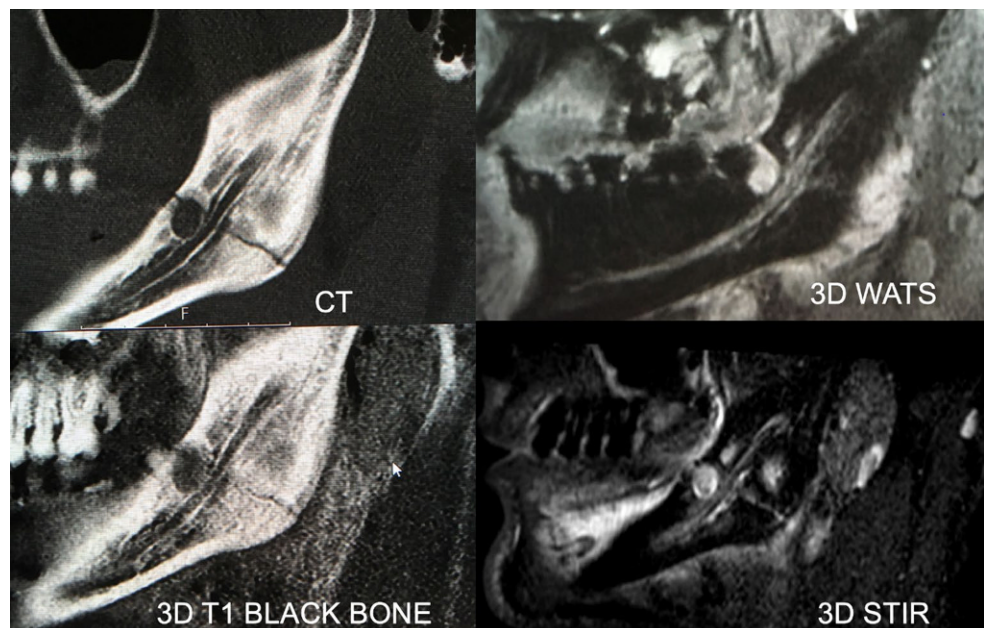
<sup>1</sup>Department of Diagnostic and Interventional Neuroradiology, Klinikum rechts der Isar, Technische Universität München, München, Deutschland

<sup>2</sup>Department of Oral and Maxillofacial Surgery and Facial Plastic Surgery, LMU München, München, Deutschland

<sup>3</sup>Department of Oral and Maxillofacial Surgery and Facial Plastic Surgery, Technische Universität München, München, Deutschland

**Background:** Radiation based imaging techniques like panoramic radiography, computed tomography (CT) or cone beam computed tomography (CBCT) are currently the standard for depicting the mandibular canal prior to surgical procedures. However, these modalities are lacking sufficient soft tissue visualization of the inferior alveolar nerve (IAN) and the lingual nerve (LN), which is particularly exposed to injury during wisdom tooth removal. Magnetic resonance imaging (MRI) using dedicated imaging sequences showed promising results in the direct visualization of the IAN and the LN with high spatial resolution and signal-to-noise-ratio (SNR) quantification. The aim of this study was to define standard specifications in MRI which allow for benchmark definition of SNR values in healthy subjects.

**Fig. 1 | 207** Fracture of the mandible depicted with CT and the conducted MRI protocol consisting of a 3D T1 TFE “black bone”, 3D WATS and 3D STIR sequence. IAN nerve continuity is preserved and SNR is within the physiological range (yellow arrow: IAN, blue arrow: vein). Scan time is 15 min



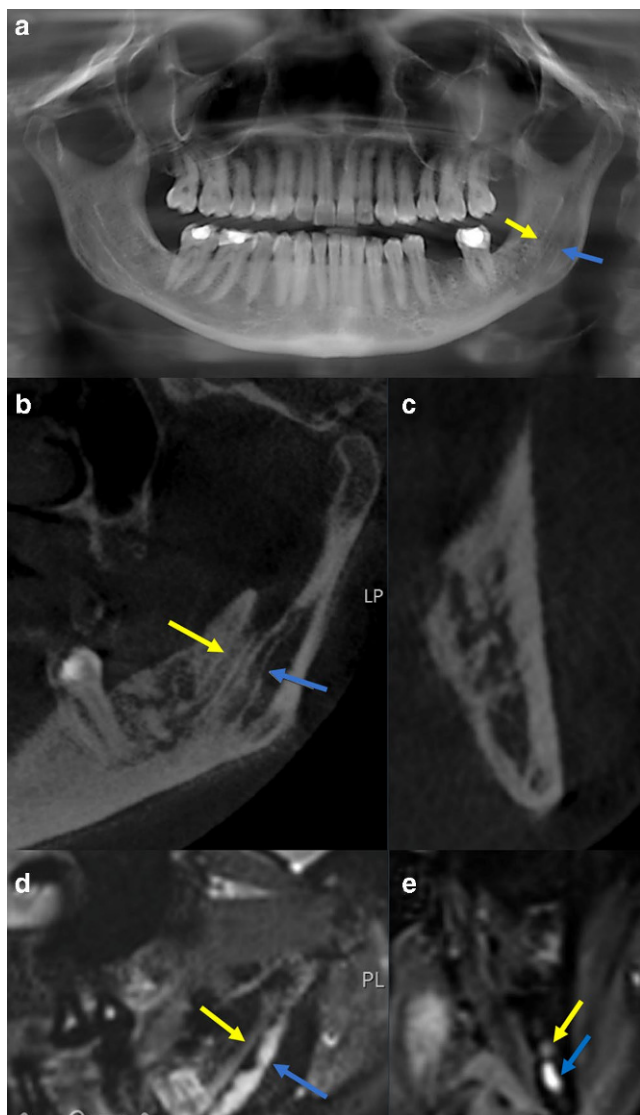


**Fig. 1 | 226.** a) panoramic radiograph, b and c) CBCT, d and e) STIR sequence; yellow arrow = IAN, blue arrow = vein

**Methods:** 33 healthy volunteers were examined on a 3T scanner. The conducted sequence protocol consisted of a 3D STIR, 3D WATS and a 3D T1 FFE “black bone”-sequence.

**Results:** The study highlights the feasibility of a direct visualization of proximal and peripheral branches of the IAN and proximal LN. STIR and WATS sequences allowed for morphological discrimination of neural and vascular components and their anatomical localization within the mandible. The STIR sequence showed significantly higher signal-to-noise-ratios for IAN as well as for the LN in the proximal and distal part of the corresponding nerves ( $p < 0.05$ ).

**Discussion:** The data presented in this study reveal, that a direct visualization of the course of the IAN and LN is feasible using high resolution STIR and WATS sequences. Furthermore, the imaging protocol conducted not only allowed for reproducible nerve diameter measurements but also for subsequent calculation of quantitative parameters like aSNR.

**Conclusion:** MRI using a dedicated sequence protocol allows for detection, nerve signal quantification and morphological characterization of the course of the IAN and the LN with its variant forms in healthy subjects.

**UNTERSUCHUNG EINES ULTRASCHNELLEN CMRT-PROTOKOLLS (5 MIN/5 SEQUENZEN) BEIM AKUTEN NEUROLOGISCHEN NOTFALL: SENSITIVITÄT, SPEZIFITÄT UND EINFLUSS AUF DIE THERAPIEENTSCHEIDUNG**

Olga Solyanik\*<sup>1</sup>, Philipp Kazmierczak<sup>1</sup>, Maximilian Patzig<sup>2</sup>, Robert Forbrig<sup>2</sup>, Max Dührsen<sup>1</sup>, Matthias Klein<sup>3</sup>, Wolfgang Kunz<sup>1</sup>, Jens Ricke<sup>1</sup>, Clemens Cyran<sup>1</sup>

<sup>1</sup>Klinik und Poliklinik für Radiologie, LMU, München, Deutschland

<sup>2</sup>Institut für Diagnostische und Interventionelle Neuroradiologie, LMU, München, Deutschland

<sup>3</sup>Neurologische Klinik und Poliklinik, LMU, München, Deutschland

**Hintergrund:** Die cMRT bietet einen deutlichen Vorteil in der neurologischen Differenzialdiagnostik, da sie einen höheren Weichteilkontrast als die cCT besitzt und somit eine höhere diagnostische Genauigkeit. Der Einsatz der cMRT in der neurologischen Notfalldiagnostik ist jedoch durch die lange Untersuchungszeit limitiert. Um adäquate Therapieentscheidungen treffen zu können, ist eine schnelle und hochauflösende Bildgebung essentiell. Ziel der Studie: Evaluation von Sensitivität und Spezifität eines 5 min/5 Sequenzen-cMRT-Protokolls zur Detektion intrakranieller Pathologien und des Einflusses auf die Therapieentscheidung beim akuten neurologischen Notfall.

**Methodens:** 449 Patienten mit akuter, nicht traumatisch bedingter neurologischer Symptomatik wurden für diese prospektive Studie evaluiert. 59 Patienten mit unauffälliger nativer cCT wurden eingeschlossen und im Anschluss an die CT am 3T-MRT untersucht. Zusätzlich zum cMRT-Kurzprotokoll (GoBrain, Siemens Healthineers: sag T1 GRE, ax T2 TSE, ax Flair, ax T2\* EPI-GRE, ax DWI SS-EPI; TA 5 min) wurde als Referenzstandard ein äquivalentes Standardprotokoll (TA 15 min) akquiriert. Zwei unabhängige verblindete Neuroradiologen bewerteten die Bildqualität auf einer 5-Punkte-Likert-Skala und befundeten die cMRT hinsichtlich intrakranieller Pathologien.

**Ergebnisse:** Verglichen mit der nativen cCT detektierte die Kurzprotokoll-cMRT 93 zusätzliche intrakranielle Läsionen (Läsionen insg.  $n = 125$ , akute Ischämie  $n = 21$ , Mikroblutung  $n = 27$ , Ödem  $n = 2$ , Marklagerläsion  $n = 38$ , alter Infarkt  $n = 3$ , sonstiges  $n = 2$ ; CT: Läsionen insg.  $n = 32$ ; Standardprotokoll:  $n = 133$ ). Die Bildqualität war dem Standardprotokoll nicht unterlegen (T2; Kurzprotokoll:  $4,04 \pm 0,331$ , Standardprotokoll  $3,93 \pm 0,262$ ,  $p = 0,083$ ) (Abb. 1). Das Kurzprotokoll zeigte eine hohe diagnostische Genauigkeit (Sen.:  $0,939 [0,881; 0,972]$ ; Spez.  $1,000 [0,895; 1,000]$ ) in der Detektion intrakranieller Pathologien und führte in 10% der Fälle zur Änderung der Therapieentscheidung verglichen mit CCT.

**Diskussion:** In 5 min erlaubt die Kurzprotokoll-cMRT eine zeitoptimierte und dem Standardprotokoll gleichwertige Diagnostik beim neurologischen Notfall. Sie besitzt direkten Einfluss auf die Therapieentscheidung und kann bei ausgewählten Patienten alternativ zur Notfall-cCT durchgeführt

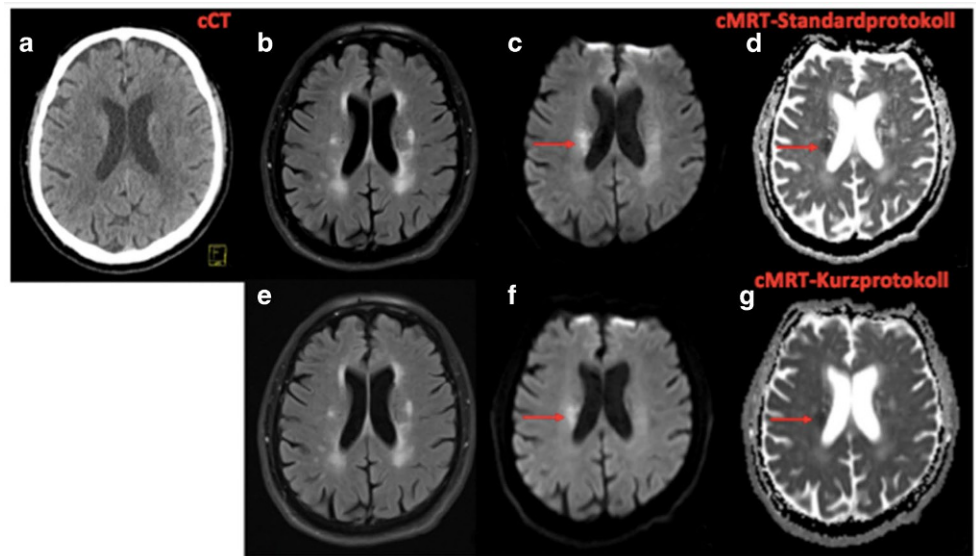
**Fazit:** Die 5 min Kurzprotokoll-cMRT ist eine adäquate und schnelle Alternative zur CCT für die Erkennung und Differenzialdiagnose intrakranieller Pathologien in akuten neurologischen Notfällen.

**OPTIMIERUNG KLINISCHER FMRT UNTERSUCHUNG DURCH DIE VERWENDUNG VON MULTIBAND EPI SEQUENZEN (SIMULTANEOUS MULTISLICE IMAGING TECHNIQUES—SMS)**

Christian Siedentopf\*<sup>1,2</sup>, Ruth Steiger<sup>1,2</sup>, Isabella Thurner<sup>1,2</sup>, Agnieszka Dabkowska-Mika<sup>1,2</sup>, Anja Ischebeck<sup>3</sup>, Elke Ruth Gizewski<sup>1,2</sup>

<sup>1</sup>Medizinische Universität Innsbruck, Neuroradiologie, Innsbruck, Österreich

**Fig. 1 | 229** a) Native CCT; b, e) FLAIR; c, f) DWI; d, g) ADC-Map des cMRT-Standardprotokolls (obere Reihe) und des cMRT-Kurzprotokolls (untere Reihe) bei einem 72-jährigen Mann mit Dysarthrie, Fazialisparese und Feinmotorikstörung links. Die CCT zeigte keine Zeichen einer frischen Ischämie oder Blutung. Die MR-Bilder zeigen einen akuten Infarkt in einer Capsula interna und in der Corona radiata rechts. Die Bildqualität des cMRT-Kurzprotokolls ist dem Standardprotokoll nicht unterlegen



<sup>2</sup>medizinische Universität Innsbruck, Neuroimaging Research Core Facility, Innsbruck, Österreich

<sup>3</sup>Institut für Psychologie, Universität Graz, Graz, Österreich

**Hintergrund:** Klinische fMRT Untersuchungen haben besonders bei der prächirurgischen Operationsplanung eine große Bedeutung erlangt. Besonders Bewegungsartefakte bei längerer Messzeit stellen ein großes Problem dar. Ziel der Studie war, ob die Verwendung von SMS Sequenzen zur Optimierung der verwendeten Paradigmen beitragen kann.

**Methoden:** An der Untersuchung nahmen 20 junge gesunde Probanden teil. Es wurde ein Standard fMRT Paradigma im Blockdesign (6 ON Blöcke) und ein motorisches Finger-Paradigma auf einem 3T MRT Siemens Skyra mit 64 Kanalspule die Single Shot EPI (SSE)-Sequenz mit einem TR von 2.5 s durchgeführt. Im Vergleich dazu die Multiband SMS Sequenzen mit einer TR von 1.25 s und 0.625 s. Die Auswertung erfolgte mit SPM 12 und Matlab R2018a. Das Blockdesignmodell wurde mit 6 ON Phasen ausgewertet und dann schrittweise jeweils um den letzten ON Block gekürzt bis auf eine Gesamtlänge von 2 ON Blöcken.

**Ergebnisse:** Es zeigten sich Aktivierungen im kontralateralen Handareal, der SMA sowie ipsilateral im Kleinhirn. Die SMS Sequenz zeigte eine signifikante Zunahme der Aktivierungsstärke (T-Werte) im Vergleich zur SSE Sequenz um bis zu 28,6%. Der T-Wert im Handareal bei der Berücksichtigung von nur 2 ON Blöcken bei SMS Sequenzen übertraf immer noch die T-Werte bei SSE Sequenz mit 6 ON Blöcken. Außerdem zeigt sich eine signifikante Abnahme der Clustergröße des Handareals bei Verwendung der SMS Sequenzen um bis zu 24,9% bei gleichzeitig stärkeren T Werten.

**Diskussion:** Die Verwendung von SMS Sequenzen führt zu einer signifikanten Zunahme der T Werte als Ausdruck einer robusteren Aktivierung bei besserer räumlicher Fokussierung. Bei einer Verkürzung des Paradigmas um 2/3 wird die Aktivierungsstärke der SSE Sequenz ohne Verkürzung übertroffen. Der so gewonnen Signalzugewinn kann in eine deutliche Verkürzung der Untersuchung ohne qualitative Einbußen investiert werden.

**Fazit:** Diese Messzeitverkürzung reduziert die Gefahr von Bewegungsartefakten deutlich, welche das Hauptproblem bei präoperativen fMRT Untersuchungen darstellt.

253

### VALIDATION OF A VIRTUAL ANEURYSM-CLIPPING SIMULATOR

Wolfgang Fenz<sup>\*1</sup>, Matthias Gmeiner<sup>2</sup>, Andreas Gruber<sup>2</sup>, Johannes Trenkler<sup>3</sup>, Michael Giretzlehner<sup>1</sup>

<sup>1</sup>RISC Software GmbH, Research Unit Medical Informatics, Hagenberg, Österreich

<sup>2</sup>Kepleruniversitätsklinikum Linz, Department of Neurosurgery, Linz, Österreich

<sup>3</sup>Kepleruniversitätsklinikum Linz, Department of Neuroradiology, Linz, Österreich

**Background:** Improving the quality and efficiency of neurosurgical education in a safe and realistic environment is highly desirable. The caseload reduction due to endovascular treatment options has led to remaining cerebral aneurysms being more complex. One way to alleviate this problem is the integration of a virtual surgical simulator for the training of both standard procedures and complex cases into resident education. Therefore, the aim of this study was to develop and evaluate a patient-specific virtual aneurysm-clipping simulator.

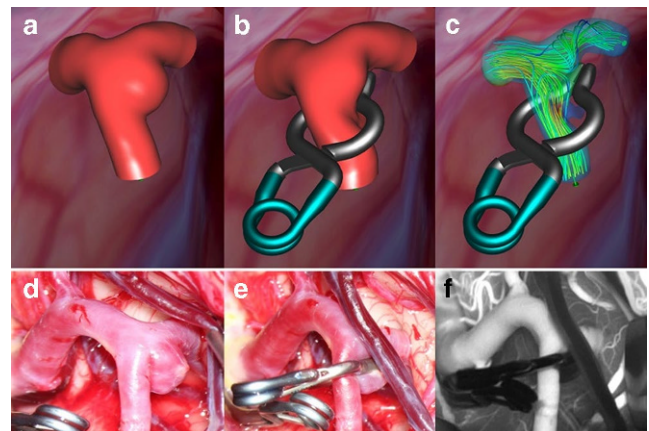


**Fig. 1 | 253** a, b Virtual cerebral aneurysm clipping using CTA data of a patient with right MCA bifurcation aneurysm; c Virtual blood flow simulation; d, e Microsurgical clipping with a ring clip; f ICG angiography showing complete occlusion of the aneurysm

**Methods:** A prototype simulator with haptic force feedback and real-time deformation of the aneurysm and vessels has been developed. Assessment of virtual clipping success via blood flow simulation was included in the system, and the prototype was evaluated by 18 neurosurgeons. Virtual clipping was performed after real-life surgery for four patients with different medial cerebral artery (MCA) aneurysms, and the surgical results were compared with respect to clip application, surgical trajectory, and blood flow.

**Result:** After positioning the patient's head and performing a virtual craniotomy, bimanual virtual aneurysm clipping was carried out using an original forceps attached to a haptic device. Residual aneurysm filling and branch stenosis was analyzed with blood flow simulation. 89% of the surveyed neurosurgeons said that the simulator improved anatomic understanding. Simulation of head positioning and craniotomy was considered realistic by 89% and 94% of users, respectively. Most participants agreed that the simulator should be integrated into neurosurgical education (94%).

**Discussion:** Using four illustrative cases, we show that virtual aneurysm surgery was possible via the same trajectory as in the real-life cases. In the case of broad-based aneurysms, both virtual clipping and blood flow simulation yielded realistic results, whereas for calcified aneurysms, virtual clipping could be performed using the same surgical trajectory, but not the same clip type.

**Conclusion:** We have successfully developed a virtual aneurysm-clipping simulator. Next, the prototype will be further improved and integrated into a hybrid simulation system. In its final form, it will also be applicable for surgical procedure planning.

267

#### EFFECTS OF ACUTE ALCOHOL INTOXICATION ON CEREBRAL WATER CONTENT

Johanna Furtmann<sup>\*1</sup>, Thorsten Sichtermann<sup>1</sup>, Ana Maria Oros-Peusquens<sup>2</sup>, Martin Wiesmann<sup>1</sup>, Nadim Jon Shah<sup>2</sup>, Omid Nikoubashmann<sup>1</sup>

<sup>1</sup>Klinik für diagnostische und interventionelle Neuroradiologie, Uniklinik RWTH Aachen, Aachen, Deutschland

<sup>2</sup>Institute of Neuroscience and Medicine 4, Forschungszentrum Jülich, Jülich, Deutschland

**Background:** Alcohol consumption influences the water balance in the brain. While the impact of chronic alcohol abuse on cerebral water content has been subject of several studies, less is known about the effects of acute alcohol abuse, with contradictory results in the literature. Therefore, we investigated the effects of acute alcohol abuse on cerebral water content using a precise quantitative MRI sequence.

**Methods:** In a prospective study we measured cerebral water content in 20 healthy volunteers before alcohol consumption and after reaching a breath alcohol concentration (BrAC) of 1‰. A quantitative MRI water mapping sequence was conducted on a clinical 3 T system. Non-alcoholic fluid in- and output were documented and accounted for. Water content was assessed for whole brain, grey and white matter and more specifically for regions known to be affected by acute or chronic alcohol abuse (occipital and frontal lobes, thalamus, and pons).

**Result:** Quantitative cerebral water content before and after acute alcohol consumption did not differ significantly ( $p \geq 0.083$ ) with changes being within the range of measurement inaccuracy.

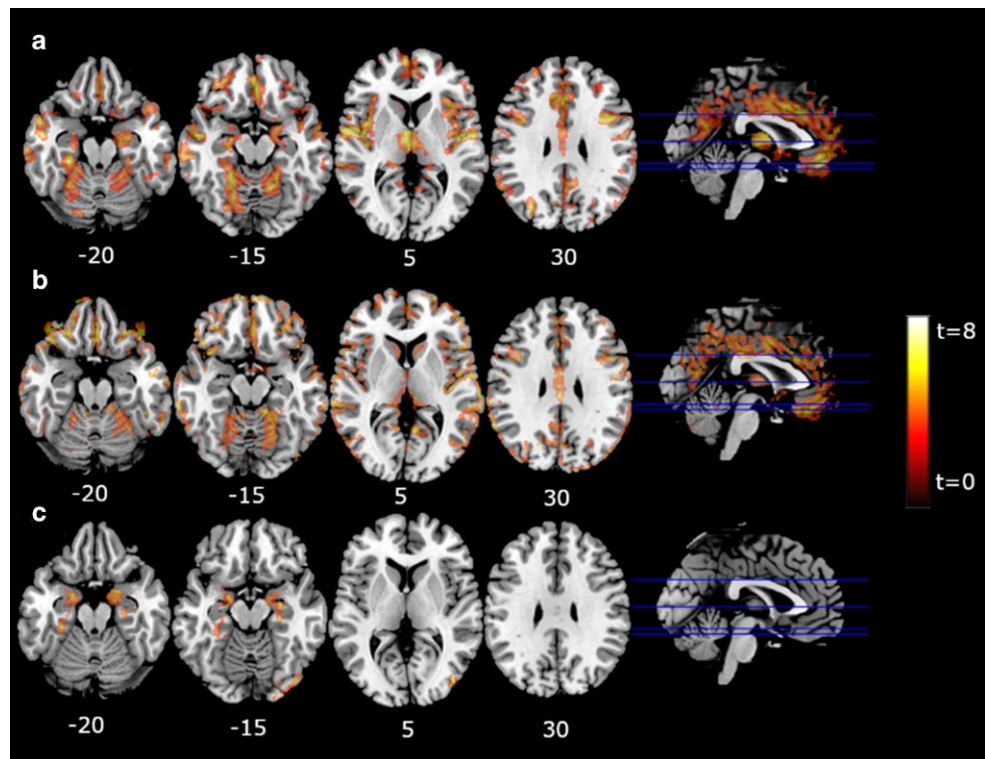
**Conclusion:** The results of our study show no significant water content change in the brain after recent alcohol intake in healthy volunteers. This accounts for the whole brain, grey and white matter, occipital and frontal lobes, thalamus, and pons.

268

#### BRAIN ALTERATIONS IN GIRLS WITH ANOREXIA NERVOSA AFTER SHORT-TERM COMBINED HIGH CALORIC AND PSYCHOTHERAPY

Lukas Lenhart<sup>\*1</sup>, Ruth Steiger<sup>1</sup>, Agnieszka Dabkowska<sup>1</sup>, Nina Haid-Stecher<sup>1</sup>, Kathrin Sevecke<sup>1</sup>, Elke Gizewski<sup>1</sup>

**Fig. 1 | 268** GM differences in AN patients ( $P < 0.001$ , FWE-corrected); **a** decreases in AN compared to HC pre therapy; **b** increases in AN pre to post therapy; **c** GM regions post therapy associated with BMI



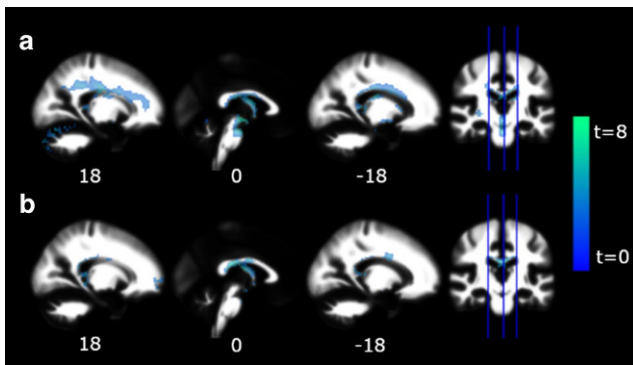


**Fig. 2 | 268** FA differences in AN patients; **a**) decreases in AN compared to HC pre therapy ( $P < 0.001$ , FWE-corrected); **b**) increases in AN pre to post therapy ( $P = 0.002$ , FWE-corrected)

<sup>1</sup>Medical University of Innsbruck, Department of Neuroradiology, Innsbruck, Österreich

**Background:** Anorexia nervosa (AN) is characterized by an abnormally low bodyweight, intense fear of weight gain and a distorted body perception. Previous studies reported significant grey matter (GM) and DTI alterations in underweight girls. However, brain regions that are critically involved in the pathophysiology of AN have not been clearly elucidated. We aimed to examine structural brain changes in a cohort of AN patients before and after short-term high caloric and psychotherapy.

**Methods:** 3T MRI, including a high-resolution T1 MPRAGE and fractional anisotropy (FA) sequences, was performed in 15 girls with AN (mean age:  $16 \pm 1.3$  years) pre and post therapy (mean duration:  $2.6 \pm 1$  months) and compared to 18 age and gender matched healthy controls (HC). SPM 12 was used to assess cross-sectional differences pre therapy and longitudinal changes after therapy. Resulting statistical maps were corrected for multiple comparisons via the FWE-method at  $P < 0.05$  level with a height-threshold set to  $P < 0.001$ .

**Result:** The global GM volume was lower in patients with AN ( $588.8 \pm 60.3 \text{ cm}^3$ ) compared to HC ( $665.1 \pm 41.1 \text{ cm}^3$ ) by approximately 13%. SPM localized GM decreases in extensive cortical areas including the insula, the prefrontal cortices, the cingulate gyrus as well as subcortical regions compared to HC ( $P < 0.001$ ), which partially increased post therapy with a relative sparing of the hippocampus and the amygdala ( $P < 0.001$ ). BMI elevations were associated with GM increases in the hippocampus, the parahippocampal gyrus and the amygdala bilaterally ( $P < 0.001$ ). Pre therapy, FA reductions were evident in the fornix and the corpus callosum, as well as white matter regions of

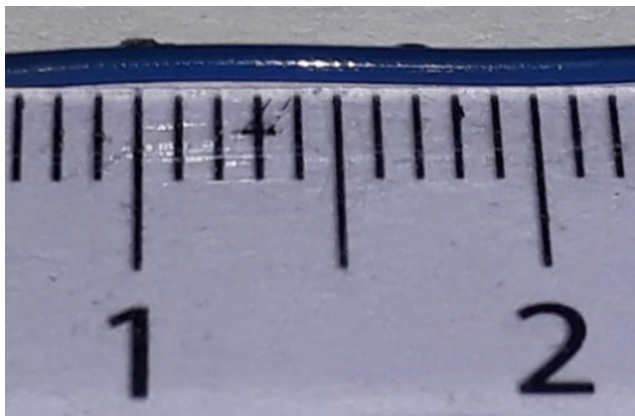


**Abb. 1 | 269**

the thalamus, the midbrain and the pons ( $P < 0.001$ ), which increased in the corpus callosum and the fornix post therapy ( $P < 0.002$ ).

**Discussion:** These findings suggest that adolescents with AN cortical GM atrophy and FA abnormalities mainly recover after combined high caloric and psychotherapy and that BMI elevations predominantly predict GM increases of subcortical regions, namely the hippocampus, the parahippocampal gyrus and the amygdala.

**Conclusion:** Weight-dependent GM and FA increases may be linked to symptom improvement.

**269**

### MIKROKATHETER-ROTATION BEI RÜCKZUG IN DER DISTALEN ACI

Bernd Turowski<sup>\*1</sup>, Christian Rubbert<sup>2,3</sup>, Andres Braschkat<sup>4</sup>, Julian Caspers<sup>3</sup>

<sup>1</sup>Diagnostische und Interventionelle Radiologie, Universitätsklinikum Düsseldorf, Neuroradiologie, Düsseldorf, Deutschland

<sup>2</sup>Diagnostische und Interventionelle Radiologie, Universitätsklinikum Düsseldorf, Düsseldorf, Deutschland

<sup>3</sup>Diagnostische und Interventionelle Radiologie, Universitätsklinikum Düsseldorf, Neuroradiologie, Düsseldorf, Deutschland

<sup>4</sup>Acandis, Pforzheim, Deutschland

**Hintergrund:** Bei Freisetzung langer geflochtener Stents in kaliberschwankenden und sehr kurvigen komplexen Gefäßanatomien kommt es häufig zu Problemen. Während ein Stent sich in geraden Gefäßen immer vollständig öffnet, kommt es bei komplexer Anatomie in vivo wie auch in vitro zu mangelhafter Öffnung mit fehlender Wandadaptation.

Stent und Mikrokatheter bilden eine dynamische Einheit. Während die mechanischen Eigenschaften geflochtener Stents untersucht sind, gibt es keine Analysen zur Dynamik des freisetzenden Mikrokatheters. Entsteht beim Rückzug eines Mikrokatheters neben der axialen Bewegung auch eine Rotationskomponente, die erhebliche Implikationen für die Freisetzung geflochtener Stents haben könnte?

**Methoden:** Ein Neuroslider-27-Mikrokatheter wurde mit 7 röntgengedichten Markierungen im Abstand von ca. 7 mm in einer Linie außen am distalen Ende markiert (Abb. 1). Der Katheter wurde im 3-D-Silikonmodell einer in vivo sehr komplexen distalen ACI-Anatomie (Abb. 2) positioniert. Mit 15 Bildern pro Sekunde wurden mehrere Angiographieserien unter Rückzug des Mikrokatheters sowohl mit innenliegendem Mikrodraht wie auch ohne Mikrodraht angefertigt.

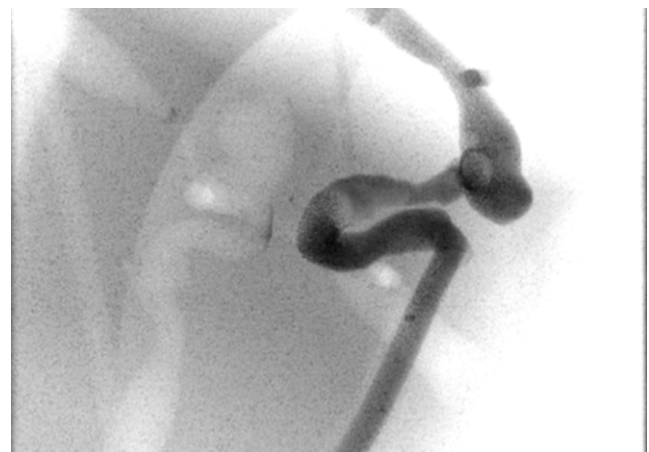
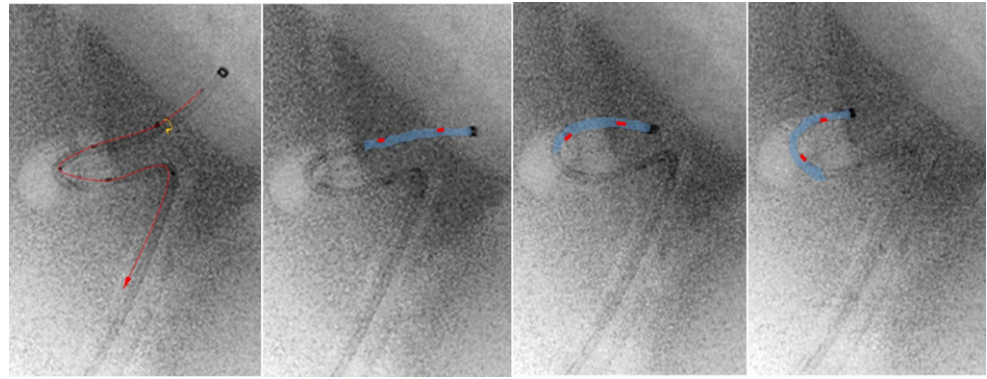


**Abb. 2 | 269**

Abb. 3 | 269



**Ergebnisse:** Beim Rückzug des Mikrokatheters durch Gefäßkurven bewegen sich die außen auf dem Mikrokatheter aufgetragenen Markierungen von der Oberseite des Mikrokatheters auf die Unterseite. Das beweist eine 180°-Drehung um die Längsachse—also eine halbe Drehung. In der nächsten Kurve erfolgt eine erneute 180°-Drehung. Es gibt keinen Unterschied zwischen Serien mit und ohne einliegenden Mikrodraht.

**Diskussion:** Es wurden viele Aspekte mangelnder Wandadaptation und sekundärer Verschlüsse insbesondere von “flow divertern” diskutiert. Die hier nachgewiesene erhebliche Rotationsbewegung ist im Zusammenhang der zirkulären Anordnung der Drähte eines geflochtenen Stents möglicherweise relevant.

**Fazit:** Torsionskräfte unter Freisetzung sollten Bestandteil zukünftiger Überlegungen sein. Es bleibt zu untersuchen, welche mechanischen Folgen die Rotation des Mikrokatheters von 180° während der Stent-Freisetzung für die Entfaltung eines geflochtenen Stents hat.

270

### BRAIN VOLUME IS REDUCED IN AMATEUR BOXERS AS COMPARED TO HEALTHY AGE-MATCHED CONTROLS

Jessica Jesser<sup>\*1</sup>, Moussa Zeidan<sup>2</sup>, Christian Herweh<sup>2</sup>, Joachim Jost<sup>3</sup>, Sabine Heiland<sup>2</sup>, Uta Meyding-Lamadé<sup>4</sup>, Martin Bendszus<sup>2</sup>, Stefan Hähnel<sup>2</sup>

<sup>1</sup>Universitätsklinikum Heidelberg, Neuroradiologie, Heidelberg, Deutschland

<sup>3</sup>Olympiastützpunkt Rhein-Neckar, Sportmedizinischer Bereich, Heidelberg, Deutschland

<sup>4</sup>Neurologische Klinik, Krankenhaus Nordwest GmbH, Frankfurt am Main, Deutschland

**Background:** Traumatic brain injuries (TBI) sustained during contact sports are being found to have long-term sequelae, being strongly linked to an increased risk of developing dementia and Alzheimer’s disease like pathologies<sup>1</sup>.

For this study we compared volumes of anatomical structures of the brain between amateur boxers and age-matched control subjects.

**Methods:** 19 amateur boxers and 19 age-matched healthy controls underwent 3T high-resolution magnetic resonance (MR) imaging. The 3D MPRAGE images were analysed using volBrain (<https://volbrain.upv.es>) to measure the volumes of the cerebral cortex, white matter, lateral ventricles and the subcortical nuclei. Statistical analysis was performed using SPSS v.25.0 software (IBM, Chicago, IL, USA).

**Results:** Total brain volume was lower in boxers as compared to controls ( $\Delta\text{rel}=7\%$ ,  $p<0.05$ ). Accordingly global cerebral grey ( $\Delta\text{rel}=6\%$ ,  $p<0.05$ ) and white matter ( $\Delta\text{rel}=9\%$ ,  $p<0.05$ ) volumes differed significantly.

Volumes of the thalamus ( $\Delta\text{rel}=8\%$ ,  $p<0.05$ ), caudate nucleus ( $\Delta\text{rel}=11\%$ ,  $p<0.05$ ), putamen ( $\Delta\text{rel}=8\%$ ,  $p<0.05$ ), globus pallidus ( $\Delta\text{rel}=9\%$ ,  $p<0.05$ ) and nucleus accumbens ( $\Delta\text{rel}=14\%$ ,  $p<0.05$ ) were lower in boxers compared to controls.

**Discussion:** To our knowledge, this is the first prospective and systematic study on brain volume in amateur boxers as compared with age-matched non-boxing controls. Our results are largely in line with other studies dealing with TBI<sup>1</sup>. We found, that brain volume regarding grey and white matter was reduced in amateur boxers as compared to controls. The most severely affected structures were cerebral white matter, caudate nucleus and nucleus accumbens. Axonal injury with consecutive neuronal loss are the most important pathologies of TBI<sup>2</sup>. Further, e. g. longitudinal, studies are needed to gain knowledge about the pathophysiological causes and the damage pattern of the diminished brain volume in boxers.

**Conclusion:** Comparing the volume of anatomical structures of the brain between amateur boxers and healthy age-matched controls we found significant differences affecting the white matter but also specific subcortical structures as the caudate nucleus and nucleus accumbens.

### References

1. Herweh C, et al. Reduced White Matter Integrity in Amateur Boxers. *Neuroradiology*. 2016;58(9):911–20. <https://doi.org/10.1007/s00234-016-1705-y>.
2. Ng TSC, et al. Neuroimaging in repetitive brain trauma. *Alzheimer’s Res Ther*. 2014;6(1):24–10. <https://doi.org/10.1186/alzrt239>.

284

### INVESTIGATING THE MYELINATION IN CHILDREN USING QUANTITATIVE T2 MAPPING

Milène Bürger<sup>\*1</sup>, Ulrich Pilatus<sup>1</sup>, Alina Jurcoane<sup>1</sup>, Ralf Deichmann<sup>2</sup>, Elke Hattingen<sup>1</sup>, Luciana Porto<sup>1</sup>

<sup>1</sup>Institute of Neuroradiology-University Hospital Frankfurt, Frankfurt am Main, Deutschland

<sup>2</sup>Brain Imaging Center Goethe University Frankfurt, Frankfurt am Main, Deutschland

**Background:** This study investigates the age-related development of myelin in healthy children using quantitative T2 mapping. In conventional T2 weighted imaging, changes are often only obvious until the age of two. The areas to myelinate last, the so-called terminal zones, were so far only described in conventional MRI. We chose these zones to observe their myelination through quantitative T2 mapping.

**Methods:** We studied T2 maps, generated by a 1.5T MRI of 13 subjects aged between 2 and 12 years. We measured T2 relaxation times in 8 different regions of interest (ROI) in the white matter of each hem-

isphere: frontal/temporal deep and subcortical, parietal, occipital, corpus callosum and peritrigonal.

**Result:** In all ROI except the corpus callosum, T2 times decreased with increasing age (pearson  $r < -0,7$ ,  $p < 0,05$ ). A monoexponential function fitted the T2 decrease best. Absolute T2 values were highest in the subcortical frontal ROI (max. 97 ms). The negative slopes of the function were steepest in the subcortical frontal ROI followed by the subcortical temporal ROI, indicating a more pronounced persistent myelination in those regions. While high T2 relaxation times could be measured in the peritrigonal zone, the exponential curve did not show a steep decrease which may indicate a slower myelination. The steepness of the T2 curve increased from the parietal, occipital and temporal up to the frontal lobes in this order. Afterwards the subcortical ROI myelinated, first temporal then frontal.

**Conclusion:** The signal changes related to myelination can be better defined after the 2nd year of life in the form of T2 relaxation time decrease correlated with increasing age. T2 mapping may provide a normal reference to pathologically altered development of myelin. The highest T2 values and the steepest slope of the exponential function were located in the subcortical frontal region, indicating a faster and therefore not yet completed myelination. The terminal zones in quantitative T2 mapping were found in the subcortical areas however not in the peritrigonal zone.

## References

1. Ding XQ, Kucinski T, Wittkugel O, et al. Normal brain maturation characterized with age-related T2 relaxation times: an attempt to develop a quantitative imaging measure for clinical use. *Invest Radiol.* 2004;39(12):740–6.
2. Liu C, Jin C, Jian Z, et al. Assessment of myelination progression in subcortical white matter of children aged 6–48 months using T2-weighted imaging. *Neuroradiology.* 2018;60(12):1343–51.

294

## A RARE CASE OF BILATERAL TEMPOROMESIAL POLYMICROGYRIA

Finn Drescher\*<sup>1</sup>, Annika Kowoll<sup>1</sup>, Sebastian Fischer<sup>1</sup>, Jörg Wellmer<sup>2</sup>, Werner Weber<sup>1</sup>

<sup>1</sup>Ruhr-Universität Bochum- Universitätsklinikum Knappschafts-Krankenhaus, Institut für Diagnostische Radiologie und Interventionelle Radiologie, Neuroradiologie und Nuklearmedizin, Bochum, Deutschland

<sup>2</sup>Ruhr-Universität Bochum- Universitätsklinikum Knappschafts-Krankenhaus, Klinik für Neurologie, Ruhr-Epileptologie, Bochum, Deutschland

**Background:** Hippocampal abnormalities are a heterogeneous group of brain abnormalities recognized as a cause of epilepsy [1]. Bilateral temporomesial polymicrogyria is an extremely rare finding marked by an irregular brain surface with multiple folded small gyri [2].

**Methods:** Clinical records and brain MRI studies of a 28-year female patient with a history of epilepsy were retrospectively reviewed.

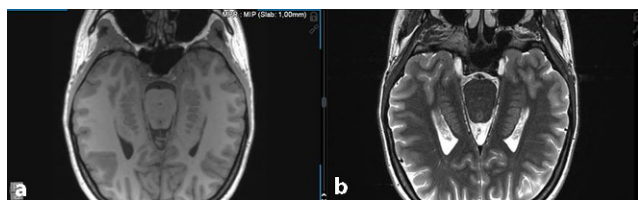


**Fig. 1 | 294** Magnetic resonance images (a) T1 axial reconstruction images and (b) T2 axial images

A cerebral MRI study was performed using a 3T MRI (Siemens Prisma, Erlangen, Germany) using a 64-channel headcoil including 3D-T1 MPR, 3D-FLAIR, T2 TSE coronal and transversal sequences.

**Result:** We report the case of a 28-year old female patient with a history of epilepsy with a manifestation age of 6 years with periods of absences. Pregnancy, delivery and early milestones were uneventful. The patient shows normal intelligence.

The patient was admitted to our Interdisciplinary Epilepsy Neuro-radiology Ambulance (IENA) in May 2019 for further clinical and MRI evaluation. Neurological and neuropsychological examinations were normal. EEG recordings showed no convincing epileptic discharges.

The MRI shows a symmetric temporomesial thickening of the cortex in the hippocampal gyrus bilaterally. There are no other suspicious findings observed on MRI. The fornix and the neocortex were morphologically normal.

**Discussion:** Bilateral temporomesial polymicrogyria is an extremely rare finding of hippocampal abnormality. Approximately 50 percent of patients with polymicrogyria have epilepsy [3]. Generally bilateral polymicrogyria have been considered sporadic although some familial cases have been reported. In this case we report the case of a young female patient with epilepsy finding of bilateral temporomesial polymicrogyria as a possible cause for the patient symptoms.

**Conclusion:** We report about a rare case of bilateral temporomesial polymicrogyria in a 28-year old female patient as cause for structural epilepsy.

## References

1. Barkovich AJ, Kuzniecky RI, Jackson GD. A developmental and genetic classification for malformations of cortical development. *Baillieres Clin Neurol.* 2005;65(12):1873–87.
2. Kuchukhidze G, Helbok R, Unterberger I, et al. Bilateral mesial temporal polymicrogyria: a case report. *J Neurol Neurosurg Psychiatry.* 2008;.
3. Barkovich AJ, Hevner R, Guerrini R. Syndromes of bilateral symmetrical polymicrogyria. *Am J Neuroradiol.* 1999;20:1814–21.

299

## ANGIOGENESIS IN UNTREATED AND IN PARTIALLY EMBOLIZED VEIN OF GALEN MALFORMATIONS

Dan Meila\*<sup>1,2</sup>, Alejandro Berenstein<sup>3</sup>

<sup>1</sup>Medizinische Hochschule Hannover, Hannover, Deutschland

<sup>2</sup>Johanna Etienne Krankenhaus, Neuss, Deutschland

<sup>3</sup>Mount Sinai Hospital, New York, United States

**Hintergrund:** In up to 30% Vein of Galen Malformation (VGM) cases DAVF development occurs. Delayed and incomplete treatment leads to additional transdural supply resulting in dural fistulas in VGM. Angiogenesis certainly plays a role. Do identify the role of pial angioarchitecture in this context.

**Methoden:** Retrospective single center data review of 120 VGM cases. Diagnosis period: 30 fetus, 42 neonates, 37 infants, 11 children. Statistical bias due to “referral center” with transferred delayed cases and partially embolized cases.

**Ergebnisse:** 14 of 120 (12%) cases identified in which angiogenesis occurred without any treatment before. 18 of 120 (15%) cases identified in which angiogenesis developed after treatment.

**Diskussion:** Reasons/trigger for angiogenesis: No treatment, delayed treatment and partial treatment. All points make a complete and definitive embolization much more difficult and time consuming.

**Fazit:** Avoid dogmatic waiting period, especially not for several years. Clinical correlation (head circumference, prominent veins) alone is not enough. Decision on an individual basis with close MRI and MRA follow-up. Goal must be curative 100% closure of all fistulas in VGM.

**References**

1. Berenstein A, Paramasivam S, Sorscher M, Molofsky W, Meila D, Ghatan S. Vein of Galen Aneurysmal Malformation: Advances in Management and Endovascular treatment. *Neurosurgery*. 2019;1:84(2):469–78. Feb.
2. Buell TJ, Ding D, Starke RM, Webster Crowley R, Liu KC. Embolization-induced angiogenesis in cerebral arteriovenous malformations. *J Clin Neurosci*. 2014;21(11):1866–71. Nov.

305

**ESTIMATION OF LESION AGE IN STROKE PATIENTS—DIRECT COMPARISON OF NON-CONTRAST ENHANCED COMPUTED TOMOGRAPHY—TO DWI-FLAIR MISMATCH**

Hannes Leischner<sup>1</sup>, Maximilian Groffmann<sup>1</sup>, Andre Kemmling<sup>2</sup>, Jens Fiehler<sup>1</sup>, Fabian Flottmann<sup>1</sup>, Uta Hanning<sup>1</sup>, Gabriel Broocks<sup>1</sup>

<sup>1</sup>Universitätsklinikum Hamburg-Eppendorf, Hamburg, Deutschland

<sup>2</sup>UK Münster, Münster, Deutschland

**Hintergrund:** In recent studies, magnetic resonance imaging (MRI) has been used to estimate lesion age in patients with wake-up stroke to enable thrombolytic therapy. However, MRI has a limited availability and feasibility, and is more time-consuming in the acute situation. As ischemic changes of the cerebral parenchyma can be detected on non-contrast enhanced computed tomography (NECT), we hypothesized that in direct comparison of the two modalities, NECT is equally sensitive and specific than MRI in identifying patients with lesion age <4.5 hours from symptom onset.

**Methoden:** 41 patients with acute anterior circulation stroke were analyzed with both imaging modalities at admission. Mismatch between diffusion-weighted MRI (DWI) and fluid-attenuated inversion recovery (FLAIR) was diagnosed by consensus reading according to the criteria of the WAKE-UP trial. NECT were analyzed for signs of ischemic parenchymal changes (loss of grey-white matter differentiation, hypattenuation of deep nuclei, cortical hypodensity with associated parenchymal swelling and gyral effacement), in a blinded approach by two experienced neuroradiologists. If ischemic parenchymal changes were detected, the patients were assigned to the group of >4.5 hours from onset and vice versa.

**Ergebnisse:** In 17 patients, the time from symptom onset to CT imaging was <4.5 h and 24 patients presented >4.5 h (range: 0.5–7.6 h). The median time from CT to MRI was 36 minutes (IQR: 24–55). DWI-FLAIR mismatch correctly assigned 28/41 patients (68%) with a sensitivity of 70% (95%CI: 51–85%) and specificity of 72% (95%CI: 47–90%). NECT analysis correctly assigned 30/41 (75%) with a sensitivity of 72% (95%CI: 69–91%) and specificity of 79% (95%CI: 53–90%).

**Fazit:** In this cohort, analysis of NECT was comparable to DWI-FLAIR mismatch in identifying patients within thrombolysis time window. Thus, future trials and a larger patient cohort are needed to investigate if NECT can be used to stratify wake-up stroke instead of MRI.

312

**VSI FÜR PLANUNGEN VON OPERATIONEN UND INTERVENTIONEN, NAVIGATION UND PATIENTENAUFKLÄRUNG**

Patrick House\*<sup>1</sup>, Sirko Pelzl<sup>2</sup>

<sup>1</sup>Epilepsiezentrum Hamburg, Ev. Krankenhaus Alsterdorf, Hamburg, Deutschland

<sup>2</sup>apoQlar GmbH, Hamburg, Deutschland

**Hintergrund:** Mit Virtual Surgery Intelligence (VSI, [www.vsi.health](http://www.vsi.health)) lassen sich MRTs und CTs durch eine Mixed Reality Brille 3-dimensional mit beliebiger Perspektive als Projektion im Raum betrachten.



Abb. 1 | 312



Abb. 2 | 312

Aufgrund der 3-Dimensionalität können Chirurgen und Neuroradiologen hiermit Operationen und Interventionen plastischer planen.

Intraoperativ kann der Chirurg nach automatischer Abtastung der Patienten-Oberfläche das 3-dimensionale MRT/CT passgenau auf den Patienten projizieren, um eine exakte Navigation zu ermöglichen. Während der Operation können Screenshots und Videos vom VSI-Sichtfeld gespeichert oder auch telemetrisch live an andernorts befindliche Kollegen oder Studenten übertragen werden.

Eine VSI-gestützte Navigation bei neuroradiologischen Interventionen ist aktuell in konzeptioneller Planung.

Tragen Arzt und Patient beide eine Mixed Reality Brille, kann der Arzt mit Hilfe des VSI seinen Patienten plastisch und laienverständlich über die bevorstehende Operation mit Demonstration der anatomischen Verhältnisse inklusive des OP-Zugangs und mit postoperativen Beispiel-MRTs/CTs aufklären. Dabei kann der Arzt in die Projektion virtuell hineinzeichnen.

**Methoden:** Navigation (VSI Surgery): um die hohe Präzision der Überlappung von Patient und Projektion für die intraoperative Navigation zu belegen, laufen derzeit zwei prospektive Studien in der Rechtsmedizin des Universitätskrankenhauses Hamburg-Eppendorf und in der Neurochirurgie des Leeds NHS Hospital.

**Patientenaufklärung (VSI Patient Education):** in einer abgeschlossenen prospektiven, randomisierten und kontrollierten klinischen Studie am Epilepsiezentrum Hamburg (House et al. 2019) wurde an 15 zu operierenden Patienten (13 Resektionen, 1 Implantation von ANT-DBS-Tiefenelektroden, 1 Implantation von Tiefenelektroden vor Stereo-EEG-Ableitung) untersucht, ob bei OP-Aufklärungen der VSI einem Kunststoff-Gehirnmodell überlegen ist.

**Ergebnisse:** Navigation (VSI Surgery): Erste Ergebnisse werden 10/2019 erwartet.

**Patientenaufklärung (VSI Patient Education):** die Patienten gaben in Fragebögen signifikant häufiger an, dass die Aufklärung mittels VSI für sie bildlich besser vorstellbar war, und sie bevorzugten hochsignifikant die VSI-Aufklärung im Vergleich zum Gehirnmodell.

**Fazit:** VSI ist eine vielversprechende Bereicherung für Chirurgen und Neuroradiologen hinsichtlich Planungen von Operationen und Interventionen, Navigation und Patientenaufklärung.

321

## EVALUATING COMPRESSED SENSE ACCELERATION FOR QUANTITATIVE MAPPING OF

### LONGITUDINAL RELAXATION RATE R1

Ronja Berg\*<sup>1</sup>, Stephan Kaczmarz<sup>1</sup>, Tobias Leutritz<sup>2</sup>, Claus Zimmer<sup>1</sup>, Christine Preibisch<sup>1</sup>

<sup>1</sup> Klinikum rechts der Isar der Technischen Universität München, Abteilung für Neuroradiologie, München, Deutschland

<sup>2</sup> Max-Planck-Institut für Kognitions- und Neurowissenschaften, Abteilung für Neurophysik, Leipzig, Deutschland

**Hintergrund:** Absolute measurements of the longitudinal relaxation rate  $R1 (= 1/T1)$  have a high potential for diagnostic applications because they are more sensitive to pathological micro-structural changes from tumors or diseases like multiple sclerosis<sup>1</sup> compared to conventional  $R1w$  or  $T1w$  imaging. Moreover, measured values are assumed to be sequence and hardware independent<sup>2,3</sup> and function as more specific markers for disease progression and contrast agent uptake<sup>1</sup>. We investigated the effect of Compressed SENSE<sup>4</sup> (CS) acceleration on the fidelity of  $R1$  mapping to foster clinical applicability by decreasing scan time.

**Methoden:** Five healthy subjects were scanned on a Philips 3T Elition. The MRI protocol consisted of  $B1$  mapping and two  $T1w$  sequences with different flip angles. Measurements were performed with standard SENSE ( $S=2.5$ , scan time: 11 min) and 2 different CS acceleration factors  $CS=4$  (9.5 min) and  $CS=6$  (6 min).  $R1$  maps were computed using the hMRI toolbox<sup>5-6</sup>. Gray matter (GM) and white matter (WM) segments were obtained using SPM12<sup>7</sup>.

**Ergebnisse:** Visually,  $R1$  maps obtained with different accelerations are very similar (Fig1). Slight artifacts from standard SENSE reconstruction (arrow Fig1a) were eliminated by CS (Fig1b-c). Subject average  $R1$  values in GM, WM, and manually defined VOIs (Fig1d) agree

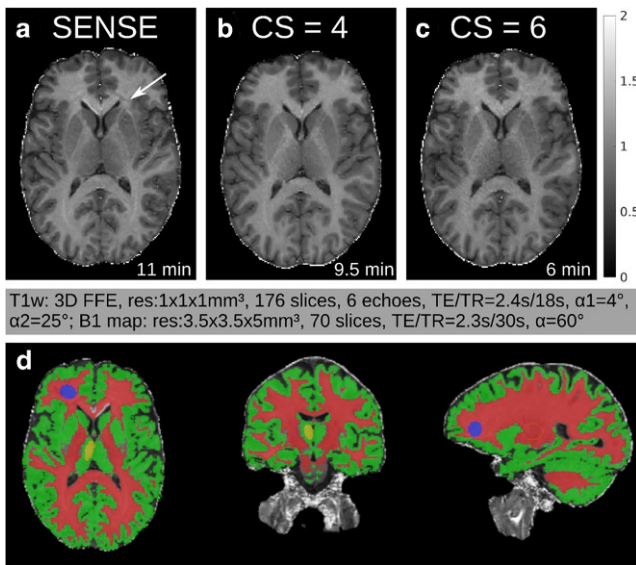


**Fig. 1 | 321** Exemplary R1 maps of a single subject with different accelerations

well between the 3 protocols (Fig2). The largest variance of R1 values across subjects is found with SENSE, while CS reduces R1 value variations across subjects (Fig2). Both CS protocols show comparable results.

**Diskussion:** Our comparison of R1 mapping protocols with different accelerations reveals R1 maps with comparable quality. Quantitative R1 values depend neither on acceleration technique (SENSE vs. CS) nor factor (CS=4 vs. CS=6).

Our results suggest that compressed SENSE, with acceleration factors up to at least 6, can be used for quantitative R1 mapping without loss of fidelity but with the advantage of clearly reduced scan times.

**Fazit:** CS is highly promising to establish quantitative R1 mapping within clinically feasible scan times.

**References**

1. Tsialios 2017 JPhys
2. Preibisch 2009 MRM
3. Baudrexel 2018 MRM
4. Geerts-Ossevoort 2018 Philips
5. Tabelow 2019 Neuroimage
6. Weiskopf 2015 CurrOpinNeurol
7. [www.fil.ion.ucl.ac.uk/spm](http://www.fil.ion.ucl.ac.uk/spm)

**333**

**TWO RARE CASES OF BRAIN ABSCESES CAUSED BY ACTINOMYCES MEYERI**

Katharina Walner<sup>2</sup>, Isabell König<sup>2</sup>, Christina Schulze<sup>3</sup>, Sebastian Fischer<sup>2</sup>, Werner Weber<sup>2</sup>, Annika Kowoll<sup>2</sup>

<sup>1</sup>Diagnostische und interventionelle Radiologie und Nuklearmedizin, Knappschaftskrankenhaus Bochum Langendreer, Bochum, Deutschland

<sup>2</sup>Diagnostische und interventionelle Radiologie und Nuklearmedizin, Knappschaftskrankenhaus Bochum-Langendreer, Bochum, Deutschland

<sup>3</sup>Medizinische Klinik, Knappschaftskrankenhaus Bochum-Langendreer, Bochum, Deutschland

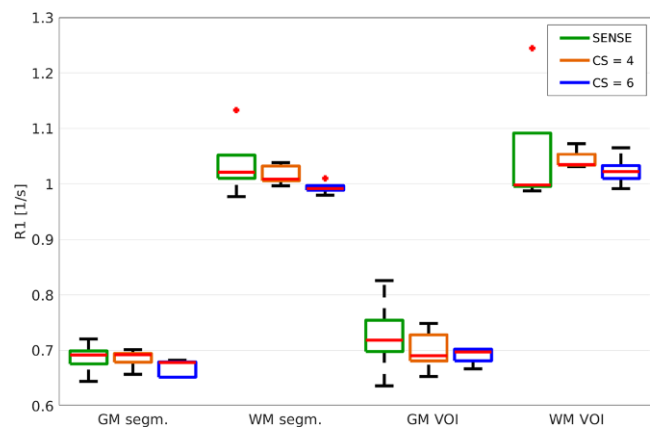


**Fig. 2 | 321** Comparison of subject average quantitative R1 values from automatically segmented and manually selected VOIs in GM and WM

**Background:** We present two cases of brain abscesses, caused by *Actinomyces meyeri*. Brain abscesses caused by *Actinomyces meyeri* are rare, only a few cases are known in literature [1].

**Methods:** Clinical information and cranial MRI studies of two patients with microbiologically confirmed *Actinomyces meyeri*-brain-abscesses were retrospectively reviewed regarding their symptoms, their predisposing factors, their imaging as well as to their response to antibiotic therapy.

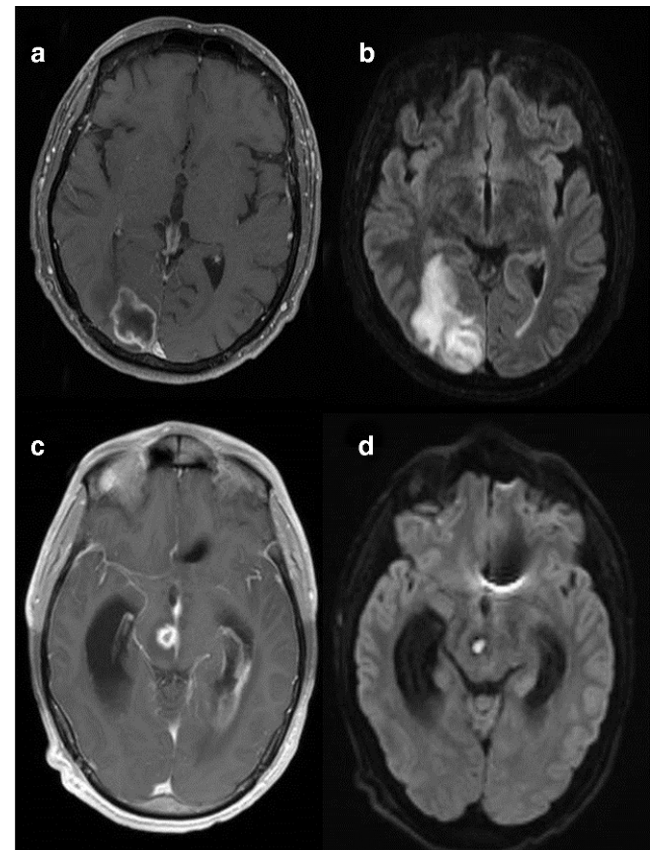


**Fig. 1 | 333** MRI of 60 Year old patient; a) T1 post-KM transversal; b) DWI transversal, 27 year old patient; e) T1 post-KM transversal; d) DWI transversal

**Result:** A 60-year old male patient and a 27-year old male patient presented at our hospital with neurological symptoms and raised temperatures. Both had no history of dental extractions, iv drug-abuse or immunosuppression. In both cases the MRI showed a singular irregular bounded lesion with a ring-enhancement as well as strong diffusion restriction and a perifocal oedema. In both cases an abscess caused by *Actinomyces meyeri* was microbiologically determined as the cause. IV antibiotic therapy was started in both cases.

**Discussion:** Brain abscesses caused by *Actinomyces meyeri* in the literature are very rare. Until now it is not explained how *Actinomyces* passes the blood brain barrier. In current literature there is described a case of *Actinomyces*-brain-abscess after dental extraction [2] but both of our patients did not have a dental intervention before suffering under brain abscesses. So in both cases the etiology remains unclear.

**Conclusion:** We report about two cases of rare brain abscesses caused by *Actinomyces meyeri*. Both patients did not have any predisposing factors.

#### References

1. Yang WT, Grant M. *Actinomyces neuii*: a case report of a rare cause of acute infective endocarditis and literature review. *BMC Infect Dis.* 2019;19(1):511. <https://doi.org/10.1186/s12879-019-4149-2>.
2. Clancy U, Ronayne A, Prentice MB, Jackson A. *Actinomyces meyeri* brain abscess following dental extraction. *Bmj Case Rep.* 2015;13:2015. <https://doi.org/10.1136/bcr-2014-207548>.

#### 343

### TRANS-RADIAL EMBOLIZATION OF MIDDLE-MENINGEAL ARTERY IN TWO PATIENTS WITH CHRONIC SUBDURAL HEMATOMAS

Johannes Hensler<sup>\*1</sup>, Jawid Madjidyar<sup>1</sup>, Fritz Wodarg<sup>1</sup>, Olav Jansen<sup>1</sup>

<sup>1</sup>Universitätsklinikum Schleswig-Holstein, Campus Kiel, Klinik für Radiologie und Neuroradiologie, Kiel, Deutschland

**Background:** Chronic subdural hematomas are a common neurosurgical disease. In addition to conventional surgical therapy, e.g. burr hole, encouraging data regarding interventional therapy with angiographic embolization of the meningeal media artery (MMA) as primary therapy or prevention of recurrence have been published recently [1]. We describe two cases with chronic subdural hematomas in which this procedure was performed under local anesthesia using the trans-radial approach.

**Methods:** Angiographic embolization of MMA in chronic subdural hematoma was performed in two patients via trans-radial approach with a 5F-Glidesheath Slender® (Terumo, Japan). A bi-axial setup with Envoy-5F guiding-catheter (Synthes, PA) was placed in common carotid artery. Embolization was performed via a 2.4F microcatheter (Progreat, Terumo) in MMA distal to spinous foramen with polyvinyl-alcohol-particles (PVA, Contour 250–355 µm, Boston Scientific, MA). In one case additional coil-embolization was performed with two pushable coils (Fig. 8–18, Boston Scientific).

**Result:** In case 1 (male, 79y) embolization of the left MMA with additional coils, in case 2 (male, y) embolization of the right MMA anterior branch was performed via the trans-radial approach in local anesthesia. In both cases a successful and complete embolization of the MMA or the anterior branch was achieved.

**Discussion:** There were no peri- or post-interventional complications. Embolization was performed to prevent recurrence 5 and 3 days after surgical burr hole and drainage or osteoplastic trepanation, respectively. Patient 1 could be discharged without neurological deficits on the day of intervention, patient 2 showed a clinical improvement at dis-

charge and a complete regression of the hematoma at 90-d follow-up CCT with no remaining neurological deficits.

**Conclusion:** Embolization of MMA via the trans-radial approach with PVA particles and coils was performed successfully and safe and may be a minimally invasive therapy option for prevention of recurrence of chronic subdural hematomas. Nevertheless, further studies regarding this procedure are necessary.

#### References

1. Link TW, Boddu S, Paine SM, et al. Middle Meningeal Artery Embolization for Chronic Subdural Hematoma: A Series of 60 Cases. *Neurosurgery.* 2018; <https://doi.org/10.1093/neuros/nyy521>.

#### 362

### KORRELATION VON RADIOLOGISCHEN PARAMETERN BEI MORBUS MENIÈRE

Desiree Grosser<sup>\*1</sup>, Friedrich Götz<sup>1</sup>, Kerstin Willenborg<sup>2</sup>, Thomas Lenarz<sup>2</sup>, Heinrich Lanfermann<sup>1</sup>, Anja Giesemann<sup>1</sup>

<sup>1</sup>Diagnostische und Interventionelle Neuroradiologie, Medizinische Hochschule Hannover, Hannover, Deutschland

<sup>2</sup>Klinik für Otorhinolaryngologie, Medizinische Hochschule Hannover, Hannover, Deutschland

**Hintergrund:** Die Diagnostik des M. Menière wurde radiologisch durch die Hydrops-Darstellung mittels MRT erweitert. Der M. Menière umfasst eine Tieftonhörmindernung, Tinnitus und Schwindel. Im MRT kann eine Differenzierung in Beteiligung von Cochlea und Vestibulum erfolgen. CT Morphologisch ist der vestibuläre Aquädukt (VA) bei M. Menière schmaler ausgeprägt. Es soll der Zusammenhang zwischen Hydropsdarstellung (vestibulär und/oder cochleär) und einem engen bzw. nicht erkennbaren VA untersucht werden.

**Methoden:** Es wurden 30 Patienten (60 Ohren) mit MR-morphologisch eindeutigem Hydrops mit der Weite des im CT sichtbaren VA ausgewertet. Der Hydrops wurde unterteilt nach Lokalisation (nur cochleär (G1), nur vestibulär oder beides (G2)). Die Graduierung des VA im CT erfolgte in nicht abgrenzbar, schmal (Weite  $\leq 1$  mm), normale Weite ( $> 1$  mm). Die Daten wurden mittels Excel korreliert.

**Ergebnisse:** Von den 60 Ohren wiesen 24 einen nur cochleären Hydrops, 4 einen isoliert vestibulären und 29 einen sowohl cochleär und vestibulären Hydrops auf. 3 kontralaterale Ohren zeigten keinen Hydrops. In G1 betrug der Anteil des nicht abgrenzbaren VA 17%, in G2 42%. Ein schmaler VA wurde in G1 in 54% gefunden, in G2 in 52%. Ein normaler VA fand sich insgesamt in nur 14%. Die 3 normalen Ohren weisen einen normal weiten VA auf. Es fand sich ein schmaler oder nicht abgrenzbarer VA auch häufiger bei vestibulärer Beteiligung als ohne.

**Diskussion:** Bei nachgewiesenem Hydrops ist auch der VA häufig schmaler ausgeprägt bzw. nicht abgrenzbar. Dies bestätigt die Daten von Krombach et al. [1]. Damit liegt mit dem CT Befund eines nicht abgrenzbaren VA ein Hinweis für M. Menière vor. Die Ätiologie des M. Menière ist weiterhin nicht geklärt. Ein Erklärungsmodell, welches einen Endolymphtransport in den Saccus endolymphaticus beinhaltet, der sicherlich bei geringem Volumen desselben eingeschränkt ist kann durch diese Daten unterstützt werden.

**Fazit:** Die Daten können die Hypothese, dass der Druckausgleich in den Saccus endolymphaticus eine Rolle für die Entstehung spielt [2], unterstützen.

#### Literatur

1. Krombach GA, van den Boom M, Di Martino E, Schmitz-Rode T, Westhofen M, Prescher A, et al. Computed tomography of the inner ear: size of anatomical structures in the normal temporal bone

and in the temporal bone of patients with Menière's disease. Eur Radiol. 2005;15(8):1505–13.

- Plontke SK, Gürkov R. Menière's Disease. Laryngorhinotologie. 2015;94(8):530–54.

367

### EARLY MRN-PARAMETERS TO PREDICT SUCCESSFUL NERVE REGENERATION FOLLOWING SEVERE INJURY

Daniel Schwarz\*<sup>1</sup>, Martin Moll<sup>1</sup>, Alfred Tessmann<sup>2</sup>, Volker Sturm<sup>1</sup>, Manuel Fischer<sup>1</sup>, Ulrich Kneser<sup>2</sup>, Martin Bendszus<sup>1</sup>, Leila Harhaus<sup>2</sup>, Sabine Heiland<sup>1</sup>, Florian Neubrech<sup>2,3</sup>

<sup>1</sup>Universitätsklinikum Heidelberg, Abteilung für Neuroradiologie, Heidelberg, Deutschland

<sup>2</sup>BG Unfallklinik Ludwigshafen, Klinik für Hand-, Plastische und Rekonstruktive Chirurgie, Schwerbrandverletzentzentrum, Klinik für Plastische und Handchirurgie der Universität Heidelberg, Ludwigshafen, Deutschland

<sup>3</sup>BG Unfallklinik Frankfurt am Main, Abteilung für Plastische, Hand- und Rekonstruktive Chirurgie, Akademisches Lehrkrankenhaus Goethe-Universität Frankfurt am Main, Frankfurt, Deutschland

**Hintergrund:** Early predictors of successful nerve regeneration are urgently needed to avoid a waste of time and thus functional outcome following severe nerve injury. Up to date, however, clinical decision making mainly relies on a watch-and-wait strategy to identify potential candidates for surgical intervention in the case of failing re-innervation [1].

We used a ultra high field magnetic resonance neurography (MRN) approach in a rodent model of peripheral nerve injury to identify early MR-parameters within the nerve which may be used to predict functional outcome.

**Methoden:** 12 female S.-Dawley rats underwent transection of the right Median nerve at upper arm level. In the gold standard group ( $n=6$ , "Gold"), an autograft of reversed Median nerve (1 cm) was re-implanted while in the negative control group ( $n=6$ , "Neg"), a 1 cm nerve gap was left in place. These two groups were imaged four times at forearm level on a 9.4 T MR-scanner 3, 10, 30 and 90 d post surgery. The protocol comprised a set of T2-w RARE, T1-w FLASH ( $\pm$  MT-pulse), DTI and MSME sequences. Groups were followed behaviourally and histological parameters were obtained after sacrifice. Results were compared longitudinally and between groups.

**Ergebnisse:** At 30 d, significant differences between Gold and Neg are noted for the magnetization transfer ratio (MTR), apparent diffusion coefficient (ADC) and radial diffusivity (RD) while other parameters show similar pathological alterations, namely T2-Time, proton density, fractional anisotropy and cross sectional area (CSA). At that time, only first signs of clinical recovery (~10% of the grip strength plateau) are present in the Gold while no function is seen in the Neg. The first time points do not show such group differences and at the last time point, only a larger CSA within the Gold is of note. Substantial phenotypical differences persist with the Neg only regaining ~20% grip strength of the Gold and showing a markedly reduced axon density.

**Fazit:** Using ultra high field MRN in a rigorous preclinical *in vivo* model we identify MTR, ADC and RD as early *in vivo* parameters of the regenerating nerve which may potentially be used in a translational setting to predict functional outcome and guide therapeutic decision making in the future.

### References

- Schwarz D, Pedro MT, Brand C, Bendszus M, Antoniadis G. Nerve injuries and traumatic lesions of the brachial plexus: Imaging diagnostics and therapeutic options. Radiologe. 2017;57:184–94. <https://doi.org/10.1007/s00117-017-0207-1>.

## Autorenverzeichnis

- A**
- Abdullayev, Nuran 218, 237  
 Abu-Fares, Omar 128  
 Albarqouni, Shadi 241  
 Alexandrou, Maria 237  
 Alonso, Angelika 112, 181, 364  
 Aludin, Schekeb 274  
 Aludin, Zarlasht 274  
 Al-Zghloul, Mansour 112, 181  
 Andresen, Gisa 277  
 Andresen, Julian Ramin 62  
 Andresen, Reimer 62, 87, 243  
 Anraths, Max 271  
 Anwar, Abdul Rauf 74  
 Arnold, Marcel 357  
 Auer, Timo Alexander 38  
 Aulmann, Linda 68  
 Aumann, Astrid 222  
 Austein, Friederike 139, 183
- B**
- Bach, Jan Philipp 293  
 Bähr, Oliver 311  
 Barg-Hock, Hannelore 126  
 Barkhof, Frederik 214  
 Barlinn, Jessica 291  
 Bartsch, Andreas 186  
 Bauknecht, Hans-Christian 341  
 Baum, Thomas 96, 109, 111, 164, 205, 314  
 Baur, Christoph 241  
 Beck, J 230  
 Becker, Lucas Ivo Emanuel 296  
 Behme, Daniel 218, 322, 324  
 Bellwald, Sebastian 357  
 Bender, Benjamin 176  
 Bendzus, Martin 65, 73, 80, 82, 86, 89, 130, 134, 135, 136, 137, 138, 174, 186, 190, 193, 194, 196, 197, 211, 270, 365, 367  
 Berberich, Anne 187  
 Berberich, Götz 105  
 Berenstein, Alejandro 299  
 Berg, Philipp 188, 301  
 Berg, Ronja 143, 321  
 Berkefeld, Joachim 313  
 Berlis, Ansgar 117, 138, 322  
 Berndt, Maria 99, 103, 125, 127, 129, 132  
 Berthold, Christoph 199  
 Beseoglu, Kerim 348  
 Bester, Maxim 110, 166, 246  
 Beuing, Oliver 188, 340  
 Bhogal, Pervinder 184  
 Birch, Giselle 214  
 Bison, Brigitte 220  
 Bittner, Stefan 74  
 Blanc, Raphael 138  
 Blüm, Philipp 132  
 Boeckh-Behrens, Tobias 99, 103, 125, 127, 129, 132  
 Böhm, Christoph 314  
 Böhme, Johannes 97, 112, 181, 364  
 Böhmer, Maik 292  
 Bohner, Georg 341  
 Bojunga, Jörg 311  
 Bonati, Leo 63  
 Bonekamp, Susanne 136, 137  
 Borggreffe, Jan 104, 218, 223, 224, 345  
 Börm, Wolfgang 277  
 Brandhofe, Annemarie 300, 313  
 Braschkat, Andres 269  
 Braun, Michael 57  
 Brawanski, Alexander 88  
 Brehm, Alex 94, 323, 324  
 Brekenfeld, Caspar 134, 203, 237, 251, 255, 347  
 Bremer, Benno 105  
 Brockmann, Carolin 147  
 Brockmann, Marc A. 147, 172  
 Bronzlik, Paul 128, 171  
 Broocks, Gabriel 42, 64, 70, 75, 79, 163, 208, 251, 305, 370  
 Bsteh, Gabriel 106  
 Buhk, Jan-Hendrik 100, 340  
 Bürger, Milène 284  
 Burian, Egon 178, 205, 207, 226
- C**
- Caldeira, Liliana 345  
 Calzà, Jessica 105  
 Cantré, Daniel 260, 358  
 Caspers, Julian 51, 67, 204, 256, 269, 287, 348  
 Cattaneo, Giorgio 188  
 Chapot, Rene 246, 340  
 Chard, Declan 214  
 Cheng, Bastian 251  
 Cho, Chang Gyu 97, 280  
 Chung, Karen 214  
 Ciccarelli, Olga 214  
 Clajus, Christin 108  
 Coras, Roland 87  
 Cordt, Justus 142  
 Cordts, Isabell 330  
 Costalat, Vincent 138  
 Cyran, Clemens 229
- D**
- Dabkowska-Mika, Agnieszka 252, 268  
 Dadak, Mete 171  
 Dargazanli, Cyril 138  
 Deb-Chatterji, Milani 203, 237, 251, 255, 347  
 Deichmann, Ralf 284, 300  
 Deisenhammer, Florian 106  
 Demerath, Theo 309, 63  
 Deschauer, Marcus 330  
 Deshmane, Anagha 176  
 Deutschmann, Hannes 69, 81  
 Dieckmeyer, Michael 157, 205  
 Dimitrov, Ivaylo 293  
 Ding, Andreas 188  
 Ding, Xiao-Qi 126, 171  
 Dinse, Bianca 130  
 Ditz, Claudia 68  
 Dobrocky, Tomas 357  
 Doenitz, Christian 88  
 Döpfert, Jörg 157  
 Dörfler, Arnd 266  
 Dorn, Franziska 223, 224, 340, 355  
 Drescher, Finn 294  
 Drumm, Jörg 199  
 Dühsen, Max 229  
 Duman, Ikram Eda 158  
 Dyrba, Martin 358
- E**
- Egger, Karl 158, 230  
 Eichinger, Paul 124  
 Eickhoff, Simon 256  
 Eisawy, Rami 360  
 Eisenberger, Hanna Josephin 94  
 Eisenhut, Felix 266  
 Elsayed, Sarah 79, 208  
 Emmer, Alexander 184  
 Engel, Jakob 183  
 Engelland, Kay 291  
 Enzinger, Christian 69  
 Epp, Samira 145  
 Eppinger, Sebastian 69  
 Ernemann, Ulrike 176  
 Ernst, Marielle Sophie 42  
 Eshaghi, Arman 214
- F**
- Faizy, Tobias D. 110, 163, 166  
 Fandler, Simon 69  
 Fandler-Höfler, Simon 81  
 Farahat, Amr 289  
 Fassbender, Klaus 192  
 Fazekas, Franz 69, 81  
 Fehrenbach, Uli 38  
 Fenz, Wolfgang 253  
 Ferrera Bertran, Pere 157  
 Fiehler, Jens 42, 64, 70, 75, 79, 110, 134, 163, 166, 203, 208, 237, 246, 251, 255, 286, 305, 347, 370  
 Finck, Tom 124, 360  
 Fischer, Antonia Carlotta 139  
 Fischer, Manuel 367  
 Fischer, Sebastian 117, 294, 333  
 Fischer, Urs 356, 357  
 Fleck, Steffen 260  
 Fleischer, Vinzenz 74  
 Flottmann, Fabian 70, 75, 134, 203, 237, 251, 255, 305, 347  
 Flüh, Charlotte 301  
 Fokas, Emmanouil 311  
 Forbrig, Robert 229, 355  
 Förster, Alex 97, 112, 181, 364  
 Franz, Daniela 205  
 Franz, Kea 311  
 Friedrich, Benjamin 99, 103, 125, 127, 129, 132, 330  
 Frysch, Robert 188  
 Fu, Tong 171  
 Fuchs, Simon 341  
 Furtmann, Johanna 267
- G**
- Ganslandt, Thomas 69, 97, 280  
 Gerber, Johannes 291  
 Gerloff, Christian 237, 251  
 Gerry, Stephen 187  
 Gersing, Alexandra S. 314  
 Gessert, Nils 244  
 Giesemann, Anja 362  
 Giretzlehner, Michael 253  
 Gizewski, Elke Ruth 106, 252, 268  
 Gliem, Michael 67, 287  
 Gmeiner, Matthias 253  
 Gnanaprakasam, Velmurugan 115  
 Gnekow, Astrid K. 220  
 Goeldlin, Martina 357  
 Golay, Xavier 176  
 Gonzalez-Escamilla, Gabriel 74  
 Görtz, Lukas 104, 223, 224, 345  
 Göttler, Jens 121, 148, 288, 290  
 Gottschalk, Hannes 183  
 Götz, Friedrich 128, 362  
 Goyal, Mayank 324  
 Gracien, René-Maxime 74, 300  
 Gralla, Jan 356, 357  
 Greve, Tobias 115, 162  
 Groden, Christoph 97, 112, 181, 280, 172, 364  
 Groffmann, Maximilian 305  
 Gröner, Jan 211  
 Groppa, Sergiu 74  
 Grosser, Desiree 362  
 Groth, Friederike 260  
 Groth, Sascha 260  
 Gruber, Andreas 253  
 Grundl, Lioba 124  
 Grundwald, Iris 192  
 Gumbinger, Christoph 135  
 Günther, René 310  
 Gürsel, Deniz A. 105

- H**
- Hadler, Felix 298  
 Hädrich, Kevin 291  
 Haensch, Carl-Albrecht 287  
 Hahn, Arthur 211  
 Hähnel, Stefan 270  
 Haider, Lukas 214  
 Haid-Stecher, Nina 268  
 Hancken, Caroline-Victoria 220  
 Hanning, Uta 42, 64, 70, 75, 79, 163, 208, 246, 251, 286, 292, 305, 347, 370  
 Hansen, Brian 110, 166  
 Hansen, Mikkel Bo 288  
 Harhaus, Leila 367  
 Harter, Patrick 311  
 Härtig, Wolfgang 184  
 Hartmann, Christian 256  
 Hartmann, Marius 259  
 Hasan, Dimah 313  
 Hasler, Mario 271  
 Hassler, Eva 69  
 Hattingen, Elke 245, 284, 300, 311  
 Hauser, Till-Karsten 53  
 Haußmann, Alena 320  
 Hedderich, Dennis 111, 132, 157  
 Heeger, Adrian 204  
 Heesen, Christoph 110, 166  
 Heiland, Dieter Henrik 189  
 Heiland, Pamela 189  
 Heiland, Sabine 194, 211, 270, 367  
 Heimann, Friederike 134  
 Heindel, Walter 292  
 Heinze, Hans-Jochen 289  
 Heldner, Mirjam Rachel 357  
 Hemmer, Bernhard 330  
 Hemmerich, Felix 65, 80, 82, 86, 89, 196, 197,  
 Hemraj, Indradeo 348  
 Hense, Katharina 88  
 Hensler, Johannes 138, 349, 343  
 Herrlinger, Ulrich 245  
 Herweh, Christian 174, 186, 187, 190, 192, 193, 270, 365, 73  
 Herz, Kai 176  
 Herzberg, Moritz 224  
 Hesse, Amelie 324  
 Hey, Silke 115  
 Hilgenfeld, Tim 211  
 Hinrichs, Hermann 289  
 Hinteregger, Nicole 69, 81  
 Hock, Andreas 115, 143, 288, 290  
 Hoffmann, Karl-Titus 184, 263  
 Hoffstaedter, Felix 256  
 Hohenhaus, M 230  
 Hölter, Philip 266  
 Hopf-Jensen, Silke 271, 276, 277  
 House, Patrick 312  
 Hövener, Jan-Bernd 329  
 Hübschle, Irene 189
- Hyder, Fahmeed 121, 288, 290  
 Hyrenbach, Sonja 136, 137
- I**
- Ikenberg, Benno 331  
 Imhoff, Detlef 311  
 Inhuber, Stephanie 205  
 Ischebeck, Anja 252  
 Ivan, Vivien Lorena 67
- J**
- Jacob, Alina 96  
 Jander, Sebastian 67, 287  
 Jannusch, Kai 348  
 Jansen, Olav 139, 142, 144 183, 225, 274, 281, 329, 343, 349  
 Janssen, Hendrik 138, 340  
 Jeibmann, Astrid 286  
 Jende, Johann 194, 211  
 Jensen-Kondering, Ulf 144  
 Jespersen, Sune 110, 166  
 Jesser, Jessica 130, 270  
 Joly, Olivier 192  
 Jost, Joachim 270  
 Juerchott, Alexander 211  
 Jung, Simon 357  
 Junge, Andreas Georg 97, 280  
 Jurcoane, Alina 284
- K**
- Kabbasch, Christoph 218, 223, 224  
 Kabiri, Reza 42, 163  
 Kaczmarz, Stephan 121, 148, 288, 290, 145, 321  
 Kadziolka, Krzysztof 340  
 Kaesmacher, Johannes 103, 125, 127, 129, 356, 357  
 Kaethner, Christian 266  
 Kalder, Johannes 297  
 Kämpgen, Benedikt 280  
 Kandels, Daniela 220  
 Karampinos, Dimitrios C. 205, 314  
 Karwacki, Grzegorz 309  
 Kaschner, Marius 67, 287, 348  
 Kastrop, Andreas 237  
 Kaufmann, Jörn 92  
 Kazmierczak, Philipp 229  
 Keil, Fee 313  
 Kellner, Elias 158, 230  
 Kemmling, Andre 64, 70, 79, 292, 305, 370  
 Kender, Zoltan 211  
 Kern, Maike 38  
 Kerz, Thomas 147  
 Khadhraoui, Eya 195  
 Khanafer, Ali 195, 285  
 Kickingereder, Philipp 73  
 Killer, Monika 138  
 Kim, Suam 230
- Kirschke, Jan S. 96, 101, 109, 111, 115, 164, 205, 314  
 Kirschner, Stefanie 172  
 Kitzler, Hagen H. 303, 310  
 Klein, Matthias 229  
 Kleine, Justus 341  
 Kleiser, Raimund 150, 262  
 Klempnauer, Jürgen 126  
 Klisch, Joachim 108  
 Klose, Uwe 53  
 Klupp, Elisabeth 205  
 Kneihs, Markus 69, 81  
 Kneser, Ulrich 367  
 Kniep, Helge 42, 70, 75, 79, 163, 208, 286  
 Koch, Caroline 358  
 Koch, Kathrin 105  
 Koehler, Caroline 303  
 Kollmer, Jennifer 194  
 König, Isabell 117, 333  
 Kopetsch, Christoph 234  
 Kopf, Stefan 211  
 Kopp, Felix K. 109, 111, 164  
 Kortmann, Rolf-Dieter 220  
 Kowoll, Annika 294, 333  
 Kraemer, Christoffer 134  
 Kramer, Andreas 147  
 Kramer, Martin 172  
 Krause, Lars Udo 246  
 Krause, Matthias 184  
 Kreiser, Kornelia 132, 162, 340  
 Kronfeld, Andrea 172  
 Kronthaler, Sophia 314  
 Krüger, Julia 244  
 Kubera, katharina 186  
 Kuchler, Jan 68  
 Kufer, Jan 121, 288  
 Kuhlentbäumer, Gregor 144  
 Kuntke, Paul 303, 310  
 Kunz, Wolfgang 229  
 Kurmann, Christoph 357  
 Kurz, Felix Tobias 211  
 Kyselyova, Anna 110, 166
- L**
- Lamplmayr, Lukas 106  
 Lanfermann, Heinrich 126, 128, 171, 362  
 Lang, Stefan 266  
 Langguth, Patrick 139, 144, 183  
 Langner, Sönke 260  
 Larsen, Naomi 139, 183, 274, 281, 301, 349  
 Laukamp, Kai Roman 104, 345  
 Lebenatus, Annett 183  
 Leblhuber, Friedrich 262  
 Lee, John-Ih 287  
 Lee, John-II 67  
 Lehrke, Stephanie 271  
 Leischner, Hannes 64, 70, 203, 237, 246, 251, 255, 305, 347  
 Leitner, Stephan 254  
 Lemke, Andreas 157  
 Lenarz, Thomas 362
- Lenhart, Lukas 106, 268  
 Lennartz, Simon 345  
 Leutritz, Tobias 321  
 Li, Hongwei 124  
 Liebig, Thomas 218, 223, 224, 355  
 Liedke, Marc Olaf 62  
 Liesche, Friederike 98  
 Liman, Jan 39, 94, 249, 323  
 Lindig, Tobias 176  
 Lindner, Thomas 183  
 Lingor, Paul 330  
 Linn, Jennifer 303, 291, 310  
 Linstedt, Ulf 277  
 Lipkova, Jana 98  
 Liu, Jian-Mín 94  
 Lobsien, Donald 108  
 Löffler, Maximilian T. 96, 109, 111, 205  
 Lowens, Stephan 246  
 Lübeck, Cindy 188  
 Luessi, Felix 74
- M**
- Madjidyar, Jawid 225, 281, 349, 343  
 Maegerlein, Christian 99, 103, 111, 125, 127, 129, 132, 330, 331  
 Maier, Ilko 94, 323, 324  
 Maier, Lisa 178, 207  
 Maintz, David 345  
 Mangesius, Stephanie 106, 214  
 Manogaran, Praveena 244  
 Margraf, Nils 144  
 Maros, Máté 97, 280, 172  
 Mathys, Christian 256  
 Mattle, Heinrich 357  
 Maurer, Christoph 117, 138, 322  
 Maus, Volker 39, 100, 218, 237, 249, 285, 322, 323, 324,  
 McTaggart, Ryan 324  
 Mei, Kai 109, 111, 164  
 Meila, Dan 299, 304, 100  
 Meineke, Jakob 143  
 Meinel, Thomas 357  
 Menze, Björn 98, 124, 360  
 Metz, Marie-Christin 98  
 Meuth, Sven G. 74  
 Meyding-Lamadé, Uta 270  
 Meyer, Bernhard 162  
 Meyer, Lukas 42, 70, 237, 246, 251, 370  
 Meyne, Johannes 183  
 Minnerup, Jens 286  
 Misch, Martin 38  
 Möhlenbruch, Markus 65, 73, 80, 82, 86, 89, 134, 135, 136, 137, 138, 174, 187, 190, 192, 193 196, 197, 365  
 Mokli, Yahia 187  
 Molina-Romero, Miguel 98  
 Moll, Martin 367

- Mönch, Sebastian 99, 125, 127, 129, 132  
 Moosbauer, Julia 360  
 Mordasini, Pasquale 357  
 Mosimann, Pascal 357  
 Mouridsen, Kim 288  
 Mpotsaris, Anastasios 218, 223, 237, 297  
 Mück, Fabian 103, 125, 127, 129  
 Mühlau, Mark 101  
 Mühl-Benninghaus, Ruben 320  
 Müller, Andreas 245  
 Müller, Angela 291  
 Müller, Mathias 245  
 Müller, Sebastian 195, 285  
 Müller-Hülsbeck, Stefan 271, 276, 277  
 Müller-Thies-Broussalis, Erasmia 138  
 Muthuraman, Muthuraman 74
- N**
- Nagel, Simon 73, 174, 186, 187, 190, 192, 193  
 Nasri, Hadi 348  
 Navab, Nassir 241  
 Nawabi, Jawed 163, 208  
 Nawroth, Peter 211  
 Nerkada, Lars 225  
 Neuberger, Ulf 73  
 Neubrech, Florian 367  
 Neumann, Alexander 68  
 Niederkorn, Kurt 69  
 Niederstadt, Thomas 292  
 Nijenhuis, Marco 115  
 Nikoubashmann, Omid 293, 297, 298, 267  
 Noel, Peter B. 109, 111, 164  
 Nösel, Patrick 126, 171  
 Nöth, Ulrike 300
- O**
- Opfer, Roland 244  
 Oros-Peusquens, Ana Maria 267  
 Osmanovic, Alma 128  
 Ostwaldt, Ann-Christin 244  
 Othman, Ahmend E 297, 298  
 Ott, Christian 88
- P**
- Paetzold, Johannes 124  
 Papanagiotou, Panagiotis 192, 237  
 Patzig, Maximilian 229  
 Pelzl, Sirko 312  
 Pennig, Lenhard 104, 345  
 Pereira-Zimmermann, Benjamin 135  
 Pereverzyev Jr., Sergiy 106  
 Perfler, Manuel 254  
 Perkuhn, Michael 104  
 Peschke, Eva 329  
 Peters, Sönke 142  
 Petr, Jan 288, 290  
 Petri, Susanne 128, 171  
 Petridis, Athanasios K. 348  
 Pfaff, Johannes 65, 73, 80, 82, 86, 89, 135, 138, 174, 187, 192, 196, 197  
 Pfeilschifter, Waltraud 300  
 Pfister, Franz MJ 360  
 Pflugrad, Henning 126  
 Pham, Mirko 220, 340  
 Piechowiak, Eike Immo 357  
 Piesch, Tim-Christian 183  
 Pietsch, Torsten 220  
 Pilatus, Ulrich 284, 311  
 Piotin, Michel 138  
 Pitzen, Tobias 199  
 Pöckler-Schöniger, Christiane 199  
 Politi, Maria 237  
 Porto, Luciana 284  
 Potthoff, Denise 150  
 Prados, Ferran 214  
 Pravdivtseva, Mariya 329  
 Pree, David 103  
 Preibisch, Christine 121, 143, 145, 148, 288, 290, 321  
 Preisner, Fabian 211  
 Preiß, Michael 276, 277  
 Probst, Florian 207, 226  
 Probst, Monika 178, 207, 226  
 Prudlo, Johannes 358  
 Psychogios, Marios 322, 323, 324  
 Psychogios, Marios-Nikos 94, 195, 285, 39, 100, 249  
 Puchta, Joana 184  
 Puetz, Volker 291  
 Pürner, Dominik 129  
 Purucker, Jan 135
- Q**
- Quäschling, Ulf 184, 268
- R**
- Radetz, Angela 74  
 Raffelsberger, Tobias 262  
 Rathmann, Eiko 260  
 Reich, Arno 293, 297, 298  
 Reimer, Robert Peter 104  
 Reinholz, Lena 105  
 Reisert, M 230  
 Reishofer, Gernot 81  
 Reith, Wolfgang 192, 320, 340  
 Riabikin, Alexander 298  
 Richter, Cindy 184, 263  
 Ricke, Jens 229  
 Ridwan, Hani 297, 298  
 Riedel, Christian 142, 363  
 Riederer, Isabelle 101, 109, 164  
 Riedl, Valentin 145  
 Rieger, Johannes 311  
 Ringel, Florian 147  
 Ringleb, Peter Arthur 73, 134, 174, 187, 190, 193  
 Ritschl, Lucas 207, 226  
 Robl, Teresa 178, 226  
 Rode, Susanne 136, 137  
 Rödel, Claus 311  
 Roder, Constantin 53  
 Roesler, Jennifer 331  
 Rohde, Veit 195  
 Rosengarh, Katharina 88  
 Roßkopf, Johannes 57  
 Roth, Christian 237  
 Rothaupt, Jan 246  
 Rother, Christian 200, 211  
 Rubbert, Christian 51, 67, 204, 256, 269, 287, 348  
 Ruf, Michael 199  
 Rummeny, Ernst J. 109, 111, 205, 314  
 Runck, Frank 138  
 Rusche, Thilo 79, 92  
 Ruschke, Stefan 314  
 Ryang, Yu-Mi 96
- S**
- S, Yang 230  
 Saalfeld, Sylvia 301  
 Sabou, Teodor Catalin 234  
 Sahlmann, Imke 249  
 Salehi Ravesh, Mona 183  
 Sallakhi, Aria 62  
 Schacht, Hannes 68  
 Schäferhenrich, Nora 297  
 Schaier, Matthias 186  
 Scheer, Fabian 62, 234  
 Scheffler, Klaus 176  
 Scherlach, Cordula 184  
 Schiffer, Mario 126  
 Schippling, Sven 244  
 Schittenhelm, Jens 176  
 Schlaefer, Alexander 244  
 Schlaeger, Sarah 205  
 Schlamann, Marc 218, 223, 224  
 Schlörcke, Erik 62  
 Schmidt, Manuel 266  
 Schmitz, Bernd 57  
 Schmitz, Birte 126, 171  
 Schmitz, Leonie 249  
 Schmitzer, Lena 148  
 Schmitz-Koep, Benita 96, 105  
 Schneider, Charlotte 314  
 Schnieder, Marlena 324  
 Schnitzbauer, Michael 259  
 Schnitzler, Alfons 256  
 Schob, Stefan 184, 263  
 Schoen, Gerhard 64, 163, 208  
 Schön, Simon 109, 164  
 Schönenberger, Silvia 135, 174, 190, 193  
 Schönfeld, Michael 42, 370  
 Schramm, Peter 68, 70, 222, 296  
 Schreiber-Katz, Olivia 128  
 Schroth, Gerhart 357  
 Schrum, Anna 87  
 Schubert, Tilman 63, 309  
 Schulze, Christina 333  
 Schüngel, Marie-Sophie 263  
 Schürmann, Kolja 293  
 Schwaiger, Benedikt J. 314  
 Schwamborn, Carolin 310  
 Schwarz, Daniel 367  
 Schwenke, Hannes 222, 296  
 Schwirtz, Ansgar 205  
 Seelhorst, Martin 264  
 Seiler, Alexander 300  
 Seitz, Rüdiger 150  
 Seker, Fatih 134, 135, 136, 137, 187, 190, 193  
 Selbach, Moritz 147  
 Sepp, Dominik 99, 103  
 Sevecke, Kathrin 268  
 Shah, Nadim Jon 267  
 Shakirin, Georgy 104  
 Shiban, Ehab 162  
 Sichtermann, Thorsten 267  
 Siebert, Eberhard 224, 341  
 Siedentopf, Christian 252  
 Siemonsen, Susanne 110, 166  
 Sigl, Benjamin 256  
 Sima, Diana 264  
 Simgen, Andreas 320  
 Singh, Raveena 297  
 Skardelly, Marco 176  
 Smeets, Dirk 264  
 Smyk, Michael 223  
 Sollmann, Nico 101, 109, 111, 115, 148, 164, 205, 290  
 Solyanik, Olga 229  
 Sommer, Clemens 172  
 Sporns, Peter 79, 208, 286, 292  
 Stark, Maria 166  
 Steidl, Eike 245  
 Steiger, Ruth 252, 268  
 Steinbach, Joachim 311  
 Steiner, Thorsten 134  
 Stellmann, Jan-Patrick 110, 166  
 Stock, Annika 220  
 Stockert, Anika 184  
 Stracke, Christian Paul 246  
 Stracke, Paul 340  
 Sträter, Ronald 292  
 Sturm, Volker 367  
 Styczen, Hanna 39, 100, 249, 323  
 Südmeyer, Martin 256  
 Sweeney-Reed, Catherine 289  
 Szymczak, Silke 271
- T**
- Tanrikulu, Levent 195  
 Tanyildizi, Yasemin 172  
 Taschner, Christian 340  
 Teichert, Nikolas 256, 348  
 Tessarek, Svenja 75  
 Tessmann, Alfred 367  
 Thaler, Christian 110, 163, 166

Thiele, Frank 104, 345  
 Thomalla, Götz 64, 75, 134, 203, 237, 246, 251, 255, 347, 370  
 Thurner, Isabella 252  
 Timmer, Marco 104  
 Timmermann, Beate 220  
 Trenkler, Johannes 150, 253, 262  
 Tritt, Stephanie 322  
 Tropine, Andrei 322  
 Trumm, Christoph 355  
 Tsogkas, Ioannis 39, 94, 100, 323, 324  
 Turowski, Bernd 51, 67, 204, 223, 256, 269, 287, 340, 348

**U**

Ulfert, Christian 174, 365  
 Urbach, Horst 158, 189, 230

**V**

Valentinitsch, Alexander 96  
 Van Hecke, Wim 264  
 van Horn, Noel 347  
 Vande Vyvere, Thijs 264  
 Velvaluri, Prasanth 329  
 Voges, Jürgen 92  
 Vollherbst, Dominik 190, 193  
 von Mettenheim, Nina 311  
 Voss, Martin 311  
 Voss, Samuel 301  
 Voß, Samuel 188

**W**

Wagner, Arthur 162  
 Wagner, Marlies 300, 311  
 Wahl, Hannes 303, 310  
 Walker-Egger, Christine 244  
 Walner, Katharina 333  
 Warmuth-Metz, Monika 220  
 Wartner, Sandra 254  
 Weber, Werner 117, 294, 333  
 Weiler, Caroline 144  
 Weiler, Markus 194  
 Weiß, Alexander 184  
 Weiß, Daniel 287  
 Weissenborn, Karin 126  
 Wellmer, Jörg 294  
 Wendl, Christina 88  
 Wenger-Alakmeh, Katharina 311  
 Wenz, Holger 97, 112, 181, 280, 364  
 Weyer, Vanessa 172  
 Weyland, Charlotte 65, 80, 89, 196, 197, 82, 86  
 Wick, Wolfgang 194  
 Widmann, Carola 150  
 Wiener, Edzard 38  
 Wiesinger, Isabel 88  
 Wiesmann, Martin 293, 297, 298, 267  
 Wießpeiner, Ulrike 81

Wiestler, Benedikt 98, 124, 241, 360  
 Wildemann, Brigitte 194  
 Wildgruber, Moritz 286, 292  
 Willenborg, Kerstin 362  
 Wilms, Guido 264  
 Wimmer, Sibylle 150, 262  
 Wirth, Stefan 103, 125, 127, 129  
 Wissgott, Christian 234  
 Wodarg, Fritz 138, 139, 274, 281, 349, 343  
 Wolf, Robert Christian 186  
 Wörtler, Klaus 314  
 Wunderlich, Silke 99, 103, 125, 127, 129, 132, 162  
 Wurm, Markus 314  
 Würtemberger, Urs 189  
 Wurth, Sebastian 106

**X**

Xenia, Kobeleva 171

**Y**

Yang, Pengfei 94  
 Yilmaz, Umut 320

**Z**

Zaiss, Moritz 176  
 Zapf, Antonia 249  
 Zapf, Julian 314  
 Zeidan, Moussa 270  
 Zeier, Martin 186  
 Zerweck, Leonie 53  
 Ziemssen, Tjalf 303  
 Zimmer, Claus 96, 98, 99, 101, 103, 109, 111, 115, 121, 124, 125, 127, 129, 132, 148, 157, 162, 164, 178, 205, 207, 226, 241, 288, 290, 330, 331, 360, 143, 321  
 Zipp, Frauke 74  
 Zöllner, Christoph 314  
 Zopfs, David 104